Understanding the biology of transforming growth factor-β in colorectal cancers

Harish Reddy Cheruku

Master of Biotechnology, Macquarie University

Faculty of Medicine and Health Sciences

Macquarie University, Sydney, Australia

MACQUARIE University
SYDNEY·AUSTRALIA

A thesis submitted to Macquarie University in fulfilment of the requirements for the degree of Doctor of Philosophy.

July 2015

Dedication

With love and gratitude

To my parents,

whose support and encouragement

made this thesis possible

&

To Trúc Thanh Lê,

whose love and support

make everything seem possible

TABLE OF CONTENTS

LIST OF TABLES

LIST OF FIGURES

STATEMENT OF DECLARATION

I certify that the work presented in this thesis titled "Understanding the biology of transforming growth factor-beta in colorectal cancers" has not previously been submitted, in either whole or part, for obtaining any other degree to any other university or institution other than Macquarie University. The work in this thesis has been carried out by the author, unless otherwise acknowledged.

Harish R Cheruku
41629191

ACKNOWLEDGEMENTS

ABSTRACT

Colorectal cancer (CRC) affects millions of people every year globally. Abnormal cells utilize several mutated proteins and perturbed pathways to progress from a benign tumour to malignant cancer. Expression of proteins such as uPAR, integrin β6 and TGFβ have been extensively implicated by us and others in CRC.

The primary aim of this thesis was to contribute additional knowledge to regarding the role TGFβ in CRC through investigation of the proposed hypothetical uPAR•αvβ6•TGFβ1 interactome. This was achieved by using six CRC cell lines as model systems where expression levels of two known activator systems of TGFβ, namely integrin β6 (SW480^{Mock}, SW480^{β6OE}, HT29^{Mock}, HT29^{β6AS}) and the uPA protease receptor uPAR (HCT116^{WT} and HT29^{uPARAS}) have been artificially expressed or down regulated. The changes in these model systems following active TGFβ1 treatment were investigated using state-of-the-art proteomics and a cell signalling assay (i.e., AlphaScreen® SureFire® Assay) technologies in conjunction with sophisticated bioinformatics. The cells expressing β6 (SW480^{β6OE}, HT29^{Mock}, HT29^{β6AS}) exhibited increased proliferation, invasion and wound healing upon treatment with TGFβ1. The cells with higher uPAR expression did not respond to (HCT116^{WT}) TGFβ treatments. These results determined that malignancy was attained in a TGFβ-dependent manner when β6 was expressed or in a TGFβ-independent manner when uPAR was expressed. Additionally, the proteomic data presented in this thesis identified several perturbed proteins and biomolecular pathways that could be associated with CRC and has given important clues to understanding the role of TGFβ and the proposed hypothetical uPAR•αvβ6•TGFβ1 interactome.

Additionally, an Olink Proseek study using Dukes' stage A-D CRC patient plasma samples (1μL of plasma) identified CEA, IL-8 and prolactin were determined to differentiate unaffected controls from non-malignant (Dukes' A + B) and malignant (Dukes' C + D) stages and were published as potential plasma Dukes'-stage CRC biomarkers.

This thesis has demonstrated the immense power of high-throughput modern proteomic and multiplexing technologies to gain insights into the TGFβ associated CRC pathogenesis at detailed molecular level and to identify avenues for disease biomarker exploration.

PUBLICATIONS AND CONTRIBUTION STATEMENT

This thesis contains material that has been published, and the percentage contribution in each of the publication by the candidate "Cheruku HR" are as follows:

Publication I (First author)

Cheruku HR, Mohamedali A, Cantor DI, Tan SH, Nice EC and Baker MS (2015). Transforming growth gactor-β, MAPK and Wnt signaling interactions in colorectal cancer. *EuPA Open proteomics. In press, Available online 2 July 2015. (doi:10.1016/j.euprot.2015.06.004)*.

The candidate contributed to all aspects of the manuscript. Concept – 90%; Writing – 70%; **Total (Average) – 80%**

Publication II (Co-author)

Cantor DI, **Cheruku HR**, Nice EC and Baker MS (2015). The β6 integrin sets the stage for colorectal cancer metastasis. *Cancer Metastasis Rev. 2015 Sep 4*. [Epub ahead of print]. PubMed ID: 23201117

The candidate contributed to all aspects of the manuscript. Concept – 25%; Writing – 25%; **Total (Average) – 25%**

Publication III (Co-first author)

Cantor DI, **Cheruku HR**, Ahn SB, Crouch MF, Nice EC and Baker MS (2015). Expression of αvβ6 integrin enhances both plasminogen and latent-transforming growth factor-β1 dependant proliferation, invasion and ERK1/2 signalling in colorectal cancer cells. *(Prepared for publication. The manuscript has been submitted to an early career researcher award competition at HUPO world congress 2015 and if accepted will be published in a HUPO affiliated journal)*.

The candidate contributed to all aspects of the manuscript. Concept – 30%; Data collection – 30%; Analysis – 30%; Writing – 30%; **Total (Average) – 30%**

Publication IV (First author)

Cheruku HR, Cantor DI, Mohamedali A, Tan SH, Nice EC and Baker MS (2015). Transforming growth factor-β signalling induces differential protein expression in colon cancer cells that varies with the level of integrin β6 expression. *(Prepared for publication to "Journal of Proteome Research")*.

The candidate contributed to all aspects of the manuscript. Concept – 50%; Data collection – 80%; Analysis – 80%; Writing – 70%; **Total (Average) – 70%**

Publication V (First author)

Cheruku HR, Cantor D, Mohamedali A, Tan SH, Nice E and Baker MS (2015). Does differential expression of cell-surface uPAR alter the effects active TGFβ has on the colorectal cancer cell membrane proteome? *(Prepared for publication to "International Journal of Oncology")*.

The candidate contributed to all aspects of the manuscript. Concept – 50%; Data collection – 90%; Analysis – 80%; Writing – 70%; **Total (Average) – 72.5%**

Publication VI (Co-author)

Mahboob S, Ahn SB, **Cheruku HR**, Cantor D, Rennel E, Fredriksson S, Edfeldt G, Breen EJ, Khan A, Mohamedali A, Muktadir MG, Ranganathan S, Tan SH, Nice E and Baker MS (2015). A novel multiplexed immunoassay identifies CEA, IL-8 and prolactin as prospective markers for Dukes' stages A-D colorectal cancers. *Clin Proteomics*. Apr 8; 12(1):10. doi: 10.1186/s12014-015-9081-x. eCollection 2015. PubMed ID: 25987887.

The candidate contributed to all aspects of the manuscript. Concept – 30%; Data collection – 30%; Analysis – 30%; Writing – 30%; **Total (Average) – 30%**

Publication VII (Co-author)

Ahn SB, Mohamedali A, Anand S, **Cheruku HR**, Birch D, Sowmya G, Cantor D, Ranganathan S, Inglis DW, Frank R, Agrez M, Nice EC and Baker MS (2014). Characterization of the interaction between heterodimeric αvβ6 integrin and urokinase plasminogen activator receptor (uPAR) using functional proteomics. *J Proteome Res*. Dec 5;13(12):5956-64. doi: 10.1021/pr500849x. Epub 2014 Oct 29. PubMed ID: 25318615.

The candidate performed the crucial structural bioinformatics analysis for the manuscript. Concept – 15%; Data collection – 20%; Analysis – 25%; Writing – 25%; **Total (Average) – 21.25%**

Publication VIII (Co-author)

Kan A, Mohamedali A, Tan SH, **Cheruku HR**, Slapetova I, Lee LY and Baker MS (2013). An improved method for the detection and enrichment of low-abundant membrane and lipid raft-residing proteins. *J Proteomics*. Feb 21;79:299-304. doi: 10.1016/j.jprot.2012.11.019. Epub 2012 Nov 29. PubMed ID: 23201117.

The candidate performed some of the western blots for the manuscript. Concept – 15%; Data collection – 20%; Analysis – 25%; Writing – 15%; **Total (Average) – 18.75%**

All the original publications have been reproduced with permission of the authors and copyright holders. Additionally, unpublished data are also presented in this thesis.

PRESENTATIONS /AWARDS

International presentations (*Oral presentations)

1. **HR Cheruku,** D Cantor, A Mohamedali, SH Tan, E Nice, MS Baker. Integrin β6 expression enhances TGFβ-1 dependent proliferation, wound healing and induces changes to membrane proteome in colorectal cancer cells. 13th World Congress of the Human Proteome Organization (HUPO) (5th – 8th Oct 2014) at Madrid, Spain.

2. Mahboob, S., S. B. Ahn, **H. R. Cheruku**, D. Cantor, E. Rennel, S. Fredriksson, G. Edfeldt, E. J. Breen, A. Khan, A. Mohamedali, M. G. Muktadir, S. Ranganathan, S. H. Tan, E. Nice and M. S. Baker (2015). A novel multiplexed immunoassay identifies CEA, IL-8 and prolactin as prospective markers for Dukes' stages A-D colorectal cancers. 13th World Congress of the Human Proteome Organization (HUPO) (5th – 8th Oct 2014) at Madrid, Spain

3. **HR Cheruku,** D Cantor, A Mohamedali, SH Tan, E Nice, MS Baker "TGFβ1 induces membrane proteome changes in colorectal cancer Cells" 14th Human Proteomics Organization World Congress (HUPO 2015), Vancouver, Canada, 29th September 2015.

4. *Invited Oral Presentation titled "TGFβ1 induces membrane proteome changes in colorectal cancer Cells" 14th Human Proteomics Organization World Congress (HUPO 2015), Vancouver, Canada, 29th September 2015

5. D Cantor, **HR Cheruku,** Ahn SB, Crouch M, E Nice, MS Baker "αvβ6, Plasminogen and Latent TGF-β Drive Colorectal Cancer Aggression" 14th Human Proteomics Organization World Congress (HUPO 2015), Vancouver, Canada, 29th September 2015

Domestic presentations

1. **HR Cheruku,** D Cantor, A Mohamedali, SH Tan, E Nice, MS Baker. TGFβ-1 increases cell proliferation, wound healing and induces changes to membrane proteome in colorectal cancer cells with varying integrin β6 expression. 20th Lorne Proteomics Symposium (5th – 8th Feb 2015), Lorne, Victoria, Australia.

2. Mahboob S, A Mohamedali, **HR Cheruku**, E Nice, MS Baker. A proteomic investigation for detection of early stage CRC biosignatures. 20th Lorne Proteomics Symposium (5th – 8th Feb 2015), Lorne, Victoria, Australia.

3. Ahn, S. B., A. Mohamedali, S. Anand, **H. R. Cheruku**, D. Birch, G. Sowmya, D. Cantor, S. Ranganathan, D. W. Inglis, R. Frank, M. Agrez, E. C. Nice and M. S. Baker. Characterization of the Interaction between Heterodimeric alphavbeta6 Integrin and Urokinase Plasminogen Activator Receptor (uPAR) Using Functional Proteomics. 20th Lorne Proteomics Symposium (5th – 8th Feb 2015), Lorne, Victoria, Australia.

4. **HR Cheruku,** D Cantor, A Mohamedali, SH Tan, E Nice, MS Baker. TGFβ-1 increases cell proliferation, wound healing and induces changes to membrane proteome in colorectal cancer cells with varying integrin β6 expression. MQ Biofocus Research Conference (11th Dec 2014), Macquarie university, Sydney, Australia.

5. **HR Cheruku,** D Cantor, A Mohamedali, SH Tan, E Nice, MS Baker. Integrin β6 expression enhances TGFβ-1 dependent proliferation, wound healing and induces changes to membrane proteome in colorectal cancer cells. 2nd Proteomics and beyond

symposium (12th Nov 2014) by APAF at Macquarie university, Sydney, Australia.

6. **HR Cheruku,** D Cantor, A Mohamedali, SH Tan, E Nice, MS Baker. Examination of TGFβ receptor II expression and interactions in colorectal cancer cell lines. 18th Lorne Proteomics Symposium (7th – 10th Feb 2013), Lorne, Victoria, Australia.

7. S Nandakumar, A Kan, SH Tan, A Mohamedali, **HR Cheruku,** MS Baker. Urokinase plasminogen activator receptor (uPAR) is down regulated as cells approach confluence in Colorectal Cancer. Proteomics and beyond symposium (7th Nov 2012) by APAF at Macquarie university, Sydney, Australia.

8. Mahboob, S., Tan S.H., S. B. Ahn, **Cheruku H. R.**, D. Cantor, A. Khan, Rennel, E., Fredriksson, S., Edfeldt, G., Breen, E. J., Ranganathan, S., Nice, E., and Baker, M. S. "Targeted proteomic immunoassays of candidate plasma biomarkers for stage A-D CRC". 19th Lorne Proteomics Symposium (6th – 9th Feb 2013), Lorne, Victoria, Australia.

Awards

- Macquarie University Postgraduate Research Fund (PGRF), 2015
- Travel grant for EMBO Targeted Proteomics Experimental Design and Data Analysis course in Barcelona, Spain, 2014.
- Skipper Early Career Researcher Travel Award awarded by Australian School of Advanced Medicine, Macquarie University, 2014.

ABBREVIATIONS

5-FU	5- Fluorouracil
ACPS	Australian clinic-pathological Staging
ACTA2	Alpha-actin-2
ACTB	Actin cytoplasmic 1
ACTN4	Alpha-actinin-4
AFAP	Attenuated familial adenomatous polyposis
ANXA2	Annexin A2
APC	Adenomatous polyposis coli
BCAM	Basal cell adhesion molecule
BMP	Bone morphogenetic proteins
BSA	Bovine serum albumin
CAMs	Cell adhesion molecules
CEA	Carcinoembryonic antigen
CEACAM1	Carcinoembryonic antigen-related cell adhesion molecule 1
CID	Collision-induced dissociation
CIN	Chromosomal instability
CRC	Colorectal cancer
CTNND1	Catenin delta 1
DCC	Deleted in colorectal carcinoma
DDA	Data-dependent acquisition
DIA	Data-independent acquisition
DIGE	Difference gel electrophoresis
DMEM	Dulbecco's Modified Eagle Medium
DNA	Deoxyribonucleic Acid
DPC4	Deletion target in pancreatic carcinoma 4
ECM	Extracellular matrix
EDTA	Ethylenediaminetetraacetic acid
EGFR	Epidermal growth factor receptor
ELISA	Enzyme-linked immunosorbent assay
EMT	Epithelial-mesenchymal transition
ERK	Extracellular signal-regulated kinases
ESI	Electrospray ionization
ETD	Electron transfer dissociation
EZR	Ezrin
FAP	Familial adenomatous polyposis
FBS	Foetal bovine serum
FDA	Food and drug administration
FDR	False discovery rate
FIT	Fecal immunochemical test
FOBT	Fecal occult blood
FPR	False positive rate
FSH	Follicle-stimulating hormone
GAIP	G Alpha Interacting Protein
GDF	Growth differentiation factors
GIPC	GAIP-interacting protein C-terminus

GPI	Glycosylphosphotidylinositol
HNPCC	Hereditary non-polyposis colon cancer
HPLC	High-performance liquid chromatography
HSP27	Heat shock 27 kDa protein
HSP60	Heat shock protein 60
HSP90B1	Endoplasmin
HSPA5	Heat shock 70 kDa protein 5
ICAT	Isotope coded protein labels
IGFR2	Insulin-like growth factor receptor 2
IHC	Immunohistochemistry
IMPs	Integral membrane proteins
IPA	Ingenuity pathway analysis
IPI	International Protein Index
ITGAV	Integrin alpha V
ITGB1	Integrin beta 1
ITGB2	Integrin beta 2
ITGB3	Integrin beta 3
ITGB6	Integrin beta 6
iTRAQ	Isobaric tags for relative and absolute quantization
K-RAS	Kirsten rat sarcoma viral oncogene homolog
KRT1	Keratin 1
KRT10	Keratin 10
KRT13	Keratin 13
KRT15	Keratin 15
KRT18	Keratin 18
KRT19	Keratin 19
KRT2	Keratin 2
KRT20	Keratin 20
KRT23	Keratin 23
KRT5	Keratin 5
KRT8	Keratin 8
LAP	Latency associated peptide
LC	Liquid chromatography
LOH	Loss of heterozygosity
LS	Lynch syndrome
MAPK	Mitogen-activated protein kinases
miRNA	microRNA
MMP	Matrix metalloprotease
MMR	Mismatch repair
MRM	Multiple reaction monitoring
MS	mass spectrometry
MS/MS	Tandem mass spectrometry
MSI	Microsatellite instability
MYL9	Myosin regulatory light polypeptide 9
NCBI	National Center for Biotechnology Information
PAGE	Polyacrylamide gel electrophoresis

PDFG	Platelet-derived growth factor
PDGF-B	B chain of PDGF
PLG	Plasminogen
pro-uPA	Pro-urokinase-type plasminogen activator
PTM	Post-translational modifications
PVDF	Polyvinylidene difluoride
QIT	Quadrupole ion-trap
Q-TOF	Quadrupole time-of-flight
RNA	Ribonucleic acid
RPMI	Roswell Park Memorial Institute medium
SCC	Squamous cell carcinomas
SCX	Strong cation exchange chromatography
SDS	Sodium dodecyl sulfate
SILAC	Stable isotope labelling by amino acids in culture
SRM	Selected reaction monitoring
SWATH	Sequential window acquisition of all theoretical fragment ion spectra
TAGLN	Transgelin
TBS	Tris buffered saline
TGFβ	Transforming growth factor-β
TGFβR1	Transforming growth factor-β type I receptor
TGFβR2	Transforming growth factor-β type II receptor
TGFβR3	Transforming growth factor-β type III receptor
TMT	Tandem mass tags
TNM	Tumor, Nodes, Metastasis
TOF	Time-of-flight
uPA	Urokinase-type plasminogen activator
uPAR	Urokinase-type plasminogen activating receptor
VEGF	Vascular endothelial growth factor
VIM	Vimentin
VTN	Vitronectin

CHAPTER 1
INTRODUCTION

1.1 Colorectal Cancer

1.1.1 Cancer – A global burden

Cancer is not a modern disease and has clearly existed for many centuries [1].Cancer can be defined as by Ruddon [2] is the *"abnormal growth of cells caused by multiple changes in gene expression leading to dysregulated balance of cell proliferation and cell death and ultimately evolving into a population of cells that can invade tissues and metastasize to distant sites, causing significant morbidity and, if untreated, death of the host"* [2].

The term 'cancer' often referred to as a single condition, is one of the most diverse class of pathologies studied and compromises of a large group of diseases that can arise and affect any part of the body. There are more than 100 types of cancer, classified primarily by the organ or the cell type of origin [3]. Histologically, cancer has been classified into five major groups: carcinoma, of epithelial origin; sarcoma, of connective tissues; leukaemia, of white-blood cells; lymphoma, of the lymphatic system; and myeloma. Carcinoma, for example, is a type cancer that arises from epithelial cells/organs. Most common cancers like breast, colorectal, prostate and lung fall under the broad categorisation of carcinoma. For cancer to survive and metastasise to other organs, it was proposed that 'normal' healthy cells need to acquire six essential "hallmark" properties - self-sufficiency in growth signals, insensitivity to growth inhibition, evasion of apoptosis, uncontrolled cell growth, sustained angiogenesis, and tissue invasion and metastasis [4]. These six properties are however mostly acquired through genetic alterations in the cancer cells which are a result of rare malfunctioning of the human genome maintenance system and are exploited by cancerous cells. Despite the difficulty in acquiring the six hallmarks of cancer and the rarity of the associated genetic mutations, cancers have become one of the most feared disease of all times.

The International Agency for Research on Cancer (IARC), estimated in 2012 that there were 14.1 million new cancer cases, 8.2 million cancer deaths and 32.6 million people living with cancer (within 5 years of diagnosis), with 57% (8 million) of the new cases and 65% (5.3 million) of the cancer deaths, and 48% (15.6 million) of the 5-year prevalent cancer occurring in the economically underdeveloped parts of the world [5, 6]. In 2014 the World Cancer Report predicted that the number of cancer cases per annum will increase to about 22 million resulting in up to 13 million deaths within the next two decades [7]. According to the IARC the three most commonly diagnosed cancers globally were lung (1.82 million), breast (1.67 million) and colorectal (1.36 million) and the most common cause of cancer deaths were lung (1.61 million), liver (745, 000), and stomach (723,000) [7], **Figure 1**.
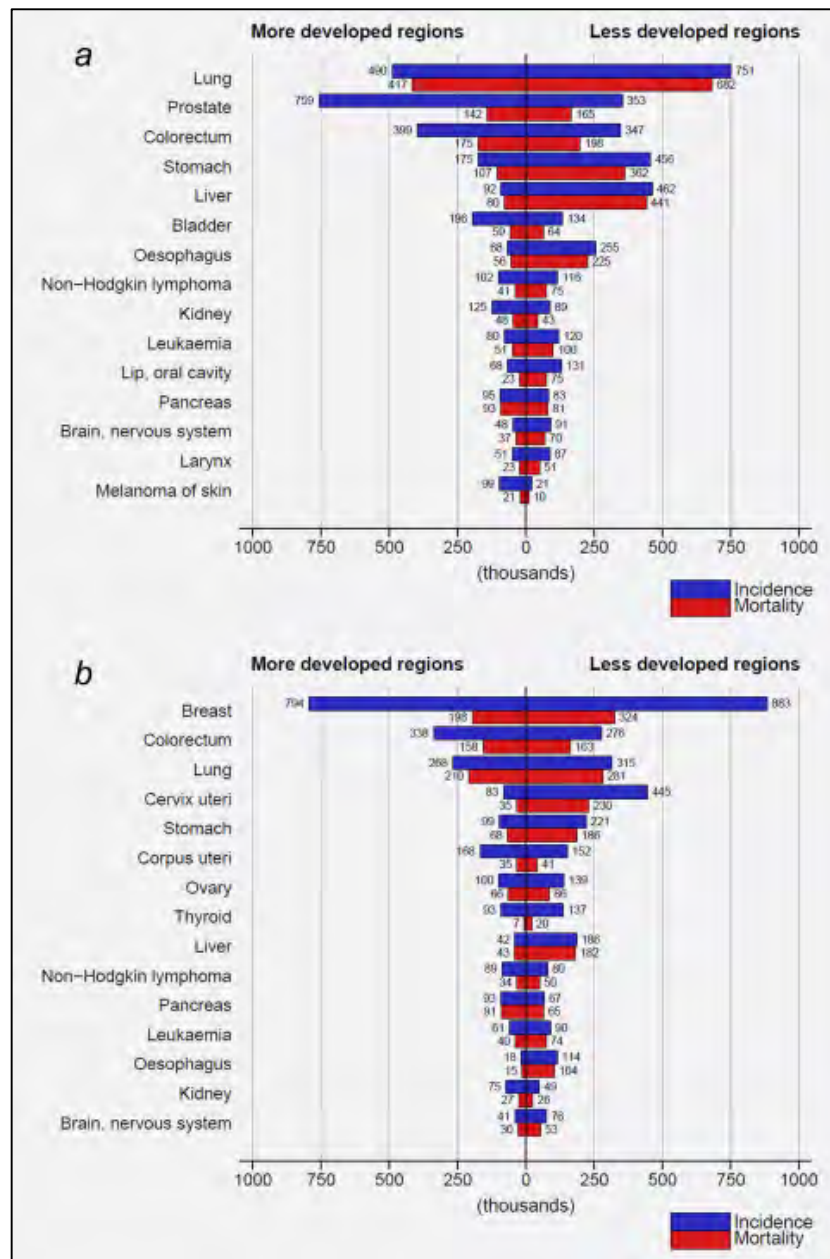
Figure 1 - Global cancer statistics. Incidence and Mortality rates comparison between more and less developed regions. a) Males, b) females. Image source [6, 7]

1.1.2 Significance of CRC: Statistics

Colorectal cancer (CRC), specifically, in 2012 was the third most common cancer globally, with 9.7% of total cancer cases, almost 55% of which occurred in well developed countries. It is the third most common cancer in men (746,000 cases, 10% of total) and the second in women (614,000 cases, 9.2% of total). The highest incidence rates of CRC were observed in Australia/New Zealand (age-standardized ratio 44.8 and 32.2 per 100,000 in men and women respectively) and lowest in western Africa (4.5 and 3.8 per 100,000), (figure 2). CRC was the fourth most common cause of cancer deaths (694,000 deaths, 8.5% of total) in 2012 with 52% of deaths in less developed countries which reflects the lack of better prognosis in those regions [6].
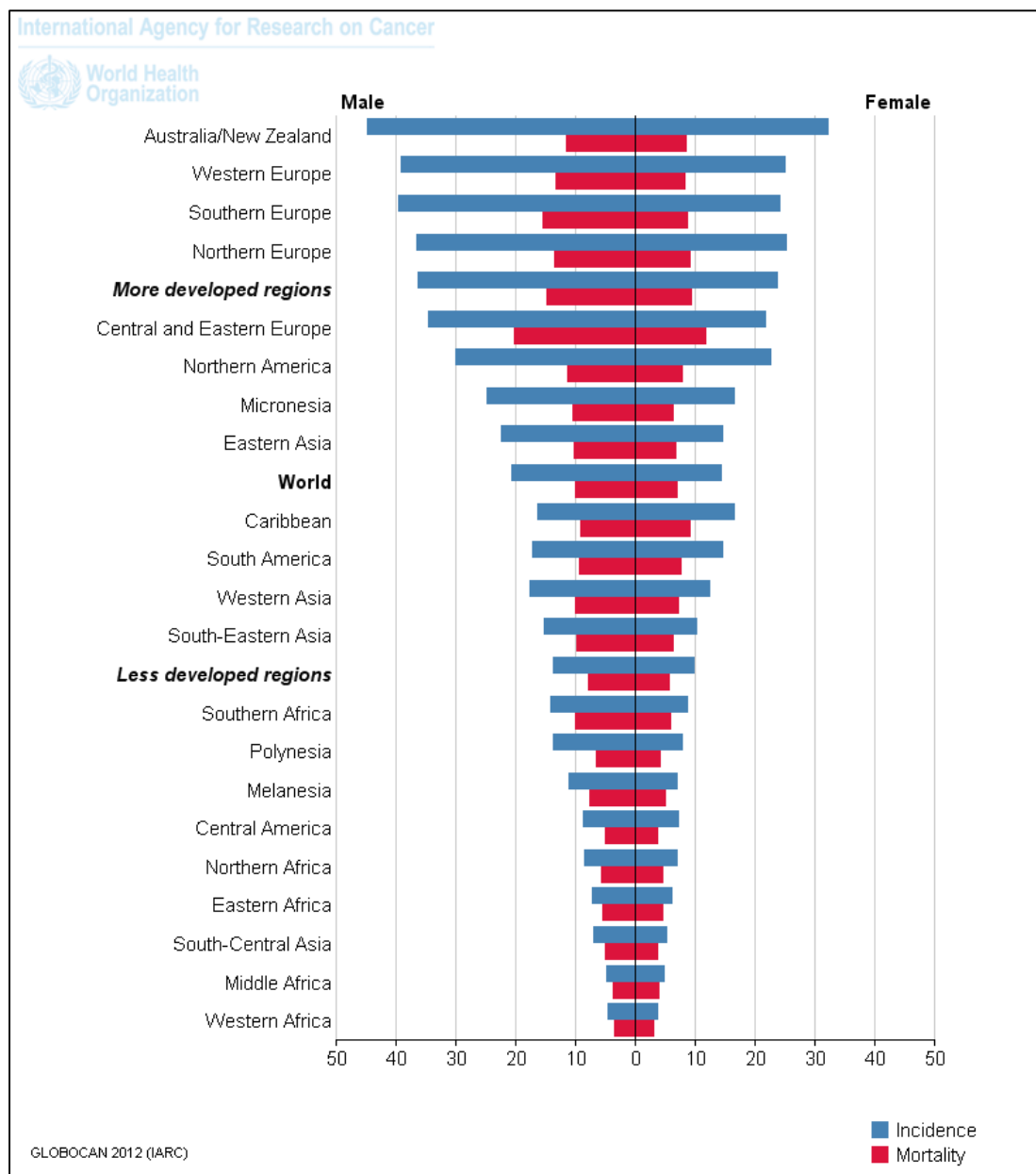
Figure 2 - Colorectal cancer statistics. Estimated (age-standardised rates (World) per 100,000) incidence, Mortality and prevalence in 2012. Image source [6, 7].

1.1.3 Aetiology of CRC

The precise cause of CRCs is not very well understood. However, a number of risk factors have been associated with CRC although the sporadic nature of this disorder continues to baffle the research community [8]. Some of these include increasing age, gender, personal and/or family history of CRC, colonic polyps, inflammatory bowel disease, ulcerative colitis or Crohn's disease, ethnic background, and various environmental factors [8, 9]. Genetic alterations have also been implicated with increased risk of CRC and are detailed in section "1.1.10 Carcinogenesis and Genetic alterations during CRC".

Advancing age is a risk factor for CRC, as more than 90% of the people diagnosed with CRC are over 50 years of age. In Australia, the lifetime risk of developing CRC before the age of 75 years is approximately 1 in 19 men and 1 in 28 women [10], which is the highest rate globally. Kim *et.al* recently showed that females over 65 years with CRC showed higher mortality and lower 5-year survival than males of the same age [11].

Most cases of CRC occur in individuals without any personal or family history of CRC or its associated diseases. Approximately 20-25% of cases occur in individuals with a familial history of CRC. The risk of developing CRC increases for the other family members either by having more than one relative with CRC, or having CRC diagnosed at a younger age [8, 9]. The diagnosis of CRC or colonic polyps, in a first-degree relative, before the age of 60 is an increased risk and may vary extensively, with none to a 6.3-8 fold increased risk [12].

Various lifestyle risk factors are involved in the development of CRC. A few important ones are diets high in fat and cholesterol and/or low in fiber, alcohol consumption, smoking, or, sedentary lifestyle. It is believed that alcohol stimulates gastro intestinal cell proliferation and promotes carcinogenesis in the presence of unabsorbed carcinogens such as nitrosamines [13, 14]. There is also strong evidence that smoking increases risk for CRC [15, 16]. Study by Giovannucci showed that long-term, heavy cigarette smokers have a 2-3 fold increased risk of CRC [16]. Carr *et.al* also showed that high consumption of beef and lamb was associated with increased risk of CRC [17].

1.1.4 Anatomy of the colon and rectum
An understanding of normal colon or large intestine anatomy is crucial to study the development of CRC. The colon is about 5 feet (150 cm) long and divided into five major segments: caecum, ascending colon, transverse colon, descending colon and sigmoid colon. The rectum is the last anatomic segment of the colon before the anus (see **Figure 3a)**. The walls, colon and rectum are composed of five distinct cellular layers – mucosa, submucosa, muscularis propria, subserosa and serosa as shown in **Figure 3b**. The serosa is absent in most of the rectum [9, 18]. The mucosa is the inner lining of the colon wall including the thin layer of epithelium, connective tissue (lamina propria) and a thin muscle layer (muscularis mucosa). In presentations of CRC, polyps are usually shown to begin in the mucosal layer and further penetrate the colon wall to metastasise. The submucosa surrounds the mucosa and contains the glands, blood and lymphatic vessels, and nerves. The muscularis propria comprises circular and longitudinal muscle layers that assists in peristalsis whist the subserosal layer consists of connective and fat tissues that supports the colon. The serosal layer derived from the visceral peritoneum, is the most superficial layer that surrounds the

colon and is made of sessile or pedunculated fat masses that protect the large intestine from damage.
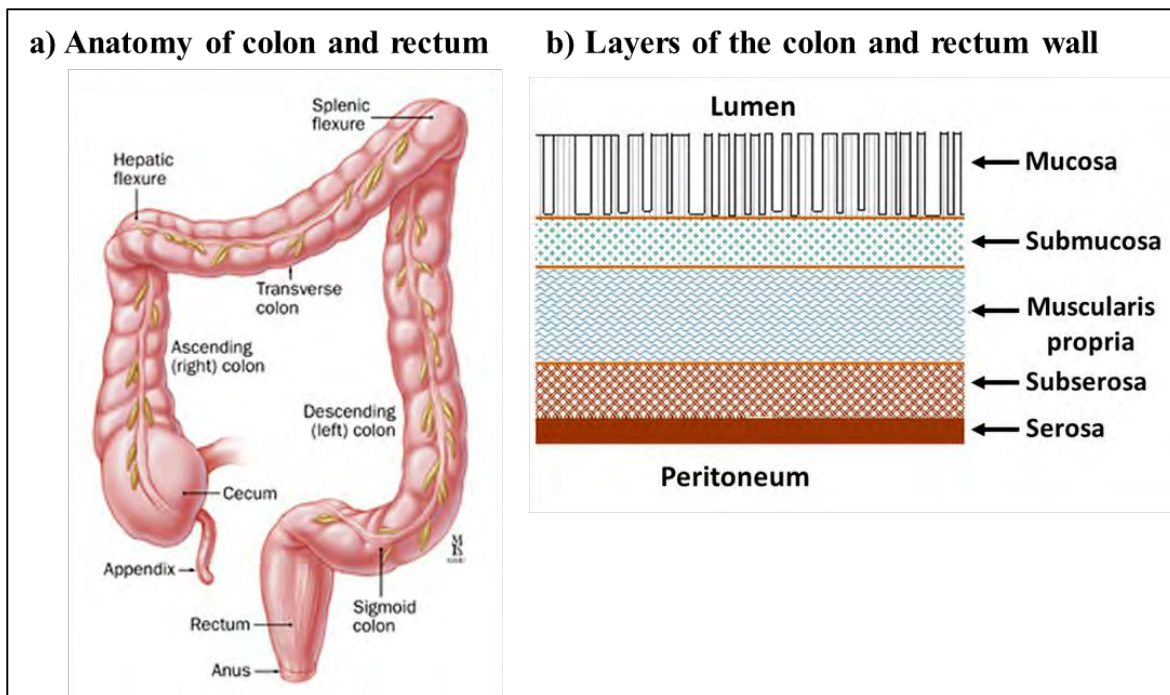
Figure 3 - (a) Basic anatomy of the colon and rectum (b) and the layers of colon and rectum wall. Images adopted from [19, 20].

1.1.5 Symptoms of CRC

Colorectal cancer presents with many common symptoms of over a long period of time. The most commonly noted symptoms of CRC are rectal bleeding, abdominal pain, change in bowel habits, anaemia and weight loss [21]. During CRC onset, these symptoms may manifest in combinations rather than in isolation [22]. Majumdar *et.al* and Astin *et.al* have showed that rectal bleeding is often accompanied by anaemia [21, 22]. However, most of these symptoms are reasonably common in general population. For example, a study by Fijten et al. showed that of the 3-15% of the population that present with rectal bleeding, only 3% of these actually are CRC patients [23]. Due to the high percentage of commonality between the symptoms exhibited by the general population and CRC patients it is very difficult to ascertain the exact observable symptoms that are specific only to the CRC patients. However, it may be possible to determine a set of "CRC specific" symptoms by evaluating the common symptoms based on severity, frequency and persistence rather than occurrence [24]. Surprisingly, duration of the symptoms do not correlate with development of CRC [25, 26] or provide any clinical utility. This lack of a "standard CRC diagnosis chart" makes it difficult for health practitioners to diagnose CRC at early stages, and can only rely upon a combination of 'unstandardized' staging systems.

1.1.6 Staging of CRC

The staging of CRC is primarily based on how deep the cancer has penetrated the bowel wall and/or spread to other organs. Colonic polyps usually begin within the mucosal layer which then penetrate the submucosal layer and enter the lymph nodes after which the cancers spread to distant organs. Regrettably, more than 75% of CRC patients present with this late stage cancer whose 5-year survival rate is very low [27, 28]. The stage of a tumour, clinical or pathological, is a description of a tumour that informs the prognosis of the disease. The two most commonly used CRC staging systems globally are: the TNM (Tumour, Nodes, Metastasis) and the Dukes' system. The TNM staging system is based on the local spread (T-stage), lymph-node spread (N-stage) and the distant metastasis to distant organs (M-stage) while the Dukes' system also assess all these features though it reports the stages in a single-lettered format. However, these two systems do not consider the size of the tumour as a factor and only consider the pathological information while staging them. A more recent, not so very commonly used alternative staging system, is the Australian Clinico-Pathological Staging (ACPS) system which is similar to Dukes' on how it reports CRC stage. ACPS uses additional clinical, radiologic, operative, and pathological data for staging along with the pathological information that is commonly used in the TNM and Dukes' staging systems [29]. The Dukes' staging system is summarised in **Figure 4** and its comparison with TNM staging is shown in **Table 1**.
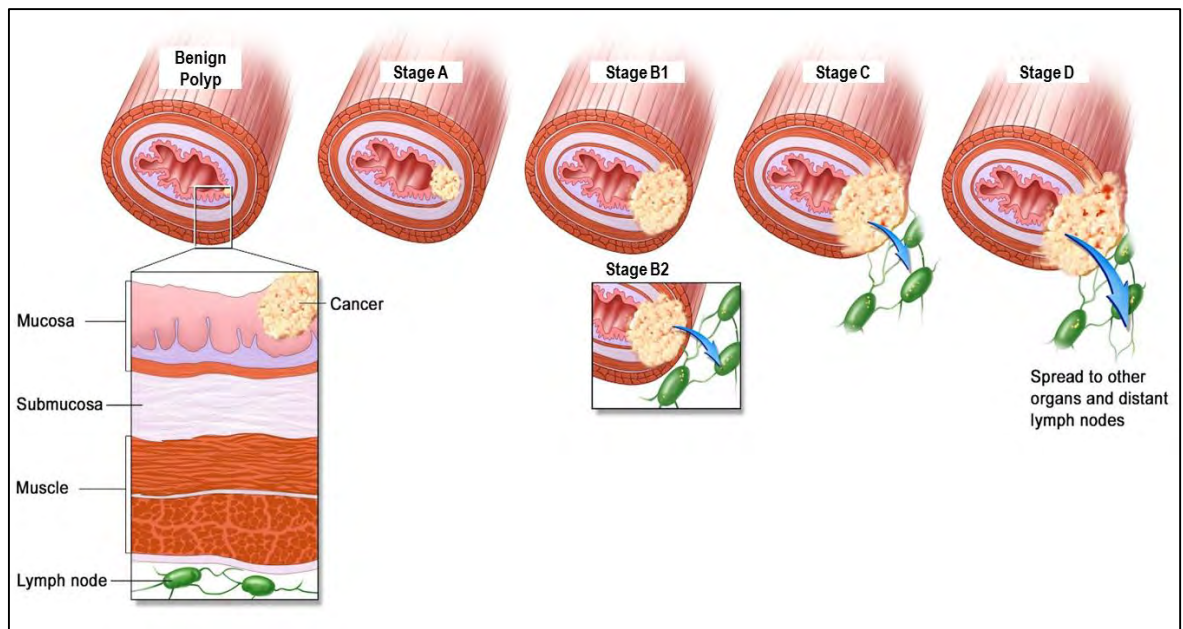
Figure 4 - The Dukes' staging system in the context of CRC. It is based on the depth of tumour progression and the presence or absence of metastasis. **Benign polyp:** Cancerous are still confined to the mucosal layer; **Stage A:** The tumour is still confined to the inner most lining of colon; **Stage B:** The tumour has spread into the muscle layer of the colon but no further; **Stage C:** The

tumour cells have spread to lymph nodes near the colon; **Stage D:** The tumour has metastasised to distant sites organs e.g. liver or lungs. Image adapted from [30].

Table 1 Comparison of Dukes' and TNM classification of CRC[§]. Key is shown at the bottom of the table.

Dukes' System	TNM System (by American Joint Commission of Cancer)				Associated 5-year survival
Stages	Stages	Primary Tumor (T)	Lymph node (N)	Distant metastasis (M)	
	Stage 0	Tis/T0	N0	M0	
A	Stage I	T1	N0	M0	>90%
B1		T2	N0	M0	>85%
B2	Stage IIA	T3	N0	M0	80%
B2	Stage IIB	T4	N0	M0	72%
C	Stage III	Any T	N1 or N2	M0	42-64%
C2		Any T	N3	M0	27-44%
D	Stage IV	Any T	Any N	M1	<10%

TX – primary tumor cannot be assessed
T0 – no evidence of primary tumor
Tis – carcinoma in situ present
T1 – tumor invades submucosa
T2 – tumor invades muscularis propria
If Serosa present (colon wall)
    T3 – tumor invades through muscularis propria into subserosa but not through Serosa
    T4 – tumor invades through serosa and spreads to adjoing organs or structures
If Serosa absent (rectal wall)
    T3 – tumor invades through muscularis propria
    T4 – tumor invades through other organs

NX – regional lymph nodes cannot be assessed
N0 – no regional node metastasis
N1 – metastasis in 1-3 regional nodes
N2 – metastasis in ≥4 regional nodes
N3 – positive for central nodes

MX – distant metastasis cannot be assessed
M0 – no distant metastasis
M1 – distant metastasis

[§]Data adapted from [31]

Despite the availability of these staging systems, it has been difficult for health practitioners and clinicians to precisely identify the stage of the disease as there are no standard histological or morphological parameters for evaluation of the samples. It would be useful to develop a standardised staging system that can be used objectively by evaluating the expression signatures of biomarkers or normal protein that are expressed in the tumour cells. Developing such a staging system will be advantageous to health practitioners and clinicians, and will substantially speed up the diagnosis of the disease and treatments that follow it.

1.1.7 Biomarkers associated with CRC

A biomarker is a characteristic that is objectively measured and evaluated as an indicator of normal biologic processes, pathogenic processes, or pharmacologic responses to a therapeutic intervention [32]. According to the National Cancer Institute (NCI) a biomarker is *"a biological molecule found in blood, other body fluids, or tissues that is a sign of a normal or abnormal process, or of a condition or disease"* such as cancer [33]. Biomarkers can typically be used to differentiate a healthy person from a diseased person and also be study the response of body to various treatments. Various molecules, such as proteins, peptides, microRNAs and DNA amongst others, can be used as biomarkers. Several studies have shown that a biomarker can also be a collection of alterations can be used in a "panel".

Biomarkers can be used to estimate risk of disease, screen for primary cancers, distinguish benign from malignant or different types of malignancies from one another, determine prognosis for patients who have been diagnosed with cancer, and monitor status the disease, either to detect recurrence or determine response or progression to therapy [34]. For example, carcinoembryonic antigen (CEA) is used to monitor CRC recurrence. Most commonly it is used to monitor CRC patients, following adjuvant therapy, with the goal of detecting liver metastases [35]. Another such example is the use of KRAS mutation as a predictive biomarker to predict response to anti-EGFR therapy in CRC patients [36].

A multitude of potential biomarkers for cancers including CRC have been identified and reported in the literature are summarised in **Table 2**. However, there are very few Food and Drug Administration (FDA) approved biomarkers for CRC [37, 38]. Despite a global research effort and reports of multi-marker panels or gene signatures, there are very few FDA diagnostic panels for CRC. Additionally, it is not possible for all the reported proteins or genes to be used as biomarkers due to the fact that majority of these are not carefully designed and tested in randomized clinical trials which is required prior to FDA approval. Therefore, it is important to scrutinize these potential biomarkers before they can be clinically translated for early stage diagnosis, where it is still resectable. Therefore, identification of a CRC-specific early stage biomarker panels could be an advantage to the patients and increase the overall survival. Importantly, these panels need to have high specificity and sensitivity for detection. The NCI defines specificity as *"the percentage of people who test negative for a specific disease among a group of people who do not have the disease"* and sensitivity *"may describe how well a test can detect a specific disease or condition in people who actually have the disease or condition"*. No test is 100% specific

nor will it be 100% sensitive because some people without the disease or the condition will test positive for it (false positive result) and those with the disease or condition will test negative for it (false negative result).

1.1.8 Early diagnosis and screening for CRC

The early detection of CRC is essential to determine the stage related prognosis. Despite the availability of numerous screening strategies aggressive surgical therapies and extensive research on the genomic, molecular and cellular basis of CRC, detection at the earliest stages remains elusive. It is very well known that CRCs develop over time, can take as long as ten years or more, which gives plenty of opportunities to diagnose the CRC at early-stages [39]. If found, early-stage CRC is associated with good 5-year survival rates (> 90%) following simple (often curative) surgical resection, while patients diagnosed with later stage cancers (ACPS C or D) experience recurrence and distant metastases leading to poor 5-year survival rates of less than 10% [4]. The early detection of CRC might be improved by implementing various 'currently' available CRC screening strategies and emerging assays, summarised in **Table 1** of **publication I**.

The most commonly used method for screening of CRC is by testing the stool using fecal occult blood test (FOBT) or fecal immunochemical test (FIT) [40-42]. Studies have shown that FOBT, when performed every 1 to 2 years in people aged 50-80, can help reduce the number of deaths due to CRC by 15-33% [43, 44]. However, FOBT and FIT have limited sensitivity compared to colonoscopy and sigmoidoscopy which have a sensitivity of >95%. Despite the high sensitivity of colonoscopy and sigmoidoscopy these are often invasive and can be painful for some patients. Other screening strategies include barium enema that used X-ray examination, rectal ultrasound and/or PET/CT scan [39-42, 45]. There are also new and emerging non-invasive screening assays that test for expression changes of proteins, microRNAs (miRNA) and DNA methylation patterns using blood or serum samples. The most promising test stool DNA test to date is comprised of a panel of four methylated genes (BMP3, NDRG4, vimentin, TFPI2), a mutant form of KRAS and α-actin as the internal reference control. This panel was able to accurately detect Stage I-III CRC patients with 87% sensitivity at 90% specificity in a training set and with 78% sensitivity at 85% specificity in a test set (combined sensitivity of 85% at 90% specificity) and is awaiting FDA approval [37]. Based on the results from one or more screening tests, CRC can be staged and the associated prognosis and available treatment options reported to the individual.

Table 2 Summary of potential CRC biomarkers identified in the last 10 years.

Candidate Biomarker	Sample Type	Mechanism	Colorectal cancer stage	Sensitivity (%)	Specificity (%)	Reference
Protein Biomarkers						
3 protein panel - IGFBP2, DKK3 and PKM2	Blood/serum			73	95	[46]
4 protein panel - DK-BLY, CEA, Ca 19-9, S-p53	Blood/Serum	Aberrantly expressed protein isoforms	CRC	61	80	[47]
6 protein panel - SULF1,NHSL1,MST1,GTF2i,SREBF2,GRN	Blood/Serum	Auto-antibodies targeting tumor-associated antigens	CRC	74	72	[48]
Alpha 1-antitrypsin	Blood/Serum			87	73	[49]
Amphiregulin	Blood/serum		Dukes' A, C from CRC	nd	nd	[50]
C3a-desArg	Blood/Serum	Auto-antibodies targeting tumor-associated antigens	CRC	61	93	[51]
			Adenoma	79	78	
CEA	Blood/Serum	Over expression of proteins in cancer tissue	CRC	22	100	[52]
			Adenoma+ Stage I CRC	21	100	
			Dukes' A, B, C, D	53	93	[49, 50, 53, 54]
Collagen type X alpha1 (CPL10A1)	Blood/serum		Controls from Adenoma and colon cancer	63	85	[55]
CXCL11	Blood/serum		Dukes' A, C from CRC	nd	nd	[50]

CXCL5	Blood/serum		Dukes' A from D	nd	nd	[50, 56]
GRN	Blood/Serum	Auto-antibodies targeting tumor-associated antigens	CRC	59	58	[48]
GTF2i	Blood/Serum	Auto-antibodies targeting tumor-associated antigens	CRC	52	58	[48]
IL6	Blood/serum		Dukes' B from Dukes' A and controls	27	95	[50]
IL8	Blood/serum		Dukes' A, D from controls	30	95	[50, 57]
MMP9	Blood/Serum	Over expression of proteolytic enzymes	CRC	79	70	[58]
			CRC	55	nd	[59]
MMP9 + CEA	Blood/Serum	Proteolytic enzyme degradation	CRC	75	nd	[59]
MMP9+TIMP-1	Blood/Serum	Proteolytic enzyme degradation	CRC	75	nd	[59]
MST1	Blood/Serum	Auto-antibodies targeting tumor-associated antigens	CRC	71	46	[48]
MUC1 + MUC4	Blood/Serum	Auto-antibodies with altered glycosylation and expression	CRC	79	92	[60]
NHSL1	Blood/Serum	Auto-antibodies targeting tumor-associated antigens	CRC	52	52	[48]

					Sensitivity	Specificity	Ref
RPH3AL auto-antibodies	Blood/Serum	Auto-antibodies targeting tumor-associated antigens	CRC		73	84	[61]
			Dukes' A+B		65	nd	
			Dukes' C+D		78	nd	
S100A8	Blood/Serum	Over expression of proteins in cancer tissue	CRC		41	95	[52]
			Adenoma+ Stage I CRC		32	95	
S100A9	Blood/Serum	Over expression of proteins in cancer tissue	CRC		44	95	[52]
			Adenoma+ Stage I CRC		40	95	[52]
sCD26	Blood/Serum	Diminished protein expression	CRC		82	79	[62]
			CRC+adenoma		58	76	
SREBF2	Blood/Serum	Auto-antibodies targeting tumor-associated antigens	CRC		61	48	[48]
SULF1	Blood/Serum	Auto-antibodies targeting tumor-associated antigens	CRC		74	50	[48]
TIMP-1	Blood/Serum	Proteolytic enzyme degradation	CRC		61	100	[59]
Transthyretin	Blood/Serum	Auto-antibodies targeting tumor-associated antigens	CRC		61	100	[51]
			Adenoma		86	68	

Transthyretin + C3a-desArg	Blood/Serum	Auto-antibodies targeting tumor-associated antigens	CRC	61	100	[51]
			Adenoma	96	70	
TuM2-PK	Stool	Isoenzyme expressionin proliferating cells	Adenoma	28	NS	[63]
			Adenoma	26	NS	[64]
			Adenoma	38	NS	
			Adenoma <1cm	20	NS	[65]
			Adenoma >1cm	60	92	
			CRC	78	74	[64]
			CRC	85	NS	[63]
			CRC	91	NS	[65]
			CRC	68	79	[66]
			CRC	81	71	[67]
			CRC	78	93	[68]
			Dukes' A/B	67	NS	[63]
			Dukes' A/B/C/D	67/61/67/100	NS	[66]
			Dukes' A/B/C/D	60/76/89/90	NS	[68]
			Dukes' C/D	89	90	[63]
Integrin β6	Tissue	Overexpression in cancer tissue	ACPS B and C	NS	NS	[69]
SATB2	Tissue	Antibody expression	CRC	85	NS	[70]
SATB2 + CK20	Tissue	Antibody expression	CRC	97	NS	[70]
uPAR	Tissue/serum	Expression in tissue samples	ACPS B and C	NS	NS	[49, 71]

mRNA Biomarkers

miR-532-3p, miR-331, miR-195, miR-17, miR-142-3p, miR-15b, miR-532, and miR-652	Blood/Plasma	RNA expression	Polyps from controls	88	64	[72]
miR-601 and miR-760	Blood/Plasma	RNA expression	CRC to normal controls	83.3	69.1	[73]
			Adenomas to normal controls	72.14	62.1	
miR17-3p	Blood/Serum	Tumor-associated RNA expression	CRC	64	70	[74]
miR-19a-3p, miR-223-3p, miR-92a-3p and miR-422a	Blood/Serum	RNA expression	CRC from Adenoma and controls	84.3	91.6	[75]
miR21	Blood/Serum	Tumor-associated RNA expression	CRC	90	90	[76]
miR29a	Blood/Serum	Tumor-associated RNA expression	CRC	69	89	[77]
			Adenoma	62	85	
miR29a + miR92a	Blood/Serum	Tumor-associated RNA expression	CRC	83	85	[77]
			Adenoma	73	80	
miR601	Blood/Serum	RNA expression	CRC	70	72	[77]
			Adenoma	72	52	
miR760	Blood/Serum	RNA expression	CRC	80	72	[73]
			Adenoma	69.8	62	
miR92	Blood/Serum	Tumor-associated RNA expression	CRC	89	70	[74]
miR92a	Blood/Serum	Tumor-associated RNA expression	CRC	84	71	[77]

			Adenoma	65	81	
Panel miR760 + miR 29a + miR92a	Blood/Serum	RNA expression	CRC	83.3	93	[73]
COX2 mRNA	Stool	Over expression of mRNA	CRC	87	100	[78]
			Dukes' A/B/C/D	77/96/82/82	NS	
MMP7 mRNA	Stool	Over expression of mRNA	CRC	65	100	[78]
			Dukes' A/B/C/D	38/78/73/55	NS	
COX2 mRNA + MMP7 mRNA	Stool	Over expression of mRNA	CRC	90	NS	[78]
DNA Biomarkers						
4 gene panel - APC, MGMT, RASSF2A, Wif-1	Serum/plasma	DNA hypermethylation	CRC	86.5	92	[79]
			Adenoma	75	91	
4 gene panel – RARB2, P16^{INK4A}, MGMT, APC	Stool	DNA hypermethylation	CRC	62	NS	[80]
			Adenoma	40	NS	
5 gene panel - CDA, MGC20553, BANK1, BCNP1, MS4A1	Serum/plasma	DNA hypermethylation	CRC	94	77	[81]
6 Gene panel - CYCD2, HIC1, PAX 5, RASSF1A, RB1, SRBC	Serum/plasma	DNA hypermethylation	CRC	83.7	68	[82]
			Adenoma	55	64	
6 Gene panel—APC, ATM, hMLH1, sFRP2, HLTF, MGMT	Stool	Overexpression of mRNA + DNA hypermethylation	CRC	75	90	[83]
ALX4 +SEPT9	Serum/plasma	DNA hypermethylation	Precancerous Colorectal lesion	71	95	[84]

APC	Serum/plasma	DNA hypermethylation	CRC	57	86	[85]
			Stage I	57	89	
BMP3, NDRG4, VIM, TFPI2 and a mutant KRAS	Stool	DNA methylation	Cancer	68-86	77-92	[86-89]
			Adenoma (Size >1 cm)	52-73	85-92	[86-89]
			Adenoma (Size ≥1 cm)	45-62	85-92	[86-89]
Calprotectin	Stool		CRC	72	75.5	[90]
			Adenoma	28	NS	
COX2 DNA + mRNA	Stool	Overexpression of mRNA + DNA hypermethylation	CRC	50	93	[83]
			Adenoma	4	NS	
DAPK1	Serum/plasma	DNA hypermethylation	CRC	50	74	[85]
			Stage I	43	70	
E-cadherin	Serum/plasma	DNA hypermethylation	CRC	60	84	[85]
			Stage I	48	87	
FHIT	Serum/plasma	DNA hypermethylation	CRC	50	84	[85]
			Stage I	29	67	
Long DNA	Stool	DNA promoter methylation	CRC	53	83.3	[91]
			CRC	79	92	
			Adenoma	17	NS	
NDRG4	Stool	DNA promoter methylation	CRC	61	93	[92]

17

NGFR	Serum/plasma	DNA hypermethylation	CRC	33	95	[93]
SEPT9	Serum/plasma		CRC	90	88	[94]
			Stage I/II/III/IV	71/90/100/100		
			Stage I + II	87		
			CRC	52	95	[93]
				67-96	81-99	[95-98]
SFRP2	Stool	DNA hypermethylation	CRC	87	NS	[99]
			Adenoma	62	76.8	
SMAD4	Serum/plasma	DNA hypermethylation	CRC	52	64	[85]
			Stage I	47	87	
SP20	Stool	DNA hypermethylation	CRC	80	100	[100]
SPG20	Tissue	DNA hypermethylation	CRC	88	NS	[101]
			Adenoma	82	NS	
TFPI2	Stool	DNA promoter methylation	CRC	68	100	[91]
			CRC	93	93	[89]
			Adenoma	21	93	
TFP12 + Long DNA	Stool	DNA promoter methylation	CRC	87	83.3	[91]
THBD-M	Serum/plasma	DNA hypermethylation	CRC	71	80	[102]
			Stage I/II	74		
TMEFF2	Serum/plasma	DNA hypermethylation	CRC	30	95	[93]

Tumor associated monocyte genetic finger print	Blood monocyte samples	Gene expression		93	92	[50]
VSX2	Tissue	DNA hypermethylation	CRC	83	92	[103]

1.1.9 Treatment of CRC

CRC is one of the most potentially curable cancers (by surgical resection) if found in the early localised (Dukes' A or B1) stages with high survival rates >90% [28]. However, most CRC (~65%) is found in Dukes' stage B2-C and require use of other treatment options that are briefly outlined here. If CRC is found at TNM stages 0, I or II, the preferred treatment is to remove the cancer by surgical resection [104]. If found at stage III, surgical resection is usually followed by adjuvant chemotherapy. If found at metastatic stages, treatment options include surgical resection, neoadjuvant chemotherapy, local ablation of CRC tissues, adjuvant chemotherapy, intra-arterial chemotherapy and targeted chemotherapy [104].

The most commonly used chemotherapeutic agents for CRC are 5- Fluorouracil (5-FU), leucovorin (LV), irinotecan, oxaliplatin, capecitabine, and bevacizumab. To improve the efficacy of the treatment these drugs are often using in combination and are affordable by families of a normal cancer patient. Depending on the stage of diagnosis various combinations of drugs are used. Briefly, a stage II patient can be treated only with 5-FU and LV and a stage III patient can be treated either with FOLFOX (5-FU, LV, and oxaliplatin) or CapeOx (capecitabine and oxaliplatin) regimens [105]. These regimens can vary with degree of CRC, age and other health needs of the patients. Stage IV metastatic CRC patients can be treated with FOLFOXIRI (LV, 5-FU, oxaliplatin, and irinotecan) plus cetuximab as first-line treatment [106].

The progress in cancer research has led to development of targeted therapies that often have less severe side effects than chemotherapy. For example, these therapies use specific monoclonal antibodies against epidermal growth factor receptor (EGFR) or vascular endothelial growth factor (VEGF). Cetuximab (Erbitux®) and panitumumab (Vectibix®) are EGFR treatments that are used in metastatic CRC patients. Phase 1 and 2 trials showed that Cetuximab is efficacious when used in combination with irinotecan- or oxaliplatin-based chemotherapy [107, 108]. Bevacizumab (Avastin®), ramucirumab (Cyramza®), and ziv-aflibercept (Zaltrap®) drugs, that target VEGF known to assist in the process of angiogenesis. A combination ramucirumab and FOLFIRI (irinotecan, folinic acid, and 5-FU) regimen is now being used to treat patients with metastatic CRC [109]. The use of multi-agent combination therapy has been associated with higher cytotoxicity than single agent administration but has a significant improvement in response rate, progression time and survival rate [110].

1.1.10 Carcinogenesis and genetic alterations during CRC

Human cancer development (carcinogenesis) is a multistep process in which epithelial cells progress through a series of premalignant phenotypes until an invasive cancer emerges [111, 112]. The concept of multi-stage carcinogenesis was proposed by various groups in the 1940s and was supported by later studies [113-115]. In 1988, Vogelstein *et al.* published a molecular analysis of 172 colorectal neoplasia, including APC-associated familial adenomatous polyposis (FAP, also known as classic FAP) and CRCs, using what they outlined the 'traditional pathway' model also known as "adenoma-carcinoma sequence". This model explained how the majority of CRCs develop [116, 117]. Since the proposal of adenoma-carcinoma sequence, CRC has been an effective model for studying multi-staged carcinogenesis [116-118].

Table 3 Oncogenes and tumour suppressor genes commonly involved in CRC.

Gene name	Type of cancer gene	Frequency of mutation	Consequences
APC	Tumor suppressor	70%	Constitutive activation of Wnt signalling pathway. Regulates cell proliferation, cell migration, cell adhesion, cytoskeletal reorganization, and chromosomal stability.
KRAS	Oncogene	35%	Constitutive activation of MAPK pathway
BRAF	Oncogene	10%	Constitutive activation of MAPK pathway
TGFBR2	Tumor suppressor	15-30%	Decreased/loss of TGFβ-mediated growth inhibition
SMAD2	Tumor suppressor	6%	Decreased/loss of TGFβ-mediated growth inhibition
SMAD4	Tumor suppressor	16-25%	Decreased/loss of TGFβ-mediated growth inhibition
TP53	Tumor suppressor	50%	Impaired DNA damage response and cellular stress
MLH1	Mismatch repair	10%	Defective DNA mismatch repair
*Data format adapted from [119]			

Carcinogenesis is a result of mutations in genes, specifically, proto-oncogenes, tumor suppressor genes and stability genes (see **Table 3**). Mutations in these genes initiate the development of CRC and are reasonably well-understood [9, 120]. The classical adenoma-carcinoma sequence and genetic changes that parallel the adenoma-carcinoma sequence during CRC can be a result of either chromosomal instability (CIN) or microsatellite instability (MSI) (see **Figure 5a**). The onset of CRC is characterised by formation of early stage dysplasia involving a single crypt (unicryptal) to formation of cluster of dysplastic crypts (adenoma) and then finally the appearance of malignancy (adenocarcinoma) [118].

However, this sequence of events are slightly different in individuals that are genetically predisposed to CRC particularly FAP and hereditary nonpolyposis CRC (HNPCC) (see **Figure 5b**). There are also other hereditary CRC syndromes such as Lynch syndrome (LS), attenuated FAP (AFAP), MUTYH-associated polyposis (MAP), and familial CRC type X [121].

CRC is considered to be more sporadic accounting for almost 80-90% of all reported cases, implying that lifestyle choices may have a more significant impact in CRC development than genetic factors [122]. Interestingly, 80% of the sporadic CRCs possess mutations in *APC* [123], suggesting these may follow the adenoma to carcinoma sequence similar to that of FAP. Although, genetic alterations are associated with higher risk of CRC they account for only 5-6% of total CRC cases [121]. Commonly, tumours with CIN are characterised with mutations in *APC*, *KRAS*, and *TP53*. In contrast, tumours with MSI are a result of both CIN and MSI, and are characterised with alterations in Wnt signalling, *BRAF*, *TGFBR2*, and *IGFR2* required for cancer progression. FAP is an example of CIN CRC and is caused by a germline mutation in the *APC* gene, located on the long arm of chromosome 5q21, which is dominant trait inherited by many individuals with adenomatous polyps in the colon. Colonic neoplastic progression and apoptosis in colonic cells are controlled by *APC* which is often referred to as the "gatekeeper" of those functions [12]. FAP is only associated with 1-2% of total CRC incidences and serves as a good model to study CRC polyp pathobiology. HNPCC makes up 5-10% of all CRCs and confers a very high lifetime risk (up to 80%) of developing CRC [124]. HNPCC is a classic example of MSI CRCs. MSI is observed in 90% and in about 10-15% of HNPCC and sporadic CRC respectively [125, 126]. With a sufficient number of mutations, a small number of cells can detach from the primary tumour site and become malignant or metastatic.
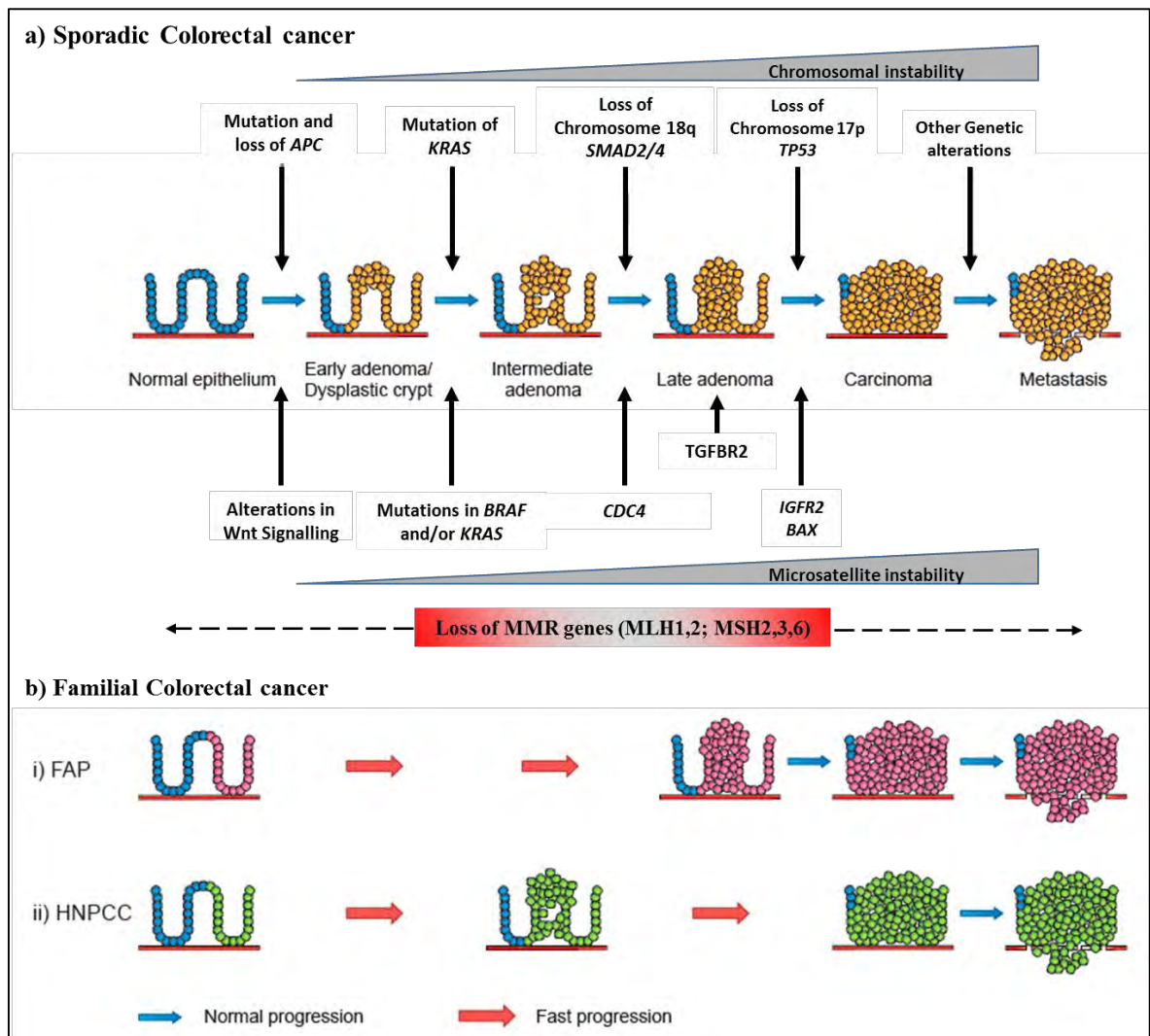
Figure 5 - The colorectal adenoma-carcinoma sequence. **a) Sporadic colorectal cancer**: Progression from normal through adenoma to carcinoma is a result of accumulated abnormalities, loss or mutation, of the genes involved at each stage of the sequence are shown. In detail, the chromosomally unstable CRC (CIN+) begins with the mutation or loss of adenomatous polyposis coli (*APC*) tumor suppressor gene results in the uncontrolled growth of normal cell sin the colon resulting in the formation of polyps or early adenoma. The activation of *KRAS* oncogene followed by the loss of chromosome 18q with Smad 4, required for transforming growth factor-β (TGFβ) signalling, and *TP53* tumor suppression genes promote the formation of carcinoma and eventually leading to metastasis. The MSI CRCs (MSI+) occur when there is loss in microsatellites that maintain genomic stability and are infrequently. Consequently, the development of CRC through MSI, must involve different, but analogous, genetic changes to those detailed in CIN+ CRC. The initial step in MSI+ CRC formation is thought be alteration of Wnt signalling pathway. This is then followed by the mutations in *BRAF*, sometimes *KRAS*, and further mutations in TGFβ receptor 2 (*TGFBR2*), insulin-like growth factor receptor 2 (*IGFR2*) and *BAX*, which then allow for p53-independent mechanism for progression to carcinoma and eventual metastasis. During, both CIN and MSI there are mutations or loss of various mismatch repair (MMR) genes. **b) Familial colorectal cancer**: These sequence of events usually occur in individuals that are genetically predisposed with cancer. More specifically, during FAP **(b.i)**, a mutation and loss of the APC gene results in the development of adenoma faster but the progression from adenoma and carcinoma happens at the same rate as of sporadic cancer. During HNPCC **(b.ii)**, the inactivation of either the MSH2 or MLH1 MMR genes along with other somatic mutations speeds up the adenoma to carcinoma progression. (Figure adopted from http://syscol-project.eu/about-syscol/ and [127]).

1.1.11 Metastasis

Metastasis can be defined as the movement of the cancerous cells to secondary sites (organs i.e. liver, heart), via circulatory or lymphatic systems, to form malignant cancer growth away from the primary site of cancer. Metastasis, rather than primary tumours, is directly responsible for the majority (almost 90%) of CRC deaths [128, 129]. It is thought to be an inefficient process since very few tumour cells escape from the primary tumour form metastasis [130-133]. Metastasis is a cascade of complex molecular interactions which alter various regulatory and signalling pathways to successfully form secondary sites of cancer [128, 134, 135]. It is thought is some way to begin with the epithelial to mesenchymal transition (EMT), which leads to invasion followed by migration and spread to distant organs.

The Epithelial to mesenchymal transition

The normal epithelial cells in an organism have two very important roles – to act as protective barrier and to secrete and absorb substances necessary for growth and metabolism. The structural integrity of the epithelial layers is maintained by the cell-cell and cell-extracellular matrix (ECM) interactions, which also define tissue polarity [136] allowing different functions for the apical and basal surfaces. In some tissues such as the colorectal epithelium, the apical surface of the cell has a role in absorption or secretion and faces into the intestinal lumen.

EMT is a key process during embryogenesis and is considered a crucial hallmark of cancer malignancy. EMT is an orchestrated series of events in which adherent epithelial cells are converted into individual migratory cells which are able to invade the ECM [137]. The term EMT is often misused to describe distinct biological events as if it were a single conserved event. However, the EMT-related processes can vary in intensity from loss of cell polarity to total cellular reprogramming [138]. The epithelial to mesenchymal transition can result in the loss of baso-apical polarization to acquire front-rear polarization required for cell migration, a modulation of the organization of the actin cytoskeleton that enhances ECM-structured communication, loss of the cell-cell adhesion structures, increased mobility, acquisition of resistance to anoikis and most importantly switch expression from keratin- to vimentin-type intermediate filaments which defines mesenchymal origin [138, 139]. The main differences in the epithelial and mesenchymal cells are summarised in **Figure 6**. These changes are all hallmarks of increased malignancy and the EMT provides a mechanism for carcinoma cells to acquire this aggressive mesenchymal phenotype.
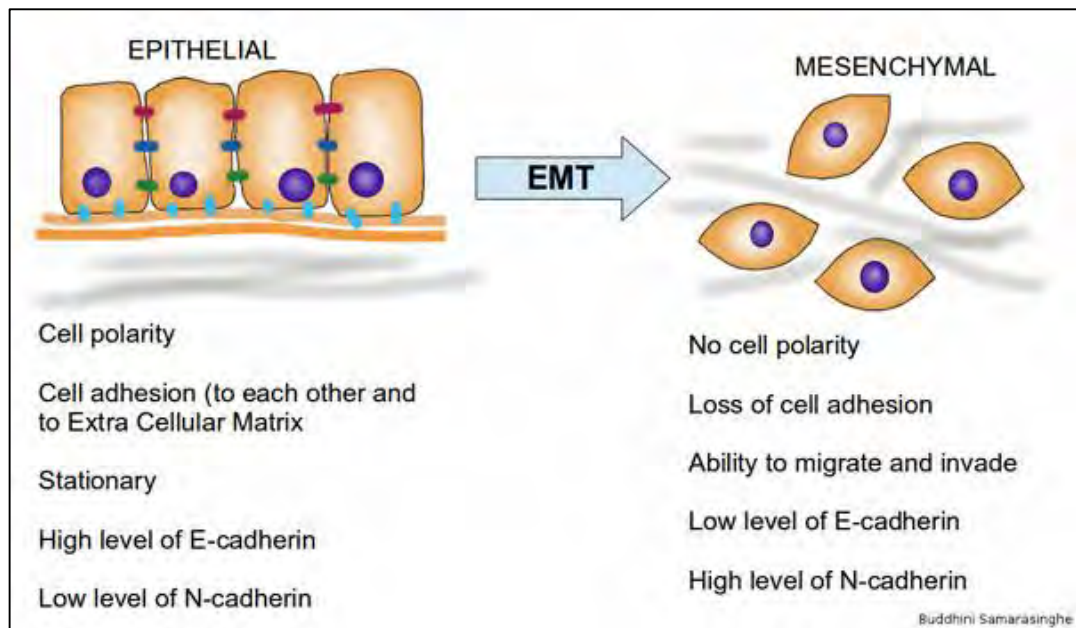
Figure 6 - Concept of the Epithelial to Mesenchymal Transition (EMT) illustrating major differences between epithelial and mesenchymal cells during the process. Image credit: Buddhini Samarasinghe [140].

The EMT is an uninterrupted process that allows the pre-malignant epithelial cells to escape the constriction of adjoining cells and the ECM, to breach the basement membrane, migrate out of the primary tumour and to locally invade surrounding tissue. This process also involves the induction of a new transcriptional program to drive and maintain the acquired mesenchymal phenotype. The EMT involves the alteration of the function, expression and distribution of proteins involved in cell adhesion and ECM remodelling. Most often the EMT has been associated with the loss of cell-cell adhesions through repression of Epithelial (E)-cadherin expression, the dissociation of desmosomes, tight- and adherens-junctions [137, 139]. Once the mesenchymal phenotype is acquired, it provides the capacity for the cells to invade surrounding tissues and metastasise to distant organs.

Invasion

Invasion is a hallmark of cancer development. Invasion can be defined as the active translocation of neoplastic cells across tissue boundaries and through host cellular and extracellular matrix barriers [141]. The majority of times the term "invasion" is used it refers to "local invasion" which compromises the function of involved tissues by compression, destruction, or prevention of normal organ functioning [142]. The process of invasion can only be achieved by breaching the basement membrane with cells entering the underlying interstitial stroma, followed by distant dissemination through lymphatics and blood vessels. It is not an innate ability of all tumour cells

Upon gaining the invasive phenotype tumour cells will acquire the ability to alter their adhesive interactions with the basement membrane, gain ability to interact with the exposed vascular or lymphatic basement membranes and finally, occupy the basement membrane from where locomotion is possible. Invasion is a dynamic process involving cyclic repetition of pseudopod protrusion, proteolysis, antiproteolysis, adhesion, and detachment, through various proteins and their associated signalling pathways [142]. It is certainly a prerequisite for metastasis [133]. The existence of an invading cancer does not necessarily imply metastasis and a fatal outcome and metastases can be prevented by averting invasion.
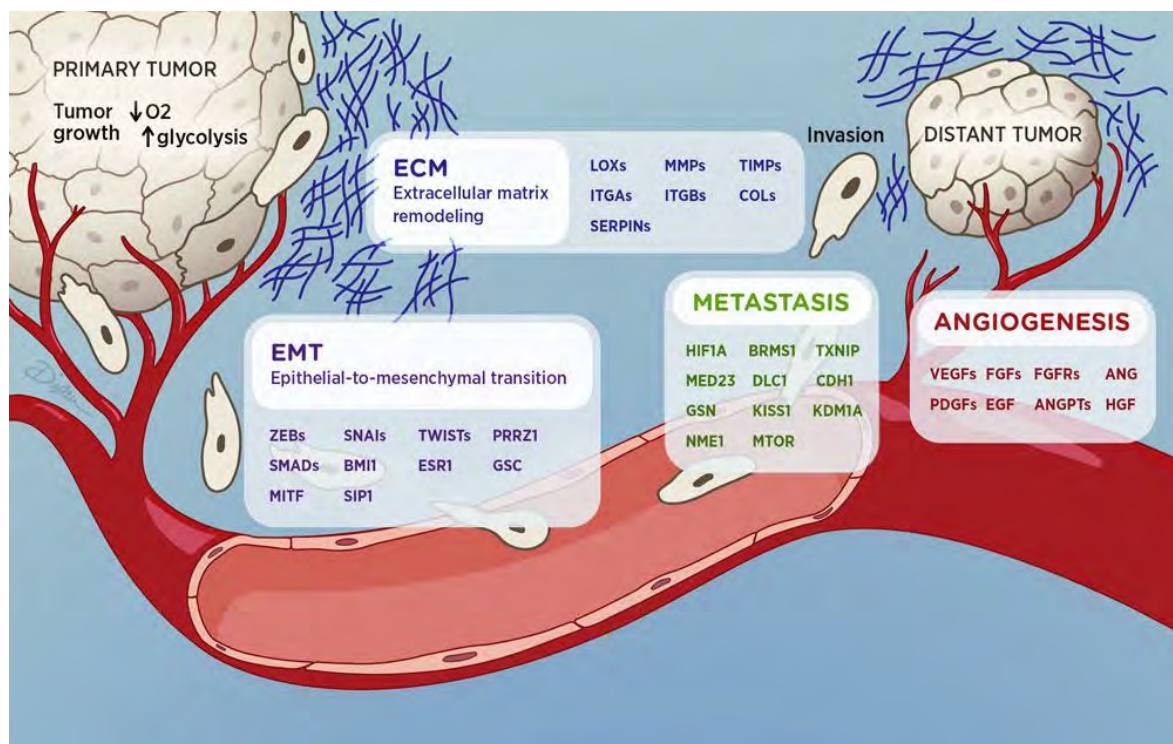
Figure 7 - Key molecules in cancer progression. The illustration shows various molecules associated with different stages of cancer development. Image source [143].

1.1.12 Key molecules in cancer progression

The complex process of metastasis relies on EMT and invasion during which various molecules that control various cellular processes such as cell adhesion, ECM degradation and cell growth are altered. These molecules associated have been reported to deviate from their normal physiological function/s and have different functional outcomes in cancer. Some key molecules or protein groups that are thought to be involved at various stages of cancer progression (see **Figure 7**) include various integrins, proteolytic enzymes and their signalling, and growth factors. The following sections will briefly focus upon the role of one integrin (αvβ6) with respect to cell adhesion, and with one protease receptor (urokinase

plasminogen activator receptor; uPAR) with respect to ECM proteolysis and a short summary of growth and signalling factors implicated in cancer.

Integrin αvβ6 as an adhesion molecule

Cell adhesion is a fundamental process for the development and functioning of a multicellular organism. There are more than 50 cell adhesion molecules (CAMs) that have been classified into various superfamilies such as integrins, cadherins, selectins, and immunoglobulin-like CAMs [144]. Various CAMs are now thought to act as both positive and negative modulators of the metastatic process [145]. Specifically, differential expression of various integrins has been implicated in multiple cancers including CRC [69, 146-150]. They are also viewed as regulators of inflammation, metastasis and drug resistance in cancer [151].

Integrins are a group of prominent transmembrane receptor proteins that were identified as cell adhesion molecules [152, 153]. Integrins can be composed from one of the 18 alpha (α-) and 8 beta (β-) subunits and form at least 24 distinct integrin heterodimer combinations known [154]. Integrins can bind to ECM proteins such as collagen IV, laminin, vitronectin, fibronectin and leukocyte-specific ligands and mediate cellular adhesion through cell-ECM and cell-cell adhesion [155, 156]. For example, α5β1, αVβ3, αVβ5 and αVβ6 heterodimers mediate cellular adhesion by binding to Arg-Gly-Asp (RGD) motifs within ECM proteins such as fibronectin, vitronectin, fibrinogen and osteopontin [155, 157]. Integrins also serve as bidirectional signalling molecules that participate in other vital cellular functions including polarity, differentiation, migration and cell division [158] wherein they associate with adapter proteins that connect the integrins to the cytoskeleton, cytoplasmic kinases, and transmembrane growth factor receptors [159]. These functions are critical during embryogenesis and maintaining cellular homeostasis during normal cell growth [158]. During cancer, however, defective integrin signalling can result in abnormal regulation of gene expression [150, 160], cell proliferation [161, 162], regulation of apoptosis [163-165], invasion and metastasis [166, 167] and angiogenesis [148, 168, 169]. Several integrin subunits and heterodimers such as αvβ6 [146, 149, 170, 171], αvβ1 [172-174], αvβ3 [175], and α6β4 [176] have been implicated in CRC.

The integrin β6 subunit is unique in three ways. Firstly, it is only expressed in wounded or transformed epithelial cells and secondly it only binds with αv subunit [158]. Lastly, the β6 has a unique C-terminal cytoplasmic tail that can bind to phospho-ERK1/2 [146, 171].The αvβ6 heterodimer is highly expressed during development of lung, skin and kidney epithelia and the expression is down-regulated in adult epithelia [177]. Elevated expression of αvβ6

has been observed in various epithelial cancers including colorectal, breast, endometrium, gastric, liver, lung, and oral and skin squamous cell carcinomas (SCC), where its expression usually correlated with poor patient survival [158]. A recent clinical study by Ahn *et al.* [69] from our group assessing surgical resections from 362 rectal cancer patients (168 Duke's stage B and 194 Duke's stage C) using tissue microarray (TMA) immunohistochemistry (IHC) reported that αvβ6 expression is significantly higher in the invasive frontal region of rectal tumours relative to the central region or adjacent non-neoplastic mucosa tissue. However, this study noted no significant difference in αvβ6 expression and overall survival between the Dukes' stage B and C patients [69].

Integrin αvβ6 is an RGD-motif binding protein. It is known to activate latent-TGFβ1 (L-TGFβ1) by binding to the RGD sequence on the latency-associated peptides (LAP) of L-TGFβ1 and L-TGFβ3 [178]. As a result of its specific expression pattern, αvβ6-mediated TGFβ activation is observed only near epithelial cells. For instance, in ovarian cancer cells, increased TGFβ1 levels was observed when αvβ6 was overexpressed [179]. Saldanha *et al.* showed that the inhibition of αvβ6 using specific antibodies resulted in the blockade of TGFβ1 and ERK activation through the αvβ6-uPAR axis [180]. Interestingly, in colon carcinoma cells, the loss of αvβ6-mediated ERK activation was abrogated when the unique 11 amino acid (EKQKVDLSTDC) cytoplasmic-tail motif of the integrin was deleted [146, 171]. Likewise, SCC9 cells expressing β6 subunit that lacked this unique cytoplasmic-tail did not develop the mesenchymal phenotype when compared to the full length β6-overexpression cell line [154]. Morgan *et al.* then showed that the expression of this unique cytoplasmic-tail sequence at the end of a different integrin subunit (β3) enhanced αvβ3 mediated tumour cell invasion thorough matrix metalloproteinases (MMP2 or MMP9) [181].

Interestingly, Ahmed *et al.* [182] also showed that increased expression of αvβ6 in ovarian cancer cells was accompanied by the secretion of high molecular weight-urokinase plasminogen activator (hmw-uPA), MMP2 and MMP9 in the tumour conditioned media and a marked reduction of these molecules was observed in the absence of αvβ6 expression. It was therefore very surprising to observe that αvβ6 interacts directly with urokinase plasminogen activating receptor (uPAR), when co-immunoprecipitation (co-IP) experiments were performed using ovarian cancer cells (OVCA429) [180]. These results from the IP experiments suggest the possibility of a αvβ6-uPAR mediated ECM degradation through activation of various proteolytic enzymes [176]. Proposed interactome associations between αvβ6, uPAR and TGFβ cascades is illustrated in **Figure 8**. The role of integrin αvβ6 in CRC metastasis has been reviewed in **Publication II** of this thesis.

Integrin β6 has also been reported to be involved in inflammation. During inflammation or epithelial injury β6 expression is rapidly induced [178, 182]. Huang XZ, et al., showed that knockout of β6 in mice resulted in increased macrophages in the skin, accumulation of lymphocytes in the lungs and showed airway hyper-responsiveness to acetylcholine (a bronchoconstrictor). These results suggest that β6 may have important anti-inflammatory effects in skin and lungs [182]. Munger S, et al., also observed that mice lacking integrin β6 developed exaggerated inflammation however, were protected from profibrotic agent bleomycin induced pulmonary fibrosis [178]. Early pre-malignant tumors are often recognised as wounds by the immune system which leads to inflammation resulting in high β6 expression. This increased β6 can then assist in the activation of L-TGFβ1 during cancer and further contribute to the growth of the tumor [183].
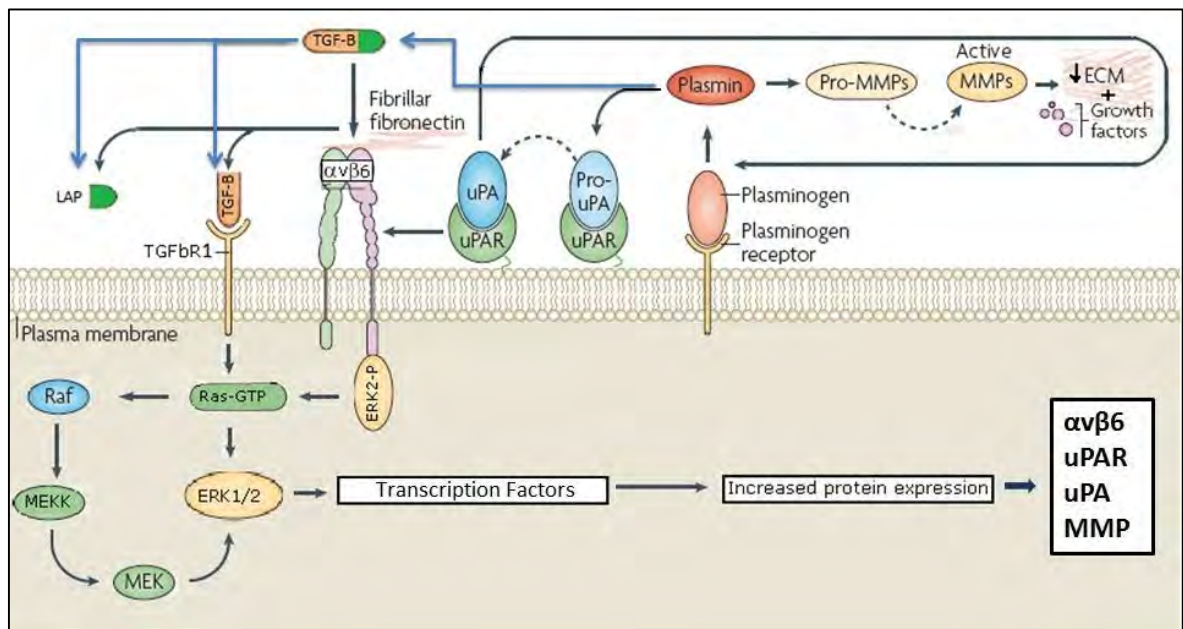
Figure 8 - The uPAR-integrin β6-TGFβ signalling pathway. uPAR binds to the inactive serine protease zymogen pro-urokinase-type plasminogen activator (pro-uPA) and converts it to active uPA. uPA can then catalyse the conversion of plasminogen into highly active plasmin[184]. The active plasmin is capable of catalysing the conversion of pro-MMPs to active MMPs. Plasmin along with the MMPs is then capable of degrading the ECM proteins such as fibronectin, vitronecton, laminin and fibrin that are key components for maintain the ECM stability. Plasmin can also activate TGFβ, through cleavage of the LAP of the L-TGFβ. Integrin αvβ6 can activate TGFβ by binding to the RGD-motif on LAP of L-TGFβ1. The active TGFβ through its receptors can activate Erk1/2 signalling alongside αvβ6. (Image modified from Smith and Marshall, 2010 [184].).

ECM proteolysis and uPAR

The ECM is a tight fabrication of multiple proteins and polysaccharides expressed by cells. Receptors such as integrins interact with ECM molecules and participate in signalling required for regulating cell adhesion, proliferation, differentiation, migration and survival. This intricate network of ECM-interactions are essential for normal functioning of an

organism. Therefore, alterations in these ECM molecules or systems can be exploited during human diseases. During cancer, loss of cell-ECM and cell-cell adhesion is a pre-requisite for increased cell motility that results in eventual migration and invasion. The majority of the times the loss in cell adhesion can be associated with increased expression of proteolytic enzymes such as plasmin and MMPs that can cleave almost all ECM related molecules. One of the ways to achieve is through the increased expression of receptors such as uPAR that are integral to plasminogen activation to plasmin which is then capable of activating various MMPs [184].

uPAR/CD87 is a cell surface glycophosphatidylinositol (GPI-) anchored protein that belongs to lymphocyte antigen 6 (Ly6) protein superfamily and is integral to the plasminogen activation cascade (see **Figure 8**). uPAR consists of a single polypeptide that is 283 amino acids in length and is composed of three domains denoted DI (residues 1-80), DII (residues 93-191) and DIII (residues 192-283). These three domains adopt a three-finger fold like tertiary structure which typically compromises of six β-strands in antiparallel and four disulphide bonds. These three domains form a concave structure and the central cavity acts as the binding site for the uPA, the primary ligand of uPAR and the outer surface is available for secondary binding partners. Apart from binding to uPA to facilitate the activation of zymogen plasmin, uPAR has also been reported to interact with αvβ6 [180] using co-IP studies. This interaction with αvβ6 was recently further investigated by Ahn *et al*. using peptide array studies and they reported six potential αvβ6 binding sites spanning across all three domains of uPAR [185]. Using homology modelling and docking studies, Sowmya *et al*. then confirmed the site of interaction to be in domain III of uPAR [186]. It is also important to note that crystal structure of αvβ6 has not been reported and therefore the homology model reported by Sowmya *et al*. only offers a glimpse of the structure of αvβ6 [186]. Various other integrins including α3β1, α4β1, α5β1, αvβ3 and αMβ2 have been reported to bind with uPAR and to facilitate downstream intracellular signalling [184].

Under normal physiological conditions, expression of uPAR is believed to be relatively limited. High expression is observed during tissue remodelling [187] and wound healing [188]. However, high expression of uPAR has been observed various cancers [189]. In CRC, specifically, elevated uPAR expression has been correlated with poor prognosis [71, 190] [189, 191-193]. A recent study by Ahn *et al*., examining the Dukes' stages B (n=170) and C (n=179) rectal cancer tissue samples showed the expression of uPAR in epithelial and stromal cells correlated with patient survival [71]. They reported that elevated epithelial uPAR expression in both the central region and invasive tumour front adversely correlated

with overall survival of stage B patients while elevated stromal uPAR at the invasive front favourably correlated with overall survival of stage C patients [71]. In contrast, another study by Boonstra *et al.*, examining CRC tumour tissue (n=262; all stages) samples showed that stromal uPAR expression was adversely associated with overall survival as well as disease free survival [191]. Another study by Illemann *et al.* also reported, similar results to Boonstra *et al.*, that uPAR expression on tumor-associated macrophages negatively correlated with overall survival in all stages (n=244) [192]. From these reports it can be inferred that high expression of uPAR during cancer result in increased levels of plasmin that may contribute to sustaining high levels of TGFβ during cancer. Therefore, it is not very surprising to observe alterations in plasmin or plasminogen binding [194], expression of MMP-2 and MMP-9 [195], integrin αvβ6 [170] and active TGFβ1 [196] which have collectively been associated with poor CRC prognosis and subsequently poor survival.

Growth and signalling factors

Growth factors are polypeptides that stimulate cell proliferation and are a major class of growth regulatory molecules for cells in culture and probably *in vivo* [197]. Under normal physiological conditions the cells receive fate-determining signals from their tissue surroundings in the form of polypeptide growth factors to control homeostasis [198]. During cancer, the departure from homeostasis and tumour initiation are instigated by oncogenic mutations rather than by growth factors [198]. However, the growth factors "are major regulators of tumour progression, namely clonal expansion, invasion across tissue barriers, angiogenesis, and colonization of distant niches" [198]. Various growth factors such as TGFβ, VEGF, EGFR and platelet-derived growth factor (PDFG) amongst others have been implicated in cancer [197, 198]. TGFβ and its signalling components have also been widely implicated in various cancers [199-207]. It has been proposed that it regulates cancer-related cellular processes such as EMT, cell proliferation, invasion and metastasis [204, 207]. Considering TGFβ is the main of focus of this thesis it will be addressed with greater detailed in the section 1.2.

Table 4 The TGFβ-superfamily ligands, tissue specificity and their major functions[§].

Names	Tissue Specificity	Molecular weight (kDa)	Representative functions
TGFβ subfamily			
TGFβ1		44.34	Control of cell growth, cell proliferation and cell differentiation in mesenchymal cells, wound healing, ECM production [208, 209]
TGFβ2	Most epithelial cells	47.74	
TGFβ3		47.32	
Activin/Inhibin/Nodal subfamily			
Activin subgroup			
Activin A		47.44	Regulates production of follicle-stimulating hormone (FSH), cell proliferation, differentiation, apoptosis, metabolism, homeostasis, immune response, wound repair, and endocrine function [210-213]
Activin B	Secreted by gonads, pituitary gland	45.12	
Activin C		38.23	
Activin E		38.56	
Inhibin subgroup			
Inhibin A	Secreted by gonads, pituitary gland		Negatively regulate FSH Secretion [214]
Inhibin B			
Nodal			
Nodal	Secreted	39.56	Essential for mesoderm formation and axial patterning during embryonic development [215]
LEFTY			
LEFTY-1		40.88	Essential for formation of mesoderm and axial patterning during embryonic development [216]
LEFTY-2		40.92	
BMP/GDF Subfamily			
BMP 2/4 subgroup			
BMP-2	Abundant in lung, spleen and colon	44.7	Participate in embryogenesis, neurogenesis, development of cartilage and bone formation [200, 209, 217, 218]

BMP-4	Liver, low levels in Kidney	46.55	
BMP 3 subgroup			
BMP-3	Adult and fetal cartilage	53.37	Negatively regulates osteogenic properties of other BMPs [219]
BMP-3b/GDF-10	Expressed in femur, brain, lung, skeletal muscle, pancreas and testis	53.12	
BMP 5 subgroup			
BMP-5	Lung and Liver	51.73	Along with BMP 2/4 subgroup theses participate in mammalian development and also take part in neurogenesis [200, 203, 209, 217, 218]
BMP-6/Vgr1		57.22	
BMP-7/OP-1	Expressed in kidney and bladder	49.31	
BMP-8a/OP-2		44.79	
BMP-8b		44.76	
BMP 9 subgroup			
BMP-9/GDF2		47.32	Acts a circulating vascular quiescence factor [220], takes part in neurogenesis like BMP 2/4 and 5 subfamilies
BMP-10		48.04	
GDF 1 subgroup			
GDF-1	Expressed in brain	39.47	Cell differentiation events during embryonic development
GDF-3/Vgr2		41.38	
GDF 5 subgroup			
GDF-5/BMP-14	Bone development	55.41	Chondrogenesis [221-223] and neurogenesis [224]
GDF-6/BMP-13	Bone development	50.66	Osteogenesis of limbs, skull and axial skeleton [225]
GDF-7	Secreted during neurogenesis	46.95	Required for the specification of neuronal identity in the dorsal spinal cord and other functions embryo development [226]
GDF 8 subgroup			
GDF-8/Myostatin	Skeletal-muscles	42.75	Negative regulator of skeletal muscle growth [227]

GDF-11/BMP-11	Secreted during embryogenesis	45.09	Facilitates temporal progression of neurogenesis in the developing spinal cord [228], controls axial vertebral development [229-231]
GDF 9 subgroup			
GDF-9	Expressed in ovarian granulosa cells	51.44	Required for ovarian folliculogenesis [232, 233], regulate ovarian functions [234]
GGDF-9b/BMP-15		44.05	
GDF-15	High expression in placenta, low expression in prostate, colon and kidney	34.14	
MIS			
MIS	Produced by Sertoli cells of the testis	59.19	Mullerian duct regression [235]

§TGFβ – transforming growth factor-β; BMP - bone morphogenetic protein; GDF - growth differentiation factor; OP - Osteogenic protein; MIS - müllerian-inhibiting substance

1.2 Transforming Growth Factor-β

Transforming Growth Factor-β (TGFβ) superfamily of growth factors and their signalling emerged with the evolution of complex multicellular organisms [236]. They are vital growth factors pathways that contribute to the increased diversity and complexity required for development and homeostasis of the metazoans [237]. The TGFβ family members have been reported to regulate various processes during embryonic development including trophoblast differentiation, endocardium, neural crest cell, lung, and palate development [238]. For example, neural crest cell morphogenesis is shown to be influenced by TGFβ1, TGFβ2, TGFβ3, BMP2/BMP4 and Wnt signalling which determines the fate of those cells [238].

The EMT, a key process during embryogenesis, is considered to be important during cancer development [238]. During embryogenesis EMT is essential for a variety of developmental processes and is regulated by TGFβ family members [236]. For instance, during the development of heart valves invasion of the heart cushion by endocardial cells from the atrioventricular canals is essential and is mediated by TGFβ signalling components [239]. However, the TGFβs function as crucial inhibitors of epithelial cell growth in adult tissues [240]. Tied to these opposing yet critical regulatory roles at various stages of the organismal growth "are the serious consequences that result when this signalling pathway malfunctions, namely tumorigenesis" [241]. The alterations to TGFβ signalling components can result in cancer cells gaining the capacity to avoid or adulterate the TGFβ growth inhibitory effects leading to TGFβ-mediated cancer cell growth. This has attracted considerable attention in recent years and efforts are being made to understand the role of TGFβ during cancer. This thesis has tried to understand the effects of TGFβ on CRC cell lines and being the main focus will details the TGFβ signal transduction and its role in cancer.

1.2.1 TGFβ superfamily of ligands

The TGFβ superfamily is found in all metazoans and is a large group of more than 30 secreted proteins that regulate a multitude of cellular functions and disease pathogenesis. The superfamily includes TGFβs, activins, inhibins, Nodal and bone morphogenetic proteins (BMP) and growth differentiation factors (GDF), all of which possess diverse and complementary physiological effects. The important functions of these ligands are summarised in **Table 4**.

TGFβs are named after their cell transforming activities (i.e., cell growth and differentiation) from *in vitro* assays and are now unequivocally known to be involved in both tumour suppression and tumour progression (i.e., proliferation, invasion and metastases). Initially,

TGFβ1 was isolated as one of two components (TGFα and TGFβ) that could induce a phenotype transformation in normal kidney rat fibroblasts [242]. Subsequently, it was understood that TGFβ was a potent growth inhibitor to most cell types whereas TGFα was a ligand for EGFR and stimulates growth in most cell types [242, 243]. The *bona fide* TGFβ subfamily consists of three TGFβ isoforms, TGFβ1, TGFβ2 and TGFβ3 encoded by genes located on different chromosomes (19q13.1, 1q41 & 14q24 respectively) but they signal through the same receptor system.

All TGFβ ligands are secreted *in vivo* as 'latent' inactive zymogen complexes in a non-covalent complex with LAPs that are bound to their respective latent TGFβ binding proteins [244]. The LAP domain ensures that 'inadvertent' activation of TGFβ does not occur in normal cells under physiological conditions. The two major ways by which activation can occur include cleavage of LAP by proteases and by conformational changes, assisted by ECM molecules such as integrins. However, L-TGFβ can also be activated *in vivo* through a variety of other mechanisms and they are summarised in **Table 5**.

Table 5 Mechanisms of TGFβ activation under different physiological conditions

Activation environment/ molecule	Mechanism of activation [Reference]
Physicochemical	
Extremes of pH (acid treatment)	Denaturing of LAP [199, 245]
Acidic cellular microenvironment	Possible denaturing of LAP [246]
Gamma-irradiation	Disabling of LAP by the hydroxyl radicals [247]
Reactive oxygen species	Disabling of LAP by the hydroxyl radicals [248, 249]
Proteases	
Plasmin	Cleaves the LAP [250]
MMP-2 and MMP-9	Cleaves the LAP [251]
Unidentified protease in Kato III cells	Unknown [252]
Physical interaction	
Thrombospondin-mediated	Disrupt non-covalent interactions between the LAP and TGFβ [253, 254]
Integrin αvβ6	Direct interaction with the RGD amino acid sequence LAP β1 and LAP β3 [178]
Integrin αvβ8	Unclear [255]
Integrin αvβ1	Direct interaction with the RGD amino acid sequence LAP β1 [256]

1.2.2 TGFβ Receptors

The TGFβ receptors were identified by affinity labelling of cells with radio-iodinated TGFβ (^{125}I-TGFβ) ligand and subsequent isolation of receptors to which it bound [257]. Three

primary TGFβ receptors, the type I receptor (53 kDa), the type II receptor (73-95 kDa) and the type III receptor (110 kDa) were identified depending on molecular weights [258]. A fourth non-proteoglycan membrane glycoprotein that co-expresses with the type I, type II, and type III TGF-β receptors in epithelial cells and other cell types but not in certain carcinoma cells was reported as the type V TGF-β receptor is a 400-kDa by O'Grady *et al.*, in 1991 [259, 260].

This thesis will only elaborate on the three primary TGFβ receptors. The structure of these three primary receptors is illustrated in **Figure 1** of this thesis' **Publication I**. Like the TGFβ ligands, there are a family of receptors (summarised in **Table 6**) that can bind to various ligands and initiate a specific signalling pathways. The three TGFβ receptors are discusses in the order of ligand presentation that occurs *in vivo*.

The TGFβ Type III Receptor
Transforming growth factor-β type III receptor (TGFβR3) is also known as betaglycan and is the most abundant of all the three TGFβ receptors followed by endoglin [261]. Betaglycan is a 851 amino acid proteoglycan comprising of a large N-terminal extracellular domain, a single-pass hydrophobic transmembrane region and a short 42 amino acid C-terminal cytoplasmic domain [261]. The cytoplasmic domain is rich in serine and threonine, but does not exhibit any kinase activity. The last three amino acids of the cytoplasmic tail comprise a class I PDZ binding motif which binds with the G Alpha Interacting Protein (GAIP)-interacting protein C-terminus (GIPC). This interaction has been found to increase stability of betaglycan at cell surface and increase TGFβ1 and TGFβ2 mediated gene expression in Mv1Lu mink lung epithelial and L6 myoblast cells expressing the GIPC [262]. Recently the GIPC-betaglycan interaction has been shown to inhibit TGFβ-mediated Smad signaling and migration in breast cancer cells [263]. However, the exact mechanism/s by which this occurs are yet to be characterized.

Betaglycan also functions as a co-receptor (accessory receptor) for TGFβ receptors and can bind to all three TGFβ ligand isoforms. Affinity-labelled saturation experiments showed that betaglycan has a 5- to 10-fold higher affinity for TGFβ2 than for TGFβ [264]. However, it has a 7-fold higher capacity for TGFβ1 than TGFβ2, which explains why betaglycan is required for mediating the binding of TGFβ1 to TGFβR2 [265]. Further increasing its functional complexity, proteolytic cleavage of the extracellular domain of betaglycan by MT1-MMP and MT3-MMP near the transmembrane region results in the release of a soluble 90kDa fragment, capable of binding and presenting TGFβ ligands to its receptors [266]. The ability to present TGFβ ligands is also affected by cleavage of the 50-amino acid linker

region extracellular domain by plasmin [267]. Plasmin mediated cleavage generates fragments of 45kDa and 55kDa which can no longer bind to and present TGFβ ligands to TGFβR1 and TGFβR2 [267].

The TGFβ Type II Receptor

Transforming growth factor-β type II receptor (TGFβR2) is a 567 amino acid serine/threonine kinase receptor which includes a 22 amino acid signal peptide, a cysteine-rich N-glycosylated extracellular domain, a transmembrane domain, and a cytoplasmic serine/threonine kinase domain flanked by a short juxtamembrane domain and C-terminal tail [268]. TGFβR2 can also bind to all three TGFβ ligands with varying affinities. It has strong affinity towards TGFβ1 followed by TGFβ3 and TGFβ2 [269]. However, the presence of the co-receptor betaglycan is essential to facilitate high affinity TGFβ1 binding to TGFβR2 to enable downstream signaling [270]. However, it cannot participate in downstream signaling in the absence of TGFβR1 [269].

The TGFβ Type I Receptor

Transforming growth factor-β type I receptor (TGFβR1) is a 503 amino acid transmembrane serine/threonine kinase receptor that closely resembles TGFβR2 in structure. TGFβR1 structure contains a 33 amino acid signal peptide, a cysteine-rich N-glycosylated extracellular domain, cytoplasmic kinase region with 41% sequence homology to TGFβR2, a very short C-terminal tail [271]. A unique feature of TGFβR1 is its highly conserved 30 amino acid region preceding the cytoplasmic kinase region called the GS domain because of the characteristic SGSGSG sequence it contains. The ligand-induced phosphorylation or serine and threonine in the GS region is required for activation of signaling [270]. TGFβR1 forms a heterodimer with TGFβR2 and this complex collectively takes part in TGFβ-mediated downstream signaling. Unlike TGFβR2, TGFβR1 has similar affinities for TGFβ1 and TGFβ3 and has 10-20 fold higher affinity for TGFβ1 than it has for TGFβ2 [269].

1.2.3 Canonical TGFβ Receptors

A well-characterized signalling pathway that is initiated by active heterodimeric TGFβ receptors is through Smads. The family of mammalian Smads consists of eight proteins divided into three subfamilies, namely receptor-activated (R-) Smads, common-mediator (Co-) Smads, and inhibitory (I-) Smads (see **Table 6**). TGFβ signalling via Smads is facilitated by TGFβR1 and TGFβR2, that form both homodimeric and heterodimeric complexes required for signalling.

Table 6 Receptors of the TGFβ superfamily**:**Nomenclature, molecular weight and their known ligand-binding partners.

Receptors	Alternative names	Molecular weight (kDa)	Ligands partners	References
Type I Receptors				
Alk-1	TSR-1, SKR3, AVCRL1	56.12	TGFβ, Activin A	[272, 273]
Alk-2 (Type 1 Activin receptor)	ActR1A, Tsk7L, SKR1	57.15	Activin A, TGFβ, BMP 2/4, BMP 6/7	[272, 274-278]
Alk-3 (BMP receptor type 1/1a)	BMPR1 (BMP type 1 receptor), BMPR1A, BRK1, Tfr11, AVCRLK3	60.198	BMP 2/4, BMP 6/7	[274, 275, 278]
Alk-4 (Type 1b Activin receptor)	ActR1B, ACVR1BSKR2	56.807	Activin A, GDF-1, Nodal, GDF-11	[272, 275, 279-281]
Alk-5 (Type 1 TGFβ receptor)	TGFβR1, SKR4	55.96	TGFβ	[282, 283]
Alk-6 (BMP receptor type 1b)	BMPR1B, BRK2	56.93	BMP2/4, GDF5/6, BMP 6/7, GDF9b, MIS	[274, 275, 278, 284-287]
Alk-7		54.87	Nodal	[288]
Type II receptors				
ActR2A (Activin type 2 receptor)	AVCR2	57.84	Activins, Inhibin A/B, BMP-6/7, GDF-1, GDF-5, GDF8/11, GDF-9b	[274-276, 279-281, 284, 287, 289]
ActR2B	AVCR2B	57.72	Activins, Inhibin A/B, BMP-6/7, GDF-1, GDF-5, GDF8/11	[274-276, 279-281, 284, 289]
TGFβR2	Type 2 TGFβ receptor	64.568	TGFβ	[282, 283]
BMPR2	BRK3	115.3	Inhibin A, BMP-2/4, BMP-6/7, GDF-5/6, GDF9b	[274, 284, 285, 287, 290-292]
MIS R2 (Mullerian inhibitory substance type 2 receptor)	AMHR2	62.75	MIS	[286]
Type III receptors				
TGFβR3	Betaglycan	93.49	TGFβ1, TGFβ2, TGFβ3, BMP 2, BMP 4, BMP7, GDF 5	[261, 283, 290, 293]

Table 7 Smad family proteins[§].

Subfamily	Name	Molecular Weight (kDa)	Associated Ligands
R-Smads	Smad1	52.26	BMP
	Smad2	52.306	TGFβ, Activin
	Smad3	48.08	TGFβ, Activin
	Smad5	52.25	BMP
	Smad8	52.49	BMP
Co-Smads	Smad4	60.43	
I-Smads	Smad6	53.49	
	Smad7	46.42	

[§]The Smad family is divided into three subfamilies. A) Receptor-activated (R-) Smads; B) Common-mediator (Co-) Smads; and C) Inhibitory (I-) Smads. Smads 2/3 signal via the TGFβ receptors and Smads 1/5/8 signal via the BMP receptors and together with Smad4 they participate in gene transcription. I-Smads can block the downstream signaling of the R-Smads by intercepting the complex formation with the Co-Smad.

Canonical TGFβ-Smad signaling is initiated by preferential binding of active TGFβ1 to TGFβR2 that then recruits, binds and transphosphorylates TGFβR1 in the GS region, inducing protein kinase activity. Active TGFβR1 then phosphorylates Smad2 and Smad3 which form a complex with Smad4 and translocate to the nucleus, where in combination with various DNA-binding co-activators, co-repressors and transcription factors, they regulate expression of TGFβ responsive genes [294]. The Smad canonical signalling is illustrated in **Figure 2** of this thesis' **Publication I**.

Under normal physiological conditions, TGFβ-activated Smad2/3/4 complex induces expression of the cyclin-dependent kinase inhibitor p21, which prevents the ability of cells to progress through the cell cycle, thereby stimulating apoptosis or differentiation. During cancer, however, TGFβ is known to participate in Smad-independent (non-canonical) pathways whereby it initiates EMT, invasion and metastasis [198],. Various TGFβ-Smad-independent signaling pathways include mitogen-activated protein kinase (MAPK), Wnt/β-catenin, PI3K/AKT, RHO/ROCK, Jagged/Notch, and mTOR [198, 241]. TGFβ crosstalk data that I have produced covering various MAPKs and Wnt signaling in CRC has been published (please refer to **Publication I** entitled *"Transforming growth factor-β, MAPK and Wnt signaling interactions in colorectal cancer"*).

1.2.4 Transforming Growth Factor-β and cancer

TGFβ signalling through its unique transmembrane receptor system controls crucial development processes during embryogenesis which are very strictly controlled in adult tissues. Given the regulatory role of TGFβ in normal tissues (growth inhibitor, tumor suppressor), any alteration in TGFβ signalling components could result in tumourigenesis (tumour promoter). Since the majority of cancer cells are genetically unstable they could have the capacity to avoid or adulterate TGFβ's growth suppressive effects. Pathological forms of TGFβ signalling are reported to promote tumour growth and invasion, evasion of immune surveillance, and cancer cell dissemination and metastasis [241]. Due to the dual tumour suppressive and promoter properties of TGFβ during cancer, it has been referred to as a "double-edged sword" by Akhurst and Derynck [295] or as "Janus, the two-faced god" by Salomon [207]. Given its dual role these terms clearly summarise the duality of its nature. How then does TGFβ, a potent tumour-suppressor, so radically deviate from its intended function? The answers could lie in the points of alterations that occur to/in the TGFβ signalling components and the context in which these occur.

1.2.5 Genetic alterations in TGFβ pathway components in CRC

Genetic alterations are key to the development of cancer. Alterations to TGFβ components are commonly observed in cancer cells. These inactivating mutations occur in response to the tumor-suppressive effects exerted by TGFβ-mediated signaling [241]. As a result almost 75% of CRC cell lines are resistant to TGFβ-mediated growth inhibition [296, 297]. The range of genetic alterations of TGFβ signaling components found in CRC are summarized in **Table 8**.

Genetic alterations in TGFβR2 are the most common and is estimated that almost 15-30% of CRCs harbor this mutation [298]. Biallelic inactivation of TGFβR2 by mutations has been observed in CRC and other cancers [299]. Very often these mutations in TGFβR2 are represented as MSI which is a result of mutation in MMR genes [201, 297]. The TGFβR2 coding region contains a 10-base poly-adenine repeat that is prone to replication errors that insert or delete one or more adenines. These poly(A) errors go uncorrected in tumors with MSI that leads to the expression of inactive or mutated receptors. Poly(A) TGFβR2 mutations are often accumulate in sporadic CRC. Alterations in TGFβR1 is often due to frameshift and missense mutations in the coding region. However, the presence of a common polymorphic variant TGFβR1*6A has been shown to increase the risk of CRC and several other cancers [205, 300].

Table 8 Genetic alterations in TGFβ signalling components in CRC.

Protein	Gene name (Locus)	Alteration type in CRC	Frequency (%) reported in the study	Association with CRC	Ref.
LIGANDS					
TGFβ1	*TGFB1* (19q13.1)	Polymorphism			
		-509C>T	46	Not associated with increased rink or progression of CRC	[301]
			Adenoma = 50 CRC = 45	Protective role in development of CRC	[302]
			56	Risk factor for developing colorectal cancer in Asians	[303]
			NS	Decreased risk of CRC susceptibility in Caucasians	[304]
				Possible risk of CRC	[305]
			42	Increased Risk of advanced CRC adenoma	[306]
		-800G>A	NS	Might contribute to increased risk of CRC	[307]
			17	NS	[306]
		Leu 10 Pro	NS	No risk association with CRC adenomatous polyps and may play a protective role in development of CRC hyperplastic polyps	[308]
			NS	Increased Risk of advanced CRC adenoma	[306]
		Overexpression	71	Disease progression to metastasis	[309, 310]
		Overexpression	58	Prognostic marker for a subgroup of patients	[311]
		High serum levels	nd	Disease progression	[204, 312, 313]
RECEPTORS					
TGFβR2	*TGFBR2* (3p22)	Mutation			

		MSI+	61	Better 5-year survival rate	[201]
		MSI+	86	NS	[314]
		MSI-	9	NS	[314]
TGFβR1	*TGFBR1* (9q33-9q34.1)	Polymorphism (TGFBR1*A6)			
		CRC metastases	29.5	May help in cancer cell growth in presence of TGFβ.	[315]
		CRC tumours	2.5	NS	[315]
SMADS					
Smad2	*SMAD2/MADH2* (18q21.1)	Homozygous deletion and intragenic mutation	6-10.3	NS	[202, 316, 317]
		Deletion	64	NS	[318]
Smad3	*SMAD3/MADH3* (15q22.33)	Mutation	NS	Very rarely seen. Associated with inactivation of TGF-β-induced transcriptional activation.	[319-321]
		Mutation	4	Loss of TGFβ-mediated transcriptional activity.	[206]
Smad4	*SMAD4/DPC4* (18q21.1)	Intragenic mutation			
		FAP	11	Carcinoma without distant metastasis	[322]
		HNPCC	11	Primary invasive carcinoma with no distant metastasis	[322]
		Sporadic	15	Carcinoma with distant metastasis	[322]
		Deletion	66	NS	[318]
		Somatic mutation	21	Higher in patients with liver metastasis	[317]

ANTAGONISTS

Smad7	*SMAD7/MADH7* (18q21)	Deletion	48	NS	[318]
		Amplification	10	NS	[318]
		Deletion	43	Better prognosis	[323]
		Amplification	15	Poor prognosis	[323]

Polymorphisms of TGFβ1 have also been associated with CRC neoplasia. Some commonly observed and studied TGFβ1 polymorphisms include -509 C>T, +869 T>C, +915 G > C, -800 G>A, Leu10Pro, Arg25Pro and Thr263Ile [306]. The -509 C>T polymorphism is thought to be present in an YY1 consensus binding site [324] and transfection with a construct containing only the *T* allele enhanced the promoter activity when compared with the *C* allele [325]. The -509T allele has been associated with increased TGFβ1 levels in plasma and is observed in approximately 8% plasma samples [326]. The Leu10Pro and Arg25Pro polymorphisms are thought to encode non-synonymous amino acid substitutions within the signal peptide sequence of TGFB1 precursor. The *10Pro* allele has been associated with elevated TGFβ1 serum levels [327]. Likewise, *in vitro* studies have associated increased TGFβ1 production with the 25Arg allele [328]. The Thr263Ile polymorphism located within the cleaved part of the TGFβ1 pro-protein is thought to affect the activation of TGFβ1 [329]. Despite numerous studies relating to TGFβ1 polymorphisms in other diseases, the most commonly studied in CRC are -509 C>T, +869 T>C, +915 G > C, -800 G>A. Various reports have reported that the -509 C>T allele is associated with decreased risk of CRC [301], [304]. However, there are reports that associate the C allele of -509 C>T and A allele of -800 G>A are associated with increased CRC risk [307] [305]. However, results from these studies are not consistent and further experimental evidence is required to gauge the role of these polymorphisms in CRC [304, 305, 307] .

Smads are crucial for TGFβ-mediated signalling and are known to undergo alterations during cancer. Very often Smad mutations are observed on Smad2 and Smad4 and are a result of allelic loss or loss of heterozygosity that is seen in up to 60% of CRCs. The Smad2 and Smad4 genes are located at chromosome 18q21 which also harbours the tumor suppressor gene DCC (deleted in colorectal cancer).The frequency of mutations of Smad2 and Smad4 in CRC are 6% and 16-25% respectively [298]. Smad4 mutations are also found in 11% of FAP and 11% of HNPCC syndromes [299, 322]. Mutations in Smad 2 occur in the MH1 or MH2 domains of the molecule affecting the phosphorylation, nuclear translocation, and/or decreasing protein stability ultimately disturbing TGFβ signalling. Rare but similar mutations or LOH of Smad3 gene (located on 15q21-q22) have been reported in a human CRC cell line (SNU-769A) [320]. A study using 36 CRC cell lines and 744 primary CRC patient tumor biopsy samples concluded that approximately 4% of them carried mutations in the Smad3 gene [206].

Interestingly, mutations in TGFβ signalling antagonist Smad7 have also been observed. Smad7 along with Smad 6 is a negative regulator of TGFβ signalling. However, the overexpression of Smad7 in the immune cells of colonic mucosa leads to chronic inflammation that predisposes the tissue to becoming cancerous. In fact, study by Boulay *et al*., have shown that the deletion of Smad7 gene has better prognosis than the amplification of Smad7 expression [323]. This suggests that Smad 7 during CRC could act as a promoter instead of an antagonist.

1.2.6 Importance of understanding the role of TGFβ in CRC
TGFβ superfamily of growth factors regulate various pathophysiological aspects including cancer. Particularly TGFβ1, has been reported to have a dual or paradoxical or Jekyll-and-Hyde role in cancer. During the early stages of cancer development TGFβ acts as a potent tumour suppressor by cell growth inhibition and by promoting apoptosis and autophagy. However, in the later stages of cancer TGFβ switches to promoting cell invasion and metastasis. These responses could be a result of TGFβ-mediated and/or the acquisition of mutations in the TGFβ signalling components to escape the growth inhibitory effects exerted by TGFβ. Although these effects have often been observed in many systems exposed to active TGFβ during experiments, the Janus-like nature of TGFβ switching to promoting cancer progression is poorly understood. This dual nature of TGFβ could likely be the product of various interrelations and correlations that simply do not have a single signature and an explanation currently remains elusive. Understanding the TGFβ switch to a tumour-promoting outcome remains an important question that is likely to be answered by exploring the in the less established interactions of TGFβ. These interactions can be studied using a combination of cell signalling and/or proteomic technologies, which are primarily used in this thesis.

1.3 Literature reviews

The manuscripts listed here have reviewed the TGFβ crosstalk with other signalling pathways and the role of β6 integrin in CRC. These reviews incorporate intricate details that contribute to understanding their roles in CRC. The manuscripts have been reproduced with permission of the authors and copyright holders

Review 1: Transforming growth factor-β, MAPK and Wnt signaling interactions in colorectal cancer. *EuPA Open proteomics (2015). In press, Available online 2 July 2015. (doi:10.1016/j.euprot.2015.06.004).* [Publication I]

Transforming growth factor-β, MAPK and Wnt signaling interactions in colorectal cancer

Harish R. Cheruku[a], Abidali Mohamedali[b], David I. Cantor[a], Sock Hwee Tan[c], Edouard C. Nice[d], Mark S. Baker[a,*]

[a] Department of Biomedical Sciences, Faculty of Health and Medical Sciences, Macquarie University, New South Wales 2109, Australia
[b] Faculty of Science, Macquarie University, New South Wales 2109, Australia
[c] National University Heart Centre, National University of Singapore, Singapore
[d] Department of Biochemistry and Molecular Biology, Monash University, Clayton, Victoria 3800, Australia

ABSTRACT

In non-cancerous cells, transforming growth factor-β (TGFβ) regulates cellular responses primarily through Smad signaling. However, during cancer progression (including colorectal) TGFβ promotes tumoral growth via Smad-independent mechanisms and is involved in crosstalk with various pathways like the mitogen-activated protein kinases (MAPK) and Wnt. Crosstalk between these pathways following activation by TGFβ and subsequent downstream signaling activity can be referred to as a crosstalk signaling signature. This review highlights the progress in understanding TGFβ signaling crosstalk involving various MAPK pathway members (e.g., extracellular signal-regulated kinase (Erk) 1/2, Ras, c-Jun N-terminal kinases (JNK) and p38) and the Wnt signaling pathway.

© 2015 The Authors. Published by Elsevier GmbH. This is an open access article under the CC BY-NC-ND license (http://creativecommons.org/licenses/by-nc-nd/4.0/).

1. Introduction

Globally, colorectal cancer (CRC) was the third most commonly diagnosed cancer in 2012 with over 1.36 million new cases (9.7% of all cancers). Then, it led to almost 694,000 deaths (i.e., 8.5% of all cancer deaths) [1]. Australia and New Zealand have one of the highest incidence rates globally (44.8 and 32.2 per 100,000 in men and women respectively), whilst the lowest rates are found in Middle Africa (4.5 and 3.5 respectively per 100,000 in men and women respectively) [1].

Diagnostically, various staging systems have been developed to describe progression of the severity of the disease (e.g., TNM Classification of Malignant Tumours, Australian Clinico-pathological Staging (ACPS) System [2] and Dukes' staging system [3]). These staging tools, usually obtained from patho-histological analyses of CRC biopsies, help clinical oncologists to assess size, location and the spread of the cancerous lesion to other parts of the body and aid in patient treatment and management. Many studies have shown that CRC survival rates primarily dependent on how advanced the cancer

is at initial diagnosis. Despite the availability of numerous screening strategies (Table 1) aggressive surgical therapies and extensive research on the genomic, molecular and cellular basis of CRC, detection at the earliest stages remains elusive.

If detected early, CRC is associated with excellent 5-year survival (>90%) following simple (often curative) surgical resection, while patients diagnosed with later stage cancers (ACPS or Dukes' C or D) experience recurrence and distant metastases leading to particularly poor 5-year survival rates of less than 10% [4]. This progressive decrease in survival rates between early to late stage CRCs (90–10%) has been shown to be associated with the disruption of a number of well-established signaling pathways (Supplementary Table 1). These include, but are not limited to, transforming growth factor-beta (TGFβ)-Smad signaling, mitogen-activated protein kinase (MAPK) signaling pathways and Wnt signaling. This review will briefly discuss TGFβ ligands, their receptors, TGFβ canonical signaling through Smads and will highlight recent findings concerning its role/s in CRC and extensively focusing on the signaling crosstalk of TGFβ with the above-mentioned pathways. TGFβ, or proteins in associated pathways, could be used as early detection biomarkers that may, in the long term, improve survival and management of the global CRC health burden. A list of potential early detection biomarkers for CRC is provided in Table 2.

* Corresponding author at: Faculty of Health and Medical Sciences, 2 Technology Place, Macquarie University, New South Wales 2109, Australia. Fax: +61 2 9850 8313.
E-mail address: mark.baker@mq.edu.au (M.S. Baker).

Table 1
Currently available/emerging CRC screening strategies. ns: not specified.

Test	Sensitivity (%)	Specificity (%)	Frequency	Year developed	Comments	Ref.
Traditional assays						
Colonoscopy	>95	95–99	Every 10 years from age 50	1969	The current gold standard, but invasive, expensive and requires bowel preparation	[5]
Sigmoidoscopy	98–100	35–70	5 years	1976	Only screens the distal colon and rectum	[6]
Double contrast barium enema (DCBE)	45	90	5 years	1920s–1930s	Detects only 30–50% of tumors detected by colonoscopy. Recommended only if endoscopic screening options are not available.	[7]
Computed tomography (CT) colonography	90	86	5 years	1994	Becoming accepted as an alternative to colonoscopy.	[8]
Guaiac fecal occult blood test (GFOBT)	16–38	98–99	Yearly	1967	Detects traces of blood released from bowel cancers or their precursors (polyps or adenomas) into the stool. Results may be affected by consumption of red meat and vitamin C. All positive FOBT tests are often followed up with colonoscopy.	[9]
Fecal immunochemical test (FIT)	56–89	91–98	Yearly	1978	Specific antibodies are used against the globin component of hemoglobin. Unaffected by dietary intake, but the epitope may be destroyed by bacterial enzymes in the stool giving false negatives	[9]
Fecal DNA	52–91	93–97	3 years	2003	Identifies genetic alterations involved in adenoma-carcinoma progression. ColoSure™ test, for example, detects methylation of the vimentin gene, an epigenetic marker.	[10]
Carcinoembryonic antigen (CEA)	43	90	ns	1969	Not suitable for routine detection, but useful for monitoring recurrence.	[11]
Emerging assays						
Colon capsule endoscopy (CCE)	>80	64–95	ns	2006	A non-invasive technique in which a capsule containing a wireless camera is swallowed and transmits images of the inside of the digestive tract to an extracorporeal monitor. Second generation colon capsule endoscopy has a diagnostic sensitivity of 89% or higher to identify polyps >5 mm.	[12,13]
MicroRNA	50–90	>70	ns	2009	miR92 reported as elevated in the plasma of CRC patients compared with controls	[14,15]
Blood RNA (ColonSentry)	72	70	Anytime	2008	Blood-based test which measures the RNA of seven-gene biomarker panel (ANXA3, CLEC4D, LMNB1, PRRG4, TNFAIP6, VNN1 and IL2RB) extracted from peripheral blood cells	[16]
SEPT9	67–96	81–99	ns	2008	Blood-based test which measures the methylated SEPT9 DNA in plasma	[16]

2. TGFβ superfamily ligands

The TGFβ superfamily consists of a large family of secreted cytokines that regulate a multitude of cellular functions and disease pathogenesis. The superfamily is divided into three major subfamilies; TGFβ, activin/inhibin/nodal branches and BMP/GDF (bone morphogenetic proteins/growth differentiation factors), all of whom possess diverse and complementary physiological effects. The TGFβ subfamily members, named for their cell transforming activities (i.e., cell growth and differentiation) from in vitro assays are now unequivocally known to be involved in both tumor suppression and tumor progression (i.e., proliferation, invasion and metastases). Activin and inhibins are well known positive and negative regulators of follicle-stimulating hormone respectively [17]. Nodal along with LEFTY-1 and LEFTY-2 is required for formation of mesoderm and axial patterning during embryonic development [18,19]. The GDF and BMP subfamily proteins have major roles in skeletal development [20], neurogenesis [21], and regulation of ovarian folliculogenesis [22].

The bona fide TGFβ subfamily consists of three TGFβ isoforms, TGFβ1, TGFβ2 and TGFβ3 encoded by three different genes located on different chromosomes (19q13.1, 1q41 and 14q24 respectively) but which are thought to function through the same receptor signaling systems. All TGFβ ligands are produced and secreted in vivo as 'latent' inactive zymogen complexes containing a mature TGFβ dimer in a non-covalent complex with latency associated peptides (LAP) that are bound to their respective latent TGFβ binding proteins [23]. The LAP domain ensures that 'inadvertent' release of TGFβ does not occur in normal cells under normal physiological conditions. Latent TGFβ can be activated in vivo through a variety of mechanisms. These include activation either by proteases (e.g., plasmin) [24] and/or various matrix metalloproteinases (MMP-2 and MMP-9) [25] by cleavage of the LAP. Alternatively, conformational changes in the LAP mediated by integrins αvβ6 [26], αvβ8 [27], and thrombospondin-1 [28] allow the release of active TGFβ1 from its associated LAP. The activation of TGFβ1 by integrin αvβ6 is restricted to epithelial tissues as αvβ6 is only expressed in those cells. Equally, the expression of TSP-1 in some epithelial tissues suggests the possibility that αvβ6 and TSP-1 may operate in tandem to activate latent TGFβ1. A recent study has shown that methylation of the TSP-1 gene results in suppression of TGFβ1 activation in CRC [29]. Integrin αvβ8-mediated activation, however, depends on the presence of MT1-MMP (MMP-14) [27]. It is therefore clear that TGFβ1 can be activated via a number of different mechanisms and in various cellular contexts. These allow it to play an important role in different cellular contexts and functions. As such, it is not surprising that alterations in plasmin or plasminogen binding [30] and alterations in expression of MMP-2 and MMP-9 [31], integrin αvβ6 [32] and active TGFβ1 [33] have been found collectively to be associated with poor CRC prognosis and subsequently poor survival.

3. TGFβ receptors

The TGFβ receptors were identified by methods involving affinity labeling of cells with radio-iodinated TGFβ (^{125}I-TGFβ) ligand and subsequent mapping of receptors to which this bound. Three different receptors, namely type I (53 kDa), type II (73–95 kDa) and type III (110 kDa) were identified depending on their molecular weights [58]. The type I and type II receptors were found to contain serine/threonine kinase domains and activity,

Table 2
Potential early detection biomarkers for CRC. nd: not determined.[a]

Candidate biomarker	Sample type	Mechanism of identification	Can discriminate	Sensitivity (%)	Specificity (%)	Ref
Individual biomarkers						
Alpha 1-antitrypsin	Serum	Protein expression levels		87	73	[34]
Amphiregulin	Blood/serum	Protein expression levels	Controls from Dukes' A CRC	nd	nd	[35]
CEA	Blood/serum	Protein expression levels	Controls from Dukes' A–D stage CRCs	53	93	[34–37]
CXCL11	Blood/serum	Protein expression levels	Controls from Dukes' A CRC	nd	nd	[35]
CXCL5	Blood/serum	Protein expression levels	Controls from Dukes' A CRC	nd	nd	[35,38]
IL6	Blood/serum	Protein expression levels		27	95	[35]
IL8	Blood/serum	Protein, mRNA expression levels	Controls from Dukes' A CRC	30	95	[35,39]
Methylated Septin 9 (SEPT9)	Blood	DNA methylation		67–96	81–99	[40–44]
MMP7	Serum	mRNA expression levels		58	100	[34]
Suppressor of cytokine signalling (SOCS)2 and SOCS6	Tumors	Protein expression levels		nd	nd	[45]
uPAR	Serum	mRNA expression levels		nd	nd	[34]
Collagen type X alpha1 (CPL10A1)	Serum	Protein expression levels	Controls from Adenoma and colon cancer	63	85	[46]
Metastasis associated in colon cancer 1 (MACC1)	Tumor samples	Protein expression levels		nd	nd	[47]
Biomarker panels						
Tumor associated monocyte genetic finger print	Blood monocyte samples	Gene expression		92.6	92.3	[48]
IGFBP2, DKK3 and PKM2	Blood	Protein expression levels		73	95	[49]
BMP3, NDRG4, VIM, TFPI2 and a mutant KRAS	Stool	DNA methylation	Cancer from controls	68–86	77–92	[50–53]
			Adenoma (size >1 cm) to controls	52–73	85–92	
			Adenoma (size >1 cm) to controls	45–62	85–92	
miR-19a-3p, miR-223-3p, miR-92a-3p and miR-422a	Serum	mRNA expression levels		84.3	91.6	[54]
miR-601 and miR-760	Plasma	mRNA expression levels	CRC to normal controls	83.3	69.1	[55]
			Adenomas to normal controls	72.1	62.1	[55]
miR-532-3p, miR-331, miR-195, miR-17, miR-142-3p, miR-15b, miR-532, and miR-652	Plasma	mRNA expression levels	Polyps from controls	88	64	[56]

[a] The data presented in this table only summarises biomarkers from research published in the last 5–6 years. For a more detailed review on this topic please see "Biomarkers for Early detection of Colorectal Cancer and Polyps: Systematic Review" by Shah et al. [57].

whilst the type III receptors lacked any similar domain [59]. The detailed structure of these three receptors is illustrated in Fig. 1.

3.1. TGFβ type III receptors

The transforming growth factor type III receptor (TGFβR3) betaglycan is the most ubiquitously expressed type III receptor. Betaglycan acts as an accessory receptor by presenting TGFβ ligands to the type II receptors and promoting signaling [60]. The short cytoplasmic tail of betaglycan consists of a class I PDZ binding motif that binds to GAIP-interacting protein C-terminus (GIPC). GIPC interaction with betaglycan increases the stability of betaglycan at the cell surface and promotes TGFβ1 and TGFβ2 mediated gene expression in Mv1Lu mink lung epithelial and L6 myoblast cells [61]. More recently the GIPC-betaglycan interaction has been shown to inhibit TGFβ-mediated Smad signaling and migration in breast cancer cells. However, the exact mechanism/s by which this occurs has yet to be characterized [62].

3.2. TGFβ type II receptor

Transforming growth factor type II receptor (TGFβR2) is a transmembrane serine/threonine kinase receptor with a signal peptide, a cysteine-rich N-glycosylated extracellular domain, a transmembrane domain, and a cytoplasmic serine/threonine kinase domain flanked by a short juxtamembrane domain and C-terminal tail [63]. TGFβR2 can bind to all three TGFβ ligands, but cannot participate in downstream signaling in the absence of TGFβR1. The presence of betaglycan is also essential to facilitate high affinity TGFβ binding to TGFβR2 which then participates in downstream signaling. As yet, only TGFβs are known to bind to TGFβR2 in any extracellular context.

3.3. TGFβ type I receptor

Transforming growth factor type I receptor (TGFβR1) is also a transmembrane serine/threonine kinase receptor and closely resembles TGFβR2 in structure. TGFβR1 contains a signal peptide,
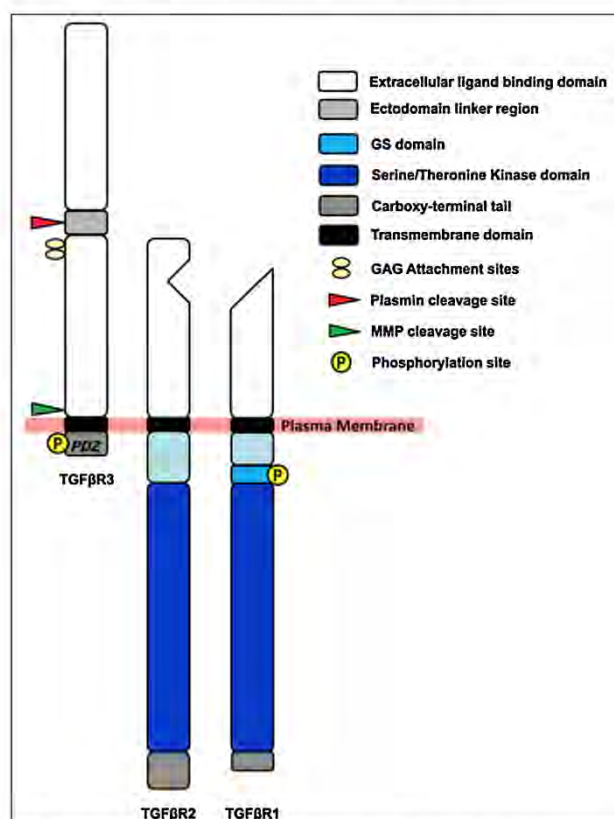
Fig. 1. Structure of TGFβ receptors type I (TGFβR1), type II (TGFβR 2) and type III (TGFβR3).

a cysteine-rich N-glycosylated extracellular domain, a cytoplasmic kinase region with 41% sequence homology to TGFβR2 and a very short C-terminal tail [64]. A unique feature of TGFβR1 is its highly conserved 30 amino acid region preceding the cytoplasmic kinase region that is called the GS domain because of the characteristic SGSGSG sequence it contains. Ligand-induced phosphorylation of serine and/or threonine residues in the GS region is required for signaling. TGFβR1 forms a heterodimer with TGFβR2 and this complex collectively takes part in TGFβ-mediated downstream signaling [64].

4. Canonical signaling of TGFβ receptors through Smads

Intracellular TGFβ signaling is complex and affects various cellular functions, both directly and indirectly. A well-character-ized signaling pathway that is initiated by active heterodimeric TGFβ receptors is through Smads, although Smad-independent TGFβ signaling pathways are also known to exist [65]. TGFβ signaling via Smads is facilitated by TGFβR1 and TGFβR2, which form both homodimeric and heterodimeric complexes required for signaling. Dysfunction in one or more components of the functional TGFβ complex has been associated with cancers (including CRC) and these are briefly discussed later in this review.

Canonical Smad signaling (Fig. 2) is initiated by preferential binding of active TGFβ1 to TGFβR2 that then recruits, binds and transphosphorylates TGFβR1 in the GS region, inducing protein kinase activity. Active TGFβR1 then phosphorylates Smad2 and Smad3 which form a complex with Smad4 and translocate to the nucleus, where in combination with various DNA-binding co-activators, co-repressors and transcription factors, they regulate expression of TGFβ responsive genes [66]. The Smad2/3/4 complex induces expression of the cyclin-dependent kinase inhibitor p21, which then leads to cell growth arrest. Puzzlingly, Smad4 can only translocate into the nucleus when bound to receptor Smads (Smad1/2/3/5/8) whilst Smad2 and Smad3 can translocate into the nucleus in a Smad4-independent manner [67] implying a regulatory role for Smad4 rather than a simple signal transmission from cytoplasm to nucleus. Studies on various tumor cells suggest that TGFβ-mediated cell migration is not always dependent on Smad signaling, but also the activation of various mitogen-activated protein kinases (MAPK) and Rho GTPases that can be activated by non-canonical Wnt signaling pathways.

5. Non-canonical signaling of TGFβ receptors

Increasing evidence over the past few years has revealed that the complexity of TGFβ signaling responses is influenced not only

51
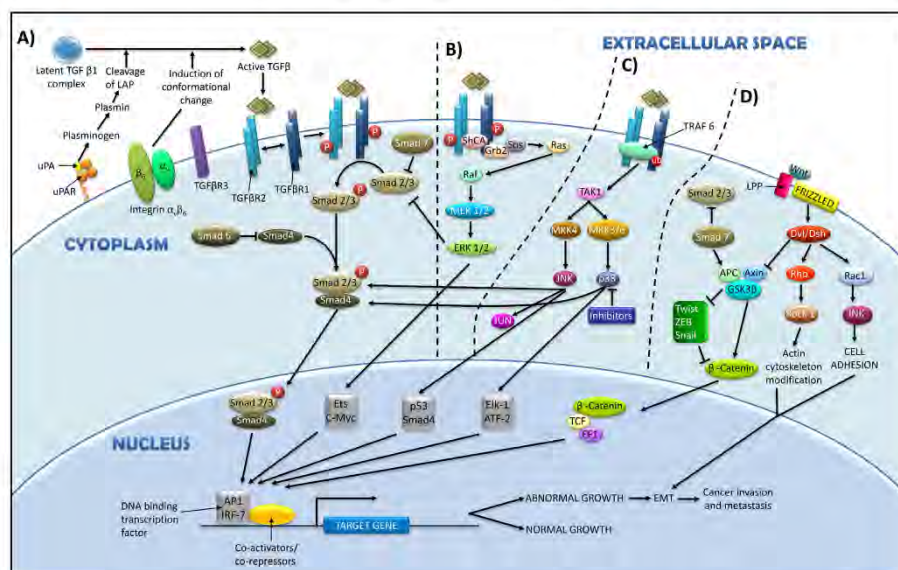
Fig. 2. Outlines the (A) Smad dependent TGFβ pathway. Latent TGFβ is activated through cleavage of LAP by plasmin or by conformational change induced by integrin αvβ6. TGFβR3 presents the active TGFβ to phosphorylated TGFβR2 which recruits, binds and phosphorylates TGFβR1. The active TGFβR1 phosphorylates Smad2 and Smad3. Active Smad2 and Smad3 form a complex with Smad 4 (Smad2/3/4) and translocate into the nucleus, where in combination with various DNA-binding co-activators, co-repressors and transcription factors regulate the expression of TGFβ target genes. Smad6 can inhibit the formation of Smad2/3/4 complex and Smad7 can inhibit the Smad2/3 interaction with TGFβR1 thereby preventing TGFβ associated Smad signaling. (B) Ras/Erk non-Smad pathway. The phosphorylated TGFβR1 and TGFβR2 recruit and phosphorylate ShcA which associated with Grb2/Sos to activate Erk through Ras, Raf and MEK1/2. Erk then regulates downstream transcription factors to control the EMT. (C) JNK/p38 non-Smad pathway. TGFβ receptors interact with polyubiquitinated TRAF6 which recruit TAK1 to activate JNK and p38 pathways via MKK4 and MKK3/6 respectively. Active JNK/p38 then regulate the EMT by controlling the downstream transcription factors. (D) Wnt pathway interactions. Smad7 and APC-Axin-GSKb3 complex interact which other to either enhance or suppress the activity of Smads. The APC-Axin-GSKβ3 complex can activate β-catenin and blocks its inhibitors Twist, Zeb and Snail. Dvl/Dsh can control two important criteria for the EMT—actin cytoskeletal modifications and cell adhesion through activation of Rho and Rac1 pathways. Rac1 then activates JNK pathway to further contribute to the EMT.

by core pathway components including ligands, receptors, Smads and Smad-dependent transcription factors, but also by the ability of TGFβ receptors to activate other Smad-independent (i.e., non-canonical) pathways through crosstalk resulting in downstream cellular responses. The mechanisms of crosstalk include, but are not restricted to, regulation of co-activators and co-repressors recruited during the process of transcription, regulation of receptor Smads activity through the mitogen-activated protein kinase (MAPK) pathway, regulation of inhibitory (I)-Smads (Smad6,7) expression and other interactions that could activate or inhibit certain molecules in the pathways [68]. A few pathways associated with TGFβ signaling crosstalk in CRC and other cancers include, but are not limited to, MAPK pathways [69] like extracellular signal-regulated kinase (Erk) 1/2 [70], Ras [70], p38 MAPK and c-Jun N-terminal kinases (JNKs), phosphoinositol-3-kinase (PI3K), protein phosphatase 2A (PP2A), Wnt [71] and RhoA [72]. This review specifically focuses on MAPK and Wnt signaling pathways.

5.1. Mitogen-activated protein kinase (MAPK) cascades

The MAPK cascades are key membrane-to-nucleus signaling modules that respond to various stimuli resulting in the phosphorylation and activation of transcription factors required for gene expression [69]. Downstream activation of distinct MAPK pathways of Erk1/2, stress-activated protein kinases (SAPK)/JNK, Ras and p38 MAPK can be regulated by TGFβ1 in either a slow or a rapid manner. Slow activation (~15 min) of these pathways is

mediated by Smad-dependent responses whilst the rapid activation is thought to be mediated by Smad-independent responses [73]. It has been shown that TGFβ has the potential to rapidly (within 3–6 min) activate Erk and Ras MAPK pathways [74]. Rapid activation of Ras by TGFβ in epithelial cells resulted in increased activity of TGFβ-induced Erk MAPK signaling leading to increased invasion and metastasis [74]. The aberrant activation of MAPK pathways by TGFβ may therefore play a key role in diverting the TGFβ response towards pro-oncogenic outcomes by promoting invasion and metastasis in CRC.

5.1.1. Erk MAPK pathway

The Erk 1/2 pathway is traditionally known to promote cell growth and survival [75], but under certain conditions it can have a pro-apoptotic effects. The Erk pathway is dysregulated in one-third of all human cancers [76] and is involved in pathogenesis, disease progression, and oncogenic behavior [77,78]. During late tumourigenesis, the activation of both Erk and Ras pathways is required for TGFβ-induced epithelial mesenchymal transition (EMT) leading to cancer progression [79,80].

The Erk/MAPK signaling cascade can be activated by a wide range of effectors including peptide growth factors involved in cell growth and differentiation and integrins [81,82]. Rapid activation of Erk mediated by TGFβ has been observed in epithelial cells, breast cancer cells and fibroblasts [83]. Smad-dependent delayed activation of Erk by TGFβ is partly accounted for, but does not completely explain the rapid activation of Erk (within 3–6 min) by

TGFβ [65]. There is evidence that TGFβR1 directly participates in the activation of Erk by recruiting and phosphorylating Src Homology 2 Domain-Containing) Transforming Protein 1 (ShcA) on its serine and tyrosine residues. The phosphorylated ShcA then associates with TGFβR1 via its phosphotyrosine-binding domain and recruits growth factor receptor binding protein 2 (Grb2) and Sos proteins, leading to activation of Erk and Ras MAPK pathways [84,85] (Fig. 2). Erk and Ras then regulate target gene transcription through their downstream transcription factors and Smads to control the EMT [84].

Treatment of TGFβ-sensitive (Hs578T) and TGFβ-responsive (MDA-MB-231) breast cancer cells with TGFβ resulted in different levels of phosphorylation of Erk 2 downstream to Erk 1. TGFβ-sensitive cells showed a significant increase in phosphorylation within 5 min of treatment as compared to the TGFβ-responsive cells, suggesting that the kinetics of Erk phosphorylation induced by TGFβ may vary with cell type and/or physiological state of the cell [83]. Interestingly, a recent study by Hough et al. [86] demonstrated that TGFβR-mediated Erk phosphorylation can be cell type specific, occurring in phenotypically normal mesenchymal cells but not in the epithelial cell phenotype. This could help to explain the dysregulated activation of Erk by TGFβ observed in epithelial cancers as they are at various stages of the epithelial–mesenchymal transition. The TGFβ-mediated phosphorylation of Erk, however, was inhibited when a specific PI3K-inhibitor, LY294002, was added. Similar inhibition was observed with the use of the MEK1/2 inhibitor U0126, suggesting that both MEK1/2 and PI3K are required for TGFβ-mediated Erk activation [86]. Hough et al. then applied small molecule inhibitors to observe their effect on the activation of the downstream PI3K-activated pathways, Akt and Erk. They found that both pathways were activated through TGFβ by PI3K, though only Erk phosphorylation was sensitive (understandably) to inhibition by the MEK1/2 inhibitor U0126 [86]. Hough et al. also proposed that TGFβ-mediated Erk phosphorylation primarily follows the PI3K/Pak2/c-Raf/MEK/Erk pathway, supported by a secondary contribution from Ras, although at a greatly reduced level. Furthermore, Erk is known to phosphorylate serine or threonine residues in the PX(S/T)P or (S/T)P motif of the linker regions in receptor Smads (Smad1,2,3,5,8) which cannot migrate into the nucleus, thus inhibiting TGFβ-Smad signaling [87]. Phosphorylation of the Smad2 linker region was found to be dependent on MEK activation, which could be increased with the rapid activation of Erk by epidermal growth factor (EGF), highlighting a direct functional connection between Erk and the Smad pathway [86]. Erk induced phosphorylation of the linker region of nuclear Smads and increased the duration of Smad-targeted gene transcription by extending the half-life of C-terminal pSmad2/3 (Ser465/467). A thymidine incorporation assay examining the biological consequences of TGFβ-mediated activation of Erk, showed a 6-fold increase in DNA synthesis with TGFβ treatment that was attenuated with MEK1/2 inhibition [86].

The TGFβRs also play an important role in the Erk-TGFβ crosstalk. Primarily, the expression levels and the ratio of TGFβR2/TGFβR1 hetero-oligomers contribute to different downstream signaling modules [88]. Bandyopadhyay et al. have established that dermal cells with high TGFβR2 expression selectively activate Erk1/2 [89]. In contrast, epidermal cells with high TGFβR1 expression favor canonical TGFβR1-Smad signaling and do not activate Erk. These two findings highlight the influence of TGFβR expression on TGFβ-mediated Erk signaling. In the context of cancer, the crosstalk between Erk, TGFβRs and Smads has been shown to directly and indirectly promote cancer growth in the early stages of cancer resulting in metastasis [90–92]. It is also important to note the tyrosine kinase activity of TGFβR1 as well as its serine/threonine kinase activity could be a key to understand the broad spectrum of TGFβR associated signaling in cancer progression.

5.1.2. Ras MAPK signaling

The Ras proteins play a key role in regulating several aspects of both normal cell growth and malignant transformation in cancer signaling. The Ras pathway is deregulated in up to about 30% of tumors [93]. Chaiyapan et al. reported that mutation of K-Ras oncogene occurred in 25–35% of CRCs at early stages of progression [94]. Abnormal activation of Ras leads to increased proliferation and reduced apoptosis, promoting progression. Similar to Erk, TGFβ-mediated activation of Ras occurs through the ShcA/Grb2/Sos complex as described earlier [84] (Fig. 2). The rapid activation of Ras, within (3–6 min) by TGFβ1 and TGFβ2 during CRC tumourigenesis causes an imbalance between Erk and JNK [74]. Ras family proteins are also known to contribute to this imbalance by suppressing JNK activation through active K-Ras or by enhancing Erk activation through H-Ras [95]. Hartsough et al. have shown that Ras activation is required for TGFβ-mediated Erk1 activation and partially required for growth inhibitory effects [96]. TGFβ growth inhibitory responses in prostate cancer and CRC cells are transmuted to Smad-independent mitogenic responses in the presence of active Ha-Ras and Ki-Ras [97,98], whereby active Ras can induce and enhance the expression of TGFβ1, which explains the frequently observed high levels of active TGFβ1 during cancer [99].

It is known that most TGFβ responses are dependent on cellular context partly due to Smad interactions with cell type specific transcription factors. For instance, active Smad3 co-occupies the genome with Oct4 in human embryonic stem cells, Myod1 in myotubes and PU.1 in pro-B cells [100]. The association between Smad2/3 and transcriptional cofactors can be regulated by the Ras MAPK pathway. Smad2/3 and tumor suppressor protein p53 can directly interact and together regulate several TGFβ target genes. Overexpression of p53 in *Xenopus* animal cap cells showed increased cooperation between endogenous Smads to induce mesoderm markers [101]. This cooperation was lost when the animal cap cells were treated with fibroblast growth factor (FGF)-receptor inhibitor SU5402, indicating a relationship between p53 and FGF. Treatment with FGF efficiently promoted association of p53 and TGFβ-activated Smad2 [101]. In this mechanism, FGF signals through Ras to regulate phosphorylation of p53 at its N-terminus, which then interacts with activated Smad2/3 to regulate TGFβ-mediated tumor suppression [101]. SW480.7 colon cancer cells deficient in Smad4 having hyperactive Ras signaling do not show TGFβ-mediated antiproliferative responses, as hyperactive Ras inhibits the function of Smad2/3 by phosphorylating them on their linker regions [102]

During their study of mammary epithelial cells, Oft et al. showed that Ras and TGFβ1 are required to work in collaboration to transform benign epithelial cells to induce invasive and metastatic phenotypes [103]. Results from a recent study by Kim et al., clearly support this outcome, demonstrating that Ras expression promoted mesenchymal morphology. Employing normal MCF-10A cells and MCF-10A/Hras cells which express pro-oncogenic H-Ras, they showed increased invasive potential with TGFβ treatment that was exacerbated when H-Ras was expressed [104]. RT-PCR analysis showed that leukotriene B_4 receptor-2 (BLT2) expression was increased by H-Ras, and the treatment with BLT2 inhibitor LY255283 or depletion of BLT2 using a BLT2-specific small interfering RNA (siBLT2) greatly reduced the morphological alterations and invasiveness of MCF-10A/Hras cells in response to TGFβ treatment. The induction of BLT2 expression in MCF-10A cells showed a marked increase in invasiveness upon TGFβ treatment. This study clearly shows that Ras controls the

expression of BLT2, which responds to TGFβ treatment to promote the adoption of the mesenchymal phenotype and invasion [104].

Various studies have shown that TGFβ and Ras cooperate to induce invasion. In the intestinal epithelium, the loss/inactivation of TGFβR2 or expression of Kras alone did not result in neoplasia. However, the combination of both lead to colorectal neoplasms and eventual metastasis which were mediated through EGF [105]. Loss of Smad4 and the presence of oncogenic K-Ras can also induce expression of MMP9 and urokinase plasminogen activator (uPA), through the EGFR/NF-κB pathway, which contributes to the invasive phenotype of cancer cells through activedegradation of the extracellular matrix (ECM), liberating the cells from cell–cell interactions and enabling extravasation from the primary site [106].

In summary, there is growing evidence of crosstalk between Ras and TGFβ pathways at various levels in cell signaling cascades leading to varying outcomes that can manipulate the EMT and promote metastatic phenotypes.

5.1.3. JNK MAPK pathway

The c-Jun N-terminal kinase (JNK) cascade regulates various transcription and non-transcription factors in response to external stimuli and has been implicated in several biological processes including cell proliferation, apoptosis and tumor development. The TGFβ system has the ability to autoregulate its own expression via the JNK pathway making it an important pathway in cancer development. TGFβ treatment rapidly increased JNK activity (within 5–10 min) and induced up-regulation of urokinase plasminogen activator receptor (uPAR) by increasing the protein--DNA complex formation at the distal Activator Protein-1 (AP-1) site in the uPAR promoter region [107]. TGFβ, however, did not affect JNK protein expression [107]. As TGFβ can activate Ras within 3–6 min of TGFβ treatment, it is conceivable Ras may be required for TGFβ-mediated JNK activation.

JNKs, like Erk, are a third layer of MAPK cascade activated by upstream MKKs—MKK4 and MKK7. The rapid Smad-independent activation of JNK through TGFβ is achieved specifically through MKK4–TGFβ-activated kinase 1 (TAK1) axis [108,109]. Further upstream, tumor necrosis factor-receptor-associated factor 6 (TRAF6) associates with TGFβR2 and TGFβR1 through its c-terminal TRAF domain to activate TAK1 in a receptor kinase-independent manner. Yue et al. also reported that TGFβR2 is required for TGFβ-mediated activation of JNK which is required for up-regulation of uPARs, suggesting a complex crosstalk between these pathways [107]. Initially, it was thought that TRAF6 can only directly interact with TGFβR2. However, the activation of TGFβR2 occurs upon homodimer formation and TGFβR1 is activated by TGFβR2. This suggests that TRAF6 binds to either the active homodimer of TGFβR2 or the hetero-complex of TGFβR2 and TGFβR1 [108]. Furthermore, TGFβR1 has a TRAF6 binding motif (basic residue-X-P-X-E-X-X-aromatic/acidic residue) and the TGFβR1–TRAF6 interaction is required for TRAF6 autoubiquitylation and subsequent activation of JNK/p38 pathways via TAK1 [109]. TRAF6 with the help of TGFβ induces Lys63-linked polyubiquitination of TGFβR1, which promotes cleavage of the intracellular domain (ICD) of TGFβR1 by TNF-alpha converting enzyme, in a PKCζ-dependent manner [110]. The ICD of TGFβR1 can then translocate into the nucleus, where in association with transcriptional regulator p300 it promotes invasion by inducing the expression of *Snail,MMP2* and *p300* genes [111].

The TRAF6–TAK1–JNK cascade, in conjunction with the Smads, is known to regulate TGFβ-mediated apoptosis and EMT [109,112] suggesting a close link between these cellular responses. Yamashita et al. showed that TRAF6 and TGFβ-mediated apoptosis and EMT were abrogated when TRAF6 expression was knocked

down [108]. A similar effect was observed with knock down of Smad3 expression. Interestingly, TAK1 also mediates TGFβ-induced signaling by phosphorylating the Smad3 linker region (pSmad3L), a feature that is also observed in CRC [113]. pSmad3L can translocate into the nucleus and regulate gene expression to mediate the development of an invasive phenotype of cancer. TGFβ can also activate JNK as part of an accessory pathway, as shown by Ventura et al., who demonstrated that JNK-deficient fibroblasts caused a significant increase in expression of TGFβ1 and TGFβR1 and decreased the expression of TGFβR2 and I-Smads [114], suggesting that JNK deficiency may cause autocrine signaling of TGFβ through a positive feedback loop. Freudlsperger et al. [115] have shown that Smad7 and TAK1 mediate TGFβ and nuclear factor-κB (NF-κB) crosstalk in head and neck cancers. TAK1 further enhances the activation of NF-κB through TGFβ. Treatment of head and neck squamous cell carcinoma (HNSCC) lines with TGFβ1 induced the phosphorylation of TAK1 along with NF-κB family member RELA (p65). RELA and TGFβ activation induced Smad7 expression that preferentially suppressed TGFβ-induced Smad and NF-κB reporters leading to malignant phenotype in HNSCC [115]. Additionally, the ability of Smad7 to interact with TGFβR1 using two modes—a three-finger-like structure in the MH2 domain and a basic groove in the MH2 domain, in contrast to only one mode for Smad6, the other I-Smad [116], suggests a dual role for Smad7: inhibition of TGFβ-Smad signaling and promotion of TGFβ-induced activation of JNK and p38 MAPK pathways.

The cooperation of Erk and JNK has been shown to jointly increase the expression of a key late stage molecule, fascin1 in gastric cancer, which promoted TGFβ-mediated invasion and metastasis [91]. Fascin1 expression was ablated by ≥75% when treated with the JNK and Erk specific inhibitors, SP6001125 or PD98059 respectively [91]. In addition to gastric cancer, a recent study by Herbest et al. reported increased fascin1 expression in late stage CRC was induced by β-catenin, an integral member of the Wnt signaling pathway, that has been associated with TGFβ-mediated crosstalk during cancer [117].

5.1.4. p38 MAPK pathway

The p38 MAPK pathway is often activated by various stress responses such as heat shock, osmotic shock and hypoxia leading to diverse roles in cell proliferation, differentiation, survival and migration in different cell types. It is unsurprising, therefore, that p38 MAPKs have been implicated in cancer development [78]. p38 signaling is required for cell migration and metastasis in both CRC and breast cancer [118,119]. As for JNKs, p38 MAPKs are activated by MKKs through autophosphorylation: specifically by MKK3 and MKK6 and sometimes by MKK4 [108,109]. Rapid Smad-independent activation of p38 MAPKs is achieved through a TAK1 and TRAF6 module [108,109] (Fig. 2). Knockdown of TRAF6 inhibited TGFβ-mediated EMT [108]. TGFβ-induced activation of TRAF6-TAK1-JNK/p38 pathways has been implicated in cell death, cell proliferation and EMT [110]. In breast cancer, ubiquitin-conjugating enzyme Ubc13 was shown to control metastasis through the TAK1-p38 MAPK pathway by activation of MEKK1 and TAK1 [119]. Silencing of Ubc13 resulted in decreased TAK1 phosphorylation, and the silencing of TAK1 or p38α resulted in a dramatic decrease of lung metastasis in a mouse model [119]. Wu et al. also showed that the using the p38 inhibitor, SB203580, resulted in decreased metastasis indicating that p38 inhibitors can be used as potential treatment for established breast cancers [119]. Safina et al. using MDA-MD-231 breast cancer cells, have showed that TGFβ-mediated TAK1 regulates MMP9 expression which involves NF-κB signaling, similar to K-Ras. The TAK1-NF-κB-MMP9 pathway as a whole, contributes to TGFβ-mediated metastasis [120]. p38 is also known to regulate cell invasion

through up regulation of MMP2 in prostate cancer [110,121]. The blockade of p38 MAPK activity using specific inhibitors, or by genetic alterations or cancer therapies like 5-fluorouracil, leads to cell cycle recovery and induction of autophagic cell death [118,122].

Activation of Smads is an important cellular response for TGFβRs. Cells with mutated TGFβR1 that are defective in Smad activation showed an increase in p38 MAPK signaling response to TGFβ1, but did not induce EMT [123]. However, cells lacking the cytoplasmic domain of TGFβR2 did not block TGFβ-mediated p38 MAPK activation, resulting in integrin αvβ1 mediated EMT [124]. This confirms that TGFβR2 is important for TGFβ-mediated EMT through the p38 MAPK cascade. The phosphorylation of TGFβR2 tyrosine (Tyr248) in the cytoplasmic domain by Src recruits Grb2 and Shc to TGFβR2, which associates these adapter proteins with p38 MAPK activation [125]. Galliher-Beckley and Schiemann also showed that Grb2 binding to Tyr248 of TGFβR2 is required for TGFβ-mediated mammary tumor growth and metastasis [126]. Northey et al. showed that ShcA expression and phosphotyrosine-dependent signaling are essential for TGFβ-mediated cell motility and invasion [127]. Galliher-Beckley and Schiemann, and Northey et al. also showed that loss, or reduced expression, of ShcA and/or Grb2, or mutations in their phosphorylation sites, no longer promoted TGFβ-mediated migration, invasion, or EMT [126,127]. Rather than the "standard" TGFβ-mediated activation of p38 through MKK3 and MKK6, the possible phosphorylation of TGFβR2 at Tyr248 has the potential to drive Shc and Grb2 through an alternative pathway that is required for TGFβ-mediated tumor growth and metastasis. This secondary activation of p38 through a pathway that would normally activate Erk/JNK compounds the complexity of TGFβ crosstalk with MAPK pathways in cancer.

5.2. Wnt signaling cascade

Along with numerous other transcriptional regulators such as the fibroblast growth factors (FGF) and Forkhead transcription factor families, the interplay between Wnt and TGFβ signaling is a feature of gut development and endoderm formation [128]. More recently, genome-wide association studies have found that both the Wnt and TGFβ pathways are active in lung cancer [129] and breast cancer cells [130]. It has previously been proposed that crosstalk between the Wnt and TGFβ pathways may be more extensive than suggested, especially in the context of malignancy and/or the EMT [128]. This crosstalk may be occurring at several points along the network, notably in the migration of cells as witnessed in cancer and also fibrosis [131,132].

Several studies have demonstrated the role of Smads, with initial studies on homeobox gene promoters showing that TGFβ mimics the effects of Wnt signaling on β-catenin, leading to cell cycle arrest through interactions with Smad7 [133]. Axin, a negative regulator of Wnt signaling has also been shown to interact with Smad3 as a putative adaptor, enhancing the efficiency of TGFβ signaling [134]. Wnt and FGF regulate the phosphorylation of the Smad4 linker region through glycogen synthase kinase-3 (GSK3) in the canonical MAPK/Erk site (PxTP) [128]. This phosphorylation event did not occur when HaCaT immortalized, human keratinocyte cells were treated with the MEK-specific inhibitor U0126, demonstrating the requirement of MAPK activity for GSK3-induced Smad4 phosphorylation [128]. MAPK/FGF and Wnt/ GSK3 mediated phosphorylation is required for the polyubiquitination and degradation of Smad4 through E3 ligase β-TrCP [128,135,136]. As stated by Demagny et al., the MAPK/Erk and GSK3 trigger the formation of a phosphodegron bound by the E3 ligase β-TrCP, resulting in the polyubiquitination of Smad4. Demagny et al. also showed that treatment of cells expressing the TGFβ-specific reporter CAGA12-luciferase with Wnt3a or

FGF2 alone did not affect TGFβ signaling activity. However, the addition of both increased TGFβ signaling activity, indicating the involvement of GSK3 [128]. This demonstrates that FGF is also required for TGFβ and Wnt crosstalk which is enhanced by activation of MAPK signaling. It is important to note that another study reported that TGFβ suppresses β-catenin/Wnt signaling and enhances cell adhesion in CRC in a Smad4-independent manner [132]. A similar study to that of Demangy et al., reported the ability of TGFβ to promote the EMT and invasion in a p38 MAPK/β-catenin/peroxisome proliferator-activated receptor γ-dependent manner in non-small cell lung cancers [137].

Numerous canonical and non-canonical Wnt signaling proteins have also been shown to act as co-factors of TGFβ signaling, including, but not limited to, Snail, Twist, β-catenin and AP-1 by either activating or suppressing the activity of various Smads (for a comprehensive review refer to [138]). These interactions have not been directly observed in CRC, though this crucial link may bridge the gap between these two signaling pathways (i.e., that of Notch, Wnt, and TGFβ/Activin signaling) which is in part mediated by the interactions of Dll1 with Smad2/3 and Tcf4 at the promoter sites [139]. A further point of interaction between the Wnt and TGFβ signaling pathways involves the regulation of the same genes independently or cooperatively. Both regulate Lef1/Tcf, which are canonical proteins involved in the EMT [140]; gastrin, a promoter of gastrointestinal cancers [141]; BAMBI, the pseudoreceptor involved in TGFβ signaling regulation in CRC [142]; and importantly Snail1 and Snail2, both of which are acknowledged as key switches that initiate the EMT in cells, and have been implicated in CRC [143–146]. Other canonical Wnt signaling molecules such as Twist and KLF8 have also been shown to be regulated by TGFβ [138].

Several other proteins involved in Wnt and TGFβ signaling have been shown to be perturbed in CRC cell lines and tissues, including Pitx2 [147], a homeodomain transcription factor, and ECM transition remodeling proteins such as heparin-degrading endosulfatases, sulfatase 1 (SULF1) and sulfatase 2 (SULF2). Recent studies have shown that FOXQ1, a member of the forkhead transcription factor family, can promote TGFβ expression and the EMT through crosstalk between the Wnt and TGFβ signaling pathways [71,148]. Fan et al. [148] showed that silencing FOXQ1 decreased cell migration and invasion which was supported by Peng et al. [71]. Interestingly, treating the cells with TGFβ1 increased FOXQ1 gene expression resulting in TGFβ-mediated the EMT within 4-days, that was suppressed upon silencing FOXQ1 expression [148]. A similar outcome was reported by Peng et al. wherein treatment of CRC cells with TGFβ1 increased FOXQ1 expression and promoted migration and invasive potential. They also demonstrated that FOXQ1 suppression by siRNA decreased the invasive and angiogenic potential and resistance to chemotherapy drugs. Peng et al. further showed that FOXQ1 is overexpressed in CRC tissues and correlates with CRC stage [71]. Indeed, other recent studies further support the fact that overexpression of FOXQ1 induces the EMT in various cancers [149–151] and has been shown to be a direct Wnt target in CRC [152].

The overall picture regarding Wnt and TGFβ signaling is that of a highly interconnected system of activators and repressors that serve to maintain cell proliferation and migration. The details of the Wnt and TGFβ pathways continue to be elucidated, with novel players such as FOXQ1 continually changing the models of potential crosstalk between these two pathways. Suffice it to say that in cancers, particularly CRC, the involvement of both these pathways is crucial not only for ECM degradation but also for metastasis as evidenced by the involvement of APC in over 60% of loss of heterozygosity (LOH) positive CRC cases [153,154]. A detailed analysis of this crosstalk system is beyond the scope of this

current review. However, there is extensive evidence indicating that such crosstalk strongly influences the EMT and metastasis.

6. Genetic alterations in TGFβ signaling components

Various intracellular signaling pathways, including the ones described above, are frequently dysregulated in CRC. Almost 75% of CRC cell lines are resistant to TGFβ-mediated growth inhibition due to the loss or mutation of one or more components of the TGFβ signaling pathway [155,156]. A detailed review of the genetic alterations of TGFβ signaling components specifically in CRC has been published by Wu et al. [158].

Genetic alterations of TGFβR2 are the most common mechanism leading to the loss of TGF-β signaling in CRC. Inactivation of TGFβR2 frequently occurs due to microsatellite instability (MSI), resulting from DNA mismatch repair defects, causing nucleotide additions or deletions in simple repeated sequences, or microsatellites in the genome [156,159]. Additionally, impairment of TGFβ-mediated anti-proliferative responses due to mutation of TGFβR1 has also been observed [160]. However, the presence of a common polymorphic variant TGFβR1*6A has been shown to increase the risk of CRC and several other cancers [161,162].

Genetic polymorphisms of TGFβ1 have also been associated with colorectal neoplasia, although meta-analyses of particular alleles demonstrated inconclusive correlation with a single mutation [163,164]. The mostly widely studied TGFβ1 genetic alterations are TGFβ1 −509 C > T, +869 T > C, +915 G > C, and −800 G > A [164]. Meta-analysis by Liu et al., has shown that the TGFβ1 −509 C > T, +869 T > C, +915 G > C, and −800 G > A polymorphisms are not associated with colorectal adenoma, but, C allele of −509 C > T and A allele of −800 G > A are associated with increased CRC risk [164]. In addition, the −509 C > T has been reported to be associated with increased risk of developing CRC by Wang et al. [165] and decreased risk of CRC by Liu et al. [163].

Mutation or deletions in Smad genes can also be an important factor during tumor development. Most commonly mutations are seen on Smad4 and Smad2, due to allelic loss or LOH that has been demonstrated in up to 60% of CRCs. Mutations in Smad4 gene (16–25%) and Smad2 gene (6%) have been associated with CRC. Smad4 and Smad2 genes along with tumor suppressor gene DCC (deleted in colorectal cancer) are localized at chromosome 18q21 [166]. Smad4 mutations are found in about 11% of familial adenomatous polyposis and 11% of hereditary non-polyposis colorectal cancer [157,167] syndromes. Smad2 mutations occur in the MH1 or MH2 domains of the molecule affecting the phosphorylation, nuclear translocation, and/or decreasing protein stability ultimately disturbing TGFβ signaling. Similar mutations or LOH of Smad3 gene (located on 15q21–q22) were reported in a human CRC cell line (SNU-769A) [160]. A later study using 36 CRC cell lines and 744 primary CRC patient tumor biopsy samples concluded that approximately 4% of them carried mutations in the Smad3 gene [168]. Concurrently, the loss of Smad3 expression in gastric cancer tumors/cells has been associated with high susceptibility to cancer [169]. This multitude of genetic mutations in TGFβ signaling components, and the signaling crosstalk with various pathways during the development of cancer, enhance its ability to invade and metastasize to various organs, resulting in decreased 5-year survival.

7. Conclusion

TGFβ signaling plays major roles in regulating normal cell growth, although various cancer studies have suggested that canonical TGFβ signaling is unfaithful. It is promiscuously involved in intracellular signaling crosstalk with various pathways, including, but not limited to, Erk, JNK, Ras, p38 and Wnt. TGFβRs play a

crucial role in non-canonical signaling which collectively result in changes that drive cancer progression and metastasis. The poorly understood Janus-like nature of TGFβ in cancer is likely the product of these interrelations and correlations that do not have simply one single signature. This may explain why understanding it remains elusive. This is potentially how a widely accepted tumor suppressor in benign cells "switches" to promote cancer progression. Understanding this switch to a tumor-promoting outcome remains an important question that is likely to be answered in the minutiae of less established interactions.

This review has explored many possible avenues of TGFβ crosstalk and their consequences in cancer. It is crucial to note that almost no TGFβ signaling component has a single function. For instance the dual kinase activity of TGFβR1 and the two modes of Smad7 interaction with TGFβR1 further add to complexity of TGFβ-crosstalk that is already poorly understood. This complex crosstalk in CRC, we propose, can be investigated by implementing a combination of sophisticated informatics, -omics technologies and in vivo studies in a spatio-temporal manner, coupled with larger protein tracking and interaction studies. Emerging multiplexed technologies such as SOMAmer® [170], proximity extension assays [35,171] and/or SureFire® assays [172] will be crucial in the coming years to perform more elaborate experiments in order to elucidate complex cell signaling behaviors within a matrix of different pathways and the crosstalk between them. It is crucial to remember that in cancer and various diseases, we cannot study these pathways in isolation but instead must transition into a matrix-oriented systems approach that more comprehensively models the spatio-temporal ramifications of signaling activities within the complexity of living cells and tissues. A better understanding of four-dimensional biology is essential to identify in vivo signaling signatures that are of clinical relevance, facilitating the development of more effective, targeted therapeutics to combat a global health burden.

Conflict of interest

Acknowledgments

Appendix A. Supplementary data

Supplementary data associated with this article can be found, in the online version, at http://dx.doi.org/10.1016/j.euprot.2015.06.004.

References

[1] J. Ferlay, et al., Cancer incidence and mortality worldwide: sources, methods and major patterns in GLOBOCAN 2012, Int. J. Cancer 136 (5) (2015) E359–86.
[2] N.C. Davis, R.C. Newland, Terminology and classification of colorectal adenocarcinoma: the Australian clinico-pathological staging system, Aust. N. Z. J. Surg. 53 (3) (1983) 211–221.
[3] C.E. Dukes, The classification of cancer of the rectum, J. Pathol. Bacteriol. 35 (3) (1932) 323–332.
[4] J.A. Meyerhardt, R.J. Mayer, Systemic therapy for colorectal cancer, N. Engl. J. Med. 352 (5) (2005) 476–487.
[5] P.E. Young, C.M. Womeldorph, Colonoscopy for colorectal cancer screening, J. Cancer 4 (3) (2013) 217–226.
[6] M. Bretthauer, Colorectal cancer screening, J. Intern. Med. 270 (2) (2011) 87–98.
[7] C. Ramos, et al., Is barium enema an adequate diagnostic test for the evaluation of patients with positive fecal occult blood? Bol. Asoc. Med. P. R. 101 (2) (2009) 23–28.

[8] C.D. Johnson, et al., Accuracy of CT colonography for detection of large adenomas and cancers, N. Engl. J. Med. 359 (12) (2008) 1207–1217.

[9] F. Stracci, M. Zorzi, G. Grazzini, Colorectal cancer screening: tests, strategies, and perspectives, Front Public Health 2 (2014) p. 210.

[10] J. Agrawal, S. Syngal, Colon cancer screening strategies, Curr. Opin. Gastroenterol. 21 (1) (2005) 59–63.

[11] M. Carpelan-Holmstrom, et al., Preoperative serum levels of CEA and CA 242 in colorectal cancer, Br. J. Cancer 71 (4) (1995) 868–872.

[12] C. Spada, et al., Second-generation colon capsule endoscopy compared with colonoscopy, Gastrointest. Endosc. 74 (3) (2011) 581–589.e1.

[13] S.N. Adler, C. Hassan, Colon capsule endoscopy: quo vadis? Colonoscopy and Colorectal Cancer Screening—Future Directions, InTechOpen, 2013, doi: http://dx.doi.org/10.5772/53055 ISBN: 978-953-51-0949-5.

[14] M. Di Lena, E. Travaglio, D.F. Altomare, New strategies for colorectal cancer screening, World J. Gastroenterol. 19 (12) (2013) 1855–1860.

[15] E.K. Ng, et al., Differential expression of microRNAs in plasma of patients with colorectal cancer: a potential marker for colorectal cancer screening, Gut 58 (10) (2009) 1375–1381.

[16] K.A. Heichman, Blood-based testing for colorectal cancer screening, Mol. Diagn. Ther. 18 (2) (2014) 127–135.

[17] N. Ling, et al., Pituitary FSH is released by a heterodimer of the beta-subunits from the two forms of inhibin, Nature 321 (6072) (1986) 779–782.

[18] K. Kosaki, et al., Characterization and mutation analysis of human LEFTY A and LEFTY B, homologues of murine genes implicated in left-right axis development, Am. J. Hum. Genet. 64 (3) (1999) 712–721.

[19] C. Meno, et al., lefty-1 is required for left-right determination as a regulator of lefty-2 and nodal, Cell 94 (3) (1998) 287–297.

[20] G. Karsenty, et al., BMP 7 is required for nephrogenesis, eye development, and skeletal patterning, Ann. N. Y. Acad. Sci. 785 (1996) 98–107.

[21] H.N. Beck, et al., Bone morphogenetic protein-5 (BMP-5) promotes dendritic growth in cultured sympathetic neurons, BMC Neurosci. 2 (2001) 12.

[22] J. Peng, et al., Growth differentiation factor 9: bone morphogenetic protein 15 heterodimers are potent regulators of ovarian functions, Proc. Natl. Acad. Sci. U. S. A. 110 (8) (2013) E776–E785.

[23] M. Shi, et al., Latent TGF-beta structure and activation, Nature 474 (7351) (2011) 343–349.

[24] R.M. Lyons, et al., Mechanism of activation of latent recombinant transforming growth factor beta 1 by plasmin, J. Cell Biol. 110 (4) (1990) 1361–1367.

[25] Q. Yu, I. Stamenkovic, Cell surface-localized matrix metalloproteinase-9 proteolytically activates TGF-beta and promotes tumor invasion and angiogenesis, Genes Dev. 14 (2) (2000) 163–176.

[26] J.S. Munger, et al., The integrin alpha v beta 6 binds and activates latent TGF beta 1: a mechanism for regulating pulmonary inflammation and fibrosis, Cell 96 (3) (1999) 319–328.

[27] D. Mu, et al., The integrin alpha(v)beta8 mediates epithelial homeostasis through MT1-MMP-dependent activation of TGF-beta1, J. Cell Biol. 157 (3) (2002) 493–507.

[28] S. Schultz-Cherry, et al., Regulation of transforming growth factor-beta activation by discrete sequences of thrombospondin 1, J. Biol. Chem. 270 (13) (1995) 7304–7310 p.

[29] A. Rojas, et al., The aberrant methylation of TSP1 suppresses TGF-beta1 activation in colorectal cancer, Int. J. Cancer 123 (1) (2008) 14–21.

[30] M. Ranson, et al., Increased plasminogen binding is associated with metastatic breast cancer cells: differential expression of plasminogen binding proteins, Br. J. Cancer 77 (10) (1998) 1586–1597.

[31] M. Hilska, et al., Prognostic significance of matrix metalloproteinases-1, -2, -7 and -13 and tissue inhibitors of metalloproteinases-1, -2, -3 and -4 in colorectal cancer, Int. J. Cancer 121 (4) (2007) 714–723.

[32] R.C. Bates, et al., Transcriptional activation of integrin beta6 during the epithelial–mesenchymal transition defines a novel prognostic indicator of aggressive colon carcinoma, J. Clin. Investig. 115 (2) (2005) 339–347.

[33] G. Sun, et al., TGF-beta promotes colorectal cancer cell growth in vitro and in vivo, Hepatogastroenterology 60 (123) (2012) .

[34] L. Bujanda, et al., Evaluation of alpha 1-antitrypsin and the levels of mRNA expression of matrix metalloproteinase 7, urokinase type plasminogen activator receptor and COX-2 for the diagnosis of colorectal cancer, PLoS One 8 (1) (2013) e51810.

[35] S. et al. Mahboob, A novel multiplexed immunoassay identifies CEA, IL-8 and prolactin as prospective markers for Dukes' stages A–D colorectal cancers, Clin. Proteomics 12 (1) (2015) 10.

[36] D. Japink, et al., CEA in activated macrophages. New diagnostic possibilities for tumor markers in early colorectal cancer, Anticancer Res. 29 (8) (2009) 3245–3251.

[37] H.J. Nielsen, et al., Plasma TIMP-1 and CEA in detection of primary colorectal cancer: a prospective, population based study of 4509 high-risk individuals, Scand. J. Gastroenterol. 46 (1) (2011) 60–69.

[38] M. Kawamura, et al., CXCL5: a promoter of cell proliferation, migration and invasion, is a novel serum prognostic marker in patients with colorectal cancer, Eur. J. Cancer 48 (14) (2012) 2244–2251.

[39] C. Rubie, et al., Correlation of IL-8 with induction: progression and metastatic potential of colorectal cancer, World J. Gastroenterol. 13 (37) (2007) 4996–5002.

[40] D.A. Johnson, et al., Plasma Septin versus fecal immunochemical testing for colorectal cancer screening: a prospective multicenter study, PLoS One 9 (6) (2014) e98238 9.

[41] K. Toth, et al., Detection of methylated SEPT9 in plasma is a reliable screening method for both left- and right-sided colon cancers, PLoS One 7 (9) (2012) e46000.

[42] J.D. Warren, et al., Septin 9 methylated DNA is a sensitive and specific blood test for colorectal cancer, BMC Med. 9 (2011) 133.

[43] T. deVos, et al., Circulating methylated SEPT9 DNA in plasma is a biomarker for colorectal cancer, Clin. Chem. 55 (7) (2009) 1337–1346.

[44] R. Grutzmann, et al., Sensitive detection of colorectal cancer in peripheral blood by septin 9 DNA methylation assay, PLoS One 3 (11) (2008) e3759.

[45] E. Letellier, et al., Identification of SOCS2 and SOCS6 as biomarkers in human colorectal cancer, Br. J. Cancer 111 (4) (2014) 726–735.

[46] X. Sole, et al., Discovery and validation of new potential biomarkers for early detection of colon cancer, PLoS One 9 (9) (2014) e106748.

[47] B. Ren, et al., MACC1 is related to colorectal cancer initiation and early-stage invasive growth, CAm. J. Clin Pathol. 140 (5) (2013) 701–707.

[48] A. Hamm, et al., Tumour-educated circulating monocytes are powerful candidate biomarkers for diagnosis and disease follow-up of colorectal cancer, Gut (2015) , doi:http://dx.doi.org/10.1136/gutjnl-2014-308988 pii: gutjnl-2014-308988.

[49] K.Y. Fung, et al., Blood-based protein biomarker panel for the detection of colorectal cancer, PLoS One 10 (3) (2015) p. e0120425.

[50] T.F. Imperiale, et al., Multitarget stool DNA testing for colorectal-cancer screening, N. Engl. J. Med. 370 (14) (2014) 1287–1297.

[51] D.A. Ahlquist, et al., Next-generation stool DNA test accurately detects colorectal cancer and large adenomas, Gastroenterology 142 (2) (2012) 248–256 quiz e25–e26..

[52] W.D. Chen, et al., Detection in fecal DNA of colon cancer-specific methylation of the nonexpressed vimentin gene, J. Natl. Cancer Inst. 97 (15) (2005) 1124–1132.

[53] S.C. Glockner, et al., Methylation of TFPI2 in stool DNA: a potential novel biomarker for the detection of colorectal cancer, Cancer Res. 69 (11) (2009) 4691–4699.

[54] G. Zheng, et al., Serum microRNA panel as biomarkers for early diagnosis of colorectal adenocarcinoma, Br. J. Cancer 111 (10) (2014) 1985–1992.

[55] Q. et al. Wang, Plasma miR-601 and miR-760 are novel biomarkers for the early detection of colorectal cancer, PLoS One 7 (9) (2012) e44398.

[56] Z. Kanaan, et al., A plasma microRNA panel for detection of colorectal adenomas: a step toward more precise screening for colorectal cancer, Ann. Surg. 258 (3) (2013) 400–408.

[57] R. Shah, et al., Biomarkers for early detection of colorectal cancer and polyps: systematic review, Cancer Epidemiol. Biomarkers Prev. 23 (9) (2014) 1712–1728.

[58] F.T. Boyd, J. Massague, Transforming growth factor-beta inhibition of epithelial cell proliferation linked to the expression of a 53-kDa membrane receptor, J. Biol. Chem. 264 (4) (1989) 2272–2278.

[59] G. De Crescenzo, et al., Real-time monitoring of the interactions of transforming growth factor-beta (TGF-beta) isoforms with latency-associated protein and the ectodomains of the TGF-beta type II and III receptors reveals different kinetic models and stoichiometries of binding, J. Biol. Chem. 276 (32) (2001) 29632–29643.

[60] F. Lopez-Casillas, et al., Structure and expression of the membrane proteoglycan betaglycan: a component of the TGF-beta receptor system, Cell 67 (4) (1991) 785–795.

[61] G.C. Blobe, et al., A novel mechanism for regulating transforming growth factor beta (TGF-beta) signaling. Functional modulation of type III TGF-beta receptor expression through interaction with the PDZ domain protein: GIPC, J. Biol. Chem. 276 (43) (2001) 39608–39617.

[62] J.D. Lee, et al., The type III TGF-beta receptor suppresses breast cancer progression through GIPC-mediated inhibition of TGF-beta signaling, Carcinogenesis 31 (2) (2010) 175–183.

[63] H.Y. Lin, et al., Expression cloning of the TGF-beta type II receptor: a functional transmembrane serine/threonine kinase, Cell 68 (4) (1992) 775–785.

[64] L. Gilboa, et al., Oligomeric structure of type I and type II transforming growth factor beta receptors: homodimers form in the ER and persist at the plasma membrane, J. Cell Biol. 140 (4) (1998) 767–777.

[65] Y.E. Zhang, Non-Smad pathways in TGF-beta signaling, Cell Res. 19 (1) (2009) 128–139.

[66] J.L. Wrana, et al., TGF beta signals through a heteromeric protein kinase receptor complex, Cell 71 (6) (1992) 1003–1014.

[67] S.P. Fink, et al., TGF-beta-induced nuclear localization of Smad2 and Smad3 in Smad4 null cancer cell lines, Oncogene 22 (9) (2003) 1317–1323.

[68] Y. Zhang, R. Derynck, Regulation of Smad signalling by protein associations and signalling crosstalk, Trends Cell Biol. 9 (7) (1999) 274–279.

[69] K. Yamaguchi, et al., Identification of a member of the MAPKKK family as a potential mediator of TGF-beta signal transduction, Science 270 (5244) (1995) 2008–2011.

[70] L. Xie, et al., Activation of the Erk pathway is required for TGF-beta1-induced EMT in vitro, Neoplasia 6 (5) (2004) 603–610.

[71] X. Peng, et al., FOXQ1 mediates the crosstalk between TGF-beta and Wnt signaling pathways in the progression of colorectal cancer, Cancer Biol. Ther. (2015) p0.

[72] N.A. Bhowmick, et al., Transforming growth factor-beta1 mediates epithelial to mesenchymal transdifferentiation through a RhoA-dependent mechanism, Mol. Biol. Cell 12 (1) (2001) 27–36.

[73] M.T. Hartsough, K.M. Mulder, Transforming growth factor beta activation of p44mapk in proliferating cultures of epithelial cells, J. Biol. Chem. 270 (13) (1995) 7117–7124.

[74] K.M. Mulder, S.L. Morris, Activation of p21ras by transforming growth factor beta in epithelial cells, J. Biol. Chem. 267 (8) (1992) 5029–5031.

[75] Z. Lu, S. Xu, ERK1/2 MAP kinases in cell survival and apoptosis, IUBMB Life 58 (11) (2006) 621–631.

[76] A.S. Dhillon, et al., MAP kinase signalling pathways in cancer, Oncogene 26 (22) (2007) 3279–3290.

[77] F. Zhu, et al., Bidirectional signals transduced by TOPK–ERK interaction increase tumorigenesis of HCT116 colorectal cancer cells, Gastroenterology 133 (1) (2007) 219–231.

[78] J.Y. Fang, B.C. Richardson, The MAPK signalling pathways and colorectal cancer, Lancet Oncol. 6 (5) (2005) 322–327.

[79] V. Ellenrieder, et al., Transforming growth factor beta1 treatment leads to an epithelial–mesenchymal transdifferentiation of pancreatic cancer cells requiring extracellular signal-regulated kinase 2 activation, Cancer Res. 61 (10) (2001) 4222–4228.

[80] M. Davies, et al., Induction of an epithelial to mesenchymal transition in human immortal and malignant keratinocytes by TGF-beta1 involves MAPK: Smad and AP-1 signalling pathways, J. Cell. Biochem. 95 (5) (2005) 918–931.

[81] K.L. Yee, V.M. Weaver, D.A. Hammer, Integrin-mediated signalling through the MAP-kinase pathway, IET Syst. Biol. 2 (1) (2008) 8–15.

[82] M.W. Renshaw, X.D. Ren, M.A. Schwartz, Growth factor activation of MAP kinase requires cell adhesion, EMBO J. 16 (18) (1997) 5592–5599.

[83] R.S. Frey, K.M. Mulder, TGFbeta regulation of mitogen-activated protein kinases in human breast cancer cells, Cancer Lett. 117 (1) (1997) 41–50.

[84] M.K. Lee, et al., TGF-beta activates Erk MAP kinase signalling through direct phosphorylation of ShcA, EMBO J. 26 (17) (2007) 3957–3967.

[85] A. Rojas, et al., TGF-beta receptor levels regulate the specificity of signaling pathway activation and biological effects of TGF-beta, Biochim. Biophys. Acta 1793 (7) (2009) 1165–1173.

[86] C. Hough, M. Radu, J.J. Dore, Tgf-beta induced Erk phosphorylation of smad linker region regulates smad signaling, PLoS One 7 (8) (2012) e42513.

[87] M. Kretzschmar, et al., A mechanism of repression of TGFbeta/Smad signaling by oncogenic Ras, Genes Dev. 13 (7) (1999) 804–816.

[88] T. Huang, et al., TGF-beta signalling is mediated by two autonomously functioning TbetaRI:TbetaRII pairs, EMBO J. 30 (7) (2011) 1263–1276.

[89] B. Bandyopadhyay, et al., TbetaRI/Alk5-independent TbetaRII signaling to ERK1/2 in human skin cells according to distinct levels of TbetaRII expression, J. Cell Sci. 124 (Pt 1) (2011) 19–24.

[90] B.W. Corn, et al., ERK signaling in colorectal cancer: a preliminary report on the expression of phosphorylated ERK and the effects of radiation therapy, Am. J. Clin. Oncol. 31 (3) (2008) 255–258.

[91] H. Fu, et al., TGF-beta promotes invasion and metastasis of gastric cancer cells by increasing fascin1 expression via ERK and JNK signal pathways, Acta Biochim. Biophys. Sin. (Shanghai) 41 (8) (2009) 648–656.

[92] K. Giehl, Y. Imamichi, A. Menke, Smad4-independent TGF-beta signaling in tumor cell migration, Cells Tissues Organs 185 (1–3) (2007) 123–130.

[93] S. Pulciani, et al., ras gene amplification and malignant transformation, Mol. Cell. Biol. 5 (10) (1985) 2836–2841.

[94] W. Chaiyapan, et al., Somatic mutations of K-Ras and BRAF in Thai colorectal cancer and their prognostic value, Asian Pac. J. Cancer Prev. 14 (1) (2013) 329–332.

[95] K. Okumura, et al., Activated Ki-Ras suppresses 12-O-tetradecanoylphorbol-13-acetate-induced activation of the c-Jun NH2-terminal kinase pathway in human colon cancer cells, Cancer Res. 59 (10) (1999) 2445–2450.

[96] M.T. Hartsough, et al., Altered transforming growth factor signaling in epithelial cells when ras activation is blocked, J. Bol. Chem. 271 (37) (1996) 22368–22375.

[97] B.J. Park, et al., Mitogenic conversion of transforming growth factor-beta1 effect by oncogenic Ha-Ras-induced activation of the mitogen-activated protein kinase signaling pathway in human prostate cancer, Cancer Res. 60 (11) (2000) 3031–3038.

[98] Z. Yan, X. Deng, E. Friedman, Oncogenic Ki-Ras confers a more aggressive colon cancer phenotype through modification of transforming growth factor-beta receptor III, J. Biol. Chem. 276 (2) (2001) 1555–1563.

[99] J. Yue, K.M. Mulder, Activation of the mitogen-activated protein kinase pathway by transforming growth factor-beta, Methods Mol. Biol. 142 (2000) 125–131.

[100] A.C. Mullen, et al., Master transcription factors determine cell-type-specific responses to TGF-beta signaling, Cell 147 (3) (2011) 565–576.

[101] M. Cordenonsi, et al., Links between tumor suppressors: p53 is required for TGF-beta gene responses by cooperating with Smads, Cell 113 (3) (2003) 301–314.

[102] M.J. Calonge, J. Massague, Smad4/DPC4 silencing and hyperactive Ras jointly disrupt transforming growth factor-beta antiproliferative responses in colon cancer cells, J. Biol. Chem. 274 (47) (1999) 33637–33643.

[103] M. Oft, et al., TGF-beta1 and Ha-Ras collaborate in modulating the phenotypic plasticity and invasiveness of epithelial tumor cells, Genes Dev. 10 (19) (1996) 2462–2477.

[104] H. Kim, J.A. Choi, J.H. Kim, Ras promotes transforming growth factor-beta (TGF-beta)-induced epithelial–mesenchymal transition via a leukotriene B4 receptor-2-linked cascade in mammary epithelial cells, J. Biol. Chem. 289 (32) (2014) 22151–22160.

[105] P. Trobridge, et al., TGF-beta receptor inactivation and mutant Kras induce intestinal neoplasms in mice via a beta-catenin-independent pathway, Gastroenterology 136 (5) (2009) 1680e7–1688e7.

[106] A. Bera, et al., Oncogenic K-Ras and loss of Smad4 mediate invasion by activating an EGFR/NF-kappaB axis that induces expression of MMP9 and uPA in human pancreas progenitor cells, PLoS One 8 (12) (2013) e82282.

[107] J. Yue, et al., Requirement of TGF-beta receptor-dependent activation of c-Jun N-terminal kinases (JNKs)/stress-activated protein kinases (Sapks) for TGF-beta up-regulation of the urokinase-type plasminogen activator receptor, J. Cell. Physiol. 199 (2) (2004) 284–292.

[108] M. Yamashita, et al., TRAF6 mediates Smad-independent activation of JNK and p38 by TGF-beta, Mol. Cell 31 (6) (2008) 918–924.

[109] A. Sorrentino, et al., The type I TGF-beta receptor engages TRAF6 to activate TAK1 in a receptor kinase-independent manner, Nat. Cell Biol. 10 (10) (2008) 1199–1207.

[110] Y. Mu, et al., TRAF6 ubiquitinates TGFbeta type I receptor to promote its cleavage and nuclear translocation in cancer, Nat. Commun. 2 (2011) 330.

[111] R. Sundar, et al., TRAF6 promotes TGFbeta-induced invasion and cell-cycle regulation via Lys63-linked polyubiquitination of Lys178 in TGFbeta type I receptor, Cell Cycle 14 (4) (2015) 554–565.

[112] Q. Liu, et al., A crosstalk between the Smad and JNK signaling in the TGF-beta-induced epithelial-mesenchymal transition in rat peritoneal mesothelial cells, PLoS One 7 (2) (2012) e32009.

[113] K. Yumoto, et al., TGF-beta-activated kinase 1 (Tak1) mediates agonist-induced Smad activation and linker region phosphorylation in embryonic craniofacial neural crest-derived cells, J. Biol. Chem. 288 (19) (2013) 13467–13480.

[114] J.J. Ventura, et al., JNK regulates autocrine expression of TGF-beta1, Mol. Cell 15 (2) (2004) 269–278.

[115] C. Freudlsperger, et al., TGF-beta and NF-kappaB signal pathway cross-talk is mediated through TAK1 and SMAD7 in a subset of head and neck cancers, Oncogene 32 (12) (2013) 1549–1559.

[116] Y. Kamiya, K. Miyazono, K. Miyazawa, Smad7 inhibits transforming growth factor-beta family type i receptors through two distinct modes of interaction, J. Biol. Chem. 285 (40) (2010) 30804–30813.

[117] A. Herbst, et al., Comprehensive analysis of beta-catenin target genes in colorectal carcinoma cell lines with deregulated Wnt/beta-catenin signaling, BMC Genomics 15 (2014) 74.

[118] F. Comes, et al., A novel cell type-specific role of p38alpha in the control of autophagy and cell death in colorectal cancer cells, Cell Death Differ. 14 (4) (2007) 693–702.

[119] X. Wu, et al., Ubiquitin-conjugating enzyme Ubc13 controls breast cancer metastasis through a TAK1-p38 MAP kinase cascade, Proc. Natl. Acad. Sci. U.S.A. 111 (38) (2014) 13870–13875.

[120] A. Safina, et al., TAK1 is required for TGF-beta 1-mediated regulation of matrix metalloproteinase-9 and metastasis, Oncogene 27 (9) (2008) 1198–1207.

[121] L. Xu, S. Chen, R.C. Bergan, MAPKAPK2 and HSP27 are downstream effectors of p38 MAP kinase-mediated matrix metalloproteinase type 2 activation and cell invasion in human prostate cancer, Oncogene 25 (21) (2006) 2987–2998.

[122] S.Y. Yang, et al., Inhibition of the p38 MAPK pathway sensitises human colon cancer cells to 5-fluorouracil treatment, Int. J. Oncol. 38 (6) (2011) 1695–1702.

[123] L. Yu, M.C. Hebert, Y.E. Zhang, TGF-beta receptor-activated p38 MAP kinase mediates Smad-independent TGF-beta responses, EMBO J. 21 (14) (2002) 3749–3759.

[124] N.A. Bhowmick, et al., Integrin beta 1 signaling is necessary for transforming growth factor-beta activation of p38MAPK and epithelial plasticity, J. Biol. Chem. 276 (50) (2001) 46707–46713.

[125] A.J. Galliher, W.P. Schiemann, Src phosphorylates Tyr284 in TGF-beta type II receptor and regulates TGF-beta stimulation of p38 MAPK during breast cancer cell proliferation and invasion, Cancer Res. 67 (8) (2007) 3752–3758.

[126] A.J. Galliher-Beckley, W.P. Schiemann, Grb2 binding to Tyr284 in TbetaR-II is essential for mammary tumor growth and metastasis stimulated by TGF-beta, Carcinogenesis 29 (2) (2008) 244–251.

[127] J.J. Northey, et al., Signaling through ShcA is required for transforming growth factor beta- and Neu/ErbB-2-induced breast cancer cell motility and invasion, Mol. Cell. Biol. 28 (10) (2008) 3162–3176.

[128] H. Demagny, T. Araki, E.M. De Robertis, The tumor suppressor Smad4/DPC4 is regulated by phosphorylations that integrate FGF, Wnt, and TGF-beta signaling, Cell Rep. 9 (2) (2014) 688–700.

[129] S.J. Ahn, et al., Microarray analysis of gene expression in lung cancer cell lines treated by fractionated irradiation, Anticancer Res. 34 (9) (2014) 4939–4948.

[130] M. Fan, et al., Systematic analysis of metastasis-associated genes identifies miR-17-5p as a metastatic suppressor of basal-like breast cancer, Breast Cancer Res. Treat. 146 (3) (2014) 487–502.

[131] Y. Liu, New insights into epithelial-mesenchymal transition in kidney fibrosis, J. Am. Soc. Nephrol. 21 (2) (2010) 212–222.

[132] H. Wang, et al., Transforming growth factor beta suppresses beta-catenin/Wnt signaling and stimulates an adhesion response in human colon carcinoma cells in a Smad4/DPC4 independent manner, Cancer Lett. 264 (2) (2008) 281–287.

[133] S. Edlund, et al., Interaction between Smad7 and beta-catenin: importance for transforming growth factor beta-induced apoptosis, Mol. Cell. Biol. 25 (4) (2005) 1475–1488.

[134] M. Furuhashi, et al., Axin facilitates Smad3 activation in the transforming growth factor beta signaling pathway, Mol. Cell. Biol. 21 (15) (2001) 5132–5141.

[135] M. Wan, et al., SCF(beta-TrCP1) controls Smad4 protein stability in pancreatic cancer cells, Am. J. Pathol. 166 (5) (2005) 1379–1392.

[136] M. Wan, et al., Smad4 protein stability is regulated by ubiquitin ligase SCF beta-TrCP1, J. Biol. Chem. 279 (15) (2004) 14484–14487.

[137] L.C. Lin, et al., TGFbeta can stimulate the p(38)/beta-catenin/PPARgamma signaling pathway to promote the EMT: invasion and migration of non-small cell lung cancer (H460 cells), Clin. Exp. Metastasis 31 (8) (2014) 881–895.

[138] J. Fuxe, T. Vincent, A. Garcia de Herreros, Transcriptional crosstalk between TGF-beta and stem cell pathways in tumor cell invasion: role of EMT promoting Smad complexes, Cell Cycle 9 (12) (2010) 2363–2374.

[139] M. Bordonaro, et al., The Notch ligand Delta-like 1 integrates inputs from TGFbeta/Activin and Wnt pathways, Exp. Cell Res. 317 (10) (2011) 1368–1381.

[140] A. Nawshad, E.D. Hay, TGFbeta3 signaling activates transcription of the LEF1 gene to induce epithelial mesenchymal transformation during mouse palate development, J. Cell Biol. 163 (6) (2003) 1291–1301.

[141] S. Lei, et al., The murine gastrin promoter is synergistically activated by transforming growth factor-beta/Smad and Wnt signaling pathways, J. Biol. Chem. 279 (41) (2004) 42492–42502.

[142] T. Sekiya, et al., Transcriptional regulation of the TGF-beta pseudoreceptor BAMBI by TGF-beta signaling, Biochem. Biophys. Res. Commun. 320 (3) (2004) 680–684.

[143] K. Horiguchi, et al., Role of Ras signaling in the induction of snail by transforming growth factor-beta, J. Biol. Chem. 284 (1) (2009) 245–253.

[144] J.I. Yook, et al., Wnt-dependent regulation of the E-cadherin repressor snail, J. Biol. Chem. 280 (12) (2005) 11740–11748.

[145] H. Peinado, M. Quintanilla, A. Cano, Transforming growth factor beta-1 induces snail transcription factor in epithelial cell lines: mechanisms for epithelial mesenchymal transitions, J. Biol. Chem. 278 (23) (2003) 21113–21123.

[146] M.J. Joseph, et al., Slug is a downstream mediator of transforming growth factor-beta1-induced matrix metalloproteinase-9 expression and invasion of oral cancer cells, J. Cell. Biochem. 108 (3) (2009) 726–736.

[147] H. Hirose, et al., The significance of PITX2 overexpression in human colorectal cancer, Ann. Surg. Oncol. 18 (10) (2011) 3005–3012.

[148] D.M. Fan, et al., Forkhead factor FOXQ1 promotes TGF-beta1 expression and induces epithelial-mesenchymal transition, Mol. Cell. Biochem. 397 (1–2) (2014) 179–186.

[149] J. Feng, et al., FoxQ1 overexpression influences poor prognosis in non-small cell lung cancer, associates with the phenomenon of EMT, PLoS One 7 (6) (2012) e39937.

[150] J. Feng, et al., Involvement of FoxQ1 in NSCLC through regulating EMT and increasing chemosensitivity, Oncotarget 5 (20) (2014) 9689–9702.

[151] Y. Qiao, et al., FOXQ1 regulates epithelial-mesenchymal transition in human cancers, Cancer Res. 71 (8) (2011) 3076–3086.

[152] J. Christensen, et al., FOXQ1, a novel target of the Wnt pathway and a new marker for activation of Wnt signaling in solid tumors, PLoS One 8 (3) (2013) e60051.

[153] F. Piard, et al., Genetic pathways in colorectal cancer: interest for the pathologist, Ann. Pathol. 22 (4) (2002) 277–288.

[154] M. Bienz, H. Clevers, Linking colorectal cancer to Wnt signaling, Cell 103 (2) (2000) 311–320.

[155] L.M. Wakefield, A.B. Roberts, TGF-beta signaling: positive and negative effects on tumorigenesis, Curr. Opin. Genet. Dev. 12 (1) (2002) 22–29.

[156] W.M. Grady, et al., Mutational inactivation of transforming growth factor beta receptor type II in microsatellite stable colon cancers, Cancer Res. 59 (2) (1999) 320–324.

[157] L. Levy, C.S. Hill, Alterations in components of the TGF-beta superfamily signaling pathways in human cancer, Cytokine Growth Factor Rev. 17 (1–2) (2006) 41–58.

[158] W.K. Wu, et al., Dysregulation and crosstalk of cellular signaling pathways in colon carcinogenesis, Crit. Rev. Oncol. Hematol. 86 (3) (2013) 251–277.

[159] R. Parsons, et al., Microsatellite instability and mutations of the transforming growth factor beta type II receptor gene in colorectal cancer, Cancer Res. 55 (23) (1995) 5548–5550.

[160] J.L. Ku, et al., Genetic alterations of the TGF-beta signaling pathway in colorectal cancer cell lines: a novel mutation in Smad3 associated with the inactivation of TGF-beta-induced transcriptional activation, Cancer Lett. 247 (2) (2007) 283–292.

[161] R.Y. Liao, et al., TGFBR1*6A/9A polymorphism and cancer risk: a meta-analysis of 13,662 cases and 14,147 controls, Mol. Biol. Rep. 37 (7) (2010) 3227–3232.

[162] D.S. Rosman, et al., TGFBR1*6A enhances the migration and invasion of MCF-7 breast cancer cells through RhoA activation, Cancer Res. 68 (5) (2008) 1319–1328.

[163] Y. Liu, et al., Transforming growth factor beta-1C-509T polymorphism and cancer risk: a meta-analysis of 55 case-control studies, Asian Pac. J. Cancer Prev. 13 (9) (2012) 4683–4688.

[164] Y. Liu, W. Zhou, D.W. Zhong, Meta-analyses of the associations between four common TGF-beta1 genetic polymorphisms and risk of colorectal tumor, Tumour Biol. 33 (4) (2012) 1191–1199.

[165] Y. Wang, et al., An updated meta-analysis on the association of TGF-beta1 gene promoter −509C/T polymorphism with colorectal cancer risk, Cytokine 61 (1) (2013) 181–187.

[166] K. Eppert, et al., MADR2 maps to 18q21 and encodes a TGFbeta-regulated MAD-related protein that is functionally mutated in colorectal carcinoma, Cell 86 (4) (1996) 543–552.

[167] M. Miyaki, et al., Higher frequency of Smad4 gene mutation in human colorectal cancer with distant metastasis, Oncogene 18 (20) (1999) 3098–3103.

[168] N.I. Fleming, et al., SMAD2: SMAD3 and SMAD4 mutations in colorectal cancer, Cancer Res. 73 (2) (2013) 725–735.

[169] S.U. Han, et al., Loss of the Smad3 expression increases susceptibility to tumorigenicity in human gastric cancer, Oncogene 23 (7) (2004) 1333–1341.

[170] Let al. Gold, Aptamer-based multiplexed proteomic technology for biomarker discovery, PLoS One 5 (12) (2010) e15004.

[171] L. Christiansson, et al., The tyrosine kinase inhibitors imatinib and dasatinib reduce myeloid suppressor cells and release effector lymphocyte responses, Mol. Cancer Ther. 14 (5) (2015) 1181–1191.

[172] R.I. Osmond, et al., G-protein-coupled receptor-mediated MAPK and PI3-kinase signaling is maintained in Chinese hamster ovary cells after gamma-irradiation, J. Biomol. Screen 17 (3) (2012) 361–369.

Review 1 – Supplemental files

Supplementary Table 1. List of selected signaling pathways that are disrupted in various cancers

Signaling pathway/components	Cancers in which implicated
c-MET	Bladder [1], Breast [2], Colorectal [3-5], gastric [6, 7], Head and neck [8, 9], Renal [10]
HER	Breast [11], Colorectal [12], Prostate [13]
Hedgehog	Colorectal [14, 15], Gastric [16, 17], Lung [18, 19], Ovarian [20], Pancreatic [21], Prostate [22]
JAK-STAT	Breast [23, 24], Colorectal [25-27], Esophageal [28], Head and neck [29]
MAP Kinases	Colorectal [30, 31], Gastric [32], Prostate [33-35],
NF-kappaB	Gastric [36, 37], Head and neck [38], Liver [39, 40], Lung [41-43], Pancreatic [44, 45], Prostate [35, 46, 47], Renal [48],
Notch	Breast [23, 49], Colorectal [50], Lung [51], Prostate [52], Pancreatic [53, 54],
PI3K/AKT/mTOR	Bladder [55], Breast [56, 57], Colorectal [58, 59], Gastric [60], Ovarian [58, 61], Prostate [33, 34], Renal [62], Skin [63]
TGFβ	Breast [64-66], Colorectal [67-69], Lung [70], Ovarian [71-73], Pancreatic [74], Prostate [75]
Smad	Colorectal [76], Ovarian [71], Pancreatic [74]
Wnt	Breast [77, 78], Colorectal [79-81], Liver [82, 83], Renal [84-86]

References

1. Yeh, C.Y., et al., *Transcriptional activation of the Axl and PDGFR-alpha by c-Met through a ras- and Src-independent mechanism in human bladder cancer.* BMC Cancer, 2011. **11**: p. 139.
2. Ponzo, M.G., et al., *Met induces mammary tumors with diverse histologies and is associated with poor outcome and human basal breast cancer.* Proc Natl Acad Sci U S A, 2009. **106**(31): p. 12903-8.
3. Liu, Y., Q. Li, and L. Zhu, *Expression of the hepatocyte growth factor and c-Met in colon cancer: correlation with clinicopathological features and overall survival.* Tumori, 2012. **98**(1): p. 105-12.
4. Moore, A.E., et al., *HGF/Met signalling promotes PGE(2) biogenesis via regulation of COX-2 and 15-PGDH expression in colorectal cancer cells.* Carcinogenesis, 2009. **30**(10): p. 1796-804.
5. Neklason, D.W., et al., *Activating mutation in MET oncogene in familial colorectal cancer.* BMC Cancer, 2011. **11**: p. 424.
6. Houldsworth, J., et al., *Gene amplification in gastric and esophageal adenocarcinomas.* Cancer Res, 1990. **50**(19): p. 6417-22.
7. Rege-Cambrin, G., et al., *Karyotypic analysis of gastric carcinoma cell lines carrying an amplified c-met oncogene.* Cancer Genet Cytogenet, 1992. **64**(2): p. 170-3.

8.	Di Renzo, M.F., et al., *Somatic mutations of the MET oncogene are selected during metastatic spread of human HNSC carcinomas.* Oncogene, 2000. **19**(12): p. 1547-55.

9.	Sen, B., et al., *Distinct interactions between c-Src and c-Met in mediating resistance to c-Src inhibition in head and neck cancer.* Clin Cancer Res, 2010. **17**(3): p. 514-24.

10.	Schmidt, L., et al., *Germline and somatic mutations in the tyrosine kinase domain of the MET proto-oncogene in papillary renal carcinomas.* Nat Genet, 1997. **16**(1): p. 68-73.

11.	Wulfkuhle, J.D., et al., *Molecular analysis of HER2 signaling in human breast cancer by functional protein pathway activation mapping.* Clin Cancer Res, 2012. **18**(23): p. 6426-35.

12.	Half, E., et al., *HER-2 receptor expression, localization, and activation in colorectal cancer cell lines and human tumors.* Int J Cancer, 2004. **108**(4): p. 540-8.

13.	Craft, N., et al., *A mechanism for hormone-independent prostate cancer through modulation of androgen receptor signaling by the HER-2/neu tyrosine kinase.* Nat Med, 1999. **5**(3): p. 280-285.

14.	Qualtrough, D., et al., *Hedgehog signalling in colorectal tumour cells: induction of apoptosis with cyclopamine treatment.* International journal of cancer. Journal international du cancer, 2004. **110**(6): p. 831-7.

15.	Varnat, F., et al., *Human colon cancer epithelial cells harbour active HEDGEHOG-GLI signalling that is essential for tumour growth, recurrence, metastasis and stem cell survival and expansion.* EMBO molecular medicine, 2009. **1**(6-7): p. 338-51.

16.	Fukaya, M., et al., *Hedgehog signal activation in gastric pit cell and in diffuse-type gastric cancer.* Gastroenterology, 2006. **131**(1): p. 14-29.

17.	Yanai, K., et al., *Hedgehog signaling pathway is a possible therapeutic target for gastric cancer.* Journal of surgical oncology, 2007. **95**(1): p. 55-62.

18.	Yuan, Z., et al., *Frequent requirement of hedgehog signaling in non-small cell lung carcinoma.* Oncogene, 2007. **26**(7): p. 1046-55.

19.	Watkins, D.N., et al., *Hedgehog signalling within airway epithelial progenitors and in small-cell lung cancer.* Nature, 2003. **422**(6929): p. 313-7.

20.	Bhattacharya, R., et al., *Role of hedgehog signaling in ovarian cancer.* Clin Cancer Res, 2008. **14**(23): p. 7659-66.

21.	Feldmann, G., et al., *Blockade of hedgehog signaling inhibits pancreatic cancer invasion and metastases: a new paradigm for combination therapy in solid cancers.* Cancer Research, 2007. **67**(5): p. 2187-96.

22.	Sheng, T., et al., *Activation of the hedgehog pathway in advanced prostate cancer.* Molecular cancer, 2004. **3**: p. 29.

23.	Reedijk, M., et al., *High-level Coexpression of JAG1 and NOTCH1 Is Observed in Human Breast Cancer and Is Associated with Poor Overall Survival.* Cancer Research, 2005. **65**(18): p. 8530-8537.

24.	Reedijk, M., et al., *JAG1 expression is associated with a basal phenotype and recurrence in lymph node-negative breast cancer.* Breast Cancer Research and Treatment, 2008. **111**(3): p. 439-448.

25.	Xiong, H., et al., *Inhibition of JAK1, 2/STAT3 signaling induces apoptosis, cell cycle arrest, and reduces tumor cell invasion in colorectal cancer cells.* Neoplasia, 2008. **10**(3): p. 287-97.

26.	Slattery, M.L., et al., *JAK/STAT/SOCS-signaling pathway and colon and rectal cancer.* Mol Carcinog, 2013. **52**(2): p. 155-66.

27.	Du, W., et al., *Inhibition of JAK2/STAT3 signalling induces colorectal cancer cell apoptosis via mitochondrial pathway.* J Cell Mol Med, 2012. **16**(8): p. 1878-88.

28.	You, Z., et al., *JAK/STAT signal pathway activation promotes progression and survival of human oesophageal squamous cell carcinoma.* Clin Transl Oncol, 2012. **14**(2): p. 143-9.

29.	Lai, S.Y., et al., *Erythropoietin-mediated activation of JAK-STAT signaling contributes to cellular invasion in head and neck squamous cell carcinoma.* Oncogene, 2005. **24**(27): p. 4442-9.

30. Wang, Q., et al., *Downregulation of mitogen-activated protein kinases in human colon cancers.* Anticancer research, 2000. **20**(1A): p. 75-83.

31. Gulmann, C., et al., *Quantitative cell signalling analysis reveals down-regulation of MAPK pathway activation in colorectal cancer.* The Journal of pathology, 2009. **218**(4): p. 514-9.

32. Liang, B., et al., *Increased expression of mitogen-activated protein kinase and its upstream regulating signal in human gastric cancer.* World journal of gastroenterology : WJG, 2005. **11**(5): p. 623-8.

33. Goc, A., et al., *PI3 kinase integrates Akt and MAP kinase signaling pathways in the regulation of prostate cancer.* International journal of oncology, 2011. **38**(1): p. 267-77.

34. Dizeyi, N., et al., *Serotonin activates MAP kinase and PI3K/Akt signaling pathways in prostate cancer cell lines.* Urologic oncology, 2011. **29**(4): p. 436-45.

35. Hermani, A., et al., *S100A8 and S100A9 activate MAP kinase and NF-kappaB signaling pathways and trigger translocation of RAGE in human prostate cancer cells.* Experimental cell research, 2006. **312**(2): p. 184-97.

36. Sasaki, N., et al., *Nuclear factor-kappaB p65 (RelA) transcription factor is constitutively activated in human gastric carcinoma tissue.* Clinical cancer research : an official journal of the American Association for Cancer Research, 2001. **7**(12): p. 4136-42.

37. Wang, W., H.S. Luo, and B.P. Yu, *Expression of NF-kappaB and human telomerase reverse transcriptase in gastric cancer and precancerous lesions.* World journal of gastroenterology : WJG, 2004. **10**(2): p. 177-81.

38. Yan, M., et al., *Correlation of NF-kappaB signal pathway with tumor metastasis of human head and neck squamous cell carcinoma.* BMC Cancer, 2010. **10**: p. 437.

39. Qiao, L., et al., *Constitutive activation of NF-kappaB in human hepatocellular carcinoma: evidence of a cytoprotective role.* Human gene therapy, 2006. **17**(3): p. 280-90.

40. Feng, Y.X., et al., *Liver cancer: EphrinA2 promotes tumorigenicity through Rac1/Akt/NF-kappaB signaling pathway 120.* Hepatology, 2010. **51**(2): p. 535-44.

41. Tsurutani, J., et al., *Tobacco components stimulate Akt-dependent proliferation and NFkappaB-dependent survival in lung cancer cells.* Carcinogenesis, 2005. **26**(7): p. 1182-95.

42. Basseres, D.S., et al., *Requirement of the NF-kappaB subunit p65/RelA for K-Ras-induced lung tumorigenesis.* Cancer Research, 2010. **70**(9): p. 3537-46.

43. Tang, X., et al., *Nuclear factor-kappaB (NF-kappaB) is frequently expressed in lung cancer and preneoplastic lesions.* Cancer, 2006. **107**(11): p. 2637-46.

44. Fujioka, S., et al., *Function of nuclear factor kappaB in pancreatic cancer metastasis.* Clinical cancer research : an official journal of the American Association for Cancer Research, 2003. **9**(1): p. 346-54.

45. Lu, Z., et al., *miR-301a as an NF-kappaB activator in pancreatic cancer cells.* The EMBO journal, 2011. **30**(1): p. 57-67.

46. Chen, F., et al., *Livin regulates prostate cancer cell invasion by impacting the NF-kappaB signaling pathway and the expression of FN and CXCR4.* IUBMB life, 2012. **64**(3): p. 274-83.

47. Garg, R., et al., *Activation of nuclear factor kappaB (NF-kappaB) in prostate cancer is mediated by protein kinase C epsilon (PKCepsilon).* The Journal of biological chemistry, 2012. **287**(44): p. 37570-82.

48. Oya, M., et al., *Increased nuclear factor-κB activation is related to the tumor development of renal cell carcinoma.* Carcinogenesis, 2003. **24**(3): p. 377-384.

49. Yamaguchi, N., et al., *NOTCH3 signaling pathway plays crucial roles in the proliferation of ErbB2-negative human breast cancer cells.* Cancer Res, 2008. **68**(6): p. 1881-8.

50. Sikandar, S.S., et al., *NOTCH signaling is required for formation and self-renewal of tumor-initiating cells and for repression of secretory cell differentiation in colon cancer.* Cancer Res, 2010. **70**(4): p. 1469-78.

51. Westhoff, B., et al., *Alterations of the Notch pathway in lung cancer.* Proc Natl Acad Sci U S A, 2009. **106**(52): p. 22293-8.

52. Wang, Z., et al., *Down-regulation of Notch-1 and Jagged-1 inhibits prostate cancer cell growth, migration and invasion, and induces apoptosis via inactivation of Akt, mTOR, and NF-kappaB signaling pathways.* J Cell Biochem, 2010. **109**(4): p. 726-36.

53. Hanlon, L., et al., *Notch1 Functions as a Tumor Suppressor in a Model of K-ras–Induced Pancreatic Ductal Adenocarcinoma.* Cancer Research, 2010.

54. Mazur, P.K., et al., *Notch2 is required for progression of pancreatic intraepithelial neoplasia and development of pancreatic ductal adenocarcinoma.* Proceedings of the National Academy of Sciences, 2010.

55. Knowles, M.A., et al., *Phosphatidylinositol 3-kinase (PI3K) pathway activation in bladder cancer.* Cancer Metastasis Rev, 2009. **28**(3-4): p. 305-16.

56. Gonzalez-Angulo, A.M., et al., *PI3K pathway mutations and PTEN levels in primary and metastatic breast cancer.* Molecular cancer therapeutics, 2011. **10**(6): p. 1093-101.

57. Sun, M., et al., *Phosphatidylinositol-3-OH Kinase (PI3K)/AKT2, activated in breast cancer, regulates and is induced by estrogen receptor alpha (ERalpha) via interaction between ERalpha and PI3K.* Cancer Research, 2001. **61**(16): p. 5985-91.

58. Philp, A.J., et al., *The phosphatidylinositol 3'-kinase p85alpha gene is an oncogene in human ovarian and colon tumors.* Cancer Research, 2001. **61**(20): p. 7426-9.

59. Johnson, S.M., et al., *Novel expression patterns of PI3K/Akt/mTOR signaling pathway components in colorectal cancer.* Journal of the American College of Surgeons, 2010. **210**(5): p. 767-76, 776-8.

60. Shi, J., et al., *Highly frequent PIK3CA amplification is associated with poor prognosis in gastric cancer.* BMC Cancer, 2012. **12**(1): p. 50.

61. Soderlund, K., G. Perez-Tenorio, and O. Stal, *Activation of the phosphatidylinositol 3-kinase/Akt pathway prevents radiation-induced apoptosis in breast cancer cells.* International journal of oncology, 2005. **26**(1): p. 25-32.

62. Hara, S., et al., *Akt activation in renal cell carcinoma: contribution of a decreased PTEN expression and the induction of apoptosis by an Akt inhibitor.* Annals of oncology : official journal of the European Society for Medical Oncology / ESMO, 2005. **16**(6): p. 928-33.

63. Slipicevic, A., et al., *Expression of activated Akt and PTEN in malignant melanomas: relationship with clinical outcome.* American journal of clinical pathology, 2005. **124**(4): p. 528-36.

64. Scollen, S., et al., *TGF-beta signaling pathway and breast cancer susceptibility.* Cancer epidemiology, biomarkers & prevention : a publication of the American Association for Cancer Research, cosponsored by the American Society of Preventive Oncology, 2011. **20**(6): p. 1112-9.

65. Wiercinska, E., et al., *The TGF-beta/Smad pathway induces breast cancer cell invasion through the up-regulation of matrix metalloproteinase 2 and 9 in a spheroid invasion model system.* Breast Cancer Research and Treatment, 2011. **128**(3): p. 657-66.

66. Shim, K.S., et al., *Elevated serum levels of transforming growth factor-beta1 in patients with colorectal carcinoma: its association with tumor progression and its significant decrease after curative surgical resection.* Cancer, 1999. **85**(3): p. 554-61.

67. Calon, A., et al., *Dependency of colorectal cancer on a TGF-beta-driven program in stromal cells for metastasis initiation.* Cancer Cell, 2012. **22**(5): p. 571-84.

68. Slattery, M.L., et al., *Genetic variation in the TGF-beta signaling pathway and colon and rectal cancer risk.* Cancer epidemiology, biomarkers & prevention : a publication of the American Association for Cancer Research, cosponsored by the American Society of Preventive Oncology, 2011. **20**(1): p. 57-69.

69. Deng, X., et al., *Overexpression of Evi-1 oncoprotein represses TGF-beta signaling in colorectal cancer.* Molecular carcinogenesis, 2013. **52**(4): p. 255-64.

70. Hasegawa, Y., et al., *Transforming growth factor-beta1 level correlates with angiogenesis, tumor progression, and prognosis in patients with nonsmall cell lung carcinoma.* Cancer, 2001. **91**(5): p. 964-71.

71. Yeh, K.T., et al., *Aberrant TGFbeta/SMAD4 signaling contributes to epigenetic silencing of a putative tumor suppressor, RunX1T1 in ovarian cancer.* Epigenetics, 2011. **6**(6): p. 727-39.

72. Yin, J., et al., *Genetic variants in TGF-beta pathway are associated with ovarian cancer risk.* PloS one, 2011. **6**(9): p. e25559.

73. Antony, M.L., et al., *Changes in expression, and/or mutations in TGF-beta receptors (TGF-beta RI and TGF-beta RII) and Smad 4 in human ovarian tumors.* Journal of cancer research and clinical oncology, 2010. **136**(3): p. 351-61.

74. Kleeff, J., et al., *Overexpression of Smad2 and colocalization with TGF-beta1 in human pancreatic cancer.* Dig Dis Sci, 1999. **44**(9): p. 1793-802.

75. Glynne-Jones, E., et al., *Transforming growth factor beta 1 expression in benign and malignant prostatic tumors.* Prostate, 1994. **25**(4): p. 210-8.

76. Zhang, B., et al., *Antimetastatic role of Smad4 signaling in colorectal cancer.* Gastroenterology, 2010. **138**(3): p. 969-80 e1-3.

77. Khramtsov, A.I., et al., *Wnt/β-Catenin Pathway Activation Is Enriched in Basal-Like Breast Cancers and Predicts Poor Outcome.* The American Journal of Pathology, 2010. **176**(6): p. 2911-2920.

78. Matsuda, Y., et al., *WNT signaling enhances breast cancer cell motility and blockade of the WNT pathway by sFRP1 suppresses MDA-MB-231 xenograft growth.* Breast Cancer Research, 2009. **11**(3): p. R32.

79. Boon, E.M., et al., *Wnt signaling regulates expression of the receptor tyrosine kinase met in colorectal cancer.* Cancer Research, 2002. **62**(18): p. 5126-8.

80. Shitashige, M., et al., *Traf2- and Nck-Interacting Kinase Is Essential for Wnt Signaling and Colorectal Cancer Growth.* Cancer Research, 2010. **70**(12): p. 5024-5033.

81. Mologni, L., et al., *Colorectal tumors are effectively eradicated by combined inhibition of {beta}-catenin, KRAS, and the oncogenic transcription factor ITF2.* Cancer Research, 2010. **70**(18): p. 7253-63.

82. Lachenmayer, A., et al., *Wnt-pathway activation in two molecular classes of hepatocellular carcinoma and experimental modulation by sorafenib.* Clinical cancer research : an official journal of the American Association for Cancer Research, 2012. **18**(18): p. 4997-5007.

83. Chiang, D.Y., et al., *Focal gains of VEGFA and molecular classification of hepatocellular carcinoma.* Cancer Research, 2008. **68**(16): p. 6779-88.

84. Kojima, T., et al., *Decreased expression of CXXC4 promotes a malignant phenotype in renal cell carcinoma by activating Wnt signaling.* Oncogene, 2009. **28**(2): p. 297-305.

85. Peruzzi, B., G. Athauda, and D.P. Bottaro, *The von Hippel-Lindau tumor suppressor gene product represses oncogenic beta-catenin signaling in renal carcinoma cells.* Proceedings of the National Academy of Sciences of the United States of America, 2006. **103**(39): p. 14531-6.

86. Kim, Y.S., et al., *beta-catenin expression and mutational analysis in renal cell carcinomas.* Pathology international, 2000. **50**(9): p. 725-30.

Review 2: The αvβ6 integrin sets the stage for colorectal cancer metastasis. [Publication II]

CrossMark

NON-THEMATIC REVIEW

Integrin αvβ6 sets the stage for colorectal cancer metastasis

D. I. Cantor[1] · H. R. Cheruku[1] · E. C. Nice[2] · M. S. Baker[1]

Abstract The β6 subunit of the αvβ6 integrin heterodimer has long been an enigma in cancer biology though recent research has provided many new insights into its biology. Collectively, these findings include discovery of the transcriptional, translational and cell biological mechanisms by which β6 acts, the identification of the cellular influences β6 exerts upon the cell proteome, the characterisation of multiple β6-centric pro-metastatic signalling systems and the search for pharmacological therapies (industry and academia) targeted against β6. Once expressional restriction is overcome in early colorectal cancer (CRC), epithelial cell surface restricted αvβ6 can physically interact with, and activate, known oncoproteins, and has the potential to enable the cross-talk through non-canonical signal transduction pathways, resulting in the adoption of an invasive/metastatic phenotype. This recent research has identified numerous interconnections and potential feedback loops, highlighting the fact that the expression of the β6 subunit may initiate a cascade of downstream effects on the CRC cell rather than acting through a single mechanism. We here review these recent studies and postulate that the existence of a cell surface uPAR/αvβ6/TGFβ "metastasome" interactome in/on a proportion of colorectal cancer cells, where β6 expression sequesters and activates multiple systems at the invasive front of tumour lesions, promoting cancer metastasis and hence explaining why β6 has been correlated with reduced patient survival in CRC.

Keywords Colorectal cancer · β6 integrin · Metastatic transformation

1 Introduction

The β6 integrin subunit of the αvβ6 integrin heterodimer (β6) has long resisted attempts to characterise its molecular biology. Despite a steady stream of insights over the past two decades into the various aspects of its roles and functions, its precise nature continues to remain elusive. The β6 subunit is a member of a large family of heterodimeric trans-plasma membrane receptors called integrins that consist of non-covalently bound α and β subunits. Integrins can be composed from 1 of 18 α- and 8 β-subunits to form 24 known heterodimer combinations (Fig. 1a) [1, 2]. Integrin subunits range from between 750 and 1000 amino acid residues in length and are constructed from several domains that are flanked by flexible linker regions, a membrane-spanning helix and a typically short, unstructured cytoplasmic tail (Fig. 1b) [3].

Integrins possess large ectodomains comprised of modular units, a single transmembrane helix and cytoplasmic tail. The external structure of the α-subunits consist of a β-propeller, thigh, calf-1 and calf-2 domains whilst β subunits are composed of a βI, hybrid, PSI (plexin-semaphorin-integrin), 1–4 I-EGF (integrin-epidermal-growth-factor, EI–4) and a β-tail domain sequence [4]. Integrins exist in an equilibrium between a "contorted" or low-affinity state that places the available ligand-binding domain near the cell membrane and a "raised" or high-affinity state when bound to any extracellular ligand found in the extracellular matrix (ECM). Interestingly, many β integrin subunits are also capable of binding intracellular

✉ M. S. Baker
mark.baker@mq.edu.au

[1] Department of Biomedical Sciences, Faculty of Medicine and Health Sciences, Macquarie University, F10A Building, 2 Technology Place, Sydney, NSW 2109, Australia

[2] Department of Biochemistry and Molecular Biology, Monash University, Clayton, VIC 5800, Australia

🖄 Springer

Fig. 1 a Schema of the various α and β subunit integrin heterodimer combinations. **b** Generic structure of the bound and unbound conformations of the αxβ2 integrin heterodimer [5]
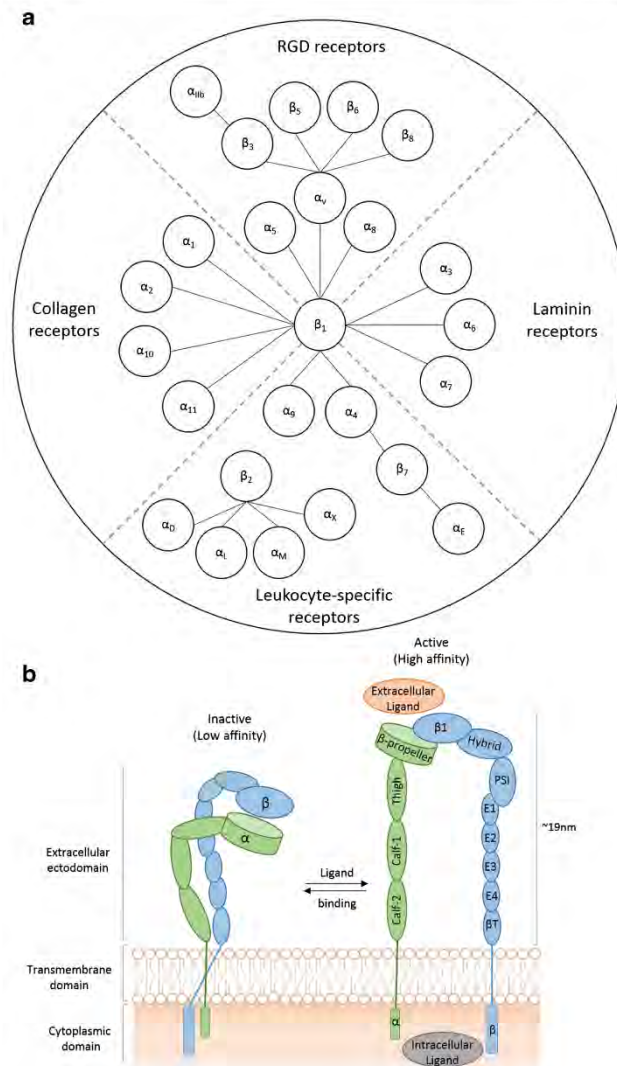
ligands on integrin domains located within the flexible cytoplasmic tail domains [5].

Predominantly thought to be cell surface ECM receptors, integrins bind to proteins such as collagen IV, laminin, vitronectin, fibronectin and leukocyte-specific ligands in order to mediate cellular adhesion through cell•ECM and also cell•cell interactions [6]. Each α/β combination confers a particular binding specificity and consequential downstream signalling capabilities which underpin the structural and functional diversity of the integrin family (Fig. 1a) [1]. For example, heterodimers such as α5β1, αVβ3, αVβ5 and αVβ6 mediate cellular adhesion by binding to Arg-Gly-Asp (RGD) sequence motifs found within a number of abundant ECM proteins, such as fibronectin, vitronectin, fibrinogen and von

67

Willebrand factor, to name a few [6]. Ligand affinity and the specificity of each individual heterodimer combination are primarily influenced by the presence of additional specific residues/sequences outside of that RGD-binding motif [6]. Ganguly et al. have presented evidence that these neighbouring residues may synergistically promote and influence the adhesion of the integrin RGD-binding domain to specific ligands [6]. Whilst the general structural features of all α and β subunits are similar (i.e., sharing 30 and 45 % sequence identity, respectively), sequencing studies have demonstrated no detectable homology between α and β subunits, suggesting that the variation within each gene family has evolved through gene duplication [6].

In mature integrin heterodimers, the large extracellular domain of the NH2-terminal tails of both subunits form an ellipsoidal head, which is responsible for binding the external ligand. Each subunit possesses a hydrophobic helical, single-pass transmembrane domain of approximately 21 residues in length and a generally short C-terminal cytoplasmic domain that is less than 60 residues in length [6, 7]. No integrin cytoplasmic tail possesses intrinsic enzymatic (kinase) function and thus integrins can only signal across the membrane through recruitment and association with a range of adaptor proteins which anchor integrins to the cytoskeleton (e.g. talin [8]) or transduce the stimulus through membrane-associated growth factor receptors (e.g. focal adhesion kinase (FAK) [9]) or cytoplasmic kinases (e.g. mitogen-activated protein kinase members (MAPK) [10]) [7, 11]. Once expressed and bound to ECM proteins, integrins cluster in-plane at the cell membrane near other heterodimers, allowing their cytoplasmic tails to associate cooperatively with the cytoskeleton [12]. This in turn promotes intracellular actin filament assembly and re-organisation in a manner that promotes further integrin clustering in a positive feedback loop mechanism, potentially enhancing cell adhesion to the ECM [6]. Integrins thereby act as cytoskeletal integrators which aggregate adaptor and cytoskeletal-associated signalling proteins into complexes called focal adhesion complexes or, put more simply, focal contacts. These provide the cell with structural support from the ECM as well as localised bi-directional signal transduction [6, 11, 13]. This transduction across the plasma membrane is mediated by conformational changes of the integrin itself, where ligand-binding to the head domains induces a separation of the cytoplasmic subunit tails (Fig. 1b), enabling interaction of intracellular potentially "signaling" ligands with nascent epitopes expressed on the separated cytoplasmic C-termini [14]. This type of signal transduction is referred to as "outside-in" signalling [13] and has been observed to involve kindlin-2 [15–17] and the tyrosine kinases of both the Src and Syk pathways [18].

Integrins are also capable of transmitting intracellular signals across the membrane outside to the extracellular environment, termed "inside-out" signalling [6]. Here, the interaction between the C-terminal cytoplasmic tails and ligands such as talin induces a conformational change that promotes the interaction of the integrin head domains with respective extracellular ligands [6, 16, 19]. Conformational changes can also stem from the mutation of a conserved glycine in the $\beta 1$ domain of the $\beta 1$, $\beta 2$ or $\beta 3$ subunit, resulting in constitutive activation through $\alpha 1/\alpha 1'$-helix unbending or protection from protein modification [4]. The interplay between ligand interaction and bi-directional signalling at focal adhesion sites generally occurs in a synchronised fashion. This synchronicity is thought to regulate several physiological cell behaviours, importantly including proliferation, survival and differentiation, migration and a process known as epithelial-mesenchymal transition (EMT) [20, 5]. However, as this synchronicity is often damaged or completely lost during pathological and developmental human conditions, like fibrosis, chronic wound healing/ulceration and cancer, these processes can exert highly detrimental effects on an organism [6]. In humans, the loss of cell regulation is a crucial step in cancer progression.

As the global population ages and continues to adopt/maintain cancer-predisposing lifestyle choices (e.g. diet, smoking, physical inactivity), the cancer burden has grown to 14.1 million new cases and 8.2 million deaths in 2012 [21]. According to the World Health Organisation's estimates for 2011, cancer now causes more deaths than coronary heart disease and stroke combined [21, 22]. One "lifestyle" cancer subtype that contributes significantly to global cancer morbidity and mortality is colorectal cancer (CRC), with over 1.36 million estimated new cases and 608,700 deaths worldwide in 2012 [21]. CRC is the third most commonly diagnosed cancer in males and the second most common in females with the highest incidence rate reported to be in Australia and New Zealand where rates of 44.8 and 32.2 per 100,000 are found respectively [21]. Morbidity and mortality from CRC invariably occurs with advanced cancers due to the progressive deterioration of normal organ function due to invasion by multiple or massive metastases (Fig. 2), as well as the development of acute complications or extensive and complete wasting/degradation of the patient in a process called cachexia [23]. Essentially, cancer lethality arises from the spread of primary tumours to secondary sites where these induce critical organ failure resulting in patient death. Once a cancer reaches a state where CRC is biologically capable of spreading to distal organs (metastasizing), the likelihood of CRC patient survival rapidly declines.

Numerous proteins and biochemical pathways are thought to enhance CRC progression towards life-threatening metastases. Many studies in the last decade have demonstrated a link between integrin subunit expression and CRC progression towards a more aggressive, metastatic phenotype

Duke's system	TNM system	Primary Tumour (T)	Regional Lymph Nodes (N)	Distal metastasis (M)	5-year survival
	Stage 0	T_{is}	N_0	M_0	
A	Stage I	T_1	N_0	M_0	>90%
B		T_2	N_0	M_0	>85%
B	Stage II	T_3	N_0	M_0	80%
B		T_4	N_0	M_0	72%
C	Stage III	T_1, T_2	N_1 or N_2	M_0	42-64%
C		T_3, T_4	N_1 or N_2	M_0	27-44%
D	Stage IV	$T_1 - T_4$	$N_0 - N_2$	M_1	<10%

Key: T_x – primary tumour can't be assessed N_x – lymph nodes can't be assessed M_x – metastasis can't be assessed

T_0 – no evidence of primary tumour N_0 – no lymph node metastasis M_0 – no distant metastasis

T_{is} – carcinoma in situ N_1 – metastasis in 1-3 lymph nodes M_1 – distant metastasis

T_1 – tumour invades submucosa N_2 – metastasis in 4+ lymph nodes

T_2 – tumour invades muscularis propria

T_3 – tumour invades into subserosa, pericolic or perirectal tissues

T_4 – tumour directly invades other organs or visceral peritoneum

Fig. 2 Duke's and Tumour-Node-Metastasis staging systems with respective survival data from the European Society for Medical Oncology [72]

[24–27]. The steadily growing numbers of CRC deaths are a reminder that there remain unmet clinical needs for a greater understanding of the molecular biology of CRC metastasis, for the discovery/validation of prognostic biomarkers and the development of improved early detection methods. Several studies have linked expression of the β6 integrin subunit with a more aggressive, invasive cancer phenotype [24–26, 28–30]. When bound to its sole binding partner αv, the β6 subunit is an epithelial cell-restricted antigen whose expression is elevated during tissue remodelling events (e.g. wound healing, fibrosis) and in epithelial cancers during EMT. It is almost invariably localised to the invasive fronts and infiltrating edges of tumour islands in cancer [25, 29, 31]. Elevated β6 expression has been observed in many cancers, including CRC, gastric, ovarian, liver, thyroid, endometrial and cervical squamous carcinoma, where expression invariably correlates with poor patient survival [32, 33]. Immunohistochemical studies have demonstrated elevated β6 expression negatively correlates with CRC patient survival [30], which was ascribed to be mediated through β6's roles in promoting cell proliferation, migration and invasion into proximal tissues eventually leading to metastasis [2, 25, 26, 30, 33–35]. Previous studies have demonstrated that the liver metastases of CRC patients exhibit significantly

elevated αvβ6 expression when compared to the primary colon cancer site and that those patients whose primary tumours were αvβ6-positive had a significantly increased rate of liver metastasis [36].

This review will explore recent developments in the characterisation of β6 integrin (as part of the αvβ6 heterodimer) and explore a potential mechanism by which this ECM receptor promotes the metastatic phenotype in CRC, reducing patient survival.

2 Characterisation of the β6 gene promoter and Ets-1 transcription factor

Under normal conditions, β6 expression is restricted to almost undetectable levels and is only expressed in epithelial tissues during large-scale tissue remodelling events, such as wound healing and carcinogenesis [25]. As such, an exciting development in β6 research has been the recent identification by Xu et al. of the previously unknown DNA elements and cognate transcription factors responsible for transcription of the β6 coding sequence (ITGB6, Fig. 3) [1].

Interestingly, Xu et al. determined that mutation of the c-Myb and AP1-binding sites did not exert significant effects on promoter activity [1]. They employed 5'-rapid amplification of cDNA ends (5'-RACE) to determine that the transcriptional
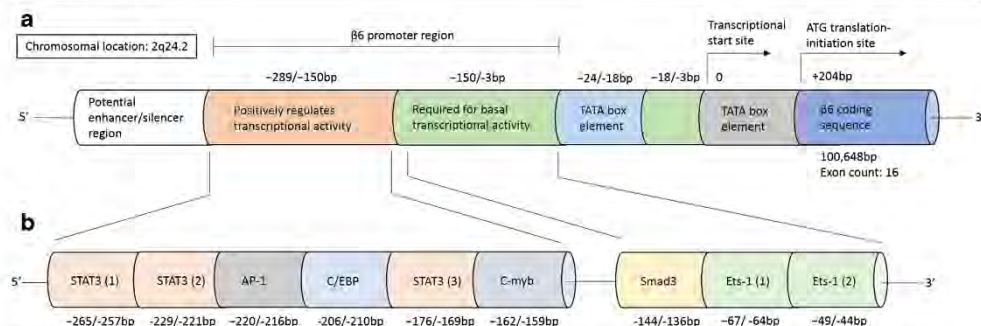
Fig. 3 a Schema of β6 gene transcriptional regions. **b** Location of putative binding sites for transcription factors based upon mutation analysis

start site was located 204 bp upstream of the ATG translation initiation site [1]. They then investigated the β6 promoter by cloning a series of truncated 5'-deletion fragments within the 5'-flanking region of the ITGB6 coding sequence into pGL2-Basic promoter-deficient luciferase reporter vectors [1]. These vectors were then transfected into a human oral squamous cell carcinoma cell line (TCA8113) and a non-human squamous cell carcinoma cell line (293T) to identify the sequence region that made the greatest contribution to gene expression [1]. Xu et al. stated that "the region between −421 and −150 is the main sequence that positively regulates ITGB6 transcription, whilst the region between −150 and −3 is necessary and minimally required for basal transcriptional activity of human ITGB6 gene" [1]. As well as identifying a functional TATA box element −24 to −18 bp upstream of the transcription start site, multiple putative transcription factor binding sites were predicted within the −289 to −150 region, including Ets-1, STAT3, C/EBPα, c-Myb and Smad3 [1]. Xu et al. then proceeded to verify that both STAT3 and C/EBPα are required for positive regulation of ITGB6 mRNA expression [1].

Of those transcription factors identified, Ets-1 and αvβ6 have recently been shown by Peng et al. to positively correlate with CRC stage along the tumour-node-metastasis (TNM) grading system and disease relapse whilst negatively correlating with patient survival [37]. Peng et al. demonstrated that out of 158 CRC tissue specimens, 91 (57.6 %) were positive for Ets-1 expression and 57 (36.1 %) positive for αvβ6 expression, whilst uninvolved colonic mucosa was negative for both Ets-1 and αvβ6 expression [37]. The Ets-1 and αvβ6 expression positively correlated with strong immunohistochemistry staining ($P=0.000$), which was always observed at the invasive front of the tumour islands and where only weak or no staining was found in the centre of tumour masses [37]. An interesting observation from this work was the additive effect of Ets-1 and αvβ6 expression on each other, wherein patients who were positive for both Ets-1 and αvβ6 expression relapsed earlier than patients who are positive for Ets-1 or αvβ6 alone [37]. These findings were supported by previous

work by Bates et al. who also demonstrated the transcriptional activation of β6 by Ets-1 correlated with poor patient survival [30]. Peng et al. investigated the interplay between Ets-1 and αvβ6 expression on the 5-year survival rates of 158 patients from Qilu Hospital (Shandong University, China), though it is important to note that patients with elevated risk factors were encouraged to take adjuvant chemotherapy, of which 87 (55.1 %) received 5-fluorouracil (5-FU)-based adjuvant chemotherapy [37]. Surgery is the preferred method for CRC treatment, though 5-FU-based therapy is the conventional care given to metastatic or lymph node-positive, stage III patients where it can reduce mortality by 25 % compared to resection alone [38]. Patients with liver metastases were encouraged to undergo radiofrequency ablation (RFA) or super γ knife radiotherapy, of which 28 (17.7 %) accepted [37]. With a 100 % follow-up rate, 71 (44.9 %) patients succumbed to cancer-specific death within 5 years of diagnosis, whilst 87 (55.1 %) of patients "were censored as their case follow up was discontinued or patients were alive beyond 60 months or died of reasons other than colon cancer" [37]. From this, Peng et al. have demonstrated that Ets-1 and αvβ6 predict relapse and poor patient survival across all CRC Duke's stages despite application of fluorouracil-based chemotherapy or RFA. However, there was no significant difference in αvβ6 expression between the clustered groups of Duke's stage A+B and C+D (representing 58.2 and 41.7 % of patients, respectively), meaning that there was no difference in αvβ6 expression between the benign and metastatic forms of the disease [37].

A similar study by Ahn et al., published just a few months ago, also explored this finding in terms of stage-dependent survival [39]. Ahn et al. assessed surgical resections from 362 rectal cancer patients (168 Duke's stage B and 194 Duke's stage C) from Concord Hospital (Sydney, Australia) that had been obtained between 1988 and 2001 [39]. Tissue microarray immunohistochemistry employed the same mouse anti-human monoclonal antibody against αvβ6 (6.2A1, Biogen, Cambridge, USA) as used by Peng et al. This study was further supported with extensive clinical data and clinical follow-

up of patients for a meritorious 25 years [39, 37]. Ahn et al. determined that αvβ6 expression is significantly higher in the invasive frontal region of rectal tumours relative to the central region or adjacent non-neoplastic mucosa tissue, as suggested by Peng et al. [39, 37]; αvβ6 expression was elevated in the central region relative to normal tissue [39]. As also observed by Peng et al., no difference was seen in αvβ6 expression between Duke's stage B or stage C rectal cancers and overall survival or clinico-pathological features were not significantly related to αvβ6 expression [39]. As noted by Ahn et al., this contrasts with other literature reports associating αvβ6 expression with poor survival in multiple cancer subtypes; however, whilst other studies such as those performed by Peng et al. have been performed across multiple stages (Duke's A–D), Ahn et al. focused exclusively on ACPS RC stages B and C with far higher sample sizes and longer follow-up time [39].

In terms of patient survival, the phenotypic transition from a lymph node negative Duke's stage B tumour to a nodal positive metastasis (Duke's stage C) is a crucial step in disease progression [40], and so this would be one likely transition where one might expect to observe upregulation of poor prognostic indicators [37, 30]. As this was not the case in either study, it is possible that other pro-metastatic factors (e.g. Ets-1 or other known β6 interactors like P-Erk-2 or urokinase-type plasminogen activator receptor (uPAR)) need to be jointly expressed with αvβ6 in order to mediate the transition, or that αvβ6 enhances its potency in their presence. This may explain the concomitant effect observed by Peng et al., whilst Ahn et al. did not observe any significant difference in survival as the only variable they measured was αvβ6 expression. These studies suggest that whilst αvβ6 does not correlate with poor survival between Duke's stages B and C without chemotherapy, when adjuvant fluorouracil-based chemotherapy or RFA is offered, αvβ6 expression does correlate with poor patient survival, suggesting that something more than just antigen expression is responsible for pro-metastatic activity.

3 Translational regulation of the β6 gene by eukaryotic initiation factor 4E

In addition to the identification of the β6 promoter, an important development in β6 research has been the discovery of the role that eukaryotic translation initiation factor 4E (eIF4E) plays in regulating β6 expression at the translational level. Enyu et al. recently identified that αvβ6 expression positively correlated with the expression of the cap-binding, translational effector eIF4E, which binds to the 5′cap structure of "weak" mRNAs and assists in the delivery of transcripts to the eIF4F translational complex [41]. Normally expressed in low-abundance and considered to be the time-limiting component of the eIF4F complex [41], eIF4E expression is increased in a

dysregulated manner in several cancers including colon [42], lung [43] and breast [44]. eIF4E expression has been associated with TNM-staged colon cancer progression, significantly reducing patient survival and also demonstrated to moderately correlate with αvβ6 expression [45]. Furthermore, when CRC patients were stratified according to low or high αvβ6 and eIF4E expression, respectively, patients with high αvβ6 and eIF4E expression had a significantly reduced survival rate compared to the other groups where only one or neither protein was upregulated [45]. eIF4E overexpression promotes the translation of mRNAs with complex secondary structures or extended 5′-untranslated regions that have central roles in metastatic cancer processes (e.g. c-myc, matrix metalloprotease (MMP)-9, cyclin-D1, fibroblast growth factor (FGF)-2 and vascular endothelial growth factor (VEGF)) [46, 47, 41]. Playing critical roles in mRNA export, stability and translation of transcripts involved in cell proliferation and survival, eIF4E functionality is influenced in concert by the ERK, MAPK, Ras, Akt and mTOR signalling pathways as well as various protein cofactors [47]. Enyu et al. demonstrated by that siRNA inhibition of eIF4E significantly decreased eIF4E mRNA expression whilst not effecting β6 mRNA expression [41]. Whilst this was not surprising, eIF4E siRNA inhibition significantly reduced the expression of both eIF4E and β6 at the protein level [41]. This inhibition was accompanied by a decreased resistance to apoptosis when treated with 5-FU and reduced the migratory capacity for HT-29 and β6-transfected SW480 (SW480^β6OE) CRC cell lines on fibronectin [41]. In the case of SW480^β6OE, eIF4E siRNA inhibition significantly returned cell migration to the same level as the non-β6-expressing wild-type (SW480^WT) and mock (SW480^Mock) transfectants [41]. As well as inhibiting cell migration, Enyu et al. highlighted that translational inhibition of eIF4E could significantly increase tumour sensitivity to 5-FU-based chemotherapies [41]. This finding complements that of Peng et al. [37], suggesting that β6 expression is regulated by Ets-1 expression at the transcriptional level and eIF4E at the translational level and that β6 expression may convey resistance to 5-FU-based chemotherapies resulting in significantly reduced patient survival.

Interestingly, as eIF4E is considered the limiting component of the eIF4F complex, our group observed that β6 overexpression in SW480^β6OE cells was accompanied with a significant upregulation of Eukaryotic translation initiation factor 4 gamma 1 (eIF4G1) which is another component of the eIF4F complex [34]. eIF4G1 is the most abundant member of the eIF4G scaffold protein family, whose elevated expression in yeast promoted direct mRNA-ribosome interaction and translation of mRNAs with longer polyA tails, thereby promoting mRNA translation efficiency [48–50]. Despite this, reduced eIF4G1 expression in yeast and mammalian cells did not inhibit the translation of multiple mRNAs, suggesting that the translation of particular mRNAs can be increased with

71

increased eIF4G expression [48, 51]. Collectively, this suggests that significant upregulation of eIF4G1 with β6 expression may facilitate an altered translational programme, influencing the expression of downstream proteins. eIFG1 is also an effector of mTOR signalling activity (following its phosphorylation) and has been observed to be elevated in breast [52], nasopharyngeal [53] and squamous cell lung cancers [54] where it is associated with metastatic progression and poor patient survival. Badura et al. identified that elevated eIF4G1 expression in breast cancer selectively increased the translation of mRNAs involved in promoting cell survival, the prevention of apoptosis and autophagy following genotoxic DNA damage [48]. In nasopharyngeal cancers, Tu et al. demonstrated that eIF4G1 mRNA and protein expression was significantly elevated in the tumour compared to nine surrounding tissue, where it positively correlated with TNM-staged tumour progression and reduced survival time [53]. Tu et al. also highlighted that inhibiting expression of eIF4G1 by shRNA resulted in the suppression of cell migration/invasion, proliferation/cell cycle progression, colony formation and xenograft tumour growth *in vivo* [53].

Taken collectively, these studies exemplify the pro-oncogenic role of β6 in cancer as it can facilitate both its own transcription and translation through the positive upregulation of Ets-1 and eIF4E, respectively, whilst upregulating the expression of the pro-oncogenic translation factor component eIF4G1. These studies not only unveil the potential transcriptional/translational mechanism of β6 expression but also demonstrate that these processes are required for the promotion of metastatic phenotypes and progression in multiple cancers, including CRC.

4 β6 neo-expression alters the membrane proteome and promotes metastatic phenotypes

The expression of the β6 subunit is the rate-limiting step in the formation of αvβ6 heterodimers at the cell surface, as the αv subunit was seen to be constitutively expressed at medium or high levels in 40 of 81 analysed normal tissue cell types, including the colon and rectum [55]. In an attempt to further illuminate the effects of β6 expression during the pivotal stage of CRC progression from Duke's stages B to C, our group recently performed a membrane-enriched proteomic study on the effect of intentional β6 neo-expression in a non-expressing cell line [34]. Utilising the SW480^{β6OE} and SW480^{Mock} cell lines, we observed that β6 expression in a Dukes' stage B CRC resulted in a significant change in the expression of 708 proteins, including 54 potential cancer biomarkers identified by the American Society of Clinical Oncology for clinical applications (e.g. diagnosis, prognosis, progression and response to therapy) [34]. One hundred thirty-four proteins were observed solely in either the β6-transfected SW480^{β6OE} or SW480^{Mock} subclone, potentially indicating a biosignature of proteins expressed/repressed in response to β6 expression [34], potentially as a result of an altered transcriptional/translational programme. Ingenuity Pathway Analysis$^©$ of the proteomic datasets revealed that the protein networks and functions most strongly affected by β6 expression were fundamentally involved in cancer metastasis. These functions included the following: (i) cell death, (ii) cellular movement, (iii) cancer phenotype, (iv) cell cycle and (v) cellular growth/proliferation [34].

Based upon the expression of signalling pathway members, the integrin-linked kinase and Ran signalling pathways were identified as being significantly altered between the SW480^{Mock} and SW480^{β6OE} cell lines as well as individual proteins within the MAPK and Wnt/β-catenin signalling pathways [34]. Interestingly, when β6 was artificially overexpressed, the expression of all other integrin subunits observable by membrane proteomics (with the exception of αv) were downregulated (α2, α6, β4 and β5, significantly) [34]. In a previous fluorescence-activated cell analysis study, both SW480^{Mock} and SW480^{β6OE} subclones were demonstrated to lack β3 subunit expression [24]. The significant downregulation of β5 with the slight upregulation of αv was an interesting observation as it suggested that β6 neo-expression inhibits the formation of a competing RGD receptor, αvβ5 (Fig. 1a) [34]. It is important to note that β1 subunit expression was also downregulated, which may reduce the expression of another competing RGD receptor, αvβ1, though this was not statistically significant [34]. Together, this suggests that once β6 is initially expressed, it may preferentially capture significant numbers of αv subunits and hence modulate formation of other available integrin heterodimers, creating a potential hierarchy. This was also postulated by Koistinen et al. who constructed cDNA coding for a single-chain, intracellular anti-αv antibody that was stably transfected into WM-266-4 melanoma subclones [56]. Koistinen et al. found that this antibody significantly reduced αv expression, selectively diminishing αvβ1 heterodimer expression on the cell surface, although it did not alter the expression of another prominent αv-containing heterodimer, αvβ3 [56]. Koistinen et al. suggested that the amount of αvβ1 on the cell surface can be selectively regulated, independently of other heterodimers [56]. In essence, αvβ3 and αvβ5 heterodimer expression was regulated at the level of the β3 and β5 genes, respectively, whilst the activity of the αv gene governs the formation of αvβ1 heterodimers [56]. It is important to note that β6 expression was not detected on these cells, although in a similar study, αvβ1-mediated adhesion to fibronectin was reduced in a β6-transfected cell line in which αvβ1 had previously been a major fibronectin receptor [56, 57]. This finding was similar to our previous study, in which β6 neo-expression reduced cell adhesion to fibronectin by 14 % as well as vitronectin, collagen I and collagen II by 16,

30 and 15 %, respectively [34]. The reduction in adhesion to fibronectin initially seemed counter-intuitive as β6 has been classically characterised as a receptor for the RGD sequence of fibronectin; however, αvβ6 has a greater binding affinity (pM) for the N-terminal RGD sequences of the latency-associated peptide (LAP) of latent transforming growth factor β1 (L-TGFβ1) [58] compared to a low nanomolar binding affinity for other ligands, like fibronectin, vitronectin or tenascin [59–62]. The LAP of TGF-β2 does not contain an RGD sequence and so does not bind to αvβ6. However, αvβ6 can bind and activate TGF-β1 and TGF-β3, whose LAPs do contain an RGD-sequence [63]. Together, this suggests that β6 neo-expression sequesters available αv subunits to establish a dominant integrin hierarchy on the cell surface, inhibiting the expression of other integrin subunits, impairing αvβ1 and αvβ5 formation and shifting adhesion from ECM constituents towards binding and activation of the LAP of L-TGFβ1.

Altered adhesion to the ECM could also help to explain how SW480^{β6OE} were significantly more capable of invasively migrating through an ECM-coated polycarbonate membrane, analogous to the epithelial basement membrane [34]. SW480^{β6OE} cells adopted a gross cellular morphology more akin to mesenchymal cells (i.e. flattened, elongated, pointed and spindly) compared to the more classically round-ed, cobble-stoned appearance of SW480^{Mock} cells [34]. β6 expression also significantly increased proliferation compared to the SW480^{Mock} controls [34]. Together, these results strongly support previous findings that EMT is promoted by β6 expression [29, 64], exerting pan-cellular consequences on the pre-metastatic CRC cell.

5 Stromal cell-derived factor 1α (SDF-1) promotes CRC migration through αvβ6

Interestingly, the same proteomic study identified that stromal cell-derived factor 2 (SDF-2) was significantly upregulated by 6.1-fold coincident with β6 neo-overexpression [34]. This appeared to contradict the literature as, although poorly characterised and ubiquitously expressed in various cancers, SDF-2 expression inversely correlates with breast cancer survival [65]. The expression of stromal cell-derived factor 1α (SDF-1) and its unique receptor (Chemokine (C-X-C Motif) Receptor 4; CXCR4) on the other hand has recently been demonstrated to correlate with αvβ6 expression, promoting CRC cell migration [66]. SDF-1 and CXCR4 have been suggested to form a signalling pathway that directs cancer cell migration [66]. Although CXCR4 does not directly contribute to cell adhesion and migration, it transmits SDF-1-induced signalling, altering integrin-dependent cell adhesion and migration [66–68]. Interestingly, recent investigations have entwined the SDF-1/CXCR4 interaction with the αvβ6

heterodimer, whereby αvβ6 mediates the pro-metastatic activity of the pathway (Fig. 4).

Wang et al. reported a significant correlation between CXCR4 and αvβ6 expression with liver metastasis after a median follow-up of 39 months, and that CXCR4-positive patients exhibited significantly increased αvβ6 expression [66]. No equivocal staining was observed in normal colon or liver tissue specimens [66]. CXCR4 and β6 mRNA and protein levels were elevated in the metastatic WiDr and HT-29 CRC cell lines whilst expressed at far lower levels in the non-metastatic Caco-2 cell line [66]. Wang et al. demonstrated that treatment of β6-expressing cell lines with SDF-1 increased cell migration on fibronectin which was ablated by antibody or siRNA-based αvβ6 inhibition [66]. Such inhibition was reported as being comparable with the use of the CXCR4-specific inhibitor, AMD3100 [66]. RT-PCR analysis then demonstrated that recombinant human SDF-1 treatment resulted in a dose-dependent increase in β6 mRNA expression in both WiDr and HT-29 cell lines whilst not affecting the mRNA levels of the αv subunit [66]. Increased β6 expression on the cell surface was confirmed by Western blotting and flow cytometry. This SDF-1-dependent upregulation of β6 was attenuated by pre-treatment with CXCR4 siRNA or the CXCR4 inhibitor, AMD3100 [66]. Increased β6 expression following SDF-1 treatment coincided with significantly increased ERK1/2 phosphorylation, which was again nullified following pre-treatment with CXCR4 siRNA, AMD3100 or the ERK-specific inhibitor U0126 [66]. Interestingly, the SDF-1-dependent increase in β6 expression and cell migration was also nullified following U0126 inhibition of ERK1/2 [66].

Wang et al. then explored whether this novel mechanism could be influenced by Ets-1 expression and function. SDF-1 treatment minimally increased Ets-1 expression; however, it significantly increased Ets-1 Thr38-phosphorylation, which was again attenuable with CXCR4 siRNA or AMD3100 pre-treatment [66]. ERK1/2 inhibition with U0126 treatment prevented the SDF-1-induced upregulation of Ets-1 expression and phosphorylation at the Thr38 residue, demonstrating that this proposed mechanism is ERK1/2-dependent [66].

Wang et al. then performed immunofluorescence analysis to show that SDF-1 treatment significantly increased nuclear levels of Thr38-phosphorylated Ets-1 which is considered as a trigger for increased DNA-binding activity, which was confirmed by an electrophoretic mobility shift assay (EMSA) [66]. The observed increase in nuclear phosphorylated Ets-1 and DNA-binding activity was reduced by AMD3100, U0126 or Ets-1 siRNA treatment [66]. Ets-1 antagonism by siRNA significantly impaired SDF-1-induced αvβ6 upregulation and cell migration on a fibronectin substrate, indicating that Ets-1 activation was required for the SDF-1/CXCR4-dependent upregulation of αvβ6 expression and the promotion of CRC cell migration [66].

73
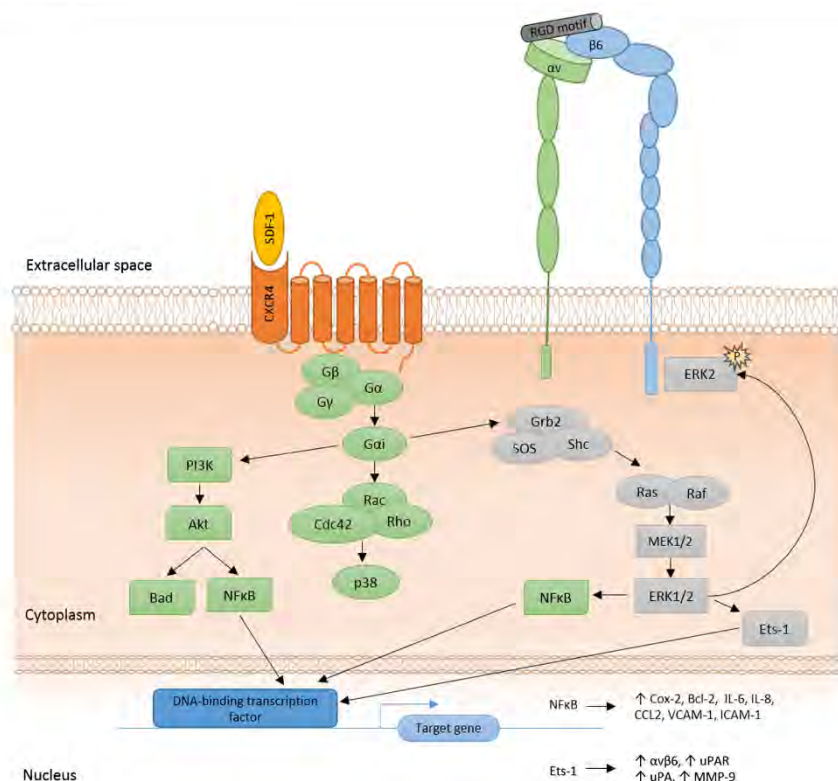
Fig. 4 Relationship between the SDF-1/CXCR4 signal transduction pathway in cancer and the αvβ6 integrin. CXCR4 is a G-protein-coupled receptor (GPCR) which associates with the heterotrimeric (Gα, Gβ, Gγ) subunits upon SDF-1-binding. The Gαi subunit inhibits adenylyl cyclase and promotes MAPK activation through Grb2/SOS/ Shc. PI3K can be activated by the Gβγ and Gα subunits, resulting in the phosphorylation of focal adhesion components (e.g. FAK, proline-rich kinase-2 (Pyk-2), Crk-associated substrate (p130Cas), Crk and paxilin). Modified from [66, 103, 104]

These experiments were repeated using non-metastatic Caco-2 CRC cells that had been transfected with a CXCR4 expression vector or a mock transfectant control. Wang et al. determined that SDF-1 treatment significantly increased β6 expression at the mRNA and protein levels, which was attenuable with AMD3100 inhibition of CXCR4 [66]. No difference in migration was observed in parental Caco-2 cells when treated with SDF-1; however, SDF-1 treatment increased the migration of CXCR4-overexpressing transfectants without affecting the mock control cell line [66]. Functional blocking of αvβ6 with the 10D5 antibody reduced the SDF-1-induced migration of CXCR4-transfected Caco-2 cells, indicating that Caco-2 cells can become migratory with CXCR4 expression, following SDF-1 treatment and the subsequent upregulation of αvβ6 [66].

Wang et al. presented a thorough explanation as to how SDF-1/CXCR4 could promote CRC metastasis via the αvβ6 integrin and this has been expanded upon by Xue et al. who demonstrated that the SDF-1/CXCR4 interaction also induces αvβ6 expression in ovarian cancer [69]. Xue et al. observed that SDF-1 enhanced ECM degradation and OVCA429 invasion through the upregulation of urokinase-type plasminogen activator (uPA) expression along with its activation of plasminogen into plasmin, all of which was once more ablated with AMD3100 or 10D5 pre-treatment [69]. In addition to mediating αvβ6-dependent invasion, SDF-1 treatment was determined to upregulate uPA through the activation of the Akt and MAPK-p38 pathways, as the effect was eliminated by treatment with the Akt inhibitor LY294002 or the p38-MAPK inhibitor SB203580 [69]. αvβ6 inhibition by the 10D5 antibody was observed to ablate the increase in uPA

expression following SDF-1 stimulation, confirming that the upregulation of uPA was also αvβ6-dependent [69].

A recent study by Sun et al. has identified yet another novel avenue of signal cross-talk between αvβ6 and interleukin 8 (IL-8), where IL-8 promoted αvβ6-dependent migration involving the related receptors CXCR1 and CXCR2 [27]. IL-8 expression was significantly correlated with αvβ6 in 139 CRC specimens where it promoted αvβ6 expression in a dose-dependent manner through the ERK/Ets-1 signalling pathway [27]. These novel mechanisms both provide new insights into β6 biology, highlighting extensive cross-talk with multiple signalling and proteolytic pathways, and identify a new ancillary system which is involved in promoting metastatic activity.

6 αvβ6 integrin is intercellularly transported via exosomes and targetable by 5-FU-containing immunoliposomes and the human therapeutic antibody 264RAD

Another recent development in the β6 research field that may be relevant to CRC has been the discovery by Fedele et al. that the αvβ6 heterodimer is transported between prostate cancer cells by cell-derived vesicles (exosomes), continuously released into the extracellular space [70]. Fedele et al. investigated whether αvβ6 can be transferred from prostate cancer cells, in which it is highly expressed, to the surrounding "normal" prostate tissue where it is not expressed [70]. Fedele et al. showed that αvβ6 is packaged into exosomes that were isolated from the RWPE and PC3 prostate cancer cell lines, where it can be transferred from a donor cell to an αvβ6-deficient recipient, whereupon it localises to the plasma membrane [70]. This was confirmed to be a result of exosome-mediated transfer rather than expression that was induced in the recipient cells as de novo αvβ6 expression as it did not result from altered mRNA expression [70]. An extremely interesting finding of this study was that when incubated with these exosomes, recipient prostate cells migrated using the αvβ6-specific ligand (TGF-β LAP) which did not occur when treated with exosomes in which αvβ6 has been repressed by either shRNA or siRNA [70]. Fedele et al. proposed a novel hypothesis in which these exosomes function to horizontally propagate αvβ6-associated phenotypes to neighbouring "normal" tissues, essentially promoting metastatic behaviour in a paracrine fashion [70]. If this is supported in CRC, it stands to reason that once β6 is expressed in a given cell, it may not require clonal expansion in order to increase the β6-expressing cell population as traditionally thought. Instead, this subpopulation may be able to "infect" neighbouring cells in the tumour microenvironment, laterally dispersing αvβ6 and potentially its pro-migratory phenotype.

Another aspect of recent vesicle-related αvβ6 research has been the use of immunoliposomes targeting β6 in order to mediate tumour-specific drug delivery in CRC. Unfortunately when used as a stand-alone therapy [71, 72], 5-FU has a patient response rate of only 10–20 % and β6 expression has been demonstrated to contribute to chemotherapeutic resistance by protecting CRC cells from 5-FU-induced growth inhibition and apoptosis [73]. As a result, the ability to direct 5-FU towards "metastatic" CRC cell populations where it might be efficiently internalised is highly attractive. Liang et al. employed polyethylene glycol containing liposomes that had been conjugated to the anti-human β6 monoclonal antibody (E7P6) to aid the internalisation of 5-FU, specifically into cells that express β6 and not surrounding epithelia where β6 is absent [74]. Liang et al. were able to enhance cellular internalisation of β6-targeted immunoliposomes into β6-expressing SW480$^{\beta6OE}$ and HT-29 cell lines compared to control liposomes. This result was dependent on the level of β6 expression found on the cell surface [74]. These immunoliposomes reduced the 5-FU IC50 for SW480$^{\beta6OE}$ and HT-29 cells by >90 % and induced a ~1.5-fold increase in the rate of 5-FU-induced apoptosis when compared to control liposomes [74]. Liang et al. observed that the growth-inhibiting activity of both the immunoliposomes and control liposomes was indistinguishable in non-β6-expressing SW480^{Mock} cells, indicating that the anti-tumour activity may be attributed to specific binding to β6 on the cell surface [74]. Interestingly, immunoliposomes or controls did not affect ERK1/2 phosphorylation, suggesting that treatment promoted 5-FU-induced apoptosis through enhanced cellular internalisation and activation of the mitochondrial cytochrome-C and caspase-3 apoptotic pathways rather than inhibiting the pro-proliferative β6·ERK2 interaction [74]. Liang et al. then went on to demonstrate that therapy with these 5-FU-containing immunoliposomes had a significantly greater therapeutic activity in vivo, reducing tumour weight by 25–35 % compared to treatment with 5-FU alone or 5-FU within control liposomes [74]. This study is an exciting development in CRC research, as 5-FU is a hydrophilic drug compound that is internalised into cells at a low efficiency and remains dependent on membrane transporters [74, 75]. The targeted and more efficient delivery of 5-FU to β6-expressing cells, where it exerts greater apoptotic activity, is an exciting leap with obvious clinical utility for treating patients with αvβ6$^+$ cancers.

Another recent method of targeting β6-expressing epithelial tumours has been the development and application of the therapeutic human antibody, 246RAD, which functionally inhibits αvβ6 [76]. 246RAD inhibits binding to all known ligands, including the LAP of TGFβ [76]. 246RAD is cross reactive with the αvβ8 heterodimer but does not bind to αvβ3, αvβ5, α5β1 or α4β1 [76]. Eberlein et al. determined through in vitro studies that 246RAD was able to prevent

75

TGFβ activation, impair MMP-9 production and inhibit invasion through a Matrigel ECM analogue using NCI-H358, Calu-3 lung and Detroit 562 pharyngeal cancer cells, respectively [76]. When applied to *in vivo* studies, 246RAD demonstrated a dose-dependent inhibition of Detroit 562 tumour growth that corresponded with a reduction in ERK1/2 phosphorylation, Ki67 and αvβ6 expression, prompting regression of well-established tumours [76]. Eberlein et al. determined that treatment with 20 mg/kg 246RAD reduced the growth and metastasis of orthotopic 4T1 mouse mammary tumours, reducing both primary tumour growth and number of lung metastases [76]. Moore et al. have further explored the use of 246RAD in a later study [77], where they noted that αvβ6 expression significantly reduced survival and 246RAD antibody treatment or β6 siRNA significantly reduced breast cancer cell invasion [77]. These observations were confirmed to be αvβ6-dependent through the use of an alternative inhibitor, 10D5 [77]. Interestingly, Moore et al. observed that αvβ6 may co-operate with HER2 to regulate intracellular invasion, and that αvβ6-inhibition using 246RAD could improve HER2-targeted antibody therapy with trastuzumab (Herceptin®) [77]. Notably, 246RAD halted BT474 growth and invasion in tumour xenografts whilst the combination of 246RAD and trastuzumab was more effective, reducing tumour size/volume by 98 % compared to trastuzumab alone where the decrease was 78 % [77]. To ensure that αvβ6-blockade was responsible for increasing the effect of trastuzumab, they repeated the experiment with trastuzumab-resistant HER2-18 xenografts and again demonstrated that joint 246RAD with trastuzumab significantly reduced tumour volume by 76 % [77]. 246RAD or trastuzumab therapy significantly reduced β6 expression in the BT474 xenografts whilst joint therapy almost completely abolished β6 expression, whilst reducing HER2, HER3, Smad2 and Akt2 expression [77].

Given that β6 can be transported between cells through exosomes, influencing cell behaviour, the ability to specifically target β6-expressing cancers through the use of immunoliposomes and therapeutic antibodies is both an exciting development and attractive area for future clinical application. The adoption and further refinement of these therapies may enhance the efficiency of current treatment methods and ultimately improve the chances of patient survival in the near future.

7 β6 expression promotes ERK2 activation

The cytoplasmic domain of β6 is involved in many important cell functions, including organisation of focal adhesion contacts, compositional regulation of the intermediate filament network, auto-phosphorylation of FAK and expression and phosphorylation of the transcription factors involved in β6 transcription (STAT3 and Notch, respectively) [78]. In addition to the recent discovery of the SDF-1/CXCR4 interaction with αvβ6, we strongly suspect that the pro-metastatic activities of β6 are complemented through interaction/s between the unique structures of the β6 subunit with uPAR and TGF-β1 (Fig. 5). The possibility of such a concept emerged from earlier work by Agrez et al. who identified that αvβ6 enhanced the proliferation of SW480 CRC cells, both *in vitro* and *in vivo*, through a unique 11-amino cytoplasmic C-terminal tail sequence [24]. Agrez et al. had previously identified that transfection of non-β6-expressing SW480 CRC cells with full-length β6 cDNA resulted in αvβ6 expression at the cell surface, altered cell/colony morphology and increased proliferation [24, 79]. In another study, they repeated their experiment with nine β6-transfected subclones and five mock controls, observing that all nine β6-transfected subclones exhibited increased proliferation relative to the mocks [24]. This pro-proliferative effect was ablated by treatment with the αv-blocking antibody L230, whilst having no effect on the mock-transfected SW480 cells [24]. They then created a new SW480 subclone which expressed a truncated β6 protein that lacked the unique 11-amino acid tail sequence (^777REKQKVDLSTDC^788), completely abolishing the β6-dependent increase in proliferation without affecting adhesion to fibronectin or localisation with focal contacts [24]. Extensive deletion of the C-terminal tail did abolish these capabilities, indicating that the regions homologous to the β1 and β3 subunits are required to support these functions [24]. Ahmed et al. expanded on this study to identify the signalling pathways responsible for the pro-proliferative effect of β6 expression in CRC and determined that antisense β6 suppression inhibited both MAPK activity and tumour growth in immune-deficient mice [28]. Using biotinylated cytoplasmic β6 peptides, they determined that the β6 subunit co-immunoprecipitates with ERK2 and that the increased MAPK activity on stimulation with EGF was accounted for by β6-bound ERK [28]. ERK2 did not co-immunoprecipitate with either the β1 or β5 integrin subunit [28]. Using a series of overlapping 20-mer peptide fragments corresponding to the β6 cytoplasmic domain (residues 737-788), they tested the ability for these fragments to bind ERK2 in a direct enzyme-linked immunosorbent assay (ELISA) and identified the region of interaction as ^749RSKAKWQTGTNPLYR^763 [28]. The direct β6●ERK2 interaction was nullified by alanine substitution, resulting in a complete loss of binding [28]. They then employed a β6 cytoplasmic domain mutant that lacked the sequence ^746EAFRSKAKWQTGTNPLYRG^764 (ERK2 binding sequence underlined) to determine the effect of its loss on ERK2 binding and tumour formation [28]. This resulted in similar levels of mutant and wild-type β6 expression at the cell surface and a <20 % reduction in adhesion to fibronectin
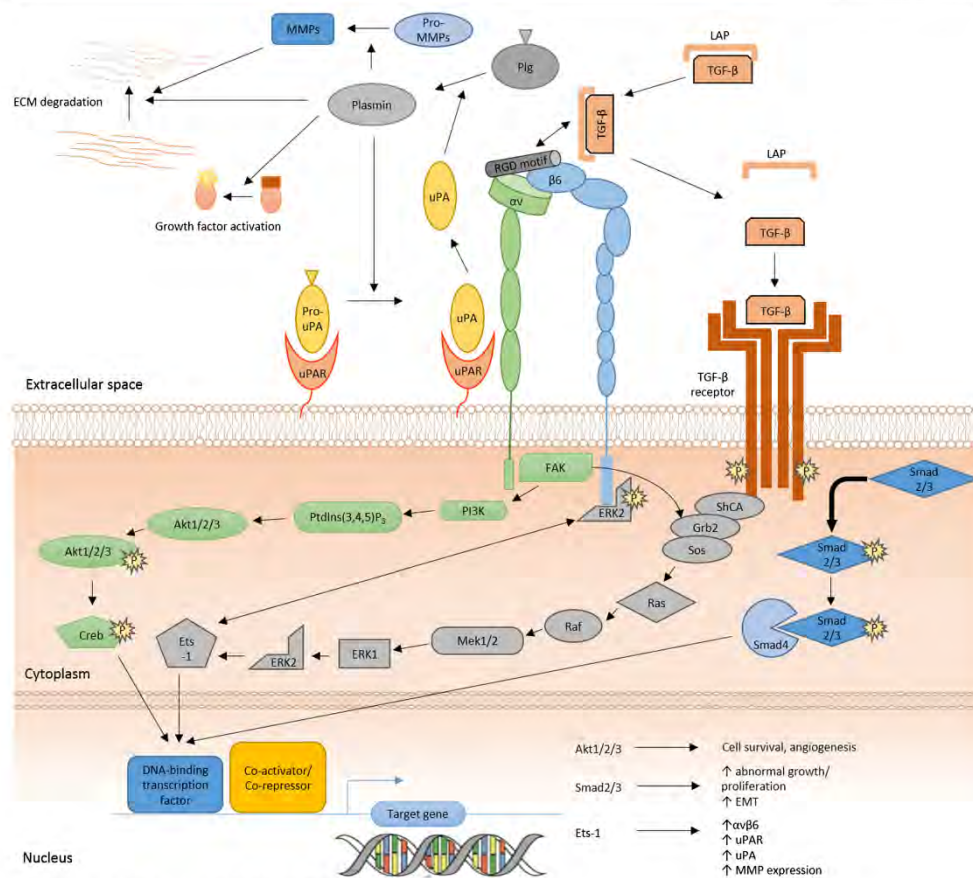
Fig. 5 Schema of the proposed uPAR/αvβ6/TGF-β metastasome

[28]. Western blotting of the immunoprecipitates with an antibody recognising phosphorylated ERK2 (pERK2) determined that truncation of the ERK2 binding sequence inhibited β6-ERK2 binding, reducing basal ERK activity in te absence of serum [28]. Deletion of the pERK2-binding sequence also reduced tumour growth by two- to threefold compared to the wild-type β6 sequence, reverting growth back to that of the non-β6-expressing SW480^Mock control [28]. Interestingly, Ahmed et al. also determined that in the absence of the ERK2 binding sequence or of full-length β6 expression, ERK2 can bind to the β5 subunit, although with lower avidly than β6 as it shares only 50 % homology with the β6●ERK2 binding sequence [28].

In another study, Ahmed et al. demonstrated that β6-expressing ovarian cancer cell lines exhibited a 3.5-fold elevation in ERK1/2 phosphorylation relative to non-β6-expressing cell lines [10]. Elevated β6 expression also correlated with increased cell surface expression of the plasminogen activation (PA) cascade members uPA and uPAR, and also promoted the secretion of zymogen matrix metalloproteases (pro-MMPs)-2 and -9 [10]. Plasmin and MMPs are produced and secreted in their inactive zymogen forms (plasminogen and pro-MMPs, respectively) where they are spatio-temporally activated into mature proteases [80]. Active plasmin is generated from plasminogen by uPA upon binding its cognate receptor, uPAR [80]. Under these conditions, uPA is relatively "shielded" from the specific serpin inhibitors (PAI-1, PAI-2 and protease nexin), as are other proteases on the cell surface in the periplasmic space [81]. Once active, plasmin is capable of driving extensive ECM component degradation

(e.g. fibronectin, fibrin, laminin and the protein core of proteoglycans [80, 81]) and the activation of the pro-MMPs-1, pro-MMPs-3, and pro-MMPs-9, which subsequently degrade additional ECM components [82, 83]. As β6 expression positively correlates with MMP-9 secretion and activity, this has been suggested to mediate the potential for CRC cells to colonise to, and survive within, liver metastases [36].

Ahmed et al. demonstrated that β6 expression regulated and enhanced plasminogen-dependent collagen IV degradation, promoting ECM degradation by a mechanism that was inhibited following treatment with antibodies against αvβ6, MMP-9 and uPA, or the uPA inhibitor amiloride [10]. This increased expression and proteolysis was demonstrated to be MAPK-dependent as it could be completely antagonised following treatment with the MAPK/extracellular signal-regulated kinase (MEK 1) inhibitors genistein or U0126 [10]. These two studies were amongst the first to demonstrate that β6 expression promotes MAPK activation in addition to the PA and MMP cascades [28, 10]. This has now been supported by CRC studies [66, 69] as well as other breast and oral cancer studies [84, 85].

8 αvβ6 interacts with domain III of uPAR through the αv subunit

Employing the same ovarian cancer cell lines, the association between β6, ERK2 and uPAR was further explored by Saldanha et al. who demonstrated by proteomics that αvβ6 co-immunoprecipitated with uPAR when using the monoclonal anti-uPAR antibody, R4 [86]. Saldanha et al. also observed that uPAR co-immunoprecipitated with several proteins of interest, including the putative plasminogen receptors thrombospondin-1, ezrin and α-enolase, as well as putative MAPK-activating protein and eukaryotic translation initiation factor 4A1 [86]. β6 co-immunoprecipitation with uPAR was confirmed by Western blotting and reverse co-immunoprecipitation using the monoclonal anti-β6 antibody, 6.3G9 [86]. As with the β6●P-ERK2 interaction [28], the expression of uPA and uPAR [87] and the secretion of soluble uPA were demonstrated to enhance tumour growth [88]. Saldanha et al. explored the effects of antagonising the uPAR●β6 interaction on cell proliferation. After performing a glycine acid wash to remove bound uPA, 48-h treatment with 10 nM uPA promoted proliferation by 46.5 %, which was not observed when the cells were pre-treated with function blocking antibodies (uPAR; R3 and β6; 6.3G9, respectively) [86]. Treatment with both antibodies produced no cumulative effect, suggesting the presence of a common pathway by which β6 supports uPAR-dependent, uPA-initiated proliferation, namely either through an interaction with uPAR and/or uPA [86]. The increase in proliferation following uPA treatment was

accompanied by a 56 % increase in ERK phosphorylation compared to control cells [86]. This uPA-dependent increase in ERK phosphorylation was eliminated following R4 and 6.3G9 pre-treatment wherein the combined antagonism of uPAR and β6 produced a synergistic inhibition of ERK1/2 phosphorylation [86]. The physical cross-talk between β6 and uPAR and/or uPA was suggested by Saldanha et al. to be an important component of MAPK activity in the OVCA 429 cell model, though they recognised that extended periods of elevated ERK activity may be attributable to the cumulative effect of several signalling pathways rather than simply a unique consequence of the β6●uPAR interaction [86].

Up until recently, no structural information was available for the complete αvβ6 heterodimer that could be used to assess the possibility of a αvβ6●uPAR interaction. X-ray crystallographic structures of specific domains of other heterodimers such as αvβ3 and αIIbβ3 are available [89], and these have recently enabled Sowmya et al. to perform structural analyses that relate to the functional significance of these ECM receptors [90]. They performed composite homology modelling to construct a 3D structural model of the large membrane protein αvβ6●uPAR complex that included the transmembrane and cytoplasmic domains of both integrin subunits [90]. Modelled structures were subjected to iterations of stereo-chemical refinements drawn from a pool of randomised potential starting conformations and made to satisfy spatial restraints [90]. The best structural model, based upon lowest current energy and best objective function, was subjected to structural quality assessment [90], providing the first glimpse into the structure of the heterodimer and its complex with uPAR. This showed that approximately 11 % of αv and β6 ectodomain residues participated in the αv●β6 interaction and thus formed an obligatory protein-protein interaction complex as the respective subunits were unstable in their monomeric states, and thus had no independent existence [90]. Sowmya et al. also suggested that the αv and β6 subunits underwent large conformational dynamics upon assembly; after which, polar interactions formed the dominant forces that promoted αv●β6 subunit interface formation as well as protein●protein interaction at the heterodimer surface [90]. Structural docking simulations were then performed between the resolved, glove-like, three-domain, glycosylphosphotidylinositol (GPI)-linked uPAR with the αvβ6 structural model, which identified a single potential interaction site between the αv subunit and the outer surface of uPAR domain III (27 residues: S299-N255) [90]. Sowmya et al. noted that the proposed αv●uPAR binding site was spatially separated from the RGD-binding site, suggesting that αvβ6 would still be independently able to bind the LAP of L-TGFβ1, fibronectin or other RGD-ligands whilst interfaced with uPAR [90].

The αvβ6●uPAR interaction originally proposed by Saldanha et al. and Sowmya et al. has now been confirmed by Ahn et al. using two orthogonal techniques: proximity ligation assays (PLA) and overlapping peptide array blots [81]. PLA is an emerging method that allows direct detection of protein●protein interactions in cellulo due to the close proximity of interacting proteins (30–40 nm) (refer to Weibrecht et al. for a comprehensive review [91]). Ahn et al. incubated paraformaldehyde-fixed OVCA 429, SW480 and HT29 CRC cell with antibodies 6.4B4 and R4 against αvβ6 and uPAR, respectively [81]. R4 and IgG1 isotype had been conjugated with the PLUS oligonucleotide probe whilst 6.4B4 and its corresponding isotype had been conjugated with the MINUS oligonucleotide probe [81]. When these proximity probes are sufficiently close together, the corresponding oligonucleotides hybridise and ligate, forming a circular DNA molecule [91, 92] which is amplified by rolling circle amplification detectable by confocal microscopy with fluorescently labelled complementary oligonucleotides [91]. Ahn et al. demonstrated that lines that express both αvβ6 and uPAR (SW480^{β6OE}, HT29^{Mock} and OVCA429) display strong interaction signals that were significantly weaker in HT29^{β6AS}, where β6 expression is suppressed (~80 %↓) [81]. No interaction signal was observed in SW480^{Mock} in which β6 is not expressed [81]. Ahn et al. cautiously noted that intermediary "bridging" proteins that may directly interact with αvβ6 and uPAR could not be excluded [81]. To address this, Ahn et al. employed a series of 108 sequential 15-mer uPAR peptides (with three residue overlap) to map potential sites of the αvβ6●uPAR interaction as well as to individual αv and β6 subunits [81]. Similar to Sowmya et al. [90], Ahn et al. determined that αvβ6 bound to six regions from all three uPAR domains (Domain I: E61-R75 and G82-D96; Domain II: G121-E141, L172-F189 and C193-E207; Domain III: S229-N255), corresponding to ~35 % of the uPAR sequence [81]. The interaction was not observed when individual αv or β6 subunits were probed, nor did β1 or β3 bind to the peptide array, suggesting the interaction required the complete αvβ6 heterodimer [81]. In agreement with Sowmya et al. [90], Ahn et al. supported the finding that the S229-N255 region of uPAR Domain III was a favourable site for αvβ6●uPAR interaction and suggested that significant external regions of uPAR remain available to other ligands such as αvβ1, αvβ3 and vitronectin whilst the receptor is bound to uPA [81, 93, 94].

The recent characterisation of the αvβ6●uPAR interaction is a long-awaited development in cancer biology. Both proteins are noted promoters of the metastatic phenotype and EMT in their own right. This interaction with αvβ6 adds to the library of proposed integrin interactions and (again) provides a route through which GPI-linked uPAR, which does not possess a transmembrane domain, can laterally signal. Additionally, the interaction potentially provides structural support and/or shields the vulnerable uPAR DI-DII linker region from cleavage by proteases, facilitating persistent expression of the active ligand (uPA) binding form on the cell surface.

9 β6 interacts with TGFβ receptor II and promotes latent TGFβ1 activation

In addition to interacting with pERK2 and uPAR, the αvβ6 integrin relates to the latent TGF-β1 complex (LTGF-β) found in the ECM, where it provides necessary traction to liberate the LAP from the zymogen L-TGFβ1 complex [95]. Once released, active TGF-β1 is able to promote cell migration and invasion in late-stage CRC [95, 30, 85]. Active TGF-β1 promotes the phosphorylation of the SMAD2/3 signalling complex and its translocation to the nucleus, where it also cyclically induces target genes that are also involved in cell migration and proliferation, including inducing the *de novo* expression of more uPAR and αvβ6 (Fig. 3) [96, 97]. Antagonism using the 6.3G9 antibody has been demonstrated by Van Aarsen et al. to ablate αvβ6 adhesion to the LAP of LTGF-β, whilst simultaneously inhibiting TGF-β activation by >90 % and significantly reducing TGF-β-mediated Smad2/3 phosphorylation *in vitro* [98]. 6.3G9 treatment also reduced basal Smad2/3 phosphorylation although it had no effect following treatment with active TGF-β1, as the LAP was no longer present. Whilst antibody blockade had no effect on Detroit 562 cell proliferation *in vitro*, 6.3G9 and a TGF-β-inhibitory antibody (rsTGF-βRII-Fc) significantly inhibited xenograft tumour growth *in vivo* by 50 %, whilst the non-function-blocking antibody 6.4B4 had no effect on tumour growth [98]. These findings by Van Aarsen et al. highlight the importance of the complex tumour microenvironment and suggest that the antagonism of αvβ6 has a greater inhibitory effect on Detroit 562 cell growth than direct TGF-β antagonism, inferring that preventing TGF-β activation by αvβ6 may be more effective than targeting active TGF-β [98].

In parallel to L-TGFβ1 activation by integrins, L-TGFβ1 can also be activated through the PA cascade where active plasmin can cleave the LAP and activate L-TGFβ1 by proteolysis [86]. Interestingly, MMP-3 and MMP-9 activation was enhanced following treatment with TGF-β1, indicating even further cross-reactivity within this novel interactome [84]. This finding was expanded upon in two recent prostate cancer studies by Dutta et al., who identified that αvβ6 selectively induces MMP-2 expression in a Smad3-mediated transcriptional programme following TGF-β1 activation, leading to osteolysis through increased matrix degradation [99]. Dutta et al. secondly determined that αvβ6 interacts with TGFβ receptor II (TGFβRII) through the β6 cytoplasmic domain, promoting Smad3 activation [83]. This observation has been

furthered by our own (unpublished) study, which identified a potential uPAR•TGFβRII interaction by immunoprecipitation. Both studies by Dutta et al. determined that these observations were β6-dependent as the αvβ5 or a chimeric β6 construct with a β3 cytoplasmic domain failed to elicit a similar response [99, 83].

We suggest that αvβ6 expression provides a structural foundation, allowing the formation of a pericellular interactome, effectively concentrating and focussing TGF-β1 and critical components of the PA cascade activity to the cell surface. This interaction axis that we term "the uPAR/αvβ6/ TGF-β metastasome" may function to sequester key metastasis-related proteins to the infiltrating edge of tumour islands, thereby concentrating immediate and downstream signalling and proteolytic activity to the invasive front of CRC tumours (Fig. 5) were co-expressed.

Figure 5 illustrates the potential role that αvβ6 plays as the nexus point within these known interactions, collaborating between multiple cell systems that have traditionally been thought of as isolated. Taken in conjunction with the novel SDF-1/CXCR4 signal transduction pathway outlined in Fig. 4, αvβ6 appears to influence multiple cell signalling

Table 1 Outline of the metastatic functions of the different signalling pathways connected to the proposed uPAR•αvβ6•TGFβ1 metastasome

	Cancer/tissue	Pathway/protein	Phenotypic consequence/s	Ref
Akt	CRC, ovarian cancer	Akt1/2/3	Akt expression and phosphorylation correlates with cell proliferation and inhibition of apoptosis. Akt (particularly Akt2) upregulation is an important event in apoptotic inhibition during early colon carcinogenesis αvβ6 promoted PI3K/Akt and p38 MAPK phosphorylation.	[105, 106, 69]
ILK	CRC	Integrin-linked kinase (ILK)	ILK was expressed in 98 % of primary tumours and in 100 % of metastatic lesions, correlating with tumour invasion, stage, increased Akt and β-catenin activation	[107]
MAPK	CRC	Phosphorylated ERK2, p38-MAPK	Binds to αvβ6, which promotes ERK1/2 activity as well as the upregulation of αvβ6 and Ets-1. Promotes proliferation and migration Promotes αvβ6 expression on SDF-1 treatment	[10, 66, 69]
mTOR	Colorectal fibrosis	Smad3, αvβ6, peroxisome proliferator-activated receptor-γ (PPARγ)	Smad3-expression upregulated αvβ6, mTOR, TGFβ and Smad3, and mTOR whilst reducing PPARγ during colorectal fibrosis. mTOR activation promotes phosphorylation of IF4E-binding protein 1, mediating protein translation, cell growth and senescence	[108, 109]
PI3K	Jurkat, HeLa, T cells	Akt, mTOR and other signalling pathways	Involved in cell cycle control, apoptosis, cell invasion, migration and angiogenesis β1 integrin ligation to collagen upregulates PI3K/Akt, protecting fibroblasts from anoikis	[110, 111]
Ras	Lung and pancreatic cancer	K-ras	Strong association between β6 expression and a well-differentiated K-Ras-addicted cancer phenotype	[64]
Smad	CRC	SMAD2/3	Potential tumour suppressor role although not fully characterised due to signalling cross-talk. Loss of Smad2/4 activity occurs in ~10 % of CRC tumours where it correlates with poor prognosis and the presence of lymph node metastases at diagnosis	[112, 113]
Wnt	Skin tissue	Kindlin-1	Initiates αvβ6-mediated TGF-β release and inhibits Wnt-β-catenin signalling The Wnt/calcium pathway antagonises β-catenin-dependent signalling, stimulating cell migration	[17, 114]
Ets-1	CRC	αvβ6 promoter	Promotes and correlates with αvβ6 expression. Regulates the expression of genes involved in proliferation, cell differentiation and transformation	[37, 1]
NFκB	CRC	P50, c-Jun N-terminal kinases (JNK)	Inhibits apoptosis and regulates gene expression involved in angiogenesis (VEGF, IL-8, COX2), proliferation (c-Myc, cyclin D1) and metastasis (MMP9) following stimulation by TNF-α, IL-1 or Toll-like receptor substrates	[115]
Stat3	Prostate epithelial cells	Stat3-C	Constitutively activated Stat3 mediates prostate tumorigenesis and enhances cell motility by downregulating E-cadherin and upregulating β6 expression Positively regulates ITGB6 mRNA expression	[1, 116]

pathways and transcription factors, which may have far-reaching consequences within a cancerous cell (some of which are briefly outlined in Table 1). The ability of β6 to influence these noted pro-oncogenic signalling pathways and transcription factors helps to explain how its expression can have such diverse, pro-metastatic effects on a CRC cell [34]. Far from simply facilitating the classical cell adhesion to fibronectin, the β6 subunit of the αvβ6 heterodimer exerts far-reaching actions across the CRC cell through its direct and indirect interactions with many key metastasis-related proteins. We have investigated this metastatic axis by treating Duke's stage B CRC cells (with varying β6 expression) with relatively low concentrations (10 ng/mL) of latent TGF-β1 and/or Plg at comparable levels to that found in human plasma (LTGF-β 136 ng/mL [100]; Plg 200 ng/mL [101]). This (unpublished) study identified that even relatively small concentrations of the zymogen ligands found in plasma can significantly enhanced proliferation, invasion/migration and ERK1/2 signalling activity in cells that express the integrin αvβ6.

10 Conclusion

The β6 integrin subunit of the αvβ6 heterodimer has remained an enigma in cancer biology, resistant to attempts at characterisation. In recent years, there has been a marked increase in understanding its biology, unveiling a wealth of correlations and potential roles in cancer. These include the discovery of its putative transcriptional/translational machinery, its ability to greatly alter the proteome and phenotypes of pre-metastatic CRC, its capability for intercellular transport and its ability to interact with several non-canonical cell systems. We postulate that the potential for β6 to make such potent, pan-cellular changes likely stems from its nature as a tissue remodeler. Integrin αvβ6 must be beneficial to be evolutionarily conserved, and as β6 is only expressed in the healthy organism during large-scale tissue remodelling events (e.g. wound healing and embryonic development), it stands to argue that when expressed in the context of cancer, β6 may in fact facilitate metastatic transformation through the induction of tissue remodelling processes [102]. Tissue remodelling involves the same processes required for a primary tumour cell to spread such as escaping the constrictions of the ECM and neighbouring cell-cell adhesions by proteolysis, infiltrative cell migration, proliferation of new cells, angiogenesis and interaction with both the immune system and tumour microenvironment. We propose that once expressed, αvβ6 initiates an out-of-context tissue remodelling system whose effects on cell regulation and signalling promote metastatic transformation. Recent investigations into β6 biology have laid the foundation to unveil the potential mechanisms of its transcription and translation during such an event and how its expression

can change the proteome of a pre-malignant cell. These findings help to explain why β6 expression correlates with poor patient survival and provides new interactions that could be targeted in the future to unravel its biology. These insights may play an important role when combined with the recent development of more effective therapeutic strategies such as the use of immunoliposomes and therapeutic antibodies that can target β6-expressing tumours. These advances in β6 research stand to facilitate more effective clinical intervention and help alleviate a global health burden.

References

1. Xu, M., Chen, X., Yin, H., Yin, L., Liu, F., Fu, Y., et al. (2015). Cloning and characterization of the human integrin beta6 gene promoter. *PloS One, 10*(3), e0121439. doi:10.1371/journal.pone.0121439.
2. Ramos, D. M., But, M., Regezi, J., Schmidt, B. L., Atakilit, A., Dang, D., et al. (2002). Expression of integrin beta 6 enhances invasive behavior in oral squamous cell carcinoma. *Matrix Biology, 21*(3), 297–307.
3. Arnaout, M. A., Goodman, S. L., & Xiong, J. P. (2007). Structure and mechanics of integrin-based cell adhesion. *Current Opinion in Cell Biology, 19*(5), 495–507. doi:10.1016/j.ceb.2007.08.002.
4. Zhang, C., Liu, J., Jiang, X., Haydar, N., Zhang, C., Shan, H., et al. (2013). Modulation of integrin activation and signaling by alpha1/alpha1'-helix unbending at the junction. *Journal of Cell Science, 126*(Pt 24), 5735–5747. doi:10.1242/jcs.137828.
5. Campbell, I. D., & Humphries, M. J. (2011). Integrin structure, activation, and interactions. *Cold Spring Harbor Perspectives in Biology, 3*(3), doi:10.1101/cshperspect.a004994.
6. Ganguly, K. K., Pal, S., Moulik, S., & Chatterjee, A. (2013). Integrins and metastasis. *Cell Adhesion & Migration, 7*(3), 251–261. doi:10.4161/cam.23840.
7. Zaidel-Bar, R., Itzkovitz, S., Ma'ayan, A., Iyengar, R., & Geiger, B. (2007). Functional atlas of the integrin adhesome. *Nature Cell Biology, 9*(8), 858–867. doi:10.1038/ncb0807-858.
8. Bouaouina, M., Harburger, D. S., & Calderwood, D. A. (2012). Talin and signaling through integrins. *Methods in Molecular Biology, 757*, 325–347. doi:10.1007/978-1-61779-166-6_20.
9. Mitra, S. K., & Schlaepfer, D. D. (2006). Integrin-regulated FAK-Src signaling in normal and cancer cells. *Current Opinion in Cell Biology, 18*(5), 516–523. doi:10.1016/j.ceb.2006.08.011.
10. Ahmed, N., Pansino, F., Baker, M., Rice, G., & Quinn, M. (2002). Association between alphavbeta6 integrin expression, elevated p42/44 kDa MAPK, and plasminogen-dependent matrix degradation in ovarian cancer. *Journal of Cellular Biochemistry, 84*(4), 675–686. doi:10.1002/jcb.10080.
11. Giancotti, F. G., & Ruoslahti, E. (1999). Integrin signaling. *Science, 285*(5430), 1028–1032.
12. Cabodi, S., Di Stefano, P., Leal Mdel, P., Tinnirello, A., Bisaro, B., Morello, V., et al. (2010). Integrins and signal transduction. *Advances in Experimental Medicine and Biology, 674*, 43–54.
13. Jones, M. C., Humphries, J. D., Byron, A., Millon-Fremillon, A., Robertson, J., Paul, N. R., et al. (2015). Isolation of integrin-based

🍀 Springer

adhesion complexes. *Current Protocols in Cell Biology, 66*, 981–9815. doi:10.1002/0471143030.cb0908s66.

14. Hynes, R. O. (2002). Integrins: bidirectional, allosteric signaling machines. *Cell, 110*(6), 673–687.

15. Montanez, E., Ussar, S., Schiffener, M., Bosl, M., Zent, R., Moser, M., et al. (2008). Kindlin-2 controls bidirectional signaling of integrins. *Genes and Development, 22*(10), 1325–1330. doi:10.1101/gad.469408.

16. Calderwood, D. A., Campbell, I. D., & Critchley, D. R. (2013). Talins and kindlins: partners in integrin-mediated adhesion. *Nature Reviews Molecular Cell Biology, 14*(8), 503–517. doi:10.1038/nrm3624.

17. Rognoni, E., Widmaier, M., Jakobson, M., Ruppert, R., Ussar, S., Katsougkri, D., et al. (2014). Kindlin-1 controls Wnt and TGF-beta availability to regulate cutaneous stem cell proliferation. *Nature Medicine, 20*(4), 350–359. doi:10.1038/nm.3490.

18. Abram, C. L., & Lowell, C. A. (2009). The ins and outs of leukocyte integrin signaling. *Annual Review of Immunology, 27*, 339–362. doi:10.1146/annurev.immunol.021908.132554.

19. Wegener, K. L., Partridge, A. W., Han, J., Pickford, A. R., Liddington, R. C., Ginsberg, M. H., et al. (2007). Structural basis of integrin activation by talin. *Cell, 128*(1), 171–182. doi:10.1016/j.cell.2006.10.048.

20. Morse, E. M., Brahme, N. N., & Calderwood, D. A. (2014). Integrin cytoplasmic tail interactions. *Biochemistry, 53*(5), 810–820. doi:10.1021/bi401596q.

21. Ferlay, J., Soerjomataram, I., Dikshit, R., Eser, S., Mathers, C., Rebelo, M., et al. (2015). Cancer incidence and mortality worldwide: sources, methods and major patterns in GLOBOCAN 2012. *International Journal of Cancer, 136*(5), E359–E386. doi:10.1002/ijc.29210.

22. Jemal, A., Bray, F., Center, M. M., Ferlay, J., Ward, E., & Forman, D. (2011). Global cancer statistics. *CA: A Cancer Journal for Clinicians, 61*(2), 69–90. doi:10.3322/caac.20107.

23. Dhanapal, R., Saraswathi, T., & Govind, R. N. (2011). Cancer cachexia. *Journal of Oral and Maxillofacial Pathology, 15*(3), 257–260. doi:10.4103/0973-029X.86670.

24. Agrez, M., Chen, A., Cone, R. I., Pytela, R., & Sheppard, D. (1994). The alpha v beta 6 integrin promotes proliferation of colon carcinoma cells through a unique region of the beta 6 cytoplasmic domain. *Journal of Cell Biology, 127*(2), 547–556.

25. Hazelbag, S., Kenter, G. G., Gorter, A., Dreef, E. J., Koopman, L. A., Violette, S. M., et al. (2007). Overexpression of the alpha v beta 6 integrin in cervical squamous cell carcinoma is a prognostic factor for decreased survival. *Journal of Pathology, 212*(3), 316–324. doi:10.1002/path.2168.

26. Ramos, D. M., Dang, D., & Sadler, S. (2009). The role of the integrin alpha v beta6 in regulating the epithelial to mesenchymal transition in oral cancer. *Anticancer Research, 29*(1), 125–130.

27. Sun, Q., Sun, F., Wang, B., Liu, S., Niu, W., Liu, E., et al. (2014). Interleukin-8 promotes cell migration through integrin alphavbeta6 upregulation in colorectal cancer. *Cancer Letters*. doi:10.1016/j.canlet.2014.08.021.

28. Ahmed, N., Niu, J., Dorahy, D. J., Gu, X., Andrews, S., Meldrum, C. J., et al. (2002). Direct integrin alphavbeta6-ERK binding: implications for tumour growth. *Oncogene, 21*(9), 1370–1380. doi:10.1038/sj.onc.1205286.

29. Bates, R. C. (2005). Colorectal cancer progression: integrin alphavbeta6 and the epithelial-mesenchymal transition (EMT). *Cell Cycle, 4*(10), 1350–1352.

30. Bates, R. C., Bellovin, D. I., Brown, C., Maynard, E., Wu, B., Kawakatsu, H., et al. (2005). Transcriptional activation of integrin beta6 during the epithelial-mesenchymal transition defines a novel prognostic indicator of aggressive colon carcinoma. *Journal of Clinical Investigation, 115*(2), 339–347. doi:10.1172/JCI23183.

31. Binder, M. A. T. M. (2009). Drugs targeting integrins for cancer therapy. *Expert Opinion on Drug Discovery, 4*(3).

32. Liu, S., Liang, B., Gao, H., Zhang, F., Wang, B., Dong, X., et al. (2013). Integrin alphavbeta6 as a novel marker for diagnosis and metastatic potential of thyroid carcinoma. *Head & Neck Oncology, 5*(1), 7.

33. Bandyopadhyay, A., & Raghavan, S. (2009). Defining the role of integrin alphavbeta6 in cancer. *Current Drug Targets, 10*(7), 645–652.

34. Cantor, D., Slapetova, I., Kan, A., McQuade, L. R., & Baker, M. S. (2013). Overexpression of alphavbeta6 integrin alters the colorectal cancer cell proteome in favor of elevated proliferation and a switching in cellular adhesion that increases invasion. *Journal of Proteome Research, 12*(6), 2477–2490. doi:10.1021/pr301099f.

35. Ahmed, N., Riley, C., Rice, G. E., Quinn, M. A., & Baker, M. S. (2002). Alpha(v)beta(6) integrin-A marker for the malignant potential of epithelial ovarian cancer. *Journal of Histochemistry and Cytochemistry, 50*(10), 1371–1380.

36. Yang, G. Y., Xu, K. S., Pan, Z. Q., Zhang, Z. Y., Mi, Y. T., Wang, J. S., et al. (2008). Integrin alpha v beta 6 mediates the potential for colon cancer cells to colonize in and metastasize to the liver. *Cancer Science, 99*(5), 879–887. doi:10.1111/j.1349-7006.2008.00762.x.

37. Peng, C., Gao, H., Niu, Z., Wang, B., Tan, Z., Niu, W., et al. (2014). Integrin alphavbeta6 and transcriptional factor Ets-1 act as prognostic indicators in colorectal cancer. *Cell & Bioscience, 4*(1), 53. doi:10.1186/2045-3701-4-53.

38. Gill, S., Loprinzi, C. L., Sargent, D. J., Thome, S. D., Alberts, S. R., Haller, D. G., et al. (2004). Pooled analysis of fluorouracil-based adjuvant therapy for stage II and III colon cancer: who benefits and by how much? *Journal of Clinical Oncology, 22*(10), 1797–1806. doi:10.1200/JCO.2004.09.059.

39. Ahn, S. B., Mohamedali, A., Chan, C., Fletcher, J., Kwun, S. Y., Clarke, C., et al. (2014). Correlations between integrin alphavnubeta6 expression and clinico-pathological features in stage B and stage C rectal cancer. *PLoS One, 9*(5), e97248. doi:10.1371/journal.pone.0097248.

40. Davis, N. C., & Newland, R. C. (1983). Terminology and classification of colorectal adenocarcinoma: the Australian clinico-pathological staging system. *Australian and New Zealand Journal of Surgery, 53*(3), 211–221.

41. Enyu, L., Zhengchuan, N., Jiayong, W., Benjia, L., Qi, S., Ruixi, Q., et al. (2015). Integrin beta6 can be translationally regulated by eukaryotic initiation factor 4E: contributing to colonic tumor malignancy. *Tumour Biology*. doi:10.1007/s13277-015-3348-8.

42. Berkel, H. J., Turbat-Herrera, E. A., Shi, R., & de Benedetti, A. (2001). Expression of the translation initiation factor eIF4E in the polyp-cancer sequence in the colon. *Cancer Epidemiology, Biomarkers and Prevention, 10*(6), 663–666.

43. Seki, N., Takasu, T., Mandai, K., Nakata, M., Saeki, H., Heike, Y., et al. (2002). Expression of eukaryotic initiation factor 4E in atypical adenomatous hyperplasia and adenocarcinoma of the human peripheral lung. *Clinical Cancer Research, 8*(10), 3046–3053.

44. Nathan, C. O., Carter, P., Liu, L., Li, B. D., Abreo, F., Tudor, A., et al. (1997). Elevated expression of eIF4E and FGF-2 isoforms during vascularization of breast carcinomas. *Oncogene, 15*(9), 1087–1094. doi:10.1038/sj.onc.1201272.

45. Niu, Z., Wang, J., Muhammad, S., Niu, W., Liu, E., Peng, C., et al. (2014). Protein expression of eIF4E and integrin alphavbeta6 in colon cancer can predict clinical significance, reveal their correlation and imply possible mechanism of interaction. *Cell & Bioscience, 4*, 23. doi:10.1186/2045-3701-4-23.

46. De Benedetti, A., & Graff, J. R. (2004). eIF-4E expression and its role in malignancies and metastases. *Oncogene, 23*(18), 3189–3199. doi:10.1038/sj.onc.1207545.

82

47. Carroll, M., & Borden, K. L. (2013). The oncogene eIF4E: using biochemical insights to target cancer. *Journal of Interferon and Cytokine Research, 33*(5), 227–238. doi:10.1089/jir.2012.0142.

48. Badura, M., Braunstein, S., Zavadil, J., & Schneider, R. J. (2012). DNA damage and eIF4G1 in breast cancer cells reprogram translation for survival and DNA repair mRNAs. *Proceedings of the National Academy of Sciences of the United States of America, 109*(46), 18767–18772. doi:10.1073/pnas.1203853109.

49. Clarkson, B. K., Gilbert, W. V., & Doudna, J. A. (2010). Functional overlap between eIF4G isoforms in *Saccharomyces cerevisiae. PloS One, 5*(2), e9114. doi:10.1371/journal.pone.0009114.

50. Park, E. H., Zhang, F., Warringer, J., Sunnerhagen, P., & Hinnebusch, A. G. (2011). Depletion of eIF4G from yeast cells narrows the range of translational efficiencies genome-wide. *BMC Genomics, 12*, 68. doi:10.1186/1471-2164-12-68.

51. Ramirez-Valle, F., Braunstein, S., Zavadil, J., Formenti, S. C., & Schneider, R. J. (2008). eIF4GI links nutrient sensing by mTOR to cell proliferation and inhibition of autophagy. *Journal of Cell Biology, 181*(2), 293–307. doi:10.1083/jcb.200710215.

52. Silvera, D., Arju, R., Darvishian, F., Levine, P. H., Zolfaghari, L., Goldberg, J., et al. (2009). Essential role for eIF4GI overexpression in the pathogenesis of inflammatory breast cancer. *Nature Cell Biology, 11*(7), 903–908. doi:10.1038/ncb1900.

53. Tu, L., Liu, Z., He, X., He, Y., Yang, H., Jiang, Q., et al. (2010). Over-expression of eukaryotic translation initiation factor 4 gamma 1 correlates with tumor progression and poor prognosis in nasopharyngeal carcinoma. *Molecular Cancer, 9*, 78. doi:10.1186/1476-4598-9-78.

54. Comtesse, N., Keller, A., Diesinger, I., Bauer, C., Kayser, K., Huwer, H., et al. (2007). Frequent overexpression of the genes FXR1, CLAPM1 and EIF4G located on amplicon 3q26-27 in squamous cell carcinoma of the lung. *International Journal of Cancer, 120*(12), 2538–2544. doi:10.1002/ijc.22585.

55. Uhlen, M., Fagerberg, L., Hallstrom, B. M., Lindskog, C., Oksvold, P., Mardinoglu, A., et al. (2015). Tissue-based map of the human proteome. *Science, 347*(6220), 1260419. doi:10.1126/science.1260419.

56. Koistinen, P., & Heino, J. (2002). The selective regulation of alpha Vbeta1 integrin expression is based on the hierarchical formation of alpha V-containing heterodimers. *Journal of Biological Chemistry, 277*(27), 24835–24841. doi:10.1074/jbc.M203149200.

57. Koivisto, L., Grenman, R., Heino, J., & Larjava, H. (2000). Integrins alpha5beta1, alphavbeta1, and alphavbeta6 collaborate in squamous carcinoma cell spreading and migration on fibronectin. *Experimental Cell Research, 255*(1), 10–17. doi:10.1006/excr.1999.4769.

58. Munger, J. S., Huang, X., Kawakatsu, H., Griffiths, M. J., Dalton, S. L., Wu, J., et al. (1999). The integrin alpha v beta 6 binds and activates latent TGF beta 1: a mechanism for regulating pulmonary inflammation and fibrosis. *Cell, 96*(3), 319–328.

59. Busk, M., Pytela, R., & Sheppard, D. (1992). Characterization of the integrin alpha v beta 6 as a fibronectin-binding protein. *Journal of Biological Chemistry, 267*(9), 5790–5796.

60. Prieto, A. L., Edelman, G. M., & Crossin, K. L. (1993). Multiple integrins mediate cell attachment to cytotactin/tenascin. *Proceedings of the National Academy of Sciences of the United States of America, 90*(21), 10154–10158.

61. Huang, X., Wu, J., Spong, S., & Sheppard, D. (1998). The integrin alphavbeta6 is critical for keratinocyte migration on both its known ligand, fibronectin, and on vitronectin. *Journal of Cell Science, 111*(Pt 15), 2189–2195.

62. Sheppard, D. (2005). Integrin-mediated activation of latent transforming growth factor beta. *Cancer and Metastasis Reviews, 24*(3), 395–402. doi:10.1007/s10555-005-5131-6.

63. Annes, J. P., Rifkin, D. B., & Munger, J. S. (2002). The integrin alphaVbeta6 binds and activates latent TGFbeta3. *FEBS Letters, 511*(1-3), 65–68.

64. Singh, A., Greninger, P., Rhodes, D., Koopman, L., Violette, S., Bardeesy, N., et al. (2009). A gene expression signature associated with "K-Ras addiction" reveals regulators of EMT and tumor cell survival. *Cancer Cell, 15*(6), 489–500. doi:10.1016/j.ccr.2009.03.022.

65. Kang, H., Escudero-Esparza, A., Douglas-Jones, A., Mansel, R. E., & Jiang, W. G. (2009). Transcript analyses of stromal cell derived factors (SDFs): SDF-2, SDF-4 and SDF-5 reveal a different pattern of expression and prognostic association in human breast cancer. *International Journal of Oncology, 35*(1), 205–211.

66. Wang, B., Wang, W., Niu, W., Liu, E., Liu, X., Wang, J., et al. (2014). SDF-1/CXCR4 axis promotes directional migration of colorectal cancer cells through upregulation of integrin alphavbeta6. *Carcinogenesis, 35*(2), 282–291. doi:10.1093/carcin/bgt331.

67. Engl, T., Relja, B., Marian, D., Blumenberg, C., Muller, I., Beecken, W. D., et al. (2006). CXCR4 chemokine receptor mediates prostate tumor cell adhesion through alpha5 and beta3 integrins. *Neoplasia, 8*(4), 290–301. doi:10.1593/neo.05694.

68. Jones, J., Marian, D., Weich, E., Engl, T., Wedel, S., Relja, B., et al. (2007). CXCR4 chemokine receptor engagement modifies integrin dependent adhesion of renal carcinoma cells. *Experimental Cell Research, 313*(19), 4051–4065. doi:10.1016/j.yexcr.2007.07.001.

69. Xue, B., Wu, W., Huang, K., Xie, T., Xu, X., Zhang, H., et al. (2013). Stromal cell-derived factor-1 (SDF-1) enhances cells invasion by alphavbeta6 integrin-mediated signaling in ovarian cancer. *Molecular and Cellular Biochemistry, 380*(1-2), 177–184. doi:10.1007/s11010-013-1671-1.

70. Fedele, C., Singh, A., Zerlanko, B. J., Iozzo, R. V., & Languino, L. R. (2015). The alphavbeta6 integrin is transferred intercellularly via exosomes. *Journal of Biological Chemistry, 290*(8), 4545–4551. doi:10.1074/jbc.C114.617662.

71. Van Cutsem, E., & Costa, F. (2005). Progress in the adjuvant treatment of colon cancer: has it influenced clinical practice? *JAMA, 294*(21), 2758–2760. doi:10.1001/jama.294.21.2758.

72. Van Cutsem, E., Oliveira, J., & Group, E. G. W. (2009). Primary colon cancer: ESMO clinical recommendations for diagnosis, adjuvant treatment and follow-up. *Annals of Oncology, 20*(Suppl 4), 49–50. doi:10.1093/annonc/mdp126.

73. Liu, S., Wang, J., Niu, W., Liu, E., Wang, J., Peng, C., et al. (2013). The beta6-integrin-ERK/MAP kinase pathway contributes to chemo resistance in colon cancer. *Cancer Letters, 328*(2), 325–334. doi:10.1016/j.canlet.2012.10.004.

74. Liang, B., Shahbaz, M., Wang, Y., Gao, H., Fang, R., Niu, Z., et al. (2015). Integrinbeta6-targeted immunoliposomes mediate tumor-specific drug delivery and enhance therapeutic efficacy in colon carcinoma. *Clinical Cancer Research, 21*(5), 1183–1195. doi:10.1158/1078-0432.CCR-14-1194.

75. Zhao, Y. Z., Dai, D. D., Lu, C. T., Chen, L. J., Lin, M., Shen, X. T., et al. (2013). Epirubicin loaded with propylene glycol liposomes significantly overcomes multidrug resistance in breast cancer. *Cancer Letters, 330*(1), 74–83. doi:10.1016/j.canlet.2012.11.031.

76. Eberlein, C., Kendrew, J., McDaid, K., Alfred, A., Kang, J. S., Jacobs, V. N., et al. (2013). A human monoclonal antibody 264RAD targeting alphavbeta6 integrin reduces tumour growth and metastasis, and modulates key biomarkers in vivo. *Oncogene, 32*(37), 4406–4416. doi:10.1038/onc.2012.460.

77. Moore, K. M., Thomas, G. J., Duffy, S. W., Warwick, J., Gabe, R., Chou, P., et al. (2014). Therapeutic targeting of integrin alphavbeta6 in breast cancer. *Journal of the National Cancer Institute, 106*(8). doi:10.1093/jnci/dju169.

83

78. Lee, C., Lee, C., Lee, S., Siu, A., & Ramos, D. M. (2014). The cytoplasmic extension of the integrin beta6 subunit regulates epithelial-to-mesenchymal transition. *Anticancer Research, 34*(2), 659–664.

79. Weinacker, A., Chen, A., Agrez, M., Cone, R. I., Nishimura, S., Wayner, E., et al. (1994). Role of the integrin alpha v beta 6 in cell attachment to fibronectin. Heterologous expression of intact and secreted forms of the receptor. *Journal of Biological Chemistry, 269*(9), 6940–6948.

80. Cox, G., Steward, W. P., & O'Byrne, K. J. (1999). The plasmin cascade and matrix metalloproteinases in non-small cell lung cancer. *Thorax, 54*(2), 169–179.

81. Ahn, S. B., Mohamedali, A., Anand, S., Cheruku, H. R., Birch, D., Sowmya, G., et al. (2014). Characterization of the interaction between heterodimeric alphavbeta6 integrin and urokinase plasminogen activator receptor (uPAR) using functional proteomics. *Journal of Proteome Research.* doi:10.1021/pr500849x.

82. Pepper, M. S. (2001). Role of the matrix metalloproteinase and plasminogen activator-plasmin systems in angiogenesis. *Arteriosclerosis, Thrombosis, and Vascular Biology, 21*(7), 1104–1117.

83. Dutta, A., Li, J., Fedele, C., Sayeed, A., Singh, A., Violette, S. M., et al. (2015). alphavbeta6 integrin is required for TGFbeta1-mediated matrix metalloproteinase2 expression. *Biochemistry Journal, 466*(3), 525–536. doi:10.1042/BJ20140698.

84. Dang, D., Yang, Y., Li, X., Atakilit, A., Regezi, J., Eisele, D., et al. (2004). Matrix metalloproteinases and TGFbeta1 modulate oral tumor cell matrix. *Biochemical and Biophysical Research Communications, 316*(3), 937–942. doi:10.1016/j.bbrc.2004.02.143.

85. Allen, M. D., Thomas, G. J., Clark, S. E., Dawoud, M. M., Vallath, S., Payne, S. J., et al. (2013). Altered microenvironment promotes progression of pre-invasive breast cancer: myoepithelial expression of alphavbeta6 integrin in DCIS identifies high-risk patients and predicts recurrence. *Clinical Cancer Research.* doi:10.1158/1078-0432.CCR-13-1504.

86. Saldanha, R. G., Molloy, M. P., Bdeir, K., Cines, D. B., Song, X., Uitto, P. M., et al. (2007). Proteomic identification of lynchpin urokinase plasminogen activator receptor protein interactions associated with epithelial cancer malignancy. *Journal of Proteome Research, 6*(3), 1016–1028. doi:10.1021/pr060518n.

87. Sidenius, N., & Blasi, F. (2003). The urokinase plasminogen activator system in cancer: recent advances and implication for prognosis and therapy. *Cancer and Metastasis Reviews, 22*(2-3), 205–222.

88. Fishman, D. A., Kearns, A., Larsh, S., Enghild, J. J., & Stack, M. S. (1999). Autocrine regulation of growth stimulation in human epithelial ovarian carcinoma by serine-proteinase-catalysed release of the urinary-type-plasminogen-activator N-terminal fragment. *Biochemistry Journal, 341*(Pt 3), 765–769.

89. Xiong, J. P., Mahalingham, B., Alonso, J. L., Borrelli, L. A., Rui, X., Anand, S., et al. (2009). Crystal structure of the complete integrin alphaVbeta3 ectodomain plus an alpha/beta transmembrane fragment. *Journal of Cell Biology, 186*(4), 589–600. doi:10.1083/jcb.200905085.

90. Sowmya, G., Khan, J. M., Anand, S., Ahn, S. B., Baker, M. S., & Ranganathan, S. (2014). A site for direct integrin alphavbeta6.uPAR interaction from structural modelling and docking. *Journal of Structural Biology.* doi:10.1016/j.jsb.2014.01.001.

91. Weibrecht, I., Leuchowius, K. J., Clausson, C. M., Conze, T., Jarvius, M., Howell, W. M., et al. (2010). Proximity ligation assays: a recent addition to the proteomics toolbox. *Expert Review of Proteomics, 7*(3), 401–409. doi:10.1586/epr.10.10.

92. Thymiakou, E., & Episkopou, V. (2011). Detection of signaling effector-complexes downstream of bmp4 using PLA, a proximity

ligation assay. *Journal of Visualized Experiments,* (49), doi:10.3791/2631.

93. Blasi, F., & Sidenius, N. (2009). The urokinase receptor: focused cell surface proteolysis, cell adhesion and signaling. *FEBS Letters.* doi:10.1016/j.febslet.2009.12.039.

94. Blasi, F., & Carmeliet, P. (2002). uPAR: a versatile signalling orchestrator. *Nature Reviews Molecular Cell Biology, 3*(12), 932–943. doi:10.1038/nrm977.

95. Annes, J. P., Chen, Y., Munger, J. S., & Rifkin, D. B. (2004). Integrin alphaVbeta6-mediated activation of latent TGF-beta requires the latent TGF-beta binding protein-1. *Journal of Cell Biology, 165*(5), 723–734. doi:10.1083/jcb.200312172.

96. Klass, B. R., Grobbelaar, A. O., & Rolfe, K. J. (2009). Transforming growth factor beta1 signalling, wound healing and repair: a multifunctional cytokine with clinical implications for wound repair, a delicate balance. *Postgraduate Medical Journal, 85*(999), 9–14. doi:10.1136/pgmj.2008.069831.

97. Zambruno, G., Marchisio, P. C., Marconi, A., Vaschieri, C., Melchiori, A., Giannetti, A., et al. (1995). Transforming growth factor-beta 1 modulates beta 1 and beta 5 integrin receptors and induces the de novo expression of the alpha v beta 6 heterodimer in normal human keratinocytes: implications for wound healing. *Journal of Cell Biology, 129*(3), 853–865.

98. Van Aarsen, L. A., Leone, D. R., Ho, S., Dolinski, B. M., McCoon, P. E., LePage, D. J., et al. (2008). Antibody-mediated blockade of integrin alpha v beta 6 inhibits tumor progression in vivo by a transforming growth factor-beta-regulated mechanism. *Cancer Research, 68*(2), 561–570. doi:10.1158/0008-5472.CAN-07-2307.

99. Dutta, A., Li, J., Lu, H., Akech, J., Pratap, J., Wang, T., et al. (2014). Integrin alphavbeta6 promotes an osteolytic program in cancer cells by upregulating MMP2. *Cancer Research, 74*(5), 1598–1608. doi:10.1158/0008-5472.CAN-13-1796.

100. Khan, S. A., Joyce, J., & Tsuda, T. (2012). Quantification of active and total transforming growth factor-beta levels in serum and solid organ tissues by bioassay. *BMC Research Notes, 5*, 636. doi:10.1186/1756-0500-5-636.

101. Leipnitz, G., Miyashita, C., Heiden, M., von Blohn, G., Kohler, M., & Wenzel, E. (1988). Reference values and variability of plasminogen in healthy blood donors and its relation to parameters of the fibrinolytic system. *Haemostasis, 18*(Suppl 1), 61–68.

102. Dvorak, H. F. (1986). Tumors: wounds that do not heal. Similarities between tumor stroma generation and wound healing. *New England Journal of Medicine, 315*(26), 1650–1659. doi:10.1056/NEJM198612253151606.

103. Teicher, B. A., & Fricker, S. P. (2010). CXCL12 (SDF-1)/CXCR4 pathway in cancer. *Clinical Cancer Research, 16*(11), 2927–2931. doi:10.1158/1078-0432.CCR-09-2329.

104. Hoesel, B., & Schmid, J. A. (2013). The complexity of NF-kappaB signaling in inflammation and cancer. *Molecular Cancer, 12*, 86. doi:10.1186/1476-4598-12-86.

105. Agarwal, E., Brattain, M. G., & Chowdhury, S. (2013). Cell survival and metastasis regulation by Akt signaling in colorectal cancer. *Cellular Signalling, 25*(8), 1711–1719. doi:10.1016/j.cellsig.2013.03.025.

106. Roy, H. K., Olusola, B. F., Clemens, D. L., Karolski, W. J., Ratashak, A., Lynch, H. T., et al. (2002). AKT proto-oncogene overexpression is an early event during sporadic colon carcinogenesis. *Carcinogenesis, 23*(1), 201–205.

107. Bravou, V., Klironomos, G., Papadaki, E., Taraviras, S., & Varakis, J. (2006). ILK over-expression in human colon cancer progression correlates with activation of beta-catenin, down-regulation of E-cadherin and activation of the Akt-FKHR pathway. *Journal of Pathology, 208*(1), 91–99. doi:10.1002/path.1860.

108. Latella, G., Vetuschi, A., Sferra, R., Speca, S., & Gaudio, E. (2013). Localization of alphanubeta6 integrin-TGF-beta1/ Smad3, mTOR and PPARgamma in experimental colorectal fibrosis. *European Journal of Histochemistry, 57*(4), e40. doi:10.4081/ ejh.2013.e40.

109. Francipane, M. G., & Lagasse, E. (2014). mTOR pathway in colorectal cancer: an update. *Oncotarget, 5*(1), 49–66.

110. Arcaro, A., & Guerreiro, A. S. (2007). The phosphoinositide 3-kinase pathway in human cancer: genetic alterations and therapeutic implications. *Current Genomics, 8*(5), 271–306. doi:10.2174/ 138920207782446160.

111. Su, C. C., Lin, Y. P., Cheng, Y. J., Huang, J. Y., Chuang, W. J., Shan, Y. S., et al. (2007). Phosphatidylinositol 3-kinase/Akt activation by integrin-tumor matrix interaction suppresses Fas-mediated apoptosis in T cells. *Journal of Immunology, 179*(7), 4589–4597.

112. Fleming, N. I., Jorissen, R. N., Mouradov, D., Christie, M., Sakthianandeswaren, A., Palmieri, M., et al. (2013). SMAD2, SMAD3 and SMAD4 mutations in colorectal cancer. *Cancer Research, 73*(2), 725–735. doi:10.1158/0008-5472.CAN-12-2706.

113. Xie, W., Rimm, D. L., Lin, Y., Shih, W. J., & Reiss, M. (2003). Loss of Smad signaling in human colorectal cancer is associated with advanced disease and poor prognosis. *Cancer Journal, 9*(4), 302–312.

114. Najdi, R., Holcombe, R. F., & Waterman, M. L. (2011). Wnt signaling and colon carcinogenesis: beyond APC. *Journal of Carcinogenesis, 10*, 5. doi:10.4103/1477-3163.78111.

115. Wang, S., Liu, Z., Wang, L., & Zhang, X. (2009). NF-kappaB signaling pathway, inflammation and colorectal cancer. *Cellular and molecular immunology, 6*(5), 327–334. doi:10.1038/cmi. 2009.43.

116. Azare, J., Leslie, K., Al-Ahmadie, H., Gerald, W., Weinreb, P. H., Violette, S. M., et al. (2007). Constitutively activated Stat3 induces tumorigenesis and enhances cell motility of prostate epithelial cells through integrin beta 6. *Molecular and Cellular Biology, 27*(12), 4444–4453. doi:10.1128/MCB.02404-06.

1.4 Mass spectrometry based cancer proteomics

1.4.1 What is proteomics?

The term 'proteome' was used for first time Wasinger et al. in 1995 [330], to describe the entire complement of PROTEins encoded by any genOME. A year later, in 1996, Wilkins et al. [331, 332] used the term 'proteomics' to describe the study of proteomes of a cell or tissue, or an entire organism and their function. Since the coining of these terms, proteomics has evolved on a great scale which is partly attributed to the development of technologies to detect and study the said proteins.

The proteome of any organism is particularly dynamic, unlike the relatively static genome. This dynamic nature of the proteome can partly be ascribed to the ability of a single gene to code for multiple isoforms of a single protein. Gene sequences or even the mRNA expression levels cannot accurately predict this protein-level information. Various post-translational modifications (PTM) such as glycosylation, methylation and phosphorylation further enhance the molecular heterogeneity of the proteome and affect the structure and function of the individual proteins. Adding to the challenge, the composition of the proteome expressed is also affected by environmental factors, physiological state of the cell/organism and their response to stimuli at any given time.

Traditionally (20 years ago), proteins were sequenced by Edman degradation which was based on the principle of chemically cleaving an amino-terminus amino acid residue followed by identification [333]. However, any modifications to the amino-terminus of a protein makes it harder to sequence using Edman degradation and thus reducing its sensitivity of this technique. This lead to the adoption of mass spectrometry (MS) technique, which had existed and was used in chemistry laboratories since its invention by Nobel laureate Sir Joseph John Thomson in 1913 [334], to identify proteins based on their mass. The protein MS came to light with the discovery of Matrix-Assisted Laser Desorption/Ionization (MALDI) [335] and Electrospray Ionization (ESI) [336] methods in the 1980s which enabled identification of intact polypeptides and proteins. The revolution of MS-based proteomics research then was boosted by the development of the nanoscale reversed-phase liquid chromatography (nanoLC) [337], tandem mass spectrometry commonly referred to as MS/MS [338] and automated sequence database search engines like SEQUEST [339] and Mascot [340]. This basic platform allowed researchers to routinely identify and quantify several hundred to thousand proteins from within a complex mixture and is known as 'shotgun' or 'bottom-up' proteomics, **Figure 9**.
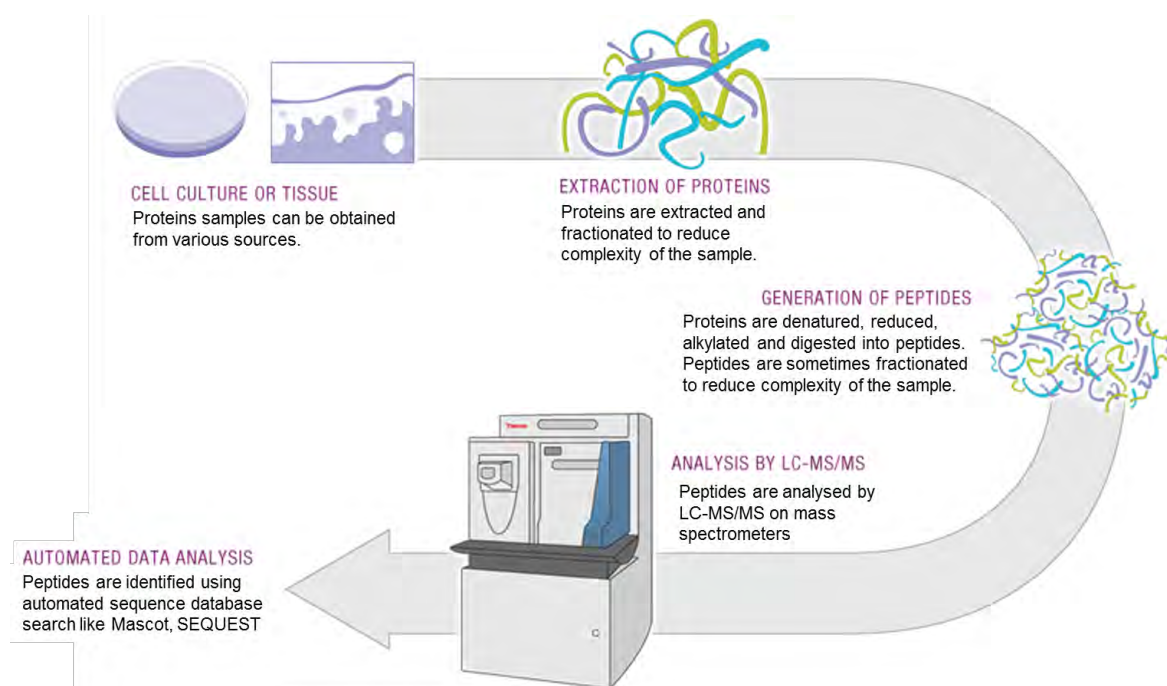
Figure 9 - Basic workflow of LC-MS/MS-based label-free shotgun proteomics. (Adapted from http://planetorbitrap.com/bottom-up-proteomics#.VYDzj_mqq2U).

In the past few decades, MS-based proteomics approaches have been extensively used in cancer research to identify proteins that may potentially be used as biomarker and/or drug targets. Hence, proteomics has become an important tool to discover new candidate biomarkers in CRC that may lead to the development of a diagnostic tools for clinicians and eventually address the complex molecular signatures that are associated with cancer (including CRC) and various diseases.

1.4.2 Colorectal cancer proteomics

Proteomics is capable of analysing the proteome deregulation associated with CRC. This can be achieved by analysing the complete proteome of a variety of samples that could reveal a subset of proteins and/or their associated pathways in CRC development, progression and metastasis. The modern proteomic technologies enable us to quantitate the changes in protein expression, protein modifications (PTM, turnover i.e. synthesis/degradation etc.) and the enzymatic activity related to CRC malignancy. Understanding these biological alterations in CRC using proteomics will allow researchers to map the molecular aspects of this disease in broad detail.

Very often CRC proteomics is performed using CRC cell lines, tissue samples and biological fluids. These studies are either performed alone or in combination to increase the confidence of the results observed. A few examples include: (a) comparison of normal epithelium

against cancerous cell lines; (b) comparison of two pathologically different CRC cell lines; (c) comparison of tissue biopsies and/or blood samples at various stage of disease progression. There could several potential combinations that could be used depending on the availability of the samples.

Human cell lines, tissues and biological fluids have been extensively explored in the quest for CRC-specific proteome changes. Often, but not always, cell lines are used as a starting point for studying cancer. Rarely, cell lines are prone to genotypic and phenotypic changes during culturing require continual assessment of their physiological and pathological relevance. Nevertheless, the unlimited sample availability and self-replicative potential of the cell lines allows researchers to re-examine a protein or pathway of interest to understand its role in CRC. Using cell lines, it is also relatively easy to perform genetic manipulations and study the associated changes. However, patient tissue samples and biological fluids have the highest pathological and physiological relevance to the disease but are hard to obtain, require large sample numbers to account for differences between individuals and have higher protein complexity. Therefore, cell line based studies make for a reasonable foundation on which other *in vivo* studies can be performed to test the performance of important molecules in the disease. This thesis utilizes three primary CRC cell lines (see **Table 9**) and their subclones to understand the biology of TGFβ in CRC. A few important MS-based proteomic studies in the recent years that use the same CRC cell lines in Table 9 and/or CRC patient plasmas are summarised in **Table 10**.

Table 9 Colorectal cancer cell lines used in this thesis[§]

Cell line	Description	Sub-clones	uPAR	β6	TGFβR1	TGFβR2
SW480	adenocarcinoma	Mock	+	-	+	+
		β6OE	+	+↑	+	+
HT29	adenocarcinoma, tumorigenic	Mock	+	+	+	+
		β6AS	+	+↓	+	+
HCT116	carcinoma, tumorigenic	WT	+	-	+	+
		uPAR-AS	+↓	-	+	+

[§] +, protein is expressed in the cell line; -, +, protein is not expressed in the cell line +↓, protein expression is stably down-regulated using plasmids; +↑, protein expression is stably up-regulated using plasmids

Table 10 Summary of recent MS-based proteomic studies performed using the CRC cell lines employed in this thesis; and CRC patient plasma/serum samples in the recent years.

Source of protein sample	Aim	Observed results and comments	Ref.
Cell line-based studies			
CRC cell line SW480 (does not express integrin β6 and SW480$^{OE\beta6}$ (stably expressing β6)	To understand how integrin αvβ6 mediated the EMT and invasive/metastatic phenotype.	74 and 60 unique proteins were identified in SW480$^{OE\beta6}$ and SW480 cell lines respectively. Important cell invasion related molecules integrins α2, α6, β1, β4, & β5, TGFβ1, CD44 and ephtin-b1 showed increased expression when β6 was expressed.	[149]
Primary SW480 cell line and lymph node metastatic variant SW620.	To identify differentially expressed proteins in whole cell lysates of SW480 and SW620 to understand molecular events of CRC metastasis.	94 down- regulated and 53 up- regulated in SW620 relative to SW480. Various cell adhesion proteins (β-catenin, NCAM1, L1CAM), cytoskeletal signalling proteins (KRT13, KRT23, tubulin-β 2A and 2B, actinin-α1, actinin-α4), cell migration inhibitor, annexin 2, and chaperones and heat shock proteins such as HSP90α and HSPH1 were down- regulated in the metastatic cell line cell line.	[341]
Primary SW480 cell line and lymph node metastatic variant SW620.	To identify potential CRC serum biomarkers through analysis of secretome of two CRC cell lines from same patient.	Reported 3 proteins TFF3, GDF15 and AGR2 to be secreted by the SW620 cells and TGM2, LCN2 and IGFBP7 were strongly expressed in SW480 cells. TFF3 and GDf15 were further examined using CRC serum and tissue samples and were reported to be associated with lymph node metastasis.	[342]
Five CRC cell lines (HT-29, Caco-2, Colo205, HCT116 and RKO).	Identification of cell surface protein biomarkers for CRC adenoma-to-carcinoma progression.	Identified EPHA1, GLUT1, ICAM1, BCAM, prion protein, SLC1A5 and HSD17B7. IHC analysis showed that GLUT1 and prion proteins to be associated with high-risk adenomas.	[343]

HCT116 cell line and its metastatic derivative E1.	To elucidate molecular mechanisms in metastasis by comparing complete proteome profiles of two CRC cell lines.	Reported over expression of DBN1, ANAX5, Lamin-A/C and TCTP in the E1 cells. High expression of DBN1 was shown by IHC analysis and they proposed further validation of this protein as a metastatic marker for CRC.	[344]
HCT8 (non-metastatic) and HCT116 cell lines.	To discover serological CRC markers by analysing the secretome of the two cell lines.	11 candidate marker proteins identified. Melanotransferrin (TRFM) was further validated in 130 plasma samples (CRC n=80; healthy n=30; other disease=20) which showed up-regulation in stages I & II of CRC compared with stages III & IV. The study suggests TRFM as a potential early serological marker.	[345]
Plasma/serum-based studies			
Serum (CRC n=91; stage I = 21, stage II = 41, stage III = 22 and IV = 7 and 33 healthy individuals).	To identify proteins involved tumourigenesis and non-invasive markers of CRC in serum.	COL1A1 and COL1A2 were most up-regulated in CRC relative to healthy controls and suggested that they might be involved in early CRC tumourigenesis and may serve as prognostic markers for CRC.	[346]
Plasma (n=32) Samples obtained from same patients at early time point (ET; before surgery) and late time point (LT; regular follow-up after surgery when distal metastasis was diagnosed).	To identify novel plasma biomarkers for CRC metastasis and to examine the possible biological relevance of the identified proteins in CRC cell migration.	Gelsolin, SERPINA3, SERPIND1, TF and C3 were increased in LT and PLG, APOA1 and F2 were decreased in LT. Further examination showed Gelsolin to be increased in plasma of more than 80% of CRC patients with distal metastasis and for stage IV vs stage I-III before treatment.	[347]
Plasma (n =90; CRC=31 and Controls=59).	To identify novel plasma biomarkers for early detection of CRC.	APOA1 and the ninth component of complement (C9) proteins were most significantly altered. C9 was proposed as a potential plasma marker for early CRC detection.	[348]

1.4.3 Protein sample preparation and handling

The separation and isolation of proteins from a cell line, tissue, or organism is the initial step in proteomics that is followed by proteolytic digestion, peptide clean-up and LC-MS/MS analysis. It is relatively easy to obtain a whole cell lysate (WCL) sample. However, WCL might be too complex for identification of certain proteins (e.g., membrane restricted proteins) which might by crucial during cancer. One of the challenges, therefore, before performing MS on a protein sample is to reduce its complexity. The complexity of WCL can be reduced by subcellular enrichment/fractionation and protein/peptide separation or both prior to MS.

Enrichment of specific proteome subsets such as proteins residing in the cytosol or membrane organelles or nucleus is important to address some specific research questions. This reduces the biological complexity of the proteome and allows examination of low abundance proteins which would, normally, otherwise not be observed by MS. The downside to this enrichment type proteomic studies is that they only reveal partial proteome. However, they are often the type of experiments that answer key biological questions and slowly but accurately lead to the mapping of key molecular aspects of the disease.

Subcellular fractionation of a WCL sample after homogenization can be efficiently performed through sucrose gradient centrifugation or liquid-liquid extraction method [349, 350]. The concept of liquid-liquid extraction is based on the differential solubility of various proteins in detergent/aqueous phases. For example, the hydrophobic membrane proteins are soluble mostly soluble in the detergent phase. This method is thought to preserve the integrity of the cytoskeletal networks if the enrichment is performed without homogenization of the cells [350]. In order to reduce the complexity of the protein samples, this thesis utilized the liquid-liquid principle to enrich for integral membrane proteins (IMPs). Briefly, the nuclear fraction is initially separated, from the cytosolic and microsomal fraction, by low speed centrifugation (2000g). The separation of microsomes from the cytosol is achieved by high speed centrifugation i.e., ultracentrifugation (120,000g), wherein the microsomes are pelleted. Now, the microsomal fraction can be enriched for IMPs either by 0.1 M sodium carbonate (pH 11.0) [351] or by triton X-114 phase partitioning [352]. The inherent challenges of working with membrane proteins include relatively low abundance, large dynamic protein range and low aqueous solubility. As described above, organic solvents and detergents can effectively solubilize membrane proteins to overcome the low aqueous solubility. However, they may be incompatible with LC-MS/MS and need to be completely removed prior to downstream analysis. Subcellular proteomics has been previously utilised

to study CRC. For instance, microsomes from CRC tissues have been analysed by proteomics [353, 354]. Cantor *et al.,* enriched and analysed the membrane proteome from SW480 CRC cells [149]; Kume *et al.,* enriched and analysed membrane proteins from CRC tissues samples to identify candidate biomarkers [355].

To further reduce the complexity of the protein samples, this thesis utilized strong cation exchange chromatography (SCX) to separate the peptides prior to analysing them on MS. Few other separation strategies include 1D or 2D gel electrophoresis, 2D differential gel electrophoresis (DIGE) and 1D and 2D off-line LC methods. In principle, the SCX stationary phase contains resins that are negatively charged in aqueous solution and therefore bind positively charged peptides or proteins. Most often, researchers use trypsin to proteolytically cleave proteins resulting in "tryptic" peptides. Most tryptic peptides have a net charge of $\geq$ 2+ and therefore can be separated by SCX [356]. The SCX also simultaneously removes any interfering substances (e.g., detergents, excess salts) that might affect the LC-MS/MS which makes it a very efficient method to use in MS-based proteomics.

1.4.4 LC MS/MS based proteomics

MS enables researchers to identify the mass of amino acid sequences and eventual identification of the associated peptide and its corresponding protein. MS can be divided into three main stages: (i) sample preparation (discussed in the previous section), (ii) sample ionization, and (iii) mass analysis.

Sample ionization

The ionization of biological samples for MS analysis is crucial and will result in charged and dry ions for analysis. Ionization is usually performed under high temperature and an electric field. This is accomplished by two most common methods – electrospray ionization (ESI) and matrix-assisted laser desorption/ionisation (MALDI). ESI was first introduced by Dole M et al., in 1968 [357] and later modified by Fenn *et al.,* in 1989 [336] and MALDI was introduced by Karas in 1987 [358]. ESI is a liquid phase ionization method where the analytes in the solvent are directly sprayed into the mass analysers. MALDI, however, relies on immobilising analytes in a matrix and then desorbed by a high energy laser for analysis. Both these methods rely upon the basic principle of converting peptides into ions by the addition or removal of one or more protons (H+). These methods result in the formation of ions without significant loss of sample integrity that allows accurate mass analysis of the peptides and proteins in their native state. As ESI was the primary method used in this thesis it will be discussed in detail below.

In ESI, the analytes in solvent flow into the orifice of the mass spectrometer through a microcapillary tube. The potential difference between the capillary and the inlet to the mass spectrometer at the orifice results in the generation of a fine mist of charged droplets. As the solvent evaporates it results in the accumulation of charged desolvated ions [359-361]. Most often MS is performed in positive ion mode simply due to the fact that most tryptic peptides are positively charged. The peptides can be doubly (2+) or triply (3+) or have higher positive charges. Furthermore, the commonly used solvent during MS analysis, 0.1% formic acid, acts as a proton donor to the basic functional groups of the peptides. The charged peptides, due to differential pressure and ion gradient, move into the mass analyser where they are separated based on their mass-to charge (m/z) ratio. The sensitivity of the ion detection depends on various factors such as the analyte concentration in the sample. The sensitivity can also be affected by any contaminants such as polymers and salts in the sample which can result in ion suppression and may lead to incorrect mass determination.

Mass Analysers

As the basic principle of mass spectrometry relies upon accurately reporting the mass of a molecule, it is a crucial component of the mass spectrometer. Mass analysers store and resolve the ions on the basis of their mass and charge in a vacuum. There are three types of mass analysers; a) Quadrupole mass analyser, b) time-of-flight (TOF) and c) ion trap (IT). Each mass analyser uses a different principle for measuring the mass of the ion. Quadrupole uses the m/z stability of the ion, the TOF uses the differential ion flight time and IT uses the m/z resonance frequency. Each mass analyser has unique performance characteristics such as resolution, mass accuracy, sensitivity, scan rate, and dynamic range [362]. The proteomic experiments in this were performed on an ABSCIEX 5600 TripleTOF which is a hybrid triple quadrupole TOF platform and therefore, the quadrupole and TOF mass analysers will be further discussed.

Quadrupole analysers are one of the most common mass analysers used. The principle of a quadrupole mass analyzer was first described in the 1950s by Paul Wolfgang [359]. Here, the desolvated ions are pulsed toward the detector by an electric field, in the range of 5 Kv, created by an array of four parallel metal rods called quadrupole [363]. The quadrupoles can also be used as mass filter whereby they only allow ions of certain m/z ratio. Therefore, combining more than one quadrupole allowed researchers to obtain information of sequence of amino acids in a peptide. This lead to the development of triple quadrupoles which had exceptional quantitative capabilities.

The ion separation principle in the TOFs is one of the simplest and was first described in the mid-20th century [364] and it was not until 1995 when it was rediscovered byBrown and Lennon [365]. It simply measures the m/z ratio of an ion by determining the time required for it to traverse the length of a flight tube. Some TOF setups have an ion mirror after the flight tube which can serve to increase the path length and correct for any small energy differences among the ions [366]. These factors contribute to increase in mass resolution when using TOFs. In addition, TOF analysers also allow the analysis of all the ions present in samples, as every ion has a charge and will eventually complete its flight and reach the detector, which is a key advantage [359]. The ABSCIEX 5600 TripleTOF used in this thesis has the quantification capabilities similar to triple quadrupoles and the high resolution with the speed and sensitivity of a TOF making it an excellent tool for proteomic studies.

1.4.5 Shotgun Quantitative proteomics using iTRAQ

The quantitative measurement of proteins along with qualitative information is crucial when comparing different proteomic samples. Quantitation in proteomics can be achieved in two ways – the non-targeted approach, where all the peptides identified by MS can be quantitated; and the targeted approach, where a selected list of peptides are quantitated. Non-targeted approaches generally use data dependant acquisition (DDA) method to analyse the peptides. In the recent years, data independent acquisition (DIA), especially SWATH MS, is being increasingly performed to analyse complete proteome in a sample [367]. Targeted approach methods such as single/multiple reaction monitoring (SRM/MRM) have also seen increasing use in cancer research [355].

Shotgun proteomics has grown to be the most common proteomics methods to analyse complex protein samples. Most often researchers choose to perform label-free proteomics as described previously, which does not require them to label their peptides samples before analysing them on a mass spectrometer and the results are not directly quantifiable. Quantitative proteomics approaches that utilize labelling techniques include isobaric Tag for Relative and Absolute Quantization (iTRAQ) [368], isotope coded protein labels (ICAT) [369], stable isotope labelling by amino acids in culture (SILAC) [370] and 18O-labelling [371]. The proteomic experiments in this thesis were performed using iTRAQ shotgun approach (see **Figure 10**), which enabled high-throughput proteomic analysis. Key advantages of iTRAQ include: a) iTRAQ reporter ions allow simultaneous identification and quantification of peptides/proteins in the sample, which is one of the key advantages; b) it allows multiple sample analysis in single MS run (from a minimum of 2 upto 8 samples); c) all tryptic peptides are labelled resulting in increased confidence and higher quality data; d)

improves MS/MS fragmentation and results in more confident peptide/protein identifications; and e) analysis of PTMs is possible [372]. A key disadvantage of iTRAQ-based proteomics is the requirement of more MS time due to the increased peptide numbers as multiple samples are combined into a single sample [372]. However, this can be easily controlled by decreasing the complexity of the sample by fractionation prior to MS.
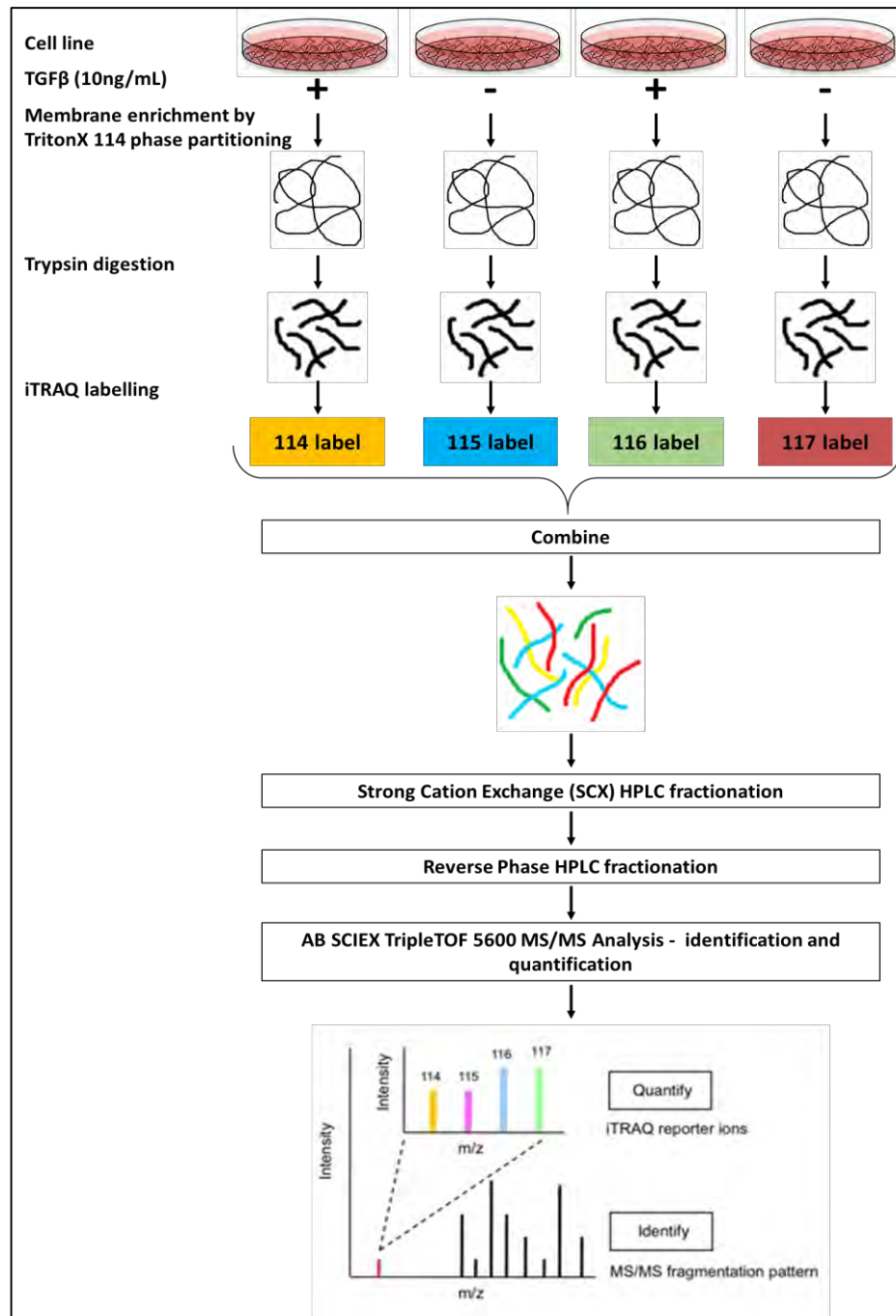
Figure 10 - Basic workflow of iTRAQ based proteomics experiments. Image modified from [373].

In brief, crude protein mixture from various samples (2 to 8 samples) is extracted from cultured cells and enriched for membrane proteins. The protein sample is then reduced, alkylated and enzymatically (using trypsin) digested into peptides. These peptides are then labelled on primary amines using 4- or 8-plex isobaric reagents. The labelled samples are then fractionated using SCX. The peptide mixture is then delivered to the ionisation chamber after the HPLC, where the iTRAQ reporter ions are detected and analysed. The MS/MS spectra obtained from the ABSCIEX Triple TOF 5600 were used to simultaneously identify and quantify the peptides and proteins using ProteinPilot^{TM}.

1.4.6 Bioinformatics tools for Data analysis

Proteomic experiments often generate vast amounts of complex data making them complicated to handle. Further adding to the complexity is the origin of the data from a various vendor specific instruments and different acquisition methods. The analysis of large amounts of data form proteomics experiments requires powerful bioinformatics tools to assist in identification, quantitation and other downstream analysis of proteins observed in the experiments. Bioinformatics tools such as protein databases, sequence comparison programs and various statistical tools make the analysis of complex proteomic datasets possible and are briefly discussed. The primary step in after mass spectrometry is to match peptide fragment spectra to their corresponding peptides and subsequently to proteins. This is primarily done by searching the acquired spectra protein against databases that match peptides based on similarity, although other methods do exist. The most commonly used database search engines include SEQUEST, Mascot and X! Tandem. These search engines allow mining for peptide or protein matches from various protein databases like National Center for Biotechnology Information (NCBI), SwissProt, Ensemble and International Protein Index (IPI). The search engines also allow researchers to set various limits prior beginning the search. Some of those limits include peptide mass tolerance, enzyme specificity, inclusion or exclusion of specific modifications and most importantly the target proteome to search against. The search engines then generate list of peptides assigned to the quarried MS/MS spectra and their associated proteins.

This peptide and protein list is usually accompanied by correlation scores (e.g., *Xcorr* for Sequest and *Evalue* for Mascot) which indicate the degree of similarity between the experimental and theoretical data; this assessment provides essentially a measure of confidence of the annotation. However, the database search engines assign peptides to MS/MS spectra irrespective of the data quality. Therefore, identification of peptide and proteins from high quality MS/MS spectra (high signal-to-noise and peptide sequence

coverage) is required to reduce the number of 'false-positive' identifications and obtain a statistical valid list of 'true-positive' identifications. The confidence of identification is measured by determining the false discovery rates (FDR), which is a measure to estimate the annotation error. Typically, FDR is calculated immediately after peptide and protein identification. Very often an FDR of 1-5% is used in proteomics experiments.

In this thesis, ProteinPilot™ that employs a robust Paragon™ algorithm [374] was used for identification of peptides and proteins from the MS/MS spectra obtained from ABSCIEX Triple TOF 5600. Additionally, the integrated FDR analysis reported to us the quality of protein and peptide identifications [375]. A typical result for iTRAQ data from protein pilot will show **N:** rank of a particular protein in respect to the other proteins identified; **Unused:** the "protscore" for a particular protein; **Total:** the "protscore" for a particular protein using all of the available peptides identified for that specific protein; **%Cov(95)**: the number of amino acids matching the identified protein sequence with confidence greater than 95%, divided by the total number of amino acids in the protein; **Accessions:** protein accession number from SwissProt protein sequence database; **Name**: protein sequence name; **Species**: shows the taxonomy of the protein; **Peptide(95%)**: the number of distinct peptides have at least 95% confidence; **Protein ratios/fold change**: the ratio of average areas measured for the respective protein ions between various labels; and ***p*-value**: from a paired t-test on the average of the areas measured. Other details such as modifications, precursor molecular weight and precursor m/z can also be obtained by manually selecting the output file options in ProteinPilot™.

Once the list of proteins is obtained, they can further be used to understand the biological relevance using functional annotation and/or pathway/network analysis tools. Some such tools include, STRING functional protein association networks (http://string-db.org/), Reactome pathway database (http://www.reactome.org/), KEGG pathway database (http://www.genome.jp/kegg/pathway.html), WEGO gene ontology annotation tool (http://wego.genomics.org.cn/cgi-bin/wego/index.pl), Ingenuity pathway analysis (IPA) (http://www.ingenuity.com/products/ipa), DAVID Functional Annotation Tool (http://david.abcc.ncifcrf.gov/), Pathway commons (http://www.pathwaycommons.org/) and ConsensusPathDB (http://cpdb.molgen.mpg.de/). IPA was used for pathway analysis of proteomic data in this thesis. The public repositories such as the ProteomeXchange (PX) consortium (http://www.proteomexchange.org/) and the PRIDE (PRoteomics IDEntifications) database (http://www.ebi.ac.uk/pride/archive/) for MS/MS spectral data

will enable researches to more confidently re-identify or re-assess a data set for more possible outcomes and will be crucial for the growth of proteomics.

1.5 Aims of the thesis

Several studies have also reported the involvement of TGFβ in cancer but there was no direct evidence to support this observation in CRC. A previous membrane proteomic study in our group) using SW480 cells which observed differential expression of TGFβ1 (↓2.9 fold) and TGFβR1 (↑>3.0 fold) when β6 was expressed. These interesting observations instigated the investigation of TGFβ and its role in regulating CRC related processes in a β6 and uPAR dependent manner.

The overall aim of this thesis was to expand the knowledge on the biology of TGFβ in CRC. This was achieved by employing state-of-the-art proteomics, cell signalling assays (i.e., AlphaScreen® SureFire® Assay) and multiplexing technologies (i.e., Proseek Multiplex Oncology I kit), in conjunction with sophisticated bioinformatics. The samples investigated in this thesis comprised of a panel of cultured human CRC cells and clinically staged CRC plasma samples.

Aim I: The first project of this thesis, a signalling study, aimed to evaluate whether expression of the β6 integrin subunit enhances the ability of CRC cells to activate recombinant zymogen TGFβ and plasmin as part the novel uPAR/αvβ6/TGFβ1 interactome. This study identified that expression of β6 integrin clearly increased the proliferation and invasion of the cells when treated with L-TGFβ and was sustained through increased Erk1/2 signalling. *(Publication IV - This work has been prepared for publication)*.

A subsequent iTRAQ-based proteomic approach was employed to explore the effects of TGFβ and its signalling on colon cancer cells that express varying levels of β6 integrin. This study was able to successfully identify various cancer related molecules and networks to be significantly altered upon TGFβ treatment. (*Publication III - This work has been prepared for publication).*

Aim II: The subsequent project then aimed to characterise proteome changes of HCT116 colon cancer cells, with differential expression of urokinase-type plasminogen activator receptor (uPAR), treated with active TGFβ1. The results from this study, demonstrate that expression of uPAR induces differential up- and down-regulation of several cancer related proteins and signalling pathways such as eIF2. (*Publication V - This work has been prepared for publication).*

Aim III: The final study of the thesis aimed to investigate the expression of LAP-TGFβ1 using an immune based analysis of EDTA-plasma samples from Dukes' stage A-D patients (n=60) and unaffected controls (n=15). The results showed no significant difference for LAP-TGFβ expression. However, the study identified three biomarkers (CEA, IL-8 and prolactin) that can significantly differentiate the unaffected controls from non-malignant (Dukes' A + B) and malignant (Dukes' C + D) stages. The findings from this study (**Publication VI**) have been published the journal of Clinical Proteomics.

During the course of this PhD project, a secondary aim that significantly contributed to determining the interaction site of uPAR and β6 integrin was also undertaken and these findings have been published in the Journal of Proteome Research (**Publication VII; Appendix II**).

Overall, the findings from this thesis (aim I and II) have reported several molecules to be deregulated in favour of or against cancer progression upon TGFβ treatments. These results will be crucial to understand the biology of TGFβ in the context of uPAR/αvβ6/TGFβ1 interactome. Additionally, the plasma study (aim III) identified CEA, IL-8 and prolactin as potential CRC biomarkers. It is believed that the results from this thesis will contribute to the effort of understanding the biology of TGFβ in cancer and aid in the development of new diagnostic and therapeutic tools to combat global CRC health burden.

CHAPTER 2: METHODS

More detailed information on the methods used in this thesis are available in the respective chapter or its associated publication in that chapter.

Method	Used in Chapter (in publication)
Proliferation assay	3,4 (III, IV, V)
Wound healing assay	3 (III)
Invasion assay	3, 4 (III, IV, V)
Cell culture	3,4 (III, IV, V, VII, VIII)
Triton X-114 phase partitioning	3,4 (III, V)
Ingenuity Pathway Analysis	3,4 (III, V)
iTRAQ-labelling	3,4 (III, V)
Strong cation exchange chromatography	3,4 (III, IV, V)
NanoLC Chromatography	3,4 (III, IV, V)
Western blotting	3,4 (III, IV, V, VII, VIII)
AlphaScreen® SureFire® assay	3 (IV)
Bio-Plex Pro™ human cytokine 27-plex immunoassay	5 (VI)
Proseek® Multiplex Oncology I proximity extension assay	5 (VI)
Immunoprecipitation	(VIII)

CHAPTER 3

This chapter incorporates two studies that are crucial for understanding the associations of TGFβ and integrin β6 in CRC biology.

3.1 - Study I:

The first study in the chapter aimed to explore the ability of β6 integrin subunit to activate recombinant L-TGFβ and plasminogen as part the novel uPAR/αvβ6/TGFβ1 interactome. This study was performed using SW480 and HT29 subclone cells that differentially express β6 integrin. This differential expression of β6 was achieved through stable cDNA transfection. Preliminary cell based studies after addition of L-TGFβ and plasminogen (PLG) showed high β6 expression resulted in increased proliferation and invasion. Surprisingly, the investigation of cell signalling activity using AlphaScreen® SureFire® assays showed higher Erk1/2 activity when the cells expressed any amount β6. The study also showed a switch in signalling from Smad to Erk when treated with plasminogen. Overall, these observations suggests that αvβ6 expression can utilize both L-TGFβ and plasminogen to induce phenotypic changes involved in cancer progression through sustained Erk1/2 activity.

3.1.1 - Expression of αvβ6 integrin enhances both plasminogen and latent-transforming growth factor-β1 dependant proliferation, invasion and ERK1/2 signalling in colorectal cancer cells. [Publication III] (*Prepared for publication*)

Expression of αvβ6 integrin enhances both plasminogen and latent-transforming growth factor-β1 dependent proliferation, invasion and ERK1/2 signalling in colorectal cancer cells

Cantor DI, Cheruku HR, Ahn SB, Crouch MF[†], Nice EC[§] and Baker MS[*].

Australian School of Advanced Medicine, Macquarie University, NSW, 2109 AUSTRALIA

[†] TGR Biosciences, Thebarton, South Australia, 5031, AUSTRALIA

[§] Monash University, Clayton, Victoria, 3800

*Corresponding Author: Prof. Mark Baker

Mailing address:

Level 1, 75 Talavera Rd

Australian School of Advanced Medicine

Macquarie University, NSW, 2109

AUSTRALIA

Phone: +61 2 9850 8211

Fax: +61 2 9812 3600

Email: mark.baker@mq.edu.au

ABSTRACT

The αvβ6 integrin, urokinase-type plasminogen activator receptor (uPAR) and transforming growth factor-β1 (TGF-β1) are crucial proteins involved in the progression of colorectal cancer (CRC) towards metastasis. Commonly upregulated in epithelial cancers, αvβ6 enhances metastatic cell attributes including proliferation, invasion, adhesion and the epithelial-mesenchymal transition (EMT). αvβ6 is suggested to physically interact with uPAR and the latency-associated peptide of TGF-β1, potentially influencing the activation of the latent TGF-β1 (L-TGFβ1) and plasminogen (Plg) zymogens. Following activation, the binding of active TGF-β1 to its receptors can initiate an amplification cascade, upregulating αvβ6 and uPAR expression through the Ets-1 transcription factor. Alternatively, αvβ6 can interact with ERK2-P through a unique C-terminal tail, promoting the plasminogen activation (PA) cascade and mitogen-activated protein kinase (MAPK) signalling pathways. The present study investigated whether αvβ6 expression enabled CRC cells to activate zymogen members of these proteolytic and growth factor pathways, inducing phenotypic changes necessary to facilitate pro-metastatic transformation. Cell-

34   based assays and signalling activity studies determined that treatment with recombinant L-

35   TGFβ1 and/or Plg significantly enhances metastatic activities in a αvβ6-dependent manner.

36   β6-overexpressing cells treated with L-TGFβ1 and/or Plg were significantly more

37   proliferative, invasive and maintained higher ERK1/2 signalling activity compared to

38   untreated control cells. In contrast, stable anti-sense suppression of β6 by ~80% did not

39   reduce the β6-dependent increases in ERK1/2 signalling activity observed when treated with

40   L-TGFβ1 and/or Plg, indicating that residual β6 could compensate for the activation. This

41   study provides evidence of a "switching" from SMAD to ERK signalling following Plg

42   treatment, promoting the metastatic phenotype.

43   **KEYWORDS:** β6 integrin; colorectal cancer; epithelial-mesenchymal transition;

44   metastasis; latent transforming growth factor-β and plasminogen activation.

45   **Abbreviations**

46   BME; basement membrane extract. BSA; bovine serum albumin. ECM; extracellular

47   matrix. EDTA; Ethylenediaminetetraacetic acid. EGF; epidermal growth factor. EMT;

48   epithelial-mesenchymal transition. ERK1/2; Extracellular signal-regulated kinase ½. FBS;

49   foetal bovine serum. HRP; horse radish peroxidase. L-TGFβ1; latent transforming growth

50   factor-β1. MAPK; mitogen-activated protein kinase. MMP; matrix metalloprotease. PA;

51   Plasminogen activation (cascade). Plg; plasminogen. PBS; phosphate buffered saline.

52   PVDF; Polyvinylidene fluoride. RPMI; Roswell Park Memorial Institute. SF; serum-free

53   (media). TBS; tris-buffered saline. TGF-β; transforming growth factor-β. VEGR; vascular

54   endothelial growth factor. uPA; urokinase-type plasminogen activator. uPAR; urokinase-

55   type plasminogen activator receptor.

56   **1. INTRODUCTION**

57   The β6 integrin subunit of the αvβ6 integrin heterodimer (β6) has long been

58   implicated as a marker of metastatic progression in colorectal cancer (CRC). Several studies

59   link β6 expression with progression towards a more aggressive, invasive and/or metastatic

60   phenotype.[1-6] The αvβ6 integrin is a member of a family of heterodimeric cell-surface

61   receptors composed of one of eighteen (18) α- and eight (8) β-subunits[2] which collectively

62   mediate cellular adhesion to ECM substrates.[1, 7] Each α/β heterodimer combination confers

63   a particular binding specificity and signalling properties.[8] The β6 subunit, when bound to

64   its sole binding partner αv, is an epithelial cell-restricted antigen whose expression is

elevated during tissue remodelling events (e.g., wound healing, fibrosis) and in epithelial cancers during EMT, where it is almost invariably localized to the invasive fronts and infiltrating edges of tumour islands.[1, 5, 9] Recent immunohistochemistry studies have demonstrated that elevated β6 expression negatively correlates with CRC patient survival[6], ascribing this to be mediated through β6's roles promoting cell proliferation, migration and invasion into proximal tissues and eventual metastasis.[1, 2, 6, 10, 11]

A recent membrane-enriched proteomic study by our group identified that deliberate β6 neo-expression into a non-expressing cell line induced a significant change in the expression of 708 proteins, including 54 potential cancer biomarkers flagged by the American Society of Clinical Oncology for clinical applications (e.g., diagnosis, prognosis, progression and response to therapy).[12] We determined that 134 proteins were observed solely in either the β6-transfected or mock subclone, potentially indicating a biosignature of proteins expressed/repressed in response to β6 expression.[12] Ingenuity Pathway Analysis© of the proteomic datasets revealed that the protein networks and functions most strongly affected by β6 expression were fundamentally involved in cancer metastasis. These functions included; (*i*) cell death, (*ii*) cellular movement, (*iii*) cancer phenotype, (*iv*) cell cycle, and (*v*) cellular growth/proliferation.[12] Based on the expression of signalling pathway members, the integrin-linked kinase and Ran signalling pathways were identified as being significantly different between the SW480$^{\text{Mock}}$ and SW480$^{\beta6\text{OE}}$ colorectal cancer cell lines as well as individual proteins found in the MAPK and Wnt/β-catenin signalling pathways.[12] Interestingly, expression of all other integrin subunits (with the exception of β6's binding partner αv) decreased (i.e., α2, α6, β4 and β5 ↓ significantly) indicating the potential existence of a subunit hierarchy. Migration and proliferation studies recapitulated previous findings demonstrating that β6 integrin expression significantly increased proliferation of SW480 cells.[12] These cells were observed to adopt a gross cellular morphology more similar to mesenchymal cells (i.e., flattened, elongated, pointed and spindly) when compared with the more classical rounded, cobble-stoned appearance of mock transfectants.[12] SW480 cells expressing β6 were significantly more capable of invasively migrating through an ECM-coated polycarbonate membrane, analogous to the epithelial tissue basement membrane.[12] Together, these findings strongly suggest that EMT is promoted by expression of the β6 integrin. This process is suspected to be driven through interaction/s between the αvβ6 integrin, uPAR and TGF-β1. This interaction axis may function to sequester key

97   metastasis-related proteins to the infiltrating edge of tumour islands, thereby concentrating

98   immediate and downstream signalling/proteolytic activity to the invasive front of a CRC

99   tumour.

100   The αvβ6 integrin anchors the latent TGF-β1 complex (LTGF-β1) to the extracellular

101   matrix (ECM), where it provides the necessary traction force to liberate TGFβ1 from its

102   zymogen complex.[13] Once released, active TGF-β1 can promote cellular migration and

103   metastatic transformation in late-stage CRC.[6, 13, 14] Active TGF-β1 promotes

104   phosphorylation and translocation of the SMAD2/3 signalling complex, which induces

105   target genes involved in cell migration and proliferation, including the *de novo* expression

106   of αvβ6.[15, 16] In parallel to activation by integrins, L-TGFβ1 can also be activated through

107   the PA cascade where uPAR binds urokinase-type Plg activator (uPA) which cleaves Plg

108   into active plasmin which subsequently can cleave and activate L-TGFβ1 by proteolysis.[17]

109   Saldanha et *al.* demonstrated that αvβ6 co-immunoprecipitates with uPAR whilst others

110   have shown that αvβ6 co-regulates proliferation through direct interactions with the MAPK

111   signalling pathway[18] (specifically pERK2). β6 expression promotes the activation of PA

112   and matrix metalloprotease (MMP) cascades through uPA and MMP family members,

113   MMP-2, MMP-3 and MMP-9.[14, 19] Interestingly, MMP-3 and MMP-9 activation was

114   enhanced following treatment with TGF-β1, indicating even further cross-reactivity within

115   this novel interactome.[19] We suggest that αvβ6 expression forms a structural foundation

116   allowing formation of a pericellular interactome, effectively concentrating TGF-β1 and PA

117   cascade activity to the cell surface. To test whether this interactome was present and capable

118   of promoting metastatic activities in αvβ6-expressing cells, we introduced relatively low

119   pathophysiological concentrations (10ng/mL) of LTGF-β1 and/or Plg compared to the

120   normal levels in human plasma (LTGF-β 136ng/mL[20]; Plg 200ng/mL[21]). These

121   concentrations were chosen to highlight the potency of the novel interactome and its ability

122   to transform relatively small concentrations of abundant zymogens in plasma into

123   significantly enhanced metastatic activity. This project aimed to determine whether

124   expression of the β6 integrin subunit enhances the ability of CRC cells to activate/implement

125   recombinant zymogens as part the novel uPAR/αvβ6/TGF-β1 interactome *in cellulo*

126   resulting in phenotypic changes crucial for metastatic progression.

127   **2. Methods and Materials**

2.1 Antibodies and reagents

This study used the commercially available ERK1/2, SMAD2 and Akt1/2/3 AlphaScreen® SureFire® assay kits (TGR Biosciences, Cat. No.'s TGRES500, TGRSM2S500 and TGRA4S500) to detect relative ERK1/2, SMAD2 and Akt1/2/3 phosphorylation respectively. All kits contained a biotinylated antibody that recognises the active phosphorylated epitope (e.g. pERK1/2, phospho-Thr202/Tyr204) and a non-biotinylated antibody that recognises a distal epitope. An anti β-actin monoclonal mouse antibody was purchased from Sigma Aldrich (Cat. No. A3854) and HRP-conjugated in-house for loading controls.[12] A monoclonal rabbit anti-human uPAR antibody was purchased from American Diagnostica (Cat. No. 3932). The inhibitors of TGFβ signalling (SB-431542; Cat. No. S4317-5MG) and plasmin (aprotinin; Cat. No. A3428) were purchased from Sigma Aldrich Australia.

2.2 Cell lines

Two Duke's stage B epithelial CRC cell lines were employed throughout this project. SW480 cells which lack endogenous β6 expression were initially established by Leibovitz et al.[22] These cells were stably transfected with a vector containing either the full-length β6 subunit coding sequence (i.e., SW480^{β6OE}) or an 'empty' vector (i.e., SW480^{Mock}) as previously described.[3] HT29 cells endogenously express the β6 integrin[4] and have been stably transfected with a vector containing either the β6 cDNA sequence in an antisense orientation (HT29^{β6AS}) or with an 'empty' vector (HT29^{Mock}) as previously described.[4] β6 expression in HT29^{β6AS} was found to be reduced by ~80% using flow cytometry.[4] Each cell line has been determined as "invasive" using Matrigel invasion assays[23] and has been previously found to express both uPAR and transforming growth factor-β1 receptor 1/2 (TGFβR1/2).[12, 24] All cell lines tested negative for *Mycoplasma* infection using the PCR-based VenorGeM Mycoplasma Detection Kit (Minerva Biolabs).[12] SW480^{Mock} and SW480^{β6OE} cells were cultured in Dulbecco's Modified Eagle Medium (DMEM; Invitrogen) supplemented with 10% foetal bovine serum (FBS) and 500μg/mL geneticin (G418 sulphate, Life Technologies). HT29^{Mock} and HT29^{β6AS} subclone cells were cultured in Roswell Park Memorial Institute medium (RPMI; Invitrogen) supplemented with 10% FBS and 2.5μg/mL puromycin (Life Technologies). Both cell lines were incubated at 37°C in 5% CO_2. Serum-free (SF) media represents 0% FBS but contains selective reagents for respective cell lines.

159 **2.3 Recombinant protein treatment protocol**

160   Recombinant, carrier-free, human L-TGFβ1 and Plg were purchased from R & D

161 Systems. Standardised recombinant protein treatments were employed for each assay.

162 Freshly passaged CRC subclones were seeded and incubated in serum-containing media for

163 24hr. Cells were washed in 1x phosphate-buffered saline (PBS) and incubated in SF media

164 for 24hrs prior to treatment with recombinant proteins followed by incubation for the time

165 period required for each assay. Four treatment conditions were employed in this study: 1)

166 SF media as a negative control; 2) SF media + 10ng/mL L-TGFβ1; 3) SF media + 10ng/mL

167 recombinant Plg; and 4) SF media + 10ng/mL L-TGFβ1 + 10ng/mL Plg. All comparisons

168 were performed against untreated mock controls and are presented as a percentage of the

169 untreated mock transfectant control. All treatments were performed in biological triplicate

170 and experiments were independently repeated at least two times. Statistical testing for

171 significance was performed using a Student's T-test with a significance cut-off of $p<0.05$.

172 **2.4 Proliferation assay**

173   Either 1×10^5 (SW480) or 5×10^4 (HT29) cells were seeded into each well of a six-

174 well plate and prepared for recombinant protein treatment as outlined above. The cells were

175 incubated in the presence of recombinant proteins for either 24hrs or 48hrswithout

176 replacement of the media. Cells were gently detached by trypsinization, mixed (1:1) with

177 0.4% Trypan Blue and the live cells enumerated using a BioRad TC-10^{TM} automated cell

178 counter. It should be noted that the trypan blue exclusion measures the steady state balance

179 between cell viability and proliferation does not measure cell death. Proliferation rate and

180 doubling time calculation methods are outlined in Supplementary Information. The

181 proliferation assay was then repeated and SW480 cell lines treated for 24hrs with specific

182 inhibitors of TGFβ (SB-431542) and/or plasmin (aprotinin) activity to a final concentration

183 of 10μM and 0.3μM respectively.

184 **2.5 Morphology assay by confocal microscopy**

185   Freshly passaged SW480 cells were seeded into each well of a Lab-Tek Chambered

186 coverglass plate (Thermo Fisher) and prepared for recombinant protein treatment as outlined

187 above. After 24hr incubation in the presence of L-TGFβ1 and/or Plg, cells were washed with

188 1x PBS and fixed with 2% paraformaldehyde in PBS for 10min at room temperature. Cells

189 were permeablised with 0.1% Triton X-100 in PBS for 5min before blocking in 1% BSA for

20min at room temperature. Fixed cells were stained with a 20nM Alexa phalloidin solution for 20min at room temperature and washed in PBS. Nuclei were counterstained with Hoechst solution (2µg/mL) and washed again with PBS. Confocal microscopy was performed using an Olympus Fluoview 300 Confocal Laser Scanning system equipped with an inverted microscope (IX70, Olympus Tokyo).

2.6 Wound-healing assays

Freshly passaged SW480^{Mock} or SW480^{β6OE} cells were seeded into a six-well plate and incubated in serum media for 24hr as part of the recombinant treatment protocol. After a 24hr incubation in SF media, a confluent monolayer had formed and each well was horizontally scraped with a 10µL pipette tip (diameter 0.35mm) to create a scratch and gently washed with PBS to remove any suspended cells. PBS was aspirated and replaced with SF media containing the respective zymogen. Cells were incubated in the presence of the recombinant proteins for 24hr and the 'wounds' imaged using 10x objective of a Leica DM-IL microscope with a Leica DFC280 digital imager. Three images were taken at random along the scratch in each well. Four scratch width measurements were taken at pre-set quarter marks for each image using the ImageJ analysis program (*http://rsbweb.nih.gov/ij/index.html*). Scratch measurements were taken from the leading cell edge only and cells that had formed islands within the scratch were excluded. Because of high variability due to differences in cell shape, the median scratch width measurement was taken for each image and used for statistical analysis as it is less susceptible to outliers.

2.7 Migration and Matrigel invasion assays

Migration and invasion assays were performed using 6.5mm diameter Transwell® permeable support inserts (8.0µm; $1x10^5$ pores/cm^2; Corning). The Transwell inserts were coated with 100µL of 12-18mg/mL Matrigel basement membrane extract (BME; Cultrex® Basement Membrane Extract) for the invasion assay as per manufacturer's instructions. Migration assay inserts were not coated with BME. Freshly passaged SW480 subclones were cultured in serum containing media for 24hr. At ~75% confluence, cells were serum deprived in SF media for 24hr. Cells were then non-enzymatically detached using 1mM EDTA in PBS and $1x10^5$ cells were inoculated into the upper chamber of inserts in SF media. L-TGFβ1 and/or Plg was introduced into the upper chamber to a final concentration of 10ng/mL, which was then placed into the lower chamber containing 1% FBS serum-media

221 and incubated for 16hr at 37ºC. Following incubation, non-migratory cells were gently

222 scraped away from inside the upper insert chamber with a cotton swab and the insert washed

223 with PBS before fixing with 2% paraformaldehyde for 2min. Excess paraformaldehyde was

224 washed away and cells were stained with 0.2% (w/v) crystal violet in 2% ethanol for 10min

225 at room temperature. Excess stain was washed away before viewing under an inverted light

226 microscope. Five random visual fields were obtained with a 40x objective and the cells that

227 were migrating through the polycarbonate membrane enumerated.

228 **2.8 Western blotting**

229 Freshly passaged SW480 and HT29 subclones were lysed in the presence of the

230 cOmplete Mini EDTA-free protease inhibitor cocktail (Roche) and phosphatase inhibitor

231 cocktail 2 (Sigma-Aldrich). Crude cell lysates were sheared by six passes through a 27G

232 needle and heated to 70ºC for 10min before 1D SDS-PAGE separation on a 4-12% NuPAGE

233 gel (Invitrogen) at 200V for 1hr. Resolved proteins were then electrophoretically transferred

234 to a PVDF membrane (Invitrogen). Non-specific binding was blocked with Tris-buffered

235 saline (TBS) containing 3% (w/v) BSA and 0.5% (v/v) Tween-20 (4ºC, 1hr) prior to primary

236 antibody probing (4ºC, overnight). The membrane was washed with TBS with 0.5% (v/v)

237 Tween-20 and incubated in horseradish peroxidase-conjugated goat or rabbit secondary

238 antibodies (room temperature, 1hr), followed by chemiluminescence detection (SuperSignal

239 West Femto Maximum Sensitivity Substrate, Thermo) and image acquisition (LAS 3000,

240 FUJI). MagicMark™ and Novex Pre-stained (Invitrogen) Western blotting protein standards

241 were used to estimate molecular weight. Signal intensity was quantified using ImageJ.

242 Western blots were performed in technical triplicate.

243 **2.9 AlphaScreen® SureFire® assays**

244 Freshly passaged SW480 cells were seeded into each well of a 96-well plate and

245 cultured using the recombinant protein treatment protocol described above. After 24hr

246 incubation in the presence of L-TGFβ1 and/or Plg, SW480 and HT29 subclones were

247 incubated in serum media for either 10 or 30mins immediately prior to cell lysis in the

248 presence of protease and phosphatase inhibitor cocktails. AlphaScreen® SureFire® assays

249 (TGR Biosciences, Australia) were performed according to the manufacturer's instructions

250 in biological triplicate with technical quadruplicates taken from each sample well.[25]

251 ERK1/2, SMAD2 and Akt1/2/3 SureFire® assays were performed on the same cell lysate

252 samples to provide relative signalling changes with treatment. Cell lysate that was either
253 negative or positive for ERK1/2, SMAD2 or Akt1/2/3 activity was provided as controls. The
254 phosphorylated epitopes measured in these assays are phospho (p)-Thr202/Tyr204 for
255 ERK1/2, p-Ser465/467 for SMAD2 and p-Ser473 for AKT1/2/3.

3. RESULTS

257   This project determined that treatment of αvβ6-expressing CRC cells with L-TGFβ1
258 and/or Plg induced or significantly promoted multiple phenotypic changes that are associated
259 with the metastatic progression of an early colorectal cancer. Overall, these results support
260 the formation of a pro-metastatic signalling "switch" involving both L-TGFβ1 and Plg that
261 is supported through elevated expression of the epithelial-restricted integrin αvβ6.

3.1 β6 expression facilitates increased proliferation when treated with L-TGFβ1 and/or Plg

264   Our previous study demonstrated that β6 overexpression enhances CRC cell
265 proliferation under standard cell culture conditions.[12] This project employed similar assays
266 to now determine whether introducing zymogen members of the uPAR/αvβ6/TGFβ1
267 interactome into these cultures induced a β6-dependent increase in cell proliferation, firstly
268 within the SW480^{Mock} and SW480^{β6OE} cell lines (Figure 1).

269   Interestingly, the SF media control had an anti-proliferative effect on SW480^{β6OE},
270 resulting in a 36% longer doubling time at 24hrs relative to SW480^{Mock}. However, L-TGFβ1
271 and/or Plg treatment significantly promoted SW480^{β6OE} proliferation by up to 65% relative
272 to the untreated SW480^{Mock} control. L-TGFβ1 and/or Plg treatment decreased cell doubling
273 times by 19% (LTGFβ1), 24% (Plg) and 35% (L-TGFβ1 + Plg) respectively, increasing the
274 live SW480^{β6OE} cell count relative to SW480^{Mock}. After 48hr, the effect of these zymogens
275 on SW480^{β6OE} proliferation was sustained though less pronounced as a 7% (L-TGFβ1), 10%
276 (Plg) and 20% (L-TGFβ1 + Plg) reduction in doubling time relative to SW480^{Mock}.
277 Comparing treatments within the SW480^{β6OE} cell line only, each zymogen treatment
278 significantly increased proliferation compared to SF control. No significant difference in
279 proliferation was observed between any zymogen protein treatment in SW480^{Mock} cells at
280 either the 24 or 48hr incubation, indicating that β6 is required for the elevated proliferation.
281 Interestingly, zymogen treatment of SW480^{β6OE} cells yields nearly the same number of live
282 cells as the SW480^{Mock} line in serum media (data not shown), suggesting that the presence

283 of these zymogens at 10ng/mL matches serum media conditions in the absence of β6. SW480

284 cell viability remained at 95.8% even after 72hr in SF media. Similar studies have shown

285 that similar sustained resistance to nutrient deprivation may correspond with increased

286 tumour aggressiveness[26], suggesting that SW480 cells are immediately pre-metastatic and

287 are a suitable models for early stages of metastasis.

288
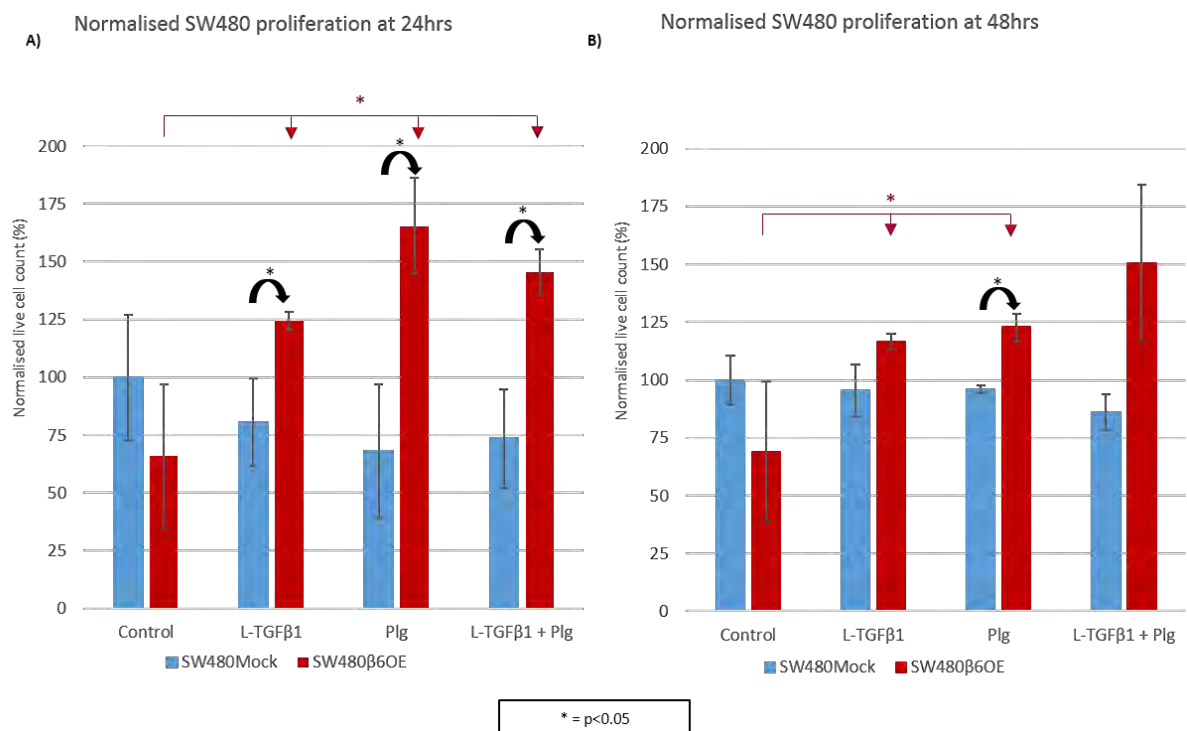
289   **Figure 1**. Proliferation of SW480 subclones after 24-48hrs normalised to untreated

290 SW480[Mock] controls. A) Live cell counts between SW480 subclones after 24hr incubation.

291 B) Live cell counts between SW480 subclones after 48hr. Error bars display one standard

292 deviation and doubling times are listed in Supplementary Table 1.

293   To determine whether these significant increases in proliferation were the direct

294 result of zymogen treatment, we repeated the proliferation assay implementing specific

295 inhibitors of TGFβ1 and plasmin activity (Figure 2).

296   Again, the SF media exerted an inhibitory effect on SW480[β6OE] proliferation.

297 Inhibitor treatment reduced SW480 subclone proliferation regardless of β6 expression,

298 indicating that TGFβ1 and plasmin activity is necessary to maintain basal SW480 cell

299 replication. When treated with one or both inhibitors, SW480[β6OE] proliferation was

300 significantly reduced compared to the SW480[Mock] cell line for each treatment except Plg +

aprotinin. This suggests that the growth-promoting effects of zymogen treatment observed in Figure 1 can be ablated when TGF-β1 and plasmin activity is inhibited. Interestingly, Figure 2 also suggests that without TGF-β1 and plasmin activity, SW480[β6OE] cells are no longer significantly more proliferative than SW480[Mock] [12] and instead become significantly less proliferative than the SW480[Mock] control. Taken together, this data suggests that the growth-promoting effects of β6 expression are conveyed through increased zymogen activation and that without TGF-β1 and plasmin activity, β6 expression exerts an anti-proliferative effect on the SW480 cell under normal tissue culture conditions.

Normalised SW480 recombinant protein proliferation at 24hrs post inhibitor treatment

L-TGFβ1	-	+	-	-	-	+	-
SB431542	-	+	+	-	-	+	-
Plg	-	-	-	+	-	+	+
AP	-	-	-	+	+	+	+

SW480Mock SW480β6OE

* = p<0.05
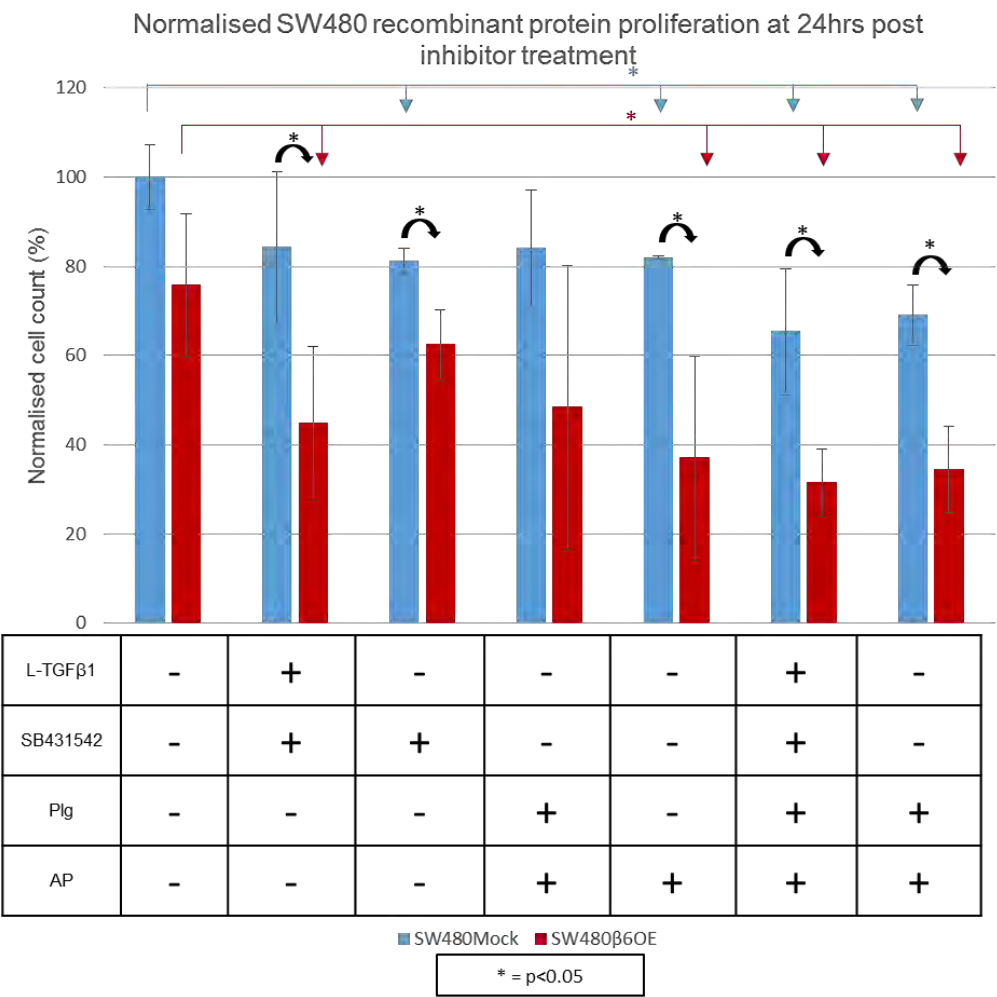
Figure 2. Proliferation of SW480 subclones after incubation with zymogens and/or inhibitors for 24hrs, normalised to untreated SW480[Mock] controls. Error bars display one standard deviation.

In order to determine whether these effects could be reversed in a β6 antisense cell model, we repeated the experiment using HT29 cell line subclones (Figure 3).

315   Antisense β6 suppression in HT29 cells significantly lowers proliferation for nearly
316   all zymogen treatments between subclones and noticeably increases HT29^{β6AS} doubling
317   times. Similar to the SW480^{β6OE} data, β6 expression in HT29^{Mock} cells significantly
318   increased proliferation when treated for 48hr with either Plg or L-TGFβ1 with Plg relative
319   to the control. This was not reflected in the HT29^{β6AS} cell line. Similar to SW480 cells, the
320   pro-proliferative effect of zymogen/s treatment on HT29 cell proliferation diminished after
321   24hr and doubling times increased as HT29 cells became less viable in SF media. Whilst
322   73% of HT29^{Mock} cells were viable after 72hr in SF media, only 33% of HT29^{β6AS} cells were
323   able to exclude Trypan Blue. As β6 overexpression in SW480^{β6OE} significantly decreased
324   tumour cell death and apoptosis [12], conversely β6 suppression may result in the absence of
325   anti-apoptotic protein networks in HT29^{β6AS}.

326
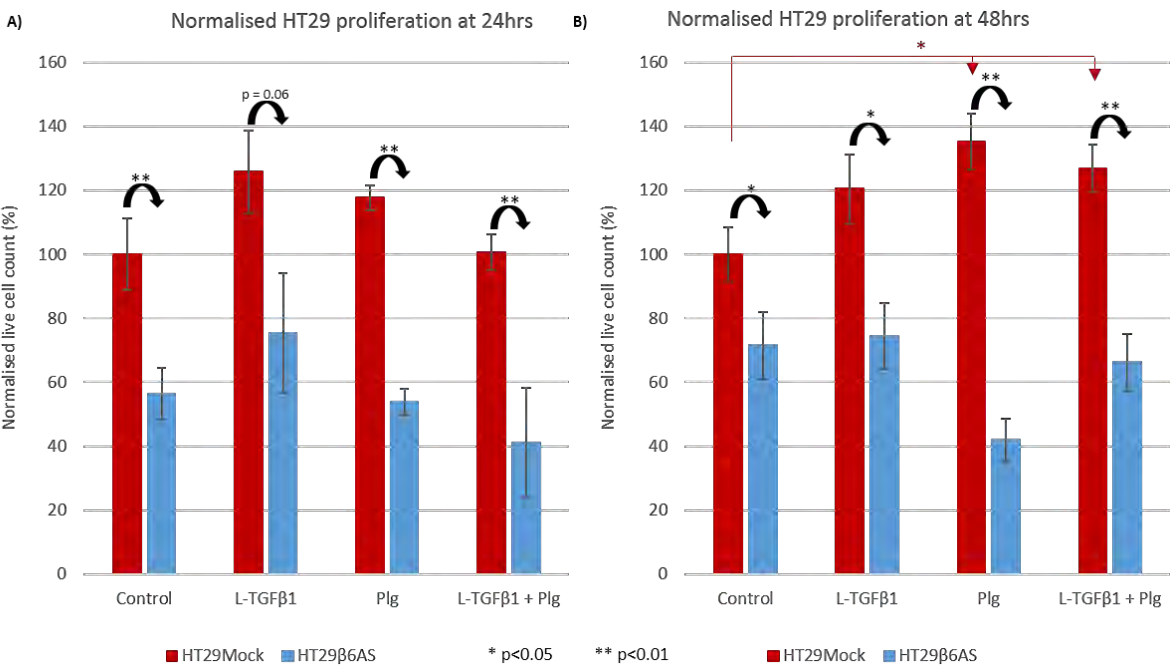
327   **Figure 3**. Proliferation assay for HT29 subclones after 24 or 48hrs, normalised to
328   untreated HT29^{Mock} controls. A) Live cell counts between HT29 subclones after 24hr
329   incubation. B) Live cell counts between HT29 subclones after 48hr incubation. Error bars
330   display one standard deviation and doubling times are listed in Supplementary Table 2.

331   These results confirm that β6 expression positively correlates with proliferation in
332   both CRC models, and that L-TGFβ1 and/or Plg treatment significantly enhances
333   proliferation further in cells which express β6 while inhibiting or exerting no effect in the
334   absence/suppression of β6.

3.2 β6 expression enables increased wound healing, migration and invasion in the presence of L-TGFβ1 and/or Plg

As β6 overexpression increases invasion [12], a preliminary 'wound' healing assay was performed to determine whether L-TGFβ1 and/or Plg treatment increased SW480 cell migration into the freshly-created 'wound' space. β6 expression enhanced SW480 cell migration across residual tissue culture surface after scratching, filling in the empty 'wound' (Figure 4).

All SW480^{Mock} 'wound' widths remained equal to those of negative controls, irrespective of zymogen treatment, and even 10% FBS containing media did not significantly reduce the width of 'wounds'. In contrast, the presence of either zymogen increased infiltrative migration of SW480^{β6OE} cells, significantly reducing scratch width over 24hr. Furthermore, zymogen treatment of SW480^{β6OE} cells significantly reduced the scratch width relative to SW480^{Mock} cells in serum media, suggesting that zymogen treatment at 10ng/mL was able to surpass that of the growth factors present in 10% FBS. To confirm that this was due increased cell migration and not simply proliferation, further cell migration and invasion assays were performed using Transwell permeable supports (Figure 5).

Cell migration and invasion studies supported the previous findings of the 'wound' healing assay, demonstrating that SW480^{β6OE} cells were significantly more invasive compared to SW480^{Mock} cells under each treatment condition. SW480^{β6OE} cells in the presence of L-TGFβ1 and/or Plg migrated faster through uncoated 8μm pores. In the BME-coated invasion model, treatment with either Plg or L-TGFβ1 with Plg significantly increased SW480^{β6OE} ECM degradation and invasive migration. These changes were not observed with SW480^{Mock} cells, where few cells were observed. As expected, the BME barrier did reduce the numbers of cells that successfully crossed through the pore. The sub-physiological treatment with 10ng/ml Plg with or without L-TGFβ1 significantly promoted invasion across the BME-coated insert by 3-4 fold. This suggests that greater proteolytic activation is occurring on the SW480^{β6OE} cell surface compared to the SW480^{Mock} cell line, despite Western blotting evidence demonstrating that uPAR expression remains unchanged across these two subclones (Supplementary Figure 1). Collectively, treatment of β6-overexpressing CRC cells with L-TGFβ1 and/or Plg significantly enhances their capacity to degrade an ECM analogue and migrate from nutrient-poor SF conditions towards chemotactic factors.
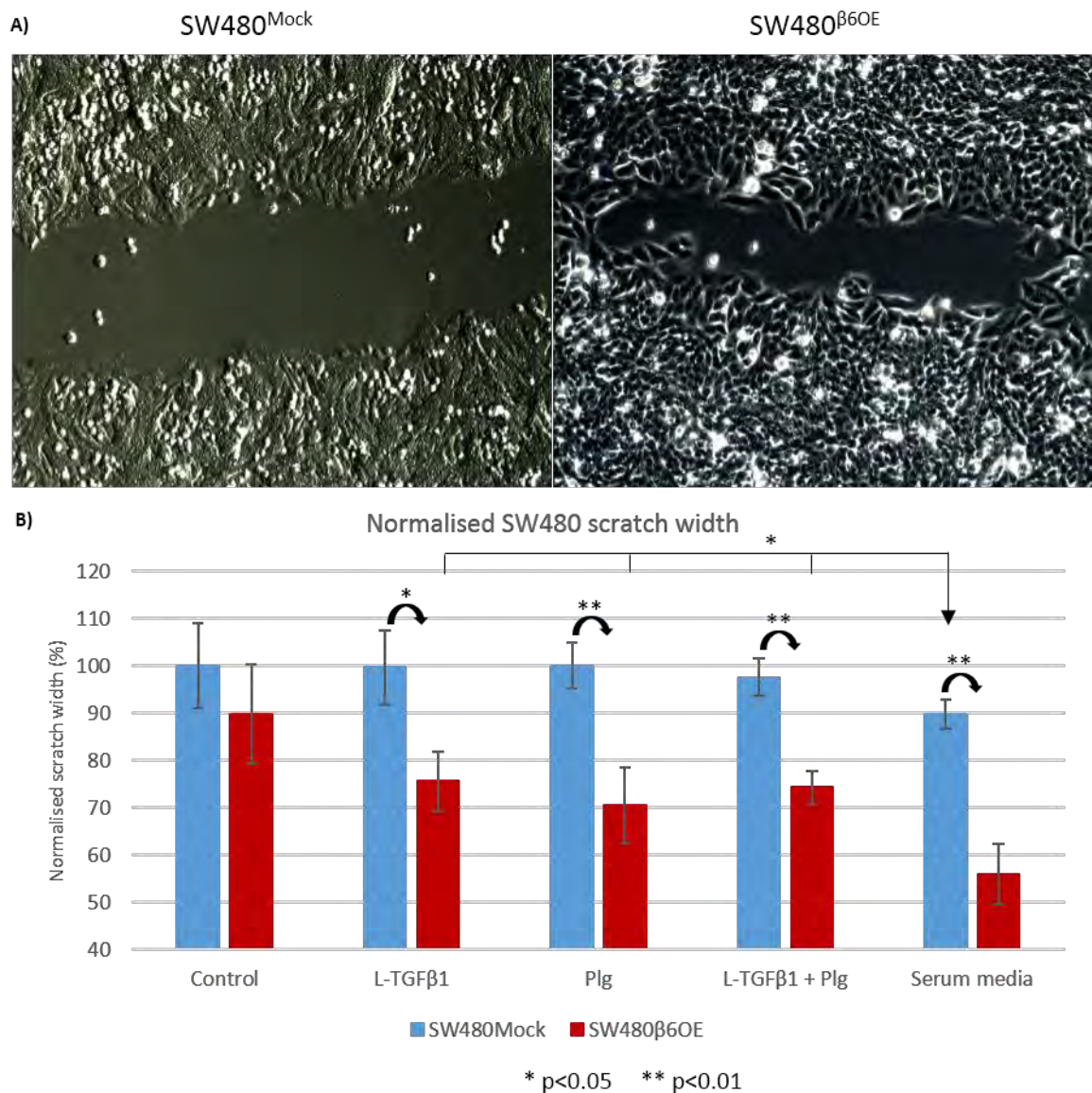
Figure 4. β6 expression significantly increases SW480 cell migration across 'wounds' when treated with L-TGFβ1 and/or Plg, normalised to untreated SW480^{Mock} controls. Error bars are set to standard error for each triplicate. A) Representative inverted light microscope image of 'wounds' after 24hr in serum containing media at 10x magnification. B) Normalised 'wound' width measurements in response to recombinant zymogen treatment.

A) Normalised SW480 cell migration

B) Normalised SW480 cell invasion

* p<0.05   ** p<0.01   ■ SW480Mock ■ SW480β6OE

374
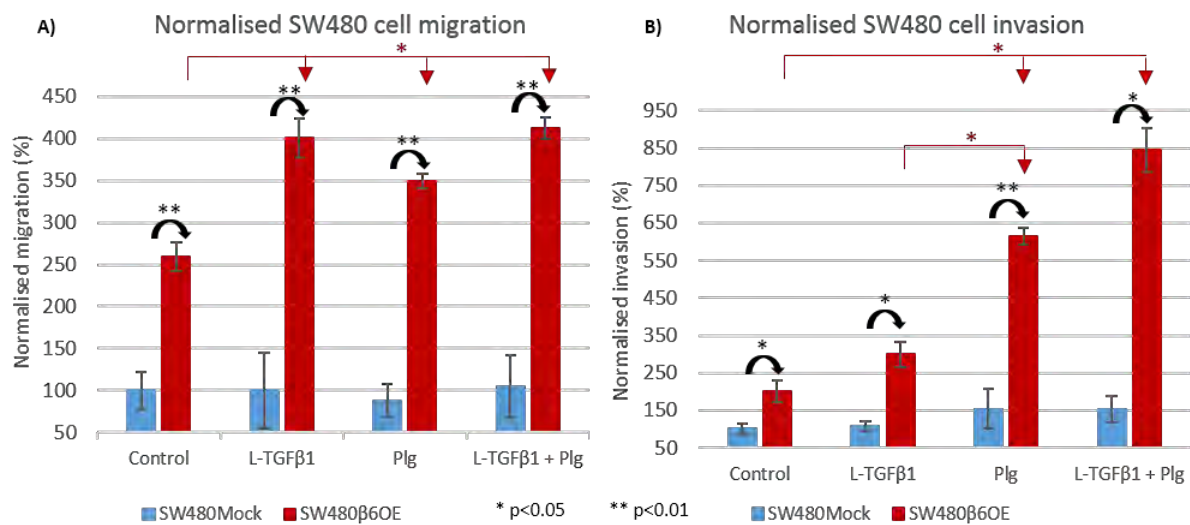
Figure 5. β6 integrin expression in SW480^{β6OE} cells significantly increases both A) chemotactic migration through the pore and B) invasive migration through the pore with an additional BME barrier. Data is normalised to untreated SW480^{Mock} controls. Migration and invasion was significantly increased further with recombinant zymogen protein treatment. Error bars display one standard deviation.

380

3.3 Recombinant protein treatment does not alter cell morphology

Confocal microscopy revealed no distinct differences in cell morphology or cytoskeletal organisation between SW480 cell lines for each respective treatment (data not shown). As a result of the treatment procedure, both subclones exhibited highly irregular, flattened, elongated and spindly morphologies similar to mesenchymal cells with irregular actin staining. The lack of a distinct cytoskeleton may be indicative of large scale cytoskeletal disruption or reorganisation of the normal support scaffold as suggested by previous proteomic analysis.[12] This may provide a greater flexibility to accommodate chemotactic migration, though this is more likely a pre-malignant migratory response to serum starvation and not a specific result of β6 expression.

391
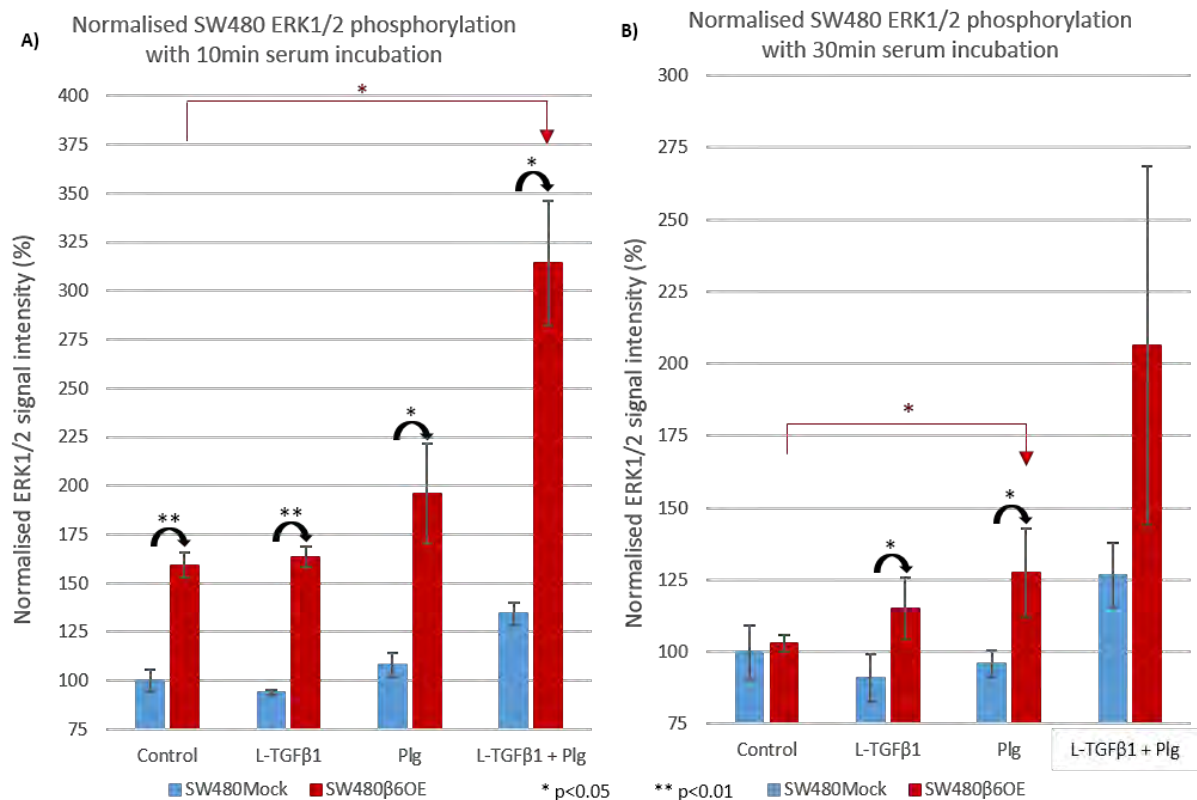
Figure 6. Normalised effect of L-TGFβ1 and/or Plg treatment on SW480 ERK1/2 signalling activity after a 10min or 30min incubation in serum media prior to lysis. A) ERK1/2 phosphorylation of SW480 cell lines in response to recombinant protein treatments after a 10min incubation in serum media. B) ERK1/2 phosphorylation of SW480 cell lines in response to recombinant protein treatments after a 30min incubation in serum media. Error bars display one standard deviation.

3.4 β6 expression increases basal ERK1/2 and SMAD2 signalling activity which is amplified further when stimulated with L-TGFβ1 and/or Plg

As β6 expression positively correlates with MAPK activity[4], we aimed to determine whether recombinant L-TGFβ1 and/or Plg treatment enhanced MAPK signalling. Preliminary Western blots were first performed to assess any relative change in ERK1/2 phosphorylation under normal cell culture conditions and as a result of the serum starvation procedure (Supplementary Figure 2). We identified differences in ERK1/2 phosphorylation between cell lines whilst total ERK1/2 expression remained unchanged. Cell lines expressing β6 demonstrated increased endogenous ERK2 phosphorylation (end product of the pro-proliferative MAPK pathway and ligand for αvβ6).[4] Although Western blots

119

indicated significant differences in ERK1/2 phosphorylation as a result of β6 expression, they were often not sensitive enough to distinguish subtle differences between subclones or technical variation between gels. Given the number of samples and treatment conditions, we employed the AlphaScreen® SureFire® assay platform to uniformly and simultaneously assess the effect of recombinant protein treatments on ERK1/2 phosphorylation. Firstly, we interrogated the effects of zymogen treatment on ERK1/2 signalling within the SW480 subclones (Figure 6).

The SW480^{β6OE} cell line exhibited a significantly higher surge in ERK1/2 phosphorylation compared to SW480^{Mock} after serum media was reintroduced for 10mins post-treatment. After 30mins, this difference between cell lines was less pronounced however SW480^{β6OE} ERK1/2 phosphorylation remained significantly higher for the L-TGFβ1 and Plg treatments. This suggested that these zymogens sustained elevated ERK1/2 phosphorylation after the initial surge that was not observed in the SF control. Due to one low outlier, the difference between cell lines for the L-TGFβ1 + Plg treatment with a 30min serum media incubation was insignificant despite the mean intensity being 80% higher in the SW480^{β6OE} cell line. Within the SW480^{β6OE} cell line there was a general trend towards increased ERK1/2 phosphorylation for each recombinant protein treatment relative to the control. These differences are weakly reflected in SW480^{Mock}, where ERK1/2 activity varied little relative to the control. ERK1/2 phosphorylation was significantly higher for both cell lines when treated with both L-TGFβ1 and Plg prior to serum media incubation relative to the SF control. The combined treatment increased ERK1/2 phosphorylation in the SW480 cell, however β6 expression significantly increased this difference further. ERK1/2 activity was significantly higher in the SW480^{β6OE} cell line in response to treatment with Plg after a 30min incubation period relative to the control. These data suggest that β6 expression significantly enhances and possibly prolongs ERK1/2 phosphorylation in SW480 cells after serum starvation and that zymogen treatment can also significantly increase ERK activity relative to the SF control.

A) Normalised HT29 ERK1/2 phosphorylation with 10min serum incubation

B) Normalised HT29 ERK1/2 phosphorylation with 30min serum incubation

* p<0.05   ** p<0.01   ■ HT29Mock   ■ HT29β6AS
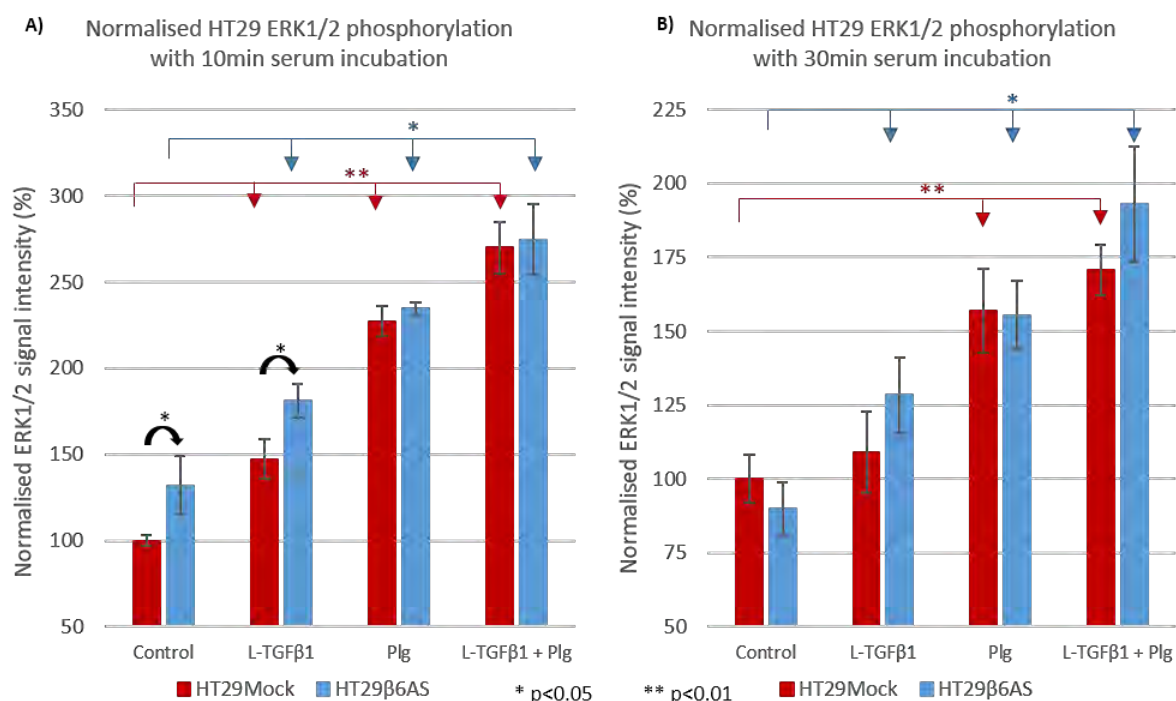
Figure 7. Normalised effect of L-TGFβ1 and/or Plg treatment on HT29 ERK1/2 signalling activity after a 10min or 30min incubation in serum media prior to lysis. A) ERK1/2 phosphorylation of HT29 cell lines in response to recombinant protein treatments after a 10min incubation in serum media. B) ERK1/2 phosphorylation of HT29 cell lines in response to recombinant protein treatments after a 30min incubation in serum media. Error bars display one standard deviation.

To determine whether the converse effect held true in the β6 antisense cell model, we examined the HT29 subclone datasets for similar differences (Figure 7).

SureFire® assay data for both cell lines suggested that β6 expression (even if reduced by antisense mutation) significantly enhanced ERK1/2 phosphorylation when treated with recombinant L-TGFβ1 and/or Plg. Given the cross-reactivity of the uPAR/αvβ6/TGF-β interactome, we expanded our study to investigate whether β6 expression altered SMAD2 and Akt1/2/3 signalling activity. When we performed SMAD2 and Akt1/2/3 SureFire® assays on the same lysate samples, we observed that basal SMAD2 and Akt1/2/3 phosphorylation was lower than that of the HEK293 cell line that is commonly used as a standard and as such, interpreted the data conservatively. We firstly assessed SMAD2 phosphorylation to identify differences in TGFβ-dependent signal transduction in response to treatment (Figure 8).

The SMAD2 SureFire® assay determined that SMAD2 signalling was significantly higher in the SW480^β6OE cell line relative to SW480^Mock for each treatment after a 10min incubation in serum media or after a 30min serum media incubation following Plg or L-TGFβ1 + Plg treatments. Despite the increased basal SMAD2 activity that accompanied β6 expression, when we compared activity between treatments within the SW480^β6OE cell line, we observed that each zymogen treatment had an inhibitory effect on SMAD2 activity. Contrary to expectations, L-TGFβ1 treatment reduced SMAD2 phosphorylation by 3% relative to the untreated control. Interestingly SMAD2 phosphorylation was further ablated by treatment with Plg, reducing SMAD2 phosphorylation by 13% (Plg) or 17% (L-TGFβ1 + Plg) relative to the untreated SW480^β6OE control. Combined with the ERK1/2 data, this suggests that although TGFβ signalling activity is intrinsically higher in the β6 expressing cell line, exposure to recombinant L-TGFβ1 and/or Plg switches signalling activity from SMAD2-dominant to MAPK-dominant signalling. SMAD2 phosphorylation in the HT29 subclones was below the limit of detection for this assay. This may suggest that HT29 cell lines preferentially signal through the ERK1/2 pathway, as overall ERK1/2 activity was much higher than that observed in the SW480 cell lines.
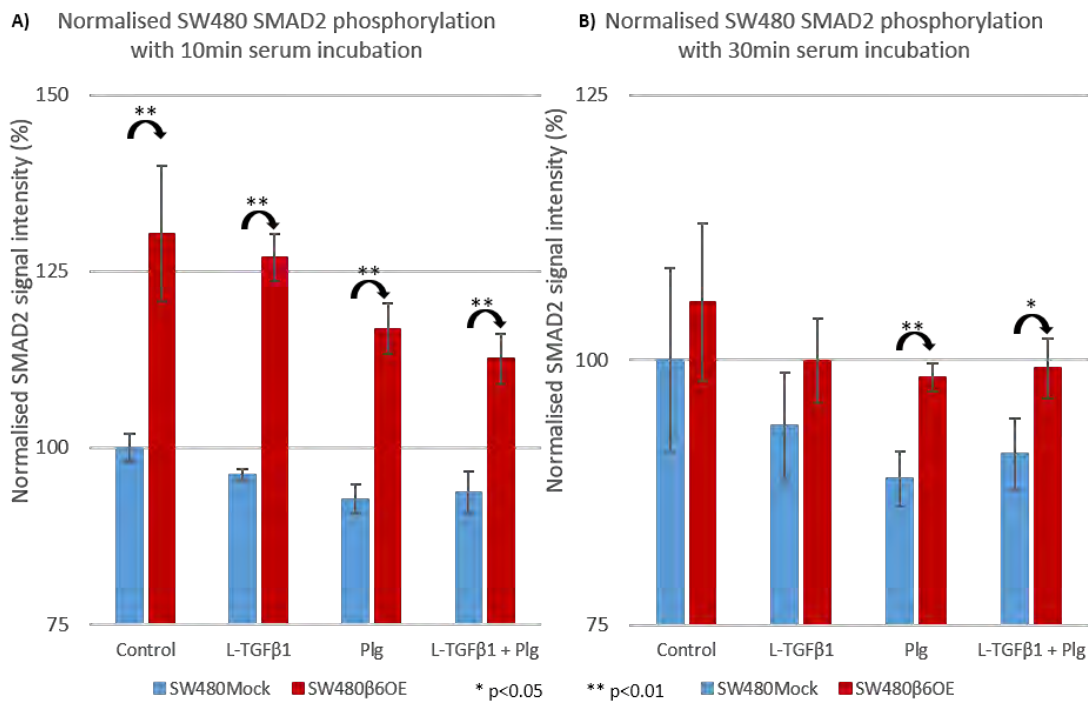
Figure 8. Normalised effect of L-TGFβ1 and/or Plg treatment on SMAD2 signalling activity of SW480 subclones after an A) 10min or B) 30min incubation in serum media prior to lysis. Error bars display one standard deviation.

475   We assessed the same samples once more for relative Akt1/2/3 phosphorylation

476   differences in response to zymogen treatment (Figure 9).

477   Similar to SMAD2 phosphorylation, the Akt1/2/3 SureFire® assay determined that

478   Akt1/2/3 signalling was significantly higher in the SW480$^{\beta 6OE}$ cell line for every treatment

479   after both a 10min and 30min incubation in serum media prior to lysis. This strongly suggests

480   that SW480 cells exhibit significantly elevated and sustained Akt1/2/3 signalling activity

481   when the β6 subunit is expressed as it was not reflected in SW480^{Mock}. Within the

482   SW480$^{\beta 6OE}$ cell line we observed that treatment with both zymogens significantly reduced

483   Akt1/2/3 phosphorylation after a 30min incubation in serum media relative to the untreated

484   control. This indicated another potential signalling switch from Akt1/2/3 to ERK1/2

485   signalling when treated with both zymogens. Once again, Akt1/2/3 phosphorylation in the

486   HT29 subclones was below the limit of detection for this assay, suggesting that ERK1/2

487   signalling is dominant in these cell lines.
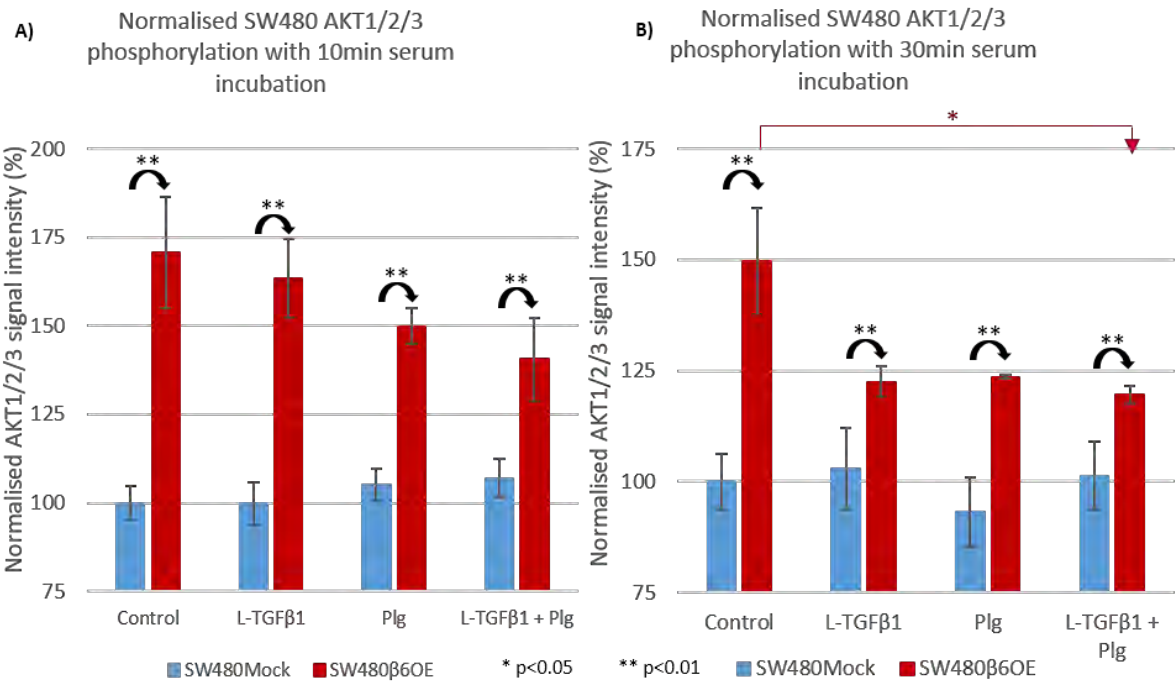
488

489   **Figure 9**. Normalised effect of L-TGFβ1 and/or Plg treatment on Akt1/2/3 signalling

490   activity of SW480 subclones after an A) 10min or B) 30min incubation in serum media prior

491   to lysis. Error bars display one standard deviation.

123

A) ERK1/2, SMAD2 and Akt1/2/3 phosphorylation ratios of SW480β6OE cells after 10min serum media incubation

B) ERK1/2, SMAD2 and Akt1/2/3 phosphorylation ratios of SW480β6OE cells after 30min serum media incubation

pERK1/2 : pSMAD2   pERK1/2 : pAKT1/2/3   pSMAD2 : pAKT1/2/3
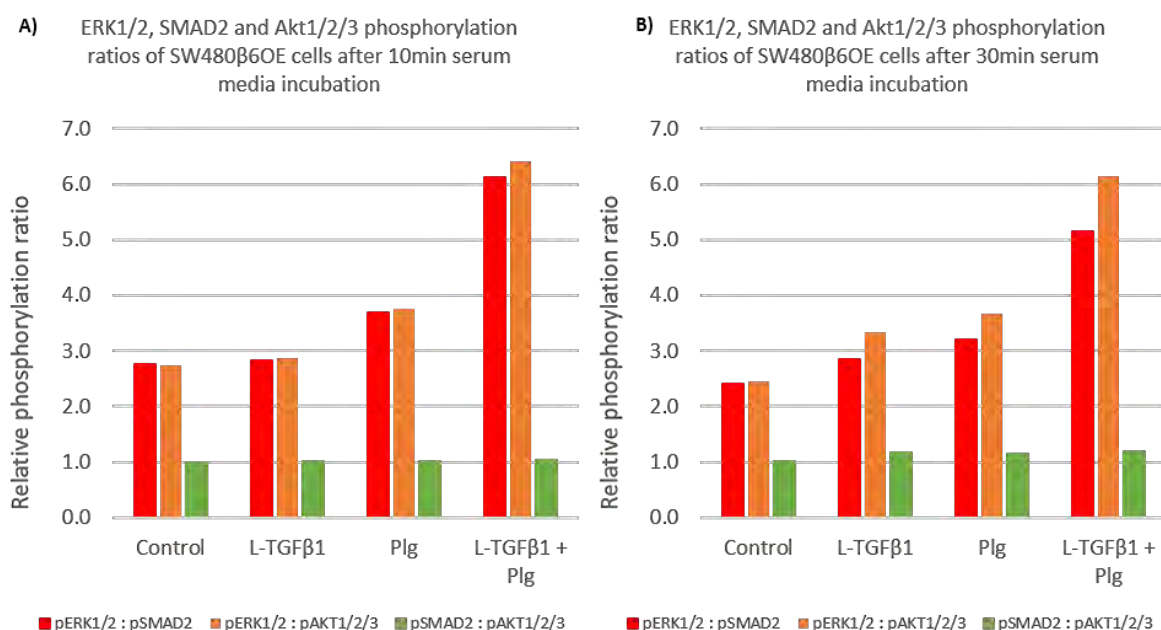
Figure 10. Ratios of ERK1/2-to-SMAD2, ERK1/2-to-Akt1/2/3 and SMAD2-to-Akt1/2/3 signalling activity in the SW480$^{\beta6OE}$ cell line following treatment and incubation in serum media for A) 10mins or B) 30mins prior to lysis.

Taking the mean intensity data obtained from each of the SureFire® assays, we then compared these values as ratios of signalling activities following zymogen treatment (Figure 10).

SureFire® assay data demonstrated that zymogen treatment promoted ERK1/2 signalling activity with converse inhibitory effects on SMAD2 and Akt1/2/3 activity in the SW480$^{\beta6OE}$ cell. As ERK1/2 activity significantly increased whilst both SMAD2 and Akt1/2/3 activity decreases with zymogen treatment (Figures 6, 8 and 9), these findings suggest a switch in signalling activity from SMAD2 and Akt1/2/3 to an ERK1/2-dependent system. Plg appears to have exerted the greater individual effect on this switch as L-TGFβ1 treatment did not alter the ERK1/2-to-SMAD2 or ERK1/2-to-Akt1/2/3 ratios relative to the SF control, however with the addition of both zymogens, ERK1/2 signalling became at least five times more active than either SMAD2 or Akt1/2/3 signalling. Collectively, ERK1/2, SMAD2 and Akt1/2/3 phosphorylation data strongly suggests that β6 expression significantly increased basal ERK1/2, SMAD2 and Akt1/2/3 signalling activity, which can be switched with L-TGFβ1 and/or Plg treatment to MAPK-dominant signalling in pre-metastatic CRC.

4. DISCUSSION

The αvβ6 integrin can be regarded as a lynchpin protein in the progression of a pre-metastatic or benign CRC cell towards the fully metastatic phenotype. In the current study, we aimed to determine whether β6 expression could translate treatment with zymogen forms of proteins we suspected to form a pro-metastatic axis with β6 into phenotypic changes. These results demonstrate that β6 expression significantly enhances the proliferative, migrative and invasive potential of CRC cells through the activation and implementation of recombinant L-TGFβ1 and/or Plg. To highlight the potency of the interactive axis on the pre-metastatic cell membrane, this study used comparatively low concentrations of each zymogen. All recombinant protein treatments were at a final concentration of 10ng/mL, whilst the normal concentration of L-TGFβ1 in healthy human plasma is 136ng/mL and active TGF-β1 is only 2.1ng/mL.[20] Treating β6-expressing CRC cells with less than 10% of the normal level of L-TGFβ1 was sufficient to significantly increase proliferation, invasion/migration and ERK1/2 signalling *in vitro*. Similar trends were observed with the 10ng/mL Plg treatment, whose normal concentration in healthy human plasma is 200ng/mL.[21] Here, 5% of this concentration was sufficient to significantly increase proliferation, invasion/migration, ERK1/2 signalling and potentially ablate SMAD2 and Akt1/2/3 signalling *in vitro*.

To ensure that these observations were the result of zymogen treatment and were not masked by the various growth factors present in FBS, this study implemented serum starvation conditions. Serum starvation prevents variation in the phenotypic response to treatment resulting from the activity of proteases, protease inhibitors, growth factors, haemoglobin and bovine serum albumin present in FBS. This allows for direct identification of β6-dependent responses resulting from zymogen treatment. Though nutrient starvation has been demonstrated to enhance tumour aggressiveness by promoting cell migration/invasion, AKT phosphorylation, morphological changes, and anchorage-independent growth [26], this study investigated how β6 expression enhances these hallmark features of the EMT beyond that of the SW480^Mock cell line which does not express β6.

Rather than being a consequence of CRC progression, αvβ6 expression may provide a 'signalling scaffold', localising and stabilising pro-metastatic protein•protein interactions. In the case of TGFβ signalling and the PA cascade, αvβ6 neo-expression on the surface of an early epithelial cancer cell could provide the structural foundation for constructing this

544   pro-metastatic axis. β6 expression is normally restricted to low or undetectable levels in

545   epithelial tissue.[1, 6] Once this repression has been ablated in the Duke's stage A or B CRC

546   cell[6], the β6 subunit forms a heterodimer with the ubiquitously expressed αv subunit. β6

547   subunit expression in these SW480 cell lines significantly downregulates the expression of

548   all other observed integrin subunits with the exception of αv.[12] The significant

549   downregulation of β5 could liberate available αv subunits, allowing the formation of αvβ6

550   heterodimers on the SW480 cell membrane as no competing β3 or β8 subunits were

551   identified in these subclones by proteomics.[12] Once expressed, αvβ6 interacts with uPAR

552   through binding to the sequestered αv subunit.[27] Ahmed et *al.* demonstrated that high

553   surface expression of αvβ6 correlates with high uPAR and uPA expression on the surface of

554   ovarian cancers.[28] This interaction may stabilise and/or shield the complex from protease

555   or phosphatase activity at the base of the heterodimer whilst leaving the β6 subunit available

556   to bind to the LAP of L-TGFβ1, activating the zymogen through mechanical torsion. Thus

557   the αvβ6 integrin centralises two pro-metastatic pathways to the SW480 cell surface, the

558   TGF-β1 pathway through β6 and the PA cascade through αv. Both pathways are capable of

559   inducing *de novo* αvβ6 expression through activation of the oncogenic transcription factor

560   Ets-1, an end-product of SMAD2/3 signalling.[6, 29] Additionally, Ets-1 also promotes the

561   expression of uPA, uPAR, epidermal growth factor (EGF), fibroblast growth factor (FGF),

562   matrix metalloproteases and vascular endothelial growth factor (VEGF).[28-30] By promoting

563   its own expression[31], αvβ6 can promote the expression of itself, its interactors and other

564   key oncogenic proteins, helping to explain its role as a negative prognostic indicator of colon

565   cancer patients in early stage CRC.[6] Though elevated αvβ6 expression does not

566   significantly reduce 5-10 year survival rates of patients with malignant CRC, elevated αvβ6

567   expression in benign CRC resulted in a significant reduction in 5 year survival by ~28%

568   with αvβ6 expression in distal metastases.[6]

569   The current study suggests that in these early CRC tumours, αvβ6 expression both

570   increases metastatic phenotypes under normal conditions and 'primes' these cells so that

571   they are ready to act upon introduced external stimuli. αvβ6 expression significantly

572   increased proliferation, invasion and cell signalling in response to L-TGFβ1 and/or Plg

573   treatment in a manner that was not reflected in the non-αvβ6 expressing cell line. We suspect

574   that the formation of the uPAR/αvβ6/TGF-β1 interactome at the CRC cell membrane has

575   mediated the rapid translation of zymogen treatment into the significant phenotypic changes

576 observed. Proliferation and ERK1/2 signalling activity significantly increased in response to

577 each treatment condition, suggesting a joint response akin to those previously demonstrated

578 by Agrez et *al.* through the unique C-terminal tail of the β6 subunit.[3] The increased

579 proliferation is likely driven through sustained ERK2 phosphorylation and additional L-

580 TGFβ1 activation that is now no longer acting as an early-stage tumour suppressor. It appears

581 that Plg treatments have the greatest effect on proliferation, potentially due to the continued

582 proteolysis of endogenously produced L-TGFβ1 compared to a single dosage of 10ng/mL.

583 To ensure that these results were due to TGF-β1 signalling and PA cascade activity, we

584 repeated the proliferation study employing specific inhibitors of these systems and observed

585 not only an ablation of pro-proliferative effects but a significant reduction in SW480^{β6OE}

586 proliferation. Aprotinin inhibits multiple serine proteases though primarily plasmin through

587 the formation of enzyme–inhibitor complexes between the lysine-15 residue of aprotinin and

588 the active serine residue of the protease.[32] SB-431542 inhibits the TGF-β-mediated

589 activation of SMAD proteins, cell proliferation and cell motility, without inhibiting kinases

590 including p38, ERK, or JNK.[33]

591 Increased proliferation through activated TGF-β1 also helps to explain the observed

592 increases in cell migration, both within a 'wound' model and through an uncoated physical

593 barrier. The significant increases in invasiveness however are likely attributable to the

594 conversion of Plg into active plasmin, which greatly enhanced the ability for SW480^{β6OE}

595 cells to degrade the BME-coated barrier and invasively migrate. The invasion assay was

596 closer to reproducing *in vivo* conditions as the BME components from an EHS sarcoma

597 include ECM proteins such as collagens and laminin, as well as proteoglycans, proteolytic

598 enzymes/inhibitors and growth factors. Increased proteolytic activity on the SW480^{β6OE} cell

599 surface is the likely explanation for the significantly higher invasion of SW480^{β6OE} cells

600 following generation of active plasmin and potential activation of downstream MMPs (e.g.

601 MMP-9 and MMP-3). The almost significant further increase in invasion when treated with

602 both L-TGFβ1 and Plg once more demonstrates the cross-reactivity within this interactive

603 axis, suggesting a cumulative effect of activating both pathways. This effect was strongly

604 observed in ERK1/2 signalling whereby β6-expressing cells demonstrated dramatic

605 increases in signalling activity in response to combined treatment. Interestingly, the SMAD2

606 activity data did not reveal any significant response to treatment with the exception of the

607 SW480^{β6OE} cell line. We observed that SMAD2 phosphorylation remains unchanged when

608   treated with L-TGFβ1, although the addition of sub-physiological Plg with L-TGFβ1 reduces

609   SMAD2 signalling, whilst significantly increasing ERK1/2 activity. This switching of

610   signalling pathways in response to Plg treatment suggests that ERK1/2 dominates SMAD2

611   and Akt1/2/3 signalling even when treated with L-TGFβ1. This phenomenon could be an

612   artefact of the pleiotropic nature of TGF-β1, now signalling via SMAD-independent

613   pathways [34] or SMAD2 signalling may be occurring more slowly than the 30min window

614   required to assess ERK1/2 activity. Slow activation of SMAD2/3 or the PA cascade

615   following zymogen treatment could promote αvβ6 expression which may explain the

616   significant increase in ERK1/2 phosphorylation when treated with both zymogens, as it

617   would increase the number of available pERK2 binding sites that are unique to β6. Once

618   bound to β6, pERK2 may be protected from phosphatases, or non-phosphorylated ERK2

619   may be more efficiently phosphorylated due to conformational changes [35] resulting in the

620   increased phosphorylation observed in this study. There is also evidence that αvβ6-bound

621   ERK2 plays a role in αvβ6 internalisation, promoting CRC cell migration and increasing

622   MMP-9 production [35, 36], again highlighting the potential of this interactive axis for cross-

623   reactivity and autocrine self-perpetuation.

5. CONCLUSION

625   In the current work we have determined that αvβ6 expression positively correlates

626   with increased metastatic behaviour in pre-malignant CRC cells and that these significant

627   changes can be promoted further with relatively minute treatments with zymogen members

628   of potential interacting pathways. The αvβ6 integrin may establish and support the novel

629   uPAR/αvβ6/TGF-β1 interactome on the CRC cell surface, enabling the activation of these

630   precursor proteins and translating their presence into significant phenotypic changes that are

631   crucial to enhance the metastatic potential of early cancer cells. We strongly suspect that

632   neo-expression of the β6 subunit is the first step in the construction of a pro-metastatic

633   autocrine signalling complex that significantly reduces patient's 5-year survival rates when

634   expressed in early stage CRC tumours.

6. CONFLICT OF INTEREST

636   The authors declare no actual or potential conflicts of interest; including any

637   financial, personal or other relationships with other people or organizations.

638

650 **REFERENCES**

651 1.   Hazelbag, S., et al., *Overexpression of the alpha v beta 6 integrin in cervical*
652   *squamous cell carcinoma is a prognostic factor for decreased survival.* J Pathol,
653   2007. **212**(3): p. 316-24.
654 2.   Ramos, D.M., D. Dang, and S. Sadler, *The role of the integrin alpha v beta6 in*
655   *regulating the epithelial to mesenchymal transition in oral cancer.* Anticancer Res,
656   2009. **29**(1): p. 125-30.
657 3.   Agrez, M., et al., *The alpha v beta 6 integrin promotes proliferation of colon*
658   *carcinoma cells through a unique region of the beta 6 cytoplasmic domain.* J Cell
659   Biol, 1994. **127**(2): p. 547-56.
660 4.   Ahmed, N., et al., *Direct integrin alphavbeta6-ERK binding: implications for tumour*
661   *growth.* Oncogene, 2002. **21**(9): p. 1370-80.
662 5.   Bates, R.C., *Colorectal cancer progression: integrin alphavbeta6 and the epithelial-*
663   *mesenchymal transition (EMT).* Cell Cycle, 2005. **4**(10): p. 1350-2.
664 6.   Bates, R.C., et al., *Transcriptional activation of integrin beta6 during the epithelial-*
665   *mesenchymal transition defines a novel prognostic indicator of aggressive colon*
666   *carcinoma.* J Clin Invest, 2005. **115**(2): p. 339-47.
667 7.   Breuss, J.M., et al., *Expression of the beta 6 integrin subunit in development,*
668   *neoplasia and tissue repair suggests a role in epithelial remodeling.* J Cell Sci, 1995.
669   **108 (Pt 6)**: p. 2241-51.
670 8.   Yang, G.Y., et al., *Integrin alpha v beta 6 mediates the potential for colon cancer*
671   *cells to colonize in and metastasize to the liver.* Cancer Sci, 2008. **99**(5): p. 879-87.
672 9.   Binder, M.a.T., M., *Drugs targeting integrins for cancer therapy.* Expert Opin. Drug
673   Discov. , 2009. **4**(3).
674 10.   Ramos, D.M., et al., *Expression of integrin beta 6 enhances invasive behavior in oral*
675   *squamous cell carcinoma.* Matrix Biol, 2002. **21**(3): p. 297-307.
676 11.   Ahmed, N., et al., *Alpha(v)beta(6) integrin-A marker for the malignant potential of*
677   *epithelial ovarian cancer.* J Histochem Cytochem, 2002. **50**(10): p. 1371-80.
678 12.   Cantor, D., et al., *Overexpression of alphavbeta6 integrin alters the colorectal*
679   *cancer cell proteome in favor of elevated proliferation and a switching in cellular*
680   *adhesion that increases invasion.* J Proteome Res, 2013. **12**(6): p. 2477-90.

681 13.   Annes, J.P., et al., *Integrin alphaVbeta6-mediated activation of latent TGF-beta*
682   *requires the latent TGF-beta binding protein-1.* J Cell Biol, 2004. **165**(5): p. 723-34.

683 14.   Allen, M.D., et al., *Altered Microenvironment Promotes Progression of Pre-Invasive*
684   *Breast Cancer: myoepithelial expression of alphavbeta6 integrin in DCIS identifies*
685   *high-risk patients and predicts recurrence.* Clin Cancer Res, 2013.

686 15.   Klass, B.R., A.O. Grobbelaar, and K.J. Rolfe, *Transforming growth factor beta1*
687   *signalling, wound healing and repair: a multifunctional cytokine with clinical*
688   *implications for wound repair, a delicate balance.* Postgrad Med J, 2009. **85**(999):
689   p. 9-14.

690 16.   Zambruno, G., et al., *Transforming growth factor-beta 1 modulates beta 1 and beta*
691   *5 integrin receptors and induces the de novo expression of the alpha v beta 6*
692   *heterodimer in normal human keratinocytes: implications for wound healing.* J Cell
693   Biol, 1995. **129**(3): p. 853-65.

694 17.   Saldanha, R.G., et al., *Proteomic identification of lynchpin urokinase plasminogen*
695   *activator receptor protein interactions associated with epithelial cancer malignancy.*
696   J Proteome Res, 2007. **6**(3): p. 1016-28.

697 18.   Waltz, D.A., et al., *Plasmin and plasminogen activator inhibitor type 1 promote*
698   *cellular motility by regulating the interaction between the urokinase receptor and*
699   *vitronectin.* J Clin Invest, 1997. **100**(1): p. 58-67.

700 19.   Dang, D., et al., *Matrix metalloproteinases and TGFbeta1 modulate oral tumor cell*
701   *matrix.* Biochem Biophys Res Commun, 2004. **316**(3): p. 937-42.

702 20.   Khan, S.A., J. Joyce, and T. Tsuda, *Quantification of active and total transforming*
703   *growth factor-beta levels in serum and solid organ tissues by bioassay.* BMC Res
704   Notes, 2012. **5**: p. 636.

705 21.   Leipnitz, G., et al., *Reference values and variability of plasminogen in healthy blood*
706   *donors and its relation to parameters of the fibrinolytic system.* Haemostasis, 1988.
707   **18 Suppl 1**: p. 61-8.

708 22.   Leibovitz, A., et al., *Classification of human colorectal adenocarcinoma cell lines.*
709   Cancer Res, 1976. **36**(12): p. 4562-9.

710 23.   Feng, B., et al., *Colorectal cancer migration and invasion initiated by microRNA-*
711   *106a.* PLoS One, 2012. **7**(8): p. e43452.

712 24.   Woodford-Richens, K.L., et al., *SMAD4 mutations in colorectal cancer probably*
713   *occur before chromosomal instability, but after divergence of the microsatellite*
714   *instability pathway.* Proc Natl Acad Sci U S A, 2001. **98**(17): p. 9719-23.

715 25.   Garbison, K.E., et al., *Phospho-ERK Assays*, in *Assay Guidance Manual*, G.S.
716   Sittampalam, et al., Editors. 2004: Bethesda (MD).

717 26.   Osawa, T., et al., *Inhibition of histone demethylase JMJD1A improves anti-*
718   *angiogenic therapy and reduces tumor-associated macrophages.* Cancer Res, 2013.
719   **73**(10): p. 3019-28.

720 27.   Sowmya, G., et al., *A site for direct integrin alphavbeta6.uPAR interaction from*
721   *structural modelling and docking.* J Struct Biol, 2014.

722 28.   Ahmed, N., et al., *Overexpression of alpha(v)beta6 integrin in serous epithelial*
723   *ovarian cancer regulates extracellular matrix degradation via the plasminogen*
724   *activation cascade.* Carcinogenesis, 2002. **23**(2): p. 237-44.

725 29.   Koinuma, D., et al., *Chromatin immunoprecipitation on microarray analysis of*
726   *Smad2/3 binding sites reveals roles of ETS1 and TFAP2A in transforming growth*
727   *factor beta signaling.* Mol Cell Biol, 2009. **29**(1): p. 172-86.

728   30.   Span, P.N., et al., *Expression of the transcription factor Ets-1 is an independent prognostic marker for relapse-free survival in breast cancer.* Oncogene, 2002. **21**(55): p. 8506-9.

731   31.   Niu, J., et al., *Integrin expression in colon cancer cells is regulated by the cytoplasmic domain of the beta6 integrin subunit.* Int J Cancer, 2002. **99**(4): p. 529-37.

734   32.   Kang, H.M., et al., *The kinetics of plasmin inhibition by aprotinin in vivo.* Thromb Res, 2005. **115**(4): p. 327-40.

736   33.   Inman, G.J., et al., *SB-431542 is a potent and specific inhibitor of transforming growth factor-beta superfamily type I activin receptor-like kinase (ALK) receptors ALK4, ALK5, and ALK7.* Mol Pharmacol, 2002. **62**(1): p. 65-74.

739   34.   Zhang, Y.E., *Non-Smad pathways in TGF-beta signaling.* Cell Res, 2009. **19**(1): p. 128-39.

741   35.   Wang, J., et al., *PKC promotes the migration of colon cancer cells by regulating the internalization and recycling of integrin alphavbeta6.* Cancer Lett, 2011. **311**(1): p. 38-47.

744   36.   Gu, X., et al., *Integrin alpha(v)beta6-associated ERK2 mediates MMP-9 secretion in colon cancer cells.* Br J Cancer, 2002. **87**(3): p. 348-51.

3.1.2 – Supplemental files

Supplementary information

Supplementary Table 1. Respective SW480 doubling times (in hr) for each treatment.

Cell doubling time (hr)	24hr Treatment			48hr Treatment		
	SW480$^{\text{Mock}}$	SW480$^{\beta6OE}$	SW480$^{\beta6OE}$ − SW480$^{\text{Mock}}$	SW480$^{\text{Mock}}$	SW480$^{\beta6OE}$	SW480$^{\beta6OE}$ − SW480$^{\text{Mock}}$
Control	31.9	43.42	11.52	28.01	33.17	5.16
L-TGFβ1	36.99	27.99	-9.00	28.58	26.3	-2.28
Plg	42.37	24.13	-18.24	28.5	25.77	-2.73
L-TGFβ1 + Plg	39.71	25.72	-13.99	29.9	23.9	-6.00

Supplementary Table 2. Respective HT29 doubling times (in hr) for each treatment.

Cell doubling time (hr)	24hr Treatment			48hr Treatment		
	HT29$^{\text{Mock}}$	HT29$^{\beta6AS}$	HT29$^{\text{Mock}}$ - HT29$^{\beta6AS}$	HT29$^{\text{Mock}}$	HT29$^{\beta6AS}$	HT29$^{\text{Mock}}$ - HT29$^{\beta6AS}$
Control	29.13	45.74	-16.61	41.34	52.21	-10.87
L-TGFβ1	26.36	67.15	-40.79	37.04	50.61	-13.57
Plg	27.32	47.77	-20.45	34.82	89.84	-55.02
L-TGFβ1 + Plg	29.90	64.48	-34.58	36.01	55.57	-19.56
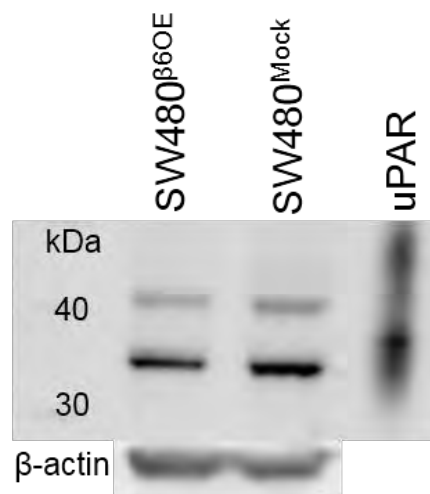
Supplementary Figure 1. Western blot of SW480 subclones probing against uPAR. 40μg of cell lysate was loaded into each lysate well with a β-actin loading control. 100ng of recombinant full-length uPAR was loaded into the uPAR lane as a positive control.
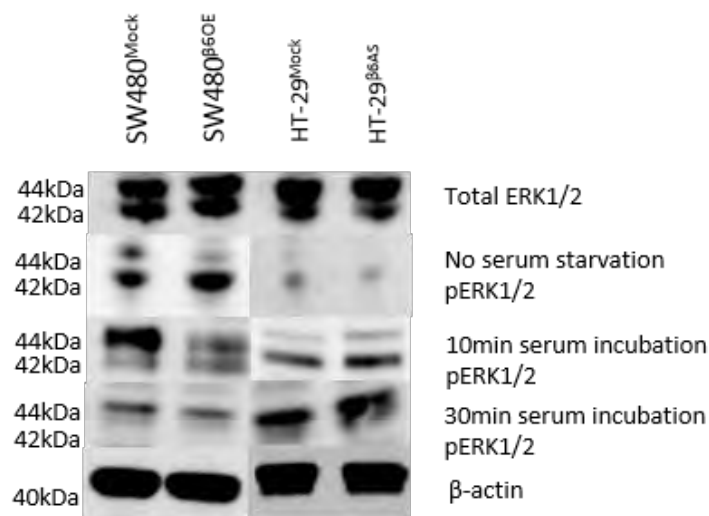
Supplementary Figure 2. Collated images of preliminary ERK1/2 western blots probing against both total ERK1/2 and active, phosphorylated ERK1/2 (pERK1/2). No serum starvation indicates normal levels of ERK phosphorylation under standard culture conditions. 20μg of cell lysate was loaded into each well with a β-actin loading control.

Proliferation assay calculations

Proliferation rate

$$f = \frac{\left\{\dfrac{\ln\left(\dfrac{Nt}{No}\right)}{\ln(2)}\right\}}{t}$$

Nt = Number of cells at a given time (t)

No = Number of cells seeded

t = Given time interval

f = Frequency of cell cycles per time interval

Doubling time = $1/f$

f = Frequency of cell cycles per time interval

3.2 - Study II:

The results from the previous study showed that β6 in a TGFβ-dependant manner can induce phenotypic changes that promote cancer progression. This second study aimed to investigate if the phenotypic changes and its associated signalling on colon cancer cells that express varying levels of β6 integrin when treated with active TGFβ. This study was also undertaken using the SW480 and HT29 subclone cells whose β6 expression has been altered using stable transfections. The SW480^{Mock} cells do not express any β6 integrin whereas SW480^{β6OE} cells have artificially induced overexpression of β6 integrin. The HT29^{Mock} cells, however, endogenously express β6 integrin and its expression has been artificially reduced by about 80% in the HT29^{β6AS} cells. These cells were treated with 10ng/mL of TGFβ and their membrane proteome was enriched using triton X-114 phase partitioning followed by iTRAQ-based proteomic analysis. The results from this study showed the expression of numerous proteins associated with cytoskeletal remodelling, cell migration/invasion, cell adhesion and cellular stress associated proteins was significantly altered in presence of TGFβ and β6 expression. Various RAS oncogene associated proteins along with a few uncharacterized proteins were also identified. Further IPA showed eIF2, mTOR and tight junction signalling pathways to be significantly altered. Additionally, upon treatment with TGFβ increased proliferation, invasion and wound healing abilities were observed in the cells that expressed β6 integrin. In conclusion, the findings from this study suggests that TGFβ in presence of β6 can promote alterations to cancer related molecules and signalling networks.

3.2.1 - Transforming growth factor-β signalling induces differential protein expression in colon cancer cells that varies with the level of integrin β6 expression. [Publication IV] *(Prepared for publication)*

Transforming growth factor-β signalling induces differential protein expression in colon cancer cells that varies with the level of integrin β6 expression

Harish R Cheruku[1], David I Cantor[1], Abidali Mohamedali[2], Sock Hwee Tan[2,3], Edouard Nice[4], Mark S Baker[1]*

[1]*Department of Biomedical Sciences, Faculty of Health and Medical Sciences, Macquarie University, NSW, 2109, Australia*

[2]*Department of Chemistry and Biomolecular Sciences, Faculty of Science, Macquarie University, NSW, 2109, Australia*

[3]*Current address: National University Heart Centre, National University of Singapore, Singapore, Singapore*

[4]*Department of Biochemistry and Molecular Biology, Monash University, Clayton, Victoria, 3800, Australia*

*Corresponding Author

Professor Mark S. Baker

Faculty of Health and Medical Sciences

2 Technology Place

Macquarie University, NSW, 2109

Australia

Telephone: +61 2 9850 8211

Fax: +61 2 9850 8313

E mail: mark.baker@mq.edu.au

Abstract

Transforming growth factor-β (TGFβ) and the αvβ6 integrin are well documented to be involved in the progression of various cancers including colorectal cancer (CRC). Despite decades of research, the role of TGFβ in CRC progression is, at best, poorly understood. Similarly, up-regulation of the integrin αvβ6 in CRC has been reported to be an important promoter of metastatic progression in CRC though its mechanism is again not very well understood. TGFβ and β6 have been demonstrated to interact, potentially concomitantly, promoting metastatic progression. To explore the role of TGFβ and β6 in CRC, the membrane-enriched proteomes of SW480 and HT29 subclones with artificially modified levels of β6 subunit expression were analysed following treatment with active TGFβ. Using iTRAQ (isobaric tags for relative and absolute quantitation) we identified 2,666 and 2,041 unique proteins for SW480 and HT29 subclones respectively. Of these, varying number of proteins were found to be significantly and differentially expressed when treated with TGFβ with a positive trend between the number of altered proteins and the level of β6 expression. Ingenuity Pathway Analysis[TM] revealed that fundamental processes like "cell growth and proliferation" were significantly altered following TGFβ treatment. Differential expression of three proteins (ezrin, annexin A2 and S100-A8) was validated by Western blotting to confirm the expression changes observed by iTRAQ. Observed proteomic changes were strongly supported by *in vitro* studies, which showed increased proliferation and wound healing was associated with elevated levels of β6 following TGFβ treatment. This study demonstrates that TGFβ can exert critical proteomic and phenotypic changes within a pre-metastatic CRC cell to promote functions crucial for metastasis, and that these changes are potentiated by expression of αvβ6.

1. INTRODUCTION

Transforming Growth Factor-β (TGFβ) was first described in 1982, and is a bi-functional protein that can positively or negatively regulate cell growth depending on its microenvironment [1, 2]. The three mammalian TGFβ isoforms (TGFβ1, TGFβ2 and TGFβ3) are encoded by genes located on different chromosomes but which have significant structural and functional similarity, and signal through the same receptor system [3, 4]. *In vivo*, all TGFβ ligands are secreted as 'latent' complexes and are primarily activated byeither plasmin, integrins (αvβ6, αvβ8), or matrix metalloproteinases (MMPs) [5]. The biological effects exerted by TGFβ are mediated through type I and type II transmembrane serine/threonine kinase receptors (TGFβR1 and TGFβR2). Canonical signalling is initiated by binding of active TGFβ to TGFβR2, which recruits and transphosphorylates TGFβR1 thereby catalysing Smad2/3 phosphorylation [6]. The phosphorylated Smad2/3 associates with Smad4 and the complex translocates to the nucleus where it controls various TGFβ-mediated gene transcriptional activities with other DNA-binding co-activators, co-repressors and transcription factors [6]. In normal cells, TGFβ canonical signalling promotes tumour suppression through cytostasis, cell differentiation and apoptosis [7]. In cancer however, TGFβ plays dual roles – promoting tumour suppression during the early stages before switching to promote growth, invasion, and metastasis in mid to late stage cancer [7, 8]. The biological mechanism/s explaining such a switch to promoting tumour growth and metastasis remain highly elusive and poorly characterised.

High levels of plasma TGFβ1 (14.8 ± 8.4 ng/mL) have previously been reported to occur in Dukes' stage B1-D CRC patients, higher to those observed in normal healthy plasma (1.9 ± 1.4 ng/mL) [9]. Additionally, Kemik *et al.,* also reported increased TGFβ expression in CRC tumor tissue samples [10].These high levels of active TGFβ can be achieved through a number of ways involving activation of latent TGFβ, including by the integrin αvβ6, which is known to be overexpressed in many cancers [11]. Various clinical immunohistochemistry (IHC) studies have demonstrated that elevated integrin β6 (herein referred to only as β6) expression negatively correlates with patient survival, ascribing this to β6's roles in promoting cell proliferation, migration and invasion into proximal tissues, eventually causing metastasis [12-14]. Interestingly, a recent study by Ahn *et al.* examining the expression of αvβ6 in Dukes' stage B and C rectal cancer tissue samples did not show any increase between stages B and C [15]. It was suggested that αvβ6 overexpression may occur before or

| 87 | during Stage B, where it can assist cancer cells in maintaining the high levels of active TGFβ |

87   during Stage B, where it can assist cancer cells in maintaining the high levels of active TGFβ

88   required to promote early tumour progression. Integrin αvβ6 is also known to promote the

89   expression of various MMPs including MMP-3 and -9 that can also active latent-TGFβ [16,

90   17]. Interestingly, treatment of β6-expressing oral squamous cell carcinoma cells (oral SCC9)

91   with active TGFβ1 further enhanced MMP-3 and MMP-9 activation, indicating further

92   cross-reactivity within this TGFβ-αvβ6 interactome [16].

93   A membrane-enriched proteomic study by Cantor *et al.* demonstrated that

94   transfection of β6 into normally non-expressing cells induced significant changes in

95   expression of 708 distinct proteins [18]. The study demonstrated that β6 overexpression

96   increased cell proliferation and invasion [18] and induced differential expression of TGFβ1

97   and TGFβR2. Ingenuity Pathway Analysis© (IPA) of the significantly altered proteins

98   showed that β6 expression greatly affects cell death, cell movement, cell

99   growth/proliferation, as well as integrin-linked kinase (ILK) and Ran signalling pathways to

100   be significantly altered, all of which are key facets in cancer metastasis [18].

101   To improve our understanding of TGFβ signalling and β6 in CRC, we have employed

102   a quantitative proteomic protocol using iTRAQ (Isobaric Tag for Relative and Absolute

103   Quantitation). The study compares active TGFβ1-treated colorectal adenocarcinoma cell

104   lines (SW480 and HT29) that were engineered to have increased or decreased expression

105   levels of cell surface β6. The use of active TGFβ eliminates any molecular changes that are

106   associated with β6-mediated Latent-TGFβ1 activation. This approach allowed us to identify

107   and quantify differentially expressed peptides/proteins in a single step, a significant

108   advantage over label-free approaches. Furthermore, iTRAQ allows multiplexing of up to 8

109   samples to identify the relative abundance of proteins in different samples within a single

110   liquid chromatography mass spectrometry (LC/MS) based proteomics experiment.

111

2. RESULTS AND DISCUSSION

2.1 Validation of integrin β6 expression by Western blotting

114   Subclones of the SW480 and HT29 colon carcinoma parental cell lines were used in

115   this study. The subclones have been engineered by stable transfection to over-express or

116   supress production of the β6 subunit. SW480^{Mock} cells do not express β6 while SW480^{β6OE}

117   cells overexpress the β6 subunit [19]. The HT29^{Mock} cells endogenously express the β6 while

118 its expression is strongly reduced in the HT29[β6AS] cells [20]. **Figure 1** illustrates the
119 differences in β6 subunit expression as detected by Western blot analysis.

120
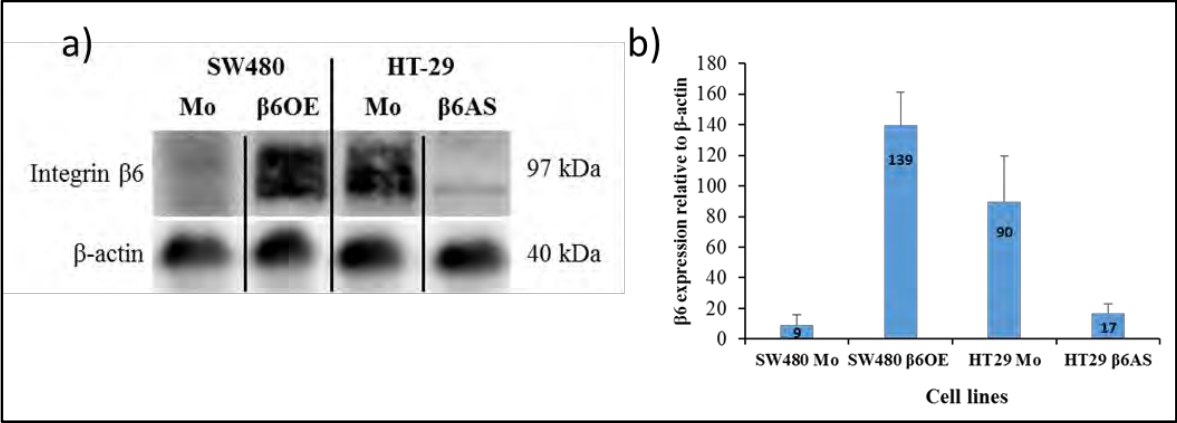
121 **Figure 1** Validation of β6 expression in the SW480 and HT29 subclones by Western blot
122 analysis. 10μg of whole cell lysate of was loaded into each well and probed with the sc-6632
123 (C-19) anti-β6 polyclonal antibody. β-actin was used as a loading control. **b)** Relative
124 abundance of β6 expression in SW480 and HT29 subclone cells (mean ± SEM) obtained by
125 quantitative analysis of the Western blot band intensities.

126 **2.2 Active TGFβ1 impairs wound healing without β6 expression**

127 We have previously demonstrated that β6 overexpression significantly increases cell
128 proliferation and invasion under normal cell culture conditions [18]. A wound healing assay
129 was used in this study to determine whether treatment with active TGFβ1 would increase the
130 ability of SW480 cells under stress to migrate into a freshly created wound (Figure 2).

131 We observed an interesting trend that at first sight seemed somewhat counter-
132 intuitive to that expected from the literature. In detail, no significant differences in wound
133 closure were observed between SW480[β6OE] and SW480[Mock] cells under SF conditions.
134 However, relative to the untreated control, TGFβ1 treatment significantly decreased the
135 ability of SW480[Mock] cells to promote wound closure. Conversely, SW480[β6OE] cells
136 exhibited a significantly faster wound closure when treated with TGFβ1, suggesting that β6
137 expression was able to ameliorate the prior anti-migrative effect. No significant differences
138 in migration were observed between the untreated and TGFβ1-treated SW480[β6OE] cells.
139 Antagonism of TGFβR1 with SB431542 (a TGFβ receptor I kinase inhibitor) was able to
140 restore SW480[Mock] cell migration to that of the SF control, whilst not significantly affecting
141 the SW480[β6OE] cell line. Interestingly, dual treatment with active TGFβ1 and SB431542
142 significantly increased SW480[β6OE] wound closure by 32% relative to the untreated control,

140

143   suggesting that active TGFβ1 may promote cell migration through other TGFβR1-
144   independent mechanisms.
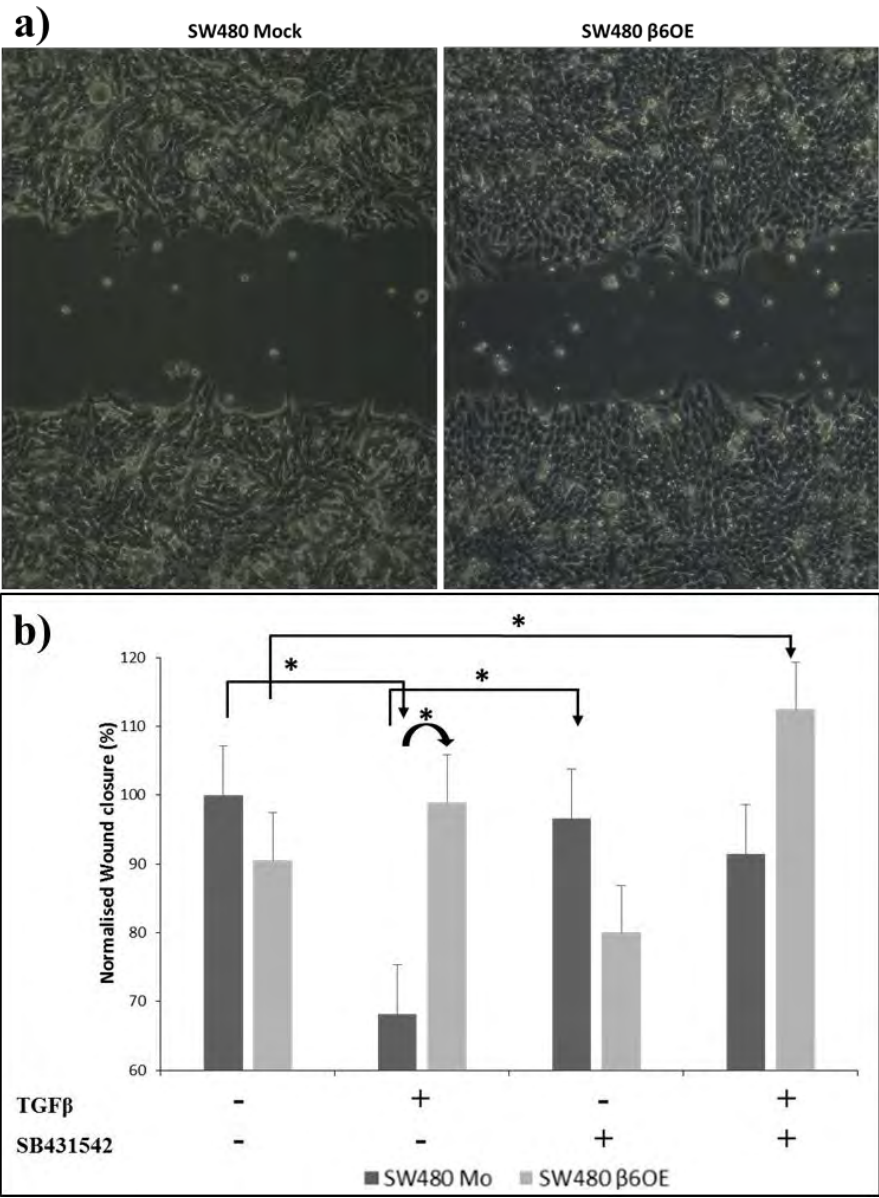
145   **Figure 2** SW480 wound healing assay. (a) Representative micrographs of wound closure
146   observed with TGFβ-treated SW480[Mock] and SW480[β6OE] cells. (b) Percentage of wound
147   closure normalised to the untreated SW480[Mock] control. TGFβ treatment significantly
148   increased SW480[β6OE] wound closure relative to the TGFβ-treated SW480[Mock] cells (*p<0.05;
149   **p<0.01). Wound width was calculated using TScratch software [21]

150   These results suggest that β6 expression influences the ability of SW480[β6OE] cells to
151   migrate into the wound compared to SW480[Mock] cells, overcoming the significant anti-
152   migrative effect of active TGFβ1.

153

2.3 β6 expression increases CRC cell invasion through an ECM analogue

Given these results and the notion that β6 overexpression directly or indirectly increases invasion in various cancers [18, 22, 23], we further assessed the influence of TGFβ1 on SW480 and HT29 invasion using Transwell invasion assays to determine whether the level of β6 expression would influence invasive potential. In addition to the SW480 subclones, in which β6 is artificially expressed, this study employed HT29 subclones which endogenously express β6 (HT29Mock) or have had β6 expression stably reduced by ~80% using antisense suppression (HT29β6AS) [20].
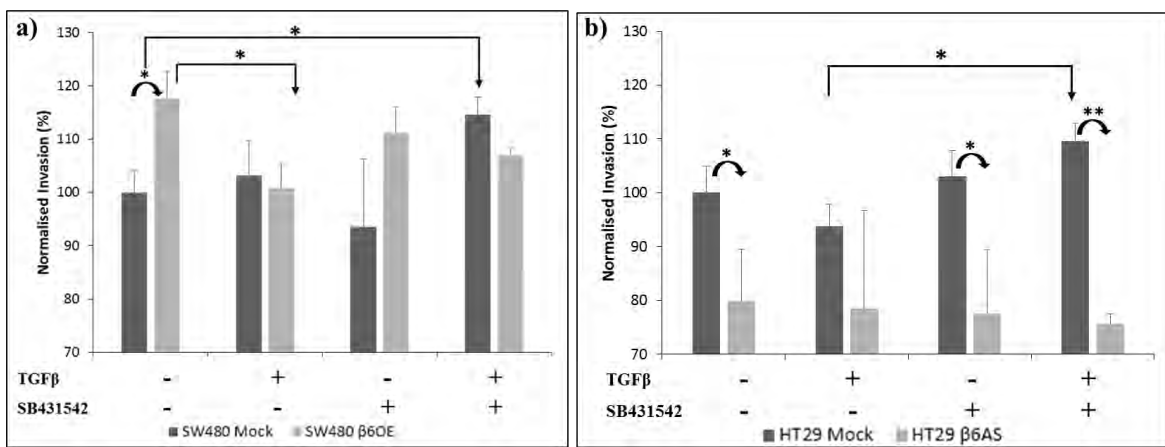
Figure 3 a) SW480 and (b) HT29 invasion assay normalised to the untreated SW480Mock and HT29Mock controls respectively (*p<0.05; **p<0.01).

We observed that SW480β6OE cells were significantly more invasive than SW480Mock cells under untreated serum-free conditions (Figure 3a), in agreement with previous observations [18]. TGFβ1 treatment significantly decreased SW480β6OE invasion relative to the untreated control, whilst SW480Mock cells did not show any noticeable change. Similarly, no significant change was observed in either cell line when treated with SB431542 alone. However, SW480Mock cells were significantly more invasive when treated with both TGFβ1 and SB431542, whilst no change was observed with SW480β6OE cells. These findings initially seemed in contradiction to those observed in the wound healing assay; however it is important to note the two assays interrogate different aspects of cell invasion. Wound-healing assays assess cell migration into an unoccupied space on a two-dimensional substrate while Transwell invasion assays assess the ability for cells to actively degrade the ECM components of a basement membrane extract and undergo chemotactic migration. Taken together, these two experiments suggest that β6 expression may protect SW480 cells from

178   TGFβ1-mediated inhibition of cell movement and significantly enhance invasion through an

179   ECM analogue via a mechanism that can be significantly impaired by active TGFβ1.

180   HT29 subclones which natively express β6 were then used to further examine the

181   TGFβ1- and β6-associated invasion. These results (Figure 3b) confirmed that high β6

182   expression promotes HT29 invasion as HT29^{Mock} cells were significantly more invasive than

183   HT29^{β6AS}. As seen with the SW480 subclones, active TGFβ1 treatment inhibited this

184   increase while TGFβR1 antagonism restored the increase in HT29^{Mock} invasion when treated

185   with TGFβ1. Interestingly, dual treatment with TGFβ1 and SB431542 significantly

186   increased HT29^{Mock} invasion compared to treatment with TGFβ1 alone, suggesting again

187   that active TGFβ1 may promote cell invasion through a TGFβR1-independent mechanism.

188   These results suggest that treatment of β6-expressing CRC cells with TGFβ1

189   promotes ECM degradation and eventually invasion. This trend was observed even when the

190   cells were treated with SB431542, which inhibits signalling through TGFβ receptors,

191   suggesting the presence of an alternative pathway other than the αvβ6-TGFβ axis for

192   invasion. This requires further investigation.

193

194   **2.4 β6 expression promotes proliferation following active TGFβ1 treatment**

195   β6 overexpression significantly enhanced SW480 cell proliferation under standard

196   cell culture conditions [18]. The ability of TGFβ to alter cell proliferation of CRC cells with

197   varying levels of β6 expression was examined by performing proliferation assays. Cell

198   counting identified significant differences in proliferation as a result of β6 expression

199   following treatment (Figure 4).

200   Interestingly, in the absence of FBS, SW480^{β6OE} cells were less proliferative than the

201   SW480^{Mock} cells grown in SF media without any treatments. However, TGFβ1 treatment

202   doubled the number of SW480^{β6OE} cells compared to the untreated control. On the other

203   hand, active TGFβ1 treatment exerted no significant effect in the SW480^{Mock} proliferation.

204   When we compared active TGFβ1-treated SW480β^{Mock} to similar SW480^{β6OE} experiments,

205   β6 expression was found to induce a ~60% increase in cell number, suggesting the anti-

206   proliferative effect of SF conditions on SW480^{β6OE} cells can be reversed with TGFβ1

207   treatment in a β6-dependent manner. To validate this observation, TGFβ antagonism with

208   SB431542 was used to ablate the pro-proliferative effect of TGFβ in SW480^{β6OE} cells,

209   significantly decreasing cell numbers by 55% relative to the active TGFβ1 treatment. While

210 SB431542 had no effect on SW480[Mock] cell numbers, the dual treatment with TGFβ1 and

211 SB431542 significantly increased SW480[Mock] proliferation by 24%, suggesting that TGFβ1

212 may be exerting an anti-proliferative effect in in the absence of β6 expression.

213
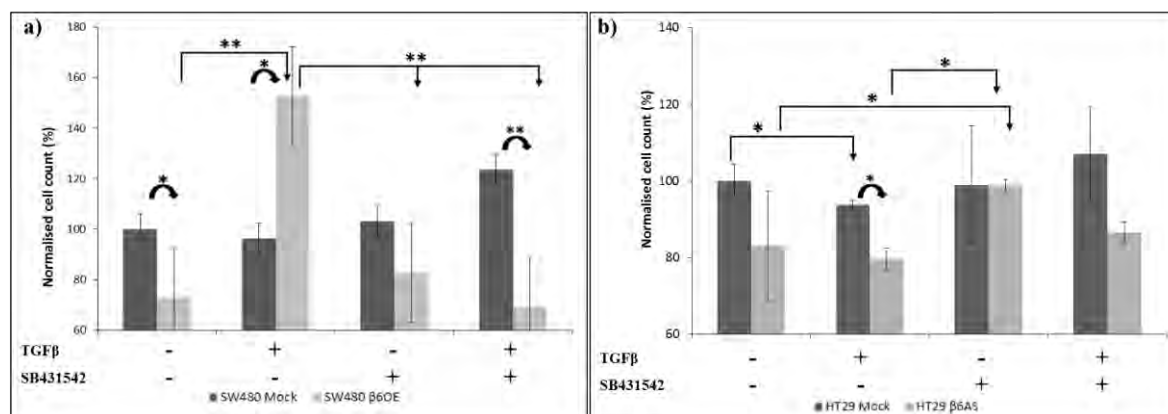
Figure 4 Proliferation assay of SW480 and HT29 subclones normalised to the untreated
SW480[Mock] and HT29[Mock] controls. (a) Live cell counts of SW480 subclones (b) Live cell
counts of HT29 subclones. Active TGFβ treatment significantly enhances the proliferation
rate of cells expressing β6 which then regresses back to normal rates when treated with
SB431542 (TGFβR1 inhibitor) (*p<0.05; **p<0.01)

219

220   This approach was subsequently repeated using the HT29 subclones. HT29[Mock] cells

221 constitutively express β6 which is reduced by ~80% in the HT29[β6AS] cell line. Unlike

222 SW480[β6OE] cells, endogenous β6 expression in HT29[Mock] cells did not experience an anti-

223 proliferative effect. Instead, antisense suppression of β6 significantly reduced HT29[β6AS]

224 proliferation. Interestingly, TGFβ1 treatment had a significant anti-proliferative effect on

225 HT29[Mock] cells compared to the untreated control. Again, this initially seemed

226 counterintuitive when considering the SW480 data. However, it should be remembered that

227 β6 is endogenously expressed in the parental cell line and so there may be considerable

228 differences in the operative cell biology. In the HT29[β6AS] cell line, TGFβ1 treatment did not

229 exert an anti-proliferative effect compared to the untreated control: instead TGFβ1

230 antagonism by SB431542 significantly increased proliferation. This was also observed when

231 HT29[β6AS] cells were treated with both TGFβ1 and SB431542, although the effect was greatly

232 reduced. TGFβ1 antagonism had no effect on HT29[Mock] cell proliferation, suggesting that

233 increased HT29[Mock] proliferation is mediated by β6 expression, albeit in a different

234 mechanism to that operating in SW480s, possibly the product of a counterbalance against β6

235 expression.

236   Data obtained from both cell lines affirm that β6 expression positively correlates with

237   cell proliferation and that TGFβ1 remains "duplicitous". Our data also suggests that TGFβ1

238   has a pro-proliferative effect on CRC cells in which β6 expression is induced while having

239   an anti-proliferative effect on CRC cells in which β6 is endogenously expressed. This,

240   coupled with the increase in invasion observed, prompted us to take a wider view of the

241   effect of TGFβ1 in CRC and therefore we adopted proteomics to gain clear insight into how

242   TGFβ and β6 expression affects CRC.

243

2.5 Membrane Proteomic analysis of CRC cell lines by iTRAQ-MS profiling

245   Having determined that TGFβ1 exerts different effects on cells with varying β6

246   expression, we investigated the membrane changes associated with TGFβ1 treatments using

247   proteomics in order to gain a greater insight into the action of TGFβ1. These molecular

248   changes were investigated using iTRAQ-based quantitative membrane proteomic analysis.

249   The protein lists obtained from the individual iTRAQ experiments were used to

250   generate a single 'library' using Stouffer's method, whereby the protein ratios across

251   experiments are combined to obtain a single Stouffer's p-value [24]. The combined protein

252   list was subjected to strict filtering criteria for the confident identification of differentially

253   expressed proteins. These filter criteria included: (1) a strict cut-off of unused protein score

254   ≥1.3, which corresponds to a 5% false discovery rate (FDR) at protein level, was used as a

255   part of Stouffer's method, (2) a protein p-value ≤ 0.05, ensuring the proteins identified were

256   seen in replicate MS runs, 3) a minimum average fold change of ≥ 20%, which corresponds

257   to a iTRAQ ratio (or fold change) of ≥ 1.2 for up-regulated and ≤ 0.83 for down-regulated

258   proteins.

259   Using the Stouffer method, we identified 2,666 and 2,041 proteins from the iTRAQ

260   MS analysis of SW480 and HT29 subclones respectively. The subcellular locations (%) of

261   the identified proteins was determined using PloGO (Figure 5). Using the workflow detailed

262   above, these lists were then used to identify differentially expressed proteins for a

263   combination of treatment comparisons as shown in Table 1. The complete list of

264   differentially regulated proteins for all comparisons can be found in the supplementary

265   information. This manuscript will not discuss any results comparing the untreated SW480

266   β6OE and SW480 Mock, as this work has been previously published by Cantor *et al*., [18].

267
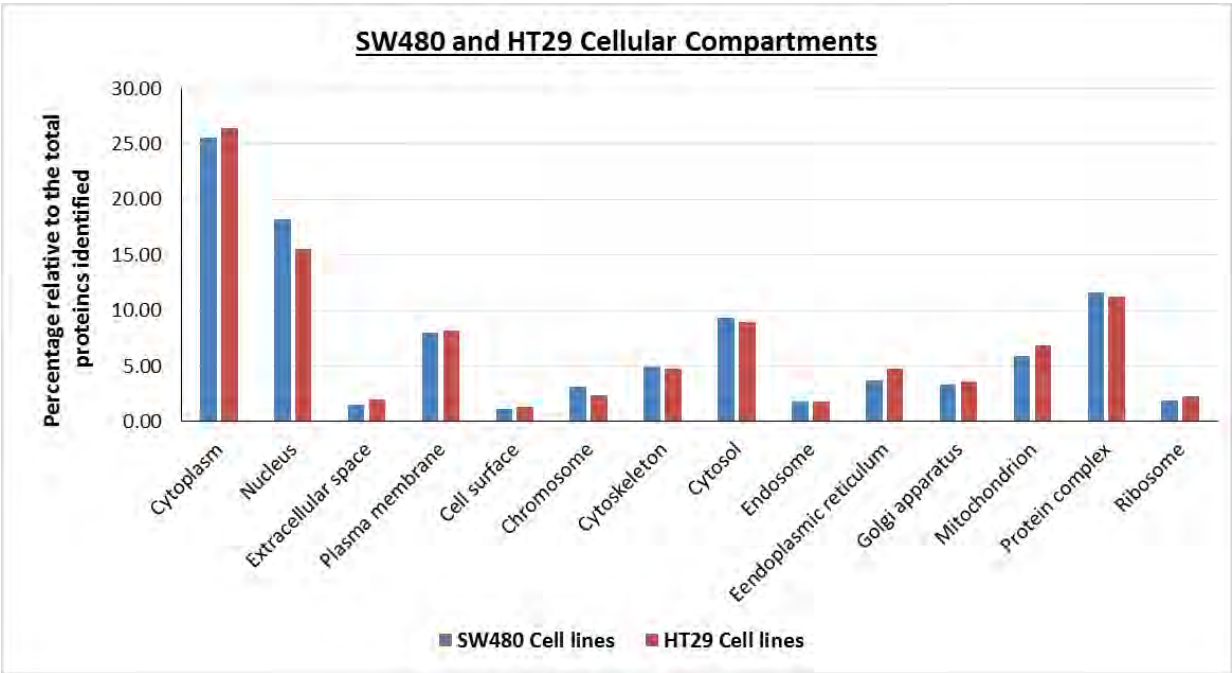
Figure 5 Cellular distribution of all the proteins identified from SW480 and HT29 iTRAQ proteomic experiments.

270

Table 1 SW480 and HT29 comparisons showing the total number of significant proteins (p≤ 0.05) and number of differentially expressed proteins

Comparison of Cell line (+/- TGFβ)	Total # of proteins with p ≤ 0.05	# up-regulated proteins (iTRAQ fold change ≥1.2)	# down-regulated proteins (iTRAQ fold change ≤0.83)
SW480 subclones			
SW480 Mo+ vs Mo-	41	11	13
SW480 β6OE+ vs β6OE-	129	30	16
SW480 β6OE+ vs Mo+	344	161	150
SW480 β6OE- vs Mo-	369	180	174
HT29 subclones			
HT29 Mo- vs β6AS-	140	69	70
HT29 Mo+ vs Mo-	161	55	70
HT29 β6AS+ vs β6AS-	94	45	35
HT29 Mo+ vs β6AS+	168	84	75

273

274

2.6 Lack of integrinβ6 expression results in minimal change to the proteome when treated with TGFβ (SW480 Mo+ vs Mo-)

TGFβ treatment of β6-deficient SW480^{Mock} cells resulted in the detectable up- and down-regulation of only a small number of proteins (11 and 13 respectively). This included proteins associated with cytoskeleton, cell adhesion and, integrin and MAPK signalling (Table 2). Various intermediate filament-associated proteins, keratin, type II cytoskeletal 1 (KRT1), keratin, type II cytoskeletal 8 (KRT8), keratin, type I cytoskeletal 9 (KRT9) and keratin, type I cytoskeletal 10 (KRT10) were identified. Walker *et al.* showed that KRT8/18 expression can be used to differentiate different subtypes of invasive ductal breast carcinoma [25]. Desmoplakin, a cell junction-associated protein was found to be slightly down-regulated. Cytoskeleton-associated protein 4 (CKAP4) was down-regulated and has been previously shown to have moderate to strong expression in cancer tissues by IHC [26]. CKAP4 is known to function as a receptor for anti-proliferative factor (APF) and has been shown to regulate tissue plasminogen activator in bladder cancer [27]. Actin filament-associated proteins myosin-9 and myosin-10 (MYH9 and MYH10), which play an important role during cell spreading and focal contact formation in the centre of spreading cells, were slightly down-regulated.

Table 2 Differentially expressed proteins observed in the TGFβ treated SW480^{Mock} cells relative to the untreated control (SW480 Mo+ vs Mo-)[a]

Accession number	Gene name	Protein Name	iTRAQ fold change	Expression pattern
P15924	DSP	desmoplakin	0.79	↓
P35580	MYH10	myosin-10	0.80	↓
Q07065	CKAP4	cytoskeleton-associated protein 4	0.80	↓
P05787	KRT8	keratin, type II cytoskeletal 8	0.81	↓
P35579	MYH9	myosin-9	0.83	↓
P13645	KRT10	keratin, type I cytoskeletal 10	1.36	↑
P35527	KRT9	keratin, type I cytoskeletal 9	1.89	↑
P04264	KRT1	keratin, type II cytoskeletal 1	1.92	↑

[a] Fold change ratios of significantly altered proteins observed in two biological replicates of iTRAQ experiment. These proteins have met the stipulated criteria (i.e., unused protein score >1.3 and change in expression level of at least 1.2 fold for aggressive (SW480^{Mock} treated with TGFβ) vs non-aggressive (SW480^{Mock} not reated with TGFβ)

IPA analysis of the significantly altered proteins identified two protein networks with high scores ["Cellular Development, Cellular Growth and Proliferation, Cell Cycle" (IPA score = 21) and "Protein Synthesis, Cell Morphology, RNA Post-Transcriptional Modification" (IPA score = 18)]. Various basic cellular functions involved in cancer, namely (i) cellular assembly and organization, (ii) cell morphology, (iii) cellular function and maintenance, (iv) cellular development, and (v) cellular growth and proliferation [28] were identified. Additionally, tight junction signalling and ILK signalling canonical pathways, that can also be associated with cancer, were identified. Unfortunately, despite this interesting observation, the number of proteins identified for each of these pathways (< 2% of the total molecules in the pathways) were insufficient for establishing conclusive biological connection.

2.7 Overexpression of integrin β6 increased the number of differentially proteins observed (SW480 OE+ vs OE-)

Treatment of SW480^{β6OE} cells with TGFβ resulted in differential up-regulation of 30 proteins and down-regulation of 16 proteins (Table 3). Among the differentially expressed proteins integrin beta-1 (β1) and integrin alpha-v (αv) were identified to be up-regulated in TGFβ-treated cells. The up-regulation of integrin αv supports the overexpression of β6 which requires integrin αv to form a heterodimer and participate in downstream signalling. Increased β1 expression could be the result of significantly increased αv expression as a result of the activation of the Ets-1 transcription factor. As shown in a previous membrane proteomic study using the same cell lines [18], the number of observed αv peptides far exceeds the number of observed β6 peptides.

It is known that epithelial cells actively trigger anoikis (cell death triggered by improper or loss of cell adhesion) during metastasis [29, 30]. Suppression of anoikis, is an important requirement for tumor cells to metastasize to distant organs [31]. Various chaperone proteins were identified, of which DnaJ homolog subfamily A member 1 (DNAJA1 or Hsp40) was significantly upregulated. Chaperone proteins play an important role in defence against cellular stress and the up-regulation of Hsp40 could reflect the suppression of anoikis. This was further supported by the fact that BAG family molecular chaperone regulator 2 (BAG-2), which directly affects the activity of Hsp70/HSC70 by promoting substrate release, was up-regulated following treatment.

327　　　　　Decreased expression of intermediate filaments keratin, type II cytoskeletal 2

328　　epidermal (KRT2) and keratin, type II cytoskeletal 8 (KRT8) was observed in the TGFβ

329　　treated cells. Interestingly, vimentin, a mesenchymal marker, was slightly down-regulated.

330　　Ragulator complex protein LAMTOR2 which indirectly regulates mTORC1 signalling and

331　　enhances MAPK signalling activity by activating MAPK2 [32], was significantly up-

332　　regulated. Nicastrin, a transmembrane glycoprotein, was also up-regulated. Nicastrin and

333　　notch4 are known to promote epithelial to mesenchymal transition (EMT) in breast cancer

334　　[33, 34].

335　　**Table 3** Differentially expressed proteins observed in the TGFβ treated SW480^{β6OE} cells

336　　relative to the untreated control (SW480 OE+ vs OE-)^a

Accession number	Gene name	Protein Name	iTRAQ fold change	Expression pattern
P35908	KRT2	keratin, type II cytoskeletal 2 epidermal	0.25	↓
P05787	KRT8	keratin, type II cytoskeletal 8	0.78	↓
P08670	VIM	vimentin	0.80	↓
Q92542	NCSTN	nicastrin	1.21	↑
O95816	BAG2	BAG family molecular chaperone regulator 2	1.21	↑
P06756	ITGAV	integrin alpha-V	1.21	↑
P31689	DNAJA1	DnaJ homolog subfamily A member 1	1.38	↑
P05556	ITGB1	integrin beta-1	1.54	↑
Q9Y2Q5	LAMTOR2	Ragulator complex protein LAMTOR2	1.85	↑

^{a} Fold change ratios of significantly altered proteins observed in two biological replicates of iTRAQ experiment. These proteins have met the stipulated criteria (i.e., unused protein score >1.3 and change in expression level of at least 1.2 fold for aggressive (SW480^{β6OE} treated with TGFβ) vs non-aggressive (SW480^{β6OE} not treated with TGFβ)

337

338　　　　　IPA identified only one protein network with score >15: the "Protein Synthesis,

339　　Developmental Disorder, Hereditary Disorder" network (IPA score of 49) (Figure 6). This

340　　network was extrapolated from 22 molecules from the list of significantly altered proteins.

341　　The network contained, amongst others, integrins – αv, β1; molecular chaperones – BAG2,

342　　HSP5A and ECM molecules – VIM, KRT8, matrin 3. The network showed associations with

343　　molecules such as Akt, p38 MAPK, MAP2K1/2 and Mek, all of which have been associated

344　　with non-Smad TGFβ signalling during cancer [35, 36].

345　　　　　IPA also suggested that fundamental cellular functions such as (i) RNA post-

346　　transcriptional modification, (ii) protein synthesis, (iii) cellular movement, and (iv) cellular

347　　growth and proliferation were altered with TGFβ1 treatment. Most of the canonical pathways

348 identified had little to no association with cancer with the exception of Eukaryotic translation

349 initiation factor 2 (eIF2) signalling. However, only 3 molecules that are part of the eIF2

350 signalling pathway were identified which is not sufficient to infer any biological relevance.

351

352

353 **Figure 6** The "Protein Synthesis, Developmental Disorder, Hereditary Disorder" network
354 identified by IPA from comparison of the TGFβ-treated SW480^{β6OE} cells relative to
355 untreated controls. The network shows the relationships between various differentially
356 expressed proteins observed by proteomics (red, up-regulated; green, down-regulated; white,
357 not observed by proteomics but crucial to the network).

358 **2.8 Integrin β6 overexpression alters a wide variety of cancer-related proteins and**
359 **functions when treated with TGFβ relative to no integrin β6 expression (SW480**
360 **β6OE+ vs Mo+)**

361   To examine the effect of TGFβ when β6 is overexpressed, we compared the

362 SW480^{β6OE} and SW480^{Mock} cell lines following treatment with TGFβ. This showed 344

363 proteins to be differentially expressed (161 proteins and 149 proteins up-regulated and

364 down-regulated respectively). These data have been functionally classified help

365 interpretation of the molecular events affected by TGFβ treatment when β6 was
366 overexpressed. Some of the key proteins observed are listed in Table 4.

367 Cytoskeletal signalling proteins such as intermediate and actin filament associated
368 proteins aid in maintaining integrity both in and between cells. Our study identified various
369 intermediate filament associated family proteins to be significantly changed in SW480^{β6OE}
370 cells. Several keratins including, keratin, type II cytoskeletal 5 (KRT5) and keratin, type I
371 cytoskeletal 18 (KRT18), all of which are integral to cytoskeletal arrangement in cells [37],
372 were down-regulated. Talin-1 and desmoplakin, which are involved in organising
373 connections between various cytoskeletal structures and plasma membrane [38UniProt, 2015 #113],
374 were up-regulated.

375 Various actin filament associated proteins such as α-actinin-4, unconventional
376 myosin-Ib, unconventional myosin-Id and ezrin (Villin-2) were significantly down-
377 regulated. The actin-binding protein, α-actinin-4, has been associated with cell motility and
378 invasion during cancer [39]. A recent study by Gosh *et al.* that showed down-regulation of α-
379 actinin-4 in the SW620 cell line, which is a metastatic lymph node progenitor of the SW480
380 cell line, supports our results [31], suggesting that SW480 cells that express β6 can adopt
381 metastatic cell line behaviour in the presence of TGFβ. Myosin regulatory light chain 12A,
382 a protein known to can play a significant role in cell cell adhesion, proliferation, migration
383 and division [40] was significantly up-regulated. Ezrin (villin-2) expression was further
384 validated by Western blot analysis (Figure 11).

385 Increased cell proliferation and migration along with decreased adhesion are
386 important biological/molecular functions required for cancer progression. Our study
387 identified various molecules involved in cell adhesion that were altered with TGFβ
388 treatment. Cell surface glycoprotein MUC18 (MCAM), integrin α6, integrin β1 and CD97
389 antigen were down-regulated. Additionally, catenin δ-1 and pinin were significantly up-
390 regulated in SW480^{β6OE}. Integrin β1 is known to affect cell adhesion and migration *in vitro*
391 as it is a receptor for fibronectin and vitronectin [41]. Down-regulation of β1, as a result αvβ1,
392 could create a shortage of receptors for fibronectin and vitronectin resulting in unstable or
393 loose ECM which may enable cell migration and proliferation [41].

394 Annexin A2, galectin-3, glypican-1, GTPase Kras and Ras GTPase-activating
395 protein-binding protein 1 which are known to regulate cell migration, were all significantly
396 down-regulated. Annexin A2, is known to inhibit cell migration *in vitro* [42] and the observed

397	down-regulation could support the increased cell migration observed in TGFβ-treated			

down-regulation could support the increased cell migration observed in TGFβ-treated SW480^{β6OE} cells (Figure 2, 3). The expression of annexin A2 was further validated by Western blot analysis (Figure 11). Liprin β1 and tight junction protein ZO-2 which are involved in the regulation of focal adhesions and tight junctions were also down-regulated. Liprin β1 could be involved in the regulation of focal adhesion disassembly [43] and was shown to be a target for metastasis-associated protein S100-A4 [44]. The down-regulation of various cell migration and adhesion associated molecules indicates that cells may have acquired the ability to spread from the primary cancer site. This is in agreement with the observation that SW480^{β6OE} cells showed increased cell proliferation and migration when treated with TGFβ (Figure 2, 3).

Table 4 Functional classification of significantly altered proteins observed upon treatment of SW480^{β6OE} cells with TGFβ relative to TGFβ treated SW480^{Mock} cells (SW480 β6OE+ vs Mo+)^a.

Accession number	Gene name	Protein Name	iTRAQ fold change	Expression pattern
Intermediate Filament associated proteins				
P35908	KRT2	keratin, type II cytoskeletal 2 epidermal	0.29	↓
P04264	KRT1	keratin, type II cytoskeletal 1	0.36	↓
P13647	KRT5	keratin, type II cytoskeletal 5	0.42	↓
P35527	KRT9	keratin, type I cytoskeletal 9	0.47	↓
P13645	KRT10	keratin, type I cytoskeletal 10	0.58	↓
P05783	KRT18	keratin, type I cytoskeletal 18	0.65	↓
P05787	KRT8	keratin, type II cytoskeletal 8	0.72	↓
Q9Y490	TLN1	talin-1	1.21	↑
P15924	DSP	desmoplakin	1.21	↑
Actin filament associated proteins				
O94832	MYO1D	unconventional myosin-Id	0.54	↓
O43707	ACTN4	alpha-actinin-4	0.70	↓
O43795	MYO1B	unconventional myosin-Ib	0.82	↓
P19105	MYL12A	myosin regulatory light chain 12A	2.66	↑
Cell Proliferation, migration and adhesion associated proteins				
P43121	MCAM	cell surface glycoprotein MUC18	0.24	↓
P15311	EZR	ezrin (Villin-2)	0.34	↓
P07355	ANXA2	annexin A2	0.39	↓
P23229	ITGA6	integrin alpha-6	0.45	↓
P17931	LGALS3	galectin-3	0.48	↓
P35052	GPC1	glypican-1	0.54	↓
P29317	EPHA2	ephrin type-A receptor 2	0.61	↓

Q86W92	PPFIBP1	liprin-beta-1	0.63	↓
Q9UDY2	TJP2	tight junction protein ZO-2	0.78	↓
P05556	ITGB1	integrin beta-1	0.79	↓
P48960	CD97	CD97 antigen	0.82	↓
O60716	CTNND1	catenin delta-1	1.24	↑
Q86UP2	KTN1	kinectin	1.48	↑
Q9H307	PNN	pinin	1.65	↑
		Cellular stress and cell death associated proteins		
P51572	BCAP31	B-cell receptor-associated protein 31	0.54	↓
P35232	PHB	prohibitin	0.48	↓
P07900	HSP90AA1	heat shock protein HSP 90-alpha	0.49	↓
Q99623	PHB2	prohibitin-2	0.57	↓
P50454	SERPINH1	serpin H1 (47 kDa heat shock protein)	0.71	↓
P08238	HSP90	heat shock protein HSP 90-beta	1.44	↑
O60884	DNAJA2	DnaJ homolog subfamily A member 2	1.63	↑
P13010	XRCC5	X-ray repair cross-complementing protein 5	1.89	↑
P12956	XRCC6	X-ray repair cross-complementing protein 6	2.09	↑
		RAS oncogene family		
P11233	RALA	Ras-related protein Ral-A	0.52	↓
P51149	RAB7A	Ras-related protein Rab-7a	0.63	↓
P51148	RAB5C	Ras-related protein Rab-5C	0.68	↓
Q13283	G3BP1	Ras GTPase-activating protein-binding protein 1	0.72	↓
P01116	KRAS	GTPase Kras	0.75	↓
		Other proteins		
O15173	PGRMC2	membrane-associated progesterone receptor component 2	0.68	↓
P02786	TFRC	transferrin receptor protein 1	0.73	↓
Q8N163	KIAA1967	DBIRD complex subunit KIAA1967	0.81	↓

[a] Fold change ratios of significantly altered proteins observed in two biological replicates of iTRAQ experiment. These proteins have met the stipulated criteria (i.e., unused protein score >1.3 and change in expression level of at least 1.2 fold for aggressive (SW480[β6OE] treated with TGFβ) vs non-aggressive (SW480[Mock] treated with TGFβ)

410

411   This study also identified various molecules that either promote or hinder cell death.

412   Similar to the SW480 β6OE+ vs β6OE- comparison, we identified various chaperone and

413   heat shock proteins such as Heat shock protein HSP 90-alpha and serpin H1 (47 kDa heat

414   shock protein) to be down-regulated. B-cell receptor-associated protein 31 (BCAP31),

415   another chaperone protein, which may be involved in CASP-8 mediated apoptosis [45] was

416   also down-regulated. Since these proteins play an important role in defence against cellular

stress, their down-regulation could be associated with activation of cell death-related pathways. However, other chaperone proteins such as Heat shock protein HSP 90-beta, DnaJ homolog subfamily A member 2, X-ray repair cross-complementing protein 5 (XRCC5) and 6 (XRCC6) were significantly up-regulated. XRCC5/6 heterodimer expression shown to be increased in gastric carcinoma and may lead to genome instability [46]. This up-regulation of cell repair molecules such as XRCC5 and XRCC6 may promote anoikis suppression and alter the genome towards a metastatic phenotype.
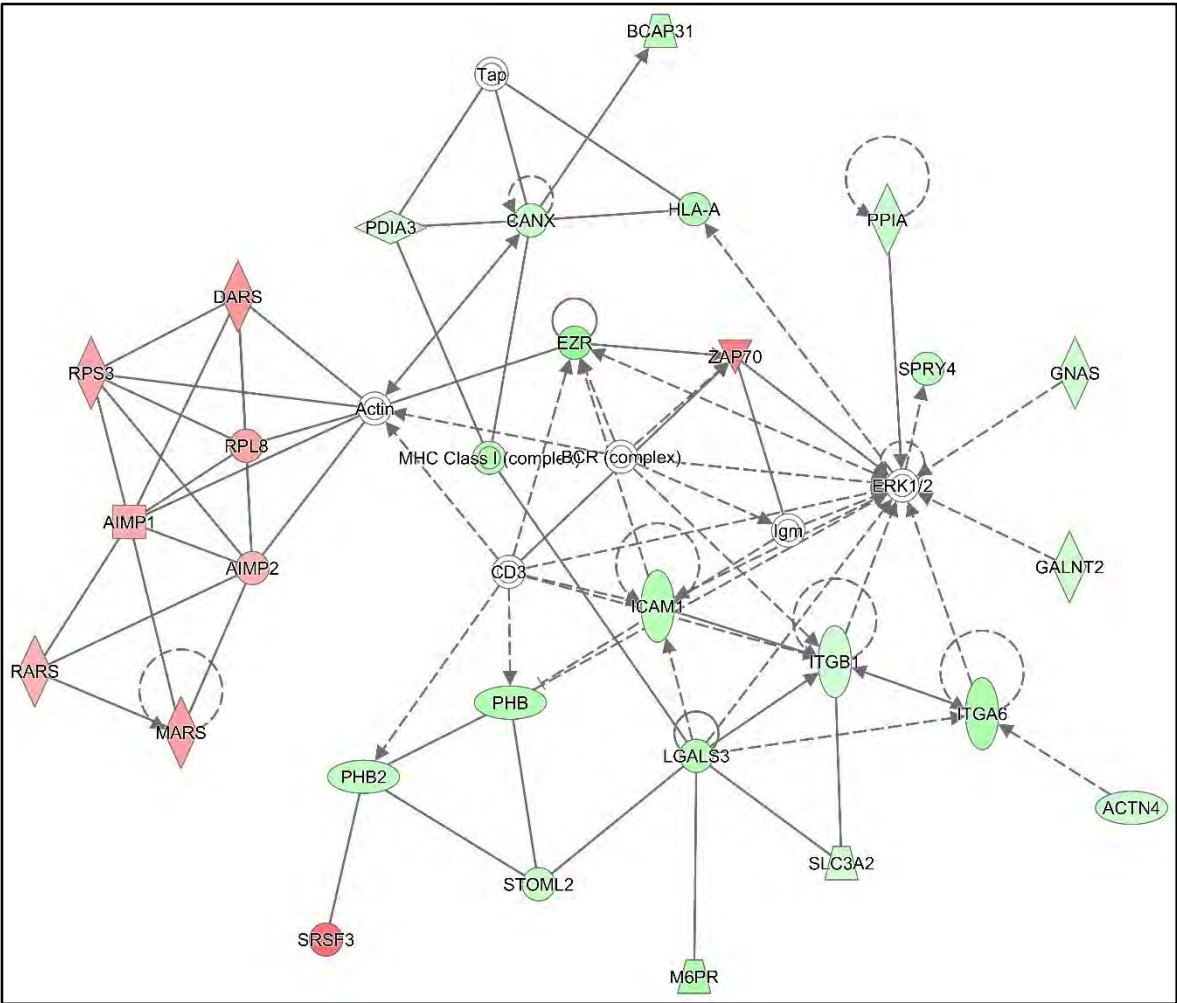
Figure 7 "Cellular Movement, Hematological System Development and Function, Immune Cell Trafficking" network identified by IPA comparing the TGFβ-treated SW480^{β6OE} cells relative to TGFβ-treated SW480^{Mock} cells. Refer to Figure 6 for legend details.

Various RAS oncogene family related proteins were down-regulated. Ras GTPase-activating protein-binding protein 1 (G3BP1) and GTPase Kras are known to play an important role in the regulation of cell proliferation [47, 48]. G3BPs are overexpressed in a number of cancers, including CRC. In breast cancer cells, G3BP1 is known to affect cell

proliferation though the regulation of PMP22 mRNA expression [49]. Interestingly, the membrane-associated progesterone receptor component 2 that is associated with malignant phenotype in breast cancer was observed to be down-regulated in CRC cell lines [50].

IPA analysis of the differentially expressed proteins identified numerous protein networks with IPA scores greater than 15. Important networks include "Cellular Movement, Hematological System Development and Function, Immune Cell Trafficking" (IPA score = 40) (Figure 7) and "Cell Cycle, Protein Synthesis, Cellular Development" (IPA score = 28), "Cellular Assembly and Organization, Dermatological Diseases and Conditions, Organismal Injury and Abnormalities" (IPA score = 24) and "Cellular Movement, Cell Morphology, Cellular Assembly and Organization" (IPA score = 16). The analysis also identified various fundamental cellular functions that are required for cancer, namely (i) RNA post-transcriptional modification, (ii) cell death and survival, (iii) cellular growth and proliferation, (iv) protein synthesis, and (v) cellular development.

Table 5 Signalling pathways that are significantly altered in the TGFβ-treated SW480^{β6OE} cells, relative to the TGFβ-treated SW480^{Mock} cells.

Pathway	Significantly altered proteins (number of molecules)	*p* value
eIF2 signalling	EIF2S1, RPL7A, RPS10, RPS26, RPS5, RPL26, RPL6, RPS13, RPS19, RPL8, EIF2S2, RPS8, RPS3A, RPL4, RPL14, RPL18A, **KRAS**, RPS6, RPL17, RPLP2, RPS2, RPL23A, EIF5, RPS3, RPS16, RPL7, EIF2S3, RPS9, RPL18, RPS17, RPL36, RPL34, RPL15, RPL27, RPL10A (35)	2.69E-28
Regulation of eIF4 and p70S6K signalling	EIF2S1, **KRAS**, RPS6, RPS10, RPS26, RPS5, RPS2, RPS3, RPS19, RPS16, RPS13, EIF2S3, EIF2S2, RPS9, RPS17, **ITGB1**, RPS8, RPS3A, PPP2R1B (19)	2.08E-12
mTOR signalling	**KRAS**, RPS6, RPS10, RPS26, RPS5, RPS2, RPS3, RPS19, RPS16, RPS13, RPS9, RPS17, RPS8, RPS3A, PPP2R1B (15)	3.44E-07

Three canonical pathways (eIF2 signalling, regulation of eIF4 and p70S6K signalling, and mammalian target of rapamycin (mTOR) signalling) that have previously been implicated in cancer [51, 52], were found to be significantly altered (p < 3.44E-07) by IPA, **Table 5**. Interestingly, KRAS was observed to be involved in all three canonical pathways, suggesting a critical role for KRAS. Additionally, integrin β1 was part of the "regulation of eIF4 and p70S6K signalling" pathway. Proteomic analysis of cells that overexpress or do not express the β6 subunit following treatment with TGFβ demonstrated

the differential expression of numerous proteins that regulate a wide variety of molecular
mechanisms required for cancer development and progression. IPA analysis identified cell
morphology, cellular assembly and organization, cellular movement, cellular growth and
proliferation and protein synthesis to be some of the important molecular functions
associated with the proteomic data sets. These results show that β6 and TGFβ together can
alter various cellular functions related to cancer. To further investigate the effect of TGFβ
when native expression of β6 is greatly reduced we next used the HT29 subclone cell lines
as models (HT29^{Mock} cells have endogenous expression of β6; HT29^{ASβ6} cells have the β6
expression greatly reduced).

2.9 Suppressing endogenous β6 expression alters various cancer-related molecules and functions (HT29 Mo- vs AS-)

Prior to examining the effects of TGFβ on the HT29 subclones, we compared the
proteomes of untreated HT29^{Mock} and HT29^{β6AS} cells. Significant differences were observed
in the expression of 139 proteins, with 69 proteins up-regulated and 70 down-regulated
respectively **(Table 6)**.

A number of intermediate filament proteins including plectin, KRT18, KRT19 and
KRT20 were down-regulated while KRT10 was up-regulated in the HT29^{Mock} cells. Various
actin filament associated proteins such as LIM domain and actin-binding protein 1 (LIAM1),
α-actinin-4, septin-2, myosin light polypeptide 6 and myosin-9 were found to be up-
regulated while Myb-binding protein 1A was down-regulated. LIAM1 is known to regulate
actin dynamics by cross-linking and stabilizing the filaments [53]. Again, α-actinin-4 has
previously been implicated in cancer cell motility and invasion [39].

Table 6 Functional classification of significantly altered proteins observed in the untreated
HT29^{Mock} cells relative to untreated HT29^{β6AS} cells (HT29 Mo- vs AS-)[a]

Accession number	Gene name	Protein Name	iTRAQ fold change	Expression pattern
		Intermediate Filament associated proteins		
P13645	KRT10	keratin, type I cytoskeletal 10	0.65	↓
Q15149	PLEC	plectin	1.22	↑
P08727	KRT19	keratin, type I cytoskeletal 19	1.49	↑
P05783	KRT18	keratin, type I cytoskeletal 18	1.55	↑
P35900	KRT20	keratin, type I cytoskeletal 20	2.39	↑
		Actin filament associated proteins		
Q9BQG0	MYBBP1A	Myb-binding protein 1A	0.47	↓

Q9UHB6	LIMA1	LIM domain and actin-binding protein 1	1.31	↑
O43707	ACTN4	alpha-actinin-4	1.50	↑
P60660	MYL6	myosin light polypeptide 6	1.55	↑
Q15019	SEPT2	septin-2	1.63	↑
P35579	MYH9	myosin-9	2.09	↑

Cell adhesion

P43121	MCAM	cell surface glycoprotein MUC18	0.32	↓
P09758	TACSTD2	Tumor-associated calcium signal transducer 2 (Cell surface glycoprotein Trop-2)	0.41	↓
P18084	ITGB5	integrin beta-5	0.59	↓
Q96AP7	ESAM	endothelial cell-selective adhesion molecule	0.66	↓
P06756	ITGAV	integrin alpha-V	0.71	↓
Q9Y653	GPR56	G-protein coupled receptor 56	1.67	↑

Cell migration

Q9NX58	LYAR	cell growth-regulating nucleolar protein	0.45	↓
P27487	DPP4	dipeptidyl peptidase 4 (CD26)	0.58	↓
P46013	MKI67	antigen KI-67	1.46	↑
P17931	LGALS3	galectin-3	2.24	↑
P06703	S100A6	S100-A6	3.42	↑

RAS Oncogene family

Q15907	RAB11B	Ras-related protein Rab-11B	0.41	↓
P51149	RAB7A	Ras-related protein Rab-7a	0.55	↓

Cellular stress and cell death associated proteins

P38646	HSPA9	Stress-70 protein, mitochondrial	1.38	↑
Q8WXX5	DNAJC9	DnaJ homolog subfamily C member 9	1.65	↑

Other significantly expressed proteins

P37059	HSD17B2	estradiol 17-beta-dehydrogenase 2	0.15	↓
Q9Y3A6	TMED5	transmembrane emp24 domain-containing protein 5	0.35	↓
O75695	RP2	XRP2	0.47	↓
P02786	TFRC	transferrin receptor protein 1	0.48	↓
Q9UHA4	LAMTOR3	Ragulator complex protein LAMTOR3	0.48	↓
P16444	DPEP1	dipeptidase 1	0.53	↓
P15529	CD46	membrane cofactor protein	0.53	↓
Q5ZPR3	CD276	CD276 antigen	0.57	↓
Q9UNN8	PROCR	endothelial protein C receptor	0.70	↓
P07339	CTSD	cathepsin D	0.79	↓
Q8N163	KIAA1967	DBIRD complex subunit KIAA1967	1.47	↑

Q9P206   KIAA1522   uncharacterized protein KIAA1522   1.52   ↑

479

480   Cellular adhesion molecules such as MCAM, Tumor-associated calcium signal

481   transducer 2 (Cell surface glycoprotein Trop-2), integrins αv and β5 were down-regulated

482   whereas GPR56 was up-regulated. Trop-2 is a paralog of epithelial cell adhesion molecule

483   (EpCAM) and is overexpressed in ovarian carcinoma and CRC [54, 55]. The overexpression

484   of Trop-2 is associated with poor prognosis in ovarian carcinomas [54]. The expression of

485   GPR56 has been shown to inhibit tumor cell growth in melanoma and to regulate VEGF

486   production and angiogenesis during melanoma progression [56].

487   Cell migration molecules such as cell growth-regulating nucleolar protein and

488   dipeptidyl peptidase 4 (CD26) were down-regulated while Antigen KI-67, Galectin-3 and

489   Protein S100-A6 were up-regulated. S100-A6 is known to be overexpressed in common

490   cancers including colorectal, breast and gastric cancers [57, 58]. It is known to affect CRC

491   adenocarcinoma tumourigenesis, invasion and metastasis [59] through the ERK and p38

492   MAPK pathways [60]. It has also been suggested to be a potential serum prognostic marker

493   for gastric cancer [61].

494   Ras-related proteins Rab-11B and Rab-7a were observed to be down-regulated. The

495   overexpression of various Ras-related proteins has been associated with increased

496   proliferation and aggressive cancer phenotypes [62]. The expression of Rab-11 in CRC

497   resulted in increased E-cadherin levels and eventual cell transformation and migration [63].

498   The over-expression of Rab-7, on the other hand, showed tumour suppressor properties in

499   prostate cancer [64]. Cellular stress associated proteins DnaJ homolog subfamily C member

500   9 and Stress-70 protein, mitochondrial were found to be up-regulated.

501   The current study also showed differential expression of various other proteins such

502   as LAMTOR3, CD276 antigen which were down-regulated while DBIRD complex subunit

503   KIAA1967 (also known as deleted in breast cancer gene 1 protein (DBC1)) and

504   uncharacterized protein KIAA1522 were up-regulated. LAMTOR3, along with LAMTOR2,

505   is part of the Ragulator complex involved in activation of mTORC1 required for MAPK2

506   activation [32]. DBC1 has been shown to interact with mutated in colorectal cancer (MCC)

507   and regulates the canonical Wnt signalling pathway through β-catenin [65] and has also been

508   reported to play an important role in tumour suppression by stabilizing the p53/TP53
509   interaction with the murine double minute 2 (MDM2) ubiquitin ligase [66]. Expression of
510   DBC1 has been observed in various cancers with varying outcomes [67-70]. For instance,
511   DBC1 deficiency in breast cancer cells has been shown to result in apoptosis [69]. In CRC
512   specifically, Zhang *et al.* reported that the overexpression of DBC1 in CRC results in poor
513   prognosis [70] whilst Kikuchi *et al.* reported that low expression of DBC1 is associated with
514   poor prognosis [71]. Although more evidence from other cancers have shown that
515   overexpression of DBC1, as we have seen, is associated poor prognosis [67-69].
516   Uncharacterized protein KIAA1522, was observed in this study and although it has not yet
517   been associated with cancer or any related functions been reported to date, a recent study has
518   observed this protein in lung cancer [72] and esophageal squamous cell carcinoma [73] and
519   indeed Chen *et al.* reported that KIAA1522 expression was elevated in squamous cell
520   carcinoma compared to squamous cell adenocarcinomas of the lung [72].

521   IPA analysis of the entire dataset of the differentially expressed proteins identified
522   four protein networks with scores >20 [i.e., "Cellular Function and Maintenance, Small
523   Molecule Biochemistry, Molecular Transport" (IPA score = 53); "Cellular Assembly and
524   Organization, Cell-To-Cell Signaling and Interaction, Reproductive System Development
525   and Function" (IPA score = 45); "Cell Cycle, Infectious Diseases, Cancer" (IPA score = 25)
526   and "Cancer, Endocrine System Disorders, Gastrointestinal Disease" (IPA score = 21)]. The
527   combination of all identified networks is shown in Supplementary Figure 1.The "Cellular
528   Function and Maintenance, Small Molecule Biochemistry, Molecular Transport" network
529   contained 29 molecules from the dataset which were involved in these processes, (Figure 8).
530   This network contains various ECM molecules such as keratins (KRT10, KRT18, KRT19),
531   actin associated proteins (MYH9, MYL6), chaperone proteins (HSPA5, HSPA9) which
532   were up-regulated and integrins (αv, β5) which were down-regulated. It is important to note
533   that "Cellular Function and Maintenance" was also identified as one of the cellular functions
534   by IPA. Other fundamental cellular functions identified by IPA include (i) RNA post-
535   transcriptional modification, (ii) cell death and survival, and (iii) cellular growth and
536   proliferation.
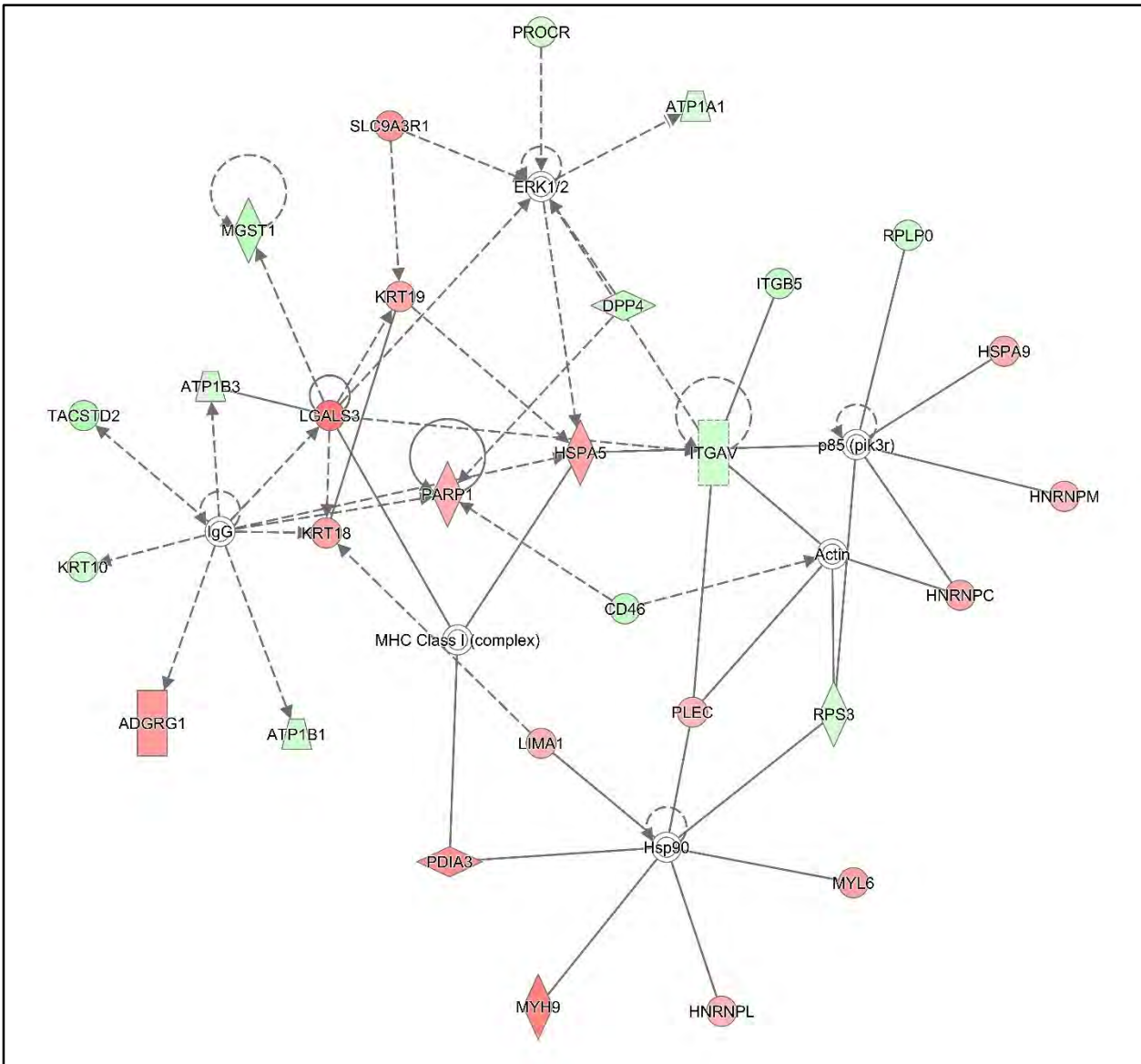
Figure 8 The "Cellular Function and Maintenance, Small Molecule Biochemistry, Molecular Transport" network identified by IPA comparing the untreated HT29^{Mock} cells relative to the untreated HT29^{β6AS} cells. Refer to Figure 6 for legend details.

IPA also identified two canonical pathways (eIF2 signalling and Granzyme B signalling) to be significantly altered in the dataset. Granzyme B is a cell death-inducing enzyme that is released from the granules of cytotoxic T lymphocytes and natural killer cells when a viral infected cell is marked for elimination [74]. The proteolytic cleavage of two key substrates, poly (ADP-ribose) polymerase 1 (PARP1) and lamin B2 (LMNB2), of granzyme B in the nucleus is essential for granzyme B-programmed cell death.[74]. Interestingly, impairment of granzyme B substrates, including, PARP1, NUMA1 (nuclear mitotic apparatus protein 1), and PRKDC (protein kinase, DNA-activated, catalytic polypeptide)

160

549   affects its signalling [75]. PARP1 and LMNB2 were found to be up-regulated while PRKDC

550   was observed to be down-regulated in proteomic data.

2.10 TGFβ induced differential expression of more proteins when β6 is natively
expressed rather than artificially induced (HT29 Mo+ vs Mo-)

553   Investigation of HT29^{Mock} cells following treatment with TGFβ showed differential

554   expression of 125 proteins relative to the untreated cells. Among the differentially expressed

555   proteins 55 were up-regulated and 70 were down-regulated. Although, this particular

556   comparison can be considered equivalent to SW480^{β6OE} + vs SW480^{β6OE} -, as both these

557   examine the effects of TGFβ when β6 is expressed, the number of differentially expressed

558   proteins was higher in the TGFβ-treated HT29^{Mock} cells (125 proteins) compared to

559   SW480^{β6OE} cells (46 proteins). To facilitate analysis of the data they were functionally

560   classified, and key proteins of interest are listed in **Table 7**. This comparison identified

561   various intermediary and actin filament proteins, cell proliferation, migration, adhesion and

562   stress-related proteins.

563   Keratins have been widely used as immunohistochemical markers in diagnostic

564   pathology. KRT8 and KRT18, have been implicated in breast cancer [25] and a wide variety

565   of other cancers, while KRT9 and KRT10 can be used to stain for cervix and squamous skin

566   carcinomas. Up-regulation of KRT10, a downstream molecule of PTEN, was shown to

567   increase cisplatin-resistance in ovarian cancer [76]. In our current study KRT8 and KRT18

568   were found to be down-regulated while KRT9 and KRT10 were up-regulated. KRT8 down-

569   regulation was also observed in the SW480 β6OE+ vs β6OE- comparison. LIAM1, which

570   regulates actin dynamics by cross-linking and stabilizing the filaments [53], was also down-

571   regulated.

572   **Table 7** Functional classification of significantly altered proteins observed upon treatment
573   of HT29^{Mock} cells with TGFβ relative to the untreated control (HT29 Mo+ vs Mo-)^a

Accession number	Gene name	Protein Name	iTRAQ fold change	Expression pattern
Intermediate Filament associated proteins				
P05787	KRT8	keratin, type II cytoskeletal 8	0.55	↓
P05783	KRT18	keratin, type I cytoskeletal 18	0.55	↓
P13645	KRT10	keratin, type I cytoskeletal 10	2.07	↑
P35527	KRT9	keratin, type I cytoskeletal 9	3.89	↑
Actin filament associated proteins				

161

| Q9UHB6 | LIMA1 | LIM domain and actin-binding protein 1 | 0.83 | ↓ |

Cell Proliferation, migration and adhesion associated proteins

P49006	MARCKSL1	MARCKS-related protein	0.45	↓
P13688	CEACAM1	carcinoembryonic antigen-related cell adhesion molecule 1	0.67	↓
Q13277	STX3	syntaxin-3	0.72	↓
Q08431	MFGE8	lactadherin	0.73	↓
P16422	EPCAM	epithelial cell adhesion molecule	0.75	↓
Q92542	NCSTN	nicastrin	0.75	↓
Q86Y82	STX12	syntaxin-12	0.75	↓
P16070	CD44	CD44 antigen	0.75	↓
Q13740	ALCAM	CD166 antigen	0.75	↓
P23229	ITGA6	integrin alpha-6	0.76	↓
P50895	BCAM	basal cell adhesion molecule	0.78	↓
P12830	CDH1	cadherin-1 (E-cadherin)	0.80	↓
P06702	S100A9	protein S100-A9	0.80	↓
P35613	BSG	basigin (CD147)	0.81	↓
P27487	DPP4	dipeptidyl peptidase 4 (CD26)	0.81	↓
Q9UQ80	PA2G4	proliferation-associated protein 2G4	1.34	↑
Q16181	SEPT7	septin-7	1.36	↑
Q9Y653	GPR56	G-protein coupled receptor 56	1.74	↑

Cellular stress and cell death associated proteins

Q969Q5	RAB24	Ras-related protein Rab-24	0.72	↓
Q92520	FAM3C	protein FAM3C	0.74	↓
Q96A26	FAM162A	protein FAM162A	0.80	↓
P51572	BCAP31	B-cell receptor-associated protein 31	0.81	↓
P13010	XRCC5	X-ray repair cross-complementing protein 5	1.36	↑
P12956	XRCC6	X-ray repair cross-complementing protein 6	1.40	↑

Proteins with unknown function

Q9BQ61	C19orf43	uncharacterized protein C19orf43	0.58	↓

[a] Fold change ratios of significantly altered proteins observed in two biological replicates of iTRAQ experiment. These proteins have met the stipulated criteria (i.e., unused protein score >1.3 and change in expression level of at least 1.2 fold for aggressive (HT29[Mock] treated with TGFβ) vs non-aggressive (HT29[Mock] not treated with TGFβ)

574

575   Various cell adhesion molecules such as CEACAM1 (carcinoembryonic antigen-

576   related cell adhesion molecule 1), EpCAM, BCAM (basal cell adhesion molecule),

577   Cadherin-1 (E-cadherin) and lactahedrin were down-regulated following TGFβ treatment

578   while GPR56 (G-protein coupled receptor 56) was up-regulated in the treated cells. Various

CEACAM molecules including CEACAM1, CEACAM5 and CEACAM6 are now considered valid clinical biomarkers and promising therapeutic targets in colorectal, melanoma, lung, and pancreatic cancers [77]. E-cadherin is typically expressed in all normal epithelial cells and regulates cell-cell adhesion, mobility and proliferation. Loss or decrease in E-cadherin expression is a well-known diagnostic biomarker for breast cancer and indicates increased invasion and epithelial-to-mesenchymal transition [78]. Lactahedrin, which is an RGD-dependent cell adhesion molecule [79] and a ligand for integrins αvβ3 and αvβ5, was shown to regulate angiogenesis in mouse models [80].

Proteins that regulate cellular proliferation and migration such as CD44 antigen, basigin (CD147), Protein S100-A9 and dipeptidyl peptidase 4 (CD26) were down-regulated and Proliferation-associated protein 2G4 (or ErbB3-binding protein 1) were up-regulated. Low preoperative serum levels of CD26 in CRC patients have been shown to correlate with poor prognosis [81]. Basigin, has been shown in various cancers to promote the production and/or release of MMPs into the surrounding ECM, which then increase the invasive potential and promotes cancer progression [82, 83]. Interestingly, septin-7, which is required for normal organization of the actin cytoskeleton, was also found to be up-regulated while MARCKS-related protein, which regulates cell movement through actin cytoskeleton reorganization, was down-regulated. The α6 integrin subunit, a receptor for laminin which is required for the structural integrity of hemidesmosomes, was found to be down-regulated. During prostate cancer, integrin α6 was shown to undergo cleavage in a urokinase-type plasminogen activator (uPA)-dependent manner [84, 85]. This resulted in an increase in laminin-dependant migration, invasion and metastasis. However, blockage of this cleavage resulted in delayed bone metastasis [84, 86]. Interestingly, ErbB3-binding protein 1 expression has also been associated with poor prognosis in prostate [87, 88] and breast cancers [89, 90]. A CRC stem cell marker, CD166 (or Activated leukocyte cell adhesion molecule) which is frequently expressed in aggressive tumours was found to be down-regulated [91]: it has been reported to be an aggressive marker for breast cancer [92] and tumor progression of malignant melanoma [93].

Chaperone protein BCAP31 was found to be down-regulated while XRCC5 and XRCC6 were up-regulated. The decreased expression for XRCC5 has been reported for colon and cervical cancers, and melanoma [94].

611
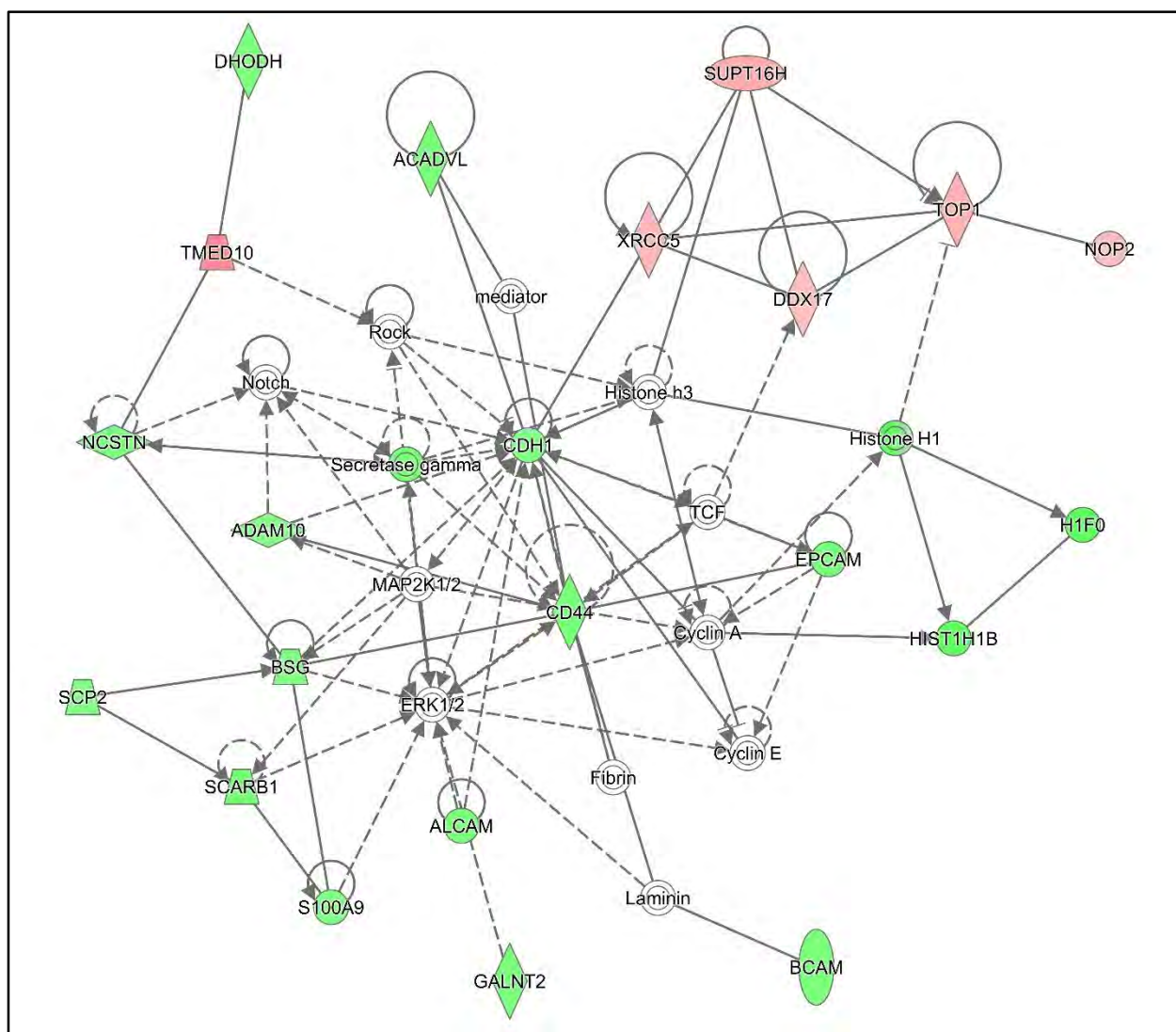
Figure 9 The "Cellular Movement, Cell-To-Cell Signalling and Interaction, Connective Tissue Development and Function" network identified by IPA comparing the treated HT29[Mock] cells relative to the untreated control. Refer to Figure 6 for legend details.

IPA of the differentially expressed proteins identified a total of seven protein networks, six of which has an IPA score ≥ 23. Amongst these networks were "Cell Morphology, Cellular Assembly and Organization, Cellular Compromise" (IPA score = 64); "Cellular Movement, Cell-To-Cell Signaling and Interaction, Connective Tissue Development and Function" (IPA score = 42) and "Cellular Function and Maintenance, Cellular Assembly and Organization, Cell Cycle" (IPA score = 23). The "Cell Morphology, Cellular Assembly and Organization, Cellular Compromise" network identified 30 proteins involved in these pathway. The jajority of these consisted of various ribosomal proteins, keratins (KRT8, 9, 10, 18) and also integrin α6. Similarly, the "Cellular Movement, Cell-

164

To-Cell Signalling and Interaction, Connective Tissue Development and Function" network identified 22 proteins from the dataset. Most of these (Figure 9) contributed to cell adhesion (ALCAM, BCAM, BSG, CD44, CDH1, EpCAM, NCSTN, S100A9, and SCARB1) and were observed to be down-regulated. Interestingly, IPA grouped these various cellular adhesion-related proteins and suggested involvement with ERK1/2, MAP2K1/2 and Notch signalling, all of which have been previously implicated in CRC and other cancers [35, 95].

It is clear from the proteomic and IPA results that native expression of integrin β6 induces differential expression of various proteins and affects cellular function when treated with TGFβ. In order to investigate if these TGFβ-induced effects are directly related to integrin β6 expression, we examined the HT29β6AS cells to determine the effect of treatment following β6 suppression.

2.11 β6 suppression reduced the number of differentially expressed proteins upon TGFβ treatment (HT29 AS+ vs AS-)

The HT29β6AS cells are an ideal model system to investigate the effects of TGFβ when only low levels of integrin β6 are present. Upon treatment with TGFβ, HT29β6AS cells showed significant differences in the expression of 80 proteins, of which 45 proteins were up-regulated and 35 proteins were down-regulated. Key proteins are listed in **Table 8**.

Various intermediate filament associated proteins such as plectin (plectin-1), and several keratins were found to be up-regulated. Bausch *et al.* showed that in pancreatic cancer plectin is expressed only in adenocarcinoma tissue and has been suggested as a potential biomarker to identify primary and metastatic pancreatic ductal adenocarcinoma [96]. Plectin has been reported to promote migration and invasion in head and neck squamous cell carcinoma (HNCC) through Erk1/2 activation [97]. Interestingly, in HNCC the overall survival of patients with higher plectin levels was significantly lower than those with low E-cadherin levels [97]. In contrast, knockdown of plectin in Chang liver cell resulted in increased cell migration and an increase in focal adhesion kinase (FAK) at the focal adhesions resulting in an invasive phenotype [98].

Actin filament related proteins such as transgelin-2 and septin-2 were observed to be down-regulated. Transgelin-2, which is rarely expressed in normal epithelia, was observed to be overexpressed in lymph nodes and distant metastases, and was associated with decreased overall survival rate in CRC [99]. Zhang *et al.* suggested the use of transgelin-2 as a marker for predicting CRC progression and prognosis [99]. Huang *et al.* also reported

656 overexpression in gastric cancer tissue samples [100]. Interestingly, TGFβ is known to
657 increase transgelin expression via direct binding of Smad3 to the Smad-binding elements
658 within the *TAGLN* promoter region [101]. Increased expression resulted in higher cell
659 proliferation and migration rates in the ATII cells [101]. Microtubule associated proteins
660 tubulin-β and tubulin-β 4B chains were found to be up-regulated in the TGFβ treated cells.

661 **Table 8** Functional classification of significantly altered proteins observed upon treatment
662 of HT29^{β6AS} cells with TGFβ relative to the untreated control (HT29 AS+ vs AS-)^a

Accession number	Gene name	Protein name	iTRAQ fold change	Expression pattern
Intermediate Filament associated proteins				
Q15149	PLEC	plectin (plectin-1)	1.25	↑
P35900	KRT20	keratin, type I cytoskeletal 20	1.31	↑
P04264	KRT1	keratin, type II cytoskeletal 1	2.01	↑
P13645	KRT10	keratin, type I cytoskeletal 10	2.23	↑
P02538	KRT6A	keratin, type II cytoskeletal 6A	4.92	↑
Q04695	KRT17	keratin, type I cytoskeletal 17	5.13	↑
P08779	KRT16	keratin, type I cytoskeletal 16	5.81	↑
Actin filament associated proteins				
P37802	TAGLN2	transgelin-2	0.78	↓
Q15019	SEPT2	septin-2	0.80	↓
P60660	MYL6	myosin light polypeptide 6	1.35	↑
Microtubule associated proteins				
P07437	TUBB	tubulin beta chain	1.94	↑
P68371	TUBB4B	tubulin beta-4B	1.97	↑
Cell Proliferation, migration and adhesion associated proteins				
P21926	CD9	CD9 antigen	0.69	↓
P16070	CD44	CD44 antigen	0.73	↓
P17301	ITGA2	integrin alpha-2	1.22	↑
Q9Y653	GPR56	G-protein coupled receptor 56	2.14	↑
P05109	S100A	protein S100-A8	9.24	↑
RAS oncogen family				
P20340	RAB6A	Ras-related protein Rab-6A	0.74	↓
Q15907	RAB11B	Ras-related protein Rab-11B	0.76	↓
Other Significantly expressed proteins				
Q96A26	FAM162A	protein FAM162A	0.57	↓
P11279	LAMP1	lysosome-associated membrane glycoprotein 1	0.63	↓

Q96KN1	FAM84B	protein FAM84B (Breast cancer membrane protein 101)	0.69	↓
Q9BYG3	MKI67IP	MKI67 FHA domain-interacting nucleolar phosphoprotein	1.22	↑
Q8N163	KIAA1967	DBIRD complex subunit KIAA1967 (Deleted in breast cancer 1 (DBC1))	1.60	↑

[a] Fold change ratios of significantly altered proteins observed in two biological replicates of iTRAQ experiment. These proteins have met the stipulated criteria (i.e., unused protein score >1.3 and change in expression level of at least 1.2 fold for aggressive (HT29^{β6AS} treated with TGFβ) vs non-aggressive (HT29^{β6AS} not treated with TGFβ)

663

CD9 and CD44 antigens were significantly down-regulated. CD9 antigen has been associated with cell adhesion, cell motility and tumor metastasis [102, 103]. For example, Murayama *et al.* have shown that CD9 can bind with epidermal growth factor receptor (EGFR) on human gastric cell line (MKN-28) and two CD9-transfected cell lines - hepatocellular carcinoma cells (HepG2/CD9) and Chinese hamster ovary cancer cells (CHO-HER/CD9) [104]. They also showed that CD9 expression in the CHO-HER cells completely attenuates the EGFR signalling and resulted in decreased EGFR expression at the cell surface [104].

Integrin α2, GPR56 and protein S100-A8 were up-regulated. Integrin α2β1 is a receptor for laminin, collagen, collagen C-propeptides, fibronectin and E-cadherin. It is known to regulate cell adhesion and invasion in prostate cancer through the FAK/src/paxillin/Rac/JNK pathway that leads to increased MMP-2 and -9 activity and eventual invasion [105]. Ramierz *et al.* showed that loss of integrin α2β1 promotes breast cancer and is associated with decreased survival in breast and prostate cancers [106], suggesting the use of α2 expression as a putative biomarker, particularly for prostate cancer [106, 107]. S100-A8 usually forms a heterodimer with S100-A9 that has been shown to be up-regulated in various cancers including CRC, gastric cancer and prostate cancer [108]. The S100-A8/A9 complex may influence tumor cell migration, invasion and metastasis. In CRC, the complex has been shown to be expressed in the invasive margins of the tumor [109]. The co-expression of S100-A8/A9 in ductal carcinomas of the breast has been associated with poor tumor differentiation, vessel invasion and node metastasis [110]. The differential expression of Protein S100-A8 in the HT29^{β6AS} cells was validated by Western blotting (Figure 11). Furthermore, we observed the up-regulation of KIAA1967 (or DBC1) and MKI67 FHA domain-interacting nucleolar phosphoprotein. The role of DBC1 has been discussed in the previous sections.

689　　　　To further understand the biological significance of these data the differentially

690　　expressed proteins were analysed using IPA. IPA identified three protein networks with

691　　scores > 20: "Cell-To-Cell Signalling and Interaction, Protein Synthesis, Cell Death and

692　　Survival" (IPA score = 47); "Cellular Movement, Hair and Skin Development and Function,

693　　Cell-To-Cell Signaling and Interaction" (IPA score = 27) and "Cell Death and Survival,

694　　Cancer, Organismal Injury and Abnormalities" (IPA score = 21). Taken together these

695　　networks (Supplementary Figure 2) identified several ECM related molecules including

696　　plectin, CD44, Keratins (KRT1, 6A, 10, 16, 17), microtubule-associated protein 4 (MAP4),

697　　MYL6, protein S100-A8, septin-2, transgelin 2, tubulin-β, tubulin-β 4B, integrin α2, Rab-

698　　6A and Rab-11B. IPA appropriately grouped these molecules showing interrelations with

699　　other molecules such as annexin A2, basigin, caveloin-1, Ras, p38 MAPK, and EGFR, which

700　　are known cancer associated proteins. The top cellular functions identified by IPA include

701　　(i) RNA post-transcriptional modification (ii) cellular assembly and organization, (iii) cell

702　　growth and proliferation, (iv) cell cycle, and (iv) cell death and survival.

703 2.12 TGFβ treatment of cells expressing different levels of β6 exhibited differential
704 expression of molecules essential for cancer-related functions (HT29 Mo+ vs AS+)

705　　　　It was clear from the two previous comparisons that β6 expression directly affects

706　　the number of differentially expressed proteins following treatment with TGFβ. The

707　　comparison of HT29^{Mock} and HT29^{β6AS} cells when both were treated with TGFβ showed

708　　differential expression of 159 proteins, of which 84 proteins were up-regulated and 75

709　　proteins were down-regulated. Similar to the previous comparisons a wide range of proteins

710　　associated with intermediate filaments, actin filaments, microtubules, cell adhesion, cell

711　　migration, cellular stress and cell death, and RAS oncogene family proteins were found to

712　　be differentially expressed (**Table 9**).

713　　　　Intermediate filament proteins KRT17 and KRT6A were down-regulated while

714　　KRT20 and KRT9 were up-regulated. Various actin filament associated proteins such as

715　　Actin, cytoplasmic 2 (γ-actin), α-actinin-4, myosin-9, septin-2, septin-7, and septin-9 were

716　　significantly down-regulated. Septin-2, -6 and -7 are required for normal organization of

717　　actin cytoskeleton. The expression of these septins is coupled, whereby up-regulation in any

718　　one member can induce the expression of the other two [111] which is the case in this study.

719　　The knockdown of these proteins in HeLa cells resulted in disintegration of stress fibres and

720　　caused cells to lose polarity [112]. Kremer *et al.* showed that these three septins are required

721 for regulation of the actin cytoskeleton and cell-cycle arrest. The cell-cycle arrest is mediated

722 by NCK which is translocated into the nucleus by SOCS7 (suppressor of cytokine signaling-

723 7). The proposed septin-SOCS7-NCK axis can then control the DNA-damage kinase cascade

724 and induce the activation of Chk2 (checkpoint kinase 2) and p53 required for cell cycle arrest

725 [112].

726 **Table 9** Functional classification of significantly altered proteins observed upon TGFβ
727 treatment of HT29^{Mock} cells relative to the TGFβ treated HT29^{β6AS} cells (HT29 Mo+ vs AS+)

Accession number	Gene name	Protein Name	iTRAQ fold change	Expression pattern
Intermediate Filament associated proteins				
Q04695	KRT17	keratin, type I cytoskeletal 17	0.19	↓
P02538	KRT6A	keratin, type II cytoskeletal 6A	0.19	↓
P35900	KRT20	keratin, type I cytoskeletal 20	1.60	↑
P35527	KRT9	keratin, type I cytoskeletal 9	1.92	↑
Actin filament associated proteins				
Q9BQG0	MYBBP1A	Myb-binding protein 1A	0.55	↓
P63261	ACTG1	actin, cytoplasmic 2	1.51	↑
O43707	ACTN4	alpha-actinin-4	1.70	↑
P35579	MYH9	myosin-9	1.74	↑
Q16181	SEPT7	septin-7	2.12	↑
Q9UHD8	SEPT9	septin-9	2.15	↑
Q15019	SEPT2	septin-2	2.25	↑
Microtubule associated proteins				
P07437	TUBB	tubulin beta chain	0.38	↓
Q71U36	TUBA1A	tubulin alpha-1A	0.38	↓
Q00610	CLTC	clathrin heavy chain 1	0.55	↓
P26038	MSN	moesin	1.52	↑
Cell adhesion				
P43121	MCAM	cell surface glycoprotein MUC18	0.36	↓
Q96AP7	ESAM	endothelial cell-selective adhesion molecule	0.62	↓
P06756	ITGAV	integrin alpha-V	0.63	↓
P18084	ITGB5	integrin beta-5	0.66	↓
P17301	ITGA2	integrin alpha-2	0.80	↓
O60716	CTNND1	catenin delta-1 (p120)	1.35	↑
Q9Y653	GPR56	G-protein coupled receptor 56	1.38	↑
P35221	CTNNA1	catenin alpha-1	1.41	↑
P13688	CEACAM1	carcinoembryonic antigen-related cell adhesion molecule 1	1.65	↑

Cell migration

P06702	S100A9	protein S100-A9	0.16	↓
P27487	DPP4	dipeptidyl peptidase 4 (CD26)	0.54	↓
Q08380	LGALS3BP	galectin-3-binding protein	0.70	↓
P46013	MKI67	antigen KI-67	1.33	↑
P17931	LGALS3	galectin-3	2.05	↑
P06703	S100A6	protein S100-A6	2.89	↑

RAS Oncogene family

Q15907	RAB11B	Ras-related protein Rab-11B	0.58	↓
P51149	RAB7A	Ras-related protein Rab-7a	0.62	↓
P57735	RAB25	Ras-related protein Rab-25	0.64	↓

Cellular stress and cell death associated proteins

P50454	SERPINH1	serpin H1 (47 kDa heat shock protein)	1.52	↑
P14625	HSP90B1	endoplasmin	1.72	↑
P11021	HSPA5	78 kDa glucose-regulated protein (Heat shock 70 kDa protein 5)	1.75	↑
Q9Y4L1	HYOU1	hypoxia up-regulated protein 1	1.90	↑
Q8WXX5	DNAJC9	DnaJ homolog subfamily C member 9	1.98	↑

Other significantly expressed proteins

P09758	TACSTD2	tumor-associated calcium signal transducer 2	0.40	↓
P55061	TMBIM6	bax inhibitor 1	0.47	↓
Q9UHA4	LAMTOR3	Ragulator complex protein LAMTOR3	0.54	↓
Q08945	SSRP1	FACT complex subunit SSRP1	1.41	↑
Q9HDC9	APMAP	adipocyte plasma membrane-associated protein	1.53	↑
P04439	HLA-A	HLA class I histocompatibility antigen, A-3 alpha chain	1.66	↑
Q53GQ0	HSD17B12	estradiol 17-beta-dehydrogenase 12	1.79	↑

[a] Fold change ratios of significantly altered proteins observed in two biological replicates of iTRAQ experiment. These proteins have met the stipulated criteria (i.e., unused protein score >1.3 and change in expression level of at least 1.2 fold for aggressive (HT29^{Mock} treated with TGFβ) vs non-aggressive (HT29^{β6AS} treated with TGFβ)

728

729   Several cell adhesion molecules such as MCAM, integrins αv, α2 and β5 were down-

730   regulated whereas catenin α-1, catenin δ-1 (or p120 catenin), GPR56 and CEACAM1were

731   significantly down-regulated. Catenins are known to associate with and regulate cell

732   adhesion properties of various cadherins that are crucial for cell stability [113]. Catenin δ-1

733   can bind to and inhibit ZBTB33, a transcriptional repressor, which may lead to activation of

734   Wnt target genes [114]. Casagolda *et al.* showed that catenin δ-1 can regulate Wnt signalling

735   when complexed with CK1ε (casein kinase 1ε) through the LRP (lipoprotein receptor-related
736   proteins) 5/6 [115].

737   Increased expression of several cellular stress and cell death related proteins
738   including serpin H1, endoplasmin, 78 kDa glucose-regulated protein (heat shock 70 kDa
739   protein 5), hypoxia up-regulated protein 1 and DnaJ homolog subfamily C member 9 was
740   observed. The up-regulation of these proteins could reflect the activation of pathways
741   required for suppression of anoikis, in turn promoting a malignant phenotype.

742   Down-regulation of Ras-related proteins Rab-11B, Rab-7a and Rab-25 was observed
743   in the HT29^{Mock} cell line. The roles of Rab-11B and Rab-7a have been discussed above. Rab-
744   25 expression has been shown to be low in human CRC independent of stage. However,
745   studies using mouse models have shown that Rab-25 deficiency promotes development of
746   colonic neoplasia [116].

747   Interestingly, the down-regulation of tumor-associated calcium signal transducer 2,
748   Bax inhibitor 1 (BI-1) and Ragulator complex protein LAMTOR3 was also observed. The
749   low expression of BAX, a downstream effector of p53, in CRC is associated with poor
750   prognosis for patients with resected liver metastases [117]. The down-regulation of Bax
751   inhibitor 1 could be a signal to increase the levels of BAX that are associated with better
752   prognosis. Additionally, Grzmil *et al.* showed different levels of BI-1 expression, which is
753   required to avert in apoptosis various breast cancers [118].

754   The biological significance of these data was examined using IPA. IPA of the
755   differentially expressed proteins identified multiple protein networks with scores > 20:
756   "Cell-To-Cell Signaling and Interaction, Cellular Movement, Protein Degradation" (IPA
757   score = 41) (Figure 10), "Cancer, Organismal Injury and Abnormalities, Respiratory
758   Disease" (IPA score = 41), "Cellular Assembly and Organization, Cell-To-Cell Signaling
759   and Interaction, Reproductive System Development and Function" (IPA score = 24),
760   "Cellular Compromise, Cell Cycle, DNA Replication, Recombination, and Repair" (IPA
761   score = 24) and "Cellular Movement, Hematological System Development and Function,
762   Immune Cell Trafficking" (IPA score = 24). The networks identified potential involvement
763   of a multitude of molecules including integrins (αv, β5), keratins (KRT6A, KRT17), heat
764   shock proteins (HSPA5, HSPD1, HSP90B1), chaperonin containing TCP1, subunits (CCT2,
765   CCT3, CCT4, CCT5, CCT6A, CCT7, CCT8), adhesion molecules (MCAM, CEACAM1,
766   DPP4), protein S100-A8 and -A9, and septins (-2, -7, -9). These molecules are known to

have crucial cellular functions including (i) cellular growth and proliferation, (ii) cell death and survival, (iii) cell-to-cell signalling and interaction, (iv) cellular compromise, and (v) cellular function and maintenance. The entire subset of CCT proteins were found to be significantly down-regulated by proteomics (iTRAQ fold change was in range of 0.54 – 0.74). It was not surprising to see IPA associate actin, ERK1/2, p38 MAPK, Akt and PI3K (complex) with these networks as they are known to mediate cancer related cellular processes.
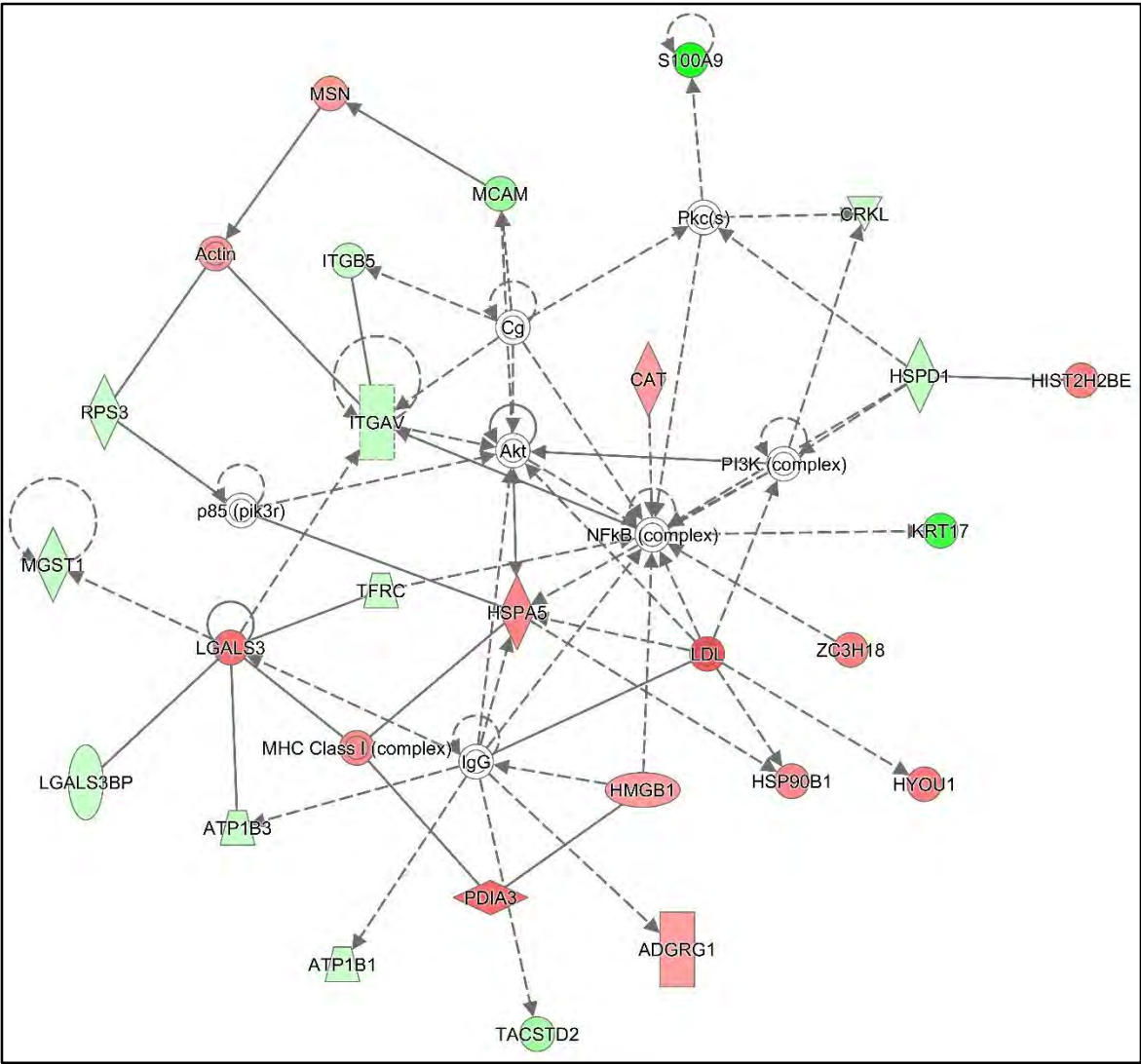
Figure 10 The top IPA network, "Cell-To-Cell Signaling and Interaction, Cellular Movement, Protein Degradation", identified when comparing the TGFβ-treated HT29^{Mock} cells relative to TGFβ-treated HT29^{β6AS} cells. The network is illustrates the relationships between various differentially expressed proteins observed by proteomics (red, up-regulated; green, down-regulated; white, not observed by proteomics but crucial to the network).

781 **2.13 Validation of proteomic results by Western blotting**

782   To validate the differential expression of ezrin, annexin-A2 and S100-A8 observed

783 by iTRAQ, these proteins were analysed by Western blotting. These results were generally

784 in agreement with the fold changes observed through iTRAQ (Figure 11), although Western

785 blot analysis of protein S100-A8 does not reflect the large fold change (↑9.24) observed by

786 proteomics. However, the intensity measurements performed using Image Studio Lite (v5.0)

787 show at least a 20% fold change which was the minimum cut-off used in the iTRAQ

788 proteomic study.

789 **Figure 11** Validation of proteomic results. The differential expression of 3 proteins were
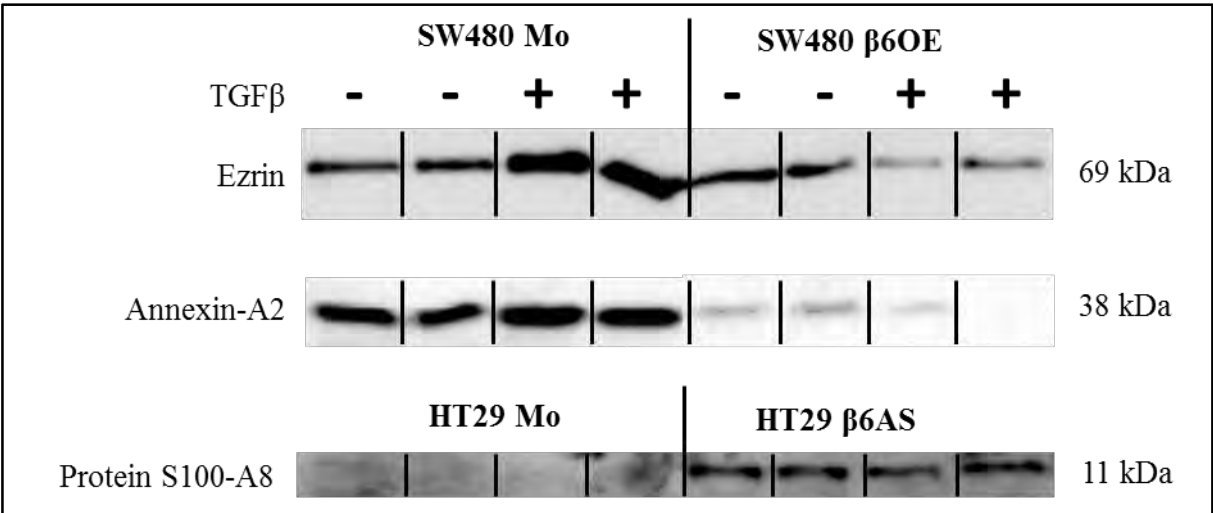
790 validated by Western-blot analysis. The down-regulation of ezrin and annexin- A2 was
791 observed in the SW480β6OE cells, relative to the TGFβ-treated SW480Mock cells, by
792 western-blot studies which confirmed the iTRAQ results shown in Table 4. The up-
793 regulation of Protein S100-A8 in the TGFβ-treated HT29β6AS cells, relative to the
794 untreated, also supported the iTRAQ results.

795 **2.14 TGFβ can alter expression of crucial cancer related networks in a β6-dependent**
796 **manner**

797   From the results obtained from both cell-based and proteomics studies, it is clear that

798 TGFβ treatment of cells expressing any amount of β6 results in differential expression of

799 basic cellular functions required for CRC. IPA provided numerous correlations between the

800 proteomic data and altered cell functions in CRC. These results demonstrate the impact of

801 TGFβ and β6 expression in CRC on many important cell functions in CRC (e.g., apoptosis,

802 cell death, adhesion, proliferation, migration, and invasion). The proteins identified by IPA

803 and significant changes in CRC cell function and listed in supplementary table 1. As would

804   be expected, some of these proteins were observed in our previous proteomics study using

805   SW480 subclones [18].

806

807   **2.15 TGFβ and β6 together alter expression of potential biomarkers**

808   Using the biomarker function in IPA, we identified 76 proteins in our proteomics

809   study that have been suggested as potential biomarkers by the American Society of Clinical

810   Oncology (ASCO) (Supplementary Table 2). Annexin A2, for example, has been suggested

811   as a diagnostic and prognostic marker for CRC [119, 120] and was also seen to be down-

812   regulated in SW620 (lymph node metastatic variant of SW480) [31]. Our observation of

813   down-regulation of annexin A2 is in agreement with the data of Ghosh *et al.* [31]. Various

814   keratins (KRT1, KRT5, KRT6A, KRT8, KRT9, KRT17, KRT18, KRT20) were also

815   identified to be markers for diagnosis, disease progression, prognosis, and efficacy. Karantza

816   *et al.* have published a detailed review on the role of keratins in cancer, and illustrated the

817   use of keratins as diagnostic and prognostic markers for various cancers including CRC [37].

818   The S100 proteins A6, A8 and A9 were also identified as potential markers for diagnosis

819   and efficacy. Yang *et al.* have shown that S100-A6 is up-regulated in gastric cancer [57] which

820   is supported by the data of Zhang *et al.* who showed that higher levels of S100-A6 in serum

821   could be used as prognostic marker in gastric cancer [61]. It is interesting to speculate that

822   some of the new potential biomarkers identified in this study could act as markers for

823   processes that are altered in a TGFβ- and β6-dependent manner during cancer progression.

824

825   **3. CONCLUSIONS**

826   TGFβ is now known to play key roles in regulating normal cell growth as well as

827   cancer cell growth. Its role in cancer is poorly understood but there are multiple reports

828   suggesting its association with various cancer-related pathways such as Erk, Ras, p38

829   MAPK, AKT, Wnt and PI3k [35, 36]. Similarly, TGFβ has also been associated with the

830   integrin αvβ6, which is known to activate latent-TGFβ1 and TGFβ3 through the RGD

831   binding domain on their latency associated peptides [121]. Interestingly, overexpression of

832   both TGFβ and the β6 have been associated with CRC [9, 122].

833   To the best of our knowledge, this is the first study to examine membrane proteome

834   changes of SW480^{Mock}, SW480^{β6OE}, HT29^{Mock} and HT29^{β6AS} cell lines after treatments with

835   active TGFβ. Our focus was to identify membrane proteomic changes associated with TGFβ

836 treatments at a concentration (10 ng/mL) that recapitulates the levels found in CRC plasma

837 [9] and tissues [10]. This study employed Triton X-114 phase partitioning to enrich for highly

838 hydrophobic integral membrane proteins that were subsequently analysed using iTRAQ.

839 Using this high-throughput quantitative proteomics approach we identified several proteins

840 as significantly altered in a TGFβ <u>and</u> β6 dependant manner. The expression changes

841 observed were validated using Western blotting.

842 IPA of the proteomic data associated TGFβ treatment with fundamental cancer-

843 related functions such as adhesion, proliferation, migration, invasion, apoptosis and cell death.

844 The differential expression of these proteins associated with these functions provides some

845 insight into the TGFβ-β6-dependent pathophysiology of CRC. Additionally, the initial cell-

846 based experiments performed as a part of this study conclusively demonstrated that TGFβ

847 mediates cell proliferation, wound healing, and invasion in a β6-dependent manner in support of

848 the proteomics results.

849 This study also demonstrated that TGFβ treatment of β6-expressing cells alters key

850 cell functions and pathways required for cancer progression. For example, the proteomic

851 data identified that the expression of numerous eIF2 and eIF4 signalling pathway members

852 including eIF2A, eIF2S1, eIF2S2, eIF2S3, and KRAS changed significantly when treated

853 with TGFβ. Using these observations, IPA identified eIF2 signalling as one of the top

854 canonical pathways for majority of the comparisons examined. The eIF2 signalling complex,

855 made up of the three essential subunits eIF2S1, eIF2S2, and eIF2S3, controls stress-related

856 signals to regulate both global and specific mRNA translation, and thus protein synthesis

857 [123]. The up-regulation of these eIF2 subunits could suggest the need to sustain increased

858 protein levels for the abnormal functioning associated with cancer. However, the increased

859 protein levels cannot be achieved without eIF4 which is necessary to deliver the mRNA to

860 eIF3 for translation into polypeptide. Although eIF4 was not observed in this proteomic

861 study, it may be up-regulated during a later stage or have been suppressed in a TGFβ-

862 dependent manner. Interestingly, eIF4G1 a member of the eIF4 complex was observed to be

863 up-regulated in our previous proteomic study using the SW480 subclones [18] and has been

864 reported to be up-regulated in breast [124] and lung [125] cancers.

865 The loss of cell adhesion is an important prerequisite for cancer cells to be able to

866 proliferate, migrate and invade into other tissues. The proteomic data provided insights into

867 how this could be achieved. Based on differential expression of various adhesion related

868 molecules identified, including EpCAM, nicastrin, CD44, DPP4, ITGA6, cadherin, MCAM,

869 ezrin, and annexin A2, IPA predicted alterations to cellular functions such as "cell movement

870 of cancer cell lines", "migration of tumour cell lines" and "invasion of tumour cell lines".

871 These functions clearly align with the cell-based experiments where treatment increased both

872 cell proliferation and wound healing ability. In contrast to the invasion assay results (Figure

873 3), where no significant change was observed following treatment with TGFβ, the

874 proteomics data suggest that the cells may have the ability to invade the ECM. This is

875 supported by the differential expression of various proteins required for cell movement,

876 proliferation, migration and invasion (Supplementary Table 1). Additionally, the differential

877 expression of various integrins such as αv, α2, β1 and β5 (key receptors for fibronectin,

878 vitronectin and fibrinogen) may contribute to altered ECM stability, potentially modulating

879 cancer cell proliferation, migration and invasion [41].

880 The loss of adhesion enables the cancer cells to spread to adjacent tissue and

881 eventually metastasise. It is known that cells trigger anoikis when cell adhesion is lost or

882 improper. The suppression of anoikis therefore becomes an important requirement for

883 tumour cells and the proteomic observations provided insights to this process. On the basis

884 of significant up-regulation of many proteins associated with this process (i.e., DNAJA1,

885 DNAJA2, Hsp40, HSP90AB1, BAG-2, XRCC5, XRCC6, HSPA5, and HSPD), IPA

886 identified "apoptosis of tumour cell lines" and "cell death of epithelial cell lines" as functions

887 that were altered following TGFβ treatment. The cancer cells that survive gain the

888 mesenchymal phenotype (thorough EMT) and metastasise.

889 EMT is an important critereon for CRC progression and metastasis [126]. It was

890 therefore not surprising to note that the epithelial cell marker, E-cadherin, was shown to be

891 down-regulated by proteomics (Table 7). However, it was interesting to note that vimentin,

892 the commonly acknowledged mesenchymal marker, was also observed to be down-regulated

893 (Table 3), as seen in our lab's previous study [18]. The down-regulation of these two proteins

894 was observed in cells with high expression of β6 (SW480^{β6OE} and HT29^{Mock}) and was

895 observed only when treated with active TGFβ. This could suggest a cancer promoting role

896 of β6 mediated indirectly through TGFβ receptor system.

897 This study also identified significant change in the expression of two uncharacterised

898 proteins, KIAA1522 and C19orf43. Interestingly there have been reports of KIAA1552

899 being involved in lung cancer and esophageal squamous cell carcinoma [72, 73]. Our data

900　supports the previous findings suggesting that KIAA1522 has a potential role to play in
901　cancer. C19orf43 has not been reported by any other cancer proteomic studies thus far. The
902　Human Protein Atlas (HPA) [127] shows the presence of both KIAA1522 and C19orf43 in
903　cancer tissues by IHC. Using the HPA032050 antibody against KIAA1522, HPA reports its
904　expression in a wide range of cancers. In CRC specifically, KIAA1522 was observed to have
905　a medium expression in > 50% of the samples (7/12) while high expression was observed in
906　normal tissues. Similarly, using the HPA059965 antibody against C19orf43, HPA has shown
907　that it too is expressed in a wide range of cancers. In CRC, it was observed to have low to
908　medium expression whereas a high to medium expression was observed in normal tissues.
909　The HPA data now needs to be further validated by proteomics and other antibody based
910　methods　such　as　Western　blotting,　enzyme-linked　immunosorbent　assay,
911　immunoprecipitation and flow cytometry to confirm their role in cancer and other diseases.

912　　　　In summary, this study analysed the membrane-enriched proteome of TGFβ-treated
913　CRC cell lines (SW480 and HT29) that exhibit varying levels of β6 expression. A
914　consortium of range of molecules that affect various fundamental cellular processes required
915　for cancer progression were identified. Among the differentially expressed proteins, 74 have
916　been previously proposed as protein biomarkers for either cancer diagnosis, prognosis,
917　progression or response to therapy. These results support the observations from the cell-
918　based experiments where TGFβ treatment in some cases promoted cell proliferation, wound
919　healing and invasion. The down-regulation of vimentin and E-cadherin upon TGFβ
920　treatment suggests a cancer-promoting role for TGFβ when associated with β6 expression.
921　Through proteomic analysis of membrane enriched samples we have identified significant
922　alteration in numerous proteins and fundamental cellular process required for cancer
923　progression. This allows, we believe, the first significant insight into the joint action of TGFβ
924　and β6 expression in CRC, detailing how these molecules can promote metastatic
925　phenotypes. This could assist in the development of targeted therapies against CRC
926　metastasis.

927　**4. CONFLICT OF INTEREST**

928　　　　The authors declare no actual or potential conflicts of interest; including any
929　financial, personal or other relationships with other people or organizations.

5. ACKNOWLEDGEMENTS

SUPPLEMENTARY INFORMATION

Details all the materials and methods used in this study are given in the Supplementary material.

The two excel files provided contain the list of all significantly up- or down-regulated proteins identified in various comparisons of this study.

Supplementary Figure 1. The top four networks identified for the HT29 Mo- vs β6AS- (merged image).

Supplementary Figure 2. The top three networks identified for the HT29 Mo- vs β6AS- (merged image).

Supplementary Table 1. Cellular function that were significantly altered in integrin β6 and TGFβ defendant manner.

Supplementary Table 2. Proteins that are significantly up- or down-regulated in this study and those that can be used as ASCO cancer biomarkers and their respective applications.

Supplementary Table 3: Complete list of proteins identified within the SW480 comparisons. Fold changes >1.2 are considered up-regulated and <0.83 are considered down-regulated.

Supplementary Table 3: Complete list of proteins identified within the HT29 comparisons. Fold changes >1.2 are considered up-regulated and <0.83 are considered down-regulated.

REFERENCES

1. Zhang, Q., N. Yu, and C. Lee, *Mysteries of TGF-beta Paradox in Benign and Malignant Cells.* Front Oncol, 2014. **4**: p. 94.
2. Weiss, A. and L. Attisano, *The TGFbeta superfamily signaling pathway.* Wiley Interdiscip Rev Dev Biol, 2013. **2**(1): p. 47-63.
3. Massague, J., *The transforming growth factor-beta family.* Annu Rev Cell Biol, 1990. **6**: p. 597-641.
4. Massague, J., *TGF-beta signal transduction.* Annu Rev Biochem, 1998. **67**: p. 753-91.
5. Annes, J.P., J.S. Munger, and D.B. Rifkin, *Making sense of latent TGFbeta activation.* Journal of cell science, 2003. **116**(Pt 2): p. 217-24.
6. Massague, J. and D. Wotton, *Transcriptional control by the TGF-beta/Smad signaling system.* EMBO J, 2000. **19**(8): p. 1745-54.
7. Massague, J., *TGFbeta in Cancer.* Cell, 2008. **134**(2): p. 215-30.
8. Fuxe, J., T. Vincent, and A. Garcia de Herreros, *Transcriptional crosstalk between TGF-beta and stem cell pathways in tumor cell invasion: role of EMT promoting Smad complexes.* Cell cycle, 2010. **9**(12): p. 2363-74.
9. Tsushima, H., et al., *High levels of transforming growth factor beta 1 in patients with colorectal cancer: association with disease progression.* Gastroenterology, 1996. **110**(2): p. 375-82.
10. Kemik, O., et al., *Transforming growth factor beta-1 in human colorectal cancer patients.* Eur J Gen Med, 2011. **8**(1): p. 53-56.
11. Munger, J.S., et al., *The integrin alpha v beta 6 binds and activates latent TGF beta 1: a mechanism for regulating pulmonary inflammation and fibrosis.* Cell, 1999. **96**(3): p. 319-28.
12. Yang, G.Y., et al., *Integrin alpha v beta 6 mediates the potential for colon cancer cells to colonize in and metastasize to the liver.* Cancer Sci, 2008. **99**(5): p. 879-87.
13. Hazelbag, S., et al., *Overexpression of the alpha v beta 6 integrin in cervical squamous cell carcinoma is a prognostic factor for decreased survival.* J Pathol, 2007. **212**(3): p. 316-24.
14. Ahmed, N., et al., *Alpha(v)beta(6) integrin-A marker for the malignant potential of epithelial ovarian cancer.* The journal of histochemistry and cytochemistry : official journal of the Histochemistry Society, 2002. **50**(10): p. 1371-80.
15. Ahn, S.B., et al., *Characterization of the interaction between heterodimeric alphavbeta6 integrin and urokinase plasminogen activator receptor (uPAR) using functional proteomics.* J Proteome Res, 2014. **13**(12): p. 5956-64.
16. Dang, D., et al., *Matrix metalloproteinases and TGFbeta1 modulate oral tumor cell matrix.* Biochem Biophys Res Commun, 2004. **316**(3): p. 937-42.
17. Allen, M.D., et al., *Altered Microenvironment Promotes Progression of Pre-Invasive Breast Cancer: myoepithelial expression of alphavbeta6 integrin in DCIS identifies high-risk patients and predicts recurrence.* Clin Cancer Res, 2013.
18. Cantor, D., et al., *Overexpression of alphavbeta6 integrin alters the colorectal cancer cell proteome in favor of elevated proliferation and a switching in cellular adhesion that increases invasion.* Journal of proteome research, 2013. **12**(6): p. 2477-90.
19. Agrez, M., et al., *The alpha v beta 6 integrin promotes proliferation of colon carcinoma cells through a unique region of the beta 6 cytoplasmic domain.* The Journal of cell biology, 1994. **127**(2): p. 547-56.

20. Ahmed, N., et al., *Direct integrin alphavbeta6-ERK binding: implications for tumour growth.* Oncogene, 2002. **21**(9): p. 1370-80.

21. Geback, T., et al., *TScratch: a novel and simple software tool for automated analysis of monolayer wound healing assays.* Biotechniques, 2009. **46**(4): p. 265-74.

22. Thomas, G.J., et al., *Expression of the alphavbeta6 integrin promotes migration and invasion in squamous carcinoma cells.* J Invest Dermatol, 2001. **117**(1): p. 67-73.

23. Thomas, G.J., et al., *AlphaVbeta6 integrin promotes invasion of squamous carcinoma cells through up-regulation of matrix metalloproteinase-9.* Int J Cancer, 2001. **92**(5): p. 641-50.

24. Pascovici, D., et al., *Combining protein ratio p-values as a pragmatic approach to the analysis of multirun iTRAQ experiments.* J Proteome Res, 2015. **14**(2): p. 738-46.

25. Walker, L.C., et al., *Cytokeratin KRT8/18 expression differentiates distinct subtypes of grade 3 invasive ductal carcinoma of the breast.* Cancer Genet Cytogenet, 2007. **178**(2): p. 94-103.

26. Ponten, F., et al., *A global view of protein expression in human cells, tissues, and organs.* Mol Syst Biol, 2009. **5**: p. 337.

27. Tuffy, K.M. and S.L. Planey, *Cytoskeleton-Associated Protein 4: Functions Beyond the Endoplasmic Reticulum in Physiology and Disease.* ISRN Cell Biology, 2012. **2012**: p. 11.

28. Hanahan, D. and R.A. Weinberg, *The hallmarks of cancer.* Cell, 2000. **100**(1): p. 57-70.

29. Frisch, S.M. and H. Francis, *Disruption of epithelial cell-matrix interactions induces apoptosis.* J Cell Biol, 1994. **124**(4): p. 619-26.

30. Meredith, J.E., Jr., B. Fazeli, and M.A. Schwartz, *The extracellular matrix as a cell survival factor.* Mol Biol Cell, 1993. **4**(9): p. 953-61.

31. Ghosh, D., et al., *Identification of key players for colorectal cancer metastasis by iTRAQ quantitative proteomics profiling of isogenic SW480 and SW620 cell lines.* J Proteome Res, 2011. **10**(10): p. 4373-87.

32. Nada, S., et al., *p18/LAMTOR1: a late endosome/lysosome-specific anchor protein for the mTORC1/MAPK signaling pathway.* Methods Enzymol, 2014. **535**: p. 249-63.

33. Lombardo, Y., et al., *Nicastrin and Notch4 drive endocrine therapy resistance and epithelial to mesenchymal transition in MCF7 breast cancer cells.* Breast Cancer Res, 2014. **16**(3): p. R62.

34. Filipovic, A., et al., *Biological and clinical implications of nicastrin expression in invasive breast cancer.* Breast Cancer Res Treat, 2011. **125**(1): p. 43-53.

35. Cheruku, H.R., et al., *Transforming growth factor-β, MAPK and Wnt signaling interactions in colorectal cancer.* EuPA Open Proteomics, 2015(0).

36. Zhang, Y.E., *Non-Smad pathways in TGF-beta signaling.* Cell Res, 2009. **19**(1): p. 128-39.

37. Karantza, V., *Keratins in health and cancer: more than mere epithelial cell markers.* Oncogene, 2011. **30**(2): p. 127-38.

38. Baumann, K., *Cell Migration Talin Heads Off.* Nature Reviews Molecular Cell Biology, 2009. **10**(6).

39. Honda, K., et al., *Actinin-4, a novel actin-bundling protein associated with cell motility and cancer invasion.* J Cell Biol, 1998. **140**(6): p. 1383-93.

40. Park, I., et al., *Myosin regulatory light chains are required to maintain the stability of myosin II and cellular integrity.* Biochem J, 2011. **434**(1): p. 171-80.

| 1056 | 41. | Ganguly, K.K., et al., *Integrins and metastasis*. Cell Adh Migr, 2013. **7**(3): p. 251-61. |

41. Ganguly, K.K., et al., *Integrins and metastasis*. Cell Adh Migr, 2013. **7**(3): p. 251-61.

42. Balch, C. and J.R. Dedman, *Annexins II and V inhibit cell migration*. Exp Cell Res, 1997. **237**(2): p. 259-63.

43. Serra-Pages, C., et al., *Liprins, a family of LAR transmembrane protein-tyrosine phosphatase-interacting proteins*. J Biol Chem, 1998. **273**(25): p. 15611-20.

44. Kriajevska, M., et al., *Liprin beta 1, a member of the family of LAR transmembrane tyrosine phosphatase-interacting proteins, is a new target for the metastasis-associated protein S100A4 (Mts1)*. J Biol Chem, 2002. **277**(7): p. 5229-35.

45. Nguyen, M., et al., *Caspase-resistant BAP31 inhibits fas-mediated apoptotic membrane fragmentation and release of cytochrome c from mitochondria*. Mol Cell Biol, 2000. **20**(18): p. 6731-40.

46. Li, W., et al., *Abnormal DNA-PKcs and Ku 70/80 expression may promote malignant pathological processes in gastric carcinoma*. World J Gastroenterol, 2013. **19**(40): p. 6894-901.

47. Zimmermann, G., et al., *Small molecule inhibition of the KRAS-PDEdelta interaction impairs oncogenic KRAS signalling*. Nature, 2013. **497**(7451): p. 638-42.

48. Yang, M.H., et al., *Regulation of RAS oncogenicity by acetylation*. Proc Natl Acad Sci U S A, 2012. **109**(27): p. 10843-8.

49. Winslow, S., K. Leandersson, and C. Larsson, *Regulation of PMP22 mRNA by G3BP1 affects cell proliferation in breast cancer cells*. Mol Cancer, 2013. **12**(1): p. 156.

50. Ji, S., A. Wu, and H. Yang, *[Expression of progesterone receptor membrane component-1 is associated with the malignant phenotypes of breast cancer]*. Nan Fang Yi Ke Da Xue Xue Bao, 2012. **32**(5): p. 635-8.

51. He, Y., et al., *The role of PKR/eIF2alpha signaling pathway in prognosis of non-small cell lung cancer*. PLoS One, 2011. **6**(11): p. e24855.

52. Sun, S.Y., et al., *Activation of Akt and eIF4E survival pathways by rapamycin-mediated mammalian target of rapamycin inhibition*. Cancer Res, 2005. **65**(16): p. 7052-8.

53. Maul, R.S., et al., *EPLIN regulates actin dynamics by cross-linking and stabilizing filaments*. J Cell Biol, 2003. **160**(3): p. 399-407.

54. Bignotti, E., et al., *Trop-2 overexpression as an independent marker for poor overall survival in ovarian carcinoma patients*. Eur J Cancer, 2010. **46**(5): p. 944-53.

55. Ohmachi, T., et al., *Clinical significance of TROP2 expression in colorectal cancer*. Clin Cancer Res, 2006. **12**(10): p. 3057-63.

56. Xu, L., et al., *GPR56, an atypical G protein-coupled receptor, binds tissue transglutaminase, TG2, and inhibits melanoma tumor growth and metastasis*. Proc Natl Acad Sci U S A, 2006. **103**(24): p. 9023-8.

57. Yang, Y.Q., et al., *Upregulated expression of S100A6 in human gastric cancer*. J Dig Dis, 2007. **8**(4): p. 186-93.

58. Cross, S.S., et al., *Expression of S100 proteins in normal human tissues and common cancers using tissue microarrays: S100A6, S100A8, S100A9 and S100A11 are all overexpressed in common cancers*. Histopathology, 2005. **46**(3): p. 256-69.

59. Komatsu, K., et al., *Expression of S100A6 and S100A4 in matched samples of human colorectal mucosa, primary colorectal adenocarcinomas and liver metastases*. Oncology, 2002. **63**(2): p. 192-200.

60.   Duan, L., et al., *S100A6 stimulates proliferation and migration of colorectal carcinoma cells through activation of the MAPK pathways.* Int J Oncol, 2014. **44**(3): p. 781-90.

61.   Zhang, J., et al., *S100A6 as a potential serum prognostic biomarker and therapeutic target in gastric cancer.* Dig Dis Sci, 2014. **59**(9): p. 2136-44.

62.   Subramani, D. and S.K. Alahari, *Integrin-mediated function of Rab GTPases in cancer progression.* Mol Cancer, 2010. **9**: p. 312.

63.   Chung, Y.C., et al., *Rab11 regulates E-cadherin expression and induces cell transformation in colorectal carcinoma.* BMC Cancer, 2014. **14**: p. 587.

64.   Steffan, J.J., et al., *Supporting a role for the GTPase Rab7 in prostate cancer progression.* PLoS One, 2014. **9**(2): p. e87882.

65.   Pangon, L., et al., *MCC inhibits beta-catenin transcriptional activity by sequestering DBC1 in the cytoplasm.* Int J Cancer, 2015. **136**(1): p. 55-64.

66.   Qin, B., et al., *DBC1 functions as a tumor suppressor by regulating p53 stability.* Cell Rep, 2015. **10**(8): p. 1324-34.

67.   Cho, D., et al., *The expression of DBC1/CCAR2 is associated with poor prognosis of ovarian carcinoma.* J Ovarian Res, 2015. **8**(1): p. 2.

68.   Bae, J.S., et al., *CK2alpha phosphorylates DBC1 and is involved in the progression of gastric carcinoma and predicts poor survival of gastric carcinoma patients.* Int J Cancer, 2015. **136**(4): p. 797-809.

69.   Kim, W. and J.E. Kim, *Deleted in breast cancer 1 (DBC1) deficiency results in apoptosis of breast cancer cells through impaired responses to UV-induced DNA damage.* Cancer Lett, 2013. **333**(2): p. 180-6.

70.   Zhang, Y., et al., *DBC1 is over-expressed and associated with poor prognosis in colorectal cancer.* Int J Clin Oncol, 2014. **19**(1): p. 106-12.

71.   Kikuchi, K., et al., *High SIRT1 expression and low DBC1 expression are associated with poor prognosis in colorectal cancer.* journal of Cancer Therapeutics and Research, 2013. **2**(1).

72.   Liu, Y.Z., et al., *A panel of protein markers for the early detection of lung cancer with bronchial brushing specimens.* Cancer Cytopathol, 2014. **122**(11): p. 833-41.

73.   Chen, Y., et al., *Screening aberrant methylation profile in esophageal squamous cell carcinoma for Kazakhs in Xinjiang area of China.* Mol Biol Rep, 2015. **42**(2): p. 457-64.

74.   Chowdhury, D. and J. Lieberman, *Death by a thousand cuts: granzyme pathways of programmed cell death.* Annu Rev Immunol, 2008. **26**: p. 389-420.

75.   Bermejo-Martin, J.F., et al., *Host adaptive immunity deficiency in severe pandemic influenza.* Crit Care, 2010. **14**(5): p. R167.

76.   Wu, H., et al., *PTEN overexpression improves cisplatin-resistance of human ovarian cancer cells through upregulating KRT10 expression.* Biochem Biophys Res Commun, 2014. **444**(2): p. 141-6.

77.   Beauchemin, N. and A. Arabzadeh, *Carcinoembryonic antigen-related cell adhesion molecules (CEACAMs) in cancer progression and metastasis.* Cancer Metastasis Rev, 2013. **32**(3-4): p. 643-71.

78.   Singhai, R., et al., *E-Cadherin as a diagnostic biomarker in breast cancer.* N Am J Med Sci, 2011. **3**(5): p. 227-33.

79.   Taylor, M.R., et al., *Lactadherin (formerly BA46), a membrane-associated glycoprotein expressed in human milk and breast carcinomas, promotes Arg-Gly-Asp (RGD)-dependent cell adhesion.* DNA Cell Biol, 1997. **16**(7): p. 861-9.

| 1151 | 80. | Neutzner, M., et al., *MFG-E8/lactadherin promotes tumor growth in an angiogenesis-dependent transgenic mouse model of multistage carcinogenesis.* Cancer Res, 2007. **67**(14): p. 6777-85. |

1151 80. Neutzner, M., et al., *MFG-E8/lactadherin promotes tumor growth in an angiogenesis-dependent transgenic mouse model of multistage carcinogenesis.* Cancer Res, 2007. **67**(14): p. 6777-85.

1154 81. Cordero, O.J., et al., *Preoperative serum CD26 levels: diagnostic efficiency and predictive value for colorectal cancer.* Br J Cancer, 2000. **83**(9): p. 1139-46.

1156 82. Kanekura, T. and X. Chen, *CD147/basigin promotes progression of malignant melanoma and other cancers.* J Dermatol Sci, 2010. **57**(3): p. 149-54.

1158 83. Muramatsu, T. and T. Miyauchi, *Basigin (CD147): a multifunctional transmembrane protein involved in reproduction, neural function, inflammation and tumor invasion.* Histol Histopathol, 2003. **18**(3): p. 981-7.

1161 84. Ports, M.O., et al., *Extracellular engagement of alpha6 integrin inhibited urokinase-type plasminogen activator-mediated cleavage and delayed human prostate bone metastasis.* Cancer Res, 2009. **69**(12): p. 5007-14.

1164 85. Pawar, S.C., et al., *Integrin alpha6 cleavage: a novel modification to modulate cell migration.* Exp Cell Res, 2007. **313**(6): p. 1080-9.

1166 86. Rabinovitz, I., R.B. Nagle, and A.E. Cress, *Integrin alpha 6 expression in human prostate carcinoma cells is associated with a migratory and invasive phenotype in vitro and in vivo.* Clin Exp Metastasis, 1995. **13**(6): p. 481-91.

1169 87. Gannon, P.O., et al., *Ebp1 expression in benign and malignant prostate.* Cancer Cell Int, 2008. **8**: p. 18.

1171 88. Zhang, Y., et al., *EBP1, an ErbB3-binding protein, is decreased in prostate cancer and implicated in hormone resistance.* Mol Cancer Ther, 2008. **7**(10): p. 3176-86.

1173 89. Zhang, Y., D. Akinmade, and A.W. Hamburger, *Inhibition of heregulin mediated MCF-7 breast cancer cell growth by the ErbB3 binding protein EBP1.* Cancer Lett, 2008. **265**(2): p. 298-306.

1176 90. Ou, K., et al., *Quantitative profiling of drug-associated proteomic alterations by combined 2-nitrobenzenesulfenyl chloride (NBS) isotope labeling and 2DE/MS identification.* J Proteome Res, 2006. **5**(9): p. 2194-206.

1179 91. Levin, T.G., et al., *Characterization of the intestinal cancer stem cell marker CD166 in the human and mouse gastrointestinal tract.* Gastroenterology, 2010. **139**(6): p. 2072-2082 e5.

1182 92. Tan, F., et al., *Enhanced down-regulation of ALCAM/CD166 in African-American Breast Cancer.* BMC Cancer, 2014. **14**: p. 715.

1184 93. van Kempen, L.C., et al., *Activated leukocyte cell adhesion molecule/CD166, a marker of tumor progression in primary malignant melanoma of the skin.* Am J Pathol, 2000. **156**(3): p. 769-74.

1187 94. Korabiowska, M., et al., *Differential expression of DNA nonhomologous end-joining proteins Ku70 and Ku80 in melanoma progression.* Mod Pathol, 2002. **15**(4): p. 426-33.

1190 95. Hu, Y.Y., et al., *Notch signaling pathway and cancer metastasis.* Adv Exp Med Biol, 2012. **727**: p. 186-98.

1192 96. Bausch, D., et al., *Plectin-1 as a novel biomarker for pancreatic cancer.* Clin Cancer Res, 2011. **17**(2): p. 302-9.

1194 97. Katada, K., et al., *Plectin promotes migration and invasion of cancer cells and is a novel prognostic marker for head and neck squamous cell carcinoma.* J Proteomics, 2012. **75**(6): p. 1803-15.

1197 98. Cheng, C.C., et al., *Transient knockdown-mediated deficiency in plectin alters hepatocellular motility in association with activated FAK and Rac1-GTPase.* Cancer Cell Int, 2015. **15**: p. 29.

99.   Zhang, Y., et al., *Identification of transgelin-2 as a biomarker of colorectal cancer by laser capture microdissection and quantitative proteome analysis.* Cancer Sci, 2010. **101**(2): p. 523-9.

100.   Huang, Q., et al., *Identification of transgelin as a potential novel biomarker for gastric adenocarcinoma based on proteomics technology.* J Cancer Res Clin Oncol, 2008. **134**(11): p. 1219-27.

101.   Yu, H., et al., *Transgelin is a direct target of TGF-beta/Smad3-dependent epithelial cell migration in lung fibrosis.* FASEB J, 2008. **22**(6): p. 1778-89.

102.   Masellis-Smith, A. and A.R. Shaw, *CD9-regulated adhesion. Anti-CD9 monoclonal antibody induce pre-B cell adhesion to bone marrow fibroblasts through de novo recognition of fibronectin.* J Immunol, 1994. **152**(6): p. 2768-77.

103.   Ikeyama, S., et al., *Suppression of cell motility and metastasis by transfection with human motility-related protein (MRP-1/CD9) DNA.* J Exp Med, 1993. **177**(5): p. 1231-7.

104.   Murayama, Y., et al., *The tetraspanin CD9 modulates epidermal growth factor receptor signaling in cancer cells.* J Cell Physiol, 2008. **216**(1): p. 135-43.

105.   Van Slambrouck, S., et al., *Reorganization of the integrin alpha2 subunit controls cell adhesion and cancer cell invasion in prostate cancer.* Int J Oncol, 2009. **34**(6): p. 1717-26.

106.   Ramirez, N.E., et al., *The alpha(2)beta(1) integrin is a metastasis suppressor in mouse models and human cancer.* J Clin Invest, 2011. **121**(1): p. 226-37.

107.   Marthick, J.R. and J.L. Dickinson, *Emerging putative biomarkers: the role of alpha 2 and 6 integrins in susceptibility, treatment, and prognosis.* Prostate Cancer, 2012. **2012**: p. 298732.

108.   Salama, I., et al., *A review of the S100 proteins in cancer.* Eur J Surg Oncol, 2008. **34**(4): p. 357-64.

109.   Stulik, J., et al., *The analysis of S100A9 and S100A8 expression in matched sets of macroscopically normal colon mucosa and colorectal carcinoma: the S100A9 and S100A8 positive cells underlie and invade tumor mass.* Electrophoresis, 1999. **20**(4-5): p. 1047-54.

110.   Arai, K., et al., *S100A8 and S100A9 overexpression is associated with poor pathological parameters in invasive ductal carcinoma of the breast.* Curr Cancer Drug Targets, 2008. **8**(4): p. 243-52.

111.   Kinoshita, M., et al., *Self- and actin-templated assembly of Mammalian septins.* Dev Cell, 2002. **3**(6): p. 791-802.

112.   Kremer, B.E., L.A. Adang, and I.G. Macara, *Septins regulate actin organization and cell-cycle arrest through nuclear accumulation of NCK mediated by SOCS7.* Cell, 2007. **130**(5): p. 837-50.

113.   Ishiyama, N., et al., *Dynamic and static interactions between p120 catenin and E-cadherin regulate the stability of cell-cell adhesion.* Cell, 2010. **141**(1): p. 117-28.

114.   UniProt, C., *UniProt: a hub for protein information.* Nucleic Acids Res, 2015. **43**(Database issue): p. D204-12.

115.   Casagolda, D., et al., *A p120-catenin-CK1epsilon complex regulates Wnt signaling.* J Cell Sci, 2010. **123**(Pt 15): p. 2621-31.

116.   Nam, K.T., et al., *Loss of Rab25 promotes the development of intestinal neoplasia in mice and is associated with human colorectal adenocarcinomas.* J Clin Invest, 2010. **120**(3): p. 840-9.

1247   117.   Sturm, I., et al., *Analysis of the p53/BAX pathway in colorectal cancer: low BAX is*
1248   *a negative prognostic factor in patients with resected liver metastases.* J Clin Oncol,
1249   1999. **17**(5): p. 1364-74.

1250   118.   Grzmil, M., et al., *Expression and functional analysis of Bax inhibitor-1 in human*
1251   *breast cancer cells.* J Pathol, 2006. **208**(3): p. 340-9.

1252   119.   Gurluler, E., et al., *Serum annexin A2 levels in patients with colon cancer in*
1253   *comparison to healthy controls and in relation to tumor pathology.* Med Sci Monit,
1254   2014. **20**: p. 1801-7.

1255   120.   Yang, T., et al., *Prognostic and diagnostic significance of annexin A2 in colorectal*
1256   *cancer.* Colorectal Dis, 2013. **15**(7): p. e373-81.

1257   121.   Annes, J.P., D.B. Rifkin, and J.S. Munger, *The integrin alphaVbeta6 binds and*
1258   *activates latent TGFbeta3.* FEBS Lett, 2002. **511**(1-3): p. 65-8.

1259   122.   Ahn, S.B., et al., *Correlations between integrin alphanubeta6 expression and*
1260   *clinico-pathological features in stage B and stage C rectal cancer.* PLoS One, 2014.
1261   **9**(5): p. e97248.

1262   123.   Stolboushkina, E.A. and M.B. Garber, *Eukaryotic type translation initiation factor*
1263   *2: structure-functional aspects.* Biochemistry (Mosc), 2011. **76**(3): p. 283-94.

1264   124.   Nathan, C.O., et al., *Elevated expression of eIF4E and FGF-2 isoforms during*
1265   *vascularization of breast carcinomas.* Oncogene, 1997. **15**(9): p. 1087-94.

1266   125.   Seki, N., et al., *Expression of eukaryotic initiation factor 4E in atypical adenomatous*
1267   *hyperplasia and adenocarcinoma of the human peripheral lung.* Clin Cancer Res,
1268   2002. **8**(10): p. 3046-53.

1269   126.   Loboda, A., et al., *EMT is the dominant program in human colon cancer.* BMC Med
1270   Genomics, 2011. **4**: p. 9.

1271   127.   Uhlen, M., et al., *Proteomics. Tissue-based map of the human proteome.* Science,
1272   2015. **347**(6220): p. 1260419.

1273

3.2.2 – Supplemental files

SUPPLEMENTARY INFORMATION

S1. MATERIALS AND METHODS

S1.1 Cell lines

Two different colorectal adenocarcinoma cell lines SW480 and HT29 were used in this study. The SW480 cells (ATCC CCL-228™) [1] devoid of endogenous β6 expression were employed to engineer two stably transfected subclones used in this study. These cells were stably transfected with a pcDNA1Neo expression vector containing either an 'empty' vector (SW480^{Mock}) or the full-length integrin β6 subunit coding sequence under control of the human cytomegalovirus immediate early enhancer (i.e., SW480^{β6OE}) as previously described [2]. HT29 cells (ATCC HTB-38™) [371] which endogenously express the β6 integrin, were stably transfected with the pEF.PGK.puro vector containing either an 'empty' vector (HT29^{Mock}) or the β6 cDNA sequence in an antisense orientation (HT29^{β6AS}) under the control of the human polypeptide chain elongation factor-1a promoter as previously described [3]. HT29^{β6AS} cells do express β6 however this is strongly reduced [3]. The stable transfectant clones of these cells were a kind gift from Prof. Michael Agrez (University of Newcastle, Australia). Each cell line has been previously found to be invasive by matrigel invasion assays [2-4] and intrinsically express uPAR, TGFβR1 and TGFβR2. Cell lines tested negative for *Mycoplasma* infection using the PCR-based VenorGeM Mycoplasma Detection Kit (Minerva Biolabs Cat. No. 11-1050).

SW480 subclone cells were cultured in Dulbecco's Modified Eagle Medium (DMEM; Invitrogen, catalogue number: 19965-092) supplemented with 10% foetal bovine serum (FBS) (Invitrogen) and 500μg/mL geneticin (G418 sulfate, Invitrogen; 11811-031). HT29 subclone cells were cultured in Roswell Park Memorial Institute medium (RPMI; Invitrogen, catalogue number: 11875-093) supplemented with 10% FBS and 2.5μg/mL puromycin (Life Technologies; A11138-02). Both cell lines were incubated at 37ºC in 5% CO_2 for each incubation step unless otherwise stated. Serum-free (SF) media for both cell lines contained 0.5% FBS.

S1.2 Recombinant protein treatment protocol

The recombinant protein treatment method employed during this study remained constant for all the assays. Freshly passaged CRC subclone cells were seeded and incubated in serum-containing media for 24 hrs. Media was then changed to SF media and serum starved for 24 hrs. At this point recombinant proteins were aseptically introduced into respective wells and incubated for the time period required for each assay. Recombinant Human TGFβ1 was purchased from R&D Systems (Minnesota, USA) and SB431542 (TGFβ Receptor I kinase inhibitor) was purchased from Abcam (Cambridge, UK).

Four treatment conditions were employed for this study: 1) SF media as a negative control, 2) SF media + 10ng/mL active TGFβ, 3) SF media + 10μM SB431542 and 4) SF media + 10ng/mL active TGFβ + 10μM SB431542. The active TGFβ1 was added to the culture 30min after treating with SB431542. All the cell based experimental comparisons were performed in biological triplicates and experiments were independently repeated at least two times. The data is presented as a percentage of the untreated mock transfectant controls.

S1.3 Wound-healing assay

A wound healing assay was performed to mimic cell migration under stress conditions. In brief, 5.0×10^5 freshly passaged SW480 subclone cells were plated in six-well plates and incubated in serum media until a confluent monolayer had formed. The cells were then wounded using a the fine end of a 10μL pipette tip (0.35mm diameter) and stimulated with 10 ng/mL TGFβ1 or 10 μM SB431542 or both in the presence of SF media for 24 h, following prior serum deprivation in SF media for 24h. The pictures of the wounds were taken at 0h and 24h after wounding. The cells were observed using a 10x objective on a Leica DM-IL microscope with a Leica DFC280 digital imager. Three images were taken at random along the 'wound' for each well. The width of the wound before and after treatments was calculated using TScratch software (http://cse-lab.ethz.ch/software/) [5]. The median width measurements were then used for statistical testing. All conditions were performed in biological triplicate and statistical testing for significance performed using a Student's t-test with a significance cut-off of $p<0.05$.

S1.4 Invasion assay

The ability of cells to invade through extra-cellular matrix (ECM) was assessed using the Chemicon QCM 96-well Invasion Assay Kit (ECM555, CHEMICON, International, CA, USA) and performed according to manufacturer's instructions. Briefly, serum starved (0.5% FBS v/v) CRC subclone cells were non-enzymatically (trypsin/EDTA) detached from the growing surface and resuspended in SF media. Then, 5×10^4 cells and recombinant proteins were placed in the invasive chamber and incubated at 37 °C for 18-24 hrs. The cells which migrated through the ECM layer and attached to the bottom of the polycarbonate membrane, were dissociated from the membrane after incubation with the 150 μL of Cell Detachment Solution (37 °C for 30 min). Next, 50 μL of lysis buffer/CyQuant GR Dye Solution (1:75) was added to each well and incubated (15 min, room temperature). Finally, 150 μL of this mixture was transferred to a new 96-well plate, and the fluorescence was measured using a FLUOstar OPTIMA microplate spectrophotometer (BMG Labtech) using 480 nm/520 nm filter set. All conditions were performed in biological triplicate and statistical testing for significance performed using a Student's t-test with a significance cut-off of $p<0.05$.

S1.5 Cell-proliferation assay

The cells were seeded at a density of 1×10^5 (SW480) or 5×10^4 (HT29) cells into six-well plates and prepared for recombinant protein treatment as outlined above. The cells were then incubated in the presence of recombinant proteins for 24hrs. Cells were detached from the plate surface by trypsinization, gently mixed in a 1:1 ratio of cell suspension to 0.4% Trypan Blue (Sigma Aldrich) and the live cells enumerated using a BioRad TC-10™ automated cell counter. It should be noted that the trypan blue exclusion measures the steady state balance between cell viability and proliferation does not measure cell death. All conditions were performed in biological triplicate and statistical testing for significance performed using a Student's t-test with a significance cut-off of $p<0.05$.

S1.6 Membrane Protein enrichment

Subclones of SW480 and HT29 cell lines were seeded in 15-cm cell culture dishes and at a confluence of 70-75%, were stimulated with 10 ng mL^{-1} of TGFβ1 in the presence of SF media for 24 h, following prior serum deprivation overnight. The cells were then collected in lysis buffer containing (50 mM Tris-HCl, 100 mM NaCl, protease inhibitor cocktail (Roche Applied Science) and phosphatase inhibitors (Sigma Aldrich)) and left on

89 ice for 30 min before proceeding to membrane enrichment. The cells were stored at -80 °C
90 if not used immediately and were thawed on ice before proceeding to membrane enrichment.

91 Membrane enrichment was performed using a previously published method [6] with
92 slight modifications. In detail, the crude cell lysate was homogenized in the lysis buffer using
93 a probe sonicator (Branson Sonifier 450; www.bransonultrasonics.com) [7]. The
94 homogenized cell lysate was centrifuged at 2000g (20 min, 4 °C) to remove nuclei and cell
95 debris. The supernatant containing the membrane and other cellular proteins was then diluted
96 to 8 mL using binding buffer (20 mM Tris-HCl, 100 mM NaCl) and subjected to
97 ultracentrifugation (Sorvall Discovery; M120 SE, S80AT3 rotor) at 120,000g (90 min, 4
98 °C). The resulting membrane pellet was washed twice with 0.1 M sodium carbonate (pH
99 11.0) and resuspended/homogenized in binding buffer. The homogenized membrane
100 proteins were diluted with 4 volumes of binding buffer containing 1% (v/v) Triton X-114
101 and chilled on ice for 10 min with intermittent vortexing. Samples were then heated at 37 °C
102 for 20 min and phase partitioned by centrifugation at 1000g (3 min). The detergent phase
103 was further diluted with 4 volumes of binding buffer containing 1% (v/v) Trition X-114 and
104 phase partition was repeated. The integral membrane proteins in the Triton X-114 detergent
105 phase were subjected to acetone precipitation. The precipitated membrane proteins were
106 resolubilized in 0.5 M triethylammonium bicarbonate (TEAB) (Sigma-Aldrich, Australia)
107 and 0.1% SDS and stored at -80 °C if not used immediately. Protein samples were
108 quantitated using Pierce™ BCA Protein Assay Kit and 100 μg of protein was used to
109 perform the iTRAQ analyses.

S1.7 iTRAQ labelling

111 iTRAQ labelling was carried out, using a 4-plex isobaric tagging kit (AB SCIEX),
112 according to manufacturer's instructions with minor modifications. iTRAQ analysis was
113 performed in biological duplicates for each cell line, where in one set of samples were not
114 treated with TGFβ1. Briefly, 100 μg of total membrane protein samples for each replicate
115 were reduced using 5 mM tris-(2-carboxyethyl) phosphine (TCEP) (60 °C, 1 h), alkylated
116 with 10 mM methyl methanethiosulfonate (MMTS) (room temperature, 10 min) and
117 digested with trypsin (Promega; 1:25 w/w, 37°C overnight). The digested peptides were then
118 dried and reconstituted in 0.5 M TEAB and ethanol (70% (v/v) final concentration). They
119 were then labelled with respective 4-plex isobaric tags and incubated at room temperature
120 for 1 h before being combined. Confirmation of labelling and mixing was carried out using
121 MALDI-MS. The iTRAQ labelled samples were dried and stored at -80°C if not used
122 immediately.

S1.8 Strong cation exchange chromatography separation

124 The strong cation-exchange chromatography (SCX) was performed to remove
125 interfering substances such as dissolution buffer, organic solvents (ethanol, acetonitrile,
126 TEAB), reducing agent (TCEP), alkylating agent (MMTS), SDS and any excess iTRAQ
127 reagents. The samples were fractionated by SCX using an Agilent 1260 quaternary HPLC
128 pump with a PolyLC polysulfoethyl aspartamide column (200 mm x 2.1 mm, 5μm, 200 Å;
129 PolyLC, Columbia, MD). The column was equilibrated with buffer A (5mM KH_2PO_4, 25%
130 v/v acetonitrile (ACN), pH 2.72), which was also used for sample resuspension, sample
131 injection and peptide adsorption to the column. Peptide elution was achieved with a step
132 gradient of 10, 45 and 100% (v/v) buffer B (5mM KH_2PO_4, 25% v/v ACN, 350mM KCl pH
133 2.72) at a flow rate of 0.3mL/min. Peptides were collected every 4.5 min between 10 and 28
134 min; 4 min between 28 and 40 min; 2 min between 40 and 70 min and; 4 min between 70

135 and 132.5 min. The resulting SCX fractionated samples were dried in a vacuum centrifuge
136 and stored at -20°C until mass spectrometry was performed.

1.9 NanoLC Chromatography

138   The dried peptides from each SCX fractions were resuspended in loading/desalting
139 solution (0.1% v/v formic acid (FA), 2% v/v ACN) and 40μL of sample was loaded onto a
140 reverse phase peptide Captrap (Michrom Bioresources, USA) for pre-concentration and
141 desalting with 0.1% v/v FA, 2% v/v ACN at 5μL/min for 10 min per fraction. The peptide
142 trap was then switched on line with the Halo C18 column (75μm x 10 cm, 2.7μm, 160Å)
143 (Advanced Materials Technology, USA). The desalted peptides in each fraction were eluted
144 from the C18 column using a linear solvent gradient, with steps, from 98:2 of mobile phase
145 A (0.1% v/v FA): mobile phase B (90% v/v ACN, 0.1% v/v FA) to 65:35, at 300 nL/min
146 over 100 min per fraction. After peptide elution, the column was cleaned with 95% buffer B
147 for 15 min and then equilibrated with buffer A for 25 min before next sample injection.

S1.10 MS/MS data acquisition

149   Mass spectra were acquired on an AB SCIEX TripleTOF 5600 mass spectrometer.
150 The reverse phase nanoLC eluent was subjected to positive ion nanoflow electrospray
151 analysis in an information dependant acquisition (IDA) mode. In the IDA mode, TOF-MS
152 survey scan spectra from m/z 400 – 1500 were acquired for each fraction every 0.25 s. The
153 ten most intense multiply charged ions (counts >150) in the survey scan were sequentially
154 subjected to MS/MS analysis. MS/MS spectra were accumulated for 200 milliseconds in the
155 mass range m/z 100 – 1500 with the total cycle time 2.3 seconds.

S1.11 Peptide and protein identification

157   The nanoLC ESI MS/MS data set (*.wiff) files were submitted into ProteinPilot
158 software (ver. 4.2b, AB SCIEX) for data processing and protein identification. This program
159 uses the Paragon Algorithm for protein database searching, identification, protein grouping
160 for the removal of redundant hits and quantitative comparisons [372]. The following search
161 parameters were selected: sample type, iTRAQ 4plex (peptide labelled); Cysteine alkylation,
162 MMTS; Digestion, trypsin; Instrument, TripleTOF 5600; Special factors, none; Species,
163 human; ID focus, biological modifications; Database, uniprot_sprot2014; and Search effort,
164 thorough. The resulting data set was auto bias corrected ProteinPilot to get rid of any
165 variations imparted due to the unequal mixing during the combination of different labelled
166 samples or loading errors. The detected protein threshold (unused ProtScore) was set to ≥
167 1.3 (95% confidence or better) and a *p-value* (p < 0.05) ensured that protein identifications
168 and subsequent quantitation were not based on single peptide hits. The results were then
169 exported into Microsoft Excel for manual data interpretation. The individual cell line and
170 treatment comparisons were performed using Stouffer's method.

S1.12 Bioinformatics analysis of proteomics data

172   To appreciate the data generated, lists of significantly altered proteins were uploaded
173 into QIAGEN's Ingenuity® Pathway Analysis (IPA®, QIAGEN Redwood City,
174 www.qiagen.com/ingenuity) software server and analysed using the Core Analysis module
175 to rank the proteins into top biological functions including disease and disorders as well as
176 molecular and cellular functions. The reference set and parameters for IPA on significantly
177 altered protein list was as follows: (i) Reference set, Ingenuity Knowledge Base (Genes
178 Only); (ii) Relationship to include, Direct and Indirect; (iii) Filter Summary, Consider only
179 molecules and/or relationships where (species = Human) AND (cell lines = All Cancer cell

180 lines in ingenuity database). Additionally, cellular location of all the identified proteins was
181 determined using PloGO, a gene ontology (GO) mapping software [373].

S1.13 Western blotting assay

183   Protein extracts used for iTRAQ analysis were separated using 4-12% NuPAGE gel
184 (Invitrogen) at 200V for 1hr. The resolved proteins were then electrophoretically transferred
185 onto to a PVDF membrane (Invitrogen). After the transfer, the PVDF membranes were
186 immediately incubated in blocking buffer, containing Tris buffered saline (TBS) with 3%
187 (w/v) bovine serum albumin (BSA) and 0.5% (v/v) Tween-20, for 1h at room temperature
188 with gentle shaking. The blots were then incubated with specific primary antibody overnight
189 (4 ºC) with gentle shaking. Following this they were then incubated with horseradish
190 peroxidase-conjugated mouse, goat or rabbit secondary antibodies (R&D Systems,
191 Minnesota, USA). The imunoreactivity was detected using chemiluminescence substrate
192 (SuperSignal West Femto Maximum Sensitivity Substrate, Thermo) and imaged using LAS
193 3000, FUJI. The following primary antibodies were used: integrin β6 (sc-6632), Ezrin (sc-
194 58758), and calgranulin A (sc-20174) were purchased from Santa Cruz Biotechnology; and
195 Annexin-A2 (ab41803) was purchased from abcam. Antibody dilutions were applied as per
196 manufacturer's recommendations. Image Studio Lite (ver 5.0) (LI-COR) was used for
197 measurement of band intensities where required.

S1.14 Statistical Analysis

199   All statistical analyses were performed using R-package and/or Microsoft Excel. All
200 the *p-values* were calculated using student's t-test followed by Bonferroni p-value
201 correction. A *p<0.05* was considered to be statistically significant for each case.

References

203 1. Leibovitz, A., et al., *Classification of human colorectal adenocarcinoma cell lines.*
204   Cancer Res, 1976. 36(12): p. 4562-9.
205 2. Agrez, M., et al., *The alpha v beta 6 integrin promotes proliferation of colon carcinoma*
206   *cells through a unique region of the beta 6 cytoplasmic domain.* The Journal of cell
207   biology, 1994. 127(2): p. 547-56.
208 3. Ahmed, N., et al., *Direct integrin alphavbeta6-ERK binding: implications for tumour*
209   *growth.* Oncogene, 2002. 21(9): p. 1370-80.
210 4. Cantor, D., et al., *Overexpression of alphavbeta6 integrin alters the colorectal cancer cell*
211   *proteome in favor of elevated proliferation and a switching in cellular adhesion that*
212   *increases invasion.* Journal of proteome research, 2013. 12(6): p. 2477-90.
213 5. Geback, T., et al., *TScratch: a novel and simple software tool for automated analysis of*
214   *monolayer wound healing assays.* Biotechniques, 2009. 46(4): p. 265-74.
215 6. Lee, A., et al., *Rat liver membrane glycoproteome: enrichment by phase partitioning and*
216   *glycoprotein capture.* Journal of proteome research, 2009. 8(2): p. 770-81.
217 7. McQuade, L.R., et al., *Improved membrane proteomics coverage of human embryonic*
218   *stem cells by peptide IPG-IEF.* Journal of proteome research, 2009. 8(12): p. 5642-9.
219 8. Shilov, I.V., et al., *The Paragon Algorithm, a next generation search engine that uses*
220   *sequence temperature values and feature probabilities to identify peptides from tandem*
221   *mass spectra.* Molecular & cellular proteomics MCP, 2007. 6(9): p. 1638-55.
222 9. Pascovici, D., et al., *PloGO: plotting gene ontology annotation and abundance in multi-*
223   *condition proteomics experiments.* Proteomics, 2012. 12(3): p. 406-10.
224

2. SUPPLEMENTARY FIGURES

Supplementary Figure 1 The top four networks identified for the HT29 Mo- vs As-(merged). The networks include "Cellular Function and Maintenance, Small Molecule Biochemistry, Molecular Transport" (IPA score = 53); "Cellular Assembly and Organization, Cell-To-Cell Signaling and Interaction, Reproductive System Development and Function" (IPA score = 45); "Cell Cycle, Infectious Diseases, Cancer" (IPA score = 25) and "Cancer, Endocrine System Disorders, Gastrointestinal Disease" (IPA score = 21).

234

Supplementary Figure 2 The top three networks identified for the HT29 Mo- vs As-(merged). The networks include "Cell-To-Cell Signalling and Interaction, Protein Synthesis, Cell Death and Survival" (IPA score = 47); "Cellular Movement, Hair and Skin Development and Function, Cell-To-Cell Signaling and Interaction" (IPA score = 27) and "Cell Death and Survival, Cancer, Organismal Injury and Abnormalities" (IPA score = 21).

3. SUPPLEMENTARY TABLES

Supplementary Table 1 Cellular function that were significantly altered in integrin β6 and TGFβ defendant manner

function	differentially expressed proteins	no. of molecules	p-value
apoptosis of colon cancer cell lines	CEACAM1,HSPD1,**ITGAV**,LGALS3,PARP1,PPIA,SFPQ	7	7.47E-03
	FASN,**ITGB1**,KRAS,KRT18,LGALS3,NAPA,NOC2L,PARP1,PPIA,**XRCC5**	10	1.37E-02
apoptosis of tumor cell lines	AIMP1,BCLAF1,CBX5,CCAR2,CCT2,CTNND1,CYB5A,ENO1,EPHA2,**EZR**,FASN,GNAS,H2AFX,HNRNPC,HNRNPK,HSP90AB1,IMMT,**ITGB1**,KHDRBS1,KRAS,KRT18,LGALS3,MDC1,MYBBP1A,NAPA,NCL,NOC2	45	2.99E-05

192

	L,NPM1,PARP1,PHB,PHB2,PPIA,PSIP1,RPS19,SLC25A5,SRSF1,SSRP1,STOML2,TFRC,TMED10,TOP2A,VDAC1,VDAC2,XPO1,**XRCC5**		
cell cycle progression	**CD44**,DDX17,EWSR1,ITGA2,NOLC1,NPM1,NUMA1,PHB2	8	2.16E-02
cell death of epithelial cell lines	CAT,DDX17,HSPA5,HSPD1,**ITGAV**,NDUFAB1,SSRP1,TFRC	8	1.96E-03
cell death of tumor cell lines	AIMP1,ANXA2,APMAP,ATP2A2,ATP5A1,BCLAF1,BUB1B,CBX5,CCAR2,CCT2,CTNND1,CYB5A,DAP3,DHCR24,EIF2S1,ENO1,EPHA2,EZR,FASN,FDFT1,GNAS,GPC1,H2AFX,HNRNPC,HNRNPK,HSP90AB1,ILF2,IMMT,**ITGB1**,KHDRBS1,KRAS,KRT18,LGALS3,LMNA,MDC1,MYBBP1A,NAPA,NCL,NOC2L,NPM1,PARP1,PHB,PHB2,PKM,PPIA,PSIP1,RPS19,SF3B3,SLC25A5,SLC3A2,SRSF1,SSB,SSRP1,STOML2,TEX10,TFRC,TMED10,TOP2A,VDAC1,VDAC2,XAB2,XPO1,**XRCC5**,XRCC6	64	1.18E-08
cell movement	**CD44**,CD9,CXADR,HNRNPK,HSPD1,ILF3,ITGA2,KRT16,MFI2,NCL,NPM1,PHB2,RTN4,S100A8,SLC2A1,TAGLN2	16	6.00E-04
cell movement of cancer cells	ADAM10,ALCAM,**CD44**,CD47,CEACAM1,**DPP4**	6	5.52E-04
cell movement of colon cancer cell lines	**CD44**,CD47,CDH1,ITGA6	4	9.57E-03
cell movement of tumor cell lines	ACTN4,AGR2,C1QBP,CAT,CRKL,**DPP4**,ITGA2,**ITGAV**,**ITGB5**,LGALS3,LGALS3BP,MCAM,MFI2,MSN,MYH9,PEBP1,PPIA,**S100A9**,SEPT9,SLC12A2,SLC9A3R1,TACSTD2	22	2.69E-05
	CD44,CD9,HNRNPK,ILF3,ITGA2,MFI2,NCL,PHB2,S100A8,SLC2A1,TAGLN2	11	2.29E-03
	ACSL4,ACTN4,ADGRE5,ANXA2,BSG,C1QBP,EPHA2,EZR,GALNT2,GNA13,GNAS,HNRNPK,HSP90AA1,ILF3,ITGA6,**ITGB1**,KHDRBS1,KRAS,KRT8,LGALS3,MCAM,NCL,PA2G4,PHB,PHB2,PPIA,RALA,SLC16A1,TLN1	29	1.99E-03
cell-cell adhesion of tumor cell lines	C1QBP,DSP,**ITGB1**,LGALS3	4	4.08E-03
invasion of tumor cell lines	AGR2,CAT,CTNND1,**DPP4**,**ITGAV**,LGALS3,MCAM,PEBP1,RAB25,S100A6,**S100A9**,SEPT9,SLC12A2,SLC9A3R1	14	3.69E-03
	ACSL4,ADGRE5,BSG,CBX5,CTNND1,EPHA2,EZR,GALNT2,GNAS,HSP90AA1,ILF3,**ITGB1**,KRAS,KRT8,LGALS3,MCAM,PA2G4,PHB,PKM,RALA,SRRM1	21	1.10E-02
invasion of tumor cells	ADGRE5,EZR,**ITGB1**,MCAM	4	1.18E-02
migration of cells	ACTN4,C1QBP,CAT,CEACAM1,CRKL,CXADR,**DPP4**,HLA-A,HMGB1,HSPA5,HSPD1,ITGA2,**ITGAV**,**ITGB5**,LGALS3,LGALS3BP,MCAM,MFI2,MSN,MYH9,PPIA,**S100A9**,SEPT9,SLC12A2,SLC9A3R1,TACSTD2	26	1.00E-04
	CD44,CD9,CXADR,HNRNPK,HSPD1,ILF3,ITGA2,KRT16,MFI2,NCL,NPM1,PHB2,RTN4,S100A8,SLC2A1	15	5.00E-04
migration of tumor cell lines	ACTN4,C1QBP,CAT,CRKL,**DPP4**,ITGA2,**ITGAV**,**ITGB5**,LGALS3,LGALS3BP,MCAM,MFI2,MSN,MYH9,**S100A9**,SEPT9,SLC12A2,SLC9A3R1,TACSTD2	19	6.60E-05
	CD44,CD9,HNRNPK,ILF3,ITGA2,MFI2,NCL,PHB2,S100A8,SLC2A1	10	2.01E-03
	ACSL4,ACTN4,ADGRE5,ANXA2,BSG,C1QBP,EPHA2,EZR,GALNT2,GNA13,GNAS,HNRNPK,HSP90AA1,ILF3,ITGA6,**ITGB1**,KHDRBS1,KRAS,KRT8,LGALS3,MCAM,NCL,PHB,PHB2,RALA,SLC16A1	26	1.32E-03
	HNRNPA2B1,HNRNPK,ILF3,**ITGAV**,**ITGB1**,KRT8,NCL,VCP,VIM	9	1.44E-04
migration of tumor cells	ACTN4,ADGRE5,EZR,**ITGB1**,LGALS3	5	5.50E-03
proliferation of cancer cells	ADAM10,BSG,**CD44**,NPM1,RPS4X,**S100A9**,TRIM25,**XRCC5**	8	4.82E-03
proliferation of cells	ACIN1,ACTG1,ACTN4,ADAR,ADGRG1,ATAD3A,ATP5A1,ATP5B,C1QBP,CAT,CCT2,CCT3,CCT5,CCT7,CD276,CD55,CEACAM1,CRKL,CTNN	63	1.97E-11

	D1,CXADR,DDX17,DLD,**DPP4**,ETFDH,H2AFY,HIST1H1B,HMGB1,HN RNPC,HNRNPF,HSPA5,HSPD1,IMMT,ITGA2,**ITGAV**,**ITGB5**,LGALS3, MCAM,MKI67,MYBBP1A,MYH9,NDUFAB1,PARP1,PDIA3,PEBP1,PLI N3,PPIA,PRKCSH,RAB25,RPS25,S100A6,**S100A9**,SEPT9,SERPINH1,SFP Q,SLC9A3R1,SRSF1,SSBP1,TACSTD2,TFRC,THRAP3,TOP1,TUBB,UBT F		
	ADGRG1,**CD44**,CD9,CXADR,DDX17,DDX21,EWSR1,HNRNPK,HNRNP M,HSPD1,ILF3,ITGA2,KRT10,KRT16,LMNA,NCL,NDUFS3,NPM1,NUM A1,PLEC,PRKCSH,RPS3A,RTN4,S100A8,SLC2A1,SNRNP200,TAGLN2, TFRC,TUBB	29	2.16E-05
	ACIN1,ADAM10,ADAR,ADGRG1,ALCAM,ALDH1A1,ATP5B,BCAP31, BSG,**CD44**,CD47,CDH1,CEACAM1,CXADR,DDX17,**DPP4**,EPCAM,ETF DH,GALNT2,H2AFY,HADHA,HIST1H1B,HNRNPM,HNRNPU,ILF2,ITG A6,KRT10,KRT8,LIMA1,LMNB1,MFGE8,NCSTN,NDUFAF2,NDUFV1,N OP2,NPM1,PA2G4,PLIN3,RPS3A,RPS4X,**S100A9**,SCARB1,SFPQ,STX3,T OP1,TRIM25,UBTF,VDAC1,**XRCC5**,XRCC6	50	1.12E-06
	DNAJA1,EEF1A1,HNRNPA1,HNRNPA2B1,HNRNPAB,HNRNPD,HNRN PK,HSPA5,ILF3,**ITGAV**,**ITGB1**,KRT2,KRT8,LAMTOR2,NCL,NCSTN,N PM1,PKM,PTBP1,RTN4,TOP2B	21	7.84E-06
proliferation of tumor cell lines	ACIN1,ACTN4,C1QBP,CAT,CEACAM1,CRKL,CTNND1,CXADR,DDX1 7,**DPP4**,H2AFY,HMGB1,HSPA5,IMMT,ITGA2,**ITGAV**,**ITGB5**,LGALS3, MKI67,MYBBP1A,PARP1,PDIA3,PEBP1,RPS25,S100A6,SEPT9,SFPQ,SL C9A3R1,SSBP1,TACSTD2,TFRC,TOP1,TUBB	33	2.28E-05

[a]Proteins in bold are members of various CRC sub-networks discussed in the main body of the manuscript

243

Supplementary Table 2 Proteins that are significantly up- or down-regulated in this study and those that can be used as ASCO cancer biomarkers and their respective applications

Symbol	Entrez Gene Name	Entrez Gene ID for Human	UniProt ID	Biomarker Application/s
AGR2	anterior gradient 2	10551	O95994	D
AIMP1	aminoacyl tRNA synthetase complex-interacting multifunctional protein 1	9255	Q12904	D
ALCAM	activated leukocyte cell adhesion molecule	214	Q13740	P
ALDH1A1	aldehyde dehydrogenase 1 family, member A1	216	P00352	D,DP
ALPL	alkaline phosphatase, liver/bone/kidney	249	P05186	E
ANXA2	annexin A2	302	P07355	D
ARSE	arylsulfatase E (chondrodysplasia punctata 1)	415	P51690	D
BCAM	basal cell adhesion molecule (Lutheran blood group)	4059	P50895	D
BSG	basigin (Ok blood group)	682	P35613	DP,P,RT
CAT	catalase	847	P04040	D
CD276	CD276 molecule	80381	Q5ZPR3	P
CD44	CD44 molecule (Indian blood group)	960	P16070	D,DP,P
CD9	CD9 molecule	928	P21926	E
CDH1	cadherin 1, type 1, E-cadherin (epithelial)	999	P12830	D,DP,E,P
CEACAM1	carcinoembryonic antigen-related cell adhesion molecule 1 (biliary glycoprotein)	634	P13688	D,E
CTNNA1	catenin (cadherin-associated protein), alpha 1, 102kDa	1495	P35221	D

DNMT1	DNA (cytosine-5-)-methyltransferase 1	1786	P26358	D
EIF2S1	eukaryotic translation initiation factor 2, subunit 1 alpha, 35kDa	1965	P05198	E
ENO1	enolase 1, (alpha)	2023	P06733	D
EPHA2	EPH receptor A2	1969	P29317	DP
EPHX1	epoxide hydrolase 1, microsomal (xenobiotic)	2052	P07099	D
EZR	ezrin	7430	P15311	P
FASN	fatty acid synthase	2194	P49327	D,E
GAPDH	glyceraldehyde-3-phosphate dehydrogenase	2597	P04406	D
H2AFX	H2A histone family, member X	3014	P16104	E
HLA-A	major histocompatibility complex, class I, A	3105	P04439	E,RT
HMGB1	high mobility group box 1	3146	P09429	D
HNRNPK	heterogeneous nuclear ribonucleoprotein K	3190	P61978	P
HSPD1	heat shock 60kDa protein 1 (chaperonin)	3329	P10809	D,P
ICAM1	intercellular adhesion molecule 1	3383	P05362	D,E,P
ITGAV	integrin, alpha V	3685	P06756	D
ITGB1	integrin, beta 1 (fibronectin receptor, beta polypeptide, antigen CD29 includes MDF2, MSK12)	3688	P05556	DP,P
ITGB5	integrin, beta 5	3693	P18084	D
KRAS	Kirsten rat sarcoma viral oncogene homolog	3845	P01116	D,E,P,RT
KRT1	keratin 1, type II	3848	P04264	D
KRT17	keratin 17, type I	3872	Q04695	D,E
KRT18	keratin 18, type I	3875	P05783	E
KRT20	keratin 20, type I	54474	P35900	D,DP,P
KRT5	keratin 5, type II	3852	P13647	D,E
KRT6A	keratin 6A, type II	3853	P02538	D
KRT8	keratin 8, type II	3856	P05787	P
KRT9	keratin 9, type I	3857	P35527	D
LDLR	low density lipoprotein receptor	3949	P01130	DP
LGALS3	lectin, galactoside-binding, soluble, 3	3958	P17931	D
LGALS3BP	lectin, galactoside-binding, soluble, 3 binding protein	3959	Q08380	P
MAP4	microtubule-associated protein 4	4134	P27816	E
MCAM	melanoma cell adhesion molecule	4162	P43121	D,P
MCM4	minichromosome maintenance complex component 4	4173	P33991	DP
MCM5	minichromosome maintenance complex component 5	4174	P33992	DP
MKI67	marker of proliferation Ki-67	4288	P46013	D,DP,E,P,RT
NPM1	nucleophosmin (nucleolar phosphoprotein B23, numatrin)	4869	P06748	DP
NUCB1	nucleobindin 1	4924	Q02818	D

PARP1	poly (ADP-ribose) polymerase 1	142	P09874	D,E,P
PDIA3	protein disulfide isomerase family A, member 3	2923	P30101	D
PHB	prohibitin	5245	P35232	D
PSIP1	PC4 and SFRS1 interacting protein 1	11168	O75475	DP
RPS4X	ribosomal protein S4, X-linked	6191	P62701	D
RPS6	ribosomal protein S6	6194	P62753	E,RT
RTN4	reticulon 4	57142	Q9NQC3	D
S100A6	S100 calcium binding protein A6	6277	P06703	D
S100A8	S100 calcium binding protein A8	6279	P05109	D,E
S100A9	S100 calcium binding protein A9	6280	P06702	D
SEPT9	septin 9	10801	Q9UHD8	D
SLC16A1	solute carrier family 16 (monocarboxylate transporter), member 1	6566	P53985	D
SLC2A1	solute carrier family 2 (facilitated glucose transporter), member 1	6513	P11166	D,E
SLC2A3	solute carrier family 2 (facilitated glucose transporter), member 3	6515	P11169	E
STOML2	stomatin (EPB72)-like 2	30968	Q9UJZ1	P
TFRC	transferrin receptor	7037	P02786	D,E
TOP1	topoisomerase (DNA) I	7150	P11387	E
TOP2A	topoisomerase (DNA) II alpha 170kDa	7153	P11388	D,E,P,RT
TPI1	triosephosphate isomerase 1	7167	P60174	D
TUBB	tubulin, beta class I	203068	P07437	E
XPO1	exportin 1	7514	O14980	D,E
ZAP70	zeta-chain (TCR) associated protein kinase 70kDa	7535	P43403	P,RT
[a] D: diagnosis; DP: disease progression; E: efficacy; P: prognosis; RT: response to therapy				

246

247

248 **Supplementary Table 3:** Complete list of proteins identified within the SW480

249 comparisons. Fold changes >1.2 are considered up-regulated and <0.83 are considered

250 down-regulated.

A: Comparison of TGFβ treated SW480 Mock/untreated SW480 Mock

Uniprot	Unused	Total	X.Cov.95.	Protein Name; Organism; Gene name	iTRAQ Fold Change	StouffersPval
P04264	14.77	18.88	12.89	Keratin, type II cytoskeletal 1 OS=Homo sapiens GN=KRT1 PE=1 SV=6	1.919	0.000
P35527	12.44	12.49	20.22	Keratin, type I cytoskeletal 9 OS=Homo sapiens GN=KRT9 PE=1 SV=3	1.890	0.002
Q9Y2Q5	5.39	5.39	38.4	Ragulator complex protein LAMTOR2 OS=Homo sapiens GN=LAMTOR2 PE=1 SV=1	1.559	0.034
P19338	33.5	33.5	26.2	Nucleolin OS=Homo sapiens GN=NCL PE=1 SV=3	1.369	0.002
P60900	2.52	2.52	7.317	Proteasome subunit alpha type-6 OS=Homo sapiens GN=PSMA6 PE=1 SV=1	1.368	0.041
P13645	8.46	10.92	15.24	Keratin, type I cytoskeletal 10 OS=Homo sapiens GN=KRT10 PE=1 SV=6	1.355	0.002
P22234	10.35	10.35	18.82	Multifunctional protein ADE2 OS=Homo sapiens GN=PAICS PE=1 SV=3	1.310	0.021
P04406	25.98	25.98	42.99	Glyceraldehyde-3-phosphate dehydrogenase OS=Homo sapiens GN=GAPDH PE=1 SV=3	1.306	0.000
P55072	11.27	13.34	15.76	Transitional endoplasmic reticulum ATPase OS=Homo sapiens GN=VCP PE=1 SV=4	1.243	0.019
O60506	32.06	32.06	37.88	Heterogeneous nuclear ribonucleoprotein Q OS=Homo sapiens GN=SYNCRIP PE=1 SV=2	1.233	0.038
Q09028	9.53	9.57	17.41	Histone-binding protein RBBP4 OS=Homo sapiens GN=RBBP4 PE=1 SV=3	1.218	0.044
P35579	111.32	111.32	36.17	Myosin-9 OS=Homo sapiens GN=MYH9 PE=1 SV=4	0.826	0.000
P04843	30.38	30.38	38.88	Dolichyl-diphosphooligosaccharide--protein glycosyltransferase subunit 1 OS=Homo sapiens GN=RPN1 PE=1 SV=1	0.817	0.006
P05787	38.55	40.45	54.24	Keratin, type II cytoskeletal 8 OS=Homo sapiens GN=KRT8 PE=1 SV=7	0.814	0.000
P14618	79.19	79.19	69.87	Pyruvate kinase PKM OS=Homo sapiens GN=PKM PE=1 SV=4	0.805	0.007
Q07065	21.23	21.38	24.58	Cytoskeleton-associated protein 4 OS=Homo sapiens GN=CKAP4 PE=1 SV=2	0.804	0.013
O00410	35.87	35.89	27.16	Importin-5 OS=Homo sapiens GN=IPO5 PE=1 SV=4	0.802	0.000
P46459	2.45	2.45	3.495	Vesicle-fusing ATPase OS=Homo sapiens GN=NSF PE=1 SV=3	0.799	0.050
P35580	48.53	68.41	24.85	Myosin-10 OS=Homo sapiens GN=MYH10 PE=1 SV=3	0.796	0.000
P15924	35.73	36.09	11.18	Desmoplakin OS=Homo sapiens GN=DSP PE=1 SV=3	0.794	0.001
O60566	7.1	9.32	8.286	Mitotic checkpoint serine/threonine-protein kinase BUB1 beta OS=Homo sapiens GN=BUB1B PE=1 SV=3	0.719	0.035
Q96RT1	7.5	7.6	4.887	Protein LAP2 OS=Homo sapiens GN=ERBB2IP PE=1 SV=2	0.709	0.040
Q9Y315	8.43	9.08	23.9	Putative deoxyribose-phosphate aldolase OS=Homo sapiens GN=DERA PE=1 SV=2	0.703	0.049
Q9NZ01	5.2	5.2	8.766	Very-long-chain enoyl-CoA reductase OS=Homo sapiens GN=TECR PE=1 SV=1	0.689	0.023

B: Comparison of TGFβ treated SW480 β6OE/untreated SW480 β6OE

Uniprot	Unused	Total	X.Cov.95.	Protein Name; Organism; Gene name	iTRAQ Fold Change	StouffersPval
Q9Y2Q5	5.39	5.39	38.4	Ragulator complex protein LAMTOR2 OS=Homo sapiens GN=LAMTOR2 PE=1 SV=1	1.855	0.018
P05387	22.58	22.58	92.17	60S acidic ribosomal protein P2 OS=Homo sapiens GN=RPLP2 PE=1 SV=1	1.826	0.023
P19338	33.5	33.5	26.2	Nucleolin OS=Homo sapiens GN=NCL PE=1 SV=3	1.745	0.000
P09651	21.27	27.51	30.38	Heterogeneous nuclear ribonucleoprotein A1 OS=Homo sapiens GN=HNRNPA1 PE=1 SV=5	1.667	0.008
P26599	16.06	16.06	44.26	Polypyrimidine tract-binding protein 1 OS=Homo sapiens GN=PTBP1 PE=1 SV=1	1.602	0.001
P55072	11.27	13.34	15.76	Transitional endoplasmic reticulum ATPase OS=Homo sapiens GN=VCP PE=1 SV=4	1.557	0.002
P27824	22.01	22.01	16.72	Calnexin OS=Homo sapiens GN=CANX PE=1 SV=2	1.553	0.000
P05556	16.57	16.63	15.04	Integrin beta-1 OS=Homo sapiens GN=ITGB1 PE=1 SV=2	1.538	0.010
Q99729	4.52	7.01	11.14	Heterogeneous nuclear ribonucleoprotein A/B OS=Homo sapiens GN=HNRNPAB PE=1 SV=2	1.499	0.011
O00629	6	6.01	9.789	Importin subunit alpha-3 OS=Homo sapiens GN=KPNA4 PE=1 SV=1	1.483	0.014
Q5JVS0	3.9	4.02	9.443	Intracellular hyaluronan-binding protein 4 OS=Homo sapiens GN=HABP4 PE=1 SV=1	1.475	0.047
O60506	32.06	32.06	37.88	Heterogeneous nuclear ribonucleoprotein Q OS=Homo sapiens GN=SYNCRIP PE=1 SV=2	1.470	0.000
P06748	15.94	17.65	43.88	Nucleophosmin OS=Homo sapiens GN=NPM1 PE=1 SV=2	1.443	0.044
P05455	6.17	6.23	9.559	Lupus La protein OS=Homo sapiens GN=SSB PE=1 SV=2	1.428	0.012
P51991	14.55	22.66	24.07	Heterogeneous nuclear ribonucleoprotein A3 OS=Homo sapiens GN=HNRNPA3 PE=1 SV=2	1.383	0.015
P05198	12.85	12.85	35.24	Eukaryotic translation initiation factor 2 subunit 1 OS=Homo sapiens GN=EIF2S1 PE=1 SV=3	1.380	0.003
O43809	8.03	8.03	40.97	Cleavage and polyadenylation specificity factor subunit 5 OS=Homo sapiens GN=NUDT21 PE=1 SV=1	1.377	0.010
P31689	24.48	24.48	48.11	DnaJ homolog subfamily A member 1 OS=Homo sapiens GN=DNAJA1 PE=1 SV=2	1.375	0.013
Q9Y2R9	6.75	6.75	21.9	28S ribosomal protein S7, mitochondrial OS=Homo sapiens GN=MRPS7 PE=1 SV=2	1.352	0.013
P22626	42.26	42.26	60.91	Heterogeneous nuclear ribonucleoproteins A2/B1 OS=Homo sapiens GN=HNRNPA2B1 PE=1 SV=2	1.344	0.030
Q14103	12.09	12.09	20	Heterogeneous nuclear ribonucleoprotein D0 OS=Homo sapiens GN=HNRNPD PE=1 SV=1	1.313	0.033
P61978	30.81	31.04	43.2	Heterogeneous nuclear ribonucleoprotein K OS=Homo sapiens GN=HNRNPK PE=1 SV=1	1.306	0.001
Q9NQC3	5.42	5.42	7.299	Reticulon-4 OS=Homo sapiens GN=RTN4 PE=1 SV=2	1.301	0.045
Q12906	18.28	18.4	15.21	Interleukin enhancer-binding factor 3 OS=Homo sapiens GN=ILF3 PE=1 SV=3	1.281	0.001
P11021	15.66	17.76	19.57	78 kDa glucose-regulated protein OS=Homo sapiens GN=HSPA5 PE=1 SV=2	1.256	0.003
P51665	12.02	12.02	32.1	26S proteasome non-ATPase regulatory subunit 7 OS=Homo sapiens GN=PSMD7 PE=1 SV=2	1.247	0.008
P61163	7.47	7.47	20.48	Alpha-centractin OS=Homo sapiens GN=ACTR1A PE=1 SV=1	1.219	0.027
Q92542	8	8	9.168	Nicastrin OS=Homo sapiens GN=NCSTN PE=1 SV=2	1.212	0.013
P06756	21.69	21.69	17.37	Integrin alpha-V OS=Homo sapiens GN=ITGAV PE=1 SV=2	1.210	0.001
O95816	12.89	12.9	45.02	BAG family molecular chaperone regulator 2 OS=Homo sapiens GN=BAG2 PE=1 SV=1	1.210	0.007
P42167	23.68	23.68	46.04	Lamina-associated polypeptide 2, isoforms beta/gamma OS=Homo sapiens GN=TMPO PE=1 SV=2	0.828	0.021
P68104	34.57	34.57	53.03	Elongation factor 1-alpha 1 OS=Homo sapiens GN=EEF1A1 PE=1 SV=1	0.818	0.004
P14618	79.19	79.19	69.87	Pyruvate kinase PKM OS=Homo sapiens GN=PKM PE=1 SV=4	0.811	0.001
Q14151	7.62	7.62	8.919	Scaffold attachment factor B2 OS=Homo sapiens GN=SAFB2 PE=1 SV=1	0.804	0.041
P43243	23.62	24.29	21.96	Matrin-3 OS=Homo sapiens GN=MATR3 PE=1 SV=2	0.796	0.003
P08670	58.18	58.18	59.01	Vimentin OS=Homo sapiens GN=VIM PE=1 SV=4	0.795	0.049
P27635	11.63	11.63	29.91	60S ribosomal protein L10 OS=Homo sapiens GN=RPL10 PE=1 SV=4	0.795	0.033
Q02880	6	8.6	5.351	DNA topoisomerase 2-beta OS=Homo sapiens GN=TOP2B PE=1 SV=3	0.786	0.023
P05787	38.55	40.45	54.24	Keratin, type II cytoskeletal 8 OS=Homo sapiens GN=KRT8 PE=1 SV=7	0.776	0.011
P61158	6.54	6.55	17.7	Actin-related protein 3 OS=Homo sapiens GN=ACTR3 PE=1 SV=3	0.768	0.039
P46063	14.63	14.63	17.72	ATP-dependent DNA helicase Q1 OS=Homo sapiens GN=RECQL PE=1 SV=3	0.760	0.013
P50213	4.68	4.68	10.93	Isocitrate dehydrogenase [NAD] subunit alpha, mitochondrial OS=Homo sapiens GN=IDH3A PE=1 SV=1	0.735	0.042
Q7Z7H5	2.11	9.55	35.68	Transmembrane emp24 domain-containing protein 4 OS=Homo sapiens GN=TMED4 PE=1 SV=1	0.672	0.040
Q9UJV9	4.14	4.14	4.502	Probable ATP-dependent RNA helicase DDX41 OS=Homo sapiens GN=DDX41 PE=1 SV=2	0.595	0.029
P68431	2	11.13	52.21	Histone H3.1 OS=Homo sapiens GN=HIST1H3A PE=1 SV=2	0.458	0.003
P35908	13.45	20.41	22.69	Keratin, type II cytoskeletal 2 epidermal OS=Homo sapiens GN=KRT2 PE=1 SV=2	0.251	0.017

C: Comparison of TGFβ treated SW480 β6OE/SW480 Mock

Uniprot	Unused	Total	X.Cov.95.	Protein Name; Organism; Gene name	iTRAQ Fold Change	StouffersPval
P62807	18.12	18.12	41.27	Histone H2B type 1-C/E/F/G/I OS=Homo sapiens GN=HIST1H2BC PE=1 SV=4	4.128	0.002
Q16629	9.44	9.44	21.43	Serine/arginine-rich splicing factor 7 OS=Homo sapiens GN=SRSF7 PE=1 SV=1	3.830	0.005
P16104	17.99	17.99	68.53	Histone H2AX OS=Homo sapiens GN=H2AFX PE=1 SV=2	3.341	0.042
P62805	17.02	17.02	56.31	Histone H4 OS=Homo sapiens GN=HIST1H4A PE=1 SV=2	2.800	0.005
P19105	14	14	57.31	Myosin regulatory light chain 12A OS=Homo sapiens GN=MYL12A PE=1 SV=2	2.663	0.000
P62906	21.72	21.72	56.68	60S ribosomal protein L10a OS=Homo sapiens GN=RPL10A PE=1 SV=2	2.645	0.000
Q13242	14.7	14.74	34.39	Serine/arginine-rich splicing factor 9 OS=Homo sapiens GN=SRSF9 PE=1 SV=1	2.618	0.000
P16401	12.33	19.86	26.55	Histone H1.5 OS=Homo sapiens GN=HIST1H1B PE=1 SV=3	2.609	0.002
Q07955	18.6	19.01	44.76	Serine/arginine-rich splicing factor 1 OS=Homo sapiens GN=SRSF1 PE=1 SV=2	2.540	0.000
Q9Y2W1	9.65	9.65	9.634	Thyroid hormone receptor-associated protein 3 OS=Homo sapiens GN=THRAP3 PE=1 SV=2	2.538	0.001
Q86V81	16	16	45.14	THO complex subunit 4 OS=Homo sapiens GN=ALYREF PE=1 SV=3	2.502	0.000
Q07666	7.09	7.09	18.28	KH domain-containing, RNA-binding, signal transduction-associated protein 1 OS=Homo sapiens GN=KHDRBS1 PE=1 S	2.473	0.000

251

252

P16403	20.39	20.39	28.17 Histone H1.2 OS=Homo sapiens GN=HIST1H1C PE=1 SV=2	2.440	0.000
P05186	13.1	13.1	24.05 Alkaline phosphatase, tissue-nonspecific isozyme OS=Homo sapiens GN=ALPL PE=1 SV=4	2.397	0.000
P38159	12.07	12.07	17.9 RNA-binding motif protein, X chromosome OS=Homo sapiens GN=RBMX PE=1 SV=3	2.335	0.012
P84103	6.43	8.5	28.66 Serine/arginine-rich splicing factor 3 OS=Homo sapiens GN=SRSF3 PE=1 SV=1	2.319	0.019
P84090	4.86	4.87	47.12 Enhancer of rudimentary homolog OS=Homo sapiens GN=ERH PE=1 SV=1	2.311	0.013
P61353	9.83	9.83	42.65 60S ribosomal protein L27 OS=Homo sapiens GN=RPL27 PE=1 SV=2	2.295	0.001
P62995	6.49	6.49	20.14 Transformer-2 protein homolog beta OS=Homo sapiens GN=TRA2B PE=1 SV=1	2.266	0.003
P62424	25.24	25.68	43.98 60S ribosomal protein L7a OS=Homo sapiens GN=RPL7A PE=1 SV=2	2.175	0.000
Q14980	59.37	59.45	22.84 Nuclear mitotic apparatus protein 1 OS=Homo sapiens GN=NUMA1 PE=1 SV=2	2.108	0.000
O75475	9.75	9.75	13.21 PC4 and SFRS1-interacting protein OS=Homo sapiens GN=PSIP1 PE=1 SV=1	2.102	0.002
P12956	33.71	33.89	37.27 X-ray repair cross-complementing protein 6 OS=Homo sapiens GN=XRCC6 PE=1 SV=2	2.094	0.000
Q722K6	6	7.48	6.748 Endoplasmic reticulum metallopeptidase 1 OS=Homo sapiens GN=ERMP1 PE=1 SV=2	2.049	0.002
P14618	79.19	79.19	69.87 Pyruvate kinase PKM OS=Homo sapiens GN=PKM PE=1 SV=4	2.049	0.000
P43403	21.2	21.35	27.79 Tyrosine-protein kinase ZAP-70 OS=Homo sapiens GN=ZAP70 PE=1 SV=1	2.043	0.000
Q15029	32.58	32.66	29.01 116 kDa U5 small nuclear ribonucleoprotein component OS=Homo sapiens GN=EFTUD2 PE=1 SV=1	2.012	0.000
Q71UI9	8.01	11.88	53.91 Histone H2A.V OS=Homo sapiens GN=H2AFV PE=1 SV=3	2.001	0.011
P18621	12.26	12.26	44.02 60S ribosomal protein L17 OS=Homo sapiens GN=RPL17 PE=1 SV=3	1.993	0.003
O75494	8	8	19.08 Serine/arginine-rich splicing factor 10 OS=Homo sapiens GN=SRSF10 PE=1 SV=1	1.992	0.001
P51398	11.67	11.67	25.63 28S ribosomal protein S29, mitochondrial OS=Homo sapiens GN=DAP3 PE=1 SV=1	1.991	0.023
O75531	4.08	4.13	40.45 Barrier-to-autointegration factor OS=Homo sapiens GN=BANF1 PE=1 SV=1	1.989	0.024
Q92665	8	8.05	15.19 28S ribosomal protein S31, mitochondrial OS=Homo sapiens GN=MRPS31 PE=1 SV=3	1.962	0.001
P62750	10.37	11.54	32.69 60S ribosomal protein L23a OS=Homo sapiens GN=RPL23A PE=1 SV=1	1.947	0.000
P82673	12.63	12.63	33.13 28S ribosomal protein S35, mitochondrial OS=Homo sapiens GN=MRPS35 PE=1 SV=1	1.910	0.001
Q02878	20.83	24.19	42.36 60S ribosomal protein L6 OS=Homo sapiens GN=RPL6 PE=1 SV=3	1.894	0.000
P13010	21.82	21.82	27.05 X-ray repair cross-complementing protein 5 OS=Homo sapiens GN=XRCC5 PE=1 SV=3	1.887	0.000
O95400	4	4	14.37 CD2 antigen cytoplasmic tail-binding protein 2 OS=Homo sapiens GN=CD2BP2 PE=1 SV=1	1.885	0.047
Q9NYF8	14.65	14.76	11.85 Bcl-2-associated transcription factor 1 OS=Homo sapiens GN=BCLAF1 PE=1 SV=2	1.866	0.000
Q8IYB3	5.28	5.28	8.739 Serine/arginine repetitive matrix protein 1 OS=Homo sapiens GN=SRRM1 PE=1 SV=2	1.860	0.015
P82933	8	8	15.91 28S ribosomal protein S9, mitochondrial OS=Homo sapiens GN=MRPS9 PE=1 SV=2	1.835	0.024
Q9H6F5	6.8	6.8	16.67 Coiled-coil domain-containing protein 86 OS=Homo sapiens GN=CCDC86 PE=1 SV=1	1.823	0.023
Q13724	13.15	13.15	16.61 Mannosyl-oligosaccharide glucosidase OS=Homo sapiens GN=MOGS PE=1 SV=5	1.817	0.000
Q9Y224	9.61	9.61	38.52 UPF0568 protein C14orf166 OS=Homo sapiens GN=C14orf166 PE=1 SV=1	1.816	0.003
Q13243	7.95	8.13	19.49 Serine/arginine-rich splicing factor 5 OS=Homo sapiens GN=SRSF5 PE=1 SV=1	1.782	0.042
Q9ULE6	12.01	12.01	11.1 Paladin OS=Homo sapiens GN=PALD1 PE=1 SV=3	1.775	0.003
P45973	4.37	4.37	21.47 Chromobox protein homolog 5 OS=Homo sapiens GN=CBX5 PE=1 SV=1	1.775	0.030
O95782	2.68	5.57	5.732 AP-2 complex subunit alpha-1 OS=Homo sapiens GN=AP2A1 PE=1 SV=3	1.770	0.006
P07910	12.14	12.14	19.61 Heterogeneous nuclear ribonucleoproteins C1/C2 OS=Homo sapiens GN=HNRNPC PE=1 SV=4	1.768	0.004
Q9Y2R9	6.75	6.75	21.9 28S ribosomal protein S7, mitochondrial OS=Homo sapiens GN=MRPS7 PE=1 SV=2	1.765	0.005
Q07065	21.23	21.38	24.58 Cytoskeleton-associated protein 4 OS=Homo sapiens GN=CKAP4 PE=1 SV=2	1.750	0.000
Q9HD33	3.55	3.55	8.8 39S ribosomal protein L47, mitochondrial OS=Homo sapiens GN=MRPL47 PE=1 SV=2	1.721	0.009
P61313	8.98	8.98	23.53 60S ribosomal protein L15 OS=Homo sapiens GN=RPL15 PE=1 SV=2	1.700	0.002
P14868	22.49	22.49	29.34 Aspartate--tRNA ligase, cytoplasmic OS=Homo sapiens GN=DARS PE=1 SV=2	1.674	0.000
P43243	23.62	24.29	21.96 Matrin-3 OS=Homo sapiens GN=MATR3 PE=1 SV=2	1.658	0.008
Q9Y3U8	10	10	35.24 60S ribosomal protein L36 OS=Homo sapiens GN=RPL36 PE=1 SV=3	1.652	0.007
Q9H307	9.47	9.47	11.3 Pinin OS=Homo sapiens GN=PNN PE=1 SV=4	1.647	0.001
P46782	11.88	11.88	32.35 40S ribosomal protein S5 OS=Homo sapiens GN=RPS5 PE=1 SV=4	1.639	0.026
Q9HCE1	7.63	7.63	7.079 Putative helicase MOV-10 OS=Homo sapiens GN=MOV10 PE=1 SV=2	1.637	0.032
Q07020	9.92	9.92	30.85 60S ribosomal protein L18 OS=Homo sapiens GN=RPL18 PE=1 SV=2	1.633	0.001
O60884	10.95	10.97	25.49 DnaJ homolog subfamily A member 2 OS=Homo sapiens GN=DNAJA2 PE=1 SV=1	1.626	0.007
Q9NUQ3	6.07	6.09	10.04 Gamma-taxilin OS=Homo sapiens GN=TXLNG PE=1 SV=2	1.616	0.008
P62241	6	6	19.71 40S ribosomal protein S8 OS=Homo sapiens GN=RPS8 PE=1 SV=2	1.608	0.026
P40222	7.34	7.39	16.85 Alpha-taxilin OS=Homo sapiens GN=TXLNA PE=1 SV=3	1.607	0.017
Q86VM9	6.03	6.05	7.45 Zinc finger CCCH domain-containing protein 18 OS=Homo sapiens GN=ZC3H18 PE=1 SV=2	1.605	0.048
P0CW22	12.29	12.48	52.59 40S ribosomal protein S17-like OS=Homo sapiens GN=RPS17L PE=1 SV=1	1.603	0.002
O76021	18.98	18.98	30.41 Ribosomal L1 domain-containing protein 1 OS=Homo sapiens GN=RSL1D1 PE=1 SV=3	1.598	0.000
P62826	12.55	12.55	35.65 GTP-binding nuclear protein Ran OS=Homo sapiens GN=RAN PE=1 SV=3	1.593	0.000
Q99848	7.42	7.42	22.22 Probable rRNA-processing protein EBP2 OS=Homo sapiens GN=EBNA1BP2 PE=1 SV=2	1.588	0.008
P50914	8.22	8.89	23.72 60S ribosomal protein L14 OS=Homo sapiens GN=RPL14 PE=1 SV=4	1.584	0.001
P25205	27.5	27.5	28.71 DNA replication licensing factor MCM3 OS=Homo sapiens GN=MCM3 PE=1 SV=3	1.571	0.000
P27816	23.17	23.32	18.66 Microtubule-associated protein 4 OS=Homo sapiens GN=MAP4 PE=1 SV=3	1.567	0.000
P39019	8.02	8.02	28.97 40S ribosomal protein S19 OS=Homo sapiens GN=RPS19 PE=1 SV=2	1.564	0.013
Q9Y5B9	23.07	23.29	18.91 FACT complex subunit SPT16 OS=Homo sapiens GN=SUPT16H PE=1 SV=1	1.561	0.000
O43143	34.22	34.72	28.55 Putative pre-mRNA-splicing factor ATP-dependent RNA helicase DHX15 OS=Homo sapiens GN=DHX15 PE=1 SV=2	1.549	0.000
P56192	23.13	23.14	24.33 Methionine--tRNA ligase, cytoplasmic OS=Homo sapiens GN=MARS PE=1 SV=2	1.539	0.005
P62277	14.15	14.15	38.41 40S ribosomal protein S13 OS=Homo sapiens GN=RPS13 PE=1 SV=2	1.534	0.001
P07814	41.94	42.1	22.16 Bifunctional glutamate/proline--tRNA ligase OS=Homo sapiens GN=EPRS PE=1 SV=5	1.532	0.000
P18124	16.63	16.63	29.44 60S ribosomal protein L7 OS=Homo sapiens GN=RPL7 PE=1 SV=1	1.526	0.000
P62753	10.24	11.8	22.89 40S ribosomal protein S6 OS=Homo sapiens GN=RPS6 PE=1 SV=1	1.519	0.001
P36578	36.43	36.8	40.28 60S ribosomal protein L4 OS=Homo sapiens GN=RPL4 PE=1 SV=5	1.504	0.000
P62917	7.28	7.28	33.07 60S ribosomal protein L8 OS=Homo sapiens GN=RPL8 PE=1 SV=2	1.497	0.003
Q96EY7	10.32	10.32	11.32 Pentatricopeptide repeat domain-containing protein 3, mitochondrial OS=Homo sapiens GN=PTCD3 PE=1 SV=3	1.497	0.013
P11388	14.19	14.19	10.65 DNA topoisomerase 2-alpha OS=Homo sapiens GN=TOP2A PE=1 SV=3	1.493	0.012
P09874	49.56	49.56	33.33 Poly [ADP-ribose] polymerase 1 OS=Homo sapiens GN=PARP1 PE=1 SV=4	1.492	0.000
Q14257	8.74	8.74	13.88 Reticulocalbin-2 OS=Homo sapiens GN=RCN2 PE=1 SV=1	1.487	0.013
A6NHR9	18.9	18.9	8.229 Structural maintenance of chromosomes flexible hinge domain-containing protein 1 OS=Homo sapiens GN=SMCHD1	1.485	0.001
Q86UP2	28.29	29.57	15.77 Kinectin OS=Homo sapiens GN=KTN1 PE=1 SV=1	1.480	0.000
P26358	21.95	22.04	11.01 DNA (cytosine-5)-methyltransferase 1 OS=Homo sapiens GN=DNMT1 PE=1 SV=2	1.479	0.001
Q9HCS7	2.76	2.8	2.339 Pre-mRNA-splicing factor SYF1 OS=Homo sapiens GN=XAB2 PE=1 SV=2	1.478	0.045
Q52LJ0	3.28	3.28	12.73 Protein FAM98B OS=Homo sapiens GN=FAM98B PE=1 SV=1	1.465	0.037
P61978	30.81	31.04	43.2 Heterogeneous nuclear ribonucleoprotein K OS=Homo sapiens GN=HNRNPK PE=1 SV=1	1.458	0.000
P49327	117.45	117.45	39.11 Fatty acid synthase OS=Homo sapiens GN=FASN PE=1 SV=3	1.452	0.000
P46783	10.78	10.86	29.09 40S ribosomal protein S10 OS=Homo sapiens GN=RPS10 PE=1 SV=1	1.446	0.001
P23396	16.88	16.88	48.97 40S ribosomal protein S3 OS=Homo sapiens GN=RPS3 PE=1 SV=2	1.441	0.001
P08238	34.19	34.19	29.97 Heat shock protein HSP 90-beta OS=Homo sapiens GN=HSP90AB1 PE=1 SV=4	1.440	0.002
Q08945	13.7	13.8	15.94 FACT complex subunit SSRP1 OS=Homo sapiens GN=SSRP1 PE=1 SV=1	1.432	0.001
Q14558	4.78	6.92	22.47 Phosphoribosyl pyrophosphate synthase-associated protein 1 OS=Homo sapiens GN=PRPSAP1 PE=1 SV=2	1.431	0.048
Q9NY12	6.43	6.44	21.66 H/ACA ribonucleoprotein complex subunit 1 OS=Homo sapiens GN=GAR1 PE=1 SV=1	1.429	0.013
P52272	43.74	43.74	42.74 Heterogeneous nuclear ribonucleoprotein M OS=Homo sapiens GN=HNRNPM PE=1 SV=3	1.428	0.000
P15880	23.36	23.36	36.52 40S ribosomal protein S2 OS=Homo sapiens GN=RPS2 PE=1 SV=2	1.426	0.000
Q8WU90	12.91	13.34	20.42 Zinc finger CCCH domain-containing protein 15 OS=Homo sapiens GN=ZC3H15 PE=1 SV=1	1.421	0.000
Q9Y3Z3	6.78	6.78	10.22 Deoxynucleoside triphosphate triphosphohydrolase SAMHD1 OS=Homo sapiens GN=SAMHD1 PE=1 SV=2	1.420	0.046

253

Q13268	8.09	8.15	27.14 Dehydrogenase/reductase SDR family member 2, mitochondrial OS=Homo sapiens GN=DHRS2 PE=1 SV=4	1.415	0.008
P48634	14.16	14.16	7.14 Protein PRRC2A OS=Homo sapiens GN=PRRC2A PE=1 SV=3	1.413	0.001
P61163	7.47	7.47	20.48 Alpha-centractin OS=Homo sapiens GN=ACTR1A PE=1 SV=1	1.409	0.005
Q9Y520	9.6	9.6	5.214 Protein PRRC2C OS=Homo sapiens GN=PRRC2C PE=1 SV=4	1.409	0.017
P41250	9.91	9.91	13.4 Glycine--tRNA ligase OS=Homo sapiens GN=GARS PE=1 SV=3	1.409	0.023
P46781	10.86	10.91	24.23 40S ribosomal protein S9 OS=Homo sapiens GN=RPS9 PE=1 SV=3	1.408	0.001
Q9NXF1	12	12.89	10.12 Testis-expressed sequence 10 protein OS=Homo sapiens GN=TEX10 PE=1 SV=2	1.407	0.002
P06733	29.98	29.98	46.77 Alpha-enolase OS=Homo sapiens GN=ENO1 PE=1 SV=2	1.406	0.021
P05387	22.58	22.58	92.17 60S acidic ribosomal protein P2 OS=Homo sapiens GN=RPLP2 PE=1 SV=1	1.405	0.003
Q92922	12.9	13.11	10.77 SWI/SNF complex subunit SMARCC1 OS=Homo sapiens GN=SMARCC1 PE=1 SV=3	1.395	0.003
P40939	27.29	27.29	33.55 Trifunctional enzyme subunit alpha, mitochondrial OS=Homo sapiens GN=HADHA PE=1 SV=2	1.387	0.001
Q92499	23.89	23.89	26.08 ATP-dependent RNA helicase DDX1 OS=Homo sapiens GN=DDX1 PE=1 SV=2	1.373	0.000
P33992	12.44	14.53	15.53 DNA replication licensing factor MCM5 OS=Homo sapiens GN=MCM5 PE=1 SV=5	1.372	0.000
P49207	5.92	5.92	20.51 60S ribosomal protein L34 OS=Homo sapiens GN=RPL34 PE=1 SV=3	1.372	0.022
P62249	13.38	13.38	38.36 40S ribosomal protein S16 OS=Homo sapiens GN=RPS16 PE=1 SV=2	1.371	0.000
P06748	15.94	17.65	43.88 Nucleophosmin OS=Homo sapiens GN=NPM1 PE=1 SV=2	1.370	0.046
Q92616	75.38	75.38	24.49 Translational activator GCN1 OS=Homo sapiens GN=GCN1L1 PE=1 SV=6	1.369	0.000
P49790	9.43	9.89	8.542 Nuclear pore complex protein Nup153 OS=Homo sapiens GN=NUP153 PE=1 SV=2	1.360	0.032
Q15393	10.58	10.58	10.27 Splicing factor 3B subunit 3 OS=Homo sapiens GN=SF3B3 PE=1 SV=4	1.358	0.040
Q96AG4	21.97	21.97	47.56 Leucine-rich repeat-containing protein 59 OS=Homo sapiens GN=LRRC59 PE=1 SV=1	1.356	0.000
Q08J23	21.17	21.17	24.9 tRNA (cytosine(34)-C(5))-methyltransferase OS=Homo sapiens GN=NSUN2 PE=1 SV=2	1.352	0.003
P62854	4.77	4.77	33.91 40S ribosomal protein S26 OS=Homo sapiens GN=RPS26 PE=1 SV=3	1.352	0.044
O60488	10.18	10.26	16.88 Long-chain-fatty-acid--CoA ligase 4 OS=Homo sapiens GN=ACSL4 PE=1 SV=2	1.349	0.002
Q9UKV3	9.15	9.26	6.339 Apoptotic chromatin condensation inducer in the nucleus OS=Homo sapiens GN=ACIN1 PE=1 SV=2	1.347	0.015
Q14676	24.12	24.12	15.27 Mediator of DNA damage checkpoint protein 1 OS=Homo sapiens GN=MDC1 PE=1 SV=3	1.345	0.038
O60566	7.1	9.32	8.286 Mitotic checkpoint serine/threonine-protein kinase BUB1 beta OS=Homo sapiens GN=BUB1B PE=1 SV=3	1.339	0.038
Q9P2J5	24.29	24.45	16.5 Leucine--tRNA ligase, cytoplasmic OS=Homo sapiens GN=LARS PE=1 SV=2	1.334	0.000
Q12904	15.44	15.44	53.85 Aminoacyl tRNA synthase complex-interacting multifunctional protein 1 OS=Homo sapiens GN=AIMP1 PE=1 SV=2	1.328	0.007
P25705	28.25	28.25	38.7 ATP synthase subunit alpha, mitochondrial OS=Homo sapiens GN=ATP5A1 PE=1 SV=1	1.328	0.000
Q14566	15.89	15.9	13.89 DNA replication licensing factor MCM6 OS=Homo sapiens GN=MCM6 PE=1 SV=1	1.327	0.001
Q92841	21.13	33.42	29.08 Probable ATP-dependent RNA helicase DDX17 OS=Homo sapiens GN=DDX17 PE=1 SV=2	1.322	0.014
Q15084	13.08	13.08	32.5 Protein disulfide-isomerase A6 OS=Homo sapiens GN=PDIA6 PE=1 SV=1	1.320	0.005
P61254	5.7	5.7	16.55 60S ribosomal protein L26 OS=Homo sapiens GN=RPL26 PE=1 SV=1	1.319	0.018
Q02543	7.95	7.95	26.7 60S ribosomal protein L18a OS=Homo sapiens GN=RPL18A PE=1 SV=2	1.308	0.003
Q9BXJ9	10.08	10.08	9.815 N-alpha-acetyltransferase 15, NatA auxiliary subunit OS=Homo sapiens GN=NAA15 PE=1 SV=1	1.307	0.022
Q9Y3I0	19.89	21.77	31.09 tRNA-splicing ligase RtcB homolog OS=Homo sapiens GN=RTCB PE=1 SV=1	1.295	0.008
P61247	21.64	21.64	44.32 40S ribosomal protein S3a OS=Homo sapiens GN=RPS3A PE=1 SV=2	1.281	0.000
Q7L2E3	15.61	16.59	11.47 Putative ATP-dependent RNA helicase DHX30 OS=Homo sapiens GN=DHX30 PE=1 SV=1	1.280	0.011
P35249	12.01	12.01	30.03 Replication factor C subunit 4 OS=Homo sapiens GN=RFC4 PE=1 SV=2	1.278	0.046
Q00839	38.09	38.13	24.73 Heterogeneous nuclear ribonucleoprotein U OS=Homo sapiens GN=HNRNPU PE=1 SV=6	1.277	0.002
Q92896	19.41	19.73	13.66 Golgi apparatus protein 1 OS=Homo sapiens GN=GLG1 PE=1 SV=2	1.271	0.006
P55084	10.74	10.74	20.68 Trifunctional enzyme subunit beta, mitochondrial OS=Homo sapiens GN=HADHB PE=1 SV=3	1.268	0.007
P14866	20.46	20.46	29.37 Heterogeneous nuclear ribonucleoprotein L OS=Homo sapiens GN=HNRNPL PE=1 SV=2	1.267	0.040
Q14683	8.65	8.69	6.488 Structural maintenance of chromosomes protein 1A OS=Homo sapiens GN=SMC1A PE=1 SV=2	1.266	0.042
Q04837	6.47	6.47	38.51 Single-stranded DNA-binding protein, mitochondrial OS=Homo sapiens GN=SSBP1 PE=1 SV=1	1.256	0.046
Q6P2Q9	51.43	51.74	17.39 Pre-mRNA-processing-splicing factor 8 OS=Homo sapiens GN=PRPF8 PE=1 SV=2	1.245	0.000
P02545	23.98	23.98	23.19 Prelamin-A/C OS=Homo sapiens GN=LMNA PE=1 SV=1	1.245	0.015
P41252	32.15	32.82	19.02 Isoleucine--tRNA ligase, cytoplasmic OS=Homo sapiens GN=IARS PE=1 SV=2	1.240	0.001
Q13155	10.08	10.12	33.44 Aminoacyl tRNA synthase complex-interacting multifunctional protein 2 OS=Homo sapiens GN=AIMP2 PE=1 SV=2	1.239	0.032
O60716	21.81	22.01	20.56 Catenin delta-1 OS=Homo sapiens GN=CTNND1 PE=1 SV=1	1.238	0.010
P20042	20.61	20.62	41.74 Eukaryotic translation initiation factor 2 subunit 2 OS=Homo sapiens GN=EIF2S2 PE=1 SV=2	1.236	0.017
P33991	28.08	28.14	26.42 DNA replication licensing factor MCM4 OS=Homo sapiens GN=MCM4 PE=1 SV=5	1.235	0.014
P41091	14.68	14.73	39.19 Eukaryotic translation initiation factor 2 subunit 3 OS=Homo sapiens GN=EIF2S3 PE=1 SV=3	1.231	0.038
P05198	12.85	12.85	35.24 Eukaryotic translation initiation factor 2 subunit 1 OS=Homo sapiens GN=EIF2S1 PE=1 SV=3	1.227	0.023
Q93009	14.07	14.16	10.44 Ubiquitin carboxyl-terminal hydrolase 7 OS=Homo sapiens GN=USP7 PE=1 SV=2	1.216	0.015
P54136	28.1	28.11	27.12 Arginine--tRNA ligase, cytoplasmic OS=Homo sapiens GN=RARS PE=1 SV=2	1.213	0.022
P15924	35.73	36.09	11.18 Desmoplakin OS=Homo sapiens GN=DSP PE=1 SV=3	1.209	0.004
Q9Y490	24.73	24.73	13.73 Talin-1 OS=Homo sapiens GN=TLN1 PE=1 SV=3	1.208	0.000
P46821	26.53	26.57	9.562 Microtubule-associated protein 1B OS=Homo sapiens GN=MAP1B PE=1 SV=2	0.832	0.038
P49748	14.26	14.26	22.6 Very long-chain specific acyl-CoA dehydrogenase, mitochondrial OS=Homo sapiens GN=ACADVL PE=1 SV=1	0.827	0.027
Q16795	12.06	12.06	24.14 NADH dehydrogenase [ubiquinone] 1 alpha subcomplex subunit 9, mitochondrial OS=Homo sapiens GN=NDUFA9 PE=	0.823	0.018
O43795	11.63	11.75	7.658 Unconventional myosin-Ib OS=Homo sapiens GN=MYO1B PE=1 SV=3	0.823	0.018
Q9NU22	12.87	13.02	2.305 Midasin OS=Homo sapiens GN=MDN1 PE=1 SV=2	0.820	0.006
Q9H0A0	16.76	16.81	14.44 N-acetyltransferase 10 OS=Homo sapiens GN=NAT10 PE=1 SV=2	0.820	0.036
O75691	14.75	14.95	4.345 Small subunit processome component 20 homolog OS=Homo sapiens GN=UTP20 PE=1 SV=3	0.817	0.009
P54920	10.3	10.3	25.08 Alpha-soluble NSF attachment protein OS=Homo sapiens GN=NAPA PE=1 SV=3	0.817	0.029
P48960	18.72	18.72	17.49 CD97 antigen OS=Homo sapiens GN=CD97 PE=1 SV=4	0.816	0.001
O00299	11.18	11.18	34.85 Chloride intracellular channel protein 1 OS=Homo sapiens GN=CLIC1 PE=1 SV=4	0.811	0.016
Q9Y3T9	5.81	5.87	6.409 Nucleolar complex protein 2 homolog OS=Homo sapiens GN=NOC2L PE=1 SV=4	0.810	0.026
Q8N163	12.59	12.59	18.42 DBIRD complex subunit KIAA1967 OS=Homo sapiens GN=KIAA1967 PE=1 SV=2	0.810	0.025
P05141	25.64	26.21	41.61 ADP/ATP translocase 2 OS=Homo sapiens GN=SLC25A5 PE=1 SV=7	0.810	0.037
Q9BVP2	9.92	10.15	16.58 Guanine nucleotide-binding protein-like 3 OS=Homo sapiens GN=GNL3 PE=1 SV=2	0.809	0.025
P30101	13.34	13.34	20.4 Protein disulfide-isomerase A3 OS=Homo sapiens GN=PDIA3 PE=1 SV=4	0.808	0.001
P08195	48.5	49.33	49.21 4F2 cell-surface antigen heavy chain OS=Homo sapiens GN=SLC3A2 PE=1 SV=3	0.801	0.001
O14980	25.36	25.43	18.58 Exportin-1 OS=Homo sapiens GN=XPO1 PE=1 SV=1	0.799	0.002
P49755	14	14.28	34.25 Transmembrane emp24 domain-containing protein 10 OS=Homo sapiens GN=TMED10 PE=1 SV=2	0.798	0.040
Q5JTH9	17.42	17.42	11.1 RRP12-like protein OS=Homo sapiens GN=RRP12 PE=1 SV=2	0.793	0.001
P05556	16.57	16.63	15.04 Integrin beta-1 OS=Homo sapiens GN=ITGB1 PE=1 SV=2	0.792	0.004
Q08AM6	6.05	7.71	6.266 Protein VAC14 homolog OS=Homo sapiens GN=VAC14 PE=1 SV=1	0.789	0.032
P42704	45	45.15	25.32 Leucine-rich PPR motif-containing protein, mitochondrial OS=Homo sapiens GN=LRPPRC PE=1 SV=3	0.785	0.000
P00387	5.13	5.13	19.93 NADH-cytochrome b5 reductase 3 OS=Homo sapiens GN=CYB5R3 PE=1 SV=3	0.781	0.047
Q9UDY2	6.06	6.06	5.21 Tight junction protein ZO-2 OS=Homo sapiens GN=TJP2 PE=1 SV=2	0.777	0.039
Q9BQG0	33.01	33.01	20.11 Myb-binding protein 1A OS=Homo sapiens GN=MYBBP1A PE=1 SV=2	0.773	0.000
P37268	6.63	6.66	11.03 Squalene synthase OS=Homo sapiens GN=FDFT1 PE=1 SV=1	0.773	0.042
P50990	22.04	22.05	24.64 T-complex protein 1 subunit theta OS=Homo sapiens GN=CCT8 PE=1 SV=4	0.764	0.000
Q9H3N1	6.49	6.49	16.43 Thioredoxin-related transmembrane protein 1 OS=Homo sapiens GN=TMX1 PE=1 SV=1	0.764	0.010
Q5RI15	4.1	4.1	22.03 Cytochrome c oxidase protein 20 homolog OS=Homo sapiens GN=COX20 PE=1 SV=2	0.757	0.041
Q5JWF2	14.95	14.96	10.32 Guanine nucleotide-binding protein G(s) subunit alpha isoforms XLas OS=Homo sapiens GN=GNAS PE=1 SV=2	0.756	0.002
P26641	9.38	9.38	18.99 Elongation factor 1-gamma OS=Homo sapiens GN=EEF1G PE=1 SV=3	0.755	0.011
P78371	39.15	39.15	50.09 T-complex protein 1 subunit beta OS=Homo sapiens GN=CCT2 PE=1 SV=4	0.754	0.000
P12268	53.65	53.65	58.95 Inosine-5'-monophosphate dehydrogenase 2 OS=Homo sapiens GN=IMPDH2 PE=1 SV=2	0.751	0.000

254

Q13823	1.81	1.81	1.778 Nucleolar GTP-binding protein 2 OS=Homo sapiens GN=GNL2 PE=1 SV=1	0.750	0.038
P01116	4.25	6.5	27.51 GTPase KRas OS=Homo sapiens GN=KRAS PE=1 SV=1	0.747	0.046
P55010	8.16	8.17	12.06 Eukaryotic translation initiation factor 5 OS=Homo sapiens GN=EIF5 PE=1 SV=2	0.744	0.016
Q12906	18.28	18.4	15.21 Interleukin enhancer-binding factor 3 OS=Homo sapiens GN=ILF3 PE=1 SV=3	0.738	0.001
Q99805	13.72	13.72	14.48 Transmembrane 9 superfamily member 2 OS=Homo sapiens GN=TM9SF2 PE=1 SV=1	0.737	0.008
P28288	12.06	12.14	13.96 ATP-binding cassette sub-family D member 3 OS=Homo sapiens GN=ABCD3 PE=1 SV=1	0.733	0.007
Q9BSJ8	38.11	38.11	29.62 Extended synaptotagmin-1 OS=Homo sapiens GN=ESYT1 PE=1 SV=1	0.733	0.000
P02786	44.49	44.49	38.82 Transferrin receptor protein 1 OS=Homo sapiens GN=TFRC PE=1 SV=2	0.733	0.000
O95573	6.94	9.68	13.75 Long-chain-fatty-acid--CoA ligase 3 OS=Homo sapiens GN=ACSL3 PE=1 SV=3	0.726	0.012
Q15392	5.78	5.81	8.915 Delta(24)-sterol reductase OS=Homo sapiens GN=DHCR24 PE=1 SV=2	0.723	0.012
P05787	38.55	40.45	54.24 Keratin, type II cytoskeletal 8 OS=Homo sapiens GN=KRT8 PE=1 SV=7	0.722	0.000
Q13283	16.43	16.43	28.76 Ras GTPase-activating protein-binding protein 1 OS=Homo sapiens GN=G3BP1 PE=1 SV=1	0.722	0.008
Q8TEM1	10.48	10.67	5.352 Nuclear pore membrane glycoprotein 210 OS=Homo sapiens GN=NUP210 PE=1 SV=3	0.720	0.003
P22234	10.35	10.35	18.82 Multifunctional protein ADE2 OS=Homo sapiens GN=PAICS PE=1 SV=3	0.715	0.000
P53985	11.42	11.42	15.8 Monocarboxylate transporter 1 OS=Homo sapiens GN=SLC16A1 PE=1 SV=3	0.714	0.020
Q9H9B4	13.66	13.66	39.44 Sideroflexin-1 OS=Homo sapiens GN=SFXN1 PE=1 SV=4	0.711	0.017
O96000	4	4	16.86 NADH dehydrogenase [ubiquinone] 1 beta subcomplex subunit 10 OS=Homo sapiens GN=NDUFB10 PE=1 SV=3	0.711	0.031
P50454	22.86	22.86	44.26 Serpin H1 OS=Homo sapiens GN=SERPINH1 PE=1 SV=2	0.709	0.000
P46063	14.63	14.63	17.72 ATP-dependent DNA helicase Q1 OS=Homo sapiens GN=RECQL PE=1 SV=3	0.708	0.001
Q10471	9.93	9.93	16.46 Polypeptide N-acetylgalactosaminyltransferase 2 OS=Homo sapiens GN=GALNT2 PE=1 SV=1	0.708	0.004
Q00325	7.59	7.67	9.945 Phosphate carrier protein, mitochondrial OS=Homo sapiens GN=SLC25A3 PE=1 SV=2	0.705	0.006
O43707	12.92	23.52	17.34 Alpha-actinin-4 OS=Homo sapiens GN=ACTN4 PE=1 SV=2	0.704	0.015
Q13308	8.47	8.47	11.87 Inactive tyrosine-protein kinase 7 OS=Homo sapiens GN=PTK7 PE=1 SV=2	0.703	0.024
Q9UQ80	21.79	21.79	36.29 Proliferation-associated protein 2G4 OS=Homo sapiens GN=PA2G4 PE=1 SV=3	0.703	0.000
Q16891	18.47	18.52	22.82 Mitochondrial inner membrane protein OS=Homo sapiens GN=IMMT PE=1 SV=1	0.695	0.002
P04843	30.38	30.38	38.88 Dolichyl-diphosphooligosaccharide--protein glycosyltransferase subunit 1 OS=Homo sapiens GN=RPN1 PE=1 SV=1	0.687	0.000
P30519	12	12	33.86 Heme oxygenase 2 OS=Homo sapiens GN=HMOX2 PE=1 SV=2	0.686	0.001
Q14344	2.52	5.12	11.94 Guanine nucleotide-binding protein subunit alpha-13 OS=Homo sapiens GN=GNA13 PE=1 SV=2	0.686	0.019
P51148	6.35	6.35	26.39 Ras-related protein Rab-5C OS=Homo sapiens GN=RAB5C PE=1 SV=2	0.681	0.046
O15173	6.17	7.66	27.35 Membrane-associated progesterone receptor component 2 OS=Homo sapiens GN=PGRMC2 PE=1 SV=1	0.675	0.008
Q9UBD5	4.79	4.84	5.907 Origin recognition complex subunit 3 OS=Homo sapiens GN=ORC3 PE=1 SV=1	0.675	0.011
P23526	9.75	9.77	13.89 Adenosylhomocysteinase OS=Homo sapiens GN=AHCY PE=1 SV=4	0.674	0.002
P50895	5.31	5.32	11.46 Basal cell adhesion molecule OS=Homo sapiens GN=BCAM PE=1 SV=2	0.672	0.027
P62937	16.42	17.72	72.12 Peptidyl-prolyl cis-trans isomerase A OS=Homo sapiens GN=PPIA PE=1 SV=2	0.671	0.042
Q07021	14.05	14.05	42.91 Complement component 1 Q subcomponent-binding protein, mitochondrial OS=Homo sapiens GN=C1QBP PE=1 SV=1	0.670	0.004
P45880	18.07	20.39	43.54 Voltage-dependent anion-selective channel protein 2 OS=Homo sapiens GN=VDAC2 PE=1 SV=2	0.667	0.000
P10606	9.28	9.28	38.76 Cytochrome c oxidase subunit 5B, mitochondrial OS=Homo sapiens GN=COX5B PE=1 SV=2	0.666	0.030
P30154	5.77	12.46	16.97 Serine/threonine-protein phosphatase 2A 65 kDa regulatory subunit A beta isoform OS=Homo sapiens GN=PPP2R1B PE=1 SV=2	0.664	0.016
P27824	22.01	22.01	16.72 Calnexin OS=Homo sapiens GN=CANX PE=1 SV=2	0.661	0.000
P78347	11.43	11.45	14.83 General transcription factor II-I OS=Homo sapiens GN=GTF2I PE=1 SV=2	0.659	0.001
P63241	5.25	5.25	31.17 Eukaryotic translation initiation factor 5A-1 OS=Homo sapiens GN=EIF5A PE=1 SV=2	0.658	0.034
Q92692	6.75	6.75	18.77 Poliovirus receptor-related protein 2 OS=Homo sapiens GN=PVRL2 PE=1 SV=1	0.654	0.028
Q9UJZ1	16.67	16.82	41.01 Stomatin-like protein 2, mitochondrial OS=Homo sapiens GN=STOML2 PE=1 SV=1	0.650	0.004
P05783	35.95	35.95	54.65 Keratin, type I cytoskeletal 18 OS=Homo sapiens GN=KRT18 PE=1 SV=2	0.650	0.000
P01130	9.62	9.67	9.651 Low-density lipoprotein receptor OS=Homo sapiens GN=LDLR PE=1 SV=1	0.646	0.023
O96008	13.25	13.34	34.35 Mitochondrial import receptor subunit TOM40 homolog OS=Homo sapiens GN=TOMM40 PE=1 SV=1	0.641	0.000
Q12905	12.13	12.13	38.72 Interleukin enhancer-binding factor 2 OS=Homo sapiens GN=ILF2 PE=1 SV=2	0.639	0.004
P16615	14.88	14.88	12.76 Sarcoplasmic/endoplasmic reticulum calcium ATPase 2 OS=Homo sapiens GN=ATP2A2 PE=1 SV=1	0.635	0.000
Q9NYL4	8	8	47.26 Peptidyl-prolyl cis-trans isomerase FKBP11 OS=Homo sapiens GN=FKBP11 PE=1 SV=1	0.634	0.043
O00116	14.07	14.07	20.36 Alkyldihydroxyacetonephosphate synthase, peroxisomal OS=Homo sapiens GN=AGPS PE=1 SV=1	0.633	0.000
P51149	24.75	24.75	52.66 Ras-related protein Rab-7a OS=Homo sapiens GN=RAB7A PE=1 SV=1	0.633	0.000
O75396	8.15	8.15	29.77 Vesicle-trafficking protein SEC22b OS=Homo sapiens GN=SEC22B PE=1 SV=4	0.632	0.020
Q86W92	11.13	11.17	10.19 Liprin-beta-1 OS=Homo sapiens GN=PPFIBP1 PE=1 SV=2	0.631	0.000
Q15758	16.94	16.94	29.39 Neutral amino acid transporter B(0) OS=Homo sapiens GN=SLC1A5 PE=1 SV=2	0.630	0.008
Q13641	6.09	6.14	10.48 Trophoblast glycoprotein OS=Homo sapiens GN=TPBG PE=1 SV=1	0.630	0.033
P35613	14.9	14.9	36.88 Basigin OS=Homo sapiens GN=BSG PE=1 SV=2	0.622	0.000
Q32MZ4	4.1	4.1	5.693 Leucine-rich repeat flightless-interacting protein 1 OS=Homo sapiens GN=LRRFIP1 PE=1 SV=2	0.620	0.018
O43776	15.36	15.36	20.07 Asparagine--tRNA ligase, cytoplasmic OS=Homo sapiens GN=NARS PE=1 SV=1	0.615	0.002
Q8NCG7	1.52	1.57	2.679 Sn1-specific diacylglycerol lipase beta OS=Homo sapiens GN=DAGLB PE=1 SV=3	0.613	0.033
Q9Y6M9	4.19	4.19	24.58 NADH dehydrogenase [ubiquinone] 1 beta subcomplex subunit 9 OS=Homo sapiens GN=NDUFB9 PE=1 SV=3	0.611	0.020
P29317	15.93	15.93	11.99 Ephrin type-A receptor 2 OS=Homo sapiens GN=EPHA2 PE=1 SV=2	0.608	0.000
Q12907	14.48	14.56	33.71 Vesicular integral-membrane protein VIP36 OS=Homo sapiens GN=LMAN2 PE=1 SV=1	0.605	0.000
Q9Y4W6	14.32	14.39	16.06 AFG3-like protein 2 OS=Homo sapiens GN=AFG3L2 PE=1 SV=2	0.602	0.000
P13073	7.34	7.34	25.44 Cytochrome c oxidase subunit 4 isoform 1, mitochondrial OS=Homo sapiens GN=COX4I1 PE=1 SV=1	0.602	0.008
Q9UGP8	9.02	9.05	10.13 Translocation protein SEC63 homolog OS=Homo sapiens GN=SEC63 PE=1 SV=2	0.601	0.000
P09669	8	8	48 Cytochrome c oxidase subunit 6C OS=Homo sapiens GN=COX6C PE=1 SV=2	0.593	0.037
P37108	5.57	5.57	27.21 Signal recognition particle 14 kDa protein OS=Homo sapiens GN=SRP14 PE=1 SV=2	0.590	0.047
Q9NVI7	6	10	13.56 ATPase family AAA domain-containing protein 3A OS=Homo sapiens GN=ATAD3A PE=1 SV=2	0.585	0.014
O75844	6.04	6.08	10.95 CAAX prenyl protease 1 homolog OS=Homo sapiens GN=ZMPSTE24 PE=1 SV=2	0.579	0.008
P13645	8.46	10.92	15.24 Keratin, type I cytoskeletal 10 OS=Homo sapiens GN=KRT10 PE=1 SV=6	0.578	0.000
P04844	22.61	22.61	29.32 Dolichyl-diphosphooligosaccharide--protein glycosyltransferase subunit 2 OS=Homo sapiens GN=RPN2 PE=1 SV=3	0.575	0.000
Q99623	9.43	9.43	21.74 Prohibitin-2 OS=Homo sapiens GN=PHB2 PE=1 SV=2	0.571	0.005
Q9C004	5.31	5.31	19.4 Protein sprouty homolog 4 OS=Homo sapiens GN=SPRY4 PE=1 SV=2	0.566	0.010
Q9HDC9	15.07	15.07	27.4 Adipocyte plasma membrane-associated protein OS=Homo sapiens GN=APMAP PE=1 SV=2	0.563	0.000
O60506	32.06	32.06	37.88 Heterogeneous nuclear ribonucleoprotein Q OS=Homo sapiens GN=SYNCRIP PE=1 SV=2	0.561	0.000
Q9Y4L1	10.74	10.86	14.61 Hypoxia up-regulated protein 1 OS=Homo sapiens GN=HYOU1 PE=1 SV=1	0.561	0.019
Q9BRR6	4	4	7.243 ADP-dependent glucokinase OS=Homo sapiens GN=ADPGK PE=1 SV=1	0.556	0.012
Q96CS3	6.68	6.73	16.85 FAS-associated factor 2 OS=Homo sapiens GN=FAF2 PE=1 SV=2	0.555	0.021
O14828	9.23	9.23	25.94 Secretory carrier-associated membrane protein 3 OS=Homo sapiens GN=SCAMP3 PE=1 SV=3	0.547	0.039
O43169	8.44	8.51	52.05 Cytochrome b5 type B OS=Homo sapiens GN=CYB5B PE=1 SV=2	0.547	0.010
Q9Y320	2.77	2.78	8.446 Thioredoxin-related transmembrane protein 2 OS=Homo sapiens GN=TMX2 PE=1 SV=1	0.545	0.014
P35052	12.05	12.05	17.74 Glypican-1 OS=Homo sapiens GN=GPC1 PE=1 SV=2	0.545	0.011
P51572	12.06	12.06	26.02 B-cell receptor-associated protein 31 OS=Homo sapiens GN=BCAP31 PE=1 SV=3	0.539	0.000
O94832	32.77	32.98	27.73 Unconventional myosin-Id OS=Homo sapiens GN=MYO1D PE=1 SV=2	0.538	0.000
Q16850	16.22	16.22	22.86 Lanosterol 14-alpha demethylase OS=Homo sapiens GN=CYP51A1 PE=1 SV=3	0.537	0.000
P05362	4.84	4.84	6.391 Intercellular adhesion molecule 1 OS=Homo sapiens GN=ICAM1 PE=1 SV=2	0.534	0.013
Q9Y3E0	4	4	10.87 Vesicle transport protein GOT1B OS=Homo sapiens GN=GOLT1B PE=1 SV=1	0.531	0.037
Q00577	4	4.1	16.15 Transcriptional activator protein Pur-alpha OS=Homo sapiens GN=PURA PE=1 SV=2	0.526	0.029
P11233	12	12.04	41.75 Ras-related protein Ral-A OS=Homo sapiens GN=RALA PE=1 SV=1	0.525	0.017
Q9Y6M7	2.3	2.3	3.377 Sodium bicarbonate cotransporter 3 OS=Homo sapiens GN=SLC4A7 PE=1 SV=2	0.513	0.037
P30447	8.49	8.49	22.47 HLA class I histocompatibility antigen, A-23 alpha chain OS=Homo sapiens GN=HLA-A PE=1 SV=1	0.501	0.015

255

P00167	4.33	4.33	25.37 Cytochrome b5 OS=Homo sapiens GN=CYB5A PE=1 SV=2	0.494	0.004
P07900	3.52	12.6	14.34 Heat shock protein HSP 90-alpha OS=Homo sapiens GN=HSP90AA1 PE=1 SV=5	0.490	0.011
Q9UJS0	24.42	24.55	30.22 Calcium-binding mitochondrial carrier protein Aralar2 OS=Homo sapiens GN=SLC25A13 PE=1 SV=2	0.486	0.000
Q09666	37.69	37.71	13.68 Neuroblast differentiation-associated protein AHNAK OS=Homo sapiens GN=AHNAK PE=1 SV=2	0.486	0.000
P17931	8.49	8.49	24 Galectin-3 OS=Homo sapiens GN=LGALS3 PE=1 SV=5	0.481	0.000
P35232	20.42	20.42	56.25 Prohibitin OS=Homo sapiens GN=PHB PE=1 SV=1	0.481	0.000
P16435	12.08	12.08	18.17 NADPH--cytochrome P450 reductase OS=Homo sapiens GN=POR PE=1 SV=2	0.480	0.000
P35527	12.44	12.49	20.22 Keratin, type I cytoskeletal 9 OS=Homo sapiens GN=KRT9 PE=1 SV=3	0.468	0.004
P12081	5.57	5.57	9.234 Histidine--tRNA ligase, cytoplasmic OS=Homo sapiens GN=HARS PE=1 SV=2	0.454	0.012
P23229	14.19	14.22	10.97 Integrin alpha-6 OS=Homo sapiens GN=ITGA6 PE=1 SV=5	0.449	0.000
P21796	24.25	24.25	61.13 Voltage-dependent anion-selective channel protein 1 OS=Homo sapiens GN=VDAC1 PE=1 SV=2	0.439	0.000
P20645	10.27	10.79	25.27 Cation-dependent mannose-6-phosphate receptor OS=Homo sapiens GN=M6PR PE=1 SV=1	0.423	0.000
P13647	4.5	6.72	6.949 Keratin, type II cytoskeletal 5 OS=Homo sapiens GN=KRT5 PE=1 SV=3	0.417	0.049
P49257	14	14	26.27 Protein ERGIC-53 OS=Homo sapiens GN=LMAN1 PE=1 SV=2	0.414	0.001
Q15836	8	8	41 Vesicle-associated membrane protein 3 OS=Homo sapiens GN=VAMP3 PE=1 SV=3	0.403	0.011
Q8TCT9	4	4	9.019 Minor histocompatibility antigen H13 OS=Homo sapiens GN=HM13 PE=1 SV=1	0.386	0.027
P07355	8.6	8.65	19.47 Annexin A2 OS=Homo sapiens GN=ANXA2 PE=1 SV=2	0.386	0.001
P05455	6.17	6.23	9.559 Lupus La protein OS=Homo sapiens GN=SSB PE=1 SV=2	0.379	0.002
P19338	33.5	33.5	26.2 Nucleolin OS=Homo sapiens GN=NCL PE=1 SV=3	0.370	0.000
P04264	14.77	18.88	12.89 Keratin, type II cytoskeletal 1 OS=Homo sapiens GN=KRT1 PE=1 SV=6	0.359	0.000
P15311	7.48	7.51	11.26 Ezrin OS=Homo sapiens GN=EZR PE=1 SV=4	0.342	0.002
P35908	13.45	20.41	22.69 Keratin, type II cytoskeletal 2 epidermal OS=Homo sapiens GN=KRT2 PE=1 SV=2	0.290	0.033
P43121	7.11	7.11	11.61 Cell surface glycoprotein MUC18 OS=Homo sapiens GN=MCAM PE=1 SV=2	0.244	0.006
P11169	22.06	22.06	11.69 Solute carrier family 2, facilitated glucose transporter member 3 OS=Homo sapiens GN=SLC2A3 PE=1 SV=1	0.161	0.000
Q9BTV4	15.34	15.34	29.5 Transmembrane protein 43 OS=Homo sapiens GN=TMEM43 PE=1 SV=1	0.149	0.000

256

257

258

259 **Supplementary Table 4:** Complete list of proteins identified within the HT29
260 comparisons§

			A: Comparison of untreated HT29 Mock/untreated HT29 β6AS		
Uniprot	Unused	Total	X.Cov.95. Protein Name; Organism; Gene name	iTRAQ Fold Change	StouffersPval
sp|P06703	6.99	7.12	30	Protein S100-A6 OS=Homo sapiens GN=S100A6 PE=1 SV=1	3.421	0.047
sp|P35900	11.54	13.58	20.99	Keratin, type I cytoskeletal 20 OS=Homo sapiens GN=KRT20 PE=1 SV=1	2.387	0.000
sp|O95994	6.62	6.62	16.57	Anterior gradient protein 2 homolog OS=Homo sapiens GN=AGR2 PE=1 SV=1	2.377	0.021
sp|P16401	19.25	32.15	42.48	Histone H1.5 OS=Homo sapiens GN=HIST1H1B PE=1 SV=3	2.299	0.030
sp|P17931	12.67	12.67	34.4	Galectin-3 OS=Homo sapiens GN=LGALS3 PE=1 SV=5	2.243	0.000
sp|P35579	66.43	66.43	23.62	Myosin-9 OS=Homo sapiens GN=MYH9 PE=1 SV=4	2.089	0.000
sp|P21589	34.93	35.06	39.37	5'-nucleotidase OS=Homo sapiens GN=NT5E PE=1 SV=1	2.024	0.000
sp|P10412	2.38	31.26	47.03	Histone H1.4 OS=Homo sapiens GN=HIST1H1E PE=1 SV=2	2.014	0.041
sp|P49756	2.07	2.17	3.559	RNA-binding protein 25 OS=Homo sapiens GN=RBM25 PE=1 SV=3	1.987	0.040
sp|P11216	8.98	9.01	9.015	Glycogen phosphorylase, brain form OS=Homo sapiens GN=PYGB PE=1 SV=5	1.986	0.000
sp|Q9HDC9	29.18	29.18	38.22	Adipocyte plasma membrane-associated protein OS=Homo sapiens GN=APMAP PE=1 SV=2	1.978	0.002
sp|Q1663C	4.12	4.16	6.897	Cleavage and polyadenylation specificity factor subunit 6 OS=Homo sapiens GN=CPSF6 PE=1 SV=2	1.932	0.001
sp|Q56VL3	10.19	10.19	31.82	OCIA domain-containing protein 2 OS=Homo sapiens GN=OCIAD2 PE=1 SV=1	1.864	0.000
sp|Q9HBR0	10.74	10.85	9.115	Putative sodium-coupled neutral amino acid transporter 10 OS=Homo sapiens GN=SLC38A10 PE=1 SV=2	1.849	0.009
sp|P30101	20.88	20.88	23.17	Protein disulfide-isomerase A3 OS=Homo sapiens GN=PDIA3 PE=1 SV=4	1.837	0.004
sp|P23786	26.46	26.46	31.16	Carnitine O-palmitoyltransferase 2, mitochondrial OS=Homo sapiens GN=CPT2 PE=1 SV=2	1.825	0.000
sp|Q9UQ3	2.32	2.32	0.6177	Serine/arginine repetitive matrix protein 2 OS=Homo sapiens GN=SRRM2 PE=1 SV=2	1.822	0.021
sp|P49750	2	2	0.8713	YLP motif-containing protein 1 OS=Homo sapiens GN=YLPM1 PE=1 SV=3	1.813	0.037
sp|P61626	7.35	7.35	39.86	Lysozyme C OS=Homo sapiens GN=LYZ PE=1 SV=1	1.808	0.017
sp|P22307	6.9	6.92	5.667	Non-specific lipid-transfer protein OS=Homo sapiens GN=SCP2 PE=1 SV=2	1.770	0.007
sp|P13667	6.31	6.34	11.94	Protein disulfide-isomerase A4 OS=Homo sapiens GN=PDIA4 PE=1 SV=2	1.755	0.004
sp|O14745	4.54	4.54	15.36	Na(+)/H(+) exchange regulatory cofactor NHE-RF1 OS=Homo sapiens GN=SLC9A3R1 PE=1 SV=4	1.748	0.002
sp|Q9UJS0	6.08	6.08	8.741	Calcium-binding mitochondrial carrier protein Aralar2 OS=Homo sapiens GN=SLC25A13 PE=1 SV=2	1.730	0.004
sp|Q13242	6.12	6.14	22.62	Serine/arginine-rich splicing factor 9 OS=Homo sapiens GN=SRSF9 PE=1 SV=1	1.719	0.017
sp|P07237	17.05	17.05	30.91	Protein disulfide-isomerase OS=Homo sapiens GN=P4HB PE=1 SV=3	1.694	0.009
sp|Q9Y653	5.18	5.18	7.071	G-protein coupled receptor 56 OS=Homo sapiens GN=GPR56 PE=1 SV=2	1.672	0.000
sp|Q05519	2.78	2.78	5.992	Serine/arginine-rich splicing factor 11 OS=Homo sapiens GN=SRSF11 PE=1 SV=1	1.666	0.016
sp|Q8WXX7	3.4	7.36	17.31	DnaJ homolog subfamily C member 9 OS=Homo sapiens GN=DNAJC9 PE=1 SV=1	1.653	0.020
sp|Q07955	15.44	15.45	34.68	Serine/arginine-rich splicing factor 1 OS=Homo sapiens GN=SRSF1 PE=1 SV=2	1.645	0.016
sp|Q02127	23.03	23.03	47.59	Dihydroorotate dehydrogenase (quinone), mitochondrial OS=Homo sapiens GN=DHODH PE=1 SV=3	1.635	0.043
sp|Q15019	20	20	47.09	Septin-2 OS=Homo sapiens GN=SEPT2 PE=1 SV=1	1.634	0.006
sp|P09622	10	10.01	15.91	Dihydrolipoyl dehydrogenase, mitochondrial OS=Homo sapiens GN=DLD PE=1 SV=2	1.630	0.012
sp|Q15084	18.06	18.06	30.91	Protein disulfide-isomerase A6 OS=Homo sapiens GN=PDIA6 PE=1 SV=1	1.628	0.012
sp|P55011	15.1	15.1	11.88	Solute carrier family 12 member 2 OS=Homo sapiens GN=SLC12A2 PE=1 SV=1	1.608	0.010
sp|Q96PK6	2.03	2.08	3.587	RNA-binding protein 14 OS=Homo sapiens GN=RBM14 PE=1 SV=2	1.604	0.033
sp|Q8NBS9	5.04	5.34	10.42	Thioredoxin domain-containing protein 5 OS=Homo sapiens GN=TXNDC5 PE=1 SV=2	1.592	0.017
sp|Q02818	6.1	6.12	12.58	Nucleobindin-1 OS=Homo sapiens GN=NUCB1 PE=1 SV=4	1.587	0.040
sp|Q96I24	9.29	13.45	25.7	Far upstream element-binding protein 3 OS=Homo sapiens GN=FUBP3 PE=1 SV=2	1.581	0.000
sp|Q03252	24.61	33.01	36.17	Lamin-B2 OS=Homo sapiens GN=LMNB2 PE=1 SV=3	1.580	0.000
sp|Q8IYB3	1.58	1.6	3.761	Serine/arginine repetitive matrix protein 1 OS=Homo sapiens GN=SRRM1 PE=1 SV=2	1.569	0.019
sp|P43304	4.45	4.45	5.089	Glycerol-3-phosphate dehydrogenase, mitochondrial OS=Homo sapiens GN=GPD2 PE=1 SV=3	1.561	0.009
sp|P05783	36.65	38.25	51.4	Keratin, type I cytoskeletal 18 OS=Homo sapiens GN=KRT18 PE=1 SV=2	1.554	0.014
sp|P60660	11.59	11.59	52.98	Myosin light polypeptide 6 OS=Homo sapiens GN=MYL6 PE=1 SV=2	1.553	0.007
sp|O60664	15.54	15.54	33.18	Perilipin-3 OS=Homo sapiens GN=PLIN3 PE=1 SV=3	1.527	0.000
sp|Q9P206	10.09	10.16	10.24	Uncharacterized protein KIAA1522 OS=Homo sapiens GN=KIAA1522 PE=1 SV=2	1.522	0.014
sp|Q8N5N7	10	10	39.24	39S ribosomal protein L50, mitochondrial OS=Homo sapiens GN=MRPL50 PE=1 SV=2	1.507	0.022
sp|O43707	22.93	22.93	19.54	Alpha-actinin-4 OS=Homo sapiens GN=ACTN4 PE=1 SV=2	1.504	0.000
sp|P11021	32.14	32.14	29.97	78 kDa glucose-regulated protein OS=Homo sapiens GN=HSPA5 PE=1 SV=2	1.501	0.000
sp|P07910	16.4	16.7	28.43	Heterogeneous nuclear ribonucleoproteins C1/C2 OS=Homo sapiens GN=HNRNPC PE=1 SV=4	1.491	0.021
sp|P08727	16.72	21.04	38.5	Keratin, type I cytoskeletal 19 OS=Homo sapiens GN=KRT19 PE=1 SV=4	1.485	0.003
sp|Q8N163	14	14	14.95	DBIRD complex subunit KIAA1967 OS=Homo sapiens GN=KIAA1967 PE=1 SV=2	1.467	0.025
sp|Q8WXF1	13.64	13.74	17.59	Paraspeckle component 1 OS=Homo sapiens GN=PSPC1 PE=1 SV=1	1.460	0.040
sp|P46013	25.52	25.52	6.357	Antigen KI-67 OS=Homo sapiens GN=MKI67 PE=1 SV=2	1.455	0.003
sp|P11387	19.44	19.44	17.12	DNA topoisomerase 1 OS=Homo sapiens GN=TOP1 PE=1 SV=2	1.438	0.004
sp|Q9UPT9	2.44	2.44	2.149	Zinc finger CCCH domain-containing protein 4 OS=Homo sapiens GN=ZC3H4 PE=1 SV=3	1.436	0.024
sp|Q9BYD6	4.18	4.18	11.25	39S ribosomal protein L4, mitochondrial OS=Homo sapiens GN=MRPL4 PE=1 SV=1	1.418	0.020
sp|P38646	8.69	10.77	10.16	Stress-70 protein, mitochondrial OS=Homo sapiens GN=HSPA9 PE=1 SV=2	1.379	0.007
sp|Q13405	6.01	6.01	23.49	39S ribosomal protein L49, mitochondrial OS=Homo sapiens GN=MRPL49 PE=1 SV=1	1.372	0.024
sp|Q9NPA0	7.18	7.37	30.99	ER membrane protein complex subunit 7 OS=Homo sapiens GN=EMC7 PE=1 SV=1	1.360	0.043
sp|O75915	12	12.02	20.74	PRA1 family protein 3 OS=Homo sapiens GN=ARL6IP5 PE=1 SV=1	1.360	0.018
sp|P55265	9.87	9.9	6.607	Double-stranded RNA-specific adenosine deaminase OS=Homo sapiens GN=ADAR PE=1 SV=4	1.352	0.007
sp|Q92841	19.88	19.88	23.05	Probable ATP-dependent RNA helicase DDX17 OS=Homo sapiens GN=DDX17 PE=1 SV=2	1.342	0.003
sp|P09874	41.41	41.41	29.78	Poly [ADP-ribose] polymerase 1 OS=Homo sapiens GN=PARP1 PE=1 SV=4	1.340	0.021
sp|Q9UHB6	13.42	13.44	15.28	LIM domain and actin-binding protein 1 OS=Homo sapiens GN=LIMA1 PE=1 SV=1	1.308	0.007
sp|P14866	8.54	8.54	13.07	Heterogeneous nuclear ribonucleoprotein L OS=Homo sapiens GN=HNRNPL PE=1 SV=2	1.291	0.027
sp|Q9BY44	4.11	4.11	6.838	Eukaryotic translation initiation factor 2A OS=Homo sapiens GN=EIF2A PE=1 SV=3	1.291	0.045
sp|Q09666	185.43	185.43	42.07	Neuroblast differentiation-associated protein AHNAK OS=Homo sapiens GN=AHNAK PE=1 SV=2	1.262	0.005
sp|P52272	22.78	22.78	25.21	Heterogeneous nuclear ribonucleoprotein M OS=Homo sapiens GN=HNRNPM PE=1 SV=3	1.242	0.040
sp|Q15149	12.21	12.29	1.601	Plectin OS=Homo sapiens GN=PLEC PE=1 SV=3	1.217	0.025
sp|P78527	18.56	19.68	3.852	DNA-dependent protein kinase catalytic subunit OS=Homo sapiens GN=PRKDC PE=1 SV=3	0.808	0.020
sp|Q16134	13.65	13.65	22.69	Electron transfer flavoprotein-ubiquinone oxidoreductase, mitochondrial OS=Homo sapiens GN=ETFDH PE=1 SV=2	0.807	0.029
sp|P07339	8.35	8.35	18.69	Cathepsin D OS=Homo sapiens GN=CTSD PE=1 SV=1	0.786	0.028
sp|Q92616	2.8	2.9	1.722	Translational activator GCN1 OS=Homo sapiens GN=GCN1L1 PE=1 SV=6	0.785	0.032
sp|P05023	15.87	15.87	10.85	Sodium/potassium-transporting ATPase subunit alpha-1 OS=Homo sapiens GN=ATP1A1 PE=1 SV=1	0.776	0.013
sp|Q99623	22.07	22.07	45.82	Prohibitin-2 OS=Homo sapiens GN=PHB2 PE=1 SV=2	0.771	0.001
sp|Q16795	9.45	9.45	20.69	NADH dehydrogenase [ubiquinone] 1 alpha subcomplex subunit 9, mitochondrial OS=Homo sapiens GN=NDUFA9 PE=1 SV=1	0.746	0.004
sp|P23396	8.06	8.06	21.4	40S ribosomal protein S3 OS=Homo sapiens GN=RPS3 PE=1 SV=2	0.739	0.014
sp|P49368	12.36	12.36	18.35	T-complex protein 1 subunit gamma OS=Homo sapiens GN=CCT3 PE=1 SV=4	0.738	0.027
sp|P78371	15.92	15.92	25.98	T-complex protein 1 subunit beta OS=Homo sapiens GN=CCT2 PE=1 SV=4	0.732	0.001
sp|P48643	16.66	16.7	21.07	T-complex protein 1 subunit epsilon OS=Homo sapiens GN=CCT5 PE=1 SV=1	0.730	0.024
sp|P49748	26.61	26.65	31.76	Very long-chain specific acyl-CoA dehydrogenase, mitochondrial OS=Homo sapiens GN=ACADVL PE=1 SV=1	0.709	0.008
sp|P06756	33.34	33.34	22.71	Integrin alpha-V OS=Homo sapiens GN=ITGAV PE=1 SV=2	0.706	0.002
sp|Q9H7Z7	8.67	8.67	19.1	Prostaglandin E synthase 2 OS=Homo sapiens GN=PTGES2 PE=1 SV=1	0.703	0.012
sp|P40227	13.61	13.61	22.03	T-complex protein 1 subunit zeta OS=Homo sapiens GN=CCT6A PE=1 SV=3	0.701	0.011
sp|Q15738	5.62	5.62	10.99	Sterol-4-alpha-carboxylate 3-dehydrogenase, decarboxylating OS=Homo sapiens GN=NSDHL PE=1 SV=2	0.695	0.045
sp|Q9UNN8	6.51	6.51	20.59	Endothelial protein C receptor OS=Homo sapiens GN=PROCR PE=1 SV=1	0.695	0.004
sp|P62888	3.56	3.56	24.35	60S ribosomal protein L30 OS=Homo sapiens GN=RPL30 PE=1 SV=2	0.694	0.011
sp|P50990	11.03	11.03	14.6	T-complex protein 1 subunit theta OS=Homo sapiens GN=CCT8 PE=1 SV=4	0.687	0.004

261

262

Uniprot Unused	Total	X.Cov.95	Protein Name; Organism; Gene name	iTRAQ Fold Change	StouffersPval
sp|P36578 29.26	29.65	36.3	60S ribosomal protein L4 OS=Homo sapiens GN=RPL4 PE=1 SV=5	0.684	0.043
sp|P54709 6.32	6.35	21.15	Sodium/potassium-transporting ATPase subunit beta-3 OS=Homo sapiens GN=ATP1B3 PE=1 SV=1	0.684	0.007
sp|P51648 5.46	5.47	9.072	Fatty aldehyde dehydrogenase OS=Homo sapiens GN=ALDH3A2 PE=1 SV=1	0.673	0.031
sp|Q96AP7 12.78	12.79	30.77	Endothelial cell-selective adhesion molecule OS=Homo sapiens GN=ESAM PE=1 SV=1	0.657	0.015
sp|O75489 16.04	16.04	40.91	NADH dehydrogenase [ubiquinone] iron-sulfur protein 3, mitochondrial OS=Homo sapiens GN=NDUFS3 PE=1 SV=1	0.657	0.008
sp|P13645 17.45	20.69	26.54	Keratin, type I cytoskeletal 10 OS=Homo sapiens GN=KRT10 PE=1 SV=6	0.650	0.003
sp|P04844 9.52	9.52	12.52	Dolichyl-diphosphooligosaccharide--protein glycosyltransferase subunit 2 OS=Homo sapiens GN=RPN2 PE=1 SV=3	0.648	0.005
sp|Q00325 10.49	10.72	13.26	Phosphate carrier protein, mitochondrial OS=Homo sapiens GN=SLC25A3 PE=1 SV=2	0.645	0.010
sp|O00116 15.48	15.48	19.76	Alkyldihydroxyacetonephosphate synthase, peroxisomal OS=Homo sapiens GN=AGPS PE=1 SV=1	0.641	0.004
sp|Q99536 13.69	13.7	26.97	Synaptic vesicle membrane protein VAT-1 homolog OS=Homo sapiens GN=VAT1 PE=1 SV=2	0.640	0.047
sp|P05026 10.07	10.07	25.41	Sodium/potassium-transporting ATPase subunit beta-1 OS=Homo sapiens GN=ATP1B1 PE=1 SV=1	0.636	0.035
sp|Q6PIU2 3.53	3.53	11.52	Neutral cholesterol ester hydrolase 1 OS=Homo sapiens GN=NCEH1 PE=1 SV=3	0.631	0.006
sp|P18621 9.26	9.26	27.72	60S ribosomal protein L17 OS=Homo sapiens GN=RPL17 PE=1 SV=3	0.627	0.034
sp|P05388 20.75	20.75	47.32	60S acidic ribosomal protein P0 OS=Homo sapiens GN=RPLP0 PE=1 SV=1	0.620	0.015
sp|Q6PL18 2.01	2.06	1.295	ATPase family AAA domain-containing protein 2 OS=Homo sapiens GN=ATAD2 PE=1 SV=1	0.618	0.041
sp|P0CW2 10.92	10.92	48.89	40S ribosomal protein S17-like OS=Homo sapiens GN=RPS17L PE=1 SV=1	0.618	0.048
sp|Q0702C 5.82	5.82	19.68	60S ribosomal protein L18 OS=Homo sapiens GN=RPL18 PE=1 SV=2	0.604	0.031
sp|P62851 10.57	10.57	24.8	40S ribosomal protein S25 OS=Homo sapiens GN=RPS25 PE=1 SV=1	0.587	0.005
sp|P04899 5.71	8.18	21.69	Guanine nucleotide-binding protein G(i) subunit alpha-2 OS=Homo sapiens GN=GNAI2 PE=1 SV=3	0.586	0.021
sp|P18084 20.32	20.32	16.9	Integrin beta-5 OS=Homo sapiens GN=ITGB5 PE=1 SV=1	0.585	0.002
sp|P27487 15.18	15.18	12.27	Dipeptidyl peptidase 4 OS=Homo sapiens GN=DPP4 PE=1 SV=2	0.579	0.000
sp|P27338 4	4	5.962	Amine oxidase [flavin-containing] B OS=Homo sapiens GN=MAOB PE=1 SV=3	0.571	0.020
sp|Q14974 8.25	8.25	7.192	Importin subunit beta-1 OS=Homo sapiens GN=KPNB1 PE=1 SV=2	0.568	0.029
sp|O00217 5.79	5.79	19.05	NADH dehydrogenase [ubiquinone] iron-sulfur protein 8, mitochondrial OS=Homo sapiens GN=NDUFS8 PE=1 SV=1	0.568	0.005
sp|Q5ZPR3 8.31	8.31	20.97	CD276 antigen OS=Homo sapiens GN=CD276 PE=1 SV=1	0.567	0.002
sp|P06576 42.27	42.27	58.6	ATP synthase subunit beta, mitochondrial OS=Homo sapiens GN=ATP5B PE=1 SV=3	0.565	0.000
sp|P51149 26.13	26.13	62.8	Ras-related protein Rab-7a OS=Homo sapiens GN=RAB7A PE=1 SV=1	0.553	0.001
sp|P39023 6.02	6.08	12.9	60S ribosomal protein L3 OS=Homo sapiens GN=RPL3 PE=1 SV=2	0.540	0.013
sp|P08754 5.55	7.72	18.93	Guanine nucleotide-binding protein G(k) subunit alpha OS=Homo sapiens GN=GNAI3 PE=1 SV=3	0.534	0.020
sp|P15529 4	4	6.122	Membrane cofactor protein OS=Homo sapiens GN=CD46 PE=1 SV=3	0.533	0.047
sp|P16444 8.23	8.23	23.6	Dipeptidase 1 OS=Homo sapiens GN=DPEP1 PE=1 SV=3	0.527	0.028
sp|Q14165 25.13	25.13	48.97	Malectin OS=Homo sapiens GN=MLEC PE=1 SV=1	0.516	0.001
sp|P10620 3.89	3.89	9.032	Microsomal glutathione S-transferase 1 OS=Homo sapiens GN=MGST1 PE=1 SV=1	0.511	0.013
sp|P08582 8.79	8.79	8.672	Melanotransferrin OS=Homo sapiens GN=MFI2 PE=1 SV=1	0.505	0.000
sp|P50991 10.25	12.1	19.85	T-complex protein 1 subunit delta OS=Homo sapiens GN=CCT4 PE=1 SV=4	0.495	0.002
sp|Q9UHA 2.31	2.31	12.9	Ragulator complex protein LAMTOR3 OS=Homo sapiens GN=LAMTOR3 PE=1 SV=1	0.478	0.019
sp|P02786 23.45	23.45	21.05	Transferrin receptor protein 1 OS=Homo sapiens GN=TFRC PE=1 SV=2	0.478	0.001
sp|Q15758 8.97	8.97	10.72	Neutral amino acid transporter B(0) OS=Homo sapiens GN=SLC1A5 PE=1 SV=2	0.477	0.010
sp|Q2VIR3 4.22	4.22	11.86	Putative eukaryotic translation initiation factor 2 subunit 3-like protein OS=Homo sapiens GN=EIF2S3L PE=5 SV=2	0.468	0.021
sp|Q9BQG 6	6.01	3.012	Myb-binding protein 1A OS=Homo sapiens GN=MYBBP1A PE=1 SV=2	0.466	0.025
sp|O75695 6.11	6.11	7.429	Protein XRP2 OS=Homo sapiens GN=RP2 PE=1 SV=4	0.466	0.035
sp|Q07021 8.45	8.45	26.6	Complement component 1 Q subcomponent-binding protein, mitochondrial OS=Homo sapiens GN=C1QBP PE=1 SV=1	0.455	0.011
sp|Q9NX51 6.57	6.57	18.21	Cell growth-regulating nucleolar protein OS=Homo sapiens GN=LYAR PE=1 SV=2	0.450	0.026
sp|P09758 4.09	4.09	10.22	Tumor-associated calcium signal transducer 2 OS=Homo sapiens GN=TACSTD2 PE=1 SV=3	0.414	0.028
sp|Q15907 17.56	17.56	46.33	Ras-related protein Rab-11B OS=Homo sapiens GN=RAB11B PE=1 SV=4	0.405	0.000
sp|Q9Y3A6 7.47	7.5	22.27	Transmembrane emp24 domain-containing protein 5 OS=Homo sapiens GN=TMED5 PE=1 SV=1	0.354	0.024
sp|P08174 29.55	29.55	38.06	Complement decay-accelerating factor OS=Homo sapiens GN=CD55 PE=1 SV=4	0.349	0.000
sp|P62979 11.47	11.47	41.03	Ubiquitin-40S ribosomal protein S27a OS=Homo sapiens GN=RPS27A PE=1 SV=2	0.345	0.003
sp|Q16563 2.69	2.69	19.69	Synaptophysin-like protein 1 OS=Homo sapiens GN=SYPL1 PE=1 SV=1	0.338	0.006
sp|P43121 18.25	18.25	27.86	Cell surface glycoprotein MUC18 OS=Homo sapiens GN=MCAM PE=1 SV=2	0.323	0.001
sp|P37059 2	2.08	3.101	Estradiol 17-beta-dehydrogenase 2 OS=Homo sapiens GN=HSD17B2 PE=1 SV=1	0.149	0.045

B: Comparison of TGFβ treated HT29 Mock/untreated HT29 Mock

Uniprot Unused	Total	X.Cov.95	Protein Name; Organism; Gene name	iTRAQ Fold Change	StouffersPval
sp|P35527 14.04	14.04	20.71	Keratin, type I cytoskeletal 9 OS=Homo sapiens GN=KRT9 PE=1 SV=3	3.885	0.002
sp|P49755 14.08	14.08	38.81	Transmembrane emp24 domain-containing protein 10 OS=Homo sapiens GN=TMED10 PE=1 SV=2	2.133	0.001
sp|P13645 17.45	20.69	26.54	Keratin, type I cytoskeletal 10 OS=Homo sapiens GN=KRT10 PE=1 SV=6	2.068	0.007
sp|P62906 17.26	17.26	42.86	60S ribosomal protein L10a OS=Homo sapiens GN=RPL10A PE=1 SV=2	1.992	0.000
sp|Q9Y653 5.16	5.18	7.071	G-protein coupled receptor 56 OS=Homo sapiens GN=GPR56 PE=1 SV=2	1.743	0.002
sp|P62424 20.51	20.51	33.08	60S ribosomal protein L7a OS=Homo sapiens GN=RPL7A PE=1 SV=2	1.734	0.000
sp|Q15233 27.2	29.48	38	Non-POU domain-containing octamer-binding protein OS=Homo sapiens GN=NONO PE=1 SV=4	1.663	0.000
sp|P48047 8.07	8.07	36.62	ATP synthase subunit O, mitochondrial OS=Homo sapiens GN=ATP5O PE=1 SV=1	1.640	0.032
sp|P18124 20.55	20.55	33.06	60S ribosomal protein L7 OS=Homo sapiens GN=RPL7 PE=1 SV=1	1.622	0.000
sp|P11182 3.06	3.06	7.261	Lipoamide acyltransferase component of branched-chain alpha-keto acid dehydrogenase complex, mitochondrial OS	1.606	0.023
sp|O75367 23.86	27.99	45.97	Core histone macro-H2A.1 OS=Homo sapiens GN=H2AFY PE=1 SV=2	1.578	0.000
sp|Q9UIGC 6.01	7.28	2.9	Tyrosine-protein kinase BAZ1B OS=Homo sapiens GN=BAZ1B PE=1 SV=2	1.563	0.030
sp|Q9Y5B9 13.1	13.1	10.6	FACT complex subunit SPT16 OS=Homo sapiens GN=SUPT16H PE=1 SV=1	1.535	0.005
sp|Q16795 9.45	9.45	20.69	NADH dehydrogenase [ubiquinone] 1 alpha subcomplex subunit 9, mitochondrial OS=Homo sapiens GN=NDUFA9 PE=1 SV	1.490	0.000
sp|P49821 8.27	8.27	11.42	NADH dehydrogenase [ubiquinone] flavoprotein 1, mitochondrial OS=Homo sapiens GN=NDUFV1 PE=1 SV=4	1.461	0.005
sp|P11387 19.44	19.44	17.12	DNA topoisomerase 1 OS=Homo sapiens GN=TOP1 PE=1 SV=2	1.434	0.013
sp|P12956 28.5	28.5	29.56	X-ray repair cross-complementing protein 6 OS=Homo sapiens GN=XRCC6 PE=1 SV=2	1.399	0.001
sp|O75306 8.58	8.58	14.47	NADH dehydrogenase [ubiquinone] iron-sulfur protein 2, mitochondrial OS=Homo sapiens GN=NDUFS2 PE=1 SV=2	1.398	0.006
sp|P22695 14.5	14.5	28.48	Cytochrome b-c1 complex subunit 2, mitochondrial OS=Homo sapiens GN=UQCRC2 PE=1 SV=3	1.387	0.000
sp|P61247 12.73	12.73	22.73	40S ribosomal protein S3a OS=Homo sapiens GN=RPS3A PE=1 SV=2	1.385	0.000
sp|P06576 42.27	42.27	58.6	ATP synthase subunit beta, mitochondrial OS=Homo sapiens GN=ATP5B PE=1 SV=3	1.383	0.000
sp|P17480 13.11	13.11	12.3	Nucleolar transcription factor 1 OS=Homo sapiens GN=UBTF PE=1 SV=1	1.377	0.000
sp|P05388 20.75	20.75	47.32	60S acidic ribosomal protein P0 OS=Homo sapiens GN=RPLP0 PE=1 SV=1	1.374	0.004
sp|Q29RF7 6.62	6.68	4.637	Sister chromatid cohesion protein PDS5 homolog A OS=Homo sapiens GN=PDS5A PE=1 SV=1	1.373	0.032
sp|P51648 5.46	5.47	9.072	Fatty aldehyde dehydrogenase OS=Homo sapiens GN=ALDH3A2 PE=1 SV=1	1.372	0.021
sp|Q0702C 5.82	5.82	19.68	60S ribosomal protein L18 OS=Homo sapiens GN=RPL18 PE=1 SV=2	1.370	0.046
sp|P06748 15.46	15.46	32.65	Nucleophosmin OS=Homo sapiens GN=NPM1 PE=1 SV=2	1.368	0.009
sp|P37108 4.03	4.03	20.59	Signal recognition particle 14 kDa protein OS=Homo sapiens GN=SRP14 PE=1 SV=2	1.366	0.016
sp|Q16181 9.73	9.73	18.99	Septin-7 OS=Homo sapiens GN=SEPT7 PE=1 SV=2	1.360	0.001
sp|P13010 11.47	11.48	12.7	X-ray repair cross-complementing protein 5 OS=Homo sapiens GN=XRCC5 PE=1 SV=3	1.359	0.016
sp|P28331 17.32	17.32	23.52	NADH-ubiquinone oxidoreductase 75 kDa subunit, mitochondrial OS=Homo sapiens GN=NDUFS1 PE=1 SV=3	1.345	0.000
sp|Q9UQ8 17.73	17.73	35.53	Proliferation-associated protein 2G4 OS=Homo sapiens GN=PA2G4 PE=1 SV=3	1.339	0.010
sp|P00352 4.33	4.51	5.589	Retinal dehydrogenase 1 OS=Homo sapiens GN=ALDH1A1 PE=1 SV=2	1.324	0.043
sp|P23246 51.95	51.95	41.73	Splicing factor, proline- and glutamine-rich OS=Homo sapiens GN=SFPQ PE=1 SV=2	1.323	0.008
sp|P43243 13.13	13.13	12.99	Matrin-3 OS=Homo sapiens GN=MATR3 PE=1 SV=2	1.321	0.000
sp|P0CW2 10.92	10.92	48.89	40S ribosomal protein S17-like OS=Homo sapiens GN=RPS17L PE=1 SV=1	1.317	0.002

263

sp|P55265 9.87	9.9	6.607	Double-stranded RNA-specific adenosine deaminase OS=Homo sapiens GN=ADAR PE=1 SV=4	1.309	0.030
sp|P40939 10.95	11.17	13.5	Trifunctional enzyme subunit alpha, mitochondrial OS=Homo sapiens GN=HADHA PE=1 SV=2	1.300	0.002
sp|P62277 12.26	12.26	43.05	40S ribosomal protein S13 OS=Homo sapiens GN=RPS13 PE=1 SV=2	1.297	0.029
sp|O00567 11.19	11.19	13.97	Nucleolar protein 56 OS=Homo sapiens GN=NOP56 PE=1 SV=4	1.296	0.005
sp|P18621 9.26	9.26	27.72	60S ribosomal protein L17 OS=Homo sapiens GN=RPL17 PE=1 SV=3	1.296	0.007
sp|O75396 6.19	6.19	20.93	Vesicle-trafficking protein SEC22b OS=Homo sapiens GN=SEC22B PE=1 SV=4	1.293	0.016
sp|P36578 29.26	29.65	36.3	60S ribosomal protein L4 OS=Homo sapiens GN=RPL4 PE=1 SV=5	1.283	0.012
sp|P62701 13.01	13.01	32.32	40S ribosomal protein S4, X isoform OS=Homo sapiens GN=RPS4X PE=1 SV=2	1.275	0.001
sp|P11216 8.98	9.01	9.015	Glycogen phosphorylase, brain form OS=Homo sapiens GN=PYGB PE=1 SV=5	1.271	0.035
sp|P52272 22.78	22.78	25.21	Heterogeneous nuclear ribonucleoprotein M OS=Homo sapiens GN=HNRNPM PE=1 SV=3	1.261	0.000
sp|Q9UH99 3.11	3.11	7.252	SUN domain-containing protein 2 OS=Homo sapiens GN=SUN2 PE=1 SV=3	1.259	0.049
sp|Q9UKV8 10.33	10.43	5.891	Apoptotic chromatin condensation inducer in the nucleus OS=Homo sapiens GN=ACIN1 PE=1 SV=2	1.248	0.029
sp|Q9Y3B7 6.25	6.25	18.23	39S ribosomal protein L11, mitochondrial OS=Homo sapiens GN=MRPL11 PE=1 SV=1	1.243	0.020
sp|Q12905 8.38	8.38	21.79	Interleukin enhancer-binding factor 2 OS=Homo sapiens GN=ILF2 PE=1 SV=2	1.235	0.008
sp|Q9Y3U8 5.8	5.8	37.14	60S ribosomal protein L36 OS=Homo sapiens GN=RPL36 PE=1 SV=3	1.232	0.023
sp|Q14258 1.4	1.42	2.222	E3 ubiquitin/ISG15 ligase TRIM25 OS=Homo sapiens GN=TRIM25 PE=1 SV=2	1.228	0.046
sp|Q15029 5.63	5.63	5.041	116 kDa U5 small nuclear ribonucleoprotein component OS=Homo sapiens GN=EFTUD2 PE=1 SV=1	1.213	0.010
sp|P46087 6.86	6.86	4.68	Putative ribosomal RNA methyltransferase NOP2 OS=Homo sapiens GN=NOP2 PE=1 SV=2	1.207	0.006
sp|Q92841 19.88	19.88	23.05	Probable ATP-dependent RNA helicase DDX17 OS=Homo sapiens GN=DDX17 PE=1 SV=2	1.206	0.018
sp|Q9UHB8 13.42	13.44	15.28	LIM domain and actin-binding protein 1 OS=Homo sapiens GN=LIMA1 PE=1 SV=1	0.825	0.013
sp|Q96DH6 7.55	7.56	17.38	RNA-binding protein Musashi homolog 2 OS=Homo sapiens GN=MSI2 PE=1 SV=1	0.823	0.026
sp|Q8IYB3 1.58	1.6	3.761	Serine/arginine repetitive matrix protein 1 OS=Homo sapiens GN=SRRM1 PE=1 SV=2	0.821	0.011
sp|P22307 6.9	6.92	5.667	Non-specific lipid-transfer protein OS=Homo sapiens GN=SCP2 PE=1 SV=2	0.819	0.031
sp|Q9BTV4 20.15	20.15	38.5	Transmembrane protein 43 OS=Homo sapiens GN=TMEM43 PE=1 SV=1	0.818	0.001
sp|Q8WWM8 8.03	8.03	8.524	Choline transporter-like protein 1 OS=Homo sapiens GN=SLC44A1 PE=1 SV=1	0.817	0.026
sp|O95721 16.37	16.37	42.64	Synaptosomal-associated protein 29 OS=Homo sapiens GN=SNAP29 PE=1 SV=1	0.816	0.007
sp|O14672 18.5	18.5	19.52	Disintegrin and metalloproteinase domain-containing protein 10 OS=Homo sapiens GN=ADAM10 PE=1 SV=1	0.812	0.016
sp|P45880 14.43	16.47	38.78	Voltage-dependent anion-selective channel protein 2 OS=Homo sapiens GN=VDAC2 PE=1 SV=2	0.811	0.005
sp|P38159 15.08	15.08	21.99	RNA-binding motif protein, X chromosome OS=Homo sapiens GN=RBMX PE=1 SV=3	0.810	0.024
sp|P27487 15.18	15.18	12.27	Dipeptidyl peptidase 4 OS=Homo sapiens GN=DPP4 PE=1 SV=2	0.809	0.000
sp|Q68D91 5.41	5.41	17.2	Metallo-beta-lactamase domain-containing protein 2 OS=Homo sapiens GN=MBLAC2 PE=1 SV=3	0.806	0.043
sp|P35613 18.02	18.02	31.69	Basigin OS=Homo sapiens GN=BSG PE=1 SV=2	0.806	0.019
sp|P51572 25.34	27.67	48.78	B-cell receptor-associated protein 31 OS=Homo sapiens GN=BCAP31 PE=1 SV=3	0.805	0.002
sp|P06702 6.02	6.04	44.74	Protein S100-A9 OS=Homo sapiens GN=S100A9 PE=1 SV=1	0.804	0.044
sp|P20645 12	12	27.44	Cation-dependent mannose-6-phosphate receptor OS=Homo sapiens GN=M6PR PE=1 SV=1	0.800	0.009
sp|Q16134 13.65	13.65	22.69	Electron transfer flavoprotein-ubiquinone oxidoreductase, mitochondrial OS=Homo sapiens GN=ETFDH PE=1 SV=2	0.797	0.010
sp|P12830 16.12	16.46	11.34	Cadherin-1 OS=Homo sapiens GN=CDH1 PE=1 SV=3	0.796	0.027
sp|Q14165 25.13	25.13	48.97	Malectin OS=Homo sapiens GN=MLEC PE=1 SV=1	0.796	0.000
sp|Q96A29 8.82	8.83	22.73	Protein FAM162A OS=Homo sapiens GN=FAM162A PE=1 SV=2	0.795	0.024
sp|P20700 51.8	54.63	47.1	Lamin-B1 OS=Homo sapiens GN=LMNB1 PE=1 SV=2	0.794	0.002
sp|P00167 14.09	14.09	47.01	Cytochrome b5 OS=Homo sapiens GN=CYB5A PE=1 SV=2	0.791	0.012
sp|P13073 11.21	11.21	31.95	Cytochrome c oxidase subunit 4 isoform 1, mitochondrial OS=Homo sapiens GN=COX4I1 PE=1 SV=1	0.791	0.041
sp|Q02127 23.03	23.03	47.59	Dihydroorotate dehydrogenase (quinone), mitochondrial OS=Homo sapiens GN=DHODH PE=1 SV=3	0.784	0.001
sp|P78310 22.64	22.64	44.11	Coxsackievirus and adenovirus receptor OS=Homo sapiens GN=CXADR PE=1 SV=1	0.782	0.000
sp|P48449 13.56	13.57	12.98	Lanosterol synthase OS=Homo sapiens GN=LSS PE=1 SV=1	0.779	0.000
sp|P50895 13.45	13.45	22.61	Basal cell adhesion molecule OS=Homo sapiens GN=BCAM PE=1 SV=2	0.776	0.008
sp|Q92945 15.56	17.61	25.18	Far upstream element-binding protein 2 OS=Homo sapiens GN=KHSRP PE=1 SV=4	0.772	0.004
sp|Q10471 9.07	9.07	16.64	Polypeptide N-acetylgalactosaminyltransferase 2 OS=Homo sapiens GN=GALNT2 PE=1 SV=1	0.770	0.017
sp|P08621 6.88	6.88	10.3	U1 small nuclear ribonucleoprotein 70 kDa OS=Homo sapiens GN=SNRNP70 PE=1 SV=2	0.764	0.018
sp|P23229 65.85	65.85	38.32	Integrin alpha-6 OS=Homo sapiens GN=ITGA6 PE=1 SV=5	0.764	0.000
sp|Q9269215	15	25.09	Poliovirus receptor-related protein 2 OS=Homo sapiens GN=PVRL2 PE=1 SV=1	0.763	0.015
sp|O60664 15.54	15.54	33.18	Perilipin-3 OS=Homo sapiens GN=PLIN3 PE=1 SV=3	0.762	0.000
sp|P49748 26.61	26.65	31.76	Very long-chain specific acyl-CoA dehydrogenase, mitochondrial OS=Homo sapiens GN=ACADVL PE=1 SV=1	0.760	0.002
sp|P51690 14.91	14.91	21.05	Arylsulfatase E OS=Homo sapiens GN=ARSE PE=1 SV=2	0.759	0.000
sp|Q9Y394 22.02	22.02	33.4	Dehydrogenase/reductase SDR family member 7 OS=Homo sapiens GN=DHRS7 PE=1 SV=1	0.755	0.002
sp|Q13740 22.75	22.75	26.24	CD166 antigen OS=Homo sapiens GN=ALCAM PE=1 SV=2	0.754	0.001
sp|P16070 30.09	30.09	16.85	CD44 antigen OS=Homo sapiens GN=CD44 PE=1 SV=3	0.753	0.002
sp|Q86Y82 7.77	7.77	22.1	Syntaxin-12 OS=Homo sapiens GN=STX12 PE=1 SV=1	0.752	0.009
sp|Q02878 18.2	18.2	36.81	60S ribosomal protein L6 OS=Homo sapiens GN=RPL6 PE=1 SV=3	0.751	0.003
sp|Q92542 11.35	11.35	11.99	Nicastrin OS=Homo sapiens GN=NCSTN PE=1 SV=2	0.751	0.021
sp|P16422 15.21	15.21	39.49	Epithelial cell adhesion molecule OS=Homo sapiens GN=EPCAM PE=1 SV=2	0.747	0.030
sp|P09669 13.05	13.05	50.67	Cytochrome c oxidase subunit 6C OS=Homo sapiens GN=COX6C PE=1 SV=1	0.746	0.029
sp|P10606 18.62	18.62	44.96	Cytochrome c oxidase subunit 5B, mitochondrial OS=Homo sapiens GN=COX5B PE=1 SV=2	0.742	0.001
sp|Q96AE4 31.22	31.22	30.12	Far upstream element-binding protein 1 OS=Homo sapiens GN=FUBP1 PE=1 SV=3	0.742	0.000
sp|Q9252C 12.67	12.69	33.48	Protein FAM3C OS=Homo sapiens GN=FAM3C PE=1 SV=1	0.737	0.001
sp|Q08431 8.05	8.06	17.83	Lactadherin OS=Homo sapiens GN=MFGE8 PE=1 SV=2	0.729	0.021
sp|Q8WTV0 5.29	5.29	5.072	Scavenger receptor class B member 1 OS=Homo sapiens GN=SCARB1 PE=1 SV=1	0.725	0.023
sp|Q969Q5 4.68	4.68	16.26	Ras-related protein Rab-24 OS=Homo sapiens GN=RAB24 PE=1 SV=1	0.720	0.032
sp|Q9HDC9 29.18	29.18	38.22	Adipocyte plasma membrane-associated protein OS=Homo sapiens GN=APMAP PE=1 SV=2	0.719	0.000
sp|Q13277 2.79	2.79	5.19	Syntaxin-3 OS=Homo sapiens GN=STX3 PE=1 SV=3	0.717	0.006
sp|P11279 9.76	9.76	17.99	Lysosome-associated membrane glycoprotein 1 OS=Homo sapiens GN=LAMP1 PE=1 SV=3	0.710	0.006
sp|Q9NYL4 6.13	6.13	23.38	Peptidyl-prolyl cis-trans isomerase FKBP11 OS=Homo sapiens GN=FKBP11 PE=1 SV=1	0.709	0.006
sp|Q86SF2 12.05	12.05	12.94	N-acetylgalactosaminyltransferase 7 OS=Homo sapiens GN=GALNT7 PE=1 SV=1	0.701	0.002
sp|Q8N183 11.96	11.96	51.48	Mimitin, mitochondrial OS=Homo sapiens GN=NDUFAF2 PE=1 SV=1	0.684	0.004
sp|P29966 14.55	14.65	45.18	Myristoylated alanine-rich C-kinase substrate OS=Homo sapiens GN=MARCKS PE=1 SV=4	0.670	0.001
sp|P13688 6.44	6.54	11.98	Carcinoembryonic antigen-related cell adhesion molecule 1 OS=Homo sapiens GN=CEACAM1 PE=1 SV=2	0.666	0.043
sp|Q00839 47.15	47.15	27.27	Heterogeneous nuclear ribonucleoprotein U OS=Homo sapiens GN=HNRNPU PE=1 SV=6	0.664	0.000
sp|P23786 26.46	26.46	31.16	Carnitine O-palmitoyltransferase 2, mitochondrial OS=Homo sapiens GN=CPT2 PE=1 SV=2	0.660	0.000
sp|P21796 24.05	24.05	47	Voltage-dependent anion-selective channel protein 1 OS=Homo sapiens GN=VDAC1 PE=1 SV=2	0.658	0.002
sp|P16401 19.25	32.15	42.48	Histone H1.5 OS=Homo sapiens GN=HIST1H1B PE=1 SV=3	0.622	0.000
sp|P07305 6.2	6.2	15.46	Histone H1.0 OS=Homo sapiens GN=H1F0 PE=1 SV=3	0.619	0.018
sp|Q08722 5.55	5.55	5.882	Leukocyte surface antigen CD47 OS=Homo sapiens GN=CD47 PE=1 SV=1	0.612	0.026
sp|Q9Y6N5 42.34	42.34	54.22	Sulfide:quinone oxidoreductase, mitochondrial OS=Homo sapiens GN=SQRDL PE=1 SV=1	0.610	0.000
sp|Q9BQ62 2.16	2.26	14.77	Uncharacterized protein C19orf43 OS=Homo sapiens GN=C19orf43 PE=1 SV=1	0.579	0.022
sp|O43169 17.82	17.82	51.37	Cytochrome b5 type B OS=Homo sapiens GN=CYB5B PE=1 SV=2	0.558	0.000
sp|P05783 36.65	38.25	51.4	Keratin, type I cytoskeletal 18 OS=Homo sapiens GN=KRT18 PE=1 SV=2	0.550	0.000
sp|P05787 68.02	68.02	63.56	Keratin, type II cytoskeletal 8 OS=Homo sapiens GN=KRT8 PE=1 SV=7	0.549	0.000
sp|P05387 38.18	38.18	85.22	60S acidic ribosomal protein P2 OS=Homo sapiens GN=RPLP2 PE=1 SV=1	0.468	0.000
sp|P49006 30.87	31.03	86.15	MARCKS-related protein OS=Homo sapiens GN=MARCKSL1 PE=1 SV=2	0.447	0.001

264

C: Comparison of TGFβ treated HT29 β6AS/untreated HT29 β6AS

Uniprot	Unused	Total	X.Cov.95.	Protein Name; Organism; Gene name	iTRAQ Fold Change	StouffersPval
sp|P05109	2.11	2.11	11.83	Protein S100-A8 OS=Homo sapiens GN=S100A8 PE=1 SV=1	9.245	0.050
sp|P08779	10.07	18.66	28.12	Keratin, type I cytoskeletal 16 OS=Homo sapiens GN=KRT16 PE=1 SV=4	5.810	0.046
sp|Q04695	11.92	21.44	30.56	Keratin, type I cytoskeletal 17 OS=Homo sapiens GN=KRT17 PE=1 SV=2	5.128	0.019
sp|P02538	30.66	36.56	33.51	Keratin, type II cytoskeletal 6A OS=Homo sapiens GN=KRT6A PE=1 SV=3	4.915	0.002
sp|P13645	17.45	20.69	26.54	Keratin, type I cytoskeletal 10 OS=Homo sapiens GN=KRT10 PE=1 SV=6	2.233	0.000
sp|Q9Y653	5.16	5.18	7.071	G-protein coupled receptor 56 OS=Homo sapiens GN=GPR56 PE=1 SV=2	2.139	0.000
sp|P04264	18.1	22.23	15.68	Keratin, type II cytoskeletal 1 OS=Homo sapiens GN=KRT1 PE=1 SV=6	2.010	0.003
sp|P68371	4.15	23.87	34.16	Tubulin beta-4B chain OS=Homo sapiens GN=TUBB4B PE=1 SV=1	1.974	0.040
sp|P07437	26.97	26.97	40.77	Tubulin beta chain OS=Homo sapiens GN=TUBB PE=1 SV=2	1.937	0.017
sp|Q8N165	14	14	14.95	DBIRD complex subunit KIAA1967 OS=Homo sapiens GN=KIAA1967 PE=1 SV=2	1.595	0.002
sp|P11166	6	6	10.16	Solute carrier family 2, facilitated glucose transporter member 1 OS=Homo sapiens GN=SLC2A1 PE=1 SV=2	1.521	0.034
sp|P19338	43.96	45.54	25.63	Nucleolin OS=Homo sapiens GN=NCL PE=1 SV=3	1.467	0.000
sp|Q01844	11.78	11.78	17.07	RNA-binding protein EWS OS=Homo sapiens GN=EWSR1 PE=1 SV=1	1.432	0.026
sp|P52272	22.78	22.78	25.21	Heterogeneous nuclear ribonucleoprotein M OS=Homo sapiens GN=HNRNPM PE=1 SV=3	1.431	0.000
sp|Q9UQ3	2.32	2.32	0.6177	Serine/arginine repetitive matrix protein 2 OS=Homo sapiens GN=SRRM2 PE=1 SV=2	1.410	0.017
sp|P62906	17.26	17.26	42.86	60S ribosomal protein L10a OS=Homo sapiens GN=RPL10A PE=1 SV=2	1.401	0.043
sp|P36578	29.26	29.65	36.3	60S ribosomal protein L4 OS=Homo sapiens GN=RPL4 PE=1 SV=5	1.392	0.004
sp|Q92665	7.51	7.53	15.19	28S ribosomal protein S31, mitochondrial OS=Homo sapiens GN=MRPS31 PE=1 SV=3	1.356	0.024
sp|Q9NR30	4.94	4.95	5.492	Nucleolar RNA helicase 2 OS=Homo sapiens GN=DDX21 PE=1 SV=5	1.355	0.022
sp|P60660	11.59	11.59	52.98	Myosin light polypeptide 6 OS=Homo sapiens GN=MYL6 PE=1 SV=2	1.353	0.016
sp|Q56VL3	10.19	10.19	31.82	OCIA domain-containing protein 2 OS=Homo sapiens GN=OCIAD2 PE=1 SV=1	1.333	0.001
sp|P42166	44.45	44.45	43.95	Lamina-associated polypeptide 2, isoform alpha OS=Homo sapiens GN=TMPO PE=1 SV=2	1.331	0.001
sp|P43243	13.13	13.13	12.99	Matrin-3 OS=Homo sapiens GN=MATR3 PE=1 SV=2	1.321	0.006
sp|Q15029	5.63	5.63	5.041	116 kDa U5 small nuclear ribonucleoprotein component OS=Homo sapiens GN=EFTUD2 PE=1 SV=1	1.320	0.005
sp|Q08211	17.96	17.96	10.08	ATP-dependent RNA helicase A OS=Homo sapiens GN=DHX9 PE=1 SV=4	1.319	0.000
sp|P02545	78.13	78.13	56.33	Prelamin-A/C OS=Homo sapiens GN=LMNA PE=1 SV=1	1.315	0.001
sp|P35900	11.54	13.58	20.99	Keratin, type I cytoskeletal 20 OS=Homo sapiens GN=KRT20 PE=1 SV=1	1.314	0.019
sp|P14866	8.54	8.54	13.07	Heterogeneous nuclear ribonucleoprotein L OS=Homo sapiens GN=HNRNPL PE=1 SV=2	1.309	0.010
sp|P18124	20.55	20.55	33.06	60S ribosomal protein L7 OS=Homo sapiens GN=RPL7 PE=1 SV=1	1.309	0.034
sp|P10809	7.98	8.04	17.63	60 kDa heat shock protein, mitochondrial OS=Homo sapiens GN=HSPD1 PE=1 SV=2	1.305	0.042
sp|O75489	16.04	16.04	40.91	NADH dehydrogenase [ubiquinone] iron-sulfur protein 3, mitochondrial OS=Homo sapiens GN=NDUFS3 PE=1 SV=1	1.305	0.011
sp|P41091	10.01	10.06	17.16	Eukaryotic translation initiation factor 2 subunit 3 OS=Homo sapiens GN=EIF2S3 PE=1 SV=3	1.303	0.017
sp|Q12906	8.56	8.56	8.389	Interleukin enhancer-binding factor 3 OS=Homo sapiens GN=ILF3 PE=1 SV=3	1.300	0.013
sp|P61247	12.73	12.73	22.73	40S ribosomal protein S3a OS=Homo sapiens GN=RPS3A PE=1 SV=2	1.288	0.020
sp|O75643	2.3	3.29	0.9831	U5 small nuclear ribonucleoprotein 200 kDa helicase OS=Homo sapiens GN=SNRNP200 PE=1 SV=2	1.277	0.024
sp|Q9UJZ1	16	16	37.36	Stomatin-like protein 2, mitochondrial OS=Homo sapiens GN=STOML2 PE=1 SV=1	1.273	0.032
sp|Q14980	32.5	32.53	14.99	Nuclear mitotic apparatus protein 1 OS=Homo sapiens GN=NUMA1 PE=1 SV=2	1.264	0.001
sp|Q92841	19.88	19.88	23.05	Probable ATP-dependent RNA helicase DDX17 OS=Homo sapiens GN=DDX17 PE=1 SV=2	1.261	0.047
sp|P27816	8.42	8.42	9.462	Microtubule-associated protein 4 OS=Homo sapiens GN=MAP4 PE=1 SV=3	1.261	0.046
sp|P06748	15.46	15.46	32.65	Nucleophosmin OS=Homo sapiens GN=NPM1 PE=1 SV=2	1.251	0.031
sp|Q15149	12.21	12.29	1.601	Plectin OS=Homo sapiens GN=PLEC PE=1 SV=3	1.251	0.004
sp|P07814	18.15	18.15	10.98	Bifunctional glutamate/proline--tRNA ligase OS=Homo sapiens GN=EPRS PE=1 SV=5	1.248	0.007
sp|P17301	23.24	23.97	18.29	Integrin alpha-2 OS=Homo sapiens GN=ITGA2 PE=1 SV=1	1.222	0.000
sp|P61978	26.64	26.64	35.42	Heterogeneous nuclear ribonucleoprotein K OS=Homo sapiens GN=HNRNPK PE=1 SV=1	1.218	0.010
sp|Q9BYG3	6.22	6.22	20.48	MKI67 FHA domain-interacting nucleolar phosphoprotein OS=Homo sapiens GN=MKI67IP PE=1 SV=1	1.218	0.009
sp|P08582	8.79	8.79	8.672	Melanotransferrin OS=Homo sapiens GN=MFI2 PE=1 SV=2	0.817	0.012
sp|Q14165	25.13	25.13	48.97	Malectin OS=Homo sapiens GN=MLEC PE=1 SV=1	0.809	0.017
sp|P51690	14.91	14.91	21.05	Arylsulfatase E OS=Homo sapiens GN=ARSE PE=1 SV=2	0.809	0.040
sp|Q15019	20	20	47.09	Septin-2 OS=Homo sapiens GN=SEPT2 PE=1 SV=1	0.803	0.006
sp|P54920	17	17	39.66	Alpha-soluble NSF attachment protein OS=Homo sapiens GN=NAPA PE=1 SV=3	0.798	0.020
sp|P04844	9.52	9.52	12.52	Dolichyl-diphosphooligosaccharide--protein glycosyltransferase subunit 2 OS=Homo sapiens GN=RPN2 PE=1 SV=3	0.796	0.020
sp|P10646	9.23	9.23	25	Tissue factor pathway inhibitor OS=Homo sapiens GN=TFPI PE=1 SV=1	0.786	0.043
sp|Q99623	22.07	22.07	45.82	Prohibitin-2 OS=Homo sapiens GN=PHB2 PE=1 SV=2	0.778	0.000
sp|Q9Y394	22.02	22.02	39.23	Dehydrogenase/reductase SDR family member 7 OS=Homo sapiens GN=DHRS7 PE=1 SV=1	0.778	0.001
sp|P37802	6.03	7.01	25.63	Transgelin-2 OS=Homo sapiens GN=TAGLN2 PE=1 SV=3	0.777	0.014
sp|Q8NBJ7	2.96	2.96	8.97	Sulfatase-modifying factor 2 OS=Homo sapiens GN=SUMF2 PE=1 SV=2	0.774	0.046
sp|O43169	17.82	17.82	51.37	Cytochrome b5 type B OS=Homo sapiens GN=CYB5B PE=1 SV=2	0.766	0.015
sp|Q14978	14.75	14.75	10.73	Nucleolar and coiled-body phosphoprotein 1 OS=Homo sapiens GN=NOLC1 PE=1 SV=2	0.758	0.009
sp|Q15907	17.56	17.56	46.33	Ras-related protein Rab-11B OS=Homo sapiens GN=RAB11B PE=1 SV=4	0.758	0.008
sp|P48449	13.56	13.57	12.98	Lanosterol synthase OS=Homo sapiens GN=LSS PE=1 SV=1	0.757	0.013
sp|Q6PIU2	3.53	3.53	11.52	Neutral cholesterol ester hydrolase 1 OS=Homo sapiens GN=NCEH1 PE=1 SV=3	0.744	0.007
sp|P20340	11.39	11.39	36.06	Ras-related protein Rab-6A OS=Homo sapiens GN=RAB6A PE=1 SV=3	0.741	0.003
sp|Q12907	24.37	24.37	44.51	Vesicular integral-membrane protein VIP36 OS=Homo sapiens GN=LMAN2 PE=1 SV=1	0.734	0.004
sp|P14314	15.33	15.35	20.64	Glucosidase 2 subunit beta OS=Homo sapiens GN=PRKCSH PE=1 SV=2	0.732	0.010
sp|P16070	30.09	30.09	16.85	CD44 antigen OS=Homo sapiens GN=CD44 PE=1 SV=3	0.730	0.033
sp|Q14697	13.76	13.76	8.263	Neutral alpha-glucosidase AB OS=Homo sapiens GN=GANAB PE=1 SV=3	0.716	0.032
sp|P78310	22.64	22.64	44.11	Coxsackievirus and adenovirus receptor OS=Homo sapiens GN=CXADR PE=1 SV=1	0.708	0.000
sp|O95721	16.37	16.37	42.64	Synaptosomal-associated protein 29 OS=Homo sapiens GN=SNAP29 PE=1 SV=1	0.706	0.003
sp|P07099	4.03	4.03	8.352	Epoxide hydrolase 1 OS=Homo sapiens GN=EPHX1 PE=1 SV=1	0.705	0.007
sp|Q96HY6	12.01	12.01	35.67	DDRGK domain-containing protein 1 OS=Homo sapiens GN=DDRGK1 PE=1 SV=2	0.701	0.003
sp|P21926	2.54	2.54	9.649	CD9 antigen OS=Homo sapiens GN=CD9 PE=1 SV=4	0.688	0.049
sp|Q96KN	3.2	3.2	13.55	Protein FAM84B OS=Homo sapiens GN=FAM84B PE=1 SV=1	0.686	0.049
sp|Q96AE4	31.22	31.22	30.12	Far upstream element-binding protein 1 OS=Homo sapiens GN=FUBP1 PE=1 SV=3	0.669	0.000
sp|P14927	16.24	16.24	45.95	Cytochrome b-c1 complex subunit 7 OS=Homo sapiens GN=UQCRB PE=1 SV=2	0.645	0.034
sp|Q9NQC	16.71	16.71	14.18	Reticulon-4 OS=Homo sapiens GN=RTN4 PE=1 SV=2	0.642	0.041
sp|P11279	9.76	9.76	17.99	Lysosome-associated membrane glycoprotein 1 OS=Homo sapiens GN=LAMP1 PE=1 SV=3	0.633	0.008
sp|Q8N4H5	3.25	3.25	27.45	Mitochondrial import receptor subunit TOM5 homolog OS=Homo sapiens GN=TOMM5 PE=1 SV=1	0.599	0.033
sp|P25398	9.32	9.32	49.24	40S ribosomal protein S12 OS=Homo sapiens GN=RPS12 PE=1 SV=3	0.586	0.002
sp|P02786	23.45	23.45	21.05	Transferrin receptor protein 1 OS=Homo sapiens GN=TFRC PE=1 SV=2	0.579	0.000
sp|Q96A26	8.82	8.83	22.73	Protein FAM162A OS=Homo sapiens GN=FAM162A PE=1 SV=2	0.568	0.012

D: Comparison of TGFβ treated HT29 Mock/TGFβ treated HT29 β6AS

Uniprot	Unused	Total	X.Cov.95.	Protein Name; Organism; Gene name	iTRAQ Fold Change	StouffersPval
sp|O95994	6.62	6.62	16.57	Anterior gradient protein 2 homolog OS=Homo sapiens GN=AGR2 PE=1 SV=1	2.963	0.016
sp|P06703	6.99	7.12	30	Protein S100-A6 OS=Homo sapiens GN=S100A6 PE=1 SV=1	2.890	0.023
sp|P11216	8.98	9.01	9.015	Glycogen phosphorylase, brain form OS=Homo sapiens GN=PYGB PE=1 SV=5	2.671	0.000
sp|P61626	7.35	7.35	39.86	Lysozyme C OS=Homo sapiens GN=LYZ PE=1 SV=1	2.427	0.009
sp|P21589	34.93	35.06	39.37	5'-nucleotidase OS=Homo sapiens GN=NT5E PE=1 SV=1	2.266	0.000

ID			Description	Ratio	p-value
sp|Q15019 20	20	47.09	Septin-2 OS=Homo sapiens GN=SEPT2 PE=1 SV=1	2.246	0.000
sp|Q99880 4.34	20.28	46.03	Histone H2B type 1-L OS=Homo sapiens GN=HIST1H2BL PE=1 SV=3	2.195	0.017
sp|P30101 20.88	20.88	23.17	Protein disulfide-isomerase A3 OS=Homo sapiens GN=PDIA3 PE=1 SV=4	2.168	0.000
sp|Q9UHD 9.57	9.57	19.97	Septin-9 OS=Homo sapiens GN=SEPT9 PE=1 SV=2	2.154	0.003
sp|Q16181 9.73	9.73	18.99	Septin-7 OS=Homo sapiens GN=SEPT7 PE=1 SV=2	2.121	0.000
sp|P17931 12.67	12.67	34.4	Galectin-3 OS=Homo sapiens GN=LGALS3 PE=1 SV=5	2.047	0.000
sp|P13667 6.31	6.34	11.94	Protein disulfide-isomerase A4 OS=Homo sapiens GN=PDIA4 PE=1 SV=2	1.987	0.002
sp|Q8WXX 7.34	7.36	17.31	DnaJ homolog subfamily C member 9 OS=Homo sapiens GN=DNAJC9 PE=1 SV=1	1.984	0.002
sp|Q9Y2W 4.53	4.53	3.351	Thyroid hormone receptor-associated protein 3 OS=Homo sapiens GN=THRAP3 PE=1 SV=2	1.980	0.008
sp|Q15233 27.2	29.48	38	Non-POU domain-containing octamer-binding protein OS=Homo sapiens GN=NONO PE=1 SV=4	1.934	0.000
sp|P35527 14.04	14.04	20.71	Keratin, type I cytoskeletal 9 OS=Homo sapiens GN=KRT9 PE=1 SV=3	1.921	0.000
sp|Q9UIG0 6.01	7.28	2.9	Tyrosine-protein kinase BAZ1B OS=Homo sapiens GN=BAZ1B PE=1 SV=2	1.913	0.012
sp|P11387 19.44	19.44	17.12	DNA topoisomerase 1 OS=Homo sapiens GN=TOP1 PE=1 SV=2	1.899	0.000
sp|Q9Y4L1 4.11	4.14	2.803	Hypoxia up-regulated protein 1 OS=Homo sapiens GN=HYOU1 PE=1 SV=1	1.899	0.030
sp|P23246 51.95	51.95	41.73	Splicing factor, proline- and glutamine-rich OS=Homo sapiens GN=SFPQ PE=1 SV=2	1.882	0.000
sp|P14314 15.33	15.35	20.64	Glucosidase 2 subunit beta OS=Homo sapiens GN=PRKCSH PE=1 SV=2	1.863	0.001
sp|Q86VM 4.08	4.11	4.512	Zinc finger CCCH domain-containing protein 18 OS=Homo sapiens GN=ZC3H18 PE=1 SV=2	1.835	0.033
sp|Q02818 6.1	6.12	12.58	Nucleobindin-1 OS=Homo sapiens GN=NUCB1 PE=1 SV=4	1.822	0.048
sp|Q16630 4.12	4.16	6.897	Cleavage and polyadenylation specificity factor subunit 6 OS=Homo sapiens GN=CPSF6 PE=1 SV=2	1.821	0.002
sp|Q15084 18.06	18.06	30.91	Protein disulfide-isomerase A6 OS=Homo sapiens GN=PDIA6 PE=1 SV=1	1.799	0.001
sp|Q14697 13.76	13.76	8.263	Neutral alpha-glucosidase AB OS=Homo sapiens GN=GANAB PE=1 SV=3	1.799	0.001
sp|Q53GQ 10.48	10.48	18.59	Estradiol 17-beta-dehydrogenase 12 OS=Homo sapiens GN=HSD17B12 PE=1 SV=2	1.786	0.024
sp|Q16778 23.63	23.64	55.56	Histone H2B type 2-E OS=Homo sapiens GN=HIST2H2BE PE=1 SV=3	1.759	0.011
sp|P11021 32.14	32.14	29.97	78 kDa glucose-regulated protein OS=Homo sapiens GN=HSPA5 PE=1 SV=2	1.754	0.000
sp|P35579 66.43	66.43	23.62	Myosin-9 OS=Homo sapiens GN=MYH9 PE=1 SV=4	1.745	0.000
sp|P11182 3.06	3.06	7.261	Lipoamide acyltransferase component of branched-chain alpha-keto acid dehydrogenase complex, mitochondrial OS	1.744	0.005
sp|P07237 17.05	17.05	30.91	Protein disulfide-isomerase OS=Homo sapiens GN=P4HB PE=1 SV=3	1.730	0.007
sp|O75367 23.86	27.99	45.97	Core histone macro-H2A.1 OS=Homo sapiens GN=H2AFY PE=1 SV=4	1.725	0.001
sp|O14745 4.54	4.54	15.36	Na(+)/H(+) exchange regulatory cofactor NHE-RF1 OS=Homo sapiens GN=SLC9A3R1 PE=1 SV=4	1.719	0.005
sp|P14625 6.53	6.53	8.468	Endoplasmin OS=Homo sapiens GN=HSP90B1 PE=1 SV=1	1.719	0.016
sp|O43707 22.93	22.93	19.54	Alpha-actinin-4 OS=Homo sapiens GN=ACTN4 PE=1 SV=2	1.701	0.000
sp|Q15424 12	12	8.852	Scaffold attachment factor B1 OS=Homo sapiens GN=SAFB PE=1 SV=4	1.689	0.042
sp|P04439 8.32	8.32	17.26	HLA class I histocompatibility antigen, A-3 alpha chain OS=Homo sapiens GN=HLA-A PE=1 SV=2	1.659	0.014
sp|Q92896 9.24	9.24	5.683	Golgi apparatus protein 1 OS=Homo sapiens GN=GLG1 PE=1 SV=2	1.654	0.004
sp|P13688 6.44	6.54	11.98	Carcinoembryonic antigen-related cell adhesion molecule 1 OS=Homo sapiens GN=CEACAM1 PE=1 SV=2	1.651	0.022
sp|P17480 13.11	13.11	12.3	Nucleolar transcription factor 1 OS=Homo sapiens GN=UBTF PE=1 SV=1	1.635	0.000
sp|P62937 18.72	20.77	69.7	Peptidyl-prolyl cis-trans isomerase A OS=Homo sapiens GN=PPIA PE=1 SV=2	1.602	0.011
sp|Q9UJS0 6.08	6.08	8.741	Calcium-binding mitochondrial carrier protein Aralar2 OS=Homo sapiens GN=SLC25A13 PE=1 SV=2	1.596	0.040
sp|P35900 11.54	13.58	20.99	Keratin, type I cytoskeletal 20 OS=Homo sapiens GN=KRT20 PE=1 SV=1	1.595	0.020
sp|P22307 6.9	6.92	5.667	Non-specific lipid-transfer protein OS=Homo sapiens GN=SCP2 PE=1 SV=2	1.581	0.016
sp|Q8WXF 13.64	13.74	17.59	Paraspeckle component 1 OS=Homo sapiens GN=PSPC1 PE=1 SV=1	1.572	0.001
sp|Q03252 24.61	33.01	36.17	Lamin-B2 OS=Homo sapiens GN=LMNB2 PE=1 SV=3	1.562	0.000
sp|P16401 19.25	32.15	42.48	Histone H1.5 OS=Homo sapiens GN=HIST1H1B PE=1 SV=3	1.558	0.041
sp|Q9UKV 10.33	10.43	5.891	Apoptotic chromatin condensation inducer in the nucleus OS=Homo sapiens GN=ACIN1 PE=1 SV=2	1.552	0.048
sp|P43304 4.45	4.45	5.089	Glycerol-3-phosphate dehydrogenase, mitochondrial OS=Homo sapiens GN=GPD2 PE=1 SV=3	1.547	0.004
sp|P55265 9.87	9.9	6.607	Double-stranded RNA-specific adenosine deaminase OS=Homo sapiens GN=ADAR PE=1 SV=4	1.532	0.019
sp|Q9HDC 29.18	29.18	38.22	Adipocyte plasma membrane-associated protein OS=Homo sapiens GN=APMAP PE=1 SV=2	1.530	0.003
sp|Q9BWF 4.04	4.04	16.48	RNA-binding protein 4 OS=Homo sapiens GN=RBM4 PE=1 SV=1	1.526	0.038
sp|P50454 6.36	6.36	15.07	Serpin H1 OS=Homo sapiens GN=SERPINH1 PE=1 SV=2	1.524	0.020
sp|P26038 24.32	24.36	24.61	Moesin OS=Homo sapiens GN=MSN PE=1 SV=3	1.523	0.001
sp|P30086 1.67	1.67	25.13	Phosphatidylethanolamine-binding protein 1 OS=Homo sapiens GN=PEBP1 PE=1 SV=3	1.516	0.039
sp|Q14676 4.25	4.28	2.489	Mediator of DNA damage checkpoint protein 1 OS=Homo sapiens GN=MDC1 PE=1 SV=3	1.515	0.010
sp|P63261 57.23	57.23	62.93	Actin, cytoplasmic 2 OS=Homo sapiens GN=ACTG1 PE=1 SV=1	1.507	0.013
sp|Q15365 8.03	8.11	22.47	Poly(rC)-binding protein 1 OS=Homo sapiens GN=PCBP1 PE=1 SV=2	1.503	0.037
sp|Q9HBR0 10.74	10.85	9.115	Putative sodium-coupled neutral amino acid transporter 10 OS=Homo sapiens GN=SLC38A10 PE=1 SV=2	1.494	0.034
sp|P07910 16.4	16.7	28.43	Heterogeneous nuclear ribonucleoproteins C1/C2 OS=Homo sapiens GN=HNRNPC PE=1 SV=4	1.476	0.002
sp|Q02127 23.03	23.03	47.59	Dihydroorotate dehydrogenase (quinone), mitochondrial OS=Homo sapiens GN=DHODH PE=1 SV=3	1.460	0.029
sp|Q07955 15.44	15.45	34.68	Serine/arginine-rich splicing factor 1 OS=Homo sapiens GN=SRSF1 PE=1 SV=2	1.459	0.006
sp|O60664 15.54	15.54	33.18	Perilipin-3 OS=Homo sapiens GN=PLIN3 PE=1 SV=3	1.447	0.000
sp|P09429 5.9	5.91	18.6	High mobility group protein B1 OS=Homo sapiens GN=HMGB1 PE=1 SV=3	1.439	0.025
sp|P55011 15.1	15.1	11.88	Solute carrier family 12 member 2 OS=Homo sapiens GN=SLC12A2 PE=1 SV=1	1.430	0.002
sp|P04040 10.07	10.07	21.44	Catalase OS=Homo sapiens GN=CAT PE=1 SV=3	1.426	0.042
sp|Q96I24 9.29	13.45	25.7	Far upstream element-binding protein 3 OS=Homo sapiens GN=FUBP3 PE=1 SV=2	1.426	0.036
sp|P35221 34.39	34.88	27.37	Catenin alpha-1 OS=Homo sapiens GN=CTNNA1 PE=1 SV=1	1.414	0.018
sp|Q08945 12.65	12.65	12.55	FACT complex subunit SSRP1 OS=Homo sapiens GN=SSRP1 PE=1 SV=1	1.409	0.028
sp|Q8NBJ7 2.96	2.96	8.97	Sulfatase-modifying factor 2 OS=Homo sapiens GN=SUMF2 PE=1 SV=2	1.404	0.017
sp|P60174 2.84	2.84	17.83	Triosephosphate isomerase OS=Homo sapiens GN=TPI1 PE=1 SV=3	1.402	0.023
sp|P09874 41.41	41.41	29.78	Poly [ADP-ribose] polymerase 1 OS=Homo sapiens GN=PARP1 PE=1 SV=4	1.380	0.000
sp|O95721 16.37	16.37	42.64	Synaptosomal-associated protein 29 OS=Homo sapiens GN=SNAP29 PE=1 SV=1	1.380	0.002
sp|Q56VL3 10.19	10.19	31.82	OCIA domain-containing protein 2 OS=Homo sapiens GN=OCIAD2 PE=1 SV=1	1.379	0.000
sp|Q9Y653 5.18	5.18	7.071	G-protein coupled receptor 56 OS=Homo sapiens GN=GPR56 PE=1 SV=2	1.377	0.004
sp|P09622 10	10.01	15.91	Dihydrolipoyl dehydrogenase, mitochondrial OS=Homo sapiens GN=DLD PE=1 SV=2	1.353	0.048
sp|Q9NQ5 6.06	6.06	25.73	39S ribosomal protein L40, mitochondrial OS=Homo sapiens GN=MRPL40 PE=1 SV=1	1.352	0.024
sp|O60716 12.95	12.95	16.43	Catenin delta-1 OS=Homo sapiens GN=CTNND1 PE=1 SV=1	1.349	0.011
sp|P46013 25.52	25.52	6.357	Antigen KI-67 OS=Homo sapiens GN=MKI67 PE=1 SV=2	1.328	0.026
sp|Q05519 2.78	2.78	5.992	Serine/arginine-rich splicing factor 11 OS=Homo sapiens GN=SRSF11 PE=1 SV=1	1.316	0.042
sp|Q92841 19.88	19.88	23.05	Probable ATP-dependent RNA helicase DDX17 OS=Homo sapiens GN=DDX17 PE=1 SV=2	1.299	0.039
sp|P23786 26.46	26.46	31.16	Carnitine O-palmitoyltransferase 2, mitochondrial OS=Homo sapiens GN=CPT2 PE=1 SV=2	1.254	0.019
sp|P22695 14.5	14.5	28.48	Cytochrome b-c1 complex subunit 2, mitochondrial OS=Homo sapiens GN=UQCRC2 PE=1 SV=3	1.206	0.009
sp|P51690 14.91	14.91	21.05	Arylsulfatase E OS=Homo sapiens GN=ARSE PE=1 SV=2	0.822	0.018
sp|Q9Y224 3.89	3.89	18.85	UPF0568 protein C14orf166 OS=Homo sapiens GN=C14orf166 PE=1 SV=1	0.813	0.027
sp|P17301 23.24	23.97	18.29	Integrin alpha-2 OS=Homo sapiens GN=ITGA2 PE=1 SV=1	0.797	0.036
sp|P45880 14.43	16.47	38.78	Voltage-dependent anion-selective channel protein 2 OS=Homo sapiens GN=VDAC2 PE=1 SV=2	0.795	0.038
sp|P78310 22.64	22.64	44.11	Coxsackievirus and adenovirus receptor OS=Homo sapiens GN=CXADR PE=1 SV=1	0.795	0.019
sp|P25705 23.79	23.79	25.68	ATP synthase subunit alpha, mitochondrial OS=Homo sapiens GN=ATP5A1 PE=1 SV=1	0.773	0.001
sp|O75533 6.09	6.09	4.831	Splicing factor 3B subunit 1 OS=Homo sapiens GN=SF3B1 PE=1 SV=3	0.742	0.042
sp|P78371 15.92	15.92	25.98	T-complex protein 1 subunit beta OS=Homo sapiens GN=CCT2 PE=1 SV=4	0.741	0.004
sp|P06576 42.27	42.27	58.6	ATP synthase subunit beta, mitochondrial OS=Homo sapiens GN=ATP5B PE=1 SV=3	0.737	0.001
sp|Q04837 8.79	8.79	41.22	Single-stranded DNA-binding protein, mitochondrial OS=Homo sapiens GN=SSBP1 PE=1 SV=1	0.735	0.015
sp|P23396 8.06	8.06	21.4	40S ribosomal protein S3 OS=Homo sapiens GN=RPS3 PE=1 SV=2	0.727	0.029

266

sp|Q16891 26.59	26.87	30.34	Mitochondrial inner membrane protein OS=Homo sapiens GN=IMMT PE=1 SV=1	0.727	0.028
sp|P50990 11.03	11.03	14.6	T-complex protein 1 subunit theta OS=Homo sapiens GN=CCT8 PE=1 SV=4	0.724	0.008
sp|P40227 13.61	13.61	22.03	T-complex protein 1 subunit zeta OS=Homo sapiens GN=CCT6A PE=1 SV=3	0.719	0.037
sp|P46109 10.13	10.44	28.05	Crk-like protein 0 OS=Homo sapiens GN=CRKL PE=1 SV=1	0.718	0.005
sp|P02786 23.45	23.45	21.05	Transferrin receptor protein 1 OS=Homo sapiens GN=TFRC PE=1 SV=2	0.710	0.001
sp|Q99832 2.41	2.41	7.182	T-complex protein 1 subunit eta OS=Homo sapiens GN=CCT7 PE=1 SV=2	0.709	0.012
sp|Q9NVI7 6.52	6.52	12.3	ATPase family AAA domain-containing protein 3A OS=Homo sapiens GN=ATAD3A PE=1 SV=2	0.704	0.012
sp|P62910 7.98	7.98	29.63	60S ribosomal protein L32 OS=Homo sapiens GN=RPL32 PE=1 SV=2	0.703	0.033
sp|Q08380 7.48	7.48	10.26	Galectin-3-binding protein OS=Homo sapiens GN=LGALS3BP PE=1 SV=1	0.702	0.014
sp|P48643 16.66	16.7	21.07	T-complex protein 1 subunit epsilon OS=Homo sapiens GN=CCT5 PE=1 SV=1	0.700	0.004
sp|P05026 10.07	10.07	25.41	Sodium/potassium-transporting ATPase subunit beta-1 OS=Homo sapiens GN=ATP1B1 PE=1 SV=1	0.699	0.025
sp|Q99536 13.69	13.7	26.97	Synaptic vesicle membrane protein VAT-1 homolog OS=Homo sapiens GN=VAT1 PE=1 SV=2	0.693	0.006
sp|Q9Y394 22.02	22.02	39.23	Dehydrogenase/reductase SDR family member 7 OS=Homo sapiens GN=DHRS7 PE=1 SV=1	0.687	0.003
sp|Q16134 13.65	13.65	22.69	Electron transfer flavoprotein-ubiquinone oxidoreductase, mitochondrial OS=Homo sapiens GN=ETFDH PE=1 SV=2	0.682	0.003
sp|Q2VIR3 4.22	4.22	11.86	Putative eukaryotic translation initiation factor 2 subunit 3-like protein OS=Homo sapiens GN=EIF2S3L PE=5 SV=2	0.680	0.042
sp|P62851 10.57	10.57	24.8	40S ribosomal protein S25 OS=Homo sapiens GN=RPS25 PE=1 SV=1	0.679	0.045
sp|P52597 12.8	12.82	23.37	Heterogeneous nuclear ribonucleoprotein F OS=Homo sapiens GN=HNRNPF PE=1 SV=3	0.675	0.017
sp|P49368 12.36	12.36	18.35	T-complex protein 1 subunit gamma OS=Homo sapiens GN=CCT3 PE=1 SV=4	0.665	0.002
sp|Q9Y6N5 42.34	42.34	54.22	Sulfide:quinone oxidoreductase, mitochondrial OS=Homo sapiens GN=SQRDL PE=1 SV=1	0.664	0.000
sp|P18084 20.32	20.32	16.9	Integrin beta-5 OS=Homo sapiens GN=ITGB5 PE=1 SV=1	0.661	0.001
sp|Q13428 5.67	5.67	6.384	Treacle protein OS=Homo sapiens GN=TCOF1 PE=1 SV=3	0.661	0.036
sp|P54709 6.32	6.35	21.15	Sodium/potassium-transporting ATPase subunit beta-3 OS=Homo sapiens GN=ATP1B3 PE=1 SV=1	0.655	0.004
sp|Q08431 8.05	8.06	17.83	Lactadherin OS=Homo sapiens GN=MFGE8 PE=1 SV=2	0.654	0.014
sp|P36578 29.26	29.65	36.3	60S ribosomal protein L4 OS=Homo sapiens GN=RPL4 PE=1 SV=5	0.649	0.024
sp|P05023 15.87	15.87	10.85	Sodium/potassium-transporting ATPase subunit alpha-1 OS=Homo sapiens GN=ATP1A1 PE=1 SV=1	0.642	0.001
sp|P49748 26.61	26.65	31.76	Very long-chain specific acyl-CoA dehydrogenase, mitochondrial OS=Homo sapiens GN=ACADVL PE=1 SV=1	0.639	0.000
sp|P57735 4.06	5.08	19.72	Ras-related protein Rab-25 OS=Homo sapiens GN=RAB25 PE=1 SV=2	0.638	0.042
sp|P42166 44.45	44.45	43.95	Lamina-associated polypeptide 2, isoform alpha OS=Homo sapiens GN=TMPO PE=1 SV=2	0.636	0.000
sp|P06756 33.34	33.34	22.71	Integrin alpha-V OS=Homo sapiens GN=ITGAV PE=1 SV=2	0.632	0.000
sp|P10620 3.89	3.89	9.032	Microsomal glutathione S-transferase 1 OS=Homo sapiens GN=MGST1 PE=1 SV=1	0.628	0.023
sp|P10809 7.98	8.04	17.63	60 kDa heat shock protein, mitochondrial OS=Homo sapiens GN=HSPD1 PE=1 SV=2	0.622	0.005
sp|Q96AP7 12.78	12.79	30.77	Endothelial cell-selective adhesion molecule OS=Homo sapiens GN=ESAM PE=1 SV=1	0.621	0.001
sp|P51149 26.13	26.13	62.8	Ras-related protein Rab-7a OS=Homo sapiens GN=RAB7A PE=1 SV=1	0.616	0.002
sp|P42167 14.49	33.01	43.39	Lamina-associated polypeptide 2, isoforms beta/gamma OS=Homo sapiens GN=TMPO PE=1 SV=2	0.614	0.008
sp|Q5ZPR3 8.31	8.31	20.97	CD276 antigen OS=Homo sapiens GN=CD276 PE=1 SV=1	0.604	0.005
sp|Q15758 8.97	8.97	10.72	Neutral amino acid transporter B(0) OS=Homo sapiens GN=SLC1A5 PE=1 SV=2	0.587	0.001
sp|P13073 11.21	11.21	31.95	Cytochrome c oxidase subunit 4 isoform 1, mitochondrial OS=Homo sapiens GN=COX4I1 PE=1 SV=1	0.580	0.048
sp|Q15907 17.56	17.56	46.33	Ras-related protein Rab-11B OS=Homo sapiens GN=RAB11B PE=1 SV=4	0.579	0.002
sp|O43570 3.22	3.23	14.97	Carbonic anhydrase 12 OS=Homo sapiens GN=CA12 PE=1 SV=1	0.578	0.013
sp|P08174 29.55	29.55	38.06	Complement decay-accelerating factor OS=Homo sapiens GN=CD55 PE=1 SV=4	0.576	0.000
sp|Q00610 10.26	10.26	5.134	Clathrin heavy chain 1 OS=Homo sapiens GN=CLTC PE=1 SV=5	0.548	0.013
sp|Q9BQG 6	6.01	3.012	Myb-binding protein 1A OS=Homo sapiens GN=MYBBP1A PE=1 SV=2	0.548	0.012
sp|Q9UHA 2.31	2.31	12.9	Ragulator complex protein LAMTOR3 OS=Homo sapiens GN=LAMTOR3 PE=1 SV=1	0.544	0.027
sp|P50991 10.25	12.1	19.85	T-complex protein 1 subunit delta OS=Homo sapiens GN=CCT4 PE=1 SV=4	0.542	0.001
sp|P27487 15.18	15.18	12.27	Dipeptidyl peptidase 4 OS=Homo sapiens GN=DPP4 PE=1 SV=2	0.537	0.000
sp|P39023 6.02	6.08	12.9	60S ribosomal protein L3 OS=Homo sapiens GN=RPL3 PE=1 SV=2	0.535	0.013
sp|P19224 10.71	10.73	13.16	UDP-glucuronosyltransferase 1-6 OS=Homo sapiens GN=UGT1A6 PE=1 SV=2	0.532	0.033
sp|P08582 8.79	8.79	8.672	Melanotransferrin OS=Homo sapiens GN=MFI2 PE=1 SV=2	0.522	0.007
sp|Q14165 25.13	25.13	48.97	Malectin OS=Homo sapiens GN=MLEC PE=1 SV=1	0.510	0.000
sp|P05387 38.18	38.18	85.22	60S acidic ribosomal protein P2 OS=Homo sapiens GN=RPLP2 PE=1 SV=1	0.497	0.025
sp|Q8N4H3.25	3.25	27.45	Mitochondrial import receptor subunit TOM5 homolog OS=Homo sapiens GN=TOMM5 PE=1 SV=1	0.496	0.029
sp|O14561 6.89	6.89	22.44	Acyl carrier protein, mitochondrial OS=Homo sapiens GN=NDUFAB1 PE=1 SV=3	0.487	0.039
sp|P55061 2.16	2.16	3.797	Bax inhibitor 1 OS=Homo sapiens GN=TMBIM6 PE=1 SV=2	0.473	0.040
sp|Q9UKS4.63	4.63	7.075	Protein kinase C and casein kinase substrate in neurons protein 3 OS=Homo sapiens GN=PACSIN3 PE=1 SV=2	0.467	0.031
sp|Q07021 8.45	8.45	26.6	Complement component 1 Q subcomponent-binding protein, mitochondrial OS=Homo sapiens GN=C1QBP PE=1 SV=0.463	0.463	0.014
sp|P09758 4.09	4.09	10.22	Tumor-associated calcium signal transducer 2 OS=Homo sapiens GN=TACSTD2 PE=1 SV=3	0.400	0.028
sp|Q71U18.86	18.86	39.47	Tubulin alpha-1A chain OS=Homo sapiens GN=TUBA1A PE=1 SV=1	0.381	0.022
sp|P07437 26.97	26.97	40.77	Tubulin beta chain OS=Homo sapiens GN=TUBB PE=1 SV=2	0.379	0.026
sp|P43121 18.25	18.25	27.86	Cell surface glycoprotein MUC18 OS=Homo sapiens GN=MCAM PE=1 SV=2	0.363	0.000
sp|P62979 11.47	11.47	41.03	Ubiquitin-40S ribosomal protein S27a OS=Homo sapiens GN=RPS27A PE=1 SV=2	0.348	0.002
sp|O75531 6.52	6.52	40.45	Barrier-to-autointegration factor OS=Homo sapiens GN=BANF1 PE=1 SV=1	0.331	0.017
sp|P02538 30.66	36.56	33.51	Keratin, type II cytoskeletal 6A OS=Homo sapiens GN=KRT6A PE=1 SV=3	0.195	0.003
sp|Q04695 11.92	21.44	30.56	Keratin, type I cytoskeletal 17 OS=Homo sapiens GN=KRT17 PE=1 SV=2	0.194	0.003
sp|P06702 6.02	6.04	44.74	Protein S100-A9 OS=Homo sapiens GN=S100A9 PE=1 SV=1	0.163	0.033

267

268

CHAPTER 4

The subsequent study then aimed to further evaluate the associations of uPAR and TGFβ in the context of CRC using HCT116 colon cancer cells. The HCT116^{WT} cells endogenously express uPAR and this expression has be artificially decreased by 35% in the HCT116^{uPARAS} cells. This study used a similar approach to that of the previous proteomics experiment in Chapter 3, Study II. Preliminary proliferation and invasion assays determined that TGFβ did not significantly affect the proliferation or invasion of HCT116 WT cells, although HCT116 ASuPAR cells, with reduced uPAR expression, exhibited significantly decreased proliferation and invasion following TGFβ treatment. The observations when investigated by proteomics showed differential up- and down-regulation of various proteins in a TGFβ-dependent or –independent manner in HCT116^{WT} cells relative to HCT116^{uPARAS} cells. Some of the cellular process that were associated with these proteins included cell adhesion, migration, invasion and cytoskeletal signalling which were also determined by IPA to be significantly altered. IPA also indicated eIF2 signalling pathway to be significantly altered and cancer was observed to be one of the top three diseases. Overall, the observations from cell-based and proteomic studies demonstrated that cells with endogenous uPAR expression do not respond to TGFβ treatment, whilst inhibiting metastatic phenotypes in cells with decrease in uPAR expression.

4.1 - Does differential expression of cell-surface uPAR alter the effects active TGFβ has on the colorectal cancer cell membrane proteome? [Publication V] *(Prepared for publication)*

Does differential expression of cell-surface uPAR alter the effects active TGFβ has on the colorectal cancer cell membrane proteome?

Harish R Cheruku[1], David I Cantor[1], Abidali Mohamedali[2], Sock Hwee Tan[2,3], Edouard C Nice[4], Mark S Baker[1]*

[1]*Department of Biomedical Sciences, Faculty of Health and Medical Sciences, Macquarie University, NSW, 2109, Australia*

[2]*Department of Chemistry and Biomolecular Sciences, Faculty of Science, Macquarie University, NSW, 2109, Australia*

[3]*Current address: National University Heart Centre, National University of Singapore, Singapore, Singapore*

[4]*Department of Biochemistry and Molecular Biology, Monash University, Clayton, Victoria, 3800, Australia*

*Corresponding Author
Professor Mark S. Baker
Faculty of Health and Medical Sciences
2 Technology Place
Macquarie University, NSW, 2109
Australia
Telephone: +61 2 9850 8211
Fax: +61 2 9850 8313
E mail: mark.baker@mq.edu.au

Abstract

Urokinase-type plasminogen activator receptor (uPAR) and transforming growth factor-β (TGFβ) have been widely implicated in different biologies in CRC, wherein the cell-surface plasminogen activation cascade (in part mediated by uPAR) has been identified as one means of latent TGFβ activation. However, the effects of TGFβ on uPAR and vice-versa remain poorly understood in CRC. To investigate the biological effect/s of TGFβ when uPAR is artificially suppressed, this study treated wild type HCT116^{WT} and uPAR-suppressed (~35%↓) HCT116$^{uPAR-AS}$ colon cancer cells with active TGFβ and then performed cell membrane-enriched quantitative proteomic analysis. Preliminary proliferation and invasion assays determined that TGFβ did not significantly affect either proliferation or invasion of HCT116^{WT} cells, although HCT116$^{uPAR-AS}$ exhibited significantly decreased proliferation (24%↓) following TGFβ treatment and invasion (~20%↓) following SB431542 inhibition or dual SB431542 and TGFβ treatment. These puzzling differential effects between cell lines were subsequently investigated by proteomics. IPA analyses of the data demonstrated that several proteins related to cytoskeletal signalling, cell adhesion, migration, cell death and survival, protein trafficking and the eIF2 signalling pathway were significantly up- or down-regulated in either in a TGFβ-dependent or a TGFβ-independent manner. Three proteins of interest (ezrin, annexin A2 and Ras-related protein Rab-10) were further validated by Western blotting to confirm that expression changes observed by iTRAQ. Overall, cell-based and proteomic studies have demonstrated that when uPAR expression is decreased, active TGFβ suppresses metastatic phenotypes though this effect is lost with increased uPAR expression. These observations demonstrate that elevated uPAR expression promotes proliferation and invasion in a TGFβ-independent manner while TGFβ exerts growth inhibitory effects when uPAR expression is decreased.

Keywords: transforming growth factor-β; uPAR; colorectal cancer; HCT116; iTRAQ

1. INTRODUCTION

World Health Organisation indicated that colorectal cancer (CRC) is the third most common malignancy (~1.36 million cases worldwide in 2012) with a mortality rate 55% [1]. Metastases, rather than primary tumours, are responsible for the majority (almost 90%) of cancer deaths [2, 3]. Metastasis is a cascade of complex molecular interactions between various proteins that can alter and regulate signalling pathways required for primary tumours to spread to distant organs [2]. Proteins such as urokinase-type plasminogen activator receptor (uPA/uPAR) [4], transforming growth factor-beta (TGFβ) [5], integrin αvβ6 [6], various mitogen-activated protein kinases (i.e., Erk, p38, Jnk, Ras) [7] and MMPs [8, 9] have been widely implicated in CRC.

In addition, the epithelial–mesenchymal transition (EMT) a key process for metastasis [10]. EMT is primarily facilitated by the loss/degradation of extracellular matrix (ECM) structure that allows for cancer cells to escape and spread to neighbouring tissues and distant organs [10]. In cancer, changes to ECM structure contribute to altered adhesion which is thought to be controlled by proteolysis [11]. uPAR, a cell surface receptor bound to the plasma membrane through a glycosyl phosphatidylinositol (GPI) anchor, is known to regulate ECM proteolysis, cell-ECM interactions and cell signalling [11]. uPAR primarily focusses plasminogen activation (PA) to the cell-surface by binding active twin chain uPA (urokinase-type plasminogen activator) as well as its single chain zymogen form sc-uPA [11]. Active uPA catalyses the conversion of zymogen plasminogen to active plasmin (a broad spectrum serine protease), which through positive-feedback can activate both zymogen forms of uPA and plasmin. Plasmin can degrade various ECM molecules such as fibrin, fibronectin and laminin while also activating matrix metalloproteinases (MMP)-1, MMP-3, MMP-9, MMP-12 and MMP-13 [11]. Interestingly, plasmin and MMPs such as MMP-2 and MMP-9 are both known to activate latent-TGFβ (L-TGFβ) [8, 12].

The (canonical) TGFβ signalling cascade in normal cells is known to promote tumour suppression through cytostasis, cell differentiation and apoptosis [13]. During cancer, however, TGFβ plays a dual role wherein it either strongly promotes cell growth suppression in the early stages but then switches to promote tumour growth, invasion, and metastasis during mid to late stages [13, 14]. The biological mechanism/s explaining this switch to promote tumour growth and metastasis are poorly characterised. However, it is known that active TGFβ during CRC is found at very high levels (14.8 ± 8.4 ng/mL) compared to healthy controls (1.9 ± 1.4 ng/mL) [15]. These high active TGFβ levels may be required to promote

86　cancer related processes and can partly be achieved through increased expression of plasmin,

87　MMPs and integrins, which are then able to activate L-TGFβ [8, 16, 17]. A recent study by

88　Ahn *et al.,* examining Dukes' stages B (n=170) and C (n=179) rectal cancer tissues showed

89　that expression of uPAR in epithelial and stromal cells differentially correlated with patient

90　survival [4]. Their results showed that elevated epithelial uPAR expression in both the

91　central region and invasive tumour front adversely correlated with overall survival of stage

92　B patients while elevated stromal uPAR (detected with a different monoclonal antibodies)

93　at the invasive front favourably correlated with overall survival of stage C patients [4]. In

94　contrast, a study by Boonstra *et al.,* examined CRC tumour tissues (n=262; all stages) and

95　showed that stromal uPAR expression was adversely associated with overall survival as well

96　as disease free survival [18]. Another study by Illemann *et al.,* also reported, similar results

97　to Boonstra *et al.,* that uPAR expression on tumour-associated macrophages negatively

98　correlated with overall survival in all stages (n=244) [19]. These high levels of uPAR can

99　lead to increased levels of plasmin which can aid in TGFβ activation during cancer.

100　Therefore, high levels of plasmin (and other suspected activators) during cancer could

101　contribute to developing high active TGFβ levels.

102　　　　Proteomics, is being widely used to study differential protein expression in response

103　to treatments with agonists or antagonists of certain processes during cancer and other

104　diseases [20]. Some of the most commonly used proteomic methods/technologies in

105　combination with mass spectrometry include one- or two-dimensional electrophoresis

106　(1/2DE) [21], two-dimensional differential in-gel electrophoresis (2D-DIGE) [22], stable

107　isotope labelling by amino acids in cell culture (SILAC) [23], and isobaric tag for relative

108　and absolute quantitation (iTRAQ)[24, 25]. This study uses iTRAQ-based technology as it

109　allows for differential labelling of peptides from 2-8 samples which are then combined

110　together and analysed in a single MS/MS run. Additionally, the differential labelling allows

111　for identification and quantitation in a single step which is a key advantage over standard

112　label-free approaches.

113　　　　In the current study, the effects of active TGFβ on HCT116 cells with differential

114　uPAR expression was investigated. The use of active TGFβ removes any molecular changes

115　that are associated with any plasmin-mediated TGFβ activation. The study compared

116　membrane enriched proteomes of TGFβ-treated and untreated HCT116^{WT} and HCT116^{uPAR-}

117　^{AS} subclone cells and the biological significance of the proteomic data evaluated using

118　Ingenuity Pathway Analysis (IPA) where a number of basic cellular pathways/functions

119 were found altered significantly. Additionally, prior to proteomic experiments proliferation
120 and invasion assays were performed.

121

2. RESULTS

2.1 Validation of uPAR expression in HCT116[WT] and HCT116[uPAR-AS] cells

124   HCT116[WT] cells used in this study natively express uPAR. However, the
125 HCT116[uPAR-AS] cell line shows decreased cell surface uPAR expression (35%↓) through
126 stable transfection [26]. **Figure 1** shows the differential expression differences of uPAR
127 between HCT116[WT] and HCT116[uPAR-AS] cell lines that was confirmed through western blot
128 analysis. These results support the reported differential expression of uPAR in these cell
129 lines [26].
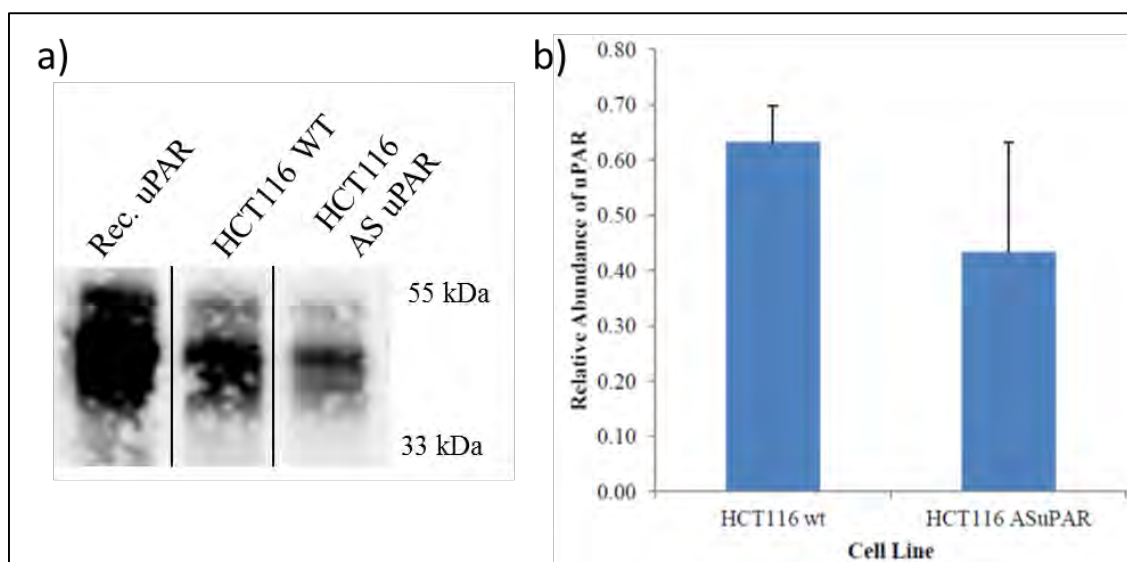
131 **Figure 1 a)** Validation of uPAR expression in HCT116[WT] and HCT116[uPAR-AS] cell lines.
132 100ng of recombinant uPAR and 20μg of cell lysates for both cell lines were separated on
133 SDS-PAGE gel followed by Western blotting using the anti-human uPAR monoclonal AF-
134 807 antibody (R&D Systems) **b)** Relative abundance of uPAR HCT116[WT] and HCT116[uPAR-]
135 [AS] cell lines (mean ± SEM) obtained by quantitative analysis of the Western blot band
136 intensities. Results indicate that HCT116[WT] expresses more uPAR than HCT116[uPAR-AS]
137 cells.

2.2 Effects of TGFβ1 on proliferation of HCT116 WT and AS cells

139   uPAR and TGFβ are key members for the uPAR/αvβ6/TGFβ1 hypothetical
140 interactome that was postulated in by group [27]. Research has shown that down-regulation
141 of uPAR correlated with decreased proliferation in papillary thyroid carcinoma cells [28]. In
142 order to evaluate the effects of TGFβ on cell proliferation (CP) of HCT116[WT] and
143 HCT116[uPAR-AS] colon cancer cells, a simple cell enumeration assay was performed. The

144 assay was performed under serum-free (SF) conditions to avoid interference from any
145 growth factors that might be present in fetal bovine serum (FBS) and that could affect
146 outcomes. The cells were treated with 10 ng/mL active TGFβ1 or 10μM SB431542 (a TGFβ
147 receptor I kinase inhibitor) or both and incubated for 24 hr, prior to analysis.

148
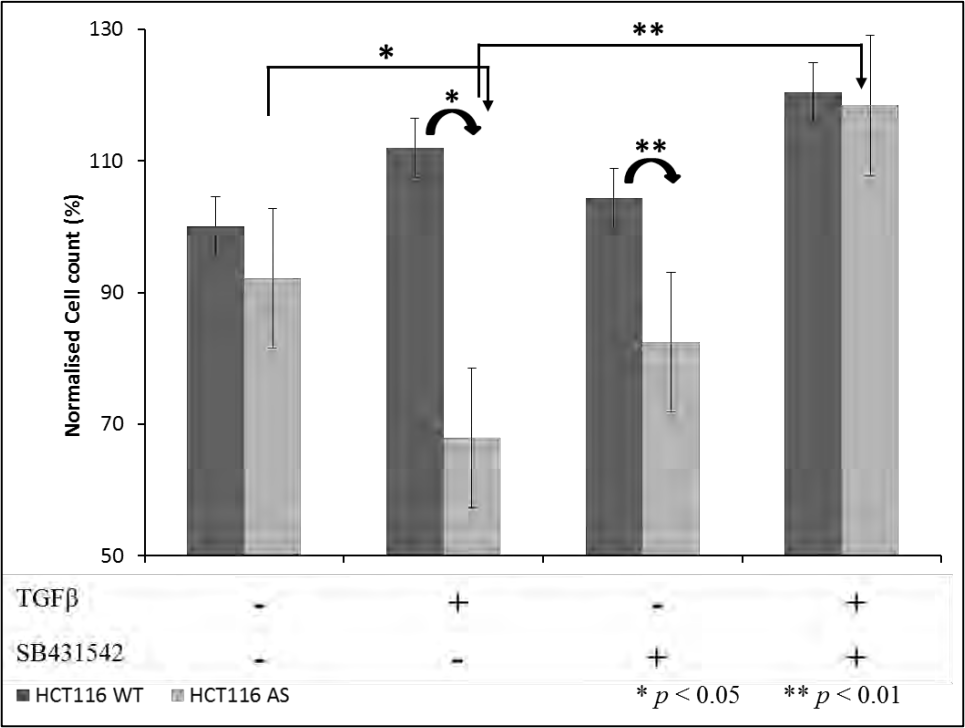
Figure 2 Proliferation assay of HCT116[WT] and HCT116[uPAR-AS] cells normalised to the
untreated HCT116[WT] control. All assays were performed in SF media and in biological
triplicate (*p<0.05; **p<0.01).

152 Both HCT116[WT] and HCT116[uPAR-AS] cells showed no significant difference in
153 proliferation under SF conditions, **Figure 2**. Interestingly, the HCT116[WT] cells showed a
154 slight increase in cell numbers upon treatment with TGFβ but failed to reach significance.
155 However, HCT116[uPAR-AS] cells, relative to untreated controls, exhibited significant changes
156 in cell numbers, decreased (24%↓) when treated with TGFβ alone or increased (26%↑)
157 when treated with TGFβ + SB431542, respectively. It is interesting to note that treatment
158 with TGFβ (alone) showed growth inhibitory responses in HCT116[uPAR-AS] cells that
159 expressed lower levels of uPAR. This growth inhibitory response was lost upon co-treatment
160 with TGFβ and SB431542 (that blocks its downstream signalling receptor TGFβR1), and
161 HCT116[uPAR-AS] cells reached high cell numbers similar to HCT116[WT] cells. Although, a
162 similar effect was observed in the HCT116[uPAR-AS] cells that were treated only with
163 SB431542, these failed to reach statistical significance. Collectively, these observations

164   demonstrate that TGFβ exerts tumour suppressive effects on HCT116 cells and this effect is

165   more pronounced when uPAR expression levels are lower.

166

167   **2.3 Effects of TGFβ1 on invasion of HCT116 WT and AS cells**

168   Previous studies using the HCT116^{WT} and HCT116$^{uPAR-AS}$ cell lines demonstrated

169   that suppression of uPAR correlated with decreased migration and invasion [26]. In the

170   current study, the possible correlation of uPAR and TGFβ that may occur during invasion

171   was evaluated using a Transwell invasion assay where the chambers are pre-coated with a

172   thin layer of ECMatrix^{TM}. Invasion was assessed in the presence of 10% FBS as a

173   chemoattractant in the lower chamber and the cells which migrated through the layer of

174   ECMatrix and through 8μm pores in the invasion chamber were scored as invasive.

175   Similar to results observed in proliferation assays, there was no significant difference

176   in invasive potential of HCT116^{WT} and HCT116$^{uPAR-AS}$ cells under SF conditions, **Figure 3**.

177   Similarly, both HCT116^{WT} and HCT116$^{uPAR-AS}$ cells relative to their untreated controls,

178   exhibited no significant difference when treated with TGFβ. However, upon treatment with

179   SB431542 (alone) or TGFβ + SB431542 (together) the HCT116$^{uPAR-AS}$ cells exhibited a

180   significant decrease in their invasive capacity relative to the untreated controls and TGFβ

181   treated cells. This decrease in invasion was more pronounced when the HCT116$^{uPAR-AS}$ cells

182   were just treated with SB431542 i.e., 17% and 18.5% relative to untreated control and TGFβ

183   treatment respectively. However, upon addition of TGFβ to SB431542 treated HCT116^{uPAR-}

184   ^{AS} cells showed only a 12.7% and 14.3% decrease in invasive potential relative to untreated

185   controls and TGFβ treated cells respectively. Despite no significant difference in invasion

186   (relative to untreated control) observed when HCT116$^{uPAR-AS}$ cells were treated with TGFβ

187   (alone) there was some loss of invasive potential upon addition of SB431542 (alone or in

188   combination with TGFβ). These observations suggest that TGFβR1 is required to regulate

189   invasion and that treatment with SB431542 greatly reduced invasion in both cell lines.
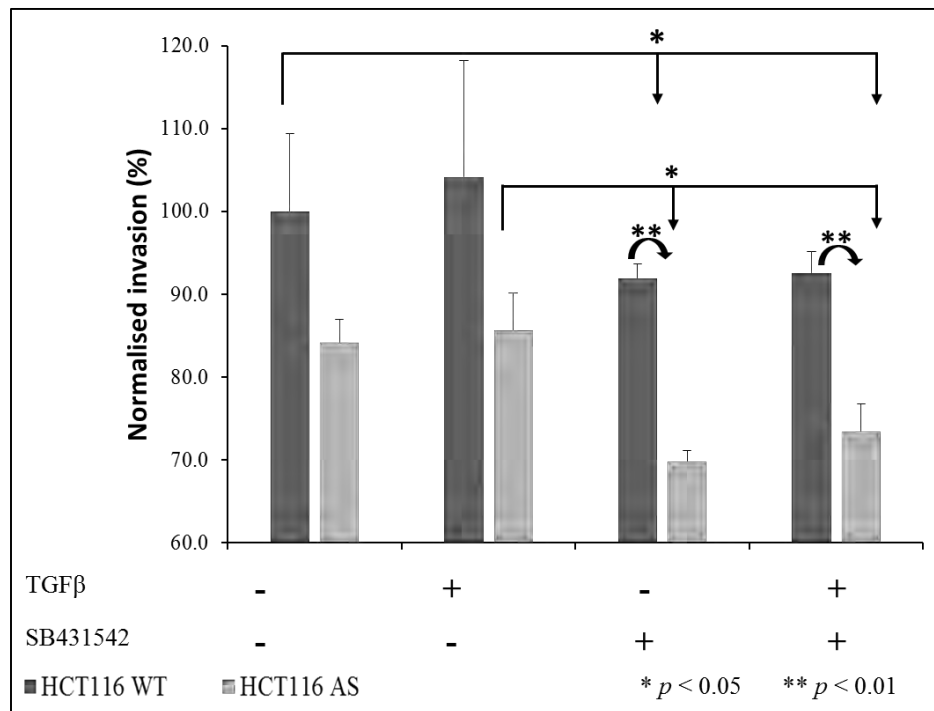
Figure 3 Effect of TGFβ on invasion of HCT116^{WT} and HCT116$^{uPAR-AS}$ cells normalised to the untreated HCT116^{WT} control. All assays were performed in SF media and in biological triplicate (*p<0.05; **p<0.01).

2.4 Proteomic analysis

The results from cell-based assays demonstrated that TGFβ does not affect proliferation or invasion of HCT116^{WT} cells. However, TGFβ showed an anti-proliferative responses in the HCT116$^{uPAR-AS}$ cells and this was abrogated upon SB431542 treatment. However, SB431542-treatment seemed to decrease the invasive potential of the HCT116$^{uPAR-AS}$ cells. These interesting observations were then expanded to examine what changes were occurring as assessed by proteomics.

To elucidate the molecular events associated with TGFβ treatment of HCT116^{WT} and HCT116$^{uPAR-AS}$ colon cancer cells, quantitative membrane proteomic analysis was performed using iTRAQ. HCT116^{WT} and HCT116$^{uPAR-AS}$ cells were treated with 10ng/mL TGFβ1 and membrane enrichment was performed using Triton X-114 phase partitioning. Following iTRAQ labelling the samples were then mixed in equal proportions and fractionated by SCX and analysed by nano LC-MS/MS using a TripleTOF mass spectrometer. The experiment was designed to examine the biological reproducibility, hence, duplicate samples were obtained for both untreated and TGFβ treated HCT116^{WT} and HCT116$^{uPAR-AS}$ cell lines and biological replicates were analysed on separate MS runs. The proteins identified from individual iTRAQ MS runs (biological replicates) were 'combined'

217

into a single list using Stouffer's method [29]. Stouffer's method, based on the observed iTRAQ protein ratios, allows for combining proteins identified across two or more MS runs and return a single combined (Stouffer's) p-value [29]. Using this approach a total of 1726 proteins were identified from two biological replicates (unused protein score ≥2.0; false discovery rate < 1% at protein level). A filter of minimum average iTRAQ fold change of ≥ 1.2 (up-regulated) or ≤ 0.83 (down-regulated) with a p < 0.05 was applied to the identified proteins and the ones that met this criteria were selected for further analysis.

Accordingly, the comparison of the untreated HCT116[WT] against the untreated HCT116[uPAR-AS] identified 222 proteins to be up- or down-regulated in the HCT116[WT] cells (**Supplementary table 1**). Likewise, the comparison of TGFβ-treated HCT116[WT] against the TGFβ-treated HCT116[uPAR-AS] identified 279 proteins to be up- or down-regulated (**Supplementary table 2**). For ease, these two protein lists were manually merged to generate a list of 346 proteins between both TGFβ treated and/or untreated conditions of HCT116[WT] and HCT116[uPAR-AS]. Furthermore, 155 of the 346 proteins were found to be differentially expressed in both conditions, while 67 and 124 proteins were found to be differentially up- or down-regulated when untreated and TGFβ-treated conditions respectively.

2.5 Gene ontology mapping of differentially expressed proteins

Gene ontology studies using PloGo [29] script classified the proteins into various groups based on their sub cellular locations, molecular function and biological processes. PloGo analysis of the 346 differentially expressed proteins is shown. These differentially expressed proteins were observed to be involved in cellular processes including cell motility, cell proliferation, cell differentiation, cell growth and cellular organisation (**Figure 4a**). The analysis also identified these proteins to be expressed in various membrane organelles including plasma membrane, Golgi apparatus, endoplasmic reticulum and mitochondria (**Figure 4b**).

2.6 Relevance of iTRAQ data to the processes of CRC

The 346 significantly altered proteins form iTRAQ experiment were functionally analysed and classified to collectively interpret the molecular events associated with CRC pathophysiology. The proteins were classified into four major categories (a) cytoskeletal signalling (b) cellular adhesion and migration (c) cellular stress and cell death and (d) membrane trafficking. For possible involvement in CRC, selected proteins from various

243 classes are listed and described below. All the protein fold changes are reported as observed

244 for HCT116$^{\text{WT}}$ cells relative to HCT116$^{\text{uPAR-AS}}$ cells (i.e., $\frac{\text{HCT116}^{\text{WT}}\ \text{fold change}}{\text{HCT116}^{\text{uPAR-AS}}\ \text{fold change}}$) and are

245 separated based on treatment.

246

A) Cell component

B) Biological process
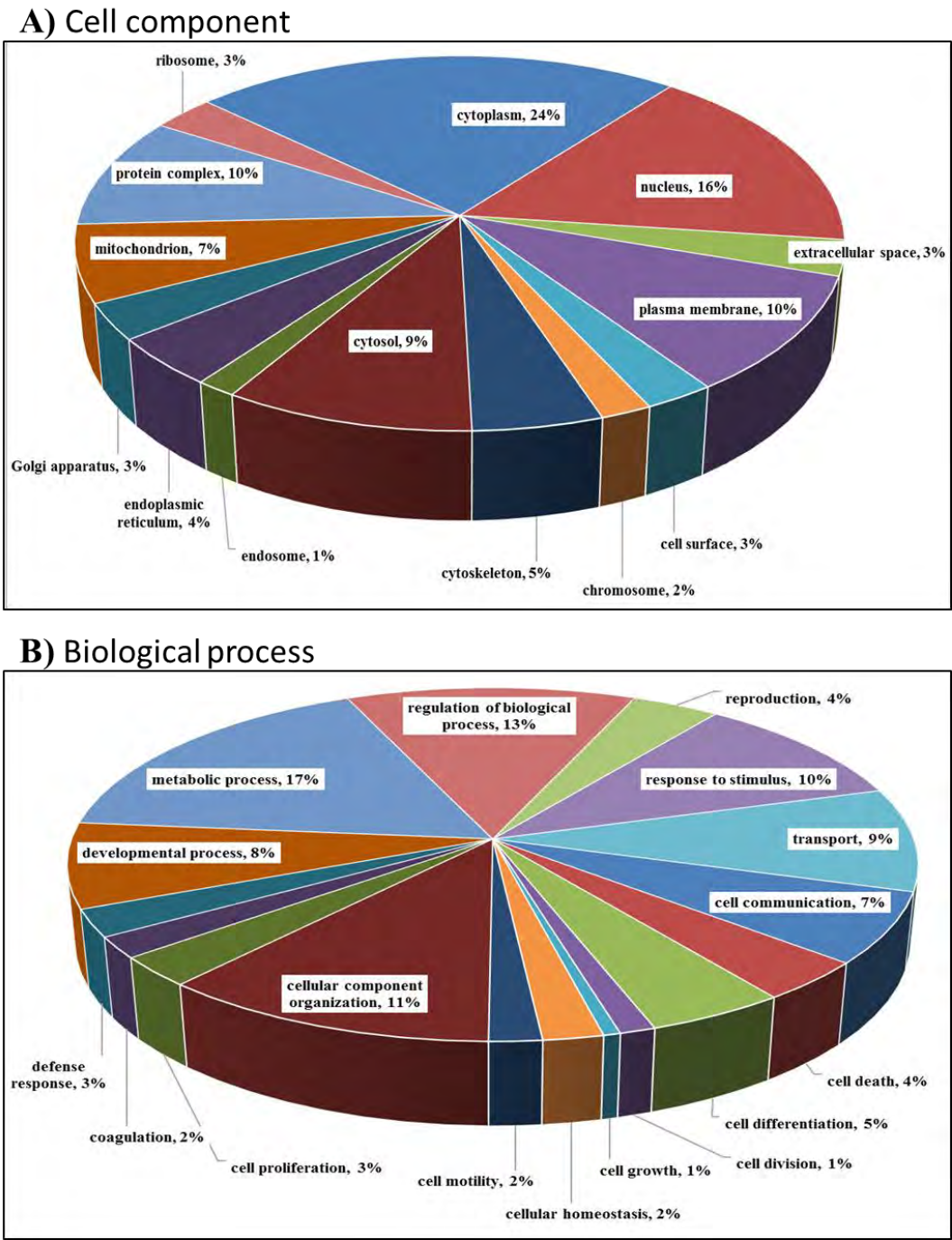
247

248 **Figure 4** Gene ontology based classification of the 346 differentially up- or down-regulated
249 proteins in the HCT116$^{\text{WT}}$ cells for TGFβ-treated and untreated conditions of HCT116$^{\text{WT}}$
250 and HCT116$^{\text{uPAR-AS}}$.

251

252

  Cytoskeletal signalling related proteins. The cytoskeletal proteins help maintain
the integrity of a cell and between cells. From the significantly altered proteins, several actin
filament, intermediate filament and microtubule associated proteins were identified.

  Actin and several actin filament associated proteins such as α-actinin-4, myosin-10,
septin-2, septin-9, septin-11, myosin regulatory light chain 12A and LIM domain and actin-
binding protein 1 were found to be significantly up-regulated in HCT116[WT] cells regardless
of TGFβ treatment (Table 1). Myosin-9 and emerin (down-regulated) and spetin-7 (up-
regulated) were observed to be significantly altered only upon TGFβ treatment.
Intermediated filament associated proteins keratin, type II cytoskeletal 8, keratin, type I
cytoskeletal 18 and keratin, type I cytoskeletal 19 were down regulated in TGFβ treated
HCT116[WT] cells, while keratin, type I cytoskeletal 9 and keratin, type I cytoskeletal 10 were
found to be up-regulated (Table 1). Plectin was also found to be down-regulated in TGFβ
treated HCT116[WT] cells. Interestingly, lamin-B1, lamin-B2 and lamina-associated
polypeptide 2, isoforms beta/gamma were found to be up-regulated in both conditions.

267

Table 1 Functional classification of significantly altered proteins related to cytoskeletal
signalling [a]

Accession number	Gene name	Protein names	iTRAQ fold change		Expression pattern
			Untreated	TGFβ treated	
Actin filament associated proteins					
O43707	ACTN4	alpha-actinin-4	1.34	1.36	↑
P35580	MYH10	myosin-10	1.47	n/o	↑
Q9UHD8	SEPT9	septin-9	1.87	3.19	↑
P19105	MYL12A	myosin regulatory light chain 12A	1.97	1.56	↑
Q9NVA2	SEPT11	septin-11	2.02	2.99	↑
Q15019	SEPT2	septin-2	2.10	3.10	↑
Q9UHB6	LIMA1	LIM domain and actin-binding protein 1	2.21	2.63	↑
P63261	ACTG1	actin, cytoplasmic 2	2.70	2.31	↑
P35579	MYH9	myosin-9	n/o	0.50	↓
P50402	EMD	emerin	n/o	0.72	↓
Q16181	SEPT7	septin-7	n/o	2.16	↑
Intermediate filament associated proteins					

P35908	KRT2	keratin, type II cytoskeletal 2 epidermal	0.58	n/o	↓
P04264	KRT1	keratin, type II cytoskeletal 1	0.64	n/o	↓
P42167	TMPO	lamina-associated polypeptide 2, isoforms beta/gamma	1.75	2.00	↑
P20700	LMNB1	lamin-B1	2.15	2.39	↑
Q03252	LMNB2	lamin-B2	2.31	1.57	↑
P13645	KRT10	keratin, type I cytoskeletal 10	n/o	1.62	↑
P35527	KRT9	keratin, type I cytoskeletal 9	n/o	1.60	↑
P05783	KRT18	keratin, type I cytoskeletal 18	n/o	0.47	↓
P08727	KRT19	keratin, type I cytoskeletal 19	n/o	0.51	↓
P05787	KRT8	keratin, type II cytoskeletal 8	n/o	0.32	↓
Q15149	PLEC	plectin	n/o	0.60	↓

Microtubule associated proteins					
P26038	MSN	moesin	n/o	1.70	↑
Q07065	CKAP4	cytoskeleton-associated protein 4	1.53	1.36	↑
P07437	TUBB	tubulin beta chain	0.37	0.23	↓
P33176	KIF5B	kinesin-1 heavy chain	0.50	0.42	↓
P27816	MAP4	microtubule-associated protein 4	0.77	n/o	↓
Q9BUF5	TUBB6	tubulin beta-6 chain	n/o	0.53	↓

[a] Fold change ratios of significantly altered proteins observed in two biological replicates of iTRAQ experiment. These proteins have met the stipulated criteria (i.e., unused protein score >2.0 and the change in expression level of at least 1.2 fold for HCT116^{WT}/HCT116$^{uPAR-AS}$ untreated and TGFβ-treated conditions. **n/o** – not observed in the treatment condition.

270

Tubulin-β and -β6 chains along with kinesin-1 heavy chain were found to be significantly down-regulated upon TGFβ treatment to HCT116^{WT} cells. Additionally, microtubule-associated protein 4 was down-regulated in the untreated HCT116^{WT} cells. Interestingly, cytoskeleton-associated protein 4 (CKAP4) that is a high affinity receptor for antiproliferative factor (APF) was found to be down-regulated upon TGFβ treatment (Table 1). Shahjee *et al.,* reported have previously reported that the knockdown of CKAP4 expression using siRNA inhibited the APF-CKAP4 driven anti-proliferative responses in T24 bladder carcinoma cells [30].

Proteins related to cell adhesion and migration. The balance of cell adhesion is a crucial factor during cancer development. The loss of cell adhesion can result in increased cell migration and invasion that is required for tumour cells dissipate to surrounding tissue and distant organs.

Cell adhesion associated molecules such as ALCAM (Activated leukocyte cell adhesion molecule or CD166 antigen), catenin α1, integrins-α2, -α3, and -β1, and CD44

286   were found to be up-regulated untreated condition (Table 2). Interestingly, the addition of
287   TGFβ resulted further up-regulation of the integrins which are key molecules for maintaining
288   cell adhesion. This TGFβ mediated up-regulation of various adhesion related molecules
289   could suggest a growth inhibition associated with TGFβ. Coxsackievirus and adenovirus
290   receptor (CXADR) a component of the epithelial apical junction complex and require for
291   tight junction integrity was observed to be up-regulated (Table 2).

292   Various cellular migration related proteins ezrin, tumour protein D54, galectin-3,
293   galectin-1, alpha-enolase and cell division control protein 42 homolog were observed to be
294   up-regulated (Table 2) in the HCT116^{WT} cells, irrespective of TGFβ treatment. Although,
295   some of these proteins showed slight up-regulation upon TGFβ treatment, the change was
296   negligible. Annexin A2 has been reported to inhibit cell migration *in vitro* [31] was observed
297   to be up-regulated regardless of TGFβ treatment. Additionally, prohibitin and prohibitin-2
298   that were shown to be required for cancer cell adhesion and proliferation [32] were observed
299   to be down-regulated significantly which further decrease upon TGFβ treatment (Table 2).
300   Once again, these observations indicate a TGFβ-mediated growth inhibition in these cells.
301   The expression of annexin A2 and ezrin was validated by Western blotting analysis (Figure
302   5).

303

304 **Table 2** Functional classification of significantly altered proteins related to cellular adhesion
305 and migration [a]

Accession number	Gene name	Protein names	iTRAQ fold change		Expression pattern
			Untreated	TGFβ treated	
		Cell adhesion related proteins			
P48960	CD97	CD97 antigen	1.32	n/o	↑
P16070	CD44	CD44 antigen	1.37	1.67	↑
P21926	CD9	CD9 antigen	1.76	n/o	↑
P35221	CTNNA1	catenin alpha-1	1.78	1.68	↑
P26006	ITGA3	integrin alpha-3	1.98	3.35	↑
P17301	ITGA2	integrin alpha-2	2.19	2.70	↑
Q13740	ALCAM	CD166 antigen	2.34	2.19	↑
P05556	ITGB1	integrin beta-1	2.70	4.04	↑
P50895	BCAM	basal cell adhesion molecule	n/o	0.67	↓
		Tight junction proteins			
P78310	CXADR	coxsackievirus and adenovirus receptor	1.62	1.56	↑

P46013	MKI67	antigen KI-67	1.25	n/o	↑
P15311	EZR	ezrin	1.46	1.99	↑
O43399	TPD52L2	tumour protein D54	2.00	3.04	↑
P17931	LGALS3	galectin-3	2.06	2.82	↑
P09382	LGALS1	galectin-1	2.14	2.61	↑
P07355	ANXA2	annexin A2	2.47	2.38	↑
P06733	ENO1	alpha-enolase	2.70	2.37	↑
P60953	CDC42	cell division control protein 42 homolog	4.34	2.48	↑
P51858	HDGF	hepatoma-derived growth factor	n/o	3.96	↑
Q99623	PHB2	prohibitin-2	0.54	0.30	↓
P35232	PHB	prohibitin	0.60	0.46	↓

[a] Fold change ratios of significantly altered proteins observed in two biological replicates of iTRAQ experiment. These proteins have met the stipulated criteria (i.e., unused protein score >2.0 and the change in expression level of at least 1.2 fold for HCT116^{WT}/HCT116$^{uPAR-AS}$ untreated and TGFβ-treated conditions. **n/o** – not observed.

306

307 **Cell death related proteins**. Tumour cells to spread to surrounding tissue and/or

308 distant organs, they require to survive the loss of cell adhesion and the stress that is

309 associated with it. However, it is known that epithelial cells can trigger apoptosis when the

310 cell adhesion is lost (i.e., anoikis) during cancer [33, 34]. Therefore, suppression of anoikis

311 becomes a crucial requirement for cancer cells. This study identified several proteins that

312 are associated with this process.

313 Various chaperone and heat shock proteins such as DnaJ homolog subfamily A

314 member 1, heat shock 70 kDa protein 1A/1B and heat shock cognate 71 kDa protein were

315 observed to be down regulated whereas DnaJ homolog subfamily B member 11, heat shock

316 70 kDa protein 4, and DnaJ homolog subfamily C member 9 were found to be down-

317 regulated in the TGFβ treated HCT116 WT cells (Table 3). Additionally, hypoxia up-

318 regulated protein 1, stress-70 protein, mitochondrial, 78 kDa glucose-regulated protein,

319 endoplasmin, and heat shock protein beta-1 were found to be up-regulated in both conditions.

320

321 **Table 3** Functional classification of significantly altered proteins related to cell death [a]

Accession number	Gene name	Protein names	iTRAQ fold change		Expression pattern
			Untreated	TGFβ treated	
		Chaperones and heat shock proteins			
P12956	XRCC6	X-ray repair cross-complementing protein 6	1.25	n/o	↑
P38646	HSPA9	stress-70 protein, mitochondrial	1.42	1.39	↑

P11021	HSPA5	78 kDa glucose-regulated protein	1.54	1.43	↑
P14625	HSP90B1	endoplasmin	1.65	1.68	↑
P04792	HSPB1	heat shock protein beta-1	4.44	3.96	↑
Q96EY1	DNAJA3	DnaJ homolog subfamily A member 3, mitochondrial	n/o	1.33	↑
Q9UBS4	DNAJB11	DnaJ homolog subfamily B member 11	n/o	1.58	↑
P34932	HSPA4	heat shock 70 kDa protein 4	n/o	1.70	↑
Q8WXX5	DNAJC9	DnaJ homolog subfamily C member 9	n/o	1.91	↑
P50454	SERPINH1	serpin H1	1.55	n/o	↑
P31689	DNAJA1	DnaJ homolog subfamily A member 1	n/o	0.36	↓
P51572	BCAP31	B-cell receptor-associated protein 31	n/o	0.50	↓
P08107	HSPA1A	heat shock 70 kDa protein 1A/1B	n/o	0.68	↓
P11142	HSPA8	heat shock cognate 71 kDa protein	n/o	0.73	↓
P50991	CCT4	T-complex protein 1 subunit delta	n/o	0.75	↓

Apoptosis-related proteins

Q9Y4L1	HYOU1	hypoxia up-regulated protein 1	1.28	1.35	↑
O95831	AIFM1	apoptosis-inducing factor 1, mitochondrial	n/o	1.35	↑
Q9UKV3	ACIN1	apoptotic chromatin condensation inducer in the nucleus	n/o	1.65	↑
Q96A26	FAM162A	protein FAM162A	n/o	1.86	↑

[a] Fold change ratios of significantly altered proteins observed in two biological replicates of iTRAQ experiment. These proteins have met the stipulated criteria (i.e., unused protein score >2.0 and the change in expression level of at least 1.2 fold for HCT116^{WT}/HCT116$^{uPAR-AS}$ untreated and TGFβ-treated conditions. **n/o** – not observed.

322

323   Interestingly, the apoptotic related molecules apoptosis-inducing factor 1,

324   mitochondrial (AIFM1) (or Programmed cell death protein 8; PDCD8), apoptotic chromatin

325   condensation inducer in the nucleus (ACIN1), and protein FAM162A (or human growth and

326   transformation-dependent protein; HGTD-P) were found to be significantly up-regulated in

327   the TGFβ treated HCT116^{WT} cells (Table 3). AIFM1 was reported by Kim *et al.,* to induce

328   apoptosis by inhibiting protein synthesis [35]. During apoptotic induction AIFM1

329   translocates from the mitochondria into the nucleus where it binds to the eukaryotic

330   translation initiation factor 3 subunit p44 (eIF3g) required for protein synthesis [35]. It is not

331   surprising to see the up-regulation of AIFM1 as IPA showed eIF4 signalling to be the top

332   canonical pathway altered in these cells. Additionally, overexpression of FAM162A a death-

333   inducing effector molecule downstream of HIF-1α (Hypoxia-inducible factor 1α) was

334   reported by Lee *et al*., to facilitate cell death by inducing mitochondrial apoptotic pathway

335   [36]. This increased expression of these apoptosis inducing proteins suggests that anoikis

336   has been triggered in the TGFβ treated HCT116^{WT} cells.

337

338 **Table 4** Functional classification of significantly altered proteins related to protein
339 trafficking [a]

Accession number	Gene name	Protein names	iTRAQ fold change		Expression pattern
			Untreated	TGFβ treated	
Ras-related Proteins					
P61026	RAB10	Ras-related protein Rab-10	7.54	4.72	↑
P51148	RAB5C	Ras-related protein Rab-5C	1.87	n/o	↑
P51149	RAB7A	Ras-related protein Rab-7a	1.73	n/o	↑
P61224	RAP1B	Ras-related protein Rap-1b	1.57	n/o	↑
Q15907	RAB11B	Ras-related protein Rab-11B	n/o	0.69	↓
Protein trafficking					
Q86Y82	STX12	syntaxin-12	1.38	1.81	↑
O15400	STX7	syntaxin-7	1.48	1.56	↑

[a] Fold change ratios of significantly altered proteins observed in two biological replicates of iTRAQ experiment. These proteins have met the stipulated criteria (i.e., unused protein score >2.0 and the change in expression level of at least 1.2 fold for HCT116^{WT}/HCT116$^{uPAR-AS}$ untreated and TGFβ-treated conditions. **n/o** – not observed

340

341   **Proteins involved in trafficking**. Several Ras-related proteins were found to be up-
342 regulated in the untreated HCT116^{WT} cells (Table 4). The identified Rab and Rap proteins
343 are GTPases that are required for protein trafficking across the membranous cell organelles
344 including endoplasmic reticulum, Golgi complex, endosomes and plasma membrane. For
345 example, Rab-10 has been reported to be involved in trafficking from the Golgi at early
346 stages of epithelial polarization [37, 38]. Additionally, Rab-10 was found to be up-regulated
347 in both untreated (7.54 fold↑) and TGFβ-treated (4.72 fold↑) conditions (Table 4).
348 Interestingly, treatment with TGFβ resulted in a 2.8-fold decrease in the expression of Rab-
349 10 and this differential expression was validated through Western blotting (**Figure 5**).
350 Surprisingly, there are very few reports that have identified Rab-10 in association with
351 cancer. However, Lee *et al*., identified Rab-10 in an HMGB1 (high mobility group box 1)
352 pull-down experiment on the same cells we use here, namely HCT116 cells [39]. This
353 observation is interesting as HMGB members have previously been associated with cell
354 migration [40]. Our study would be the second after Lee *et al*., [39] to report the
355 identification of Rab-10 in the context of CRC.

356   Two other proteins, syntaxin-7 and syntaxin-12, that regulate protein trafficking from
357 the plasma membrane to the early endosomes [41] were observed to be up-regulated (Table
358 4). Decreased expression of Syntaxin-7 in melanoma is associated with more aggressive

359 tumours [42]. In contrast, up-regulation of Syntaxin-7 in this study could indicate a less

360 aggressive phenotype or even growth inhibition.

361   This study also identified other proteins such as plasminogen activator inhibitor 1

362 RNA-binding protein, transforming protein RhoA, uncharacterized protein C19orf43, and

363 scavenger receptor class B member 1 to be up-regulated while transferrin receptor protein 1,

364 protein FAM3C, Ragulator complex protein LAMTOR1, membrane-associated

365 progesterone receptor component 1, DBIRD complex subunit KIAA1967, and

366 uncharacterized protein KIAA2013 to be down-regulated (Supplementary tables 3).

367 Interestingly, KIAA1967 or deleted in breast cancer gene 1 protein (DBC1) expression has

368 been observed in various cancers with varying outcomes [43-46]. Zhang *et al*., reported that

369 the overexpression of DBC1 in CRC results in poor prognosis [46], which confers with this

370 study. However, low expression of DBC1 was associated with poor prognosis in CRC as

371 reported by Kikuchi *et al*., [47]. In contrast, several studies report the overexpression of

372 DBC1 in other cancers to be associated poor prognosis [43-45].

373 **2.7 Validation of selected protein candidates by western blotting**

374   To confirm that the fold changes values of proteins observed through iTRAQ was

375 real, the differential expression of three proteins – ezrin, annexin A2 and Ras-related protein

376 Rab-10, were validated using Western blotting. As shown in Figure 5, the relative expression

377 of these proteins was assayed using specific antibodies. The results observed here were in

378 agreement with the fold changes observed through iTRAQ.

379
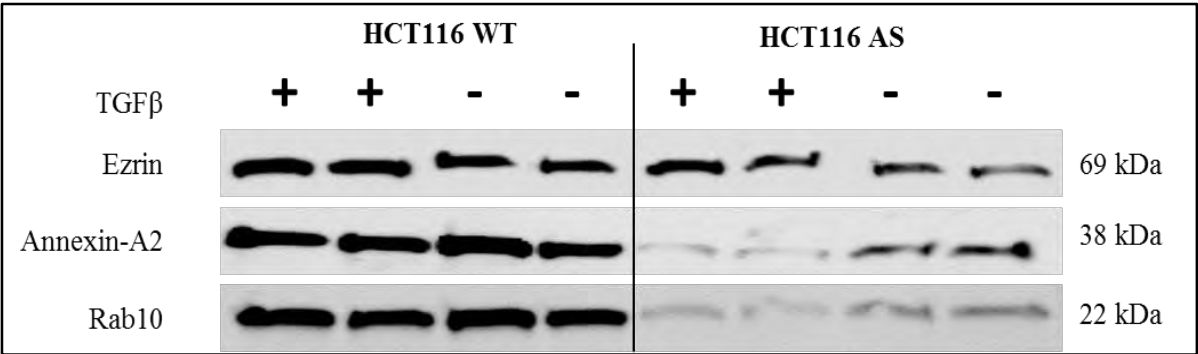
380

381 **Figure 5** Validation of proteomic results. The differential expression of 3 proteins was
382 validated by Western-blot analysis. 20 μg of protein sample for TGFβ –treated and untreated
383 HCT116^{WT} and HCT116$^{uPAR-AS}$ cells were separated on SDS-PAGE gel followed by
384 Western blotting using ezrin (sc-58758), annexin A2 (ab41803) and Rab-10 (ab181367)
385 antibodies.

386

387   Leiphrakpam *et al*., recently reported that the expression of ezrin and the

388   phosphorylatiaon at its T567 site was increased during CRC liver metastasis [48]. From the

389   Western blot analysis, it is clear that the HCT116^{WT} cells endogenously have higher ezrin

390   levels compared to the HCT116$^{uPAR-AS}$ cells that have lower uPAR expression. However, the

391   addition of TGFβ to either cells increased ezrin expression, suggesting a TGFβ-mediated

392   growth of these cells. Other studies on breast cancer and tongue squamous cell carcinoma

393   have shown that the expression of ezrin is required during proliferation, migration and

394   invasion during cancer [49, 50].

395   Annexin A2 overexpression has been observed in pancreatic, colorectal and brain

396   tumours and correlated with advanced clinical stage [51]. Likewise, high expression of

397   annexin A2 was observed in metastatic CRC cells compared with non-metastatic cells [52].

398   Similar to ezrin, annexin A2 was found to be expressed at high levels when uPAR was

399   expressed (HCT116^{WT}) and decreased with uPAR expression (HCT116$^{uPAR-AS}$). However,

400   the addition of TGFβ showed very little difference in the expression.

401   The increased expression of these proteins in cells with high uPAR expression,

402   regardless of TGFβ treatment, suggests that uPAR primarily could be responsible for the

403   cancer progression propertied observed within these cell lines.

404   **2.8 Network analysis of proteomic data using Ingenuity Pathway Analysis**

405   To examine the biological significance, the proteomic data was examined using IPA

406   server. The differentially expressed proteins from the untreated and TGFβ-treated were

407   analysed separately. The untreated dataset contained 222 proteins and the TGFβ-treated

408   dataset contained 279 proteins. It is important to note that 155 proteins were found to be

409   observed in both datasets. Despite the large overlap, the network aimed to differentiate

410   changes associated with TGFβ treatment. First we examined the untreated dataset.

411   **IPA of untreated dataset**. IPA identified various fundamental cellular functions

412   including (i) cellular growth and proliferation (ii) cell death and survival (iii) protein

413   synthesis (iv) cell morphology and (v) cellular function and maintenance to be significantly

414   altered in either of the untreated HCT116 subclone cell lines. Likewise, several networks

415   related to these cellular processes were also seen to be altered significantly. They include,

416   "Protein Synthesis, Cell Death and Survival, Drug Metabolism" (IPA score=41), "Cell-To-

417   Cell Signaling and Interaction, Cancer, Organismal Injury and Abnormalities" (IPA

score=35), "Cell Death and Survival, Cell-To-Cell Signaling and Interaction, Cardiovascular System Development and Function" (IPA score=31) and "Cell Cycle, Cancer, Organismal Injury and Abnormalities" (IPA score=25).

IPA also showed eIF2 signalling, regulation of eIF4 and p70S6K signalling to be the top two canonical pathways to be altered with this data set. Majority of the molecules that were associated with these pathways were various ribosomal proteins. IPA showed eukaryotic translation initiation factor 4 gamma 1 (eIF4G1) to be associated with both these pathways and was observed to be down-regulated by proteomics (iTRAQ-fold change, 0.60↓). eIF4G1 is the most abundant member of the eIF4G scaffold protein family, whose elevated expression in yeast promoted direct mRNA-ribosome interaction and translation of mRNAs with longer polyA tails, thereby promoting mRNA translation efficiency [53-55]. eIF4G1 is a component of the eIF4F complex that is essential for mRNA translation. The down-regulation of eIF4G1 in mammalian and yeast cells showed a decrease in mRNA translation of multiple mRNAs but was not completely inhibited [53, 56]. This suggest that eIF4G1 is crucial for increasing mRNA translation under stress conditions and the observed down-regulation in this study could mean a normal functioning of the cells.

To further investigate the regulators associated with the proteomic changes observed, the upstream regulator analysis in IPA was implemented. Interestingly, TGFβ1 system was found to be activated (activation z-score, 2.2; p-value, 0.041), despite any treatment. This shows that TGFβ is endogenously expressed in these cells. Furthermore, IPA associated the IgG and TGFβ regulators with several diseases and functions including adhesion of colon cancer cell lines, attachment of tumour cell lines binding of tumour cell lines, and cell movement of carcinoma cell lines. Rightly, IPA identified CALR, CD44, EZR, HSPB1, ITGA2, ITGA3, ITGB1, LGALS1, LGALS3, and SCARB1 to be involved in these functions.

IPA of TGFβ-treated dataset. IPA identified cancer as the top disease while (i) RNA post-translational modification, (ii) cellular growth and proliferation, (iii) cell death and survival, (iv) protein synthesis and (v) cellular development were found to be the top cellular functions associated with the dataset. IPA also identified several networks associated with these cellular functions. The top three networks are "Protein Synthesis, Cancer, Hematological Disease" (IPA score=43), "RNA Post-Transcriptional Modification, Carbohydrate Metabolism, Cell Morphology" (IPA score=36) and "Cell Death and Survival,

450 Cancer, Organismal Injury and Abnormalities" (IPA score=36). IPA also showed eIF2

451 signalling to be the top canonical pathway that is significantly altered. Interestingly, no eIFs

452 were found to be altered upon treating HCT116^{WT} and HCT116$^{uPAR-AS}$ cells with TGFβ. Like

453 the untreated cells, the TGFβ1 system was found to be activated (activation z-score, 2.2) but

454 was not significant.

455 The IPA showed several basic cellular functions to be altered when uPAR is

456 differentially expressed in the HCT116 cells. Similar observations were also seen when the

457 HCT116 cells were treated with TGFβ.

3. DISCUSSION

459 Colorectal cancer is the third most common cancer globally with mortality rates over

460 50% [1] with majority of the deaths being due to metastasis [3]. Several proteins including

461 uPAR and TGFβ have been implicated in CRC biology. Likewise, several studies have

462 shown that increased uPAR expression is associated with poor overall survival of cancer

463 patients [4, 18, 19]. However, several reports have implicated TGFβ in CRC, but its exact

464 mechanism is not very well understood. This study aimed to investigate the effects of TGFβ

465 on HCT116 subclone cells with differential uPAR expression.

466 The observations from initial cell proliferation (CP) and invasion studies showed that

467 TGFβ did not significantly affect these processes. In contrast, the HCT116$^{uPAR-AS}$ cells

468 showed significant decrease in CP upon addition of TGFβ alone or with SB431542.

469 Although, the HCT116$^{uPAR-AS}$ showed no difference in invasion upon TGFβ treatment, this

470 invasion was significantly decreased upon treatment with SB431542 alone or with TGFβ.

471 These observations suggest that the proliferation of the HCT116^{WT} cells with high uPAR

472 expression could happen independent of TGFβ. In contrast, the increased proliferation

473 associated with HCT116$^{uPAR-AS}$ cells upon treatment with SB431542 could be through non-

474 TGFβ mediated pathways such as mitogen-activated protein kinases (MAPKs). Overall, the

475 cell based assays showed that high uPAR expression by itself can promote malignant

476 phenotypes whereas lower uPAR expressing cells/tumours require assistance to attain the

477 malignant phenotype. Interestingly, Brattain *et al*., had reported the parent HCT116 cells to

478 be tumourigenic, when trypsinized or scrapped cells in tissue culture medium without any

479 serum given as subcutaneous injections, to athymic nude mice [57]. Wang *et al*., also

480 reported pulmonary metastases to occur in 63-78% of athymic nude mice injected with the

481 parent HCT116 cells [58]. However, injection of the antisense transfected clones, 3′-AS7

and 5′-AS, showed pulmonary metastases only in 19% and 9% of the mice respectively [58]. The observations from our cell based studies seem to align with these mice studies, where proliferation and invasion was more pronounced in HCT116[WT] cells with high uPAR expression and reduced when uPAR expression was artificially decreased by ~50%. These interesting observations were then examined by proteomics.

Our focus in this study was to identify membrane proteomic changes in the HCT116[WT] and HCT116[uPAR-AS] cells associated with TGFβ treatment at a concentration (10 ng/mL) that recapitulates the levels during CRC Dukes' stage B-D [15]. Following Triton X-114 phase partitioning for enrichment of highly hydrophobic integral membrane proteins they were subsequently analysed using iTRAQ. Using this high-throughput quantitative proteomics approach we identified several proteins as significantly altered. Proteomic results and the IPA of the data showed several proteins associated with the cytoskeletal signalling, cell adhesion and migration, cell death and survival, and protein trafficking were found to be up- or down-regulated either in a TGFβ-dependant or a TGFβ-independent manner when uPAR was differentially expressed. Three proteins of interest – ezrin, annexin A2 and Ras-related protein Rab-10 were further validated by western blotting. Interestingly, the increased expression of ezrin and annexin A2 was reported to be crucial for metastasis in several cancers and their blockade or deficiency significantly reduced cell proliferation, migration and invasiveness [49-51, 59]. Prior to this study, Rab-10 was observed in only one other study in the context of CRC [39], which is an interesting observation.

In conclusion, the observations from cell based studies and proteomics study suggest that the cells expressing uPAR (HCT116[WT]) do not significantly respond to TGFβ treatments in contrast to those with lower uPAR levels (HCT116[uPAR-AS]). These observations suggest a possible malignant phenotype of the HCT116[WT] cells in a TGFβ-independent manner and TGFβ-dependant growth suppression in the HCT116[uPAR-AS] cells. Furthermore, the identification of Rab-10 is interesting and it warrants further investigation. Finally, the identification of important protein networks offer valuable information toward future research on role of TGFβ in CRC.

4. MATERIALS AND METHODS

4.1 Cell lines

This study utilised the subclones of HCT116 cells (ATCC® CCL-247™). The HCT116 wild-type (HCT116[WT]) and HCT116 uPAR anti-sense (HCT116[uPAR-AS]) were a kind gift from Professor Yao Wang (Orthopaedic Research Institute, St George Hospital,

514   Sydney, Australia). The HCT116[uPAR-AS] subclone has shown approximately 35% decreased

515   cell surface uPAR [26]. This decreased expression was achieved by stable transfection of

516   the HCT116[WT] cells with a pDR2 vector which expresses 5′ uPAR cDNA in an antisense

517   orientation [26]. HCT116 WT cells were maintained in complete Dulbecco's Modified

518   Eagle's Medium (DMEM; cat. no. D5796, Sigma-Aldrich Pty. Ltd, NSW, Australia)

519   supplemented with 10% FBS and incubated at 37°C in the presence of 5% CO_2. Complete

520   media for HCT116 AS cells contained an additional 400 μg/mL hygromycin B as a selective

521   antibiotic. Serum-free (SF) media used for both cell lines contained only 0.5% FBS. The

522   primary HCT116 cell has been previously found to be tumourigenic to athymic nude mice

523   when they were given subcutaneous injections with trypsinized or scrapped cells in tissue

524   culture medium without any serum [57]. Cell lines tested negative for *Mycoplasma* infection

525   using the PCR-based VenorGeM Mycoplasma Detection Kit (Minerva Biolabs Cat. No. 11-

526   1050).

527   **4.2 Recombinant protein treatment protocol**

528   The recombinant protein treatment method employed during this study remained

529   constant for all the assays. Freshly passaged HCT116 cells were seeded and incubated in

530   complete media for 24 hr and then serum starved using SF media for 24 hrs. At this point

531   recombinant proteins were aseptically added and incubated as required. Recombinant

532   Human TGFβ1 was purchased from R&D Systems (Minnesota, USA) and SB431542 (TGFβ

533   Receptor I kinase inhibitor) was purchased from Abcam (Cambridge, UK). Four treatment

534   conditions were employed during this study: 1) SF media as a negative control, 2) SF media

535   + 10ng/mL active TGFβ, 3) SF media + 10μM SB431542 and 4) SF media + 10ng/mL active

536   TGFβ + 10μM SB431542. TGFβ1 was added to the cells 30 min after treating with

537   SB431542. All the cell based experimental comparisons were performed in biological

538   triplicates and were repeated at least twice and are presented as a percentage of the untreated

539   HCT116 WT cells.

540   **4.3 Cell-proliferation assay**

541   The cells were seeded at a density of 1×10^5 cells into six-well plates and prepared for

542   recombinant protein treatment as outlined above. The cells were then incubated in presence

543   of recombinant proteins for 24hr. They were then detached from the well surface by

544   trypsinization, gently mixed in a 1:1 ratio of cell suspension to 0.4% Trypan Blue (Sigma

545   Aldrich) and the live cells enumerated using a BioRad TC-10[TM] automated cell counter. It

should be noted that the trypan blue exclusion measures the steady state balance between cell viability and proliferation does not measure cell death. All conditions were performed in biological triplicate and statistical testing for significance performed using a Student's t-test with a significance cut-off of $p<0.05$.

4.4 Invasion assay

The ability of cells to invade through extra-cellular matrix (ECM) was assessed using the Chemicon QCM 96-well Invasion Assay Kit (ECM555, CHEMICON, International, CA, USA) and performed according to manufacturer's instructions. Briefly, serum starved HCT116 cells were non-enzymatically (trypsin/EDTA) detached from the growing surface and resuspended in SF media. Then, 5×10^4 cells and recombinant proteins were placed in the invasive chamber and incubated at 37 °C for 18 hrs. The cells which migrated through the ECM layer and attached to the bottom of the polycarbonate membrane, were dissociated from the membrane after incubation with the 150 μL of Cell Detachment Solution (37 °C for 30 min). Next, 50 μL of lysis buffer/CyQuant GR Dye Solution (1:75) was added to each well and incubated (15 min, room temperature). Finally, 150 μL of this mixture was transferred to a new 96-well plate, and the fluorescence was measured using a FLUOstar OPTIMA microplate spectrophotometer (BMG Labtech) using 480 nm/520 nm filter set. All conditions were performed in biological triplicate and statistical testing for significance performed using a Student's t-test with a significance cut-off of $p<0.05$.

4.5 Membrane Protein Enrichment

The HCT116 cells were seeded in 15-cm cell culture dishes and at a confluence of 70-75%, were stimulated with 10 ng mL^{-1} of TGFβ1 for 24 hrs in the presence of SF media. The cells were then collected in lysis buffer containing 50 mM Tris-HCl, 100 mM NaCl, protease inhibitor cocktail (Roche Applied Science) and phosphatase inhibitors (Sigma Aldrich) and left on ice for 30 min before proceeding to membrane enrichment. The cells were stored at -80 °C if not used immediately and were thawed on ice before proceeding to membrane enrichment.

Membrane enrichment was performed using a previously published method [60] with slight modifications. In detail, the crude cell lysate was homogenized in the lysis buffer using a probe sonicator (Branson Sonifier 450; www.bransonultrasonics.com). The homogenized cell lysate was centrifuged at 2000g (20 min, 4 °C) to remove nuclei and cell debris. The

577 supernatant containing the membrane and other cellular proteins was then diluted to 8 mL

578 using binding buffer (20 mM Tris-HCl, 100 mM NaCl) and subjected to ultracentrifugation

579 (Sorvall Discovery; M120 SE, S80AT3 rotor) at 120,000g (90 min, 4 °C). The resulting

580 membrane pellet was washed twice with 0.1 M sodium carbonate (pH 11.0) and

581 resuspended/homogenized in binding buffer. The homogenized membrane proteins were

582 diluted with 4 volumes of binding buffer containing 1% (v/v) Triton X-114 and chilled on

583 ice for 10 min with intermittent vortexing. Samples were then heated at 37 °C for 20 min

584 and phase partitioned by centrifugation at 1000g (3 min). The detergent phase was further

585 diluted with 4 volumes of binding buffer containing 1% (v/v) Triton X-114 and phase

586 partition was repeated. The integral membrane proteins in the Triton X-114 detergent phase

587 were subjected to acetone precipitation. The precipitated membrane proteins were

588 resolubilized in 0.5 M triethyl ammonium bicarbonate (TEAB) (Sigma-Aldrich, Australia)

589 and 0.1% SDS and stored at -80 °C if not used immediately. Protein samples were

590 quantitated using Pierce™ BCA Protein Assay Kit and 100 μg of protein was used to

591 perform the iTRAQ analyses.

4.6 iTRAQ isobaric labelling

593 iTRAQ labelling was carried out, using a 4-plex isobaric tagging kit (AB SCIEX),

594 according to manufacturer's instructions with minor modifications. iTRAQ analysis was

595 performed in biological duplicates for each cell line, where in one set of samples were not

596 treated with TGFβ1. Briefly, 100 μg of total membrane protein samples for each replicate

597 were reduced using 5 mM Tris-(2-carboxyethyl) phosphine (TCEP) (60 °C, 1 h), alkylated

598 with 10 mM methyl methanethiosulfonate (MMTS) (room temperature, 10 min) and

599 digested with trypsin (Promega; 1:25 w/w, 37°C overnight). The digested peptides were then

600 dried and reconstituted in 0.5 M TEAB and ethanol (70% (v/v) final concentration). They

601 were then labelled with respective 4-plex isobaric tags and incubated at room temperature

602 for 1 hr before being combined. Confirmation of labelling and mixing was carried out using

603 MALDI-MS. The iTRAQ labelled samples were dried and stored at -80°C if not used

604 immediately.

4.7 Strong cation exchange chromatography separation

606 The strong cation-exchange chromatography (SCX) was performed to remove

607 interfering substances such as dissolution buffer, organic solvents (ethanol, acetonitrile,

608 TEAB), reducing agent (TCEP), alkylating agent (MMTS), SDS and any excess iTRAQ

609 reagents. The samples were fractionated by SCX using an Agilent 1260 quaternary HPLC

610 pump with a PolyLC polysulfoethyl aspartamide column (200 mm x 2.1 mm, 5μm, 200 Å;

611 PolyLC, Columbia, MD). The column was equilibrated with buffer A (5mM KH_2PO_4, 25%

612 v/v acetonitrile (ACN), pH 2.72), which was also used for sample resuspension, sample

613 injection and peptide adsorption to the column. Peptide elution was achieved with a step

614 gradient of 10, 45 and 100% (v/v) buffer B (5mM KH_2PO_4, 25% v/v ACN, 350mM KCl pH

615 2.72) at a flow rate of 0.3mL/min. Peptides were collected every 4.5 min between 10 and 28

616 min; 4 min between 28 and 40 min; 2 min between 40 and 70 min and; 4 min between 70

617 and 132.5 min. The resulting SCX fractionated samples were dried in a vacuum centrifuge

618 and stored at -20°C until mass spectrometry was performed.

619 **4.8 Nano-LC MS/MS analysis**

620 The dried peptides from each SCX fractions were resuspended in loading/desalting

621 solution (0.1% v/v formic acid (FA), 2% v/v ACN) and 40μL of sample was loaded onto a

622 reverse phase peptide Captrap (Michrom Bioresources, USA) for pre-concentration and

623 desalting with 0.1% v/v FA, 2% v/v ACN at 5μL/min for 10 min per fraction. The peptide

624 trap was then switched on line with the Halo C18 column (75μm x 10 cm, 2.7μm, 160Å)

625 (Advanced Materials Technology, USA). The desalted peptides in each fraction were eluted

626 from the C18 column using a linear solvent gradient, with steps, from 98:2 of mobile phase

627 A (0.1% v/v FA): mobile phase B (90% v/v ACN, 0.1% v/v FA) to 65:35, at 300 nL/min

628 over 100 min per fraction. After peptide elution, the column was cleaned with 95% buffer B

629 for 15 min and then equilibrated with buffer A for 25 min before next sample injection.

630 Mass spectra were acquired on an AB SCIEX TripleTOF 5600 mass spectrometer.

631 The reverse phase nanoLC eluent was subjected to positive ion nanoflow electrospray

632 analysis in an information dependant acquisition (IDA) mode. In the IDA mode, TOF-MS

633 survey scan spectra from m/z 400 – 1500 were acquired for each fraction every 0.25 s. The

634 ten most intense multiply charged ions (counts >150) in the survey scan were sequentially

635 subjected to MS/MS analysis. MS/MS spectra were accumulated for 200 milliseconds in the

636 mass range m/z 100 – 1500 with the total cycle time 2.3 seconds.

637 **4.9 Protein identification**

The nanoLC ESI MS/MS data set (*.wiff) files were submitted into ProteinPilot software (ver. 4.2b, AB SCIEX) for data processing and protein identification. This program uses the Paragon Algorithm for protein database searching, identification, protein grouping for the removal of redundant hits and quantitative comparisons [61]. The following search parameters were selected: sample type, iTRAQ 4plex (peptide labelled); Cysteine alkylation, MMTS; Digestion, trypsin; Instrument, TripleTOF 5600; Special factors, none; Species, human; ID focus, biological modifications; Database, uniprot_sprot2014; and Search effort, thorough. The resulting data set was auto bias corrected ProteinPilot to get rid of any variations imparted due to the unequal mixing during the combination of different labelled samples or loading errors. The detected protein threshold (unused ProtScore) was set to $\geq$ 1.3 (95% confidence or better) and a *p-value* (p < 0.05) ensured that protein identifications and subsequent quantitation were not based on single peptide hits. The results were then exported into Microsoft Excel for manual data interpretation and other statistical analysis.

4.10 Bioinformatics Analysis of Proteomic Data

To appreciate the data generated, lists of significantly altered proteins were uploaded into QIAGEN's Ingenuity® Pathway Analysis (IPA®, QIAGEN Redwood City, www.qiagen.com/ingenuity) software server and analysed using the Core Analysis module to rank the proteins into top biological functions including disease and disorders as well as molecular and cellular functions. The reference set and parameters for IPA on significantly altered protein list was as follows: (i) Reference set, Ingenuity Knowledge Base (Genes Only); (ii) Relationship to include, Direct and Indirect; (iii) Filter Summary, Consider only molecules and/or relationships where (species = Human) AND (cell lines = All Cancer cell lines in ingenuity database). Additionally, cellular location of all the identified proteins was determined using PloGO, a gene ontology (GO) mapping software [62].

4.11 Western blotting assay

Protein extracts used for iTRAQ analysis were separated using 4-12% NuPAGE gel (Invitrogen) at 200V for 1hr. The resolved proteins were then electrophoretically transferred onto to a PVDF membrane (Invitrogen). After the transfer, the PVDF membranes were immediately incubated in blocking buffer, containing Tris buffered saline (TBS) with 3% (w/v) bovine serum albumin (BSA) and 0.5% (v/v) Tween-20, for 1 hr at room temperature with gentle shaking. The blots were then incubated with specific primary antibody overnight

669 (4 °C) with gentle shaking. Following this they were then incubated with horseradish
670 peroxidase-conjugated mouse, goat or rabbit secondary antibodies (R&D Systems,
671 Minnesota, USA). The imunoreactivity was detected using chemiluminescence substrate
672 (SuperSignal West Femto Maximum Sensitivity Substrate, Thermo) and imaged using LAS
673 3000, FUJI. The following primary antibodies were used: uPAR antibody (AF807) was
674 purchased from R&D Systems; annexin A2 (ab41803) and RAB10 (ab181367) were
675 purchased from abcam; and ezrin (sc-58758) was purchased from Santa Cruz Biotechnology.
676 Antibody dilutions were applied as per manufacturer's recommendations. Image Studio Lite
677 (ver 5.0) (LI-COR, http://www.licor.com/bio/products/software/image_studio_lite/) was
678 used for measurement of signal intensities where required.

679 **4.12 Statistical Analysis**

680   All statistical analyses were performed using R-package and/or Microsoft Excel. All
681 the p-values were calculated using student's t-test followed by Bonferroni p-value
682 correction. A $p<0.05$ was considered to be statistically significant for each case.

683 **SUPPLEMENTARY INFORMATION**

684   **Supplementary Table 1.** The complete list of 222 proteins that were significantly
685 up- or down-regulated in the untreated HCT116^{WT} cells relative to the untreated
686 HCT116$^{uPAR-AS}$ cells (HCT116^{WT}-/ HCT116$^{uPAR-AS}$-); **Supplementary Table 2.** The
687 complete list of 279 proteins that were significantly up- or down-regulated in TGFβ treated
688 HCT116^{WT} cells relative to TGFβ treated HCT116$^{uPAR-AS}$ cells (HCT116^{WT}+/HCT116^{uPAR-}
689 ^{AS}+); **Supplementary Table 3.** List of other important proteins identified from untreated
690 and TGFβ treated conditions.

691 **CONFLICT OF INTEREST**

692   The authors declare no actual or potential conflicts of interest; including any
693 financial, personal or other relationships with other people or organizations.

694 **ACKNOWLEDGEMENTS**

700 was written with all authors making academic contributions. All authors have given approval
701 to the final version of this manuscript.

702

703 **REFERENCES**

704 1.   Ferlay, J., et al., *Cancer incidence and mortality worldwide: Sources, methods and*
705   *major patterns in GLOBOCAN 2012.* Int J Cancer, 2015. **136**(5): p. E359-86.
706 2.   Chambers, A.F., A.C. Groom, and I.C. MacDonald, *Dissemination and growth of*
707   *cancer cells in metastatic sites.* Nature reviews. Cancer, 2002. **2**(8): p. 563-72.
708 3.   Mehlen, P. and A. Puisieux, *Metastasis: a question of life or death.* Nature reviews.
709   Cancer, 2006. **6**(6): p. 449-58.
710 4.   Ahn, S.B., et al., *Epithelial and stromal cell urokinase plasminogen activator*
711   *receptor expression differentially correlates with survival in rectal cancer stages B*
712   *and C patients.* PLoS One, 2015. **10**(2): p. e0117786.
713 5.   Bellam, N. and B. Pasche, *Tgf-beta signaling alterations and colon cancer.* Cancer
714   Treat Res, 2010. **155**: p. 85-103.
715 6.   Ahn, S.B., et al., *Correlations between integrin alphanubeta6 expression and*
716   *clinico-pathological features in stage B and stage C rectal cancer.* PLoS One, 2014.
717   **9**(5): p. e97248.
718 7.   Urosevic, J., A.R. Nebreda, and R.R. Gomis, *MAPK signaling control of colon*
719   *cancer metastasis.* Cell Cycle, 2014. **13**(17): p. 2641-2.
720 8.   Yu, Q. and I. Stamenkovic, *Cell surface-localized matrix metalloproteinase-9*
721   *proteolytically activates TGF-beta and promotes tumor invasion and angiogenesis.*
722   Genes Dev, 2000. **14**(2): p. 163-76.
723 9.   Zeng, Z.S., et al., *Matrix metalloproteinase-7 expression in colorectal cancer liver*
724   *metastases: evidence for involvement of MMP-7 activation in human cancer*
725   *metastases.* Clin Cancer Res, 2002. **8**(1): p. 144-8.
726 10.   Voulgari, A. and A. Pintzas, *Epithelial-mesenchymal transition in cancer metastasis:*
727   *mechanisms, markers and strategies to overcome drug resistance in the clinic.*
728   Biochimica et biophysica acta, 2009. **1796**(2): p. 75-90.
729 11.   Smith, H.W. and C.J. Marshall, *Regulation of cell signalling by uPAR.* Nature
730   reviews. Molecular cell biology, 2010. **11**(1): p. 23-36.
731 12.   Lyons, R.M., et al., *Mechanism of activation of latent recombinant transforming*
732   *growth factor beta 1 by plasmin.* J Cell Biol, 1990. **110**(4): p. 1361-7.
733 13.   Massague, J., *TGFbeta in Cancer.* Cell, 2008. **134**(2): p. 215-30.
734 14.   Fuxe, J., T. Vincent, and A. Garcia de Herreros, *Transcriptional crosstalk between*
735   *TGF-beta and stem cell pathways in tumor cell invasion: role of EMT promoting*
736   *Smad complexes.* Cell cycle, 2010. **9**(12): p. 2363-74.
737 15.   Tsushima, H., et al., *High levels of transforming growth factor beta 1 in patients with*
738   *colorectal cancer: association with disease progression.* Gastroenterology, 1996.
739   **110**(2): p. 375-82.
740 16.   Allen, M.D., et al., *Altered Microenvironment Promotes Progression of Pre-Invasive*
741   *Breast Cancer: myoepithelial expression of alphavbeta6 integrin in DCIS identifies*
742   *high-risk patients and predicts recurrence.* Clin Cancer Res, 2013.
743 17.   Dang, D., et al., *Matrix metalloproteinases and TGFbeta1 modulate oral tumor cell*
744   *matrix.* Biochem Biophys Res Commun, 2004. **316**(3): p. 937-42.

745 18. Boonstra, M.C., et al., *Expression of uPAR in tumor-associated stromal cells is*
746 *associated with colorectal cancer patient prognosis: a TMA study.* BMC Cancer,
747 2014. **14**: p. 269.

748 19. Illemann, M., et al., *Urokinase-type plasminogen activator receptor (uPAR) on*
749 *tumor-associated macrophages is a marker of poor prognosis in colorectal cancer.*
750 Cancer Med, 2014. **3**(4): p. 855-64.

751 20. Blackstock, W.P. and M.P. Weir, *Proteomics: quantitative and physical mapping of*
752 *cellular proteins.* Trends Biotechnol, 1999. **17**(3): p. 121-7.

753 21. Rabilloud, T. and C. Lelong, *Two-dimensional gel electrophoresis in proteomics: a*
754 *tutorial.* J Proteomics, 2011. **74**(10): p. 1829-41.

755 22. Friedman, D.B., et al., *Proteome analysis of human colon cancer by two-dimensional*
756 *difference gel electrophoresis and mass spectrometry.* Proteomics, 2004. **4**(3): p.
757 793-811.

758 23. Ong, S.E., et al., *Stable isotope labeling by amino acids in cell culture, SILAC, as a*
759 *simple and accurate approach to expression proteomics.* Mol Cell Proteomics, 2002.
760 **1**(5): p. 376-86.

761 24. Ghosh, D., et al., *Identification of key players for colorectal cancer metastasis by*
762 *iTRAQ quantitative proteomics profiling of isogenic SW480 and SW620 cell lines.* J
763 Proteome Res, 2011. **10**(10): p. 4373-87.

764 25. Chen, H., et al., *iTRAQ-based proteomic analysis of dioscin on human HCT-116*
765 *colon cancer cells.* Proteomics, 2014. **14**(1): p. 51-73.

766 26. Ahmed, N., et al., *Downregulation of urokinase plasminogen activator receptor*
767 *expression inhibits Erk signalling with concomitant suppression of invasiveness due*
768 *to loss of uPAR-beta1 integrin complex in colon cancer cells.* Br J Cancer, 2003.
769 **89**(2): p. 374-84.

770 27. Saldanha, R.G., et al., *Proteomic identification of lynchpin urokinase plasminogen*
771 *activator receptor protein interactions associated with epithelial cancer malignancy.*
772 J Proteome Res, 2007. **6**(3): p. 1016-28.

773 28. Nowicki, T.S., et al., *Downregulation of uPAR inhibits migration, invasion,*
774 *proliferation, FAK/PI3K/Akt signaling and induces senescence in papillary thyroid*
775 *carcinoma cells.* Cell Cycle, 2011. **10**(1): p. 100-7.

776 29. Pascovici, D., et al., *Combining protein ratio p-values as a pragmatic approach to*
777 *the analysis of multirun iTRAQ experiments.* J Proteome Res, 2015. **14**(2): p. 738-
778 46.

779 30. Shahjee, H.M., et al., *Antiproliferative factor decreases Akt phosphorylation and*
780 *alters gene expression via CKAP4 in T24 bladder carcinoma cells.* J Exp Clin Cancer
781 Res, 2010. **29**: p. 160.

782 31. Balch, C. and J.R. Dedman, *Annexins II and V inhibit cell migration.* Exp Cell Res,
783 1997. **237**(2): p. 259-63.

784 32. Sievers, C., et al., *Prohibitins are required for cancer cell proliferation and*
785 *adhesion.* PLoS One, 2010. **5**(9): p. e12735.

786 33. Meredith, J.E., Jr., B. Fazeli, and M.A. Schwartz, *The extracellular matrix as a cell*
787 *survival factor.* Mol Biol Cell, 1993. **4**(9): p. 953-61.

788 34. Frisch, S.M. and H. Francis, *Disruption of epithelial cell-matrix interactions induces*
789 *apoptosis.* J Cell Biol, 1994. **124**(4): p. 619-26.

790 35. Kim, J.T., et al., *Apoptosis-inducing factor (AIF) inhibits protein synthesis by*
791 *interacting with the eukaryotic translation initiation factor 3 subunit p44 (eIF3g).*
792 FEBS Lett, 2006. **580**(27): p. 6375-83.

793   36.   Lee, M.J., et al., *Identification of the hypoxia-inducible factor 1 alpha-responsive*
794   *HGTD-P gene as a mediator in the mitochondrial apoptotic pathway.* Mol Cell Biol,
795   2004. **24**(9): p. 3918-27.
796   37.   Schuck, S., et al., *Rab10 is involved in basolateral transport in polarized Madin-*
797   *Darby canine kidney cells.* Traffic, 2007. **8**(1): p. 47-60.
798   38.   Babbey, C.M., et al., *Rab10 regulates membrane transport through early endosomes*
799   *of polarized Madin-Darby canine kidney cells.* Mol Biol Cell, 2006. **17**(7): p. 3156-
800   75.
801   39.   Lee, H., et al., *Analysis of nuclear high mobility group box 1 (HMGB1)-binding*
802   *proteins in colon cancer cells: clustering with proteins involved in secretion and*
803   *extranuclear function.* J Proteome Res, 2010. **9**(9): p. 4661-70.
804   40.   Yanai, H., et al., *HMGB proteins function as universal sentinels for nucleic-acid-*
805   *mediated innate immune responses.* Nature, 2009. **462**(7269): p. 99-103.
806   41.   Prekeris, R., et al., *Differential roles of syntaxin 7 and syntaxin 8 in endosomal*
807   *trafficking.* Mol Biol Cell, 1999. **10**(11): p. 3891-908.
808   42.   Stromberg, S., et al., *Selective expression of Syntaxin-7 protein in benign*
809   *melanocytes and malignant melanoma.* J Proteome Res, 2009. **8**(4): p. 1639-46.
810   43.   Cho, D., et al., *The expression of DBC1/CCAR2 is associated with poor prognosis of*
811   *ovarian carcinoma.* J Ovarian Res, 2015. **8**(1): p. 2.
812   44.   Bae, J.S., et al., *CK2alpha phosphorylates DBC1 and is involved in the progression*
813   *of gastric carcinoma and predicts poor survival of gastric carcinoma patients.* Int J
814   Cancer, 2015. **136**(4): p. 797-809.
815   45.   Kim, W. and J.E. Kim, *Deleted in breast cancer 1 (DBC1) deficiency results in*
816   *apoptosis of breast cancer cells through impaired responses to UV-induced DNA*
817   *damage.* Cancer Lett, 2013. **333**(2): p. 180-6.
818   46.   Zhang, Y., et al., *DBC1 is over-expressed and associated with poor prognosis in*
819   *colorectal cancer.* Int J Clin Oncol, 2014. **19**(1): p. 106-12.
820   47.   Kikuchi, K., et al., *High SIRT1 expression and low DBC1 expression are associated*
821   *with poor prognosis in colorectal cancer.* journal of Cancer Therapeutics and
822   Research, 2013. **2**(1).
823   48.   Leiphrakpam, P.D., et al., *Ezrin expression and cell survival regulation in colorectal*
824   *cancer.* Cell Signal, 2014. **26**(5): p. 868-79.
825   49.   Ghaffari, A., et al., *A novel role for ezrin in breast cancer angio/lymphangiogenesis.*
826   Breast Cancer Res, 2014. **16**(5): p. 438.
827   50.   Saito, S., et al., *Mechanisms underlying cancer progression caused by ezrin*
828   *overexpression in tongue squamous cell carcinoma.* PLoS One, 2013. **8**(1): p.
829   e54881.
830   51.   Lokman, N.A., et al., *The role of annexin A2 in tumorigenesis and cancer*
831   *progression.* Cancer Microenviron, 2011. **4**(2): p. 199-208.
832   52.   Yeatman, T.J., et al., *Expression of annexins on the surfaces of non-metastatic and*
833   *metastatic human and rodent tumor cells.* Clin Exp Metastasis, 1993. **11**(1): p. 37-
834   44.
835   53.   Badura, M., et al., *DNA damage and eIF4G1 in breast cancer cells reprogram*
836   *translation for survival and DNA repair mRNAs.* Proc Natl Acad Sci U S A, 2012.
837   **109**(46): p. 18767-72.
838   54.   Clarkson, B.K., W.V. Gilbert, and J.A. Doudna, *Functional overlap between eIF4G*
839   *isoforms in Saccharomyces cerevisiae.* PLoS One, 2010. **5**(2): p. e9114.
840   55.   Park, E.H., et al., *Depletion of eIF4G from yeast cells narrows the range of*
841   *translational efficiencies genome-wide.* BMC Genomics, 2011. **12**: p. 68.

842 56. Ramirez-Valle, F., et al., *eIF4GI links nutrient sensing by mTOR to cell proliferation*
843 *and inhibition of autophagy.* J Cell Biol, 2008. **181**(2): p. 293-307.
844 57. Brattain, M.G., et al., *Heterogeneity of malignant cells from a human colonic*
845 *carcinoma.* Cancer Res, 1981. **41**(5): p. 1751-6.
846 58. Wang, Y., et al., *Inhibition of colon cancer metastasis by a 3'- end antisense*
847 *urokinase receptor mRNA in a nude mouse model.* Int J Cancer, 2001. **92**(2): p. 257-
848 62.
849 59. Wang, C.Y. and C.F. Lin, *Annexin A2: Its Molecular Regulation and Cellular*
850 *Expression in Cancer Development.* Disease Markers, 2014.
851 60. Lee, A., et al., *Rat liver membrane glycoproteome: enrichment by phase partitioning*
852 *and glycoprotein capture.* Journal of proteome research, 2009. **8**(2): p. 770-81.
853 61. Shilov, I.V., et al., *The Paragon Algorithm, a next generation search engine that uses*
854 *sequence temperature values and feature probabilities to identify peptides from*
855 *tandem mass spectra.* Molecular & cellular proteomics : MCP, 2007. **6**(9): p. 1638-
856 55.
857 62. Pascovici, D., et al., *PloGO: plotting gene ontology annotation and abundance in*
858 *multi-condition proteomics experiments.* Proteomics, 2012. **12**(3): p. 406-10.

859

860

4.2 – Supplemental files

Supplementary Table 1: Comparison of TGFβ untreated HCT116 WT/HCT116AS

Uniprot	Unused	Total	X.Cov.95.	Protein Name; Organism; Gene name	iTRAQ Fold Change	StouffersPval
P61026	9.45	11.04	33	Ras-related protein Rab-10 OS=Homo sapiens GN=RAB10 PE=1 SV=1	7.542	0.012
P04792	20.12	20.12	69.76	Heat shock protein beta-1 OS=Homo sapiens GN=HSPB1 PE=1 SV=2	4.443	0.000
P60953	6	6	21.47	Cell division control protein 42 homolog OS=Homo sapiens GN=CDC42 PE=1 SV=2	4.342	0.021
Q07021	12.14	12.14	36.17	Complement component 1 Q subcomponent-binding protein, mitochondrial OS=Homo sapiens GN=C1QBP PE=1 SV=1	3.418	0.000
P62158	7.65	7.65	57.72	Calmodulin OS=Homo sapiens GN=CALM1 PE=1 SV=2	3.317	0.004
P09429	14.62	14.62	38.6	High mobility group protein B1 OS=Homo sapiens GN=HMGB1 PE=1 SV=3	3.153	0.005
P07602	16.96	16.96	28.05	Proactivator polypeptide OS=Homo sapiens GN=PSAP PE=1 SV=2	3.059	0.000
P09622	6.16	6.16	8.644	Dihydrolipoyl dehydrogenase, mitochondrial OS=Homo sapiens GN=DLD PE=1 SV=2	2.920	0.014
P63261	48.37	48.37	62.4	Actin, cytoplasmic 2 OS=Homo sapiens GN=ACTG1 PE=1 SV=1	2.705	0.000
P05556	27.88	28.34	22.06	Integrin beta-1 OS=Homo sapiens GN=ITGB1 PE=1 SV=2	2.702	0.000
P06733	17.46	17.46	29.03	Alpha-enolase OS=Homo sapiens GN=ENO1 PE=1 SV=2	2.698	0.000
Q02952	25.73	25.73	19.08	A-kinase anchor protein 12 OS=Homo sapiens GN=AKAP12 PE=1 SV=4	2.648	0.000
P06748	17.94	17.94	33.67	Nucleophosmin OS=Homo sapiens GN=NPM1 PE=1 SV=2	2.595	0.000
P50151	6.81	6.81	52.94	Guanine nucleotide-binding protein G(I)/G(S)/G(O) subunit gamma-10 OS=Homo sapiens GN=GNG10 PE=1 SV=1	2.509	0.029
P62937	19.61	19.99	69.09	Peptidyl-prolyl cis-trans isomerase A OS=Homo sapiens GN=PPIA PE=1 SV=2	2.469	0.000
P07355	16.25	16.25	42.18	Annexin A2 OS=Homo sapiens GN=ANXA2 PE=1 SV=2	2.466	0.000
P18669	6.2	6.2	22.05	Phosphoglycerate mutase 1 OS=Homo sapiens GN=PGAM1 PE=1 SV=2	2.441	0.012
P07237	33.59	33.59	40.16	Protein disulfide-isomerase OS=Homo sapiens GN=P4HB PE=1 SV=3	2.438	0.000
P26583	4.37	8.7	25.36	High mobility group protein B2 OS=Homo sapiens GN=HMGB2 PE=1 SV=2	2.382	0.001
Q13740	29.32	29.33	39.62	CD166 antigen OS=Homo sapiens GN=ALCAM PE=1 SV=2	2.338	0.000
P26885	5.92	5.92	49.3	Peptidyl-prolyl cis-trans isomerase FKBP2 OS=Homo sapiens GN=FKBP2 PE=1 SV=2	2.338	0.001
O14561	9.62	9.62	30.13	Acyl carrier protein, mitochondrial OS=Homo sapiens GN=NDUFAB1 PE=1 SV=3	2.314	0.019
Q03252	36.98	43.54	40.17	Lamin-B2 OS=Homo sapiens GN=LMNB2 PE=1 SV=3	2.313	0.000
P15531	2.08	8.49	29.61	Nucleoside diphosphate kinase A OS=Homo sapiens GN=NME1 PE=1 SV=1	2.276	0.040
Q14978	23.05	23.05	18.03	Nucleolar and coiled-body phosphoprotein 1 OS=Homo sapiens GN=NOLC1 PE=1 SV=2	2.262	0.000
Q9UHB6	6.02	6.48	7.378	LIM domain and actin-binding protein 1 OS=Homo sapiens GN=LIMA1 PE=1 SV=1	2.205	0.044
Q09666	38.54	38.61	7.301	Neuroblast differentiation-associated protein AHNAK OS=Homo sapiens GN=AHNAK PE=1 SV=2	2.194	0.000
P17301	11.95	12.3	7.959	Integrin alpha-2 OS=Homo sapiens GN=ITGA2 PE=1 SV=1	2.193	0.000
P27797	16.02	16.02	30.7	Calreticulin OS=Homo sapiens GN=CALR PE=1 SV=1	2.177	0.001
P20700	45.35	50.54	45.39	Lamin-B1 OS=Homo sapiens GN=LMNB1 PE=1 SV=2	2.155	0.000
P09382	9.39	9.39	45.19	Galectin-1 OS=Homo sapiens GN=LGALS1 PE=1 SV=2	2.142	0.008
P49748	14.53	14.53	24.12	Very long-chain specific acyl-CoA dehydrogenase, mitochondrial OS=Homo sapiens GN=ACADVL PE=1 SV=1	2.103	0.000
Q15019	18.25	18.35	44.88	Septin-2 OS=Homo sapiens GN=SEPT2 PE=1 SV=1	2.102	0.000
O15347	8.12	8.12	30.5	High mobility group protein B3 OS=Homo sapiens GN=HMGB3 PE=1 SV=4	2.101	0.033
P37235	2.32	2.32	14.51	Hippocalcin-like protein 1 OS=Homo sapiens GN=HPCAL1 PE=1 SV=3	2.083	0.024
O43181	4.07	4.07	14.29	NADH dehydrogenase [ubiquinone] iron-sulfur protein 4, mitochondrial OS=Homo sapiens GN=NDUFS4 PE=1 SV=1	2.072	0.040
P17931	10.44	10.44	32.8	Galectin-3 OS=Homo sapiens GN=LGALS3 PE=1 SV=5	2.061	0.000
Q14697	16.75	16.75	13.35	Neutral alpha-glucosidase AB OS=Homo sapiens GN=GANAB PE=1 SV=3	2.036	0.000
P30040	3.36	3.38	15.33	Endoplasmic reticulum resident protein 29 OS=Homo sapiens GN=ERP29 PE=1 SV=4	2.027	0.002
Q9NVA2	7.19	7.23	11.19	Septin-11 OS=Homo sapiens GN=SEPT11 PE=1 SV=3	2.019	0.002
Q15233	37.63	39.78	46.28	Non-POU domain-containing octamer-binding protein OS=Homo sapiens GN=NONO PE=1 SV=4	2.014	0.000
O43399	7.85	7.85	37.86	Tumor protein D54 OS=Homo sapiens GN=TPD52L2 PE=1 SV=2	1.999	0.002
P26006	12.44	12.67	8.278	Integrin alpha-3 OS=Homo sapiens GN=ITGA3 PE=1 SV=5	1.983	0.000
P19105	12.08	12.08	46.78	Myosin regulatory light chain 12A OS=Homo sapiens GN=MYL12A PE=1 SV=2	1.972	0.012
Q99733	8.8	8.8	17.6	Nucleosome assembly protein 1-like 4 OS=Homo sapiens GN=NAP1L4 PE=1 SV=1	1.968	0.047
O43169	13.2	13.5	63.01	Cytochrome b5 type B OS=Homo sapiens GN=CYB5B PE=1 SV=2	1.952	0.002
Q8WXF1	13.79	14.5	19.5	Paraspeckle component 1 OS=Homo sapiens GN=PSPC1 PE=1 SV=1	1.909	0.000
P16403	2	23.86	36.62	Histone H1.2 OS=Homo sapiens GN=HIST1H1C PE=1 SV=2	1.900	0.005
Q9UHD8	10.07	10.09	16.89	Septin-9 OS=Homo sapiens GN=SEPT9 PE=1 SV=2	1.870	0.006
P51148	7.03	7.1	32.87	Ras-related protein Rab-5C OS=Homo sapiens GN=RAB5C PE=1 SV=2	1.867	0.005
Q9UGP8	5.27	5.29	5.526	Translocation protein SEC63 homolog OS=Homo sapiens GN=SEC63 PE=1 SV=2	1.863	0.030
Q16630	8.84	8.87	15.43	Cleavage and polyadenylation specificity factor subunit 6 OS=Homo sapiens GN=CPSF6 PE=1 SV=2	1.857	0.003
P23284	27.01	27.01	54.63	Peptidyl-prolyl cis-trans isomerase B OS=Homo sapiens GN=PPIB PE=1 SV=2	1.835	0.000
O60664	16.09	16.09	33.41	Perilipin-3 OS=Homo sapiens GN=PLIN3 PE=1 SV=3	1.805	0.000
P60174	4.32	4.32	17.13	Triosephosphate isomerase OS=Homo sapiens GN=TPI1 PE=1 SV=3	1.803	0.031
P49821	19.33	19.44	37.72	NADH dehydrogenase [ubiquinone] flavoprotein 1, mitochondrial OS=Homo sapiens GN=NDUFV1 PE=1 SV=4	1.793	0.001
P23246	46.04	46.04	42.29	Splicing factor, proline- and glutamine-rich OS=Homo sapiens GN=SFPQ PE=1 SV=2	1.784	0.000
P35221	18.22	18.22	17.66	Catenin alpha-1 OS=Homo sapiens GN=CTNNA1 PE=1 SV=1	1.779	0.000
P40926	8.03	8.03	20.12	Malate dehydrogenase, mitochondrial OS=Homo sapiens GN=MDH2 PE=1 SV=3	1.774	0.000
P21926	7.41	7.45	12.72	CD9 antigen OS=Homo sapiens GN=CD9 PE=1 SV=4	1.756	0.034
P42167	6.84	23.82	40.97	Lamina-associated polypeptide 2, isoforms beta/gamma OS=Homo sapiens GN=TMPO PE=1 SV=2	1.746	0.008
P09110	11.74	11.74	31.6	3-ketoacyl-CoA thiolase, peroxisomal OS=Homo sapiens GN=ACAA1 PE=1 SV=2	1.739	0.004
P51149	27.08	27.08	66.67	Ras-related protein Rab-7a OS=Homo sapiens GN=RAB7A PE=1 SV=1	1.729	0.000
P63104	6.65	6.65	24.9	14-3-3 protein zeta/delta OS=Homo sapiens GN=YWHAZ PE=1 SV=1	1.725	0.020
P61769	5.88	5.88	28.57	Beta-2-microglobulin OS=Homo sapiens GN=B2M PE=1 SV=1	1.701	0.034
Q13765	5.89	5.89	19.07	Nascent polypeptide-associated complex subunit alpha OS=Homo sapiens GN=NACA PE=1 SV=1	1.694	0.037
Q9Y5B9	12.47	12.51	7.832	FACT complex subunit SPT16 OS=Homo sapiens GN=SUPT16H PE=1 SV=1	1.687	0.015
P19404	10.31	10.31	33.33	NADH dehydrogenase [ubiquinone] flavoprotein 2, mitochondrial OS=Homo sapiens GN=NDUFV2 PE=1 SV=2	1.686	0.001
P14314	20.47	20.47	25.95	Glucosidase 2 subunit beta OS=Homo sapiens GN=PRKCSH PE=1 SV=2	1.682	0.000
P10606	15.58	15.58	46.51	Cytochrome c oxidase subunit 5B, mitochondrial OS=Homo sapiens GN=COX5B PE=1 SV=2	1.675	0.006
P14625	21.02	23.41	21.54	Endoplasmin OS=Homo sapiens GN=HSP90B1 PE=1 SV=1	1.654	0.000
P30101	27.36	27.7	37.03	Protein disulfide-isomerase A3 OS=Homo sapiens GN=PDIA3 PE=1 SV=4	1.649	0.000
P61586	11.39	13.47	45.08	Transforming protein RhoA OS=Homo sapiens GN=RHOA PE=1 SV=1	1.644	0.037
Q13185	5.55	6.06	29.51	Chromobox protein homolog 3 OS=Homo sapiens GN=CBX3 PE=1 SV=4	1.628	0.024
P78310	10.28	10.28	23.84	Coxsackievirus and adenovirus receptor OS=Homo sapiens GN=CXADR PE=1 SV=1	1.623	0.008
P31040	5.82	5.82	8.735	Succinate dehydrogenase [ubiquinone] flavoprotein subunit, mitochondrial OS=Homo sapiens GN=SDHA PE=1 SV=2	1.604	0.024
P00558	6.6	7.11	11.99	Phosphoglycerate kinase 1 OS=Homo sapiens GN=PGK1 PE=1 SV=3	1.598	0.035
P61224	12.38	14.13	49.46	Ras-related protein Rap-1b OS=Homo sapiens GN=RAP1B PE=1 SV=1	1.573	0.009
P51970	8	8.08	30.23	NADH dehydrogenase [ubiquinone] 1 alpha subcomplex subunit 8 OS=Homo sapiens GN=NDUFA8 PE=1 SV=3	1.568	0.017
P06576	50.5	50.5	64.08	ATP synthase subunit beta, mitochondrial OS=Homo sapiens GN=ATP5B PE=1 SV=3	1.566	0.000
P17480	13.97	13.97	12.7	Nucleolar transcription factor 1 OS=Homo sapiens GN=UBTF PE=1 SV=1	1.559	0.000
Q8WTV0	5.83	5.89	6.703	Scavenger receptor class B member 1 OS=Homo sapiens GN=SCARB1 PE=1 SV=1	1.550	0.015
P50454	15.62	15.68	31.34	Serpin H1 OS=Homo sapiens GN=SERPINH1 PE=1 SV=2	1.548	0.001
O43852	6.77	6.82	14.29	Calumenin OS=Homo sapiens GN=CALU PE=1 SV=2	1.544	0.024
P11021	42.64	46.82	40.37	78 kDa glucose-regulated protein OS=Homo sapiens GN=HSPA5 PE=1 SV=2	1.537	0.000
Q07065	12.45	12.45	19.1	Cytoskeleton-associated protein 4 OS=Homo sapiens GN=CKAP4 PE=1 SV=2	1.528	0.000
P28331	16.16	16.22	22.42	NADH-ubiquinone oxidoreductase 75 kDa subunit, mitochondrial OS=Homo sapiens GN=NDUFS1 PE=1 SV=3	1.499	0.000
O15400	8	8.05	20.31	Syntaxin-7 OS=Homo sapiens GN=STX7 PE=1 SV=4	1.482	0.004
O75915	5.77	5.77	14.36	PRA1 family protein 3 OS=Homo sapiens GN=ARL6IP5 PE=1 SV=1	1.475	0.047

P04040	10.16	10.16	21.44	Catalase OS=Homo sapiens GN=CAT PE=1 SV=3	1.470	0.024
P35580	10.1	25.14	7.743	Myosin-10 OS=Homo sapiens GN=MYH10 PE=1 SV=3	1.469	0.014
Q10471	8.99	9.03	14.36	Polypeptide N-acetylgalactosaminyltransferase 2 OS=Homo sapiens GN=GALNT2 PE=1 SV=1	1.466	0.019
Q06830	11.14	11.14	33.67	Peroxiredoxin-1 OS=Homo sapiens GN=PRDX1 PE=1 SV=1	1.465	0.019
P15311	32.66	32.68	32.94	Ezrin OS=Homo sapiens GN=EZR PE=1 SV=4	1.461	0.002
Q12797	6.55	6.55	10.29	Aspartyl/asparaginyl beta-hydroxylase OS=Homo sapiens GN=ASPH PE=1 SV=3	1.452	0.017
P48739	2.71	2.71	9.225	Phosphatidylinositol transfer protein beta isoform OS=Homo sapiens GN=PITPNB PE=1 SV=2	1.450	0.035
P24534	10.57	10.6	34.67	Elongation factor 1-beta OS=Homo sapiens GN=EEF1B2 PE=1 SV=3	1.449	0.002
Q99986	6.04	6.06	11.62	Serine/threonine-protein kinase VRK1 OS=Homo sapiens GN=VRK1 PE=1 SV=1	1.445	0.030
Q96AG4	18.33	18.33	33.88	Leucine-rich repeat-containing protein 59 OS=Homo sapiens GN=LRRC59 PE=1 SV=1	1.445	0.005
P48047	13.28	13.36	46.95	ATP synthase subunit O, mitochondrial OS=Homo sapiens GN=ATP5O PE=1 SV=1	1.439	0.035
O14949	4.55	4.55	37.8	Cytochrome b-c1 complex subunit 8 OS=Homo sapiens GN=UQCRQ PE=1 SV=4	1.430	0.027
Q15637	8	8	11.74	Splicing factor 1 OS=Homo sapiens GN=SF1 PE=1 SV=4	1.428	0.013
O75947	11.81	11.97	59.01	ATP synthase subunit d, mitochondrial OS=Homo sapiens GN=ATP5H PE=1 SV=3	1.424	0.001
Q96PD2	11.83	11.83	15.61	Discoidin, CUB and LCCL domain-containing protein 2 OS=Homo sapiens GN=DCBLD2 PE=1 SV=1	1.422	0.004
P38646	12.81	12.81	13.11	Stress-70 protein, mitochondrial OS=Homo sapiens GN=HSPA9 PE=1 SV=2	1.421	0.014
Q99536	8.13	8.13	21.63	Synaptic vesicle membrane protein VAT-1 homolog OS=Homo sapiens GN=VAT1 PE=1 SV=2	1.411	0.028
Q16795	10.76	10.76	27.59	NADH dehydrogenase [ubiquinone] 1 alpha subcomplex subunit 9, mitochondrial OS=Homo sapiens GN=NDUFA9 PE=1	1.411	0.004
P14927	9.85	9.85	43.24	Cytochrome b-c1 complex subunit 7 OS=Homo sapiens GN=UQCRB PE=1 SV=2	1.409	0.026
Q8WWI5	9.46	9.46	11.11	Choline transporter-like protein 1 OS=Homo sapiens GN=SLC44A1 PE=1 SV=1	1.408	0.007
P11387	21.58	21.58	15.95	DNA topoisomerase 1 OS=Homo sapiens GN=TOP1 PE=1 SV=2	1.406	0.000
P29692	7.82	7.97	23.13	Elongation factor 1-delta OS=Homo sapiens GN=EEF1D PE=1 SV=5	1.404	0.047
Q08945	10.78	10.78	13.68	FACT complex subunit SSRP1 OS=Homo sapiens GN=SSRP1 PE=1 SV=1	1.390	0.000
Q9NC51	20.51	20.51	22.3	Plasminogen activator inhibitor 1 RNA-binding protein OS=Homo sapiens GN=SERBP1 PE=1 SV=2	1.385	0.009
Q86Y82	10	10.01	28.26	Syntaxin-12 OS=Homo sapiens GN=STX12 PE=1 SV=1	1.380	0.008
P04844	12.95	12.95	18.38	Dolichyl-diphosphooligosaccharide--protein glycosyltransferase subunit 2 OS=Homo sapiens GN=RPN2 PE=1 SV=3	1.374	0.017
Q9HDC9	29.54	29.54	44.71	Adipocyte plasma membrane-associated protein OS=Homo sapiens GN=APMAP PE=1 SV=2	1.369	0.025
P13667	9.32	9.52	13.64	Protein disulfide-isomerase A4 OS=Homo sapiens GN=PDIA4 PE=1 SV=2	1.368	0.011
P16070	18.14	18.14	12.13	CD44 antigen OS=Homo sapiens GN=CD44 PE=1 SV=3	1.366	0.002
Q99653	12.67	12.71	54.36	Calcineurin B homologous protein 1 OS=Homo sapiens GN=CHP1 PE=1 SV=3	1.354	0.009
P09874	51.2	51.2	34.02	Poly [ADP-ribose] polymerase 1 OS=Homo sapiens GN=PARP1 PE=1 SV=4	1.349	0.000
O43707	12.01	12.01	9.001	Alpha-actinin-4 OS=Homo sapiens GN=ACTN4 PE=1 SV=2	1.343	0.010
O75489	13.37	13.37	35.23	NADH dehydrogenase [ubiquinone] iron-sulfur protein 3, mitochondrial OS=Homo sapiens GN=NDUFS3 PE=1 SV=1	1.328	0.003
P62316	11.55	11.55	46.61	Small nuclear ribonucleoprotein Sm D2 OS=Homo sapiens GN=SNRPD2 PE=1 SV=1	1.324	0.028
Q9Y639	8.02	8.02	13.57	Neuroplastin OS=Homo sapiens GN=NPTN PE=1 SV=2	1.323	0.030
P48960	9.02	9.02	10.78	CD97 antigen OS=Homo sapiens GN=CD97 PE=1 SV=4	1.320	0.046
P21589	12.23	12.33	20.38	5'-nucleotidase OS=Homo sapiens GN=NT5E PE=1 SV=1	1.319	0.035
Q9BTV4	12.64	12.64	31	Transmembrane protein 43 OS=Homo sapiens GN=TMEM43 PE=1 SV=1	1.313	0.001
Q8IWA5	10.55	10.55	8.64	Choline transporter-like protein 2 OS=Homo sapiens GN=SLC44A2 PE=1 SV=3	1.308	0.023
Q9Y6M1	12.96	12.96	19.2	Insulin-like growth factor 2 mRNA-binding protein 2 OS=Homo sapiens GN=IGF2BP2 PE=1 SV=2	1.301	0.006
P62899	7.83	7.83	31.2	60S ribosomal protein L31 OS=Homo sapiens GN=RPL31 PE=1 SV=1	1.290	0.040
Q9Y4L1	21.83	21.88	18.52	Hypoxia up-regulated protein 1 OS=Homo sapiens GN=HYOU1 PE=1 SV=1	1.276	0.013
P19338	67.49	67.49	34.23	Nucleolin OS=Homo sapiens GN=NCL PE=1 SV=3	1.273	0.005
O75367	14.93	15.59	30.11	Core histone macro-H2A.1 OS=Homo sapiens GN=H2AFY PE=1 SV=4	1.269	0.008
Q15084	6.52	7.36	13.18	Protein disulfide-isomerase A6 OS=Homo sapiens GN=PDIA6 PE=1 SV=1	1.262	0.046
P12956	38.3	38.3	39.9	X-ray repair cross-complementing protein 6 OS=Homo sapiens GN=XRCC6 PE=1 SV=2	1.252	0.000
P46013	30.79	30.79	8.968	Antigen KI-67 OS=Homo sapiens GN=MKI67 PE=1 SV=2	1.248	0.005
Q14165	17.5	17.5	26.71	Malectin OS=Homo sapiens GN=MLEC PE=1 SV=1	1.240	0.041
Q09028	4.55	4.69	11.76	Histone-binding protein RBBP4 OS=Homo sapiens GN=RBBP4 PE=1 SV=3	1.225	0.018
Q15029	17.23	17.44	18.72	116 kDa U5 small nuclear ribonucleoprotein component OS=Homo sapiens GN=EFTUD2 PE=1 SV=1	1.212	0.045
Q14444	5.1	5.26	13.12	Caprin-1 OS=Homo sapiens GN=CAPRIN1 PE=1 SV=2	0.806	0.016
Q01085	2	2	4.8	Nucleolysin TIAR OS=Homo sapiens GN=TIAL1 PE=1 SV=1	0.796	0.021
P43304	10.6	10.6	12.1	Glycerol-3-phosphate dehydrogenase, mitochondrial OS=Homo sapiens GN=GPD2 PE=1 SV=3	0.788	0.002
P62851	8.66	8.66	29.6	40S ribosomal protein S25 OS=Homo sapiens GN=RPS25 PE=1 SV=1	0.787	0.041
Q9UJZ1	15.85	15.85	34.55	Stomatin-like protein 2, mitochondrial OS=Homo sapiens GN=STOML2 PE=1 SV=1	0.773	0.013
P62263	10.29	10.29	48.34	40S ribosomal protein S14 OS=Homo sapiens GN=RPS14 PE=1 SV=3	0.773	0.048
P27816	21.6	21.6	19.7	Microtubule-associated protein 4 OS=Homo sapiens GN=MAP4 PE=1 SV=3	0.769	0.025
P52272	34.25	34.25	31.1	Heterogeneous nuclear ribonucleoprotein M OS=Homo sapiens GN=HNRNPM PE=1 SV=3	0.768	0.013
Q9NR30	16.62	16.62	16.73	Nucleolar RNA helicase 2 OS=Homo sapiens GN=DDX21 PE=1 SV=5	0.766	0.022
P38159	8.83	8.83	9.719	RNA-binding motif protein, X chromosome OS=Homo sapiens GN=RBMX PE=1 SV=3	0.761	0.026
Q14204	33.07	33.54	6.608	Cytoplasmic dynein 1 heavy chain 1 OS=Homo sapiens GN=DYNC1H1 PE=1 SV=5	0.745	0.001
Q8IYS2	10	10	11.51	Uncharacterized protein KIAA2013 OS=Homo sapiens GN=KIAA2013 PE=2 SV=1	0.740	0.016
P43686	9.82	11.92	20.1	26S protease regulatory subunit 6B OS=Homo sapiens GN=PSMC4 PE=1 SV=2	0.739	0.023
O94901	8.27	8.27	8.498	SUN domain-containing protein 1 OS=Homo sapiens GN=SUN1 PE=1 SV=3	0.738	0.015
O00571	6.04	6.82	9.063	ATP-dependent RNA helicase DDX3X OS=Homo sapiens GN=DDX3X PE=1 SV=3	0.729	0.045
Q9GZR7	4.63	4.63	6.636	ATP-dependent RNA helicase DDX24 OS=Homo sapiens GN=DDX24 PE=1 SV=1	0.721	0.045
P08195	26.44	26.51	29.21	4F2 cell-surface antigen heavy chain OS=Homo sapiens GN=SLC3A2 PE=1 SV=3	0.714	0.014
Q6IAA8	16.55	16.55	75.16	Ragulator complex protein LAMTOR1 OS=Homo sapiens GN=LAMTOR1 PE=1 SV=2	0.714	0.006
Q9BVJ6	8.04	8.09	7.782	U3 small nucleolar RNA-associated protein 14 homolog A OS=Homo sapiens GN=UTP14A PE=1 SV=1	0.714	0.001
P62847	6.44	6.44	29.32	40S ribosomal protein S24 OS=Homo sapiens GN=RPS24 PE=1 SV=1	0.713	0.005
P62917	10.07	10.07	24.12	60S ribosomal protein L8 OS=Homo sapiens GN=RPL8 PE=1 SV=2	0.712	0.013
Q9BVK6	17.86	17.86	37.02	Transmembrane emp24 domain-containing protein 9 OS=Homo sapiens GN=TMED9 PE=1 SV=2	0.710	0.030
P27708	13.71	13.96	6.292	CAD protein OS=Homo sapiens GN=CAD PE=1 SV=3	0.710	0.042
Q9NZ45	2	2	12.04	CDGSH iron-sulfur domain-containing protein 1 OS=Homo sapiens GN=CISD1 PE=1 SV=1	0.707	0.048
Q15046	12.53	12.53	17.76	Lysine--tRNA ligase OS=Homo sapiens GN=KARS PE=1 SV=3	0.706	0.024
P15880	22.77	22.77	38.23	40S ribosomal protein S2 OS=Homo sapiens GN=RPS2 PE=1 SV=2	0.705	0.009
P40429	12.21	12.21	23.15	60S ribosomal protein L13a OS=Homo sapiens GN=RPL13A PE=1 SV=2	0.702	0.028
Q14344	7.52	7.55	11.94	Guanine nucleotide-binding protein subunit alpha-13 OS=Homo sapiens GN=GNA13 PE=1 SV=2	0.702	0.024
P62701	20.49	20.49	39.16	40S ribosomal protein S4, X isoform OS=Homo sapiens GN=RPS4X PE=1 SV=2	0.699	0.031
P02786	25.35	25.35	23.42	Transferrin receptor protein 1 OS=Homo sapiens GN=TFRC PE=1 SV=2	0.696	0.003
Q00839	39.08	39.08	28.36	Heterogeneous nuclear ribonucleoprotein U OS=Homo sapiens GN=HNRNPU PE=1 SV=6	0.696	0.003
Q02127	15.5	15.5	40	Dihydroorotate dehydrogenase (quinone), mitochondrial OS=Homo sapiens GN=DHODH PE=1 SV=3	0.694	0.005
Q13895	6.22	6.24	14.19	Bystin OS=Homo sapiens GN=BYSL PE=1 SV=3	0.693	0.030
Q12907	19.4	19.4	38.2	Vesicular integral-membrane protein VIP36 OS=Homo sapiens GN=LMAN2 PE=1 SV=1	0.692	0.003
Q96I24	18.98	19.41	30.42	Far upstream element-binding protein 3 OS=Homo sapiens GN=FUBP3 PE=1 SV=2	0.686	0.007
P51665	5.12	5.12	28.09	26S proteasome non-ATPase regulatory subunit 7 OS=Homo sapiens GN=PSMD7 PE=1 SV=2	0.682	0.049
Q9UHG3	9.42	9.42	19.6	Prenylcysteine oxidase 1 OS=Homo sapiens GN=PCYOX1 PE=1 SV=3	0.677	0.000
P41252	12.56	12.62	9.271	Isoleucine--tRNA ligase, cytoplasmic OS=Homo sapiens GN=IARS PE=1 SV=2	0.675	0.025
P36578	30.91	30.91	39.58	60S ribosomal protein L4 OS=Homo sapiens GN=RPL4 PE=1 SV=5	0.674	0.000
P68104	25.32	25.32	38.1	Elongation factor 1-alpha 1 OS=Homo sapiens GN=EEF1A1 PE=1 SV=1	0.673	0.002
P61353	8.28	8.28	52.21	60S ribosomal protein L27 OS=Homo sapiens GN=RPL27 PE=1 SV=2	0.670	0.032

P61247	31.73	31.73	45.83	40S ribosomal protein S3a OS=Homo sapiens GN=RPS3A PE=1 SV=2	0.663	0.028
Q9NX63	7.33	7.36	24.23	Coiled-coil-helix-coiled-coil-helix domain-containing protein 3, mitochondrial OS=Homo sapiens GN=CHCHD3 PE=1 SV	0.663	0.005
P62191	5.16	5.32	9.773	26S protease regulatory subunit 4 OS=Homo sapiens GN=PSMC1 PE=1 SV=1	0.661	0.039
P56192	4.49	4.51	4.556	Methionine--tRNA ligase, cytoplasmic OS=Homo sapiens GN=MARS PE=1 SV=2	0.661	0.006
P52292	10.04	10.05	11.34	Importin subunit alpha-1 OS=Homo sapiens GN=KPNA2 PE=1 SV=1	0.657	0.005
P05023	14.63	14.63	11.53	Sodium/potassium-transporting ATPase subunit alpha-1 OS=Homo sapiens GN=ATP1A1 PE=1 SV=1	0.657	0.027
P23396	13.81	13.81	32.1	40S ribosomal protein S3 OS=Homo sapiens GN=RPS3 PE=1 SV=2	0.643	0.007
Q9ULC5	9.6	9.6	20.06	Long-chain-fatty-acid--CoA ligase 5 OS=Homo sapiens GN=ACSL5 PE=1 SV=1	0.641	0.005
P04264	24.35	27.4	21.43	Keratin, type II cytoskeletal 1 OS=Homo sapiens GN=KRT1 PE=1 SV=6	0.641	0.022
Q8WWM7	8	8	6.977	Ataxin-2-like protein OS=Homo sapiens GN=ATXN2L PE=1 SV=2	0.630	0.010
P62277	13.84	13.84	46.36	40S ribosomal protein S13 OS=Homo sapiens GN=RPS13 PE=1 SV=2	0.625	0.014
P54136	15.92	15.94	12.58	Arginine--tRNA ligase, cytoplasmic OS=Homo sapiens GN=RARS PE=1 SV=2	0.624	0.000
P62280	7.44	7.44	17.72	40S ribosomal protein S11 OS=Homo sapiens GN=RPS11 PE=1 SV=3	0.619	0.034
Q6ZRP7	2.07	2.13	2.292	Sulfhydryl oxidase 2 OS=Homo sapiens GN=QSOX2 PE=1 SV=3	0.608	0.037
P46778	11.17	11.61	37.5	60S ribosomal protein L21 OS=Homo sapiens GN=RPL21 PE=1 SV=2	0.603	0.029
P35232	25.97	25.97	62.13	Prohibitin OS=Homo sapiens GN=PHB PE=1 SV=1	0.597	0.000
Q04637	14.8	14.97	6.504	Eukaryotic translation initiation factor 4 gamma 1 OS=Homo sapiens GN=EIF4G1 PE=1 SV=4	0.595	0.007
Q12904	11.52	11.52	34.62	Aminoacyl tRNA synthase complex-interacting multifunctional protein 1 OS=Homo sapiens GN=AIMP1 PE=1 SV=2	0.590	0.028
P35908	5.14	8.77	14.71	Keratin, type II cytoskeletal 2 epidermal OS=Homo sapiens GN=KRT2 PE=1 SV=2	0.579	0.014
P12532	8	8.2	17.99	Creatine kinase U-type, mitochondrial OS=Homo sapiens GN=CKMT1A PE=1 SV=1	0.573	0.044
P21796	30.29	30.29	70.67	Voltage-dependent anion-selective channel protein 1 OS=Homo sapiens GN=VDAC1 PE=1 SV=2	0.562	0.023
P62241	16	16	38.94	40S ribosomal protein S8 OS=Homo sapiens GN=RPS8 PE=1 SV=2	0.560	0.033
P62266	4.98	5.08	19.58	40S ribosomal protein S23 OS=Homo sapiens GN=RPS23 PE=1 SV=3	0.558	0.023
P32969	8.1	8.31	29.69	60S ribosomal protein L9 OS=Homo sapiens GN=RPL9 PE=1 SV=1	0.556	0.044
Q99623	26.26	26.26	51.51	Prohibitin-2 OS=Homo sapiens GN=PHB2 PE=1 SV=2	0.540	0.000
O00264	14.16	14.16	28.72	Membrane-associated progesterone receptor component 1 OS=Homo sapiens GN=PGRMC1 PE=1 SV=3	0.539	0.005
P18621	12.06	12.06	32.07	60S ribosomal protein L17 OS=Homo sapiens GN=RPL17 PE=1 SV=3	0.514	0.001
P33176	4.31	4.32	3.531	Kinesin-1 heavy chain OS=Homo sapiens GN=KIF5B PE=1 SV=1	0.502	0.025
Q92520	21.64	21.64	64.32	Protein FAM3C OS=Homo sapiens GN=FAM3C PE=1 SV=1	0.501	0.001
Q15365	5.9	10.53	27.25	Poly(rC)-binding protein 1 OS=Homo sapiens GN=PCBP1 PE=1 SV=2	0.497	0.005
P49327	33.79	34.14	12.58	Fatty acid synthase OS=Homo sapiens GN=FASN PE=1 SV=3	0.495	0.000
P14618	16.11	16.79	24.67	Pyruvate kinase PKM OS=Homo sapiens GN=PKM PE=1 SV=4	0.453	0.000
Q8N5K1	6.09	6.09	31.11	CDGSH iron-sulfur domain-containing protein 2 OS=Homo sapiens GN=CISD2 PE=1 SV=1	0.435	0.031
P62753	11.11	11.11	19.28	40S ribosomal protein S6 OS=Homo sapiens GN=RPS6 PE=1 SV=1	0.423	0.003
P49792	6.67	6.94	1.055	E3 SUMO-protein ligase RanBP2 OS=Homo sapiens GN=RANBP2 PE=1 SV=2	0.402	0.008
P46781	10.65	10.65	25.26	40S ribosomal protein S9 OS=Homo sapiens GN=RPS9 PE=1 SV=3	0.395	0.001
P07437	42.77	42.91	65.54	Tubulin beta chain OS=Homo sapiens GN=TUBB PE=1 SV=2	0.369	0.047
P62249	12.69	12.69	45.89	40S ribosomal protein S16 OS=Homo sapiens GN=RPS16 PE=1 SV=2	0.351	0.001
P12268	32.34	32.34	37.74	Inosine-5'-monophosphate dehydrogenase 2 OS=Homo sapiens GN=IMPDH2 PE=1 SV=2	0.338	0.000
P45880	12.14	16.11	40.14	Voltage-dependent anion-selective channel protein 2 OS=Homo sapiens GN=VDAC2 PE=1 SV=2	0.281	0.000
P62244	8.28	8.28	40	40S ribosomal protein S15a OS=Homo sapiens GN=RPS15A PE=1 SV=2	0.279	0.026
P49411	4.03	4.03	7.743	Elongation factor Tu, mitochondrial OS=Homo sapiens GN=TUFM PE=1 SV=2	0.242	0.011

866

Supplementary Table 2: Comparison of TGFβ treated HCT116 WT/HCT116AS

Uniprot	Unused	Total	X.Cov.95.	Protein Name; Organism; Gene name	iTRAQ Fold Change	StouffersPval
P61026	9.45	11.04	33	Ras-related protein Rab-10 OS=Homo sapiens GN=RAB10 PE=1 SV=1	4.716	0.026
P62158	7.65	7.65	57.72	Calmodulin OS=Homo sapiens GN=CALM1 PE=1 SV=2	4.508	0.001
P17096	7.15	7.15	41.12	High mobility group protein HMG-I/HMG-Y OS=Homo sapiens GN=HMGA1 PE=1 SV=3	4.280	0.019
P07602	16.96	16.96	28.05	Proactivator polypeptide OS=Homo sapiens GN=PSAP PE=1 SV=2	4.278	0.000
Q07021	12.14	12.14	36.17	Complement component 1 Q subcomponent-binding protein, mitochondrial OS=Homo sapiens GN=C1QBP PE=1 SV=1	4.111	0.000
P05556	27.88	28.34	22.06	Integrin beta-1 OS=Homo sapiens GN=ITGB1 PE=1 SV=2	4.040	0.000
P18859	11.5	11.57	58.33	ATP synthase-coupling factor 6, mitochondrial OS=Homo sapiens GN=ATP5J PE=1 SV=1	4.036	0.003
P04792	20.12	20.12	69.76	Heat shock protein beta-1 OS=Homo sapiens GN=HSPB1 PE=1 SV=2	3.963	0.000
P51858	3.31	3.31	13.75	Hepatoma-derived growth factor OS=Homo sapiens GN=HDGF PE=1 SV=1	3.960	0.047
Q02952	25.73	25.73	19.08	A-kinase anchor protein 12 OS=Homo sapiens GN=AKAP12 PE=1 SV=4	3.901	0.000
O43809	2.03	2.03	7.93	Cleavage and polyadenylation specificity factor subunit 5 OS=Homo sapiens GN=NUDT21 PE=1 SV=1	3.893	0.023
P06748	17.94	17.94	33.67	Nucleophosmin OS=Homo sapiens GN=NPM1 PE=1 SV=2	3.751	0.000
P09429	14.62	14.62	38.6	High mobility group protein B1 OS=Homo sapiens GN=HMGB1 PE=1 SV=3	3.621	0.002
P26006	12.44	12.67	8.278	Integrin alpha-3 OS=Homo sapiens GN=ITGA3 PE=1 SV=5	3.354	0.000
P50151	6.81	6.81	52.94	Guanine nucleotide-binding protein G(I)/G(S)/G(O) subunit gamma-10 OS=Homo sapiens GN=GNG10 PE=1 SV=1	3.350	0.002
Q16630	8.84	8.87	15.43	Cleavage and polyadenylation specificity factor subunit 6 OS=Homo sapiens GN=CPSF6 PE=1 SV=2	3.300	0.000
O60664	16.09	16.09	33.41	Perilipin-3 OS=Homo sapiens GN=PLIN3 PE=1 SV=3	3.289	0.002
P16403	2	23.86	36.62	Histone H1.2 OS=Homo sapiens GN=HIST1H1C PE=1 SV=2	3.219	0.002
O75531	8	8	48.31	Barrier-to-autointegration factor OS=Homo sapiens GN=BANF1 PE=1 SV=1	3.195	0.001
Q9UHD8	10.07	10.09	16.89	Septin-9 OS=Homo sapiens GN=SEPT9 PE=1 SV=2	3.193	0.000
P62857	3.74	3.74	30.43	40S ribosomal protein S28 OS=Homo sapiens GN=RPS28 PE=1 SV=1	3.125	0.048
Q15019	18.25	18.35	44.88	Septin-2 OS=Homo sapiens GN=SEPT2 PE=1 SV=1	3.096	0.000
O43399	7.85	7.85	37.86	Tumor protein D54 OS=Homo sapiens GN=TPD52L2 PE=1 SV=2	3.042	0.002
Q9NVA2	7.19	7.23	11.19	Septin-11 OS=Homo sapiens GN=SEPT11 PE=1 SV=3	2.991	0.018
P18669	6.2	6.2	22.05	Phosphoglycerate mutase 1 OS=Homo sapiens GN=PGAM1 PE=1 SV=2	2.963	0.013
P07237	33.59	33.59	40.16	Protein disulfide-isomerase OS=Homo sapiens GN=P4HB PE=1 SV=3	2.935	0.000
P26885	5.92	5.92	49.3	Peptidyl-prolyl cis-trans isomerase FKBP2 OS=Homo sapiens GN=FKBP2 PE=1 SV=2	2.932	0.023
P17931	10.44	10.44	32.8	Galectin-3 OS=Homo sapiens GN=LGALS3 PE=1 SV=5	2.822	0.000
Q00688	6.12	6.12	22.77	Peptidyl-prolyl cis-trans isomerase FKBP3 OS=Homo sapiens GN=FKBP3 PE=1 SV=1	2.739	0.016
P17301	11.95	12.3	7.959	Integrin alpha-2 OS=Homo sapiens GN=ITGA2 PE=1 SV=1	2.698	0.000
P62937	19.61	19.99	69.09	Peptidyl-prolyl cis-trans isomerase A OS=Homo sapiens GN=PPIA PE=1 SV=2	2.688	0.000
Q01130	2.72	2.87	14.48	Serine/arginine-rich splicing factor 2 OS=Homo sapiens GN=SRSF2 PE=1 SV=4	2.664	0.007
P10606	15.58	15.58	46.51	Cytochrome c oxidase subunit 5B, mitochondrial OS=Homo sapiens GN=COX5B PE=1 SV=2	2.650	0.000
O43181	4.07	4.07	14.29	NADH dehydrogenase [ubiquinone] iron-sulfur protein 4, mitochondrial OS=Homo sapiens GN=NDUFS4 PE=1 SV=1	2.643	0.008
Q9UHB6	6.02	6.48	7.378	LIM domain and actin-binding protein 1 OS=Homo sapiens GN=LIMA1 PE=1 SV=1	2.633	0.017
Q09666	38.54	38.61	7.301	Neuroblast differentiation-associated protein AHNAK OS=Homo sapiens GN=AHNAK PE=1 SV=2	2.630	0.000
P09382	9.39	9.39	45.19	Galectin-1 OS=Homo sapiens GN=LGALS1 PE=1 SV=2	2.610	0.002
P09622	6.16	6.16	8.644	Dihydrolipoyl dehydrogenase, mitochondrial OS=Homo sapiens GN=DLD PE=1 SV=2	2.602	0.029
P19404	10.31	10.31	33.33	NADH dehydrogenase [ubiquinone] flavoprotein 2, mitochondrial OS=Homo sapiens GN=NDUFV2 PE=1 SV=2	2.525	0.000
P60953	6	6	21.47	Cell division control protein 42 homolog OS=Homo sapiens GN=CDC42 PE=1 SV=2	2.483	0.001
P14314	20.47	20.47	25.95	Glucosidase 2 subunit beta OS=Homo sapiens GN=PRKCSH PE=1 SV=2	2.481	0.000
Q8NBJ4	2.08	2.12	9.726	Golgi membrane protein 1 OS=Homo sapiens GN=GOLM1 PE=1 SV=1	2.447	0.011
P20700	45.35	50.54	45.39	Lamin-B1 OS=Homo sapiens GN=LMNB1 PE=1 SV=2	2.392	0.000
P07355	16.25	16.25	42.18	Annexin A2 OS=Homo sapiens GN=ANXA2 PE=1 SV=2	2.384	0.018
P06733	17.46	17.46	29.03	Alpha-enolase OS=Homo sapiens GN=ENO1 PE=1 SV=2	2.370	0.000
P23284	27.01	27.01	54.63	Peptidyl-prolyl cis-trans isomerase B OS=Homo sapiens GN=PPIB PE=1 SV=2	2.340	0.000
P49748	14.53	14.53	24.12	Very long-chain specific acyl-CoA dehydrogenase, mitochondrial OS=Homo sapiens GN=ACADVL PE=1 SV=1	2.314	0.005
P63261	48.37	48.37	62.4	Actin, cytoplasmic 2 OS=Homo sapiens GN=ACTG1 PE=1 SV=1	2.311	0.001
O15347	8.12	8.12	30.5	High mobility group protein B3 OS=Homo sapiens GN=HMGB3 PE=1 SV=4	2.306	0.040
Q9BQ61	2.59	2.69	14.77	Uncharacterized protein C19orf43 OS=Homo sapiens GN=C19orf43 PE=1 SV=1	2.294	0.047
O43169	13.2	13.5	63.01	Cytochrome b5 type B OS=Homo sapiens GN=CYB5B PE=1 SV=2	2.287	0.004
P26583	4.37	8.7	25.36	High mobility group protein B2 OS=Homo sapiens GN=HMGB2 PE=1 SV=2	2.255	0.003
P61769	5.88	5.88	28.57	Beta-2-microglobulin OS=Homo sapiens GN=B2M PE=1 SV=1	2.239	0.001
P30040	3.36	3.38	15.33	Endoplasmic reticulum resident protein 29 OS=Homo sapiens GN=ERP29 PE=1 SV=4	2.236	0.001
Q13740	29.32	29.33	39.62	CD166 antigen OS=Homo sapiens GN=ALCAM PE=1 SV=2	2.185	0.000
O14561	9.62	9.62	30.13	Acyl carrier protein, mitochondrial OS=Homo sapiens GN=NDUFAB1 PE=1 SV=3	2.173	0.021
Q16181	10.1	10.1	17.85	Septin-7 OS=Homo sapiens GN=SEPT7 PE=1 SV=2	2.161	0.002
Q71UI9	5.31	5.9	31.25	Histone H2A.V OS=Homo sapiens GN=H2AFV PE=1 SV=3	2.137	0.036
P26368	7.05	7.05	13.89	Splicing factor U2AF 65 kDa subunit OS=Homo sapiens GN=U2AF2 PE=1 SV=4	2.110	0.022
P68431	20.78	20.78	59.56	Histone H3.1 OS=Homo sapiens GN=HIST1H3A PE=1 SV=2	2.106	0.001
P14854	6.53	6.53	47.67	Cytochrome c oxidase subunit 6B1 OS=Homo sapiens GN=COX6B1 PE=1 SV=2	2.052	0.039
P24534	10.57	10.6	34.67	Elongation factor 1-beta OS=Homo sapiens GN=EEF1B2 PE=1 SV=3	2.025	0.004
Q8WXF1	13.79	14.5	19.5	Paraspeckle component 1 OS=Homo sapiens GN=PSPC1 PE=1 SV=1	2.020	0.001
P42167	6.84	23.82	40.97	Lamina-associated polypeptide 2, isoforms beta/gamma OS=Homo sapiens GN=TMPO PE=1 SV=2	2.004	0.003
Q15637	8	8	11.74	Splicing factor 1 OS=Homo sapiens GN=SF1 PE=1 SV=4	2.002	0.002
Q8WWI5	9.46	9.46	11.11	Choline transporter-like protein 1 OS=Homo sapiens GN=SLC44A1 PE=1 SV=1	1.999	0.036
P15311	32.66	32.68	32.94	Ezrin OS=Homo sapiens GN=EZR PE=1 SV=4	1.995	0.000
P49821	19.33	19.44	37.72	NADH dehydrogenase [ubiquinone] flavoprotein 1, mitochondrial OS=Homo sapiens GN=NDUFV1 PE=1 SV=4	1.988	0.000
Q13765	5.89	5.89	19.07	Nascent polypeptide-associated complex subunit alpha OS=Homo sapiens GN=NACA PE=1 SV=1	1.987	0.016
P09012	6.42	6.42	15.25	U1 small nuclear ribonucleoprotein A OS=Homo sapiens GN=SNRPA PE=1 SV=3	1.984	0.005
P13987	10	10	35.94	CD59 glycoprotein OS=Homo sapiens GN=CD59 PE=1 SV=1	1.977	0.023
Q96AE4	8.41	17.77	21.74	Far upstream element-binding protein 1 OS=Homo sapiens GN=FUBP1 PE=1 SV=3	1.940	0.011
P48739	2.71	2.71	9.225	Phosphatidylinositol transfer protein beta isoform OS=Homo sapiens GN=PITPNB PE=1 SV=2	1.931	0.029
Q8WXX5	9.37	9.37	19.23	DnaJ homolog subfamily C member 9 OS=Homo sapiens GN=DNAJC9 PE=1 SV=1	1.905	0.006
P29966	10.03	10.1	29.52	Myristoylated alanine-rich C-kinase substrate OS=Homo sapiens GN=MARCKS PE=1 SV=4	1.895	0.041
P21579	6.47	6.59	11.14	Synaptotagmin-1 OS=Homo sapiens GN=SYT1 PE=1 SV=1	1.888	0.016
P19338	67.49	67.49	34.23	Nucleolin OS=Homo sapiens GN=NCL PE=1 SV=3	1.882	0.000
P30049	7.35	7.44	37.5	ATP synthase subunit delta, mitochondrial OS=Homo sapiens GN=ATP5D PE=1 SV=2	1.878	0.022
Q14978	23.05	23.05	18.03	Nucleolar and coiled-body phosphoprotein 1 OS=Homo sapiens GN=NOLC1 PE=1 SV=2	1.866	0.000
Q96A26	3.21	3.21	16.23	Protein FAM162A OS=Homo sapiens GN=FAM162A PE=1 SV=2	1.857	0.035
O43852	6.77	6.82	14.29	Calumenin OS=Homo sapiens GN=CALU PE=1 SV=2	1.844	0.001
P51970	8	8.08	30.23	NADH dehydrogenase [ubiquinone] 1 alpha subcomplex subunit 8 OS=Homo sapiens GN=NDUFA8 PE=1 SV=3	1.816	0.000
Q86Y82	10	10.01	28.26	Syntaxin-12 OS=Homo sapiens GN=STX12 PE=1 SV=1	1.811	0.045
Q8NC51	20.51	20.51	22.3	Plasminogen activator inhibitor 1 RNA-binding protein OS=Homo sapiens GN=SERBP1 PE=1 SV=2	1.771	0.000
Q99733	8.8	8.8	17.6	Nucleosome assembly protein 1-like 4 OS=Homo sapiens GN=NAP1L4 PE=1 SV=1	1.763	0.006
O75475	7.56	7.56	10.94	PC4 and SFRS1-interacting protein OS=Homo sapiens GN=PSIP1 PE=1 SV=1	1.762	0.006
P52815	7.41	7.41	33.33	39S ribosomal protein L12, mitochondrial OS=Homo sapiens GN=MRPL12 PE=1 SV=2	1.739	0.031
P62316	11.55	11.55	46.61	Small nuclear ribonucleoprotein Sm D2 OS=Homo sapiens GN=SNRPD2 PE=1 SV=1	1.734	0.003
P04040	10.16	10.16	21.44	Catalase OS=Homo sapiens GN=CAT PE=1 SV=3	1.728	0.006

867

P14927	9.85	9.85	43.24	Cytochrome b-c1 complex subunit 7 OS=Homo sapiens GN=UQCRB PE=1 SV=2	1.720	0.001
Q09028	4.55	4.69	11.76	Histone-binding protein RBBP4 OS=Homo sapiens GN=RBBP4 PE=1 SV=3	1.709	0.005
P22307	6.24	6.53	6.947	Non-specific lipid-transfer protein OS=Homo sapiens GN=SCP2 PE=1 SV=2	1.708	0.030
P26038	6.41	15.68	15.6	Moesin OS=Homo sapiens GN=MSN PE=1 SV=3	1.705	0.040
Q9HBR0	8.04	8.59	6.971	Putative sodium-coupled neutral amino acid transporter 10 OS=Homo sapiens GN=SLC38A10 PE=1 SV=2	1.705	0.015
Q14697	16.75	16.75	13.35	Neutral alpha-glucosidase AB OS=Homo sapiens GN=GANAB PE=1 SV=3	1.698	0.001
P34932	4.39	4.41	8.452	Heat shock 70 kDa protein 4 OS=Homo sapiens GN=HSPA4 PE=1 SV=4	1.698	0.035
O14949	4.55	4.55	37.8	Cytochrome b-c1 complex subunit 8 OS=Homo sapiens GN=UQCRQ PE=1 SV=4	1.696	0.010
Q06830	11.14	11.14	33.67	Peroxiredoxin-1 OS=Homo sapiens GN=PRDX1 PE=1 SV=1	1.691	0.003
P08621	9.4	9.4	14.87	U1 small nuclear ribonucleoprotein 70 kDa OS=Homo sapiens GN=SNRNP70 PE=1 SV=2	1.689	0.019
P35637	16.6	16.62	15.97	RNA-binding protein FUS OS=Homo sapiens GN=FUS PE=1 SV=1	1.683	0.005
P14625	21.02	23.41	21.54	Endoplasmin OS=Homo sapiens GN=HSP90B1 PE=1 SV=1	1.681	0.002
P35221	18.22	18.22	17.66	Catenin alpha-1 OS=Homo sapiens GN=CTNNA1 PE=1 SV=1	1.678	0.003
P16070	18.14	18.14	12.13	CD44 antigen OS=Homo sapiens GN=CD44 PE=1 SV=3	1.674	0.004
P48730	3.71	3.71	8.916	Casein kinase I isoform delta OS=Homo sapiens GN=CSNK1D PE=1 SV=2	1.670	0.036
Q13185	5.55	6.06	29.51	Chromobox protein homolog 3 OS=Homo sapiens GN=CBX3 PE=1 SV=4	1.661	0.024
Q9UKV3	8.15	8.17	6.115	Apoptotic chromatin condensation inducer in the nucleus OS=Homo sapiens GN=ACIN1 PE=1 SV=2	1.652	0.031
P09651	23.02	30.35	38.44	Heterogeneous nuclear ribonucleoprotein A1 OS=Homo sapiens GN=HNRNPA1 PE=1 SV=5	1.648	0.005
P40926	8.03	8.03	20.12	Malate dehydrogenase, mitochondrial OS=Homo sapiens GN=MDH2 PE=1 SV=3	1.645	0.004
Q8IWA5	10.55	10.55	8.64	Choline transporter-like protein 2 OS=Homo sapiens GN=SLC44A2 PE=1 SV=3	1.637	0.009
P28066	5.64	5.64	26.56	Proteasome subunit alpha type-5 OS=Homo sapiens GN=PSMA5 PE=1 SV=3	1.631	0.030
Q9NX40	22.97	23.35	58.37	OCIA domain-containing protein 1 OS=Homo sapiens GN=OCIAD1 PE=1 SV=1	1.629	0.008
P13645	9.86	14.06	15.58	Keratin, type I cytoskeletal 10 OS=Homo sapiens GN=KRT10 PE=1 SV=6	1.623	0.014
P27695	6.45	6.48	23.27	DNA-(apurinic or apyrimidinic site) lyase OS=Homo sapiens GN=APEX1 PE=1 SV=2	1.622	0.047
Q9Y639	8.02	8.02	13.57	Neuroplastin OS=Homo sapiens GN=NPTN PE=1 SV=2	1.606	0.006
Q99729	6.39	8.59	17.17	Heterogeneous nuclear ribonucleoprotein A/B OS=Homo sapiens GN=HNRNPAB PE=1 SV=2	1.604	0.009
P35527	11.58	13.35	17.34	Keratin, type I cytoskeletal 9 OS=Homo sapiens GN=KRT9 PE=1 SV=3	1.599	0.048
P37108	11.37	11.38	43.38	Signal recognition particle 14 kDa protein OS=Homo sapiens GN=SRP14 PE=1 SV=2	1.597	0.032
O00217	4.06	4.06	13.81	NADH dehydrogenase [ubiquinone] iron-sulfur protein 8, mitochondrial OS=Homo sapiens GN=NDUFS8 PE=1 SV=1	1.590	0.010
Q96PD2	11.83	11.83	15.61	Discoidin, CUB and LCCL domain-containing protein 2 OS=Homo sapiens GN=DCBLD2 PE=1 SV=1	1.589	0.005
P27797	16.02	16.02	30.7	Calreticulin OS=Homo sapiens GN=CALR PE=1 SV=1	1.586	0.008
Q9UBS4	10	10	23.18	DnaJ homolog subfamily B member 11 OS=Homo sapiens GN=DNAJB11 PE=1 SV=1	1.578	0.045
P23246	46.04	46.04	42.29	Splicing factor, proline- and glutamine-rich OS=Homo sapiens GN=SFPQ PE=1 SV=2	1.575	0.001
Q03252	36.98	43.54	40.17	Lamin-B2 OS=Homo sapiens GN=LMNB2 PE=1 SV=3	1.568	0.000
P78310	10.28	10.28	23.84	Coxsackievirus and adenovirus receptor OS=Homo sapiens GN=CXADR PE=1 SV=1	1.565	0.004
O15400	8	8.05	20.31	Syntaxin-7 OS=Homo sapiens GN=STX7 PE=1 SV=4	1.561	0.033
P19105	12.08	12.08	46.78	Myosin regulatory light chain 12A OS=Homo sapiens GN=MYL12A PE=1 SV=2	1.555	0.017
Q9NUP9	3.06	3.07	14.72	Protein lin-7 homolog C OS=Homo sapiens GN=LIN7C PE=1 SV=1	1.544	0.037
P23786	8.2	8.2	11.7	Carnitine O-palmitoyltransferase 2, mitochondrial OS=Homo sapiens GN=CPT2 PE=1 SV=2	1.538	0.005
Q9BQ67	6.14	6.14	11.66	Glutamate-rich WD repeat-containing protein 1 OS=Homo sapiens GN=GRWD1 PE=1 SV=1	1.535	0.030
P61586	11.89	13.47	45.08	Transforming protein RhoA OS=Homo sapiens GN=RHOA PE=1 SV=1	1.527	0.003
P09661	5.75	5.75	20.39	U2 small nuclear ribonucleoprotein A' OS=Homo sapiens GN=SNRPA1 PE=1 SV=2	1.527	0.037
Q9NQ50	6.17	6.25	29.61	39S ribosomal protein L40, mitochondrial OS=Homo sapiens GN=MRPL40 PE=1 SV=1	1.527	0.031
Q9P2B2	6.01	6.01	7.964	Prostaglandin F2 receptor negative regulator OS=Homo sapiens GN=PTGFRN PE=1 SV=2	1.513	0.010
Q14011	3.81	3.81	20.35	Cold-inducible RNA-binding protein OS=Homo sapiens GN=CIRBP PE=1 SV=1	1.512	0.047
Q9Y5B9	12.47	12.51	7.832	FACT complex subunit SPT16 OS=Homo sapiens GN=SUPT16H PE=1 SV=1	1.505	0.002
P55209	6.31	8.26	17.39	Nucleosome assembly protein 1-like 1 OS=Homo sapiens GN=NAP1L1 PE=1 SV=1	1.488	0.033
O75947	11.81	11.97	59.01	ATP synthase subunit d, mitochondrial OS=Homo sapiens GN=ATP5H PE=1 SV=3	1.477	0.002
O14818	6.77	6.77	20.16	Proteasome subunit alpha type-7 OS=Homo sapiens GN=PSMA7 PE=1 SV=1	1.475	0.019
P36873	24.13	24.13	47.37	Serine/threonine-protein phosphatase PP1-gamma catalytic subunit OS=Homo sapiens GN=PPP1CC PE=1 SV=1	1.454	0.050
P62750	10.47	10.47	32.69	60S ribosomal protein L23a OS=Homo sapiens GN=RPL23A PE=1 SV=1	1.449	0.048
P30101	27.36	27.7	37.03	Protein disulfide-isomerase A3 OS=Homo sapiens GN=PDIA3 PE=1 SV=4	1.441	0.003
P13667	9.32	9.52	13.64	Protein disulfide-isomerase A4 OS=Homo sapiens GN=PDIA4 PE=1 SV=2	1.441	0.009
Q99653	12.67	12.71	54.36	Calcineurin B homologous protein 1 OS=Homo sapiens GN=CHP1 PE=1 SV=3	1.440	0.001
P09110	11.74	11.74	31.6	3-ketoacyl-CoA thiolase, peroxisomal OS=Homo sapiens GN=ACAA1 PE=1 SV=2	1.431	0.016
P11021	42.64	46.82	40.37	78 kDa glucose-regulated protein OS=Homo sapiens GN=HSPA5 PE=1 SV=2	1.429	0.000
P38646	12.81	12.81	13.11	Stress-70 protein, mitochondrial OS=Homo sapiens GN=HSPA9 PE=1 SV=2	1.393	0.009
Q92485	14.29	14.29	23.52	Acid sphingomyelinase-like phosphodiesterase 3b OS=Homo sapiens GN=SMPDL3B PE=2 SV=2	1.391	0.003
Q9NX58	10.75	10.81	17.94	Cell growth-regulating nucleolar protein OS=Homo sapiens GN=LYAR PE=1 SV=2	1.389	0.033
P17480	13.97	13.97	12.7	Nucleolar transcription factor 1 OS=Homo sapiens GN=UBTF PE=1 SV=1	1.379	0.038
Q15233	37.63	39.78	46.28	Non-POU domain-containing octamer-binding protein OS=Homo sapiens GN=NONO PE=1 SV=4	1.376	0.002
O43707	12.01	12.01	9.001	Alpha-actinin-4 OS=Homo sapiens GN=ACTN4 PE=1 SV=2	1.361	0.035
Q07065	12.45	12.45	19.1	Cytoskeleton-associated protein 4 OS=Homo sapiens GN=CKAP4 PE=1 SV=2	1.360	0.008
Q9UQB8	9.88	10.15	18.84	Brain-specific angiogenesis inhibitor 1-associated protein 2 OS=Homo sapiens GN=BAIAP2 PE=1 SV=1	1.359	0.014
Q9Y6M1	12.96	12.96	19.2	Insulin-like growth factor 2 mRNA-binding protein 2 OS=Homo sapiens GN=IGF2BP2 PE=1 SV=2	1.358	0.009
Q9Y4L1	21.83	21.88	18.52	Hypoxia up-regulated protein 1 OS=Homo sapiens GN=HYOU1 PE=1 SV=1	1.354	0.024
O95831	2.93	2.94	8.646	Apoptosis-inducing factor 1, mitochondrial OS=Homo sapiens GN=AIFM1 PE=1 SV=1	1.351	0.039
Q96EY1	8.13	8.13	11.67	DnaJ homolog subfamily A member 3, mitochondrial OS=Homo sapiens GN=DNAJA3 PE=1 SV=2	1.335	0.018
Q14165	17.5	17.5	26.71	Malectin OS=Homo sapiens GN=MLEC PE=1 SV=1	1.332	0.028
P09874	51.2	51.2	34.02	Poly [ADP-ribose] polymerase 1 OS=Homo sapiens GN=PARP1 PE=1 SV=4	1.297	0.000
Q15459	11.84	11.84	14.25	Splicing factor 3A subunit 1 OS=Homo sapiens GN=SF3A1 PE=1 SV=1	1.286	0.008
P21589	12.23	12.33	20.38	5'-nucleotidase OS=Homo sapiens GN=NT5E PE=1 SV=1	1.284	0.033
Q92945	29.45	29.55	34.32	Far upstream element-binding protein 2 OS=Homo sapiens GN=KHSRP PE=1 SV=4	1.269	0.010
Q9Y224	6.95	6.95	23.36	UPF0568 protein C14orf166 OS=Homo sapiens GN=C14orf166 PE=1 SV=1	1.259	0.038
O60506	27.69	27.81	30.82	Heterogeneous nuclear ribonucleoprotein Q OS=Homo sapiens GN=SYNCRIP PE=1 SV=2	1.235	0.008
Q9BTV4	12.64	12.64	31	Transmembrane protein 43 OS=Homo sapiens GN=TMEM43 PE=1 SV=1	1.228	0.003
Q9P0J0	8.03	8.03	36.11	NADH dehydrogenase [ubiquinone] 1 alpha subcomplex subunit 13 OS=Homo sapiens GN=NDUFA13 PE=1 SV=3	0.805	0.047
P55795	10.54	13.02	26.5	Heterogeneous nuclear ribonucleoprotein H2 OS=Homo sapiens GN=HNRNPH2 PE=1 SV=1	0.798	0.046
Q9BSJ8	8.97	9.21	10.78	Extended synaptotagmin-1 OS=Homo sapiens GN=ESYT1 PE=1 SV=1	0.790	0.018
P62917	10.07	10.07	24.12	60S ribosomal protein L8 OS=Homo sapiens GN=RPL8 PE=1 SV=2	0.786	0.024
P62269	12.15	12.15	39.47	40S ribosomal protein S18 OS=Homo sapiens GN=RPS18 PE=1 SV=3	0.767	0.019
Q12906	36.26	36.93	25.84	Interleukin enhancer-binding factor 3 OS=Homo sapiens GN=ILF3 PE=1 SV=3	0.762	0.022
Q15046	12.53	12.53	17.76	Lysine--tRNA ligase OS=Homo sapiens GN=KARS PE=1 SV=3	0.761	0.009
Q9BVJ6	8.04	8.09	7.782	U3 small nucleolar RNA-associated protein 14 homolog A OS=Homo sapiens GN=UTP14A PE=1 SV=1	0.750	0.006
P50991	21.28	23.4	34.32	T-complex protein 1 subunit delta OS=Homo sapiens GN=CCT4 PE=1 SV=4	0.748	0.030
P05388	26.46	26.46	49.21	60S acidic ribosomal protein P0 OS=Homo sapiens GN=RPLP0 PE=1 SV=1	0.729	0.032
P11142	47.94	47.94	44.27	Heat shock cognate 71 kDa protein OS=Homo sapiens GN=HSPA8 PE=1 SV=1	0.726	0.001
Q13308	15.34	15.34	11.4	Inactive tyrosine-protein kinase 7 OS=Homo sapiens GN=PTK7 PE=1 SV=2	0.724	0.023
P38159	8.83	8.83	9.719	RNA-binding motif protein, X chromosome OS=Homo sapiens GN=RBMX PE=1 SV=3	0.723	0.001
P50402	6.43	6.43	23.23	Emerin OS=Homo sapiens GN=EMD PE=1 SV=1	0.717	0.025
P04899	14.04	14.1	30.14	Guanine nucleotide-binding protein G(i) subunit alpha-2 OS=Homo sapiens GN=GNAI2 PE=1 SV=3	0.705	0.039

868

P62424	28.91	29.04	45.11	60S ribosomal protein L7a OS=Homo sapiens GN=RPL7A PE=1 SV=2	0.705	0.009
Q8N163	12.07	12.07	11.48	DBIRD complex subunit KIAA1967 OS=Homo sapiens GN=KIAA1967 PE=1 SV=2	0.701	0.008
Q15717	6.12	6.12	19.02	ELAV-like protein 1 OS=Homo sapiens GN=ELAVL1 PE=1 SV=2	0.698	0.018
Q15907	22.5	22.5	53.67	Ras-related protein Rab-11B OS=Homo sapiens GN=RAB11B PE=1 SV=4	0.694	0.023
P08107	18.15	25.2	29.8	Heat shock 70 kDa protein 1A/1B OS=Homo sapiens GN=HSPA1A PE=1 SV=5	0.685	0.002
Q92499	8.57	8.57	9.189	ATP-dependent RNA helicase DDX1 OS=Homo sapiens GN=DDX1 PE=1 SV=2	0.683	0.001
P62851	8.66	8.66	29.6	40S ribosomal protein S25 OS=Homo sapiens GN=RPS25 PE=1 SV=1	0.683	0.034
P43304	10.6	10.6	12.1	Glycerol-3-phosphate dehydrogenase, mitochondrial OS=Homo sapiens GN=GPD2 PE=1 SV=3	0.671	0.046
P26373	13.33	13.33	30.81	60S ribosomal protein L13 OS=Homo sapiens GN=RPL13 PE=1 SV=4	0.669	0.012
P36578	30.91	30.91	39.58	60S ribosomal protein L4 OS=Homo sapiens GN=RPL4 PE=1 SV=5	0.668	0.001
Q96I24	18.98	19.41	30.42	Far upstream element-binding protein 3 OS=Homo sapiens GN=FUBP3 PE=1 SV=2	0.668	0.035
P50895	10.54	10.54	15.45	Basal cell adhesion molecule OS=Homo sapiens GN=BCAM PE=1 SV=2	0.667	0.017
P61353	8.28	8.28	52.21	60S ribosomal protein L27 OS=Homo sapiens GN=RPL27 PE=1 SV=2	0.652	0.016
P04406	17.41	17.41	42.69	Glyceraldehyde-3-phosphate dehydrogenase OS=Homo sapiens GN=GAPDH PE=1 SV=3	0.651	0.026
P49257	15.08	15.08	25.49	Protein ERGIC-53 OS=Homo sapiens GN=LMAN1 PE=1 SV=2	0.648	0.012
O00116	15.01	15.08	19.3	Alkyldihydroxyacetonephosphate synthase, peroxisomal OS=Homo sapiens GN=AGPS PE=1 SV=1	0.643	0.000
Q9H727	8.19	8.19	23.08	Prostaglandin E synthase 2 OS=Homo sapiens GN=PTGES2 PE=1 SV=1	0.642	0.004
Q9NX63	7.33	7.36	24.23	Coiled-coil-helix-coiled-coil-helix domain-containing protein 3, mitochondrial OS=Homo sapiens GN=CHCHD3 PE=1 SV=1	0.641	0.024
Q9NR30	16.62	16.62	16.73	Nucleolar RNA helicase 2 OS=Homo sapiens GN=DDX21 PE=1 SV=5	0.640	0.037
Q99805	8.75	8.75	11.76	Transmembrane 9 superfamily member 2 OS=Homo sapiens GN=TM9SF2 PE=1 SV=1	0.638	0.028
P18621	12.06	12.06	32.07	60S ribosomal protein L17 OS=Homo sapiens GN=RPL17 PE=1 SV=3	0.637	0.008
P23396	13.81	13.81	32.1	40S ribosomal protein S3 OS=Homo sapiens GN=RPS3 PE=1 SV=2	0.636	0.002
P62191	5.16	5.32	9.773	26S protease regulatory subunit 4 OS=Homo sapiens GN=PSMC1 PE=1 SV=1	0.631	0.015
P48444	1.5	1.5	2.153	Coatomer subunit delta OS=Homo sapiens GN=ARCN1 PE=1 SV=1	0.628	0.030
P52272	34.25	34.25	31.1	Heterogeneous nuclear ribonucleoprotein M OS=Homo sapiens GN=HNRNPM PE=1 SV=3	0.617	0.001
Q9Y3B3	7.61	7.61	24.11	Transmembrane emp24 domain-containing protein 7 OS=Homo sapiens GN=TMED7 PE=1 SV=2	0.613	0.014
P62847	6.44	6.44	29.32	40S ribosomal protein S24 OS=Homo sapiens GN=RPS24 PE=1 SV=1	0.612	0.003
Q14204	33.07	33.54	6.608	Cytoplasmic dynein 1 heavy chain 1 OS=Homo sapiens GN=DYNC1H1 PE=1 SV=5	0.600	0.001
P25705	34.85	34.85	44.48	ATP synthase subunit alpha, mitochondrial OS=Homo sapiens GN=ATP5A1 PE=1 SV=1	0.600	0.000
Q15149	55.27	55.27	10.25	Plectin OS=Homo sapiens GN=PLEC PE=1 SV=3	0.599	0.000
Q92616	16.37	16.66	6.702	Translational activator GCN1 OS=Homo sapiens GN=GCN1L1 PE=1 SV=5	0.594	0.005
Q8TDD1	8.74	8.74	9.648	ATP-dependent RNA helicase DDX54 OS=Homo sapiens GN=DDX54 PE=1 SV=2	0.592	0.038
P52292	10.04	10.05	11.34	Importin subunit alpha-1 OS=Homo sapiens GN=KPNA2 PE=1 SV=1	0.592	0.031
P54136	15.92	15.94	12.58	Arginine--tRNA ligase, cytoplasmic OS=Homo sapiens GN=RARS PE=1 SV=2	0.592	0.001
Q6IAA8	16.55	16.55	75.16	Ragulator complex protein LAMTOR1 OS=Homo sapiens GN=LAMTOR1 PE=1 SV=2	0.587	0.000
P40429	12.21	12.21	23.15	60S ribosomal protein L13a OS=Homo sapiens GN=RPL13A PE=1 SV=2	0.579	0.003
P41252	12.56	12.62	9.271	Isoleucine--tRNA ligase, cytoplasmic OS=Homo sapiens GN=IARS PE=1 SV=2	0.578	0.003
P62081	12.95	12.95	39.18	40S ribosomal protein S7 OS=Homo sapiens GN=RPS7 PE=1 SV=1	0.575	0.035
Q8WWM7	8	8	6.977	Ataxin-2-like protein OS=Homo sapiens GN=ATXN2L PE=1 SV=2	0.566	0.017
P16435	17.06	17.09	23.04	NADPH--cytochrome P450 reductase OS=Homo sapiens GN=POR PE=1 SV=2	0.564	0.000
P46778	11.17	11.61	37.5	60S ribosomal protein L21 OS=Homo sapiens GN=RPL21 PE=1 SV=2	0.562	0.006
P00403	2.2	2.2	13.22	Cytochrome c oxidase subunit 2 OS=Homo sapiens GN=MT-CO2 PE=1 SV=1	0.559	0.004
Q9H9B4	6	6	16.46	Sideroflexin-1 OS=Homo sapiens GN=SFXN1 PE=1 SV=4	0.558	0.003
P04843	9.69	9.72	11.04	Dolichyl-diphosphooligosaccharide--protein glycosyltransferase subunit 1 OS=Homo sapiens GN=RPN1 PE=1 SV=1	0.558	0.000
Q9BVK6	17.86	17.86	37.02	Transmembrane emp24 domain-containing protein 9 OS=Homo sapiens GN=TMED9 PE=1 SV=2	0.554	0.001
P63096	6	8.09	16.95	Guanine nucleotide-binding protein G(i) subunit alpha-1 OS=Homo sapiens GN=GNAI1 PE=1 SV=2	0.551	0.034
P62701	20.49	20.49	39.16	40S ribosomal protein S4, X isoform OS=Homo sapiens GN=RPS4X PE=1 SV=2	0.550	0.001
O00571	6.04	6.82	9.063	ATP-dependent RNA helicase DDX3X OS=Homo sapiens GN=DDX3X PE=1 SV=3	0.544	0.001
Q9BUF5	6.04	15.79	31.17	Tubulin beta-6 chain OS=Homo sapiens GN=TUBB6 PE=1 SV=1	0.533	0.029
Q92544	3.28	3.28	5.14	Transmembrane 9 superfamily member 4 OS=Homo sapiens GN=TM9SF4 PE=1 SV=2	0.532	0.029
P68104	25.32	25.32	38.1	Elongation factor 1-alpha 1 OS=Homo sapiens GN=EEF1A1 PE=1 SV=1	0.531	0.004
P36542	4.23	4.25	7.718	ATP synthase subunit gamma, mitochondrial OS=Homo sapiens GN=ATP5C1 PE=1 SV=1	0.521	0.040
P08727	33.51	37.57	56.5	Keratin, type I cytoskeletal 19 OS=Homo sapiens GN=KRT19 PE=1 SV=4	0.515	0.000
P62979	11.32	11.37	50.64	Ubiquitin-40S ribosomal protein S27a OS=Homo sapiens GN=RPS27A PE=1 SV=2	0.514	0.043
P62854	6	6	33.91	40S ribosomal protein S26 OS=Homo sapiens GN=RPS26 PE=1 SV=3	0.510	0.022
Q16891	19.86	20.04	32.45	Mitochondrial inner membrane protein OS=Homo sapiens GN=IMMT PE=1 SV=1	0.507	0.002
P51572	16.06	16.5	29.67	B-cell receptor-associated protein 31 OS=Homo sapiens GN=BCAP31 PE=1 SV=3	0.504	0.016
P05023	14.63	14.63	11.53	Sodium/potassium-transporting ATPase subunit alpha-1 OS=Homo sapiens GN=ATP1A1 PE=1 SV=1	0.503	0.004
O75964	5.81	5.81	47.57	ATP synthase subunit g, mitochondrial OS=Homo sapiens GN=ATP5L PE=1 SV=3	0.502	0.018
P35579	80.73	80.73	26.99	Myosin-9 OS=Homo sapiens GN=MYH9 PE=1 SV=4	0.499	0.000
P62266	4.98	5.08	19.58	40S ribosomal protein S23 OS=Homo sapiens GN=RPS23 PE=1 SV=3	0.499	0.013
O00410	6.12	6.87	5.014	Importin-5 OS=Homo sapiens GN=IPO5 PE=1 SV=4	0.496	0.004
P49327	33.79	34.14	12.58	Fatty acid synthase OS=Homo sapiens GN=FASN PE=1 SV=3	0.484	0.000
Q07020	9.47	9.47	30.85	60S ribosomal protein L18 OS=Homo sapiens GN=RPL18 PE=1 SV=2	0.483	0.038
Q9Y3A6	5.38	3.39	13.1	Transmembrane emp24 domain-containing protein 5 OS=Homo sapiens GN=TMED5 PE=1 SV=1	0.479	0.026
P54709	16.71	16.83	33.69	Sodium/potassium-transporting ATPase subunit beta-3 OS=Homo sapiens GN=ATP1B3 PE=1 SV=1	0.474	0.000
P21796	30.29	30.29	70.67	Voltage-dependent anion-selective channel protein 1 OS=Homo sapiens GN=VDAC1 PE=1 SV=2	0.474	0.013
P05783	41.73	41.73	59.3	Keratin, type I cytoskeletal 18 OS=Homo sapiens GN=KRT18 PE=1 SV=2	0.472	0.000
P49755	13.89	13.89	39.73	Transmembrane emp24 domain-containing protein 10 OS=Homo sapiens GN=TMED10 PE=1 SV=2	0.465	0.000
P35232	25.97	25.97	62.13	Prohibitin OS=Homo sapiens GN=PHB PE=1 SV=1	0.459	0.000
Q01813	8.83	8.83	10.71	6-phosphofructokinase type C OS=Homo sapiens GN=PFKP PE=1 SV=2	0.450	0.014
Q92520	21.64	21.64	64.32	Protein FAM3C OS=Homo sapiens GN=FAM3C PE=1 SV=1	0.448	0.001
P27338	6	6.03	10	Amine oxidase [flavin-containing] B OS=Homo sapiens GN=MAOB PE=1 SV=3	0.440	0.031
Q9UHG3	9.42	9.42	19.6	Prenylcysteine oxidase 1 OS=Homo sapiens GN=PCYOX1 PE=1 SV=3	0.435	0.000
Q16563	2.39	2.39	10.04	Synaptophysin-like protein 1 OS=Homo sapiens GN=SYPL1 PE=1 SV=1	0.425	0.013
P33176	4.31	4.32	3.531	Kinesin-1 heavy chain OS=Homo sapiens GN=KIF5B PE=1 SV=1	0.424	0.036
Q15365	5.9	10.53	27.25	Poly(rC)-binding protein 1 OS=Homo sapiens GN=PCBP1 PE=1 SV=2	0.424	0.017
P62244	8.28	8.28	40	40S ribosomal protein S15a OS=Homo sapiens GN=RPS15A PE=1 SV=2	0.423	0.003
Q6ZRP7	2.07	2.13	2.292	Sulfhydryl oxidase 2 OS=Homo sapiens GN=QSOX2 PE=1 SV=2	0.421	0.036
P49792	6.67	6.94	1.055	E3 SUMO-protein ligase RanBP2 OS=Homo sapiens GN=RANBP2 PE=1 SV=2	0.419	0.009
P00387	10.06	10.07	32.56	NADH-cytochrome b5 reductase 3 OS=Homo sapiens GN=CYB5R3 PE=1 SV=3	0.405	0.004
Q9UJZ1	15.85	15.85	34.55	Stomatin-like protein 2, mitochondrial OS=Homo sapiens GN=STOML2 PE=1 SV=1	0.404	0.000
Q14344	7.52	7.55	11.94	Guanine nucleotide-binding protein subunit alpha-13 OS=Homo sapiens GN=GNA13 PE=1 SV=2	0.401	0.000
P14618	16.11	16.79	24.67	Pyruvate kinase PKM OS=Homo sapiens GN=PKM PE=1 SV=4	0.382	0.000
P62913	3.12	4.94	16.85	60S ribosomal protein L11 OS=Homo sapiens GN=RPL11 PE=1 SV=2	0.368	0.049
P62753	11.11	11.11	19.28	40S ribosomal protein S6 OS=Homo sapiens GN=RPS6 PE=1 SV=1	0.365	0.002
P31689	9.03	9.22	22.42	DnaJ homolog subfamily A member 1 OS=Homo sapiens GN=DNAJA1 PE=1 SV=2	0.360	0.015
P11166	3.51	3.54	5.285	Solute carrier family 2, facilitated glucose transporter member 1 OS=Homo sapiens GN=SLC2A1 PE=1 SV=2	0.359	0.048
P08195	26.44	26.51	29.21	4F2 cell-surface antigen heavy chain OS=Homo sapiens GN=SLC3A2 PE=1 SV=3	0.355	0.000
P02786	25.35	25.35	23.42	Transferrin receptor protein 1 OS=Homo sapiens GN=TFRC PE=1 SV=2	0.353	0.000
P12268	32.34	32.34	37.74	Inosine-5'-monophosphate dehydrogenase 2 OS=Homo sapiens GN=IMPDH2 PE=1 SV=2	0.337	0.000

869

P62241	16	16	38.94	40S ribosomal protein S8 OS=Homo sapiens GN=RPS8 PE=1 SV=2	0.324	0.023
P05787	56.49	56.49	53.42	Keratin, type II cytoskeletal 8 OS=Homo sapiens GN=KRT8 PE=1 SV=7	0.323	0.000
P62249	12.69	12.69	45.89	40S ribosomal protein S16 OS=Homo sapiens GN=RPS16 PE=1 SV=2	0.311	0.000
Q99623	26.26	26.26	51.51	Prohibitin-2 OS=Homo sapiens GN=PHB2 PE=1 SV=2	0.305	0.000
Q15363	5.1	5.1	20.4	Transmembrane emp24 domain-containing protein 2 OS=Homo sapiens GN=TMED2 PE=1 SV=1	0.265	0.026
P46781	10.65	10.65	25.26	40S ribosomal protein S9 OS=Homo sapiens GN=RPS9 PE=1 SV=3	0.260	0.000
P45880	12.14	16.11	40.14	Voltage-dependent anion-selective channel protein 2 OS=Homo sapiens GN=VDAC2 PE=1 SV=2	0.234	0.000
P07437	42.77	42.91	65.54	Tubulin beta chain OS=Homo sapiens GN=TUBB PE=1 SV=2	0.229	0.011

870

247

Supplementary Table 3: The list 346 proteins of manually generated from Supplementary tables 2 and 3

Uniprot ID	Protein Name; Organism; Gene name	TGFβ treated fold change	untreated fold change	expression pattern
P62191	26S protease regulatory subunit 4 OS=Homo sapiens GN=PSMC1 PE=1 SV=1	0.631	0.661	↓
P09110	3-ketoacyl-CoA thiolase, peroxisomal OS=Homo sapiens GN=ACAA1 PE=1 SV=2	1.431	1.739	↑
P62244	40S ribosomal protein S15a OS=Homo sapiens GN=RPS15A PE=1 SV=2	0.423	0.279	↓
P62249	40S ribosomal protein S16 OS=Homo sapiens GN=RPS16 PE=1 SV=2	0.311	0.351	↓
P62266	40S ribosomal protein S23 OS=Homo sapiens GN=RPS23 PE=1 SV=3	0.499	0.558	↓
P62847	40S ribosomal protein S24 OS=Homo sapiens GN=RPS24 PE=1 SV=1	0.612	0.713	↓
P62851	40S ribosomal protein S25 OS=Homo sapiens GN=RPS25 PE=1 SV=1	0.683	0.787	↓
P23396	40S ribosomal protein S3 OS=Homo sapiens GN=RPS3 PE=1 SV=2	0.636	0.643	↓
P62701	40S ribosomal protein S4, X isoform OS=Homo sapiens GN=RPS4X PE=1 SV=2	0.550	0.699	↓
P62753	40S ribosomal protein S6 OS=Homo sapiens GN=RPS6 PE=1 SV=1	0.365	0.423	↓
P62241	40S ribosomal protein S8 OS=Homo sapiens GN=RPS8 PE=1 SV=2	0.324	0.560	↓
P46781	40S ribosomal protein S9 OS=Homo sapiens GN=RPS9 PE=1 SV=3	0.260	0.395	↓
P08195	4F2 cell-surface antigen heavy chain OS=Homo sapiens GN=SLC3A2 PE=1 SV=3	0.355	0.714	↓
P21589	5'-nucleotidase OS=Homo sapiens GN=NT5E PE=1 SV=1	1.284	1.319	↑
P40429	60S ribosomal protein L13a OS=Homo sapiens GN=RPL13A PE=1 SV=2	0.579	0.702	↓
P18621	60S ribosomal protein L17 OS=Homo sapiens GN=RPL17 PE=1 SV=3	0.637	0.514	↓
P46778	60S ribosomal protein L21 OS=Homo sapiens GN=RPL21 PE=1 SV=2	0.562	0.603	↓
P61353	60S ribosomal protein L27 OS=Homo sapiens GN=RPL27 PE=1 SV=2	0.652	0.670	↓
P36578	60S ribosomal protein L4 OS=Homo sapiens GN=RPL4 PE=1 SV=5	0.668	0.674	↓
P62917	60S ribosomal protein L8 OS=Homo sapiens GN=RPL8 PE=1 SV=2	0.786	0.712	↓
P11021	78 kDa glucose-regulated protein OS=Homo sapiens GN=HSPA5 PE=1 SV=2	1.429	1.537	↑
P63261	Actin, cytoplasmic 2 OS=Homo sapiens GN=ACTG1 PE=1 SV=1	2.311	2.705	↑
O14561	Acyl carrier protein, mitochondrial OS=Homo sapiens GN=NDUFAB1 PE=1 SV=3	2.173	2.314	↑
Q02952	A-kinase anchor protein 12 OS=Homo sapiens GN=AKAP12 PE=1 SV=4	3.901	2.648	↑
O43707	Alpha-actinin-4 OS=Homo sapiens GN=ACTN4 PE=1 SV=2	1.361	1.343	↑
P06733	Alpha-enolase OS=Homo sapiens GN=ENO1 PE=1 SV=2	2.370	2.698	↑
P07355	Annexin A2 OS=Homo sapiens GN=ANXA2 PE=1 SV=2	2.384	2.466	↑
P54136	Arginine--tRNA ligase, cytoplasmic OS=Homo sapiens GN=RARS PE=1 SV=2	0.592	0.624	↓
Q8WWM7	Ataxin-2-like protein OS=Homo sapiens GN=ATXN2L PE=1 SV=2	0.566	0.630	↓
O75947	ATP synthase subunit d, mitochondrial OS=Homo sapiens GN=ATP5H PE=1 SV=3	1.477	1.424	↑
O00571	ATP-dependent RNA helicase DDX3X OS=Homo sapiens GN=DDX3X PE=1 SV=3	0.544	0.729	↓
P61769	Beta-2-microglobulin OS=Homo sapiens GN=B2M PE=1 SV=1	2.239	1.701	↑
Q99653	Calcineurin B homologous protein 1 OS=Homo sapiens GN=CHP1 PE=1 SV=3	1.440	1.354	↑
P62158	Calmodulin OS=Homo sapiens GN=CALM1 PE=1 SV=2	4.508	3.317	↑
P27797	Calreticulin OS=Homo sapiens GN=CALR PE=1 SV=1	1.586	2.177	↑
O43852	Calumenin OS=Homo sapiens GN=CALU PE=1 SV=2	1.844	1.544	↑
P04040	Catalase OS=Homo sapiens GN=CAT PE=1 SV=3	1.728	1.470	↑
P35221	Catenin alpha-1 OS=Homo sapiens GN=CTNNA1 PE=1 SV=1	1.678	1.779	↑
Q13740	CD166 antigen OS=Homo sapiens GN=ALCAM PE=1 SV=2	2.185	2.338	↑
P16070	CD44 antigen OS=Homo sapiens GN=CD44 PE=1 SV=3	1.674	1.366	↑
P60953	Cell division control protein 42 homolog OS=Homo sapiens GN=CDC42 PE=1 SV=2	2.483	4.342	↑
Q8WWI5	Choline transporter-like protein 1 OS=Homo sapiens GN=SLC44A1 PE=1 SV=1	1.999	1.408	↑
Q8IWA5	Choline transporter-like protein 2 OS=Homo sapiens GN=SLC44A2 PE=1 SV=3	1.637	1.308	↑
Q13185	Chromobox protein homolog 3 OS=Homo sapiens GN=CBX3 PE=1 SV=4	1.661	1.628	↑
Q16630	Cleavage and polyadenylation specificity factor subunit 6 OS=Homo sapiens GN=CPSF6 PE=1 S\	3.300	1.857	↑
Q9NX63	Coiled-coil-helix-coiled-coil-helix domain-containing protein 3, mitochondrial OS=Homo sapien	0.641	0.663	↓
Q07021	Complement component 1 Q subcomponent-binding protein, mitochondrial OS=Homo sapiens	4.111	3.418	↑
P78310	Coxsackievirus and adenovirus receptor OS=Homo sapiens GN=CXADR PE=1 SV=1	1.565	1.623	↑
O43169	Cytochrome b5 type B OS=Homo sapiens GN=CYB5B PE=1 SV=2	2.287	1.952	↑
P14927	Cytochrome b-c1 complex subunit 7 OS=Homo sapiens GN=UQCRB PE=1 SV=2	1.720	1.409	↑
O14949	Cytochrome b-c1 complex subunit 8 OS=Homo sapiens GN=UQCRQ PE=1 SV=4	1.696	1.430	↑
P10606	Cytochrome c oxidase subunit 5B, mitochondrial OS=Homo sapiens GN=COX5B PE=1 SV=2	2.650	1.675	↑
Q14204	Cytoplasmic dynein 1 heavy chain 1 OS=Homo sapiens GN=DYNC1H1 PE=1 SV=5	0.600	0.745	↓
Q07065	Cytoskeleton-associated protein 4 OS=Homo sapiens GN=CKAP4 PE=1 SV=2	1.360	1.528	↑
P09622	Dihydrolipoyl dehydrogenase, mitochondrial OS=Homo sapiens GN=DLD PE=1 SV=2	2.602	2.920	↑
Q96PD2	Discoidin, CUB and LCCL domain-containing protein 2 OS=Homo sapiens GN=DCBLD2 PE=1 SV=	1.589	1.422	↑
P49792	E3 SUMO-protein ligase RanBP2 OS=Homo sapiens GN=RANBP2 PE=1 SV=2	0.419	0.402	↓
P68104	Elongation factor 1-alpha 1 OS=Homo sapiens GN=EEF1A1 PE=1 SV=1	0.531	0.673	↓
P24534	Elongation factor 1-beta OS=Homo sapiens GN=EEF1B2 PE=1 SV=3	2.025	1.449	↑
P30040	Endoplasmic reticulum resident protein 29 OS=Homo sapiens GN=ERP29 PE=1 SV=4	2.236	2.027	↑
P14625	Endoplasmin OS=Homo sapiens GN=HSP90B1 PE=1 SV=1	1.681	1.654	↑
P15311	Ezrin OS=Homo sapiens GN=EZR PE=1 SV=4	1.995	1.461	↑
Q9Y5B9	FACT complex subunit SPT16 OS=Homo sapiens GN=SUPT16H PE=1 SV=1	1.505	1.687	↑
Q96I24	Far upstream element-binding protein 3 OS=Homo sapiens GN=FUBP3 PE=1 SV=2	0.668	0.686	↓
P49327	Fatty acid synthase OS=Homo sapiens GN=FASN PE=1 SV=3	0.484	0.495	↓
P09382	Galectin-1 OS=Homo sapiens GN=LGALS1 PE=1 SV=2	2.610	2.142	↑
P17931	Galectin-3 OS=Homo sapiens GN=LGALS3 PE=1 SV=5	2.822	2.061	↑
P14314	Glucosidase 2 subunit beta OS=Homo sapiens GN=PRKCSH PE=1 SV=2	2.481	1.682	↑
P43304	Glycerol-3-phosphate dehydrogenase, mitochondrial OS=Homo sapiens GN=GPD2 PE=1 SV=3	0.671	0.788	↓
P50151	Guanine nucleotide-binding protein G(I)/G(S)/G(O) subunit gamma-10 OS=Homo sapiens GN=C	3.350	2.509	↑

871

Q14344	Guanine nucleotide-binding protein subunit alpha-13 OS=Homo sapiens GN=GNA13 PE=1 SV=2	0.401	0.702	↓
P04792	Heat shock protein beta-1 OS=Homo sapiens GN=HSPB1 PE=1 SV=2	3.963	4.443	↑
P52272	Heterogeneous nuclear ribonucleoprotein M OS=Homo sapiens GN=HNRNPM PE=1 SV=3	0.617	0.768	↓
P09429	High mobility group protein B1 OS=Homo sapiens GN=HMGB1 PE=1 SV=3	3.621	3.153	↑
P26583	High mobility group protein B2 OS=Homo sapiens GN=HMGB2 PE=1 SV=2	2.255	2.382	↑
O15347	High mobility group protein B3 OS=Homo sapiens GN=HMGB3 PE=1 SV=4	2.306	2.101	↑
P16403	Histone H1.2 OS=Homo sapiens GN=HIST1H1C PE=1 SV=2	3.219	1.900	↑
Q09028	Histone-binding protein RBBP4 OS=Homo sapiens GN=RBBP4 PE=1 SV=3	1.709	1.225	↑
Q9Y4L1	Hypoxia up-regulated protein 1 OS=Homo sapiens GN=HYOU1 PE=1 SV=1	1.354	1.276	↑
P52292	Importin subunit alpha-1 OS=Homo sapiens GN=KPNA2 PE=1 SV=1	0.592	0.657	↓
P12268	Inosine-5'-monophosphate dehydrogenase 2 OS=Homo sapiens GN=IMPDH2 PE=1 SV=2	0.337	0.338	↓
Q9Y6M1	Insulin-like growth factor 2 mRNA-binding protein 2 OS=Homo sapiens GN=IGF2BP2 PE=1 SV=2	1.358	1.301	↑
P17301	Integrin alpha-2 OS=Homo sapiens GN=ITGA2 PE=1 SV=1	2.698	2.193	↑
P26006	Integrin alpha-3 OS=Homo sapiens GN=ITGA3 PE=1 SV=5	3.354	1.983	↑
P05556	Integrin beta-1 OS=Homo sapiens GN=ITGB1 PE=1 SV=2	4.040	2.702	↑
P41252	Isoleucine--tRNA ligase, cytoplasmic OS=Homo sapiens GN=IARS PE=1 SV=2	0.578	0.675	↓
P33176	Kinesin-1 heavy chain OS=Homo sapiens GN=KIF5B PE=1 SV=1	0.424	0.502	↓
P42167	Lamina-associated polypeptide 2, isoforms beta/gamma OS=Homo sapiens GN=TMPO PE=1 SV	2.004	1.746	↑
P20700	Lamin-B1 OS=Homo sapiens GN=LMNB1 PE=1 SV=2	2.392	2.155	↑
Q03252	Lamin-B2 OS=Homo sapiens GN=LMNB2 PE=1 SV=3	1.568	2.313	↑
Q9UHB6	LIM domain and actin-binding protein 1 OS=Homo sapiens GN=LIMA1 PE=1 SV=1	2.633	2.205	↑
Q15046	Lysine--tRNA ligase OS=Homo sapiens GN=KARS PE=1 SV=3	0.761	0.706	↓
P40926	Malate dehydrogenase, mitochondrial OS=Homo sapiens GN=MDH2 PE=1 SV=3	1.645	1.774	↑
Q14165	Malectin OS=Homo sapiens GN=MLEC PE=1 SV=1	1.332	1.240	↑
P19105	Myosin regulatory light chain 12A OS=Homo sapiens GN=MYL12A PE=1 SV=2	1.555	1.972	↑
P51970	NADH dehydrogenase [ubiquinone] 1 alpha subcomplex subunit 8 OS=Homo sapiens GN=NDUI	1.816	1.568	↑
P49821	NADH dehydrogenase [ubiquinone] flavoprotein 1, mitochondrial OS=Homo sapiens GN=NDUF	1.988	1.793	↑
P19404	NADH dehydrogenase [ubiquinone] flavoprotein 2, mitochondrial OS=Homo sapiens GN=NDUF	2.525	1.686	↑
O43181	NADH dehydrogenase [ubiquinone] iron-sulfur protein 4, mitochondrial OS=Homo sapiens GN=	2.643	2.072	↑
Q13765	Nascent polypeptide-associated complex subunit alpha OS=Homo sapiens GN=NACA PE=1 SV=	1.987	1.694	↑
Q09666	Neuroblast differentiation-associated protein AHNAK OS=Homo sapiens GN=AHNAK PE=1 SV=2	2.630	2.194	↑
Q9Y639	Neuroplastin OS=Homo sapiens GN=NPTN PE=1 SV=2	1.606	1.323	↑
Q14697	Neutral alpha-glucosidase AB OS=Homo sapiens GN=GANAB PE=1 SV=3	1.698	2.036	↑
Q15233	Non-POU domain-containing octamer-binding protein OS=Homo sapiens GN=NONO PE=1 SV=4	1.376	2.014	↑
Q14978	Nucleolar and coiled-body phosphoprotein 1 OS=Homo sapiens GN=NOLC1 PE=1 SV=2	1.866	2.262	↑
Q9NR30	Nucleolar RNA helicase 2 OS=Homo sapiens GN=DDX21 PE=1 SV=5	0.640	0.766	↓
P17480	Nucleolar transcription factor 1 OS=Homo sapiens GN=UBTF PE=1 SV=1	1.379	1.559	↑
P19338	Nucleolin OS=Homo sapiens GN=NCL PE=1 SV=3	1.882	1.273	↑
P06748	Nucleophosmin OS=Homo sapiens GN=NPM1 PE=1 SV=2	3.751	2.595	↑
Q99733	Nucleosome assembly protein 1-like 4 OS=Homo sapiens GN=NAP1L4 PE=1 SV=1	1.763	1.968	↑
Q8WXF1	Paraspeckle component 1 OS=Homo sapiens GN=PSPC1 PE=1 SV=1	2.020	1.909	↑
P62937	Peptidyl-prolyl cis-trans isomerase A OS=Homo sapiens GN=PPIA PE=1 SV=2	2.688	2.469	↑
P23284	Peptidyl-prolyl cis-trans isomerase B OS=Homo sapiens GN=PPIB PE=1 SV=2	2.340	1.835	↑
P26885	Peptidyl-prolyl cis-trans isomerase FKBP2 OS=Homo sapiens GN=FKBP2 PE=1 SV=2	2.932	2.338	↑
O60664	Perilipin-3 OS=Homo sapiens GN=PLIN3 PE=1 SV=3	3.289	1.805	↑
Q06830	Peroxiredoxin-1 OS=Homo sapiens GN=PRDX1 PE=1 SV=1	1.691	1.465	↑
P48739	Phosphatidylinositol transfer protein beta isoform OS=Homo sapiens GN=PITPNB PE=1 SV=2	1.931	1.450	↑
P18669	Phosphoglycerate mutase 1 OS=Homo sapiens GN=PGAM1 PE=1 SV=2	2.963	2.441	↑
Q8NC51	Plasminogen activator inhibitor 1 RNA-binding protein OS=Homo sapiens GN=SERBP1 PE=1 SV=	1.771	1.385	↑
P09874	Poly [ADP-ribose] polymerase 1 OS=Homo sapiens GN=PARP1 PE=1 SV=4	1.297	1.349	↑
Q15365	Poly(rC)-binding protein 1 OS=Homo sapiens GN=PCBP1 PE=1 SV=2	0.424	0.497	↓
Q9UHG3	Prenylcysteine oxidase 1 OS=Homo sapiens GN=PCYOX1 PE=1 SV=3	0.435	0.677	↓
P07602	Proactivator polypeptide OS=Homo sapiens GN=PSAP PE=1 SV=2	4.278	3.059	↑
P35232	Prohibitin OS=Homo sapiens GN=PHB PE=1 SV=1	0.459	0.597	↓
Q99623	Prohibitin-2 OS=Homo sapiens GN=PHB2 PE=1 SV=2	0.305	0.540	↓
P30101	Protein disulfide-isomerase A3 OS=Homo sapiens GN=PDIA3 PE=1 SV=4	1.441	1.649	↑
P13667	Protein disulfide-isomerase A4 OS=Homo sapiens GN=PDIA4 PE=1 SV=2	1.441	1.368	↑
P07237	Protein disulfide-isomerase OS=Homo sapiens GN=P4HB PE=1 SV=3	2.935	2.438	↑
Q92520	Protein FAM3C OS=Homo sapiens GN=FAM3C PE=1 SV=1	0.448	0.501	↓
P14618	Pyruvate kinase PKM OS=Homo sapiens GN=PKM PE=1 SV=4	0.382	0.453	↓
Q6IAA8	Ragulator complex protein LAMTOR1 OS=Homo sapiens GN=LAMTOR1 PE=1 SV=2	0.587	0.714	↓
P61026	Ras-related protein Rab-10 OS=Homo sapiens GN=RAB10 PE=1 SV=1	4.716	7.542	↑
P38159	RNA-binding motif protein, X chromosome OS=Homo sapiens GN=RBMX PE=1 SV=3	0.723	0.761	↓
Q9NVA2	Septin-11 OS=Homo sapiens GN=SEPT11 PE=1 SV=3	2.991	2.019	↑
Q15019	Septin-2 OS=Homo sapiens GN=SEPT2 PE=1 SV=1	3.096	2.102	↑
Q9UHD8	Septin-9 OS=Homo sapiens GN=SEPT9 PE=1 SV=2	3.193	1.870	↑
P62316	Small nuclear ribonucleoprotein Sm D2 OS=Homo sapiens GN=SNRPD2 PE=1 SV=1	1.734	1.324	↑
P05023	Sodium/potassium-transporting ATPase subunit alpha-1 OS=Homo sapiens GN=ATP1A1 PE=1 S	0.503	0.657	↓
Q15637	Splicing factor 1 OS=Homo sapiens GN=SF1 PE=1 SV=4	2.002	1.428	↑
P23246	Splicing factor, proline- and glutamine-rich OS=Homo sapiens GN=SFPQ PE=1 SV=2	1.575	1.784	↑
Q9UJZ1	Stomatin-like protein 2, mitochondrial OS=Homo sapiens GN=STOML2 PE=1 SV=1	0.404	0.773	↓
P38646	Stress-70 protein, mitochondrial OS=Homo sapiens GN=HSPA9 PE=1 SV=2	1.393	1.421	↑
Q6ZRP7	Sulfhydryl oxidase 2 OS=Homo sapiens GN=QSOX2 PE=1 SV=3	0.421	0.608	↓

872

Q86Y82	Syntaxin-12 OS=Homo sapiens GN=STX12 PE=1 SV=1	1.811	1.380	↑
O15400	Syntaxin-7 OS=Homo sapiens GN=STX7 PE=1 SV=4	1.561	1.482	↑
P02786	Transferrin receptor protein 1 OS=Homo sapiens GN=TFRC PE=1 SV=2	0.353	0.696	↓
P61586	Transforming protein RhoA OS=Homo sapiens GN=RHOA PE=1 SV=1	1.527	1.644	↑
Q9BVK6	Transmembrane emp24 domain-containing protein 9 OS=Homo sapiens GN=TMED9 PE=1 SV=2	0.554	0.710	↓
Q9BTV4	Transmembrane protein 43 OS=Homo sapiens GN=TMEM43 PE=1 SV=1	1.228	1.313	↑
P07437	Tubulin beta chain OS=Homo sapiens GN=TUBB PE=1 SV=2	0.229	0.369	↓
O43399	Tumor protein D54 OS=Homo sapiens GN=TPD52L2 PE=1 SV=2	3.042	1.999	↑
Q9BVJ6	U3 small nucleolar RNA-associated protein 14 homolog A OS=Homo sapiens GN=UTP14A PE=1	0.750	0.714	↓
P49748	Very long-chain specific acyl-CoA dehydrogenase, mitochondrial OS=Homo sapiens GN=ACADV	2.314	2.103	↑
P21796	Voltage-dependent anion-selective channel protein 1 OS=Homo sapiens GN=VDAC1 PE=1 SV=2	0.474	0.562	↓
P45880	Voltage-dependent anion-selective channel protein 2 OS=Homo sapiens GN=VDAC2 PE=1 SV=2	0.234	0.281	↓
P52815	39S ribosomal protein L12, mitochondrial OS=Homo sapiens GN=MRPL12 PE=1 SV=2	1.739	n/o	↑
Q9NQ50	39S ribosomal protein L40, mitochondrial OS=Homo sapiens GN=MRPL40 PE=1 SV=1	1.527	n/o	↑
P62269	40S ribosomal protein S18 OS=Homo sapiens GN=RPS18 PE=1 SV=3	0.767	n/o	↓
P62854	40S ribosomal protein S26 OS=Homo sapiens GN=RPS26 PE=1 SV=3	0.510	n/o	↓
P62857	40S ribosomal protein S28 OS=Homo sapiens GN=RPS28 PE=1 SV=1	3.125	n/o	↑
P62081	40S ribosomal protein S7 OS=Homo sapiens GN=RPS7 PE=1 SV=1	0.575	n/o	↓
P05388	60S acidic ribosomal protein P0 OS=Homo sapiens GN=RPLP0 PE=1 SV=1	0.729	n/o	↓
P62913	60S ribosomal protein L11 OS=Homo sapiens GN=RPL11 PE=1 SV=2	0.368	n/o	↓
P26373	60S ribosomal protein L13 OS=Homo sapiens GN=RPL13 PE=1 SV=4	0.669	n/o	↓
Q07020	60S ribosomal protein L18 OS=Homo sapiens GN=RPL18 PE=1 SV=2	0.483	n/o	↓
P62750	60S ribosomal protein L23a OS=Homo sapiens GN=RPL23A PE=1 SV=1	1.449	n/o	↑
P62424	60S ribosomal protein L7a OS=Homo sapiens GN=RPL7A PE=1 SV=2	0.705	n/o	↓
Q01813	6-phosphofructokinase type C OS=Homo sapiens GN=PFKP PE=1 SV=2	0.450	n/o	↓
Q92485	Acid sphingomyelinase-like phosphodiesterase 3b OS=Homo sapiens GN=SMPDL3B PE=2 SV=2	1.391	n/o	↑
O00116	Alkyldihydroxyacetonephosphate synthase, peroxisomal OS=Homo sapiens GN=AGPS PE=1 SV=	0.643	n/o	↓
P27338	Amine oxidase [flavin-containing] B OS=Homo sapiens GN=MAOB PE=1 SV=3	0.440	n/o	↓
O95831	Apoptosis-inducing factor 1, mitochondrial OS=Homo sapiens GN=AIFM1 PE=1 SV=1	1.351	n/o	↑
Q9UKV3	Apoptotic chromatin condensation inducer in the nucleus OS=Homo sapiens GN=ACIN1 PE=1 S	1.652	n/o	↑
P25705	ATP synthase subunit alpha, mitochondrial OS=Homo sapiens GN=ATP5A1 PE=1 SV=1	0.600	n/o	↓
P30049	ATP synthase subunit delta, mitochondrial OS=Homo sapiens GN=ATP5D PE=1 SV=2	1.878	n/o	↑
O75964	ATP synthase subunit g, mitochondrial OS=Homo sapiens GN=ATP5L PE=1 SV=3	0.502	n/o	↓
P36542	ATP synthase subunit gamma, mitochondrial OS=Homo sapiens GN=ATP5C1 PE=1 SV=1	0.521	n/o	↓
P18859	ATP synthase-coupling factor 6, mitochondrial OS=Homo sapiens GN=ATP5J PE=1 SV=1	4.036	n/o	↑
Q92499	ATP-dependent RNA helicase DDX1 OS=Homo sapiens GN=DDX1 PE=1 SV=2	0.683	n/o	↓
Q8TDD1	ATP-dependent RNA helicase DDX54 OS=Homo sapiens GN=DDX54 PE=1 SV=2	0.592	n/o	↓
O75531	Barrier-to-autointegration factor OS=Homo sapiens GN=BANF1 PE=1 SV=1	3.195	n/o	↑
P50895	Basal cell adhesion molecule OS=Homo sapiens GN=BCAM PE=1 SV=2	0.667	n/o	↓
P51572	B-cell receptor-associated protein 31 OS=Homo sapiens GN=BCAP31 PE=1 SV=3	0.504	n/o	↓
Q9UQB8	Brain-specific angiogenesis inhibitor 1-associated protein 2 OS=Homo sapiens GN=BAIAP2 PE=1	1.359	n/o	↑
P23786	Carnitine O-palmitoyltransferase 2, mitochondrial OS=Homo sapiens GN=CPT2 PE=1 SV=2	1.538	n/o	↑
P48730	Casein kinase I isoform delta OS=Homo sapiens GN=CSNK1D PE=1 SV=2	1.670	n/o	↑
P13987	CD59 glycoprotein OS=Homo sapiens GN=CD59 PE=1 SV=1	1.977	n/o	↑
Q9NX58	Cell growth-regulating nucleolar protein OS=Homo sapiens GN=LYAR PE=1 SV=2	1.389	n/o	↑
O43809	Cleavage and polyadenylation specificity factor subunit 5 OS=Homo sapiens GN=NUDT21 PE=1	3.893	n/o	↑
P48444	Coatomer subunit delta OS=Homo sapiens GN=ARCN1 PE=1 SV=1	0.628	n/o	↓
Q14011	Cold-inducible RNA-binding protein OS=Homo sapiens GN=CIRBP PE=1 SV=1	1.512	n/o	↑
P00403	Cytochrome c oxidase subunit 2 OS=Homo sapiens GN=MT-CO2 PE=1 SV=1	0.559	n/o	↓
P14854	Cytochrome c oxidase subunit 6B1 OS=Homo sapiens GN=COX6B1 PE=1 SV=2	2.052	n/o	↑
Q8N163	DBIRD complex subunit KIAA1967 OS=Homo sapiens GN=KIAA1967 PE=1 SV=2	0.701	n/o	↓
P27695	DNA-(apurinic or apyrimidinic site) lyase OS=Homo sapiens GN=APEX1 PE=1 SV=2	1.622	n/o	↑
P31689	DnaJ homolog subfamily A member 1 OS=Homo sapiens GN=DNAJA1 PE=1 SV=2	0.360	n/o	↓
Q96EY1	DnaJ homolog subfamily A member 3, mitochondrial OS=Homo sapiens GN=DNAJA3 PE=1 SV=2	1.335	n/o	↑
Q9UBS4	DnaJ homolog subfamily B member 11 OS=Homo sapiens GN=DNAJB11 PE=1 SV=1	1.578	n/o	↑
Q8WXX5	DnaJ homolog subfamily C member 9 OS=Homo sapiens GN=DNAJC9 PE=1 SV=1	1.905	n/o	↑
P04843	Dolichyl-diphosphooligosaccharide--protein glycosyltransferase subunit 1 OS=Homo sapiens GI	0.558	n/o	↓
Q15717	ELAV-like protein 1 OS=Homo sapiens GN=ELAVL1 PE=1 SV=2	0.698	n/o	↓
P50402	Emerin OS=Homo sapiens GN=EMD PE=1 SV=1	0.717	n/o	↓
Q9BSJ8	Extended synaptotagmin-1 OS=Homo sapiens GN=ESYT1 PE=1 SV=1	0.790	n/o	↓
Q96AE4	Far upstream element-binding protein 1 OS=Homo sapiens GN=FUBP1 PE=1 SV=3	1.940	n/o	↑
Q92945	Far upstream element-binding protein 2 OS=Homo sapiens GN=KHSRP PE=1 SV=4	1.269	n/o	↑
Q9BQ67	Glutamate-rich WD repeat-containing protein 1 OS=Homo sapiens GN=GRWD1 PE=1 SV=1	1.535	n/o	↑
P04406	Glyceraldehyde-3-phosphate dehydrogenase OS=Homo sapiens GN=GAPDH PE=1 SV=3	0.651	n/o	↓
Q8NBJ4	Golgi membrane protein 1 OS=Homo sapiens GN=GOLM1 PE=1 SV=1	2.447	n/o	↑
P63096	Guanine nucleotide-binding protein G(i) subunit alpha-1 OS=Homo sapiens GN=GNAI1 PE=1 SV	0.551	n/o	↓
P04899	Guanine nucleotide-binding protein G(i) subunit alpha-2 OS=Homo sapiens GN=GNAI2 PE=1 SV	0.705	n/o	↓
P08107	Heat shock 70 kDa protein 1A/1B OS=Homo sapiens GN=HSPA1A PE=1 SV=5	0.685	n/o	↓
P34932	Heat shock 70 kDa protein 4 OS=Homo sapiens GN=HSPA4 PE=1 SV=4	1.698	n/o	↑
P11142	Heat shock cognate 71 kDa protein OS=Homo sapiens GN=HSPA8 PE=1 SV=1	0.726	n/o	↓
P51858	Hepatoma-derived growth factor OS=Homo sapiens GN=HDGF PE=1 SV=1	3.960	n/o	↑
Q99729	Heterogeneous nuclear ribonucleoprotein A/B OS=Homo sapiens GN=HNRNPAB PE=1 SV=2	1.604	n/o	↑
P09651	Heterogeneous nuclear ribonucleoprotein A1 OS=Homo sapiens GN=HNRNPA1 PE=1 SV=5	1.648	n/o	↑

873

P55795	Heterogeneous nuclear ribonucleoprotein H2 OS=Homo sapiens GN=HNRNPH2 PE=1 SV=1	0.798	n/o	↓
O60506	Heterogeneous nuclear ribonucleoprotein Q OS=Homo sapiens GN=SYNCRIP PE=1 SV=2	1.235	n/o	↑
P17096	High mobility group protein HMG-I/HMG-Y OS=Homo sapiens GN=HMGA1 PE=1 SV=3	4.280	n/o	↑
Q71UI9	Histone H2A.V OS=Homo sapiens GN=H2AFV PE=1 SV=3	2.137	n/o	↑
P68431	Histone H3.1 OS=Homo sapiens GN=HIST1H3A PE=1 SV=2	2.106	n/o	↑
O00410	Importin-5 OS=Homo sapiens GN=IPO5 PE=1 SV=4	0.496	n/o	↓
Q13308	Inactive tyrosine-protein kinase 7 OS=Homo sapiens GN=PTK7 PE=1 SV=2	0.724	n/o	↓
Q12906	Interleukin enhancer-binding factor 3 OS=Homo sapiens GN=ILF3 PE=1 SV=3	0.762	n/o	↓
P13645	Keratin, type I cytoskeletal 10 OS=Homo sapiens GN=KRT10 PE=1 SV=6	1.623	n/o	↑
P05783	Keratin, type I cytoskeletal 18 OS=Homo sapiens GN=KRT18 PE=1 SV=2	0.472	n/o	↓
P08727	Keratin, type I cytoskeletal 19 OS=Homo sapiens GN=KRT19 PE=1 SV=4	0.515	n/o	↓
P35527	Keratin, type I cytoskeletal 9 OS=Homo sapiens GN=KRT9 PE=1 SV=3	1.599	n/o	↑
P05787	Keratin, type II cytoskeletal 8 OS=Homo sapiens GN=KRT8 PE=1 SV=7	0.323	n/o	↓
Q16891	Mitochondrial inner membrane protein OS=Homo sapiens GN=IMMT PE=1 SV=1	0.507	n/o	↓
P26038	Moesin OS=Homo sapiens GN=MSN PE=1 SV=3	1.705	n/o	↑
P35579	Myosin-9 OS=Homo sapiens GN=MYH9 PE=1 SV=4	0.499	n/o	↓
P29966	Myristoylated alanine-rich C-kinase substrate OS=Homo sapiens GN=MARCKS PE=1 SV=4	1.895	n/o	↑
Q9P0J0	NADH dehydrogenase [ubiquinone] 1 alpha subcomplex subunit 13 OS=Homo sapiens GN=NDL	0.805	n/o	↓
O00217	NADH dehydrogenase [ubiquinone] iron-sulfur protein 8, mitochondrial OS=Homo sapiens GN=	1.590	n/o	↑
P00387	NADH-cytochrome b5 reductase 3 OS=Homo sapiens GN=CYB5R3 PE=1 SV=3	0.405	n/o	↓
P16435	NADPH--cytochrome P450 reductase OS=Homo sapiens GN=POR PE=1 SV=2	0.564	n/o	↓
P22307	Non-specific lipid-transfer protein OS=Homo sapiens GN=SCP2 PE=1 SV=2	1.708	n/o	↑
P55209	Nucleosome assembly protein 1-like 1 OS=Homo sapiens GN=NAP1L1 PE=1 SV=1	1.488	n/o	↑
Q9NX40	OCIA domain-containing protein 1 OS=Homo sapiens GN=OCIAD1 PE=1 SV=1	1.629	n/o	↑
O75475	PC4 and SFRS1-interacting protein OS=Homo sapiens GN=PSIP1 PE=1 SV=1	1.762	n/o	↑
Q00688	Peptidyl-prolyl cis-trans isomerase FKBP3 OS=Homo sapiens GN=FKBP3 PE=1 SV=1	2.739	n/o	↑
Q15149	Plectin OS=Homo sapiens GN=PLEC PE=1 SV=3	0.599	n/o	↓
Q9H7Z7	Prostaglandin E synthase 2 OS=Homo sapiens GN=PTGES2 PE=1 SV=1	0.642	n/o	↓
Q9P2B2	Prostaglandin F2 receptor negative regulator OS=Homo sapiens GN=PTGFRN PE=1 SV=2	1.513	n/o	↑
P28066	Proteasome subunit alpha type-5 OS=Homo sapiens GN=PSMA5 PE=1 SV=3	1.631	n/o	↑
O14818	Proteasome subunit alpha type-7 OS=Homo sapiens GN=PSMA7 PE=1 SV=1	1.475	n/o	↑
P49257	Protein ERGIC-53 OS=Homo sapiens GN=LMAN1 PE=1 SV=2	0.648	n/o	↓
Q96A26	Protein FAM162A OS=Homo sapiens GN=FAM162A PE=1 SV=2	1.857	n/o	↑
Q9NUP9	Protein lin-7 homolog C OS=Homo sapiens GN=LIN7C PE=1 SV=1	1.544	n/o	↑
Q9HBR0	Putative sodium-coupled neutral amino acid transporter 10 OS=Homo sapiens GN=SLC38A10 P	1.705	n/o	↑
Q15907	Ras-related protein Rab-11B OS=Homo sapiens GN=RAB11B PE=1 SV=4	0.694	n/o	↓
P35637	RNA-binding protein FUS OS=Homo sapiens GN=FUS PE=1 SV=1	1.683	n/o	↑
Q16181	Septin-7 OS=Homo sapiens GN=SEPT7 PE=1 SV=2	2.161	n/o	↑
Q01130	Serine/arginine-rich splicing factor 2 OS=Homo sapiens GN=SRSF2 PE=1 SV=4	2.664	n/o	↑
P36873	Serine/threonine-protein phosphatase PP1-gamma catalytic subunit OS=Homo sapiens GN=PPI	1.454	n/o	↑
Q9H9B4	Sideroflexin-1 OS=Homo sapiens GN=SFXN1 PE=1 SV=4	0.558	n/o	↓
P37108	Signal recognition particle 14 kDa protein OS=Homo sapiens GN=SRP14 PE=1 SV=2	1.597	n/o	↑
P54709	Sodium/potassium-transporting ATPase subunit beta-3 OS=Homo sapiens GN=ATP1B3 PE=1 SV	0.474	n/o	↓
P11166	Solute carrier family 2, facilitated glucose transporter member 1 OS=Homo sapiens GN=SLC2A1	0.359	n/o	↓
Q15459	Splicing factor 3A subunit 1 OS=Homo sapiens GN=SF3A1 PE=1 SV=1	1.286	n/o	↑
P26368	Splicing factor U2AF 65 kDa subunit OS=Homo sapiens GN=U2AF2 PE=1 SV=4	2.110	n/o	↑
Q16563	Synaptophysin-like protein 1 OS=Homo sapiens GN=SYPL1 PE=1 SV=1	0.425	n/o	↓
P21579	Synaptotagmin-1 OS=Homo sapiens GN=SYT1 PE=1 SV=1	1.888	n/o	↑
P50991	T-complex protein 1 subunit delta OS=Homo sapiens GN=CCT4 PE=1 SV=4	0.748	n/o	↓
Q92616	Translational activator GCN1 OS=Homo sapiens GN=GCN1L1 PE=1 SV=6	0.594	n/o	↓
Q99805	Transmembrane 9 superfamily member 2 OS=Homo sapiens GN=TM9SF2 PE=1 SV=1	0.638	n/o	↓
Q92544	Transmembrane 9 superfamily member 4 OS=Homo sapiens GN=TM9SF4 PE=1 SV=2	0.532	n/o	↓
P49755	Transmembrane emp24 domain-containing protein 10 OS=Homo sapiens GN=TMED10 PE=1 SV	0.465	n/o	↓
Q15363	Transmembrane emp24 domain-containing protein 2 OS=Homo sapiens GN=TMED2 PE=1 SV=1	0.265	n/o	↓
Q9Y3A6	Transmembrane emp24 domain-containing protein 5 OS=Homo sapiens GN=TMED5 PE=1 SV=1	0.479	n/o	↓
Q9Y3B3	Transmembrane emp24 domain-containing protein 7 OS=Homo sapiens GN=TMED7 PE=1 SV=2	0.613	n/o	↓
Q9BUF5	Tubulin beta-6 chain OS=Homo sapiens GN=TUBB6 PE=1 SV=1	0.533	n/o	↓
P08621	U1 small nuclear ribonucleoprotein 70 kDa OS=Homo sapiens GN=SNRNP70 PE=1 SV=2	1.689	n/o	↑
P09012	U1 small nuclear ribonucleoprotein A OS=Homo sapiens GN=SNRPA PE=1 SV=3	1.984	n/o	↑
P09661	U2 small nuclear ribonucleoprotein A' OS=Homo sapiens GN=SNRPA1 PE=1 SV=2	1.527	n/o	↑
P62979	Ubiquitin-40S ribosomal protein S27a OS=Homo sapiens GN=RPS27A PE=1 SV=2	0.514	n/o	↓
Q9BQ61	Uncharacterized protein C19orf43 OS=Homo sapiens GN=C19orf43 PE=1 SV=1	2.294	n/o	↑
Q9Y224	UPF0568 protein C14orf166 OS=Homo sapiens GN=C14orf166 PE=1 SV=1	1.259	n/o	↑
Q15029	116 kDa U5 small nuclear ribonucleoprotein component OS=Homo sapiens GN=EFTUD2 PE=1 S	n/o	1.212	↑
P63104	14-3-3 protein zeta/delta OS=Homo sapiens GN=YWHAZ PE=1 SV=1	n/o	1.725	↑
P43686	26S protease regulatory subunit 6B OS=Homo sapiens GN=PSMC4 PE=1 SV=2	n/o	0.739	↓
P51665	26S proteasome non-ATPase regulatory subunit 7 OS=Homo sapiens GN=PSMD7 PE=1 SV=2	n/o	0.682	↓
P62280	40S ribosomal protein S11 OS=Homo sapiens GN=RPS11 PE=1 SV=3	n/o	0.619	↓
P62277	40S ribosomal protein S13 OS=Homo sapiens GN=RPS13 PE=1 SV=2	n/o	0.625	↓
P62263	40S ribosomal protein S14 OS=Homo sapiens GN=RPS14 PE=1 SV=3	n/o	0.773	↓
P15880	40S ribosomal protein S2 OS=Homo sapiens GN=RPS2 PE=1 SV=2	n/o	0.705	↓
P61247	40S ribosomal protein S3a OS=Homo sapiens GN=RPS3A PE=1 SV=2	n/o	0.663	↓
P62899	60S ribosomal protein L31 OS=Homo sapiens GN=RPL31 PE=1 SV=1	n/o	1.290	↑

874

P32969	60S ribosomal protein L9 OS=Homo sapiens GN=RPL9 PE=1 SV=1	n/o	0.556	↓
Q9HDC9	Adipocyte plasma membrane-associated protein OS=Homo sapiens GN=APMAP PE=1 SV=2	n/o	1.369	↑
Q12904	Aminoacyl tRNA synthase complex-interacting multifunctional protein 1 OS=Homo sapiens GN=	n/o	0.590	↓
P46013	Antigen KI-67 OS=Homo sapiens GN=MKI67 PE=1 SV=2	n/o	1.248	↑
Q12797	Aspartyl/asparaginyl beta-hydroxylase OS=Homo sapiens GN=ASPH PE=1 SV=3	n/o	1.452	↑
P06576	ATP synthase subunit beta, mitochondrial OS=Homo sapiens GN=ATP5B PE=1 SV=3	n/o	1.566	↑
P48047	ATP synthase subunit O, mitochondrial OS=Homo sapiens GN=ATP5O PE=1 SV=1	n/o	1.439	↑
Q9GZR7	ATP-dependent RNA helicase DDX24 OS=Homo sapiens GN=DDX24 PE=1 SV=1	n/o	0.721	↓
Q13895	Bystin OS=Homo sapiens GN=BYSL PE=1 SV=3	n/o	0.693	↓
P27708	CAD protein OS=Homo sapiens GN=CAD PE=1 SV=3	n/o	0.710	↓
Q14444	Caprin-1 OS=Homo sapiens GN=CAPRIN1 PE=1 SV=2	n/o	0.806	↓
P21926	CD9 antigen OS=Homo sapiens GN=CD9 PE=1 SV=4	n/o	1.756	↑
P48960	CD97 antigen OS=Homo sapiens GN=CD97 PE=1 SV=4	n/o	1.320	↑
Q9NZ45	CDGSH iron-sulfur domain-containing protein 1 OS=Homo sapiens GN=CISD1 PE=1 SV=1	n/o	0.707	↓
Q8N5K1	CDGSH iron-sulfur domain-containing protein 2 OS=Homo sapiens GN=CISD2 PE=1 SV=1	n/o	0.435	↓
O75367	Core histone macro-H2A.1 OS=Homo sapiens GN=H2AFY PE=1 SV=4	n/o	1.269	↑
P12532	Creatine kinase U-type, mitochondrial OS=Homo sapiens GN=CKMT1A PE=1 SV=1	n/o	0.573	↓
Q02127	Dihydroorotate dehydrogenase (quinone), mitochondrial OS=Homo sapiens GN=DHODH PE=1 :	n/o	0.694	↓
P11387	DNA topoisomerase 1 OS=Homo sapiens GN=TOP1 PE=1 SV=2	n/o	1.406	↑
P04844	Dolichyl-diphosphooligosaccharide--protein glycosyltransferase subunit 2 OS=Homo sapiens GI	n/o	1.374	↑
P29692	Elongation factor 1-delta OS=Homo sapiens GN=EEF1D PE=1 SV=5	n/o	1.404	↑
P49411	Elongation factor Tu, mitochondrial OS=Homo sapiens GN=TUFM PE=1 SV=2	n/o	0.242	↓
Q04637	Eukaryotic translation initiation factor 4 gamma 1 OS=Homo sapiens GN=EIF4G1 PE=1 SV=4	n/o	0.595	↓
Q08945	FACT complex subunit SSRP1 OS=Homo sapiens GN=SSRP1 PE=1 SV=1	n/o	1.390	↑
Q00839	Heterogeneous nuclear ribonucleoprotein U OS=Homo sapiens GN=HNRNPU PE=1 SV=6	n/o	0.696	↓
P37235	Hippocalcin-like protein 1 OS=Homo sapiens GN=HPCAL1 PE=1 SV=3	n/o	2.083	↑
P04264	Keratin, type II cytoskeletal 1 OS=Homo sapiens GN=KRT1 PE=1 SV=6	n/o	0.641	↓
P35908	Keratin, type II cytoskeletal 2 epidermal OS=Homo sapiens GN=KRT2 PE=1 SV=2	n/o	0.579	↓
Q96AG4	Leucine-rich repeat-containing protein 59 OS=Homo sapiens GN=LRRC59 PE=1 SV=1	n/o	1.445	↑
Q9ULC5	Long-chain-fatty-acid--CoA ligase 5 OS=Homo sapiens GN=ACSL5 PE=1 SV=1	n/o	0.641	↓
O00264	Membrane-associated progesterone receptor component 1 OS=Homo sapiens GN=PGRMC1 PE	n/o	0.539	↓
P56192	Methionine--tRNA ligase, cytoplasmic OS=Homo sapiens GN=MARS PE=1 SV=2	n/o	0.661	↓
P27816	Microtubule-associated protein 4 OS=Homo sapiens GN=MAP4 PE=1 SV=3	n/o	0.769	↓
P35580	Myosin-10 OS=Homo sapiens GN=MYH10 PE=1 SV=3	n/o	1.469	↑
Q16795	NADH dehydrogenase [ubiquinone] 1 alpha subcomplex subunit 9, mitochondrial OS=Homo sa	n/o	1.411	↑
O75489	NADH dehydrogenase [ubiquinone] iron-sulfur protein 3, mitochondrial OS=Homo sapiens GN=	n/o	1.328	↑
P28331	NADH-ubiquinone oxidoreductase 75 kDa subunit, mitochondrial OS=Homo sapiens GN=NDUF!	n/o	1.499	↑
Q01085	Nucleolysin TIAR OS=Homo sapiens GN=TIAL1 PE=1 SV=1	n/o	0.796	↓
P15531	Nucleoside diphosphate kinase A OS=Homo sapiens GN=NME1 PE=1 SV=1	n/o	2.276	↑
P00558	Phosphoglycerate kinase 1 OS=Homo sapiens GN=PGK1 PE=1 SV=3	n/o	1.598	↑
Q10471	Polypeptide N-acetylgalactosaminyltransferase 2 OS=Homo sapiens GN=GALNT2 PE=1 SV=1	n/o	1.466	↑
O75915	PRA1 family protein 3 OS=Homo sapiens GN=ARL6IP5 PE=1 SV=1	n/o	1.475	↑
Q15084	Protein disulfide-isomerase A6 OS=Homo sapiens GN=PDIA6 PE=1 SV=1	n/o	1.262	↑
P51148	Ras-related protein Rab-5C OS=Homo sapiens GN=RAB5C PE=1 SV=2	n/o	1.867	↑
P51149	Ras-related protein Rab-7a OS=Homo sapiens GN=RAB7A PE=1 SV=1	n/o	1.729	↑
P61224	Ras-related protein Rap-1b OS=Homo sapiens GN=RAP1B PE=1 SV=1	n/o	1.573	↑
Q8WTV0	Scavenger receptor class B member 1 OS=Homo sapiens GN=SCARB1 PE=1 SV=1	n/o	1.550	↑
Q99986	Serine/threonine-protein kinase VRK1 OS=Homo sapiens GN=VRK1 PE=1 SV=1	n/o	1.445	↑
P50454	Serpin H1 OS=Homo sapiens GN=SERPINH1 PE=1 SV=2	n/o	1.548	↑
P31040	Succinate dehydrogenase [ubiquinone] flavoprotein subunit, mitochondrial OS=Homo sapiens	n/o	1.604	↑
O94901	SUN domain-containing protein 1 OS=Homo sapiens GN=SUN1 PE=1 SV=3	n/o	0.738	↓
Q99536	Synaptic vesicle membrane protein VAT-1 homolog OS=Homo sapiens GN=VAT1 PE=1 SV=2	n/o	1.411	↑
Q9UGP8	Translocation protein SEC63 homolog OS=Homo sapiens GN=SEC63 PE=1 SV=2	n/o	1.863	↑
P60174	Triosephosphate isomerase OS=Homo sapiens GN=TPI1 PE=1 SV=3	n/o	1.803	↑
Q8IYS2	Uncharacterized protein KIAA2013 OS=Homo sapiens GN=KIAA2013 PE=2 SV=1	n/o	0.740	↓
Q12907	Vesicular integral-membrane protein VIP36 OS=Homo sapiens GN=LMAN2 PE=1 SV=1	n/o	0.692	↓
P12956	X-ray repair cross-complementing protein 6 OS=Homo sapiens GN=XRCC6 PE=1 SV=2	n/o	1.252	↑

875

Supplementary Table 4: List of other important proteins identified from untreated and TGFβ-treated HCT116 WT/HCT116AS comparisions

Uniprot ID	Gene name	Protein names	iTRAQ fold change		Expression pattern
			Untreated	TGFβ treated	
Q8NC51	SERBP1	Plasminogen activator inhibitor 1 RNA-binding protein	1.385	1.771	↑
P61586	RHOA	Transforming protein RhoA	1.644	1.527	↑
Q9BQ61	C19orf43	Uncharacterized protein C19orf43	n/o	2.294	↑
Q8WTV0	SCARB1	Scavenger receptor class B member 1	1.550	n/o	↑
P02786	TFRC	Transferrin receptor protein 1	0.696	0.353	↓
Q92520	FAM3C	Protein FAM3C	0.501	0.448	↓
Q6IAA8	LAMTOR1	Ragulator complex protein LAMTOR1	0.714	0.587	↓
Q8N163	KIAA1967	DBIRD complex subunit KIAA1967	n/o	0.701	↓
O00264	PGRMC1	Membrane-associated progesterone receptor component 1	0.539	n/o	↓
Q8IYS2	KIAA2013	Uncharacterized protein KIAA2013	0.740	n/o	↓

n/o - not observed

876

877

878

CHAPTER 5

The observations from studies in the previous chapters clearly indicated that TGFβ can promote alterations in cancer related molecules and pathways upon expression of β6 integrin and uPAR. Therefore, it is important to further understand/investigate the expression levels of these molecules in biological samples. This prompted the investigation of TGFβ and uPAR expression levels in a clinical setting using human blood plasma samples from Dukes' stage A-D CRC patients (n=60) and unaffected normal control plasmas (n=15). These samples were analysed using the Proseek Multiplex Oncology I kit that evaluated the expression of 92 putative cancer-related proteins including Latency-associated peptide TGFβ1 (LAP TGFβ1) and uPAR from just 1μL of human plasma. The observations from this study indicated no significant difference in expression of LAP-TGFβ1 and uPAR in plasma between various stages. However, this study identified CEA, IL-8 and prolactin as potential CRC biomarkers that significantly differentiate the unaffected controls from non-malignant (Dukes' A + B) and malignant (Dukes' C + D) stages. These findings are an important step towards identifying and developing a CRC biomarker panel that can in the future be used for diagnostic and therapeutic purposes.

The study was conducted under Macquarie University Human Ethics Committee approval (Approval No. 5201200702).

5.1 - A novel multiplexed immunoassay identifies CEA, IL-8 and prolactin as prospective markers for Dukes' stages A-D colorectal cancers. *Clin Proteomics*. **Apr 8; 12(1):10. doi: 10.1186/s12014-015-9081-x. eCollection 2015.** [Publication VI]

CLINICAL PROTEOMICS

A novel multiplexed immunoassay identifies CEA, IL-8 and prolactin as prospective markers for Dukes' stages A-D colorectal cancers

Sadia Mahboob[1], Seong Beom Ahn[1], Harish R Cheruku[1], David Cantor[1], Emma Rennel[3], Simon Fredriksson[3], Gabriella Edfeldt[3], Edmond J Breen[4], Alamgir Khan[4], Abidali Mohamedali[2], Md Golam Muktadir[5], Shoba Ranganathan[2], Sock-Hwee Tan[1], Edouard Nice[6] and Mark S Baker[1*]

Abstract

Background: Current methods widely deployed for colorectal cancers (CRC) screening lack the necessary sensitivity and specificity required for population-based early disease detection. Cancer-specific protein biomarkers are thought to be produced either by the tumor itself or other tissues in response to the presence of cancers or associated conditions. Equally, known examples of cancer protein biomarkers (e.g., PSA, CA125, CA19-9, CEA, AFP) are frequently found in plasma at very low concentration (pg/mL-ng/mL). New sensitive and specific assays are therefore urgently required to detect the disease at an early stage when prognosis is good following surgical resection. This study was designed to meet the longstanding unmet clinical need for earlier CRC detection by measuring plasma candidate biomarkers of cancer onset and progression in a clinical stage-specific manner. EDTA plasma samples (1 μL) obtained from 75 patients with Dukes' staged CRC or unaffected controls (age and sex matched with stringent inclusion/exclusion criteria) were assayed for expression of 92 human proteins employing the Proseek® Multiplex Oncology I proximity extension assay. An identical set of plasma samples were analyzed utilizing the Bio-Plex Pro™ human cytokine 27-plex immunoassay.

Results: Similar quantitative expression patterns for 13 plasma antigens common to both platforms endorsed the potential efficacy of Proseek as an immune-based multiplex assay for proteomic biomarker research. Proseek found that expression of Carcinoembryonic Antigen (CEA), IL-8 and prolactin are significantly correlated with CRC stage.

Conclusions: CEA, IL-8 and prolactin expression were found to identify between control (unaffected), non-malignant (Dukes' A + B) and malignant (Dukes' C + D) stages.

Keywords: Multiplex immunoassay, Plasma biomarker, Colorectal cancer

Background

CRC is the third most commonly diagnosed cancer worldwide with over 694,000 deaths (8.5% of all cancer deaths) in 2012, with Australia and New Zealand having the highest incidence rates (44.8 and 32.2 per 100,000 in men and women respectively) [1].

Various staging systems have been developed to describe the progression of the disease based on the size, location and spread of the tumour to distant organs (e.g., Tumour-Node-Metastasis (TNM) staging systems,

Australian Clinico-pathological staging (ACPS) system and Dukes' staging system [2,3]). Patient prognosis inversely correlates with tumour stage at the time of diagnosis [4,5]. Once metastases becomes clinically observable, prognosis is extremely poor with survival often measured in months [6]. Currently, we are unable to detect patients with clinically silent metastases, possibly linked to poor outcome. Despite the availability of numerous screening strategies, aggressive surgical therapy and extensive research on the molecular basis of CRC, early detection of the disease remains problematic. Population-based CRC screening programmes can reduce morbidity and mortality through the early identification of surgically-treatable disease. However, there is currently a gap in translational

* Correspondence: mark.baker@mq.edu.au
[1]Australian School of Advanced Medicine, Faculty of Medicine and Human Sciences, Macquarie University, Rm1, Level 1, 75 Talavera Road, Sydney, NSW 2109, Australia
Full list of author information is available at the end of the article

Mahboob et al. Clinical Proteomics (2015) 12:10

Page 2 of 12

research between identification of potential new biomarkers and development of Food and Drug Association (FDA) approved diagnostic tests [7]. Most diagnostic tests available to date are based on a single protein biomarker [8]. This concept is hazardous in the clinical setting as biological systems are interdependent and highly complex with inherent false positives subject to the genomic instability of cancers [9]. It is now widely accepted that panels of biomarkers will be required to achieve the increased sensitivity and specificity necessary for population-based screening [10]. The use of a pan-cellular field such as proteomics could help identify protein expression profiles associated with CRC progression that may prove to be more reliable than single biomarker based assessment.

Simultaneous assessment using a multiple biomarker strategy necessitates the development of multiplex high-throughput technologies with sufficient sensitivity and specificity to detect CRC early [9]. Multiplexing or simultaneous quantitation of several biomarkers in plasma can indicate the protein expression profiles involved in tumour formation, progression and metastasis. Under carefully controlled experimental conditions, multiplexed assays can identify many (96) low abundance candidate proteins using minimal sample volumes (1 μl) [11]. An example of this technology is the proximity extension assay (PEA) which has recently been developed by Olink Biosciences from Uppsala, Sweden [12].

This study was designed to meet a longstanding clinical need for earlier CRC detection by identifying plasma biomarkers of CRC onset and progression using the Proseek® Multiplex Oncology kit I (Proseek assay). In detail, Proseek assay employs PEA technology to quantitate 92 potential oncoproteins using only 1 μL of human plasma [12], where samples are treated with matched antibody pairs that are tagged with DNA reporter molecules. Once the antibodies are bound to their respective antigen the corresponding DNA tails form an amplicon that can be quantified by high-throughput real time PCR which generates a measurable fluorescent signal that directly correlates with abundance [13]. This PEA-based approach provides a platform for accurate quantification of multiple (96) low abundance oncoproteins from biological samples. Here, we aimed to validate PEA results with an existing benchmark multiplexed technology, namely the Bio-Plex Pro™ human cytokine 27-plex kit [14] (Bio-Plex), which is a bead-based multiplex immunoassay, measures the concentrations of 27 cytokines, chemokines or growth factors.

Results

Proseek® multiplex oncology I assay

The expression levels of 92 potential protein biomarkers (Additional file 1: Table S3) in each of the 75 plasma samples from CRC patients and healthy controls were evaluated simultaneously using the Proseek assay. The levels of 8 oncoproteins (CEA, IL-8, prolactin, amphiregulin, PDGF-BB, IL-6, CXCL11 and CXCL5) differed significantly between various individual CRC stages (Table 1).

Additional file 1: Tables S3 and S4 list the complete statistical analyses on this data. Twelve (12) of the target biomarkers were found to have expression levels below the Proseek LOD.

Specifically, CEA was found to be the overexpressed protein measured in stage D when compared with any other CRC stage (i.e., either Dukes' A, B or C) and/or healthy unaffected controls (for all stage D comparisons Ps were ≤ 0.0001). In addition, CEA was also overexpressed in stage C when compared with stage A ($P = 0.0076$) and/or healthy controls ($P = 0.0304$). Previous studies have also shown elevated CEA expression in Dukes' stage C and D CRC [15-21].

Differences in IL-8 expression were observed in stage A to D comparisons ($P = 2.96E-05$) and stage D to healthy control comparisons ($P = 1.23E-06$). Interestingly, levels of prolactin were elevated in Dukes' stage C compared with stage D ($P = 1.24E-05$) and healthy controls ($P = 2.89E-05$). Prolactin levels were found to consistently increase as disease progressed from controls through CRC Dukes' stages A-C (Figure 1, P5). Amphiregulin was overexpressed in stage D when compared with stages A ($P = 8.96E-07$) and

Table 1 Tukey-honest significant differences post-hoc test for Proseek data [Stage specific (A-D)] and healthy unaffected control (group E)

Candidate Biomarker	Comparison	Up/Down of expression	Adjusted p-value	Previous studies referring CRC associations
CEA	D/A	↑	0	[15-21]
	D/E	↑	1.70E-12	
	D/B	↑	4.13E-12	
	D/C	↑	0.0001	
	C/A	↑	0.0076	
	C/E	↑	0.0304	
IL-8	D/E	↑	1.23E-06	[44,47]
	D/A	↑	2.96E-05	
Prolactin	C/D	↑	1.24E-05	[49-51]
	C/E	↑	2.89E-05	
Amphiregulin	D/A	↑	8.95E-07	[54]
	D/C	↑	1.46E-06	
PDGF-BB	D/A	↑	3.02E-05	[22,55]
IL-6	B/A	↑	0.0024	[43,56]
	B/E	↑	0.0124	
CXCL11	D/C	↑	0.0155	[57]
	D/A	↑	0.0387	
CXCL5	D/A	↑	0.0424	[58-61]

Mahboob *et al. Clinical Proteomics* (2015) 12:10

Page 3 of 12

Figure 1 Panels (P) (A, B, C, D & E) representing protein abundance data for CEA (A), IL-8 (B) prolactin (C), amphiregulin (D) and PDGF-BB (E) in individual Dukes' stage A, B, C & D with E controls; pooled group (defined control, non-malignant, malignant groups). Values were determined by Proseek PFA using CRC patient EDTA plasmas and was based on z-scores (log2 scale).

C ($P = 1.46E\text{-}06$), while PDGF-BB was elevated in stage D compared with stage A ($P = 3.02E\text{-}05$). It was also noted that IL-6 showed a higher expression in stage B when compared to stage A and healthy unaffected controls ($P \leq 0.0024$). Chemokine (C-X-C motif) ligand CXCL11 and CXCL5 had a higher expression at stage D when compared with stage A ($P = 0.0155$). It was interesting to note that some of the previously reported biomarker oncoproteins (e.g., IL-4, CAIX, TNF-α, MCP-1, GM-CSF, VEGF, TIE2, IL17, IL-6, IFNG) did not display differential expression between Dukes' CRC stages ($P \approx 1.0$) [22-32].

To determine whether changes were observed when CRC data were pooled into control (group E), non-malignant (stages A + B combined) or malignant groups (stages C + D combined), a Tukey honest significant differences post-hoc ANOVA (Type II) test was performed and Q values calculated, where Q values are a measure of statistical significance in terms of false discovery rate (Table 2).

This study showed expression of three biomarker oncoproteins (CEA, IL-8 and prolactin) were altered when pooled CRC groups (i.e., control, non-malignant, malignant) were considered.

Comparison between pooled controls, non-malignant and malignant groups with individually staged patients indicated CEA and IL-8 were both considerably upregulated in malignant compared to healthy controls. Additionally, as expected [20] CEA was overexpressed in comparisons between non-malignant and malignant groups (Q-value = 0). In contrast, prolactin demonstrated a noticeable Dukes' stage-dependant increase in expression until metastasis occurred beyond lymph nodes (i.e., is elevated up to stage C). Once metastasized to distal organs (Dukes' stage D), plasma prolactin expression levels returned to approximately normal control (group E) levels. Additionally, an increase was found between control and non-malignant pooled groups for prolactin values.

258

Mahboob *et al. Clinical Proteomics* (2015) 12:10

Page 4 of 12

Table 2 Q values of significantly altered potential biomarker proteins between pooled CRC groups

Candidate Biomarker	Comparison	Difference	Lower CI	Upper CI	Q-value
CEA	Malignant/Non-malignant	1.97	1.08	2.85	0
CEA	Malignant/Healthy	2.11	1.02	3.19	0
IL-8	Malignant/Healthy	1.22	0.14	2.31	0
Prolactin	Non-malignant/Healthy	1.1	0.02	2.19	0.04

The Proseek multiplexed assay data strongly suggests the combined use of CEA, IL-8 and prolactin expression as potential combined diagnostic indicators of Dukes' stage with their abundance positively correlating with metastatic progression. However, as target proteins display differences in expression trends, SOMs were used to cluster and visualise pooled data into one of six discernible expression trends (Figure 2).

SOMs assembled the data into the six trends (Figure 2), where median values were used as they are less susceptible to variation [33]. The largest differences were observed between either the non-malignant or the malignant patient groups against control patients' plasmas. SOM trend A biomarkers decrease between controls and non-malignant plasmas but increase again to similar levels when malignant plasmas are compared to controls. All trend B biomarkers show no major change irrespective of stage. In an opposite manner to trend A, trend D biomarkers increase in non-malignant but decrease again in malignancy. Trend C biomarkers steadily decreased biomarker expression

from healthy to malignant and may be useful to distinguish healthy patients from malignant cancers. A converse trend pattern was observed for both trends E (amphiregulin, CA19, caspase 3, CD30, CD40, CD69, EGF, GDF15, Il-6, Il-7, Il-8, PDGF-BB) and F (CEA) with strong steady increases observed during progression. Data shown in trend F demonstrates the power CEA has over all other protein biomarkers examined in the Proseek panel for distinguishing malignant from either non-malignant CRC and/or healthy patients.

Bio-Plex Pro™ human cytokine 27-plex immunoassay
Where possible the significant differences observed using the Proseek assay were reproduced/validated using an established antibody-based multiplexed detection system, namely the Bio-plex Pro™ human cytokine 27-plex immunoassay. The Dukes' CRC stage specific analyses identified 6 target proteins (IFN-G, IL-4, IL-8, MCP-1, MIP-1 and PDGF-BB) that were each significantly elevated in stage D plasmas compared with healthy unaffected

Figure 2 SOMs trends (A-F) of control, non-malignant and malignant CRC groups normalised median Proseek biomarker protein expression scores, showing these can be clustered into six distinct trends.

259

Mahboob et al. Clinical Proteomics (2015) 12:10

Page 5 of 12
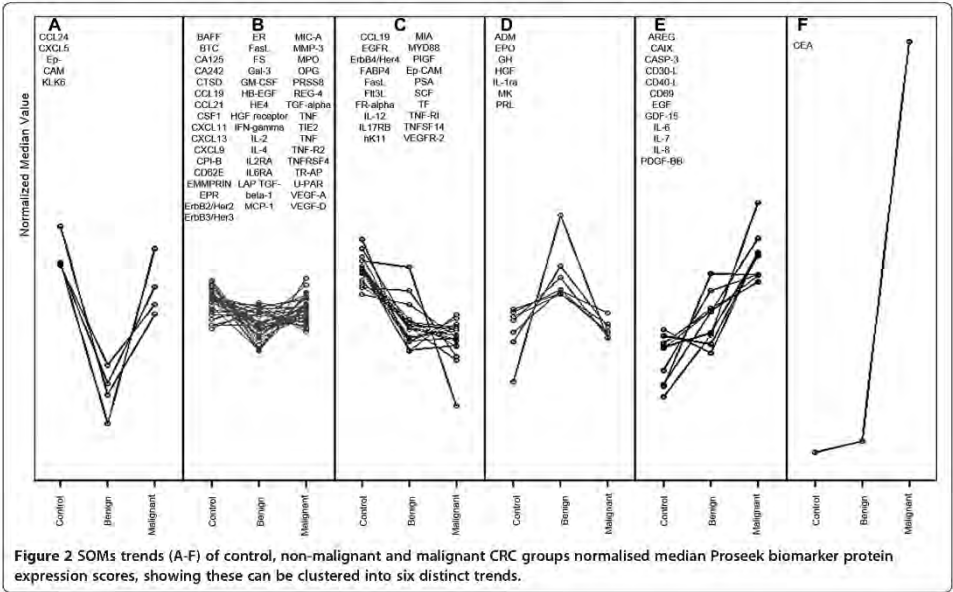
controls ($P < 0.05$) (Table 3). Additional file 1: Tables S5 and S6 summarize the statistical analyses conducted on the Bio-plex data.

In detail, significant differences in IL-8 expression were observed in stage A, B and D when compared to healthy controls ($P = 6.00E-05$, $6.00E-03$ and $2.00E-03$ respectively). Additionally, PDGF-BB was significantly elevated in stage D compared with healthy controls or stage A ($Ps = 2.00E-07$ and $4.00E-03$ respectively). It was also noted that monocyte chemotactic protein-1/C-C motif chemokine 2 (CCL2) showed a significantly higher expression in stage D when compared to healthy unaffected controls ($P = 5.00E-04$). Furthermore, IFNG, IL-4 and monocyte chemotactic protein-1/C-C motif chemokine 3 (CCL3) also exhibited significant overexpression in stage D when compared to healthy controls ($P \le 0.05$).

Comparison between pooled control, non-malignant and malignant groups with individually staged patients indicated that four proteins (i.e., G-CSF, IL-4, IL-8 and MCP-1) were more highly expressed between non-malignant and healthy cohorts whilst nine proteins (G-CSF, IFN-G, IL-4, IL-6, IL-8, IL-9, MCP-1, MIP-1B and PDGF-BB) were higher in the metastatic group compared to healthy cohorts (Additional file 1: Table S6). SOM analyses of the same data was performed (Figure 3).

Analysis of the SOM data highlights six different trends (A-F) of patient plasma cytokine response to CRC progression. Trend A shows a variable response, whilst trend B shows an increase in cytokine/chemokine expression in both non-malignant and malignant CRC groups above healthy controls. Trend C also displays increased expression in both cancer groups compared to healthy controls with additional slight increases in malignant above non-malignant groups. The tendency for increased expression as cancers progress was more pronounced in trends D and E, whilst in trend F the increase in non-malignant over control groups was

Table 3 Tukey-honest significant differences post-hoc test for Bio-Plex data [Stage specific (A-D)] and healthy unaffected control (group E)

Candidate Biomarker	Comparison	Adjusted p-value	Previous studies referencing CRC association
IL-8	D/E	6.00E-05	[44,47]
	A/E	6.00E-03	
	B/E	2.00E-03	
PDGF-BB	D/E	2.00E-07	[22,55]
	D/A	4.00E-03	
CCL2	D/E	5.00E-04	[61-63]
IFNG	D/E	0.002	[63]
IL-4	D/E	0.004	[64]
CCL3	D/E	0.004	[63]

followed by a small decrease when the malignant group was compared to the non-malignant group. Collectively, these observations may hold some prognostic value for evaluation of CRC over healthy controls using Bio-Plex analysis of plasma G-CSF, IFN-G, IL-4, IL-6, IL-8, IL-9, MCP-1, MIP-1B and PDGF-BB in a clinical setting.

Comparison of Proseek with Bio-plex data

The 13 common proteins that were available across both the Proseek and Bio-Plex platforms were evaluated by pairing and subsequently analysing the combined data by Spearman's rank-order correlation (Figure 4). The X-Y comparisons for the Bio-Plex (X) and Proseek (Y) data for these common 13 plasma proteins are provided in Additional file 1: Table S7.

When comparing the two multiplexed immunoassay platforms, there were significant differences between outputs. For a number of proteins (GM-CSF, IL-2, IL-4 and TNF), the correlation was highly skewed as the target biomarker fell below LOD in one or both of the platforms. However, IL-8 and MCP-1 scatter plots suggested there was a positive correlation between data derived from both platforms. The scatter plot data for plasma IL-7, IFN-g, IL-6, VEGF-A levels also suggested moderate correlation. However, the correlation between Proseek and Bio-Plex analyses for PDGF-BB was particularly strong (p and q values = 0) (Additional file 1: Table S7).

In summary, out of the 13 proteins common to both immunoassay platforms, two proteins were identified whose plasma abundance were differentially correlated with Dukes' CRC clinical stage (IL-8 between samples for Dukes' D/healthy controls and PDGF-BB between Dukes' D/A). The remaining eleven proteins did not show major expression difference ($P > 0.05$) across all comparisons made between Dukes' stage A-D CRC and themselves or healthy controls. For those proteins only available for assay in a single kit, a small number of proteins showed significantly higher expression profiles (8 proteins by Proseek CEA, IL-8, prolactin, amphiregulin, PDGF-BB, IL-6, CXCL11 & CXCL5 and 6 proteins by Bio-Plex: G-CSF, IFN-G, IL-4, IL-8, MCP-1, MIP-1 & PDGF-BB).

Collectively, these differentially expressed plasma proteins epitomise potential Dukes' stage- and progression-specific CRC biomarkers. The significant differentially expressed proteins identified in this study should now be progressed to a much larger double-blind, multi-centre biomarker trial for further validation of their potential as "combinatorial signatures" of Dukes' stage-specific CRC.

Discussion

To the best of our knowledge, this study is one of the first to simultaneously evaluate two independent multiplexed biomarker detection technologies using the same

Mahboob *et al. Clinical Proteomics* (2015) 12:10

Page 6 of 12

Figure 3 SOMs trends (A-F) of control, non-malignant and malignant CRC groups normalised median Bio-Plex biomarker protein expression scores showing these can clustered into six distinct patterns/trends.

clinical CRC plasma samples. Choi *et al.,* undertook an EDTA (Ethylenediaminetetraacetic acid) plasma proteomic study using 2DE/MALDI MS combined with Milliplex MAP Human 26 Plex Cytokine/Chemokine Kit to investigate CRC biomarker signatures [34], but have been heavily criticized for lacking comparison with age- and other criteria-matched healthy controls [35]. In contrast, the current study reports the expression profile of 92 potential oncoproteins biomarkers from patient EDTA plasmas across the four Dukes' CRC stages combined with an age-, sex-, smoking- and other contraindication-matched healthy group using the recently developed Olink PEA technology. The combined data emanating from the use of this novel multiplexed platform combined with stringent clinical exclusion and inclusion criteria, sample processing and analysis indicates some proteins may be representative of different aspects of progression through Dukes' staging and potentially reflect real differences in CRC biology *in vivo* during these stages. As such, this study proposes a potential biomarker "signature" of clinical relevance that could be utilised to evaluate Dukes' CRC stage and progression.

The Proseek® Multiplex Oncology I assay is a high throughput, high sensitivity, specific assay developed for cancer research. It is now realised that the limiting factor in multiplexed immunoassays is antibody cross-reactivity that typically limits the degree of assay multiplexing [36]. Problems with cross-reactivity are virtually eliminated in PEA assays since only matched DNA reporter pairs (i.e., mirroring the presence of two distinct epitopes on the protein) are amplified at the real-time PCR step [12]. Additionally, the small sample volume required (1 μL) to simultaneously quantitatively assay 92 oncoproteins in a multiplexed format is significantly lower than required for alternative platforms (e.g., Luminex-based platforms). This is important as clinical samples are frequently volume limited, particularly when multiple assays (e.g., biomarker "signature" panels) are required or only limited plasma sources (e.g. young children/neonates) are available. As the PEA technology has only recently been commercialized, it was important to validate the platform against an existing benchmark technology (e.g., Bio-Plex multiplex immunoassay) which has FDA approval [37]. The expression profiles of 13 common oncoproteins were compared between both platforms. Nine of those common proteins showed reasonable correlation between platforms, thereby supporting/validating the potential use of the Proseek assay for cancer biomarker research (Figure 4).

261

Mahboob *et al. Clinical Proteomics* (2015) 12:10

Page 7 of 12

Figure 4 Spearman correlation scatter plots for 13 individual common biomarkers (PDGF-BB, IL-8, MCP1, IL-6, IL-7, VEGFA, IFNG, IL-2, GM-CSF, IL-4, IL-1ra, IL-12, and TNF) common to the Proseek and Bio-Plex multiplexed immunoassays.
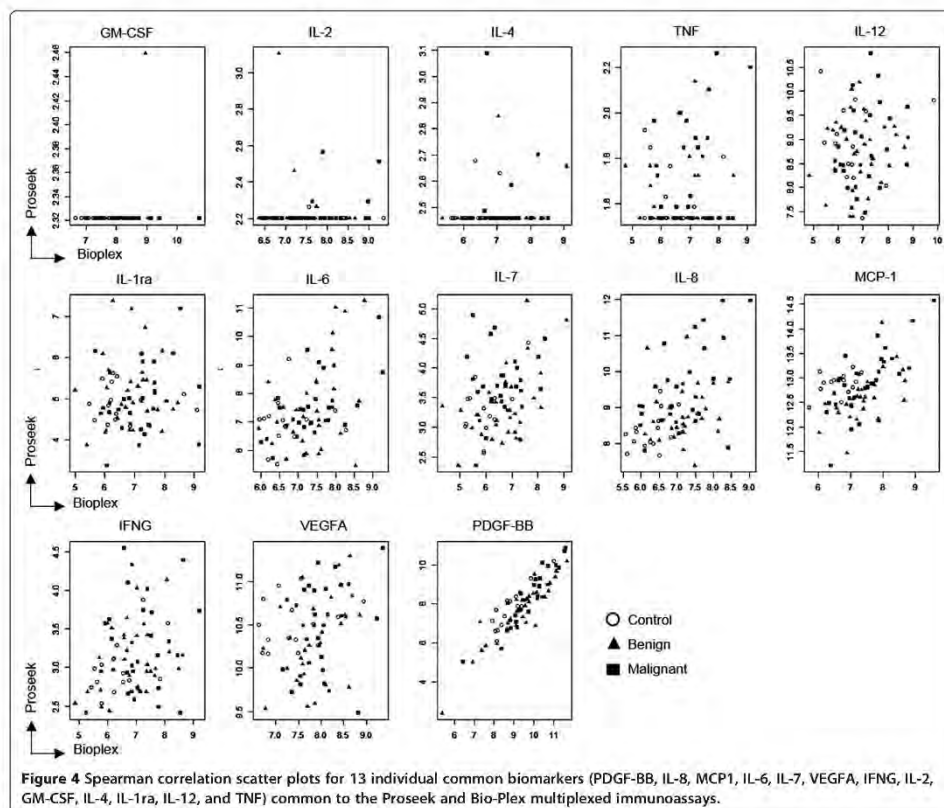
Typically immunoassays involve conformational/shape recognition. As such, the knowledge of epitope location or structure is crucial for designing targeted, multiple epitope-based immune assays that can tag multiple sequences for antigen detection. Inadequate mapping can yield false positive or negative results. The Proseek assay uses two proximal epitopes to recognize a single antigen thereby reducing false positive rates which then fall below the LOD (GM-CSF, IL2, IL4 & TNF; Figure 4). However, this may not be a general phenomenon. Proseek technology uses unique sequence-based tagging of every antibody in the assay. By contrast, although the Bio-Plex utilizes a dual antibody system, lack of sequence tagging can create a higher possibility of cross-reactivity and non-specificity [38]. It should be noted that both platforms employ automated software and calibration updates to reduce the need for operator input.

Investigation of individual CRC stage differences in the expression of 92 oncoproteins assessed by the Proseek assay, identified eight oncoproteins that appear to be differentially expressed in plasma as a result of CRC progression (Table 1). CEA, IL-8 and prolactin demonstrated the greatest potential use as diagnostic CRC Dukes' stage-specific biomarkers (Figure 1). It was interesting to note that except for CEA, none of the other significantly expressed oncoproteins matched with the list of serological CRC indicators identified in a similar study utilizing a 74-plex PEA platform [39]. In that study, Thorsen et al., investigated 74 different protein biomarkers and found carcinoembryonic antigen (CEA), transferrin receptor-1 (TFRC), macrophage migration inhibitory factor (MIF), osteopontin (OPN/SPP1) and cancer antigen 242 (CA242) as CRC discriminators. CEA, TFRC and CA242 were suggested to be early stage

262

Mahboob et al. Clinical Proteomics (2015) 12:10

Page 8 of 12

CRC indicators. Intriguingly, Choi et al., identified 24 significantly elevated proteins in CRC, of which IL-8, TNF-alpha, and IP-10 (interferon gamma-induced protein) were elevated in the CRC group relative to the adenoma group [34]. Surprisingly, CEA was not a selected as a potential oncoprotein in the Milliplex MAP Human 26 Plex Cytokine/Chemokine Kit used in that study.

CEA is currently employed as a routine marker for CRC prognosis, disease-free survival and therapeutic response [40] and as an independent predictor of patients at higher risk of CRC recurrence and/or metastases during postoperative follow-up [41]. Our study supports aspects of this contention - namely that high plasma CEA expression significantly correlates with the presence of metastatic CRC, though (as previously proposed) it was not found to be an effective plasma biomarker of very early stage disease (Dukes' A). Another differentially expressed protein (IL-8) is recognized as a pro-inflammatory cytokine and an important chemoattractant factor for leukocytes. IL-8 has been reported to contribute to cancer progression through potential motility-stimulating, mitogenic and angiogenic functions [29]. It has been previously demonstrated that IL-8 is elevated at both the mRNA and plasma protein levels and in CRC tumour tissues compared to adjacent normal colonic mucosa [42-44]. IL-8 is a soluble mediator released by tumor cells that functions within the tumor microenvironment [45]. A number of studies have confirmed the effects of elevated IL-8 on signalling that promotes the angiogenic response and that eventually leads to infiltration of neutrophils to the tumor site [46]. IL-8 expression in tumour tissues significantly correlates with tumour size, depth of infiltration, liver metastasis and tumour stage [24,47]. The present study also confirms that plasma IL-8 concentration significantly discriminates Dukes' stage D (those with metastatic disease) from either healthy controls or Dukes' stage A patients.

A number of studies have found that prolactin actively participates in tumorigenesis and that it is overexpressed in several cancer cell lines including those derived from reproductive and non-reproductive tissues [48]. Hence scientists have been interested in developing therapies for controlling tumor growth through suppression of prolactin production [48]. Elevated serum prolactin has been shown to correlate with CRC malignancy [49,50] and is observed in many CRC cell lines and tumour specimens [51,52]. Our data strongly suggests that plasma prolactin significantly correlates with CRC tumour progression through Dukes' stage A, B and C, being continuously upregulated until distal metastasis occurs. Our data encourage further studies on larger clinical cohorts to evaluate the plasma expression of prolactin during CRC progression as a stage-specific biomarker.

Conclusions

New, improved and volume-sparing plasma biomarkers/biomarker signature panels are urgently required for cancer screening and surveillance using minimally invasive techniques. Multiplexing represents a powerful platform for the qualitative and quantitative assessment of cancer biomarker signatures, giving the opportunity for sensitive and specific detection of multiple oncoproteins in plasma samples, providing a suite of biomarkers with potential for use as stage-specific indicators of CRC progression.

The emerging PEA technology has received increasing interest considering the large number of target biomarkers that can be measured quantitatively with the advantage of minimum cross-reactivity over benchmark multiplexing platforms. This study has identified eight proteins (CEA, IL-8, prolactin, amphiregulin, PDGF-BB, IL-6, CXCL11 and CXCL5) whose expression trends are of great interest for developing a "biosignatures" of CRC progression that could potentially be translated into a diagnostic/prognostic. Finally, we recognized three prospective novel markers of CRC progression (CEA, IL-8 and prolactin) that hold potential to be utilised in clinical oncology, as they significantly increase with CRC progression and correlate with Dukes' stage. We recognize the importance of performing further multi-centred large study analysis of marker combinations and in developing new algorithms that confirm improved performance of CEA, perhapsby addition of IL-8 and/or prolactin. As such, we highly recommend the use of these oncoproteins in patient screening as well as for further investigation as potential CRC plasma biomarkers in large multicentric multisample controlled CRC study cohorts.

Materials & methods

Patient plasma samples

Clinically staged CRC (Dukes' A, B, C, D) and control EDTA-plasma samples were obtained from 75 patients. Patients were Dukes' staged CRC (15 patients each stage A-D) or apparently healthy disease unaffected controls at Victoria Cancer Biobank (n = 15, called group E subsequently). Samples were stringently age and sex matched with strict inclusion/exclusion criteria applied to minimize variation within the study population. In detail, the study population was a mixture (50:50) of females/males, aged between 50 and 80 for each CRC stage and for the healthy unaffected controls. Samples were collected from CRC patients diagnosed with non-malignant/malignant tumors, before they underwent any treatment and surgery for CRC. The control or unaffected plasma samples were collected from 15 individuals who were aged-matched to the clinical CRC plasma and had no apparent evidence of diseases (i.e., with no

Mahboob *et al. Clinical Proteomics* (2015) 12:10

Page 9 of 12

evidence of inflammation or metastatic conditions, no previous history of tumor, cancer or major therapy. Clinical details about CRC patients are provided in Additional file 1: Table S8).

Plasma handling conditions

The samples were collected in 2 EDTA tubes (9 ml each), centrifuged at room temperature (RT) at 1,200 g for 10 mins and plasma fractions transferred to a single 10 ml tube. The combined plasma fractions were centrifuged at RT 1,800 g for 10 mins and aliquoted into $8 \times$ 250 µl tubes that were stored and frozen at -80oC. The entire process was completed within 2 h of plasma collection to meet the VCB protocols required for proteomic experiments.

Proseek® multiplex oncology I assay

Proseek assays were performed to evaluate the expression of a panel of potential biomarkers within the plasma samples (n = 75) in a 96-well plate. This assay measured 92 potential protein biomarkers (Additional file 1: Table S1) and 4 internal controls generating 9,216 data points per run. The investigation was performed according to manufacturer's instructions (www.olink.com) with minimal changes. The complete experiment was conducted on a single 96 well plate to minimize variation, with one EDTA plasma sample from each group (number 15) examined in duplicate. Briefly, 1 µl of each sample or negative control was incubated with the conjugated antibodies at 4°C overnight. The next day, the extension mixture was added and the products were extended and pre-amplified using PCR (ABI 2720 Thermal cycler, Life Technologies). The detection reagent and a fraction (2.8 µl) of the extended and pre-amplified product were mixed and loaded into an oil-loaded Fluidigm Gene Expression 96 × 96 Dynamic arrays (Fluidigm Corporation) on one side and the Primer plate with specific primers on the other side of the chip. The chip was primed using Fluidigm IFC controller HX (Fluidigm Corporation) and afterwards loaded into a Fluidigm Biomarker system (Fluidigm Corporation).

Raw data was annotated using Real Time PCR software (Fluidigm Corporation). The Proseek assay generated Cq values that represent the cycle values in the PCR amplification where the signal is above background. This is calculated on a log 2 scale as PCR amplification is increased by 2 fold up during each cycle. To even out variation between and within runs, data was normalized using the extension control and a background value. The data used for further statistical analysis were expressed in Normalized Protein eXpression (NPX) units on log2 scale, where a high value corresponded to high protein concentration. The limit of detection (mean negative control plus $3 \times$ standard deviation) was determined for each protein

assay. Data was normalized and analysed using GenEx software (MultiD, Gothenburg, Sweden). All statistical analyses (dynamic principal component analysis and one way ANOVA) were performed on normalized data. For each biomarker, the limit of detection (LOD) was defined as the mean of negative control plus 3 standard deviations of the 38 negative controls.

Bio-plex Pro™ human cytokine 27-plex immunoassay

Bio-Plex assay (Bio-Rad, CA, USA, Cat No: M500KCA-FoY) was utilised according to manufacturer's instructions and also as reported earlier [23] to measure the concentrations of 27 target proteins (Additional file 1: Table S2) using identical CRC plasma samples as used in the Proseek assay. Samples were prepared using a robotic liquid handling workstation (epMotion 5075, Eppendorf, Germany) and incubated with antibody-coupled beads for 60 min followed by incubation with a detection antibody for 30 min. The conjugates were then incubated with streptavidin for 10 min, washed using the Bio-Plex Pro II wash station (Bio-Rad, CA, USA), resuspended and vortexed prior to fluorescent measurement on a Bio-Plex® 200 system (Bio-Rad, Hercules, CA). Data were acquired with the Bio-Plex Systems 100 (Bio-Rad, CA, USA), analysed and standard curves (Log (x) – Linear(y)) generated using the Bio-Rad Bio-Plex Manager v6.0 software [53].

Statistical analysis and correlation

Biomarker expression values were analysed using the statistical analytical package RStudio version 0.97.551 across each of stages A-D CRC and E (apparently healthy unaffected controls). In addition, to determine if protein expression could distinguish non-malignant from malignant CRC, individually staged data were pooled into three groups, namely controls (Group E; n = 15), non-malignant CRC (Groups/stage A and B; n = 30) and malignant CRC (Groups/stage C and D; n = 30). This subsequent analysis was performed to determine if significant protein expression differences were found between non-malignant and malignant CRC or when each group was compared to control patients. A two-way ANOVA using type II sums of squares was used for analysis as the control group was now smaller than the combined non-metastatic and metastatic groups implementing an R notation given as: Log2 (Response) ~ Group*Proteins + Sample, where response is the protein expression value, Group is a factor with 3 levels (control, non-metastatic and metastatic), Proteins is a factor with 92 levels for Proseek data set and 27 levels for the Bio-Plex data set and Sample is a factor with 15 levels. Sample represents the plasma samples from CRC patient and unaffected controls that were included in the analysis to allow for any individual differences between patients that might mask the difference in expression

Mahboob et al. Clinical Proteomics (2015) 12:10

Page 10 of 12

levels between CRC stages. P value < 0.05 was considered significant.

To identify which proteins were differentially expressed between collated CRC groups (control, non-malignant and malignant), a Tukey honest significant differences post-hoc test was also performed with respect to the interaction between Protein and Group factors. To discover which proteins exhibited similar expression profiles during CRC progression, self-organizing maps (SOM) were employed to present a discrete representation of the input space of the protein expression values. Raw data was transformed by taking the median expression value for the patient data for each protein within each group. This data was log2 transformed and then each group was normalized by setting each group's mean value to zero. Expression data was clustered into 6 groups using the SOM and displayed as a plot of the normalized median expressions for each protein with respect to its group values.

To investigate the complementarity of Proseek and Bio-Plex data sets, the expression of 13 proteins that are common to both platforms were paired and analysed by Spearman's rank-order correlation. This was performed to investigate any potential differences between multiplexed platforms by pairing the expression values and transforming p-values into q-values using the Benjamini and Hochberg procedure for multiple test correction.

Additional file

Additional file 1: Table S1. List of oncoproteins analyzed by Proseek Assay with Limit of Detection (LOD) in pg/ ml, working range (Lower Limit of Quantification, LLOQ, Upper Limit of Quantification, ULOQ). **Table S2.** List of cytokines analyzed by Bio-plex Assay with Limit of Detection (LOD) in pg/ ml, Lower Limit of Quantification (LLOQ) and Upper Limit of Quantification (ULOQ) (Proteins in bold letters indicate common target proteins between two platforms). **Table S3.** Q-values calculated for stage specific protein expressions analyzed by PEA technology. **Table S4.** Anova Table (Type II tests) or 2-Way Anova factor analysis for Proseek Assay. **Table S5.** p- values calculated for stage specific protein expressions analyzed by Bio-Plex Assay (Stage specific (A-D, n = 15) and healthy group). **Table S6.** Tukey honest significant differences post-hoc test for Bio-plex assay (Group- specific analysis). **Table S7.** Spearman Correlation between Proseek and Bio-plex assay (with p and q-values). **Table S8.** Clinical Details of CRC patients.

Competing interests
The authors declare that they have no competing interests.

Authors' contributions
(1) Conception and design of the study: MS, ASB, CHR, CD, TS-H, NE, BMS. (2) Generation, collection, assembly, analysis and/or interpretation of data: MS, AS B, CH R, CD, R E, FS, EG, BE J, KA, RS, MM G, MA, TS-H, NE, BM S, (3) Drafting or revision of the manuscript, MS, AS B, CH R, CD, RE, FS, EG, BE J, KA, MM G, MA, T S-H, NE, BM S, (4) Approval of the final version of the manuscript: MS, AS B, CHR, CD, R E, F S, EG, BE J, KA, RS, MM G, MA, TS-H, NE, BM S. All authors read and approved the final manuscript.

Author details
[1]Australian School of Advanced Medicine, Faculty of Medicine and Human Sciences, Macquarie University, Rm1, Level 1, 75 Talavera Road, Sydney, NSW 2109, Australia. [2]Department of Chemistry and Biomolecular Sciences, Faculty of Science, Macquarie University, Sydney, NSW 2109, Australia. [3]Olink Bioscience, Dag Hammarskjölds Väg, 54A, 75183 Uppsala, Sweden. [4]Australian Proteome Analysis Facility, Macquarie University, Sydney, NSW 2109, Australia. [5]School of Science and Health, University of Western Sydney, NSW, Australia. [6]Department of Biochemistry and Molecular Biology, Monash University, Clayton Campus, Melbourne, VIC 3800, Australia.

References
1. Ferlay J, Soerjomataram I, Ervik M, Dikshit R, Eser S, Mathers C, et al. Cancer Incidence and Mortality Worldwide: IARC CancerBase No. 11 [Internet]. GLOBOCAN 2012, v1.0.
2. Dukes CE. The classification of cancer of the rectum. J Pathol Bacteriol. 1932;35:323–32.
3. Beattie T. Classification of colorectal cancer to aid the stomal therapy nurse in practice. Journal of Stomal Therapy Australia 2012, 32.
4. Peeters M, Price T, Van Laethem JL. Anti-epidermal growth factor receptor monotherapy in the treatment of metastatic colorectal cancer: where are we today? Oncologist. 2009;14:29–39.
5. Loberg M, Kalager M, Holme O, Hoff G, Adami HO, Bretthauer M. Long-term colorectal cancer mortality after adenoma removal. N Engl J Med. 2014;371:799–807.
6. Langan RC, Mullinax JE, Raiji MT, Upham T, Summers T, Stojadinovic A, et al. Colorectal cancer biomarkers and the potential role of cancer stem cells. J Cancer 2013;4:241–50.
7. Heichman KA. Blood-based testing for colorectal cancer screening. Mol Diagn Ther. 2014;18:127–35.
8. Duffy MJ, van Dalen A, Haglund C, Hansson L, Klapdor R, Lamerz R, et al. Clinical utility of biochemical markers in colorectal cancer: European Group on Tumour Markers (EGTM) guidelines. Eur J Cancer. 2003;39:718–27.
9. Ang CS, Rothacker J, Patsiouras H, Gibbs P, Burgess AW, Nice EC. Use of multiple reaction monitoring for multiplex analysis of colorectal cancer associated proteins in human feces. Electrophoresis. 2011;32:1926–38.
10. Nice E. Biomarker discovery and validation: the tide is turning. Expert Rev Proteomics. 2013;10:505–7.
11. Lea P, Keystone E, Mudumba S, Kahama A, Ding SF, Hansen J, et al. Advantages of multiplex proteomics in clinical immunology: the case of rheumatoid arthritis: novel IgXPLEX: planar microarray diagnosis. Clin Rev Allergy Immunol. 2011;41:20–35.
12. Assarsson E, Lundberg M, Holmquist G, Björkesten J, Bucht Thorsen S, Ekman D, et al. Homogenous 96-Plex PEA Immunoassay Exhibiting High Sensitivity, Specificity, and Excellent Scalability. PLoS One. 2014;9:e95192.
13. Hjelm F, Tran B, Fredriksson S. Sensitive detection of cytokines in 1-[mu]l serum samples using Proseek[reg]. Nat Meth 2011, 8.
14. Li D, Chiu H, Gupta V, Chan DW. Validation of a multiplex immunoassay for serum angiogenic factors as biomarkers for aggressive prostate cancer. Clin Chim Acta. 2012;413:1506–11.
15. Nielsen HJ, Brunner N, Jorgensen LN, Olsen J, Rahr HB, Thygesen K, et al. Plasma TIMP-1 and CEA in detection of primary colorectal cancer: a prospective, population based study of 4509 high-risk individuals. Scand J Gastroenterol. 2011;46:60–9.
16. Japink D, Leers MP, Sosef MN, Nap M. CEA in activated macrophages. New diagnostic possibilities for tumor markers in early colorectal cancer. Anticancer Res. 2009;29:3245–51.

Mahboob *et al. Clinical Proteomics* (2015) 12:10

Page 11 of 12

17. National Institutes of Health consensus development conference statement CEA (carcinoembryonic antigen): its role as a marker in the management of cancer. J Ark Med Soc 1981, 78:65-68. (Accessed online: 12th March, 2015).

18. CEA (Carcinoembryonic Antigen): Its Role as a Marker in the Management of Cancer. NIH Consens Statement Online 1980 Sep 29-Oct 1 [cited 15/03/12]; 3(7):1-4.

19. Ahlemann LM, Staab HJ, Koch HL, Anderer FA. Carcinoembryonic antigen (CEA) measurements as an aid to management of patients with lung cancer treated by radiotherapy. Oncodev Biol Med. 1980;1:143–50.

20. Bray PF, Wu JT, Madsen AC. Carcinoembryonic antigen (CEA) assay. In diagnosis and management of cancer. Rocky Mt Med J. 1975;72:21–3.

21. Hansen HJ, Snyder JJ, Miller E, Vandevoorde JP, Miller ON, Hines LR, et al. Carcinoembryonic antigen (CEA) assay. A laboratory adjunct in the diagnosis and management of cancer. Hum Pathol. 1974;5:139–47.

22. Peterson JE, Zurakowski D, Italiano Jr JE, Michel LV, Connors S, Oenick M, et al. VEGF, PF4 and PDGF are elevated in platelets of colorectal cancer patients. Angiogenesis. 2012;15:265–73.

23. Liu J, Duan Y, Cheng X, Chen X, Xie W, Long H, et al. IL-17 is associated with poor prognosis and promotes angiogenesis via stimulating VEGF production of cancer cells in colorectal carcinoma. Biochem Biophys Res Commun. 2011;407:348–54.

24. Bunger S, Haug U, Kelly FM, Klempt-Giessing K, Cartwright A, Posorski N, et al. Toward standardized high-throughput serum diagnostics: multiplex-protein array identifies IL-8 and VEGF as serum markers for colon cancer. J Biomol Screen. 2011;16:1018–26.

25. Kirman I, Belizon A, Balik E, Feingold D, Arnell T, Horst P, et al. Perioperative sargramostim (recombinant human GM-CSF) induces an increase in the level of soluble VEGFR1 in colon cancer patients undergoing minimally invasive surgery. Eur J Surg Oncol. 2007;33:1169–76.

26. Malaguarnera L, Imbesi RM, Scuto A, D'Amico F, Licata F, Messina A, et al. Prolactin increases HO-1 expression and induces VEGF production in human macrophages. J Cell Biochem. 2004;93:197–206.

27. Chin KF, Greenman J, Reusch P, Gardiner E, Marme D, Monson J. Changes in serum soluble VEGFR-1 and Tie-2 receptors in colorectal cancer patients following surgical resections. Anticancer Res. 2004;24:2353–7.

28. Chin KF, Greenman J, Reusch P, Gardiner E, Marme D, Monson JR. Vascular endothelial growth factor and soluble Tie-2 receptor in colorectal cancer: associations with disease recurrence. Eur J Surg Oncol. 2003;29:497–505.

29. Kantola T, Klintrup K, Vayrynen JP, Vornanen J, Bloigu R, Karhu T, et al. Stage-dependent alterations of the serum cytokine pattern in colorectal carcinoma. Br J Cancer. 2012;107:1729–36.

30. TaghipourFardArdekani M, Malekzadeh M, Hosseini SV, Bordbar E, Doroudchi M, Ghaderi A. Evaluation of Pre-Treatment Serum Levels of IL-7 and GM-CSF in Colorectal Cancer Patients. Int J Mol Cell Med. 2014;3:27–34.

31. Tilg H, Trehu E, Atkins MB, Dinarello CA, Mier JW. Interleukin-6 (IL-6) as an anti-inflammatory cytokine: induction of circulating IL-1 receptor antagonist and soluble tumor necrosis factor receptor p55. Blood. 1994;83:113–8.

32. Ortea I, Roschitzki B, Ovalles JG, Longo JL, de la Torre I, Gonzalez I, et al. Discovery of serum proteomic biomarkers for prediction of response to infliximab (a monoclonal anti-TNF antibody) treatment in rheumatoid arthritis: an exploratory analysis. J Proteomics. 2012;77:372–82.

33. Georgakis A, Kotropoulos C, Xafopoulos A, Pitas I. Marginal median SOM for document organization and retrieval. Neural Netw. 2004;17:365–77.

34. Choi JW, Liu H, Shin DH, Yu GI, Hwang JS, Kim ES, et al. Proteomic and cytokine plasma biomarkers for predicting progression from colorectal adenoma to carcinoma in human patients. Proteomics. 2013;13:2361–74.

35. Coghlin C, Murray GI. Progress in the identification of plasma biomarkers of colorectal cancer. Proteomics. 2013;13:2227–8.

36. Ellington AA, Kullo IJ, Bailey KR, Klee GG. Antibody-based protein multiplex platforms: technical and operational challenges. Clin Chem. 2010;56:186–93.

37. Marianelli P, Bassi Luciani L, Micera S. Electrical potential distribution within the inner ear: a preliminary study for vestibular prosthesis design. Conf Proc IEEE Eng Med Biol Soc. 2012;2012:3017–20.

38. Juncker D, Bergeron S, Laforte V, Li H. Cross-reactivity in antibody microarrays and multiplexed sandwich assays: shedding light on the dark side of multiplexing. Curr Opin Chem Biol. 2014;18:29–37.

39. Thorsen SB, Lundberg M, Villablanca A, Christensen SL, Belling KC, Nielsen BS, et al. Detection of serological biomarkers by proximity extension assay for detection of colorectal neoplasias in symptomatic individuals. J Transl Med. 2013;11:253.

40. Ward U, Primrose JN, Finan PJ, Perren TJ, Selby P, Purves DA, et al. The use of tumour markers CEA, CA-195 and CA-242 in evaluating the response to

41. chemotherapy in patients with advanced colorectal cancer. Br J Cancer. 1993;67:1132–5.

41. Litvka A, Cercek A, Segal N, Reidy-Lagunes D, Stadler ZK, Yaeger RD, et al. False-positive elevations of carcinoembryonic antigen in patients with a history of resected colorectal cancer. J Natl Compr Canc Netw. 2014;12:907–13.

42. Ning Y, Manegold PC, Hong YK, Zhang W, Pohl A, Lurje G, et al. Interleukin-8 is associated with proliferation, migration, angiogenesis and chemosensitivity in vitro and in vivo in colon cancer cell line models. Int J Cancer. 2011;128:2038–49.

43. Malicki S, Winiarski M, Matlok M, Kostarczyk W, Guzdek A, Konturek PC. IL-6 and IL-8 responses of colorectal cancer in vivo and in vitro cancer cells subjected to simvastatin. J Physiol Pharmacol. 2009;60:141–6.

44. Rubie C, Frick VO, Pfeil S, Wagner M, Kollmar O, Kopp B, et al. Correlation of IL-8 with induction, progression and metastatic potential of colorectal cancer. World J Gastroenterol. 2007;13:4996–5002.

45. Fernando RI, Castillo MD, Litzinger M, Hamilton DH, Palena C. IL-8 signaling plays a critical role in the epithelial–mesenchymal transition of human carcinoma cells. Cancer Res. 2011;71:5296–306.

46. Waugh DJ, Wilson C. The interleukin-8 pathway in cancer. Clin Cancer Res. 2008;14:6735–41.

47. Terada H, Urano T, Konno H. Association of interleukin-8 and plasminogen activator system in the progression of colorectal cancer. Eur Surg Res. 2005;37:166–72.

48. Ben-Jonathan N, Liby K, McFarland M, Zinger M. Prolactin as an autocrine/paracrine growth factor in human cancer. Trends Endocrinol Metab. 2002;13:245–50.

49. Bhatavdekar JM, Patel DD, Giri DD, Karelia NH, Vora HH, Ghosh N, et al. Comparison of plasma prolactin and CEA in monitoring patients with adenocarcinoma of colon and rectum. Br J Cancer. 1992;66:977–80.

50. Bhatavdekar JM, Patel DD, Chikhlikar PR, Shah NG, Vora HH, Ghosh N, et al. Ectopic production of prolactin by colorectal adenocarcinoma. Dis Colon Rectum. 2001;44:119–27.

51. Neradugomma NK, Subramaniam D, Tawfik OW, Goffin V, Kumar TR, Jensen RA, et al. Prolactin signaling enhances colon cancer stemness by modulating Notch signaling in a Jak2-STAT3/ERK manner. Carcinogenesis. 2014;35:795–806.

52. Sun Q, Sun F, Wang B, Liu S, Niu W, Liu E, et al. Interleukin-8 promotes cell migration through integrin alphavbeta6 upregulation in colorectal cancer. Cancer Lett. 2014;2:161–74.

53. Khan A. Detection and quantitation of forty eight cytokines, chemokines, growth factors and nine acute phase proteins in healthy human plasma, saliva and urine. J Proteomics. 2012;75:4802–19.

54. Yamada M, Ichikawa Y, Yamagishi S, Momiyama N, Ota M, Fujii S, et al. Amphiregulin is a promising prognostic marker for liver metastases of colorectal cancer. Clin Cancer Res. 2008;14:2351–6.

55. McCarty MF, Somcio RJ, Stoeltzing O, Wey J, Fan F, Liu W, et al. Overexpression of PDGF-BB decreases colorectal and pancreatic cancer growth by increasing tumor pericyte content. J Clin Invest. 2007;117:2114–22.

56. Galizia G, Orditura M, Romano C, Lieto E, Castellano P, Pelosio L, et al. Prognostic significance of circulating IL-10 and IL-6 serum levels in colon cancer patients undergoing surgery. Clin Immunol. 2002;102:169–78.

57. Rupertus K, Sinistra J, Scheuer C, Nickels RM, Schilling MK, Menger MD, et al. Interaction of the chemokines I-TAC (CXCL11) and SDF-1 (CXCL12) in the regulation of tumor angiogenesis of colorectal cancer. Clin Exp Metastasis. 2014;31:447–59.

58. Kawamura M, Toiyama Y, Tanaka K, Saigusa S, Okugawa Y, Hiro J, et al. CXCL5, a promoter of cell proliferation, migration and invasion, is a novel serum prognostic marker in patients with colorectal cancer. Eur J Cancer. 2012;48:2244–51.

59. Speetjens FM, Kuppen PJ, Sandel MH, Menon AG, Burg D, van de Velde CJ, et al. Disrupted expression of CXCL5 in colorectal cancer is associated with rapid tumor formation in rats and poor prognosis in patients. Clin Cancer Res. 2008;14:2276–84.

60. Dimberg J, Dienus O, Lofgren S, Hugander A, Wagsater D. Expression and gene polymorphisms of the chemokine CXCL5 in colorectal cancer patients. Int J Oncol. 2007;31:97–102.

61. Baier PK, Eggstein S, Wolff-Vorbeck G, Baumgartner U, Hopt UT. Chemokines in human colorectal carcinoma. Anticancer Res. 2005;25:3581–4.

62. Crittenden M, Gough M, Harrington K, Olivier K, Thompson J, Vile RG. Expression of inflammatory chemokines combined with local tumor destruction enhances tumor regression and long-term immunity. Cancer Res. 2003;63:5505–12.

266

Mahboob et al. Clinical Proteomics (2015) 12:10

Page 12 of 12

63. Turner PK, Houghton JA, Petak I, Tillman DM, Douglas L, Schwartzberg L, et al. Interferon-gamma pharmacokinetics and pharmacodynamics in patients with colorectal cancer. Cancer Chemother Pharmacol. 2004;53:253–60.
64. Kang M, Edmundson P, Araujo-Perez F, McCoy AN, Galanko J, Keku TO. Association of plasma endotoxin, inflammatory cytokines and risk of colorectal adenomas. BMC Cancer. 2013;13:91.
65. Neagu S, Lerescu L, Costea R, Tucureanu C, Caras I, Gangura G, et al. Salageanu A: [Perioperative immunologic changes in colorectal cancer patients]. Chirurgia (Bucur). 2012;107:59–65.

5.2 – Supplemental files

Supplementary Data

Table S1: List of oncoproteins analyzed by Proseek Assay with Limit of Detection (LOD) in pg/ ml, working range (Lower Limit of Quantification, LLOQ, Upper Limit of Quantification, ULOQ)					
Olink Abbreviations	Gene Name	Target Protein Name	UniProt No	LOD (pg/mL)	Assay Working Range (pg/ml)
Adrenomedullin	ADM	Adrenomedullin	P35318	227.1	976.6-250000
Amphiregulin	AREG	Amphiregulin	P15514	1.58	15.3-15625
TIE2	TIE2	Angiopoietin-1 receptor	Q02763	486.3	976.6-250000
BAFF	BAFF	B-cell activating factor	Q9Y275	56	244.1-250000
Betacellulin	BTC	Betacellulin	P35070	7.9	61.0-3906
CA242	CA242	CA242 tumor marker		NR	NR-NR
CAIX	CAIX	Carbonic Anhydrase IX	Q16790	9.9	61.0-15625
CEA	CEA	Carcinoembryonic antigen	P06731	46.6	61.0-62500
Caspase-3	CASP-3	Caspase-3	P42574	18.7	61.0-62500

Cathepsin D	CTSD	Cathepsin D	P07339	6684.7	15625.0-1000000
CCL19	CCL19	C-C motif chemokine 19	Q99731	5.7	15.3-15625
CCL21	CCL21	C-C motif chemokine 21	O00585	54.5	244.1-3906
CCL24	CCL24	C-C motif chemokine 24	O00175	0.44	3.8-3906
CD40 ligand	CD40-L	CD40 ligand	P29965	0.66	3.8-15625
CXCL10	CXCL10	C-X-C motif chemokine 10	P02778	4.6	15.3-15625
CXCL11	CXCL11	C-X-C motif chemokine 11	O14625	14	61.0-15625
CXCL13	CXCL13	C-X-C motif chemokine 13	O43927	1.16	15.3-3906
CXCL5	CXCL5	C-X-C motif chemokine 5	P42830	3	15.3-15625
CXCL9	CXCL9	C-X-C motif chemokine 9	Q07325	4.2	61.0-62500
Cystatin B	CPI-B	Cystatin B	P04080	207.7	976.6-250000
CD69	CD69	Benign activation antigen CD69	Q07108	1.15	15.3-62500
EGF	EGF	Epidermal growth factor	P01133	0.17	0.95-3906
EGFR	EGFR	Epidermal growth factor receptor	P00533	149.6	976.6-250000
HE4	HE4	Epididymal secretory protein E4	Q14508	18.8	61.0-62500
Epiregulin	EPR	Epiregulin	O14944	5.1	61.0-15625

Ep-CAM	Ep-CAM	Epithelial cell adhesion molecule	P16422	0.44	3.8-15625
EPO	EPO	Erythropoietin	P01588	81.6	244.1-62500
E-selectin	CD62E	E-selectin	P16581	1250.5	3906.3-250000
Estrogen receptor	ER	Estrogen receptor	P03372	375	3906.3-250000
EMMPRIN	EMMPRIN	Extracellular matrix metalloproteinase inducer	P35613	0.16	3.8-15625
FasL	FasL	Fas antigen ligand	P48023	2.6	15.3-15625
FABP4	FABP4	Fatty acid binding protein 4 adipocyte	P15090	635.6	976.6-250000
Flt3L	Flt3L	Fms-reMalignantd tyrosine kinase 3 ligand	P49771	0.18	0.95-3906
FR-alpha	FR-alpha	FoMalignant receptor alpha	P15328	8.7	61.0-62500
Follistatin	FS	Follistatin	P19883	31.5	244.1-250000
Galectin-3	Gal-3	Galectin-3	P17931	3584.5	15625.0-1000000
GM-CSF	GM-CSF	Granulocyte-macrophage colonystimulating factor	P04141	42	244.1-250000
Growth Hormone	GH	Growth Hormone	P01241	0.34	0.95-15625

Hormone					
GDF-15	GDF-15	Growth/differentiation factor 15	Q99988	21.2	244.1-62500
HB-EGF	HB-EGF	Heparin-binding EGF-like growth factor	Q99075	0.16	3.8-3906
HGF	HGF	Hepatocyte growth factor	P14210	1.85	15.3-15625
HGF receptor	HGF receptor	Hepatocyte growth factor receptor	P08581	20.5	61.0-62500
IFN-gamma	IFN-gamma	Interferon gamma	P01579	14.2	61.0-15625
IL-1ra	IL-1ra	Interleukin 1 receptor antagonist protein	P18510	105.1	244.1-15625
IL-12	IL-12	Interleukin 12	P29460	0.77	3.8-3906
IL17RB	IL17RB	Interleukin 17 receptor B	Q9NRM	3.9	15.3-62500
IL-2	IL-2	Interleukin 2	P60568	55.8	244.1-250000
IL2RA	IL2RA	Interleukin 2 receptor subunit alpha	P01589	0.19	0.95-3906
IL-4	IL-4	Interleukin 4	P05112	0.63	3.8-15625
IL-6	IL-6	Interleukin 6	P05231	0.06	0.24-15625
IL6RA	IL6RA	Interleukin 6 receptor subunit alpha	P08887	121.2	976.6-250000

269

IL-7	IL-7	Interleukin 7	P13232	1.09	3.8-15625
IL-8	IL-8	Interleukin 8	P10145	0.06	0.24-3906
Kallikrein-11	hK11	Kallikrein-11	Q9UBX7	145	244.1-15625
Kallikrein-6	KLK6	Kallikrein-6	Q92876	11	61.0-62500
CSF-1	CSF-1	Macrophage colony-stimulating factor 1	P09603	0.09	0.95-15625
MMP-3	MMP-3	Matrix metalloproteinase-3	P08254	NR	NR-NR
'MIA	MIA	Melanoma-derived growth regulatory protein	Q16674	97.4	244.1-62500
MIC-A	MIC-A	MHC class I polypeptide-reMalignantd sequence A	Q29983	17.1	61.0-3906
Midkine	MK	Midkine	P21741	232.9	976.6-62500
MCP-1	MCP-1	Monocyte chemotactic protein-1	P13500	0.11	0.95-3906
MYD88	MYD88	Myeloid differentiation primary response protein MyD88	Q99836	69.7	244.1-250000
MPO	MPO	Myeloperoxidase	P05164	137.8	976.6-250000
Osteoprotegerin	OPG	Osteoprotegerin	O00300	0.14	0.24-15625
CA-125	CA-125	Ovarian cancer-reMalignantd tumor marker 125	Q8WXI7	NR	NR-NR

PIGF	PIGF	Placenta Growth Factor	P49763	0.2	0.95-15625
PECAM-1		PMalignantlet endothelial cell adhesion molecule	P16284	463.4	976.6-250000
PDGF subunit B	PDGF subunit B	PMalignantlet-derived growth factor subunit B	P01127	92.7	244.1-250000
Prolactin	PRL	Prolactin	P01236	1925.4	3906.3-1000000
Prostasin	PRSS8	Prostasin	Q16651	9.5	15.3-15625
PSA	PSA	Prostate-specific antigen	P07288	48.6	244.1-62500
ErbB2/Her2	ErbB2/Her2	Receptor tyrosine-protein kinase ErbB-2	P04626	86.1	244.1-62500
ErbB3/Her3	ErbB3/Her3	Receptor tyrosine-protein kinase ErbB-3	P21860	16.8	61.0-62500
ErbB4/Her4	ErbB4/Her4	Receptor tyrosine-protein kinase ErbB-4	Q15303	11.1	61.0-62500
REG-4	REG-4	Regenerating islet-derived protein 4	Q9BYZ8	259.9	3906.3-1000000
Stem cell factor	SCF	Stem cell factor	P21583	6.2	61.0-62500

TR-AP	TR-AP	Tartrate-resistant acid phosphatase type 5	P13686	58.8	244.1-250000
Thrombopoietin	THPO	Thrombopoietin	P40225	146.6	244.1-62500
Tissue Factor	TF	Tissue Factor	P13726	0.81	3.8-15625
TGF-alpha	TGF-alpha	Transforming growth factor alpha	P01135	0.8	3.8-15625
LAP TGF-beta-1	LAP TGF-beta-1	Transforming growth factor beta 1	P01137	56.1	244.1-250000
TNF	TNF	Tumor necrosis factor alpha	P01375	77.4	244.1-250000
TNFSF14	TNFSF14	Tumor necrosis factor ligand superfamily member 14	O43557	4.5	15.3-15625
CD30-L	CD30-L	Tumor necrosis factor ligand superfamily member 8	P32971	9.7	61.0-15625
TNF-RI	TNF-RI	Tumor necrosis factor receptor 1	P19438	0.88	3.8-15625
TNF-R2	TNF-R2	Tumor necrosis factor receptor 2	P20333	247.4	976.6-250000
TNFRSF4	TNFRSF4	Tumor necrosis factor receptor superfamily	P43489	4.7	15.3-15625

		member 4			
FAS	FAS	Tumor necrosis factor receptor superfamily member 6	P25445	12.5	244.1-250000
U-PAR	U-PAR	Urokinase plasminogen activator surface receptor	Q03405	0.81	3.8-15625
VEGF-A	VEGF-A	Vascular endothelial growth factor A	P15692	0.32	0.95-15625
VEGF-D	VEGF-D	Vascular endothelial growth factor D	O43915	22.7	61.0-62500
VEGFR-2	VEGFR-2	Vascular endothelial growth factor receptor 2	P35968	12.2	61.0-62500

Table S2: List of cytokines analyzed by Bio-plex Assay with Limit of Detection (LOD) in pg/ ml, Lower Limit of Quantification (LLOQ) and Upper Limit of Quantification (ULOQ) (Proteins in bold letters indicate common target proteins between two platforms)					
Cytokine	Gene name	Target Protein Name	UNIPROT ID	LOD	Assay Working range (pg/ml)
Eotaxin	CCL11	C-C motif chemokine 11	P51671	2.5	40.9-5,824
FGF basic	FGF2	Fibroblast growth factor 2	P09038	1.9	27.2-7,581
G-CSF	CSF3	Granulocyte colony-stimulating factor	P09919	1.7	2.4-11,565
GM-CSF	**CSF2**	**Granulocyte-macrophage colony-stimulating factor**	**P04141**	**2.2**	**63.3-6,039**
IFN-gamma	**IFNG**	**Interferon gamma**	**P01579**	**6.4**	**92.6-52,719**
IL-1 beta	IL1B	Interleukin-1 beta	P01584	0.6	3.2-3,261

IL-1ra	IL1RN	Interleukin 1 receptor antagonist protein	P18510	5.5	81.1-70,487
IL-2	IL2	Interleukin 2	P60568	1.6	2.1-17,772
IL-4	IL4	Interleukin 4	P05112	0.7	2.2-3,467
IL-5	IL5	Interleukin-5	P05113	0.6	3.1-7,380
IL-6	IL6	Interleukin 6	P05231	2.6	2.3-18,880
IL-7	IL7	Interleukin 7	P13232	1.1	3.1-6,001
IL-8	IL8	Interleukin 8	P10145	1	1.9-26,403
IL-9	IL9	Interleukin-9	P15248	2.5	2.1-7,989
IL-10	IL10	Interleukin-10	P22301	0.3	2.2-8,840
IL12 (p70)	IL12	Interleukin-12	P29460	3.5	3.3-13,099
IL-13	IL13	Interleukin-13	P35225	0.7	3.7-3,137
IL-15	IL15	Interleukin-15	P40933	2.4	2.1-2,799
IL-17	IL17A	Interleukin-17A	Q16552	3.3	4.9-12,235
IP-10	CXCL10	C-X-C motif chemokine 10	P02778	6.1	18.8-26,867
MCP-1	CCL2	Monocyte chemotactic protein-1/ C-C	P13500	1.1	2.1-1,820

		motif chemokine 2			
MIP-1 alpha	CCL3	Macrophage inflammatory protein 1-alpha/ C-C motif chemokine 3	P10147	1.6	1.4-836
MIP-1 beta	CCL4	Macrophage inflammatory protein 1-beta/ C-C motif chemokine 4	P13236	2.4	2-1,726
PDGF-BB	PDGFB	PMalignantlet-derived growth factor subunit B	P01127	2.9	7-51,933
RANTES	CCL5	C-C motif chemokine 5	P13501	1.8	2.2-8,617
TNF-alpha	TNF	Tumor necrosis factor alpha	P01375	6	5.8-95,484
VEGF	VEGFA	Vascular endothelial growth factor A	P15692	3.1	5.5-56,237

Table S3: Q- values calculated for stage specific protein expressions analyzed by PEA technology					
Candidate Biomarker	Comparison	Difference	Lower CI	Upper CI	Q-value
Adrenomedullin	A/E	-0.37343	-1.66099	0.914138	1
Adrenomedullin	B/E	0.042987	-1.24458	1.330551	1
Adrenomedullin	C/E	-0.22955	-1.51712	1.058009	1
Adrenomedullin	D/E	-0.17962	-1.46718	1.107945	1
Adrenomedullin	B/A	0.416413	-0.87115	1.703976	1
Adrenomedullin	C/A	0.143871	-1.14369	1.431434	1
Adrenomedullin	D/A	0.193806	-1.09376	1.48137	1
Adrenomedullin	C/B	-0.27254	-1.56011	1.015022	1
Adrenomedullin	D/B	-0.22261	-1.51017	1.064957	1
Adrenomedullin	D/C	0.049936	-1.23763	1.337499	1
Amphiregulin	A/E	-0.22732	-1.51489	1.06024	1
Amphiregulin	B/E	0.340724	-0.94684	1.628288	1
Amphiregulin	C/E	-0.20858	-1.49614	1.078988	1
Amphiregulin	D/E	1.5605	0.272936	2.848063	0.000236
Amphiregulin	B/A	0.568048	-0.71952	1.855611	1
Amphiregulin	C/A	0.018748	-1.26882	1.306311	1
Amphiregulin	D/A	1.787823	0.50026	3.075387	8.95E-07
Amphiregulin	C/B	-0.5493	-1.83686	0.738263	1
Amphiregulin	D/B	1.219775	-0.06779	2.507339	0.138034
Amphiregulin	D/C	1.769075	0.481512	3.056639	1.46E-06

BAFF	A/E	-0.42231	-1.70988	0.86525	1
BAFF	B/E	-0.22192	-1.50948	1.065645	1
BAFF	C/E	-0.50774	-1.7953	0.779828	1
BAFF	D/E	0.044072	-1.24349	1.331635	1
BAFF	B/A	0.200395	-1.08717	1.487958	1
BAFF	C/A	-0.08542	-1.37299	1.202141	1
BAFF	D/A	0.466385	-0.82118	1.753948	1
BAFF	C/B	-0.28582	-1.57338	1.001746	1
BAFF	D/B	0.26599	-1.02157	1.553553	1
BAFF	D/C	0.551807	-0.73576	1.83937	1
Betacellulin	A/E	0.017737	-1.26983	1.305301	1
Betacellulin	B/E	0.062329	-1.22523	1.349893	1
Betacellulin	C/E	-4.22E-15	-1.28756	1.287563	1
Betacellulin	D/E	-1.53E-14	-1.28756	1.287563	1
Betacellulin	B/A	0.044592	-1.24297	1.332156	1
Betacellulin	C/A	-0.01774	-1.3053	1.269826	1
Betacellulin	D/A	-0.01774	-1.3053	1.269826	1
Betacellulin	C/B	-0.06233	-1.34989	1.225234	1
Betacellulin	D/B	-0.06233	-1.34989	1.225234	1
Betacellulin	D/C	-1.11E-14	-1.28756	1.287563	1
CA.125	A/E	-0.32782	-1.61538	0.959745	1
CA.125	B/E	-0.33964	-1.62721	0.947919	1
CA.125	C/E	-0.30166	-1.58922	0.985908	1
CA.125	D/E	-0.00804	-1.29561	1.279521	1

CA.125	B/A	-0.01183	-1.29939	1.275738	1
CA.125	C/A	0.026163	-1.2614	1.313727	1
CA.125	D/A	0.319777	-0.96779	1.60734	1
CA.125	C/B	0.037989	-1.24957	1.325552	1
CA.125	D/B	0.331602	-0.95596	1.619166	1
CA.125	D/C	0.293613	-0.99395	1.581177	1
CA242	A/E	0.180915	-1.10665	1.468478	1
CA242	B/E	0.048157	-1.23941	1.335721	1
CA242	C/E	0.148181	-1.13938	1.435744	1
CA242	D/E	0.557591	-0.72997	1.845154	1
CA242	B/A	-0.13276	-1.42032	1.154806	1
CA242	C/A	-0.03273	-1.3203	1.254829	1
CA242	D/A	0.376676	-0.91089	1.664239	1
CA242	C/B	0.100024	-1.18754	1.387587	1
CA242	D/B	0.509434	-0.77813	1.796997	1
CA242	D/C	0.40941	-0.87815	1.696973	1
CAIX	A/E	0.065766	-1.2218	1.35333	1
CAIX	B/E	0.182975	-1.10459	1.470539	1
CAIX	C/E	-0.01831	-1.30587	1.269255	1
CAIX	D/E	0.884121	-0.40344	2.171685	0.998262
CAIX	B/A	0.117209	-1.17035	1.404772	1
CAIX	C/A	-0.08408	-1.37164	1.203488	1
CAIX	D/A	0.818355	-0.46921	2.105919	0.999979
CAIX	C/B	-0.20128	-1.48885	1.08628	1

CAIX	D/B	0.701146	-0.58642	1.98871	1
CAIX	D/C	0.90243	-0.38513	2.189994	0.995655
Caspase.3	A/E	-0.30713	-1.59469	0.980435	1
Caspase.3	B/E	0.333613	-0.95395	1.621176	1
Caspase.3	C/E	0.114641	-1.17292	1.402205	1
Caspase.3	D/E	0.670484	-0.61708	1.958048	1
Caspase.3	B/A	0.640741	-0.64682	1.928305	1
Caspase.3	C/A	0.42177	-0.86579	1.709333	1
Caspase.3	D/A	0.977613	-0.30995	2.265176	0.935363
Caspase.3	C/B	-0.21897	-1.50653	1.068592	1
Caspase.3	D/B	0.336872	-0.95069	1.624435	1
Caspase.3	D/C	0.555843	-0.73172	1.843406	1
Cathepsin.D	A/E	-0.50432	-1.79188	0.783243	1
Cathepsin.D	B/E	-0.10476	-1.39232	1.182807	1
Cathepsin.D	C/E	-0.364	-1.65157	0.923561	1
Cathepsin.D	D/E	-0.24864	-1.5362	1.038927	1
Cathepsin.D	B/A	0.399564	-0.888	1.687128	1
Cathepsin.D	C/A	0.140318	-1.14725	1.427881	1
Cathepsin.D	D/A	0.255684	-1.03188	1.543247	1
Cathepsin.D	C/B	-0.25925	-1.54681	1.028317	1
Cathepsin.D	D/B	-0.14388	-1.43144	1.143683	1
Cathepsin.D	D/C	0.115366	-1.1722	1.40293	1
CCL19	A/E	-0.67464	-1.96221	0.61292	1
CCL19	B/E	-0.51097	-1.79853	0.776596	1

CCL19	C/E	-0.57792	-1.86549	0.70964	1
CCL19	D/E	-0.27511	-1.56267	1.012454	1
CCL19	B/A	0.163676	-1.12389	1.451239	1
CCL19	C/A	0.09672	-1.19084	1.384284	1
CCL19	D/A	0.399534	-0.88803	1.687097	1
CCL19	C/B	-0.06696	-1.35452	1.220608	1
CCL19	D/B	0.235858	-1.05171	1.523422	1
CCL19	D/C	0.302814	-0.98475	1.590377	1
CCL21	A/E	-0.15568	-1.44324	1.131884	1
CCL21	B/E	0.141274	-1.14629	1.428837	1
CCL21	C/E	-0.18085	-1.46841	1.106717	1
CCL21	D/E	0.003103	-1.28446	1.290666	1
CCL21	B/A	0.296953	-0.99061	1.584517	1
CCL21	C/A	-0.02517	-1.31273	1.262396	1
CCL21	D/A	0.158782	-1.12878	1.446346	1
CCL21	C/B	-0.32212	-1.60968	0.965443	1
CCL21	D/B	-0.13817	-1.42573	1.149392	1
CCL21	D/C	0.18395	-1.10361	1.471513	1
CCL24	A/E	-0.37707	-1.66464	0.91049	1
CCL24	B/E	-0.52457	-1.81213	0.762996	1
CCL24	C/E	-0.59621	-1.88377	0.691356	1
CCL24	D/E	-0.50964	-1.7972	0.777928	1
CCL24	B/A	-0.14749	-1.43506	1.140069	1
CCL24	C/A	-0.21913	-1.5067	1.068429	1

CCL24	D/A	-0.13256	-1.42013	1.155002	1
CCL24	C/B	-0.07164	-1.3592	1.215923	1
CCL24	D/B	0.014932	-1.27263	1.302496	1
CCL24	D/C	0.086572	-1.20099	1.374136	1
CD30.L	A/E	0.208145	-1.07942	1.495708	1
CD30.L	B/E	0.328648	-0.95892	1.616212	1
CD30.L	C/E	0.256961	-1.0306	1.544525	1
CD30.L	D/E	0.315992	-0.97157	1.603555	1
CD30.L	B/A	0.120503	-1.16706	1.408067	1
CD30.L	C/A	0.048816	-1.23875	1.33638	1
CD30.L	D/A	0.107847	-1.17972	1.39541	1
CD30.L	C/B	-0.07169	-1.35925	1.215877	1
CD30.L	D/B	-0.01266	-1.30022	1.274907	1
CD30.L	D/C	0.05903	-1.22853	1.346594	1
CD40.ligand	A/E	-0.51146	-1.79903	0.776101	1
CD40.ligand	B/E	-0.22448	-1.51204	1.063083	1
CD40.ligand	C/E	-0.44517	-1.73273	0.842397	1
CD40.ligand	D/E	0.327277	-0.96029	1.614841	1
CD40.ligand	B/A	0.286982	-1.00058	1.574545	1
CD40.ligand	C/A	0.066296	-1.22127	1.353859	1
CD40.ligand	D/A	0.838739	-0.44882	2.126303	0.999898
CD40.ligand	C/B	-0.22069	-1.50825	1.066877	1
CD40.ligand	D/B	0.551757	-0.73581	1.839321	1
CD40.ligand	D/C	0.772443	-0.51512	2.060007	1

CD69	A/E	-0.08868	-1.37625	1.198881	1
CD69	B/E	0.550041	-0.73752	1.837604	1
CD69	C/E	0.281364	-1.0062	1.568927	1
CD69	D/E	0.574976	-0.71259	1.86254	1
CD69	B/A	0.638723	-0.64884	1.926286	1
CD69	C/A	0.370046	-0.91752	1.657609	1
CD69	D/A	0.663658	-0.62391	1.951222	1
CD69	C/B	-0.26868	-1.55624	1.018886	1
CD69	D/B	0.024935	-1.26263	1.312499	1
CD69	D/C	0.293613	-0.99395	1.581176	1
CEA	A/E	-0.07688	-1.36444	1.210688	1
CEA	B/E	0.357538	-0.93003	1.645101	1
CEA	C/E	1.317497	0.029933	2.60506	0.030429
CEA	D/E	2.899803	1.612239	4.187366	1.70E-12
CEA	B/A	0.434413	-0.85315	1.721976	1
CEA	C/A	1.394372	0.106808	2.681935	0.007576
CEA	D/A	2.976678	1.689114	4.264241	0
CEA	C/B	0.959959	-0.3276	2.247522	0.960883
CEA	D/B	2.542265	1.254701	3.829828	4.13E-12
CEA	D/C	1.582306	0.294743	2.869869	0.000143
CSF.1	A/E	-0.19372	-1.48129	1.09384	1
CSF.1	B/E	-0.01191	-1.29947	1.275657	1
CSF.1	C/E	-0.35253	-1.6401	0.935029	1
CSF.1	D/E	-0.03133	-1.3189	1.256229	1

CSF.1	B/A	0.181817	-1.10575	1.469381	1
CSF.1	C/A	-0.15881	-1.44638	1.128752	1
CSF.1	D/A	0.162389	-1.12517	1.449952	1
CSF.1	C/B	-0.34063	-1.62819	0.946935	1
CSF.1	D/B	-0.01943	-1.30699	1.268135	1
CSF.1	D/C	0.3212	-0.96636	1.608764	1
CXCL10	A/E	-0.68081	-1.96837	0.606753	1
CXCL10	B/E	-0.47845	-1.76602	0.809112	1
CXCL10	C/E	-0.7874	-2.07496	0.500167	0.999999
CXCL10	D/E	0.029593	-1.25797	1.317156	1
CXCL10	B/A	0.202359	-1.0852	1.489922	1
CXCL10	C/A	-0.10659	-1.39415	1.180978	1
CXCL10	D/A	0.710403	-0.57716	1.997967	1
CXCL10	C/B	-0.30894	-1.59651	0.978619	1
CXCL10	D/B	0.508045	-0.77952	1.795608	1
CXCL10	D/C	0.816989	-0.47057	2.104552	0.999981
CXCL11	A/E	-0.48886	-1.77642	0.798705	1
CXCL11	B/E	0.259621	-1.02794	1.547184	1
CXCL11	C/E	-0.54156	-1.82912	0.746005	1
CXCL11	D/E	0.814415	-0.47315	2.101979	0.999985
CXCL11	B/A	0.748479	-0.53908	2.036043	1
CXCL11	C/A	-0.0527	-1.34026	1.234863	1
CXCL11	D/A	1.303274	0.01571	2.590837	0.038658
CXCL11	C/B	-0.80118	-2.08874	0.486384	0.999995

CXCL11	D/B	0.554794	-0.73277	1.842358	1
CXCL11	D/C	1.355974	0.06841	2.643537	0.015472
CXCL13	A/E	-0.62111	-1.90868	0.666451	1
CXCL13	B/E	-0.32926	-1.61682	0.958302	1
CXCL13	C/E	-0.06465	-1.35222	1.222911	1
CXCL13	D/E	0.179172	-1.10839	1.466735	1
CXCL13	B/A	0.291851	-0.99571	1.579415	1
CXCL13	C/A	0.556459	-0.7311	1.844023	1
CXCL13	D/A	0.800284	-0.48728	2.087847	0.999996
CXCL13	C/B	0.264608	-1.02296	1.552172	1
CXCL13	D/B	0.508433	-0.77913	1.795996	1
CXCL13	D/C	0.243825	-1.04374	1.531388	1
CXCL5	A/E	-0.92751	-2.21508	0.360049	0.987274
CXCL5	B/E	-0.13596	-1.42352	1.151606	1
CXCL5	C/E	-0.17444	-1.462	1.113127	1
CXCL5	D/E	0.370127	-0.91744	1.657691	1
CXCL5	B/A	0.791557	-0.49601	2.07912	0.999998
CXCL5	C/A	0.753078	-0.53449	2.040641	1
CXCL5	D/A	1.297642	0.010078	2.585205	0.04243
CXCL5	C/B	-0.03848	-1.32604	1.249084	1
CXCL5	D/B	0.506085	-0.78148	1.793649	1
CXCL5	D/C	0.544564	-0.743	1.832128	1
CXCL9	A/E	-0.31503	-1.60259	0.972536	1
CXCL9	B/E	0.305379	-0.98218	1.592943	1

CXCL9	C/E	-0.26451	-1.55207	1.023054	1
CXCL9	D/E	0.62695	-0.66061	1.914514	1
CXCL9	B/A	0.620407	-0.66716	1.90797	1
CXCL9	C/A	0.050518	-1.23705	1.338082	1
CXCL9	D/A	0.941978	-0.34559	2.229542	0.978272
CXCL9	C/B	-0.56989	-1.85745	0.717675	1
CXCL9	D/B	0.321571	-0.96599	1.609135	1
CXCL9	D/C	0.89146	-0.3961	2.179023	0.997454
Cystatin.B	A/E	-0.39287	-1.68043	0.894697	1
Cystatin.B	B/E	0.074363	-1.2132	1.361927	1
Cystatin.B	C/E	-0.21858	-1.50615	1.06898	1
Cystatin.B	D/E	-0.04773	-1.33529	1.239836	1
Cystatin.B	B/A	0.46723	-0.82033	1.754793	1
Cystatin.B	C/A	0.174283	-1.11328	1.461847	1
Cystatin.B	D/A	0.34514	-0.94242	1.632703	1
Cystatin.B	C/B	-0.29295	-1.58051	0.994617	1
Cystatin.B	D/B	-0.12209	-1.40965	1.165473	1
Cystatin.B	D/C	0.170856	-1.11671	1.45842	1
E.selectin	A/E	-0.00044	-1.288	1.287128	1
E.selectin	B/E	-0.00074	-1.28831	1.28682	1
E.selectin	C/E	-0.29272	-1.58028	0.994846	1
E.selectin	D/E	0.432712	-0.85485	1.720276	1
E.selectin	B/A	-0.00031	-1.28787	1.287256	1
E.selectin	C/A	-0.29228	-1.57984	0.995282	1

E.selectin	D/A	0.433148	-0.85442	1.720712	1
E.selectin	C/B	-0.29197	-1.57954	0.99559	1
E.selectin	D/B	0.433456	-0.85411	1.721019	1
E.selectin	D/C	0.725429	-0.56213	2.012993	1
EGF	A/E	-0.54822	-1.83578	0.739342	1
EGF	B/E	0.081633	-1.20593	1.369197	1
EGF	C/E	-0.15077	-1.43834	1.13679	1
EGF	D/E	0.480911	-0.80665	1.768474	1
EGF	B/A	0.629854	-0.65771	1.917418	1
EGF	C/A	0.397448	-0.89012	1.685011	1
EGF	D/A	1.029132	-0.25843	2.316695	0.803702
EGF	C/B	-0.23241	-1.51997	1.055157	1
EGF	D/B	0.399277	-0.88829	1.686841	1
EGF	D/C	0.631684	-0.65588	1.919247	1
EGFR	A/E	-0.3328	-1.62037	0.954759	1
EGFR	B/E	-0.40615	-1.69371	0.881415	1
EGFR	C/E	-0.41663	-1.70419	0.870933	1
EGFR	D/E	-0.24693	-1.53449	1.040633	1
EGFR	B/A	-0.07334	-1.36091	1.21422	1
EGFR	C/A	-0.08383	-1.37139	1.203738	1
EGFR	D/A	0.085875	-1.20169	1.373438	1
EGFR	C/B	-0.01048	-1.29805	1.277081	1
EGFR	D/B	0.159218	-1.12835	1.446781	1
EGFR	D/C	0.1697	-1.11786	1.457264	1

EMMPRIN	A/E	0.320567	-0.967	1.60813	1
EMMPRIN	B/E	-0.15027	-1.43783	1.137292	1
EMMPRIN	C/E	0.34046	-0.9471	1.628023	1
EMMPRIN	D/E	0.333331	-0.95423	1.620895	1
EMMPRIN	B/A	-0.47084	-1.7584	0.816725	1
EMMPRIN	C/A	0.019893	-1.26767	1.307456	1
EMMPRIN	D/A	0.012764	-1.2748	1.300328	1
EMMPRIN	C/B	0.490731	-0.79683	1.778294	1
EMMPRIN	D/B	0.483602	-0.80396	1.771166	1
EMMPRIN	D/C	-0.00713	-1.29469	1.280435	1
Ep.CAM	A/E	-0.48613	-1.7737	0.801431	1
Ep.CAM	B/E	-0.43517	-1.72274	0.852389	1
Ep.CAM	C/E	-0.35947	-1.64704	0.928091	1
Ep.CAM	D/E	0.421201	-0.86636	1.708765	1
Ep.CAM	B/A	0.050958	-1.23661	1.338521	1
Ep.CAM	C/A	0.12666	-1.1609	1.414224	1
Ep.CAM	D/A	0.907334	-0.38023	2.194897	0.994555
Ep.CAM	C/B	0.075703	-1.21186	1.363266	1
Ep.CAM	D/B	0.856376	-0.43119	2.143939	0.999659
Ep.CAM	D/C	0.780673	-0.50689	2.068237	0.999999
Epiregulin	A/E	3.33E-14	-1.28756	1.287563	1
Epiregulin	B/E	1.27E-14	-1.28756	1.287563	1
Epiregulin	C/E	0.010219	-1.27734	1.297782	1
Epiregulin	D/E	0.027725	-1.25984	1.315289	1

Epiregulin	B/A	-2.07E-14	-1.28756	1.287563	1
Epiregulin	C/A	0.010219	-1.27734	1.297782	1
Epiregulin	D/A	0.027725	-1.25984	1.315289	1
Epiregulin	C/B	0.010219	-1.27734	1.297782	1
Epiregulin	D/B	0.027725	-1.25984	1.315289	1
Epiregulin	D/C	0.017507	-1.27006	1.30507	1
EPO	A/E	-0.14463	-1.43219	1.142938	1
EPO	B/E	0.188557	-1.09901	1.47612	1
EPO	C/E	-0.06631	-1.35387	1.221252	1
EPO	D/E	-0.20288	-1.49044	1.084683	1
EPO	B/A	0.333182	-0.95438	1.620746	1
EPO	C/A	0.078314	-1.20925	1.365878	1
EPO	D/A	-0.05826	-1.34582	1.229308	1
EPO	C/B	-0.25487	-1.54243	1.032696	1
EPO	D/B	-0.39144	-1.679	0.896126	1
EPO	D/C	-0.13657	-1.42413	1.150994	1
ErbB2.Her2	A/E	-0.15048	-1.43805	1.137081	1
ErbB2.Her2	B/E	-0.23611	-1.52368	1.05145	1
ErbB2.Her2	C/E	-0.38065	-1.66822	0.906911	1
ErbB2.Her2	D/E	-0.09415	-1.38171	1.193415	1
ErbB2.Her2	B/A	-0.08563	-1.37319	1.201933	1
ErbB2.Her2	C/A	-0.23017	-1.51773	1.057393	1
ErbB2.Her2	D/A	0.056334	-1.23123	1.343897	1
ErbB2.Her2	C/B	-0.14454	-1.4321	1.143024	1

ErbB2.Her2	D/B	0.141965	-1.1456	1.429528	1
ErbB2.Her2	D/C	0.286504	-1.00106	1.574067	1
ErbB3.Her3	A/E	-0.20242	-1.48998	1.085144	1
ErbB3.Her3	B/E	-0.22752	-1.51509	1.060041	1
ErbB3.Her3	C/E	-0.21303	-1.5006	1.074529	1
ErbB3.Her3	D/E	-0.13316	-1.42072	1.154407	1
ErbB3.Her3	B/A	-0.0251	-1.31267	1.262461	1
ErbB3.Her3	C/A	-0.01061	-1.29818	1.276949	1
ErbB3.Her3	D/A	0.069264	-1.2183	1.356827	1
ErbB3.Her3	C/B	0.014488	-1.27308	1.302051	1
ErbB3.Her3	D/B	0.094366	-1.1932	1.38193	1
ErbB3.Her3	D/C	0.079878	-1.20768	1.367442	1
ErbB4.Her4	A/E	-0.39023	-1.67779	0.897332	1
ErbB4.Her4	B/E	-0.40493	-1.6925	0.882632	1
ErbB4.Her4	C/E	-0.4994	-1.78696	0.788164	1
ErbB4.Her4	D/E	-0.38354	-1.6711	0.904022	1
ErbB4.Her4	B/A	-0.0147	-1.30226	1.272863	1
ErbB4.Her4	C/A	-0.10917	-1.39673	1.178395	1
ErbB4.Her4	D/A	0.00669	-1.28087	1.294253	1
ErbB4.Her4	C/B	-0.09447	-1.38203	1.193096	1
ErbB4.Her4	D/B	0.02139	-1.26617	1.308954	1
ErbB4.Her4	D/C	0.115858	-1.17171	1.403421	1
Estrogen.receptor	A/E	2.31E-14	-1.28756	1.287563	1
Estrogen.receptor	B/E	2.22E-15	-1.28756	1.287563	1

Estrogen.receptor	C/E	0.003838	-1.28373	1.291401	1
Estrogen.receptor	D/E	0.011243	-1.27632	1.298807	1
Estrogen.receptor	B/A	-2.09E-14	-1.28756	1.287563	1
Estrogen.receptor	C/A	0.003838	-1.28373	1.291401	1
Estrogen.receptor	D/A	0.011243	-1.27632	1.298807	1
Estrogen.receptor	C/B	0.003838	-1.28373	1.291401	1
Estrogen.receptor	D/B	0.011243	-1.27632	1.298807	1
Estrogen.receptor	D/C	0.007406	-1.28016	1.294969	1
FABP4	A/E	-0.02496	-1.31252	1.262608	1
FABP4	B/E	0.213661	-1.0739	1.501225	1
FABP4	C/E	0.220405	-1.06716	1.507969	1
FABP4	D/E	-0.22565	-1.51321	1.061914	1
FABP4	B/A	0.238617	-1.04895	1.52618	1
FABP4	C/A	0.245361	-1.0422	1.532924	1
FABP4	D/A	-0.20069	-1.48826	1.086869	1
FABP4	C/B	0.006744	-1.28082	1.294307	1
FABP4	D/B	-0.43931	-1.72687	0.848253	1
FABP4	D/C	-0.44605	-1.73362	0.841509	1
FAS	A/E	-0.36378	-1.65134	0.923786	1
FAS	B/E	-0.20395	-1.49151	1.083614	1
FAS	C/E	-0.34914	-1.6367	0.938426	1
FAS	D/E	-0.18012	-1.46768	1.107444	1
FAS	B/A	0.159829	-1.12773	1.447392	1
FAS	C/A	0.01464	-1.27292	1.302204	1

FAS	D/A	0.183658	-1.10391	1.471221	1
FAS	C/B	-0.14519	-1.43275	1.142375	1
FAS	D/B	0.023829	-1.26373	1.311393	1
FAS	D/C	0.169018	-1.11855	1.456581	1
FasL	A/E	-0.03079	-1.31835	1.256778	1
FasL	B/E	-0.04012	-1.32768	1.247448	1
FasL	C/E	0.049413	-1.23815	1.336976	1
FasL	D/E	0.001596	-1.28597	1.28916	1
FasL	B/A	-0.00933	-1.29689	1.278233	1
FasL	C/A	0.080198	-1.20737	1.367761	1
FasL	D/A	0.032381	-1.25518	1.319945	1
FasL	C/B	0.089528	-1.19804	1.377092	1
FasL	D/B	0.041712	-1.24585	1.329275	1
FasL	D/C	-0.04782	-1.33538	1.239747	1
Flt3L	A/E	-0.49858	-1.78614	0.788983	1
Flt3L	B/E	-0.2944	-1.58197	0.993161	1
Flt3L	C/E	-0.59173	-1.8793	0.695832	1
Flt3L	D/E	-0.30745	-1.59502	0.980109	1
Flt3L	B/A	0.204178	-1.08339	1.491742	1
Flt3L	C/A	-0.09315	-1.38071	1.194412	1
Flt3L	D/A	0.191126	-1.09644	1.478689	1
Flt3L	C/B	-0.29733	-1.58489	0.990234	1
Flt3L	D/B	-0.01305	-1.30062	1.274511	1
Flt3L	D/C	0.284277	-1.00329	1.571841	1

288

Follistatin	A/E	-0.20524	-1.49281	1.082319	1
Follistatin	B/E	0.316564	-0.971	1.604127	1
Follistatin	C/E	0.137673	-1.14989	1.425237	1
Follistatin	D/E	0.056123	-1.23144	1.343686	1
Follistatin	B/A	0.521808	-0.76576	1.809372	1
Follistatin	C/A	0.342918	-0.94465	1.630482	1
Follistatin	D/A	0.261367	-1.0262	1.548931	1
Follistatin	C/B	-0.17889	-1.46645	1.108673	1
Follistatin	D/B	-0.26044	-1.548	1.027123	1
Follistatin	D/C	-0.08155	-1.36911	1.206013	1
FR.alpha	A/E	-0.3325	-1.62006	0.955062	1
FR.alpha	B/E	-0.12797	-1.41553	1.159598	1
FR.alpha	C/E	-0.35417	-1.64173	0.933396	1
FR.alpha	D/E	-0.32852	-1.61609	0.95904	1
FR.alpha	B/A	0.204536	-1.08303	1.492099	1
FR.alpha	C/A	-0.02167	-1.30923	1.265897	1
FR.alpha	D/A	0.003978	-1.28359	1.291541	1
FR.alpha	C/B	-0.2262	-1.51377	1.061361	1
FR.alpha	D/B	-0.20056	-1.48812	1.087006	1
FR.alpha	D/C	0.025644	-1.26192	1.313208	1
Galectin.3	A/E	-0.39005	-1.67761	0.897516	1
Galectin.3	B/E	-0.23158	-1.51915	1.05598	1
Galectin.3	C/E	-0.20829	-1.49585	1.079276	1
Galectin.3	D/E	0.23005	-1.05751	1.517614	1

Galectin.3	B/A	0.158464	-1.1291	1.446028	1
Galectin.3	C/A	0.18176	-1.1058	1.469323	1
Galectin.3	D/A	0.620098	-0.66747	1.907661	1
Galectin.3	C/B	0.023295	-1.26427	1.310859	1
Galectin.3	D/B	0.461633	-0.82593	1.749197	1
Galectin.3	D/C	0.438338	-0.84923	1.725902	1
GDF.15	A/E	-0.36566	-1.65322	0.921907	1
GDF.15	B/E	0.69645	-0.59111	1.984014	1
GDF.15	C/E	0.075028	-1.21254	1.362591	1
GDF.15	D/E	0.649793	-0.63777	1.937357	1
GDF.15	B/A	1.062107	-0.22546	2.34967	0.679682
GDF.15	C/A	0.440684	-0.84688	1.728248	1
GDF.15	D/A	1.01545	-0.27211	2.303013	0.847039
GDF.15	C/B	-0.62142	-1.90899	0.666141	1
GDF.15	D/B	-0.04666	-1.33422	1.240906	1
GDF.15	D/C	0.574766	-0.7128	1.862329	1
GM.CSF	A/E	0.008594	-1.27897	1.296157	1
GM.CSF	B/E	-3.55E-15	-1.28756	1.287563	1
GM.CSF	C/E	-1.78E-15	-1.28756	1.287563	1
GM.CSF	D/E	-1.24E-14	-1.28756	1.287563	1
GM.CSF	B/A	-0.00859	-1.29616	1.278969	1
GM.CSF	C/A	-0.00859	-1.29616	1.278969	1
GM.CSF	D/A	-0.00859	-1.29616	1.278969	1
GM.CSF	C/B	1.78E-15	-1.28756	1.287563	1

GM.CSF	D/B	-8.88E-15	-1.28756	1.287563	1
GM.CSF	D/C	-1.07E-14	-1.28756	1.287563	1
Growth.Hormone	A/E	0.729487	-0.55808	2.017051	1
Growth.Hormone	B/E	0.576355	-0.71121	1.863919	1
Growth.Hormone	C/E	0.79832	-0.48924	2.085883	0.999996
Growth.Hormone	D/E	0.362469	-0.92509	1.650033	1
Growth.Hormone	B/A	-0.15313	-1.4407	1.134431	1
Growth.Hormone	C/A	0.068832	-1.21873	1.356396	1
Growth.Hormone	D/A	-0.36702	-1.65458	0.920545	1
Growth.Hormone	C/B	0.221965	-1.0656	1.509528	1
Growth.Hormone	D/B	-0.21389	-1.50145	1.073677	1
Growth.Hormone	D/C	-0.43585	-1.72341	0.851713	1
HB.EGF	A/E	-0.20058	-1.48814	1.086988	1
HB.EGF	B/E	-0.00285	-1.29041	1.284715	1
HB.EGF	C/E	-0.2012	-1.48876	1.086365	1
HB.EGF	D/E	0.358139	-0.92942	1.645702	1
HB.EGF	B/A	0.197728	-1.08984	1.485291	1
HB.EGF	C/A	-0.00062	-1.28819	1.286941	1
HB.EGF	D/A	0.558715	-0.72885	1.846278	1
HB.EGF	C/B	-0.19835	-1.48591	1.089213	1
HB.EGF	D/B	0.360987	-0.92658	1.64855	1
HB.EGF	D/C	0.559337	-0.72823	1.8469	1
HE4	A/E	-0.20184	-1.4894	1.085728	1
HE4	B/E	-0.0913	-1.37886	1.196264	1

HE4	C/E	-0.16483	-1.45239	1.122736	1
HE4	D/E	-0.10764	-1.39521	1.179919	1
HE4	B/A	0.110536	-1.17703	1.398099	1
HE4	C/A	0.037009	-1.25055	1.324572	1
HE4	D/A	0.094192	-1.19337	1.381755	1
HE4	C/B	-0.07353	-1.36109	1.214036	1
HE4	D/B	-0.01634	-1.30391	1.271219	1
HE4	D/C	0.057183	-1.23038	1.344747	1
HGF	A/E	0.018823	-1.26874	1.306387	1
HGF	B/E	0.532771	-0.75479	1.820335	1
HGF	C/E	-0.34026	-1.62783	0.947301	1
HGF	D/E	-0.06215	-1.34972	1.22541	1
HGF	B/A	0.513948	-0.77362	1.801511	1
HGF	C/A	-0.35909	-1.64665	0.928477	1
HGF	D/A	-0.08098	-1.36854	1.206587	1
HGF	C/B	-0.87303	-2.1606	0.41453	0.99906
HGF	D/B	-0.59492	-1.88249	0.692639	1
HGF	D/C	0.27811	-1.00945	1.565673	1
HGF.receptor	A/E	-0.02215	-1.30972	1.26541	1
HGF.receptor	B/E	-0.1043	-1.39186	1.183263	1
HGF.receptor	C/E	-0.23358	-1.52115	1.05398	1
HGF.receptor	D/E	-0.11026	-1.39783	1.177301	1
HGF.receptor	B/A	-0.08215	-1.36971	1.205417	1
HGF.receptor	C/A	-0.21143	-1.49899	1.076133	1

HGF.receptor	D/A	-0.08811	-1.37567	1.199454	1
HGF.receptor	C/B	-0.12928	-1.41685	1.15828	1
HGF.receptor	D/B	-0.00596	-1.29353	1.281601	1
HGF.receptor	D/C	0.123321	-1.16424	1.410885	1
IFN.gamma	A/E	0.06658	-1.22098	1.354144	1
IFN.gamma	B/E	0.091151	-1.19641	1.378715	1
IFN.gamma	C/E	0.25105	-1.03651	1.538613	1
IFN.gamma	D/E	0.063843	-1.22372	1.351406	1
IFN.gamma	B/A	0.024571	-1.26299	1.312134	1
IFN.gamma	C/A	0.184469	-1.10309	1.472032	1
IFN.gamma	D/A	-0.00274	-1.2903	1.284826	1
IFN.gamma	C/B	0.159898	-1.12767	1.447462	1
IFN.gamma	D/B	-0.02731	-1.31487	1.260255	1
IFN.gamma	D/C	-0.18721	-1.47477	1.100357	1
IL.12	A/E	-0.41984	-1.7074	0.867725	1
IL.12	B/E	0.306472	-0.98109	1.594036	1
IL.12	C/E	-0.13656	-1.42412	1.151007	1
IL.12	D/E	-0.1022	-1.38976	1.185365	1
IL.12	B/A	0.726311	-0.56125	2.013875	1
IL.12	C/A	0.283283	-1.00428	1.570846	1
IL.12	D/A	0.31764	-0.96992	1.605204	1
IL.12	C/B	-0.44303	-1.73059	0.844535	1
IL.12	D/B	-0.40867	-1.69623	0.878892	1
IL.12	D/C	0.034357	-1.25321	1.321921	1

IL.1ra	A/E	0.231602	-1.05596	1.519165	1
IL.1ra	B/E	0.401115	-0.88645	1.688678	1
IL.1ra	C/E	-0.29876	-1.58632	0.988808	1
IL.1ra	D/E	0.279447	-1.00812	1.56701	1
IL.1ra	B/A	0.169513	-1.11805	1.457077	1
IL.1ra	C/A	-0.53036	-1.81792	0.757207	1
IL.1ra	D/A	0.047845	-1.23972	1.335409	1
IL.1ra	C/B	-0.69987	-1.98743	0.587694	1
IL.1ra	D/B	-0.12167	-1.40923	1.165895	1
IL.1ra	D/C	0.578202	-0.70936	1.865765	1
IL.2	A/E	-0.00384	-1.2914	1.283726	1
IL.2	B/E	0.072531	-1.21503	1.360095	1
IL.2	C/E	0.037938	-1.24963	1.325501	1
IL.2	D/E	0.007556	-1.28001	1.295119	1
IL.2	B/A	0.076369	-1.21119	1.363932	1
IL.2	C/A	0.041776	-1.24579	1.329339	1
IL.2	D/A	0.011393	-1.27617	1.298957	1
IL.2	C/B	-0.03459	-1.32216	1.25297	1
IL.2	D/B	-0.06498	-1.35254	1.222588	1
IL.2	D/C	-0.03038	-1.31795	1.257181	1
IL.4	A/E	-0.0338	-1.32137	1.25376	1
IL.4	B/E	-0.00952	-1.29708	1.278045	1
IL.4	C/E	0.007073	-1.28049	1.294637	1
IL.4	D/E	0.00135	-1.28621	1.288914	1

IL.4	B/A	0.024285	-1.26328	1.311849	1
IL.4	C/A	0.040877	-1.24669	1.32844	1
IL.4	D/A	0.035154	-1.25241	1.322717	1
IL.4	C/B	0.016591	-1.27097	1.304155	1
IL.4	D/B	0.010868	-1.2767	1.298432	1
IL.4	D/C	-0.00572	-1.29329	1.28184	1
IL.6	A/E	-0.08436	-1.37193	1.203201	1
IL.6	B/E	1.368284	0.080721	2.655848	0.012356
IL.6	C/E	0.270008	-1.01756	1.557571	1
IL.6	D/E	0.75137	-0.53619	2.038933	1
IL.6	B/A	1.452647	0.165083	2.74021	0.002396
IL.6	C/A	0.35437	-0.93319	1.641933	1
IL.6	D/A	0.835732	-0.45183	2.123295	0.999918
IL.6	C/B	-1.09828	-2.38584	0.189287	0.527659
IL.6	D/B	-0.61691	-1.90448	0.670649	1
IL.6	D/C	0.481362	-0.8062	1.768925	1
IL.7	A/E	-0.18069	-1.46826	1.10687	1
IL.7	B/E	0.150554	-1.13701	1.438117	1
IL.7	C/E	0.346557	-0.94101	1.634121	1
IL.7	D/E	0.491123	-0.79644	1.778686	1
IL.7	B/A	0.331247	-0.95632	1.618811	1
IL.7	C/A	0.527251	-0.76031	1.814814	1
IL.7	D/A	0.671816	-0.61575	1.95938	1
IL.7	C/B	0.196004	-1.09156	1.483567	1

IL.7	D/B	0.340569	-0.94699	1.628132	1
IL.7	D/C	0.144565	-1.143	1.432129	1
IL.8	A/E	0.126378	-1.16119	1.413941	1
IL.8	B/E	0.693238	-0.59432	1.980802	1
IL.8	C/E	0.668738	-0.61883	1.956301	1
IL.8	D/E	1.775656	0.488093	3.06322	1.23E-06
IL.8	B/A	0.56686	-0.7207	1.854424	1
IL.8	C/A	0.54236	-0.7452	1.829923	1
IL.8	D/A	1.649278	0.361715	2.936842	2.96E-05
IL.8	C/B	-0.0245	-1.31206	1.263063	1
IL.8	D/B	1.082418	-0.20515	2.369981	0.594911
IL.8	D/C	1.106919	-0.18064	2.394482	0.491408
IL17RB	A/E	-0.3459	-1.63346	0.941665	1
IL17RB	B/E	-0.32447	-1.61203	0.963093	1
IL17RB	C/E	-0.47892	-1.76649	0.808641	1
IL17RB	D/E	-0.27818	-1.56574	1.009386	1
IL17RB	B/A	0.021428	-1.26614	1.308991	1
IL17RB	C/A	-0.13302	-1.42059	1.15454	1
IL17RB	D/A	0.067721	-1.21984	1.355285	1
IL17RB	C/B	-0.15445	-1.44201	1.133112	1
IL17RB	D/B	0.046294	-1.24127	1.333857	1
IL17RB	D/C	0.200745	-1.08682	1.488308	1
IL2RA	A/E	-0.11799	-1.40555	1.169577	1
IL2RA	B/E	-0.06306	-1.35063	1.2245	1

IL2RA	C/E	-0.12032	-1.40789	1.167241	1
IL2RA	D/E	-0.00278	-1.29034	1.284785	1
IL2RA	B/A	0.054923	-1.23264	1.342486	1
IL2RA	C/A	-0.00234	-1.2899	1.285227	1
IL2RA	D/A	0.115208	-1.17236	1.402771	1
IL2RA	C/B	-0.05726	-1.34482	1.230304	1
IL2RA	D/B	0.060285	-1.22728	1.347848	1
IL2RA	D/C	0.117544	-1.17002	1.405108	1
IL6RA	A/E	-0.33998	-1.62754	0.947587	1
IL6RA	B/E	-0.33233	-1.61989	0.955234	1
IL6RA	C/E	-0.49598	-1.78354	0.791583	1
IL6RA	D/E	0.152035	-1.13553	1.439598	1
IL6RA	B/A	0.007647	-1.27992	1.29521	1
IL6RA	C/A	-0.156	-1.44357	1.131559	1
IL6RA	D/A	0.492011	-0.79555	1.779574	1
IL6RA	C/B	-0.16365	-1.45121	1.123912	1
IL6RA	D/B	0.484364	-0.8032	1.771928	1
IL6RA	D/C	0.648016	-0.63955	1.935579	1
Kallikrein.11	A/E	-0.44654	-1.7341	0.841022	1
Kallikrein.11	B/E	-0.31073	-1.5983	0.97683	1
Kallikrein.11	C/E	-0.50939	-1.79696	0.77817	1
Kallikrein.11	D/E	-0.3087	-1.59627	0.978861	1
Kallikrein.11	B/A	0.135808	-1.15176	1.423371	1
Kallikrein.11	C/A	-0.06285	-1.35042	1.224711	1

Kallikrein.11	D/A	0.137839	-1.14972	1.425403	1
Kallikrein.11	C/B	-0.19866	-1.48622	1.088903	1
Kallikrein.11	D/B	0.002031	-1.28553	1.289595	1
Kallikrein.11	D/C	0.200692	-1.08687	1.488255	1
Kallikrein.6	A/E	-0.57193	-1.85949	0.715635	1
Kallikrein.6	B/E	-0.23184	-1.51941	1.055719	1
Kallikrein.6	C/E	-0.24759	-1.53516	1.039971	1
Kallikrein.6	D/E	-0.10984	-1.3974	1.177724	1
Kallikrein.6	B/A	0.340084	-0.94748	1.627648	1
Kallikrein.6	C/A	0.324337	-0.96323	1.6119	1
Kallikrein.6	D/A	0.46209	-0.82547	1.749653	1
Kallikrein.6	C/B	-0.01575	-1.30331	1.271816	1
Kallikrein.6	D/B	0.122005	-1.16556	1.409569	1
Kallikrein.6	D/C	0.137753	-1.14981	1.425316	1
LAP.TGF.beta.1	A/E	-0.38507	-1.67264	0.902491	1
LAP.TGF.beta.1	B/E	-0.07898	-1.36654	1.208587	1
LAP.TGF.beta.1	C/E	-0.24775	-1.53532	1.039809	1
LAP.TGF.beta.1	D/E	0.264267	-1.0233	1.551831	1
LAP.TGF.beta.1	B/A	0.306097	-0.98147	1.59366	1
LAP.TGF.beta.1	C/A	0.137319	-1.15024	1.424882	1
LAP.TGF.beta.1	D/A	0.64934	-0.63822	1.936903	1
LAP.TGF.beta.1	C/B	-0.16878	-1.45634	1.118786	1
LAP.TGF.beta.1	D/B	0.343243	-0.94432	1.630807	1
LAP.TGF.beta.1	D/C	0.512021	-0.77554	1.799585	1

MCP.1	A/E	-0.38498	-1.67254	0.902586	1
MCP.1	B/E	-0.07715	-1.36471	1.210416	1
MCP.1	C/E	-0.25963	-1.54719	1.027937	1
MCP.1	D/E	0.341067	-0.9465	1.62863	1
MCP.1	B/A	0.30783	-0.97973	1.595393	1
MCP.1	C/A	0.12535	-1.16221	1.412914	1
MCP.1	D/A	0.726044	-0.56152	2.013607	1
MCP.1	C/B	-0.18248	-1.47004	1.105084	1
MCP.1	D/B	0.418214	-0.86935	1.705778	1
MCP.1	D/C	0.600694	-0.68687	1.888257	1
MIA	A/E	-0.63378	-1.92134	0.653783	1
MIA	B/E	-0.64632	-1.93388	0.641247	1
MIA	C/E	-0.603	-1.89056	0.684566	1
MIA	D/E	-0.2945	-1.58207	0.99306	1
MIA	B/A	-0.01254	-1.3001	1.275027	1
MIA	C/A	0.030784	-1.25678	1.318347	1
MIA	D/A	0.339277	-0.94829	1.62684	1
MIA	C/B	0.04332	-1.24424	1.330883	1
MIA	D/B	0.351813	-0.93575	1.639376	1
MIA	D/C	0.308493	-0.97907	1.596057	1
MIC.A	A/E	-0.34743	-1.63499	0.940134	1
MIC.A	B/E	0.068764	-1.2188	1.356327	1
MIC.A	C/E	-0.82032	-2.10788	0.467242	0.999975
MIC.A	D/E	0.200954	-1.08661	1.488517	1

MIC.A	B/A	0.416193	-0.87137	1.703757	1
MIC.A	C/A	-0.47289	-1.76046	0.814671	1
MIC.A	D/A	0.548383	-0.73918	1.835947	1
MIC.A	C/B	-0.88909	-2.17665	0.398478	0.997745
MIC.A	D/B	0.13219	-1.15537	1.419754	1
MIC.A	D/C	1.021275	-0.26629	2.308839	0.829279
Midkine	A/E	0.098438	-1.18913	1.386001	1
Midkine	B/E	0.714716	-0.57285	2.00228	1
Midkine	C/E	0.164197	-1.12337	1.451761	1
Midkine	D/E	0.399948	-0.88762	1.687511	1
Midkine	B/A	0.616278	-0.67129	1.903842	1
Midkine	C/A	0.065759	-1.2218	1.353323	1
Midkine	D/A	0.30151	-0.98605	1.589073	1
Midkine	C/B	-0.55052	-1.83808	0.737044	1
Midkine	D/B	-0.31477	-1.60233	0.972795	1
Midkine	D/C	0.235751	-1.05181	1.523314	1
MMP.3	A/E	-0.05737	-1.34493	1.230195	1
MMP.3	B/E	-0.04233	-1.32989	1.245236	1
MMP.3	C/E	-0.04818	-1.33574	1.239386	1
MMP.3	D/E	0.079491	-1.20807	1.367054	1
MMP.3	B/A	0.015041	-1.27252	1.302604	1
MMP.3	C/A	0.009191	-1.27837	1.296754	1
MMP.3	D/A	0.136859	-1.1507	1.424422	1
MMP.3	C/B	-0.00585	-1.29341	1.281713	1

MMP.3	D/B	0.121818	-1.16575	1.409382	1
MMP.3	D/C	0.127668	-1.1599	1.415232	1
MPO	A/E	-0.09423	-1.38179	1.193336	1
MPO	B/E	0.001222	-1.28634	1.288785	1
MPO	C/E	-0.17332	-1.46089	1.114242	1
MPO	D/E	0.184051	-1.10351	1.471614	1
MPO	B/A	0.09545	-1.19211	1.383013	1
MPO	C/A	-0.07909	-1.36666	1.20847	1
MPO	D/A	0.278278	-1.00929	1.565842	1
MPO	C/B	-0.17454	-1.46211	1.11302	1
MPO	D/B	0.182829	-1.10473	1.470392	1
MPO	D/C	0.357372	-0.93019	1.644936	1
MYD88	A/E	-0.40192	-1.68948	0.885647	1
MYD88	B/E	0.000381	-1.28718	1.287945	1
MYD88	C/E	-0.24244	-1.53	1.045125	1
MYD88	D/E	-0.14605	-1.43361	1.141514	1
MYD88	B/A	0.402298	-0.88527	1.689862	1
MYD88	C/A	0.159479	-1.12808	1.447042	1
MYD88	D/A	0.255868	-1.0317	1.543431	1
MYD88	C/B	-0.24282	-1.53038	1.044744	1
MYD88	D/B	-0.14643	-1.43399	1.141133	1
MYD88	D/C	0.096389	-1.19117	1.383953	1
Osteoprotegerin	A/E	-0.32379	-1.61136	0.963771	1
Osteoprotegerin	B/E	-0.02155	-1.30911	1.266012	1

Osteoprotegerin	C/E	-0.27586	-1.56342	1.011706	1
Osteoprotegerin	D/E	-0.02826	-1.31583	1.259302	1
Osteoprotegerin	B/A	0.302241	-0.98532	1.589805	1
Osteoprotegerin	C/A	0.047936	-1.23963	1.335499	1
Osteoprotegerin	D/A	0.295531	-0.99203	1.583094	1
Osteoprotegerin	C/B	-0.25431	-1.54187	1.033258	1
Osteoprotegerin	D/B	-0.00671	-1.29427	1.280853	1
Osteoprotegerin	D/C	0.247595	-1.03997	1.535159	1
PDGF.subunit.B	A/E	-0.73187	-2.01943	0.555694	1
PDGF.subunit.B	B/E	-0.14729	-1.43485	1.140275	1
PDGF.subunit.B	C/E	-0.23398	-1.52154	1.053586	1
PDGF.subunit.B	D/E	0.916642	-0.37092	2.204206	0.991819
PDGF.subunit.B	B/A	0.584581	-0.70298	1.872144	1
PDGF.subunit.B	C/A	0.497891	-0.78967	1.785455	1
PDGF.subunit.B	D/A	1.648511	0.360948	2.936075	3.02E-05
PDGF.subunit.B	C/B	-0.08669	-1.37425	1.200874	1
PDGF.subunit.B	D/B	1.06393	-0.22363	2.351494	0.672233
PDGF.subunit.B	D/C	1.15062	-0.13694	2.438184	0.322841
PECAM.1	A/E	-0.48737	-1.77494	0.800192	1
PECAM.1	B/E	-0.25059	-1.53815	1.036972	1
PECAM.1	C/E	-0.4692	-1.75676	0.818366	1
PECAM.1	D/E	-0.15511	-1.44267	1.132458	1
PECAM.1	B/A	0.236781	-1.05078	1.524344	1
PECAM.1	C/A	0.018174	-1.26939	1.305738	1

PECAM.1	D/A	0.332266	-0.9553	1.619829	1
PECAM.1	C/B	-0.21861	-1.50617	1.068957	1
PECAM.1	D/B	0.095485	-1.19208	1.383049	1
PECAM.1	D/C	0.314092	-0.97347	1.601655	1
PIGF	A/E	-0.64893	-1.93649	0.638636	1
PIGF	B/E	-0.36402	-1.65158	0.923547	1
PIGF	C/E	-0.56469	-1.85226	0.72287	1
PIGF	D/E	-0.31558	-1.60314	0.971987	1
PIGF	B/A	0.284912	-1.00265	1.572475	1
PIGF	C/A	0.084234	-1.20333	1.371798	1
PIGF	D/A	0.333351	-0.95421	1.620914	1
PIGF	C/B	-0.20068	-1.48824	1.086886	1
PIGF	D/B	0.048439	-1.23912	1.336003	1
PIGF	D/C	0.249117	-1.03845	1.53668	1
Prolactin	A/E	1.228535	-0.05903	2.516098	0.122194
Prolactin	B/E	0.975752	-0.31181	2.263315	0.938496
Prolactin	C/E	1.650283	0.36272	2.937847	2.89E-05
Prolactin	D/E	-0.03449	-1.32206	1.253071	1
Prolactin	B/A	-0.25278	-1.54035	1.03478	1
Prolactin	C/A	0.421749	-0.86581	1.709312	1
Prolactin	D/A	-1.26303	-2.55059	0.024536	0.073555
Prolactin	C/B	0.674532	-0.61303	1.962095	1
Prolactin	D/B	-1.01024	-2.29781	0.277319	0.862
Prolactin	D/C	-1.68478	-2.97234	-0.39721	1.24E-05

Prostasin	A/E	-0.09506	-1.38262	1.192506	1
Prostasin	B/E	-0.0761	-1.36367	1.211462	1
Prostasin	C/E	-0.21866	-1.50622	1.068907	1
Prostasin	D/E	0.081616	-1.20595	1.36918	1
Prostasin	B/A	0.018956	-1.26861	1.306519	1
Prostasin	C/A	-0.1236	-1.41116	1.163964	1
Prostasin	D/A	0.176673	-1.11089	1.464237	1
Prostasin	C/B	-0.14256	-1.43012	1.145008	1
Prostasin	D/B	0.157718	-1.12985	1.445281	1
Prostasin	D/C	0.300273	-0.98729	1.587836	1
PSA	A/E	0.730205	-0.55736	2.017768	1
PSA	B/E	-0.24568	-1.53324	1.041882	1
PSA	C/E	-0.34369	-1.63125	0.943872	1
PSA	D/E	0.125083	-1.16248	1.412646	1
PSA	B/A	-0.97589	-2.26345	0.311677	0.938273
PSA	C/A	-1.0739	-2.36146	0.213667	0.630876
PSA	D/A	-0.60512	-1.89269	0.682441	1
PSA	C/B	-0.09801	-1.38557	1.189553	1
PSA	D/B	0.370764	-0.9168	1.658327	1
PSA	D/C	0.468774	-0.81879	1.756337	1
REG.4	A/E	-0.01744	-1.30501	1.27012	1
REG.4	B/E	-0.0483	-1.33586	1.239265	1
REG.4	C/E	-0.1459	-1.43346	1.141667	1
REG.4	D/E	0.288647	-0.99892	1.57621	1

REG.4	B/A	-0.03085	-1.31842	1.256709	1
REG.4	C/A	-0.12845	-1.41602	1.15911	1
REG.4	D/A	0.30609	-0.98147	1.593654	1
REG.4	C/B	-0.0976	-1.38516	1.189965	1
REG.4	D/B	0.336945	-0.95062	1.624508	1
REG.4	D/C	0.434544	-0.85302	1.722107	1
Stem.cell.factor	A/E	-0.25866	-1.54622	1.028906	1
Stem.cell.factor	B/E	-0.26823	-1.55579	1.019333	1
Stem.cell.factor	C/E	-0.44963	-1.73719	0.837933	1
Stem.cell.factor	D/E	-0.40021	-1.68778	0.887349	1
Stem.cell.factor	B/A	-0.00957	-1.29714	1.27799	1
Stem.cell.factor	C/A	-0.19097	-1.47854	1.09659	1
Stem.cell.factor	D/A	-0.14156	-1.42912	1.146006	1
Stem.cell.factor	C/B	-0.1814	-1.46896	1.106163	1
Stem.cell.factor	D/B	-0.13198	-1.41955	1.155579	1
Stem.cell.factor	D/C	0.049416	-1.23815	1.336979	1
TGF.alpha	A/E	0.01454	-1.27302	1.302104	1
TGF.alpha	B/E	-0.05146	-1.33903	1.2361	1
TGF.alpha	C/E	-0.2037	-1.49126	1.083867	1
TGF.alpha	D/E	-0.16417	-1.45173	1.123398	1
TGF.alpha	B/A	-0.066	-1.35357	1.22156	1
TGF.alpha	C/A	-0.21824	-1.5058	1.069327	1
TGF.alpha	D/A	-0.17871	-1.46627	1.108857	1
TGF.alpha	C/B	-0.15223	-1.4398	1.13533	1

TGF.alpha	D/B	-0.1127	-1.40027	1.174861	1
TGF.alpha	D/C	0.039531	-1.24803	1.327094	1
Thrombopoietin	A/E	-0.37393	-1.66149	0.913635	1
Thrombopoietin	B/E	-0.14577	-1.43334	1.141791	1
Thrombopoietin	C/E	-0.33228	-1.61984	0.955288	1
Thrombopoietin	D/E	-0.11724	-1.4048	1.170322	1
Thrombopoietin	B/A	0.228157	-1.05941	1.51572	1
Thrombopoietin	C/A	0.041654	-1.24591	1.329217	1
Thrombopoietin	D/A	0.256687	-1.03088	1.544251	1
Thrombopoietin	C/B	-0.1865	-1.47407	1.10106	1
Thrombopoietin	D/B	0.028531	-1.25903	1.316094	1
Thrombopoietin	D/C	0.215034	-1.07253	1.502597	1
TIE2	A/E	-0.22035	-1.50791	1.067217	1
TIE2	B/E	-0.22496	-1.51252	1.062603	1
TIE2	C/E	-0.22292	-1.51048	1.064642	1
TIE2	D/E	0.048792	-1.23877	1.336356	1
TIE2	B/A	-0.00461	-1.29218	1.282949	1
TIE2	C/A	-0.00257	-1.29014	1.284989	1
TIE2	D/A	0.269139	-1.01842	1.556702	1
TIE2	C/B	0.002039	-1.28552	1.289603	1
TIE2	D/B	0.273753	-1.01381	1.561316	1
TIE2	D/C	0.271714	-1.01585	1.559277	1
Tissue.Factor	A/E	-0.39283	-1.68039	0.894736	1
Tissue.Factor	B/E	-0.24589	-1.53345	1.041678	1

Tissue.Factor	C/E	-0.44157	-1.72913	0.845997	1
Tissue.Factor	D/E	-0.44497	-1.73254	0.842591	1
Tissue.Factor	B/A	0.146941	-1.14062	1.434505	1
Tissue.Factor	C/A	-0.04874	-1.3363	1.238824	1
Tissue.Factor	D/A	-0.05215	-1.33971	1.235418	1
Tissue.Factor	C/B	-0.19568	-1.48324	1.091882	1
Tissue.Factor	D/B	-0.19909	-1.48665	1.088477	1
Tissue.Factor	D/C	-0.00341	-1.29097	1.284158	1
TNF	A/E	-0.00529	-1.29286	1.28227	1
TNF	B/E	-0.03084	-1.31841	1.25672	1
TNF	C/E	0.068782	-1.21878	1.356346	1
TNF	D/E	0.112691	-1.17487	1.400255	1
TNF	B/A	-0.02555	-1.31311	1.262014	1
TNF	C/A	0.074076	-1.21349	1.361639	1
TNF	D/A	0.117985	-1.16958	1.405548	1
TNF	C/B	0.099626	-1.18794	1.387189	1
TNF	D/B	0.143535	-1.14403	1.431098	1
TNF	D/C	0.043909	-1.24365	1.331472	1
TNF.R2	A/E	-0.41884	-1.70641	0.868721	1
TNF.R2	B/E	-0.0639	-1.35146	1.223665	1
TNF.R2	C/E	-0.3718	-1.65936	0.915762	1
TNF.R2	D/E	0.006443	-1.28112	1.294006	1
TNF.R2	B/A	0.354944	-0.93262	1.642507	1
TNF.R2	C/A	0.047041	-1.24052	1.334605	1

TNF.R2	D/A	0.425286	-0.86228	1.712849	1
TNF.R2	C/B	-0.3079	-1.59547	0.979661	1
TNF.R2	D/B	0.070342	-1.21722	1.357905	1
TNF.R2	D/C	0.378244	-0.90932	1.665808	1
TNF.RI	A/E	-0.27892	-1.56648	1.008647	1
TNF.RI	B/E	0.016103	-1.27146	1.303666	1
TNF.RI	C/E	-0.18978	-1.47734	1.097785	1
TNF.RI	D/E	-0.06358	-1.35114	1.223986	1
TNF.RI	B/A	0.29502	-0.99254	1.582583	1
TNF.RI	C/A	0.089138	-1.19843	1.376702	1
TNF.RI	D/A	0.21534	-1.07222	1.502903	1
TNF.RI	C/B	-0.20588	-1.49344	1.081682	1
TNF.RI	D/B	-0.07968	-1.36724	1.207883	1
TNF.RI	D/C	0.126201	-1.16136	1.413765	1
TNFRSF4	A/E	-0.45869	-1.74625	0.828874	1
TNFRSF4	B/E	-0.0136	-1.30116	1.273963	1
TNFRSF4	C/E	-0.20048	-1.48805	1.087082	1
TNFRSF4	D/E	-0.05732	-1.34488	1.230248	1
TNFRSF4	B/A	0.445089	-0.84247	1.732652	1
TNFRSF4	C/A	0.258208	-1.02936	1.545771	1
TNFRSF4	D/A	0.401374	-0.88619	1.688937	1
TNFRSF4	C/B	-0.18688	-1.47444	1.100682	1
TNFRSF4	D/B	-0.04371	-1.33128	1.243849	1
TNFRSF4	D/C	0.143166	-1.1444	1.43073	1

TNFSF14	A/E	0.040668	-1.2469	1.328231	1
TNFSF14	B/E	0.299366	-0.9882	1.58693	1
TNFSF14	C/E	0.009446	-1.27812	1.297009	1
TNFSF14	D/E	0.276483	-1.01108	1.564047	1
TNFSF14	B/A	0.258699	-1.02886	1.546262	1
TNFSF14	C/A	-0.03122	-1.31879	1.256341	1
TNFSF14	D/A	0.235815	-1.05175	1.523379	1
TNFSF14	C/B	-0.28992	-1.57748	0.997643	1
TNFSF14	D/B	-0.02288	-1.31045	1.26468	1
TNFSF14	D/C	0.267037	-1.02053	1.554601	1
TR.AP	A/E	-0.35322	-1.64079	0.934339	1
TR.AP	B/E	-0.19405	-1.48161	1.093517	1
TR.AP	C/E	-0.28759	-1.57516	0.999971	1
TR.AP	D/E	0.055106	-1.23246	1.34267	1
TR.AP	B/A	0.159178	-1.12839	1.446742	1
TR.AP	C/A	0.065632	-1.22193	1.353196	1
TR.AP	D/A	0.408331	-0.87923	1.695894	1
TR.AP	C/B	-0.09355	-1.38111	1.194017	1
TR.AP	D/B	0.249153	-1.03841	1.536716	1
TR.AP	D/C	0.342699	-0.94486	1.630262	1
U.PAR	A/E	-0.11941	-1.40697	1.168158	1
U.PAR	B/E	-0.00132	-1.28888	1.286246	1
U.PAR	C/E	-0.26198	-1.54954	1.025584	1
U.PAR	D/E	0.0469	-1.24066	1.334463	1

U.PAR	B/A	0.118089	-1.16947	1.405652	1
U.PAR	C/A	-0.14257	-1.43014	1.14499	1
U.PAR	D/A	0.166306	-1.12126	1.453869	1
U.PAR	C/B	-0.26066	-1.54823	1.026902	1
U.PAR	D/B	0.048217	-1.23935	1.33578	1
U.PAR	D/C	0.308879	-0.97868	1.596442	1
VEGF.A	A/E	-0.38499	-1.67255	0.902576	1
VEGF.A	B/E	-0.01992	-1.30749	1.26764	1
VEGF.A	C/E	-0.24658	-1.53414	1.040988	1
VEGF.A	D/E	0.092884	-1.19468	1.380447	1
VEGF.A	B/A	0.365065	-0.9225	1.652628	1
VEGF.A	C/A	0.138413	-1.14915	1.425976	1
VEGF.A	D/A	0.477872	-0.80969	1.765435	1
VEGF.A	C/B	-0.22665	-1.51422	1.060912	1
VEGF.A	D/B	0.112807	-1.17476	1.40037	1
VEGF.A	D/C	0.339459	-0.9481	1.627022	1
VEGF.D	A/E	-0.16086	-1.44842	1.126708	1
VEGF.D	B/E	-0.23253	-1.52009	1.055032	1
VEGF.D	C/E	-0.17385	-1.46142	1.11371	1
VEGF.D	D/E	-0.1297	-1.41726	1.157868	1
VEGF.D	B/A	-0.07168	-1.35924	1.215887	1
VEGF.D	C/A	-0.013	-1.30056	1.274565	1
VEGF.D	D/A	0.03116	-1.2564	1.318723	1
VEGF.D	C/B	0.058678	-1.22889	1.346242	1

VEGF.D	D/B	0.102836	-1.18473	1.390399	1
VEGF.D	D/C	0.044158	-1.24341	1.331721	1
VEGFR.2	A/E	-0.15969	-1.44725	1.127876	1
VEGFR.2	B/E	-0.26163	-1.5492	1.02593	1
VEGFR.2	C/E	-0.24783	-1.53539	1.039737	1
VEGFR.2	D/E	-0.15742	-1.44499	1.13014	1
VEGFR.2	B/A	-0.10195	-1.38951	1.185617	1
VEGFR.2	C/A	-0.08814	-1.3757	1.199424	1
VEGFR.2	D/A	0.002264	-1.2853	1.289827	1
VEGFR.2	C/B	0.013807	-1.27376	1.301371	1
VEGFR.2	D/B	0.10421	-1.18335	1.391773	1
VEGFR.2	D/C	0.090403	-1.19716	1.377966	1

311

Table S4: Anova Table (Type II tests) or 2-Way Anova factor analysis for Proseek Assay						
	SS	Df	F-value	Pr(>F)	Sig	
Group	73	2	6.49E+01	2.20E-16	***	
Proteins	65377	91	1.28E+03	2.20E-16	***	
Sample	766	72	1.89E+01	2.20E-16	***	
Group:Proteins	228	182	2.23E+00	2.20E-16	***	
Residuals	3942	7012				

Sig Codes: 0 '***', 0.001 '**', 0.01 '*'

Comparison		Protein	Difference	Lower CI	Upper CI	Q-value
Malignant	Benign	CEA	1.97	1.08	2.85	0.00
Malignant	Healthy	CEA	2.11	1.02	3.19	0.00
Malignant	Healthy	IL.8	1.22	0.14	2.31	0.00
Benign	Healthy	Prolactin	1.10	0.02	2.19	0.04
Malignant	Benign	IL.8	0.81	-0.07	1.70	0.21
Malignant	Benign	PDGF.subunit.B	0.78	-0.10	1.67	0.34
Malignant	Healthy	Prolactin	0.81	-0.28	1.89	0.92

Malignant	Benign	CXCL5	0.63	-0.26	1.52	0.98
Malignant	Benign	Amphiregulin	0.62	-0.27	1.51	0.99

Table S5: p- values calculated for stage specific protein expressions analyzed by Bio-Plex Assay (Stage specific (A-D, n=15) and healthy group E											
Comparison	Target Biomarker	p-adju	Comparison	Target Biomarker	p-adju	Comparison	Target Biomarker	p-adju	Comparison	Target Biomarker	p-adju
A/E	Hu.IL.8..54.	0.006	B/E	Hu.IL.8..54.	0.002	C/E	Hu.MIP.1b..18.	0.017	D/E	Hu.PDGF.bb..47.	2E-07
A/E	Hu.MCP.1.MCAF...53.	0.053	B/E	Hu.MCP.1.MCAF...53.	0.074	C/E	Hu.IL.8..54.	0.066	D/E	Hu.IL.8..54.	6E-05
A/E	Hu.IL.4..52.	0.113	B/E	Hu.IL.4..52.	0.210	C/E	Hu.IL.4..52.	0.215	D/E	Hu.MCP.1.MCAF...53.	5E-04
A/E	Hu.G.CSF..57.	0.275	B/E	Hu.IL.6..19.	0.223	C/E	Hu.IL.15..73.	0.376	D/E	Hu.IFN.g..21.	2E-03
A/E	Hu.MIP.1b..18.	0.522	B/E	Hu.PDGF.bb..47.	0.739	C/E	Hu.IL.2..38.	0.712	D/E	Hu.IL.4..52.	4E-03
A/E	Hu.IL.7..74.	0.954	B/E	Hu.G.CSF..57.	0.741	C/E	Hu.PDGF.bb..47.	0.744	D/A	Hu.PDGF.bb..47.	4E-03
A/E	Hu.IL.6..19.	0.978	B/E	Hu.IL.9..77.	1.000	C/E	Hu.G.CSF..57.	0.757	D/E	Hu.MIP.1a..55.	4E-03
A/E	Hu.IL.5..33.	0.986	B/E	Hu.VEGF..45.	1.000	C/E	Hu.GM.CSF..3 4.	0.796	D/E	Hu.IL.1b..39.	1E-02
A/E	Hu.VEGF..45.	0.992	B/E	Hu.IL.7..74.	1.000	C/E	Hu.MCP.1.MCAF...53.	0.887	D/E	Hu.IL.9..77.	2E-02
A/E	Hu.IL.13..51.	0.995	B/E	Hu.GM.CSF..34.	1.000	C/E	Hu.IL.9..77.	0.987	D/E	Hu.IL.6..19.	3E-02
A/E	Hu.IFN.g..21.	1.000	B/E	Hu.IFN.g..21.	1.000	C/E	Hu.IL.6..19.	0.993	D/E	Hu.IL.7..74.	6E-02
A/E	Hu.IL.10..56.	1.000	B/E	Hu.MIP.1b..18.	1.000	C/E	Hu.VEGF..45.	0.998	D/E	Hu.IL.17..76.	9E-02
A/E	Hu.IL.15..73.	1.000	B/E	Hu.TNF.a..36.	1.000	C/E	Hu.IL.5..33.	0.998	D/A	Hu.MIP.1a..55.	9E-02
A/E	Hu.IL.9..77.	1.000	B/A	Hu.IL.13..51.	1.000	C/B	Hu.IL.2..38.	0.999	D/C	Hu.MIP.1a..55.	1E-01
A/E	Hu.GM.CSF..34.	1.000	B/A	Hu.IL.5..33.	1.000	C/E	Hu.IL.1ra..25.	1.000	D/E	Hu.G.CSF..57.	1E-01
A/E	Hu.TNF.a..36.	1.000	B/E	Hu.IL.10..56.	1.000	C/E	Hu.IFN.g..21.	1.000	D/E	Hu.MIP.1b..18.	2E-01
A/E	Hu.Eotaxin..43.	1.000	B/E	Hu.IL.1b..39.	1.000	C/B	Hu.MIP.1b..18.	1.000	D/E	Hu.TNF.a..36.	2E-01
A/E	Hu.IL.1b..39.	1.000	B/E	Hu.Eotaxin..43.	1.000	C/E	Hu.Eotaxin..43.	1.000	D/E	Hu.IL.5..33.	2E-01
A/E	Hu.FGF.basic..44.	1.000	B/A	Hu.Eotaxin..43.	1.000	C/E	Hu.IL.17..76.	1.000	D/E	Hu.VEGF..45.	3E-01
A/E	Hu.IL.12.p70	1.000	B/A	Hu.FGF.basic..44.	1.000	C/A	Hu.IL.2..38.	1.000	D/E	Hu.FGF.basic..	5E-01

	...75.							44.	
A/E	Hu.IL.17..76.	1.000	B/A	Hu.FGF.basic..44.	1.000	C/B	Hu.IL.15..73.	1.000	D/B	Hu.MIP.1a..55.	5E-01
A/E	Hu.IL.1ra..25.	1.000	B/A	Hu.G.CSF..57.	1.000	C/E	Hu.IL.7..74.	1	D/E	Hu.IL.1ra..25.	6E-01
A/E	Hu.IL.2..38.	1.000	B/A	Hu.GM.CSF..34.	1.000	C/E	Hu.TNF.a..36.	1	D/E	Hu.IL.10..56.	8E-01
A/E	Hu.IP.10..48.	1.000	B/A	Hu.IFN.g..21.	1.000	C/E	Hu.IL.10..56.	1	D/C	Hu.PDGF.bb..47.	8E-01
A/E	Hu.MIP.1a..55.	1.000	B/A	Hu.IL.10..56.	1.000	C/E	Hu.IL.13..51.	1	D/B	Hu.PDGF.bb..47.	8E-01
A/E	Hu.PDGF.bb..47.	1.000	B/E	Hu.IL.12.p70..75.	1.000	C/A	Hu.Eotaxin..43.	1	D/A	Hu.FGF.basic..44.	9E-01
A/E	Hu.RANTES..37.	1.000	B/A	Hu.IL.12.p70..75.	1.000	C/B	Hu.Eotaxin..43.	1	D/C	Hu.IL.1b..39.	1E+00
			B/E	Hu.IL.13..51.	1.000	C/E	Hu.FGF.basic..44.	1	D/A	Hu.IL.1b..39.	1E+00
			B/E	Hu.IL.15..73.	1.000	C/A	Hu.FGF.basic..44.	1	D/B	Hu.IL.1b..39.	1E+00
			B/A	Hu.IL.15..73.	1.000	C/B	Hu.FGF.basic..44.	1	D/E	Hu.IL.2..38.	1E+00

			B/E	Hu.IL.17..76.	1.000	C/A	Hu.G.CSF..57.	1	D/E	Hu.GM.CSF..34.	1E+00
			B/A	Hu.IL.17..76.	1.000	C/B	Hu.G.CSF..57.	1	D/A	Hu.IL.17..76.	1E+00
			B/A	Hu.IL.1b..39.	1.000	C/A	Hu.GM.CSF..34.	1	D/C	Hu.FGF.basic..44.	1E+00
			B/E	Hu.IL.1ra..25.	1.000	C/B	Hu.GM.CSF..34.	1	D/E	Hu.IL.15..73.	1E+00
			B/A	Hu.IL.1ra..25.	1.000	C/A	Hu.IFN.g..21.	1	D/B	Hu.IFN.g..21.	1E+00
			B/E	Hu.IL.2..38.	1.000	C/B	Hu.IFN.g..21.	1	D/C	Hu.IFN.g..21.	1E+00
			B/A	Hu.IL.2..38.	1.000	C/A	Hu.IL.10..56.	1	D/B	Hu.FGF.basic..44.	1E+00
			B/A	Hu.IL.4..52.	1.000	C/B	Hu.IL.10..56.	1	D/A	Hu.IFN.g..21.	1E+00
			B/A	Hu.IL.5..33.	1.000	C/E	Hu.IL.12.p70..75.	1	D/B	Hu.IL.17..76.	1E+00
			B/A	Hu.IL.6..19.	1.000	C/A	Hu.IL.12.p70..75.	1	D/A	Hu.IL.9..77.	1E+00
			B/A	Hu.IL.7..74.	1.000	C/B	Hu.IL.12.p70..75.	1	D/E	Hu.IL.12.p70..75.	1E+00
			B/A	Hu.IL.8..54.	1.000	C/A	Hu.IL.13..51.	1	D/C	Hu.MCP.1.MC	1E+00

314

									AF...53.	
			B/A	Hu.IL.9..77.	1.000	C/B	Hu.IL.13..51.	1	D/C	Hu.IL.7..74.	1E+00
			B/E	Hu.IP.10..48.	1.000	C/A	Hu.IL.15..73.	1	D/B	Hu.IL.1ra..25.	1E+00
			B/A	Hu.IP.10..48.	1.000	C/A	Hu.IL.17..76.	1	D/B	Hu.IL.9..77.	1E+00
			B/A	Hu.MCP.1.MCAF...53.	1.000	C/B	Hu.IL.17..76.	1	D/C	Hu.IL.17..76.	1E+00
			B/E	Hu.MIP.1a..55.	1.000	C/E	Hu.IL.1b..39.	1	D/B	Hu.IL.5..33.	1E+00
			B/A	Hu.MIP.1a..55.	1.000	C/A	Hu.IL.1b..39.	1	D/A	Hu.TNF.a..36.	1E+00
			B/A	Hu.MIP.1b..18.	1.000	C/B	Hu.IL.1b..39.	1	D/B	Hu.IL.2..38.	1E+00
			B/A	Hu.PDGF.bb..47.	1.000	C/A	Hu.IL.1ra..25.	1	D/C	Hu.TNF.a..36.	1E+00
			B/E	Hu.RANTES..37.	1.000	C/B	Hu.IL.1ra..25.	1	D/B	Hu.TNF.a..36.	1E+00
			B/A	Hu.RANTES..37.	1.000	C/A	Hu.IL.4..52.	1	D/B	Hu.MIP.1b..18.	1E+00
			B/A	Hu.TNF.a..36.	1.000	C/B	Hu.IL.4..52.	1	D/A	Hu.IP.10..48.	1E+00
			B/A	Hu.VEGF..45.	1.000	C/A	Hu.IL.5..33.	1	D/B	Hu.IL.7..74.	1E+00
						C/B	Hu.IL.5..33.	1	D/E	Hu.Eotaxin..43.	1E+00
						C/A	Hu.IL.6..19.	1	D/A	Hu.Eotaxin..43.	1E+00
						C/B	Hu.IL.6..19.	1	D/B	Hu.Eotaxin..43	1E+00

									.	
						C/A	Hu.IL.7..74.	1	D/C	Hu.Eotaxin..43.	1E+00
						C/B	Hu.IL.7..74.	1	D/A	Hu.G.CSF..57.	1E+00
						C/A	Hu.IL.8..54.	1	D/B	Hu.G.CSF..57.	1E+00
						C/B	Hu.IL.8..54.	1	D/C	Hu.G.CSF..57.	1E+00
						C/A	Hu.IL.9..77.	1	D/A	Hu.GM.CSF..34.	1E+00
						C/B	Hu.IL.9..77.	1	D/B	Hu.GM.CSF..34.	1E+00
						C/E	Hu.IP.10..48.	1	D/C	Hu.GM.CSF..34.	1E+00
						C/A	Hu.IP.10..48.	1	D/A	Hu.IL.10..56.	1E+00
						C/B	Hu.IP.10..48.	1	D/B	Hu.IL.10..56.	1E+00
						C/A	Hu.MCP.1.MCAF...53.	1	D/C	Hu.IL.10..56.	1E+00
						C/B	Hu.MCP.1.MCAF...53.	1	D/A	Hu.IL.12.p70...75.	1E+00
						C/E	Hu.MIP.1a..55.	1	D/B	Hu.IL.12.p70...	1E+00

										75.	
					C/A	Hu.MIP.1a..55.	1	D/C	Hu.IL.12.p70...75.	1E+00	
					C/B	Hu.MIP.1a..55.	1	D/E	Hu.IL.13..51.	1E+00	
					C/A	Hu.MIP.1b..18.	1	D/A	Hu.IL.13..51.	1E+00	
					C/A	Hu.PDGF.bb..47.	1	D/B	Hu.IL.13..51.	1	
					C/B	Hu.PDGF.bb..47.	1	D/C	Hu.IL.13..51.	1	
					C/E	Hu.RANTES..37.	1	D/A	Hu.IL.15..73.	1	
					C/A	Hu.RANTES..37.	1	D/B	Hu.IL.15..73.	1	
					C/B	Hu.RANTES..37.	1	D/C	Hu.IL.15..73.	1	
					C/A	Hu.TNF.a..36.	1	D/A	Hu.IL.1ra..25.	1	
					C/B	Hu.TNF.a..36.	1	D/C	Hu.IL.1ra..25.	1	
					C/A	Hu.VEGF..45.	1	D/A	Hu.IL.2..38.	1	
					C/B	Hu.VEGF..45.	1	D/C	Hu.IL.2..38.	1	

								D/A	Hu.IL.4..52.	1
								D/B	Hu.IL.4..52.	1
								D/C	Hu.IL.4..52.	1
								D/A	Hu.IL.5..33.	1
								D/C	Hu.IL.5..33.	1
								D/A	Hu.IL.6..19.	1
								D/B	Hu.IL.6..19.	1
								D/C	Hu.IL.6..19.	1
								D/A	Hu.IL.7..74.	1
								D/A	Hu.IL.8..54.	1
								D/B	Hu.IL.8..54.	1
								D/C	Hu.IL.8..54.	1
								D/C	Hu.IL.9..77.	1
								D/E	Hu.IP.10..48.	1
								D/B	Hu.IP.10..48.	1
								D/C	Hu.IP.10..48.	1
								D/A	Hu.MCP.1.MCAF...53.	1
								D/B	Hu.MCP.1.MC	1

316

								AF...53.	
								D/A	Hu.MIP.1b..18.	1
								D/C	Hu.MIP.1b..18.	1
								D/E	Hu.RANTES..37.	1
								D/A	Hu.RANTES..37.	1
								D/B	Hu.RANTES..37.	1
								D/C	Hu.RANTES..37.	1
								D/A	Hu.VEGF..45.	1
								D/B	Hu.VEGF..45.	1
								D/C	Hu.VEGF..45.	1
								D/C	Hu.VEGF..45.	1

Table S6: Tukey honest significant differences post-hoc test for Bio-plex assay [Group- specific analysis]						
Comparison		Protein	Difference	Lower CI	Upper CI	Q-value
Malignant	Healthy	Hu.IL.8..54.	0.95	0.27	1.64	0
Malignant	Healthy	Hu.PDGF.bb..47.	0.95	0.26	1.63	0
Benign	Healthy	Hu.IL.8..54.	0.94	0.25	1.63	0
Malignant	Healthy	Hu.IL.4..52.	0.85	0.16	1.53	0
Malignant	Healthy	Hu.MIP.1b..18.	0.82	0.13	1.51	0
Benign	Healthy	Hu.MCP.1.MCAF...53.	0.82	0.13	1.5	0
Malignant	Healthy	Hu.MCP.1.MCAF...53.	0.81	0.12	1.5	0
Benign	Healthy	Hu.IL.4..52.	0.77	0.08	1.46	0.01
Malignant	Healthy	Hu.IFN.g..21.	0.71	0.03	1.4	0.03
Malignant	Healthy	Hu.IL.9..77.	0.71	0.02	1.4	0.03
Malignant	Healthy	Hu.G.CSF..57.	0.71	0.02	1.39	0.03
Malignant	Healthy	Hu.IL.6..19.	0.69	0.01	1.38	0.04
Benign	Healthy	Hu.G.CSF..57.	0.69	0	1.37	0.05
Benign	Healthy	Hu.IL.6..19.	0.65	-0.04	1.34	0.11

Malignant	Healthy	Hu.IL.5..33.	0.63	-0.06	1.31	0.17
Malignant	Healthy	Hu.IL.1b..39.	0.61	-0.07	1.3	0.21
Malignant	Healthy	Hu.VEGF..45.	0.61	-0.07	1.3	0.22
Malignant	Healthy	Hu.IL.7..74.	0.61	-0.08	1.3	0.23
Malignant	Healthy	Hu.IL.17..76.	0.61	-0.08	1.29	0.23
Malignant	Healthy	Hu.IL.15..73.	0.6	-0.08	1.29	0.25
Malignant	Healthy	Hu.IL.2..38.	0.59	-0.1	1.27	0.33
Malignant	Benign	Hu.PDGF.bb..47.	0.47	-0.09	1.03	0.37
Malignant	Healthy	Hu.TNF.a..36.	0.57	-0.11	1.26	0.39

Table S7: Spearman Correlation between Proseek and Bio-plex assay (with p and q-values)			
Target Protein	Correlation	p.value	q.value
PDGF.subunit.B	0.87	0.00	0.00
IL.8	0.45	0.00	0.00
MCP.1	0.46	0.00	0.00
IL.6	0.39	0.00	0.00
IL.7	0.31	0.01	0.02
VEGF.A	0.28	0.02	0.04
IFN.gamma	0.25	0.03	0.05
IL.2	0.21	0.08	0.12
GM.CSF	0.18	0.13	0.19
IL.4	0.13	0.28	0.37
IL.1ra	0.11	0.34	0.41
IL.12	0.10	0.38	0.41
TNF	0.04	0.72	0.72

Table S8: Clinical Details of CRC patients				
Dukes' stage **(n=)**	**A** **(15)**	**B** **(15)**	**C** **(15)**	**D** **(15)**
Age				
Median $\pm$ SD	65 $\pm$ 7.2	70 $\pm$ 7.9	65 $\pm$ 9.0	62 $\pm$ 8.0
Sex				
Male	66.7%	53.3%	46.7%	60%
Female	22.2%	46.7%	53.3%	40%
Location of tumor/cancer				
Sigmoid	6 (40%)	6 (40%)	11	8 (53.3%)
Low Rectal	2 (13.3%)	0	1 (6.7%)	1 (6.7%)
Caecal	2 (13.3%)	3 (20%)	3 (20%)	3 (20%)
Ascending colon	2 (13.3%)	2 (13.3%)	0	1 (6.7%)
Transverse colon	2 (13.3%)	4 (26.7%)	0	0
Descending colon	0	0	0	2 (13.3%)
Adenoma	1 (6.7%)	0	0	0
Metastasis/Location				
Lymph Node	0	0	15	0
Liver	0	0	0	8
Gall Bladder/Lung	0	0	0	1
Ovary	0	0	0	1
Other Colonic Regions	0	0	0	5

CHAPTER 6
GENERAL DISCUSSION, FUTURE DIRECTIONS AND CONCLUSION

6.1 General discussion

Colorectal cancer (CRC) is the third most prevalent cancer globally with mortality rates over 50% with cancer spread (metastasis) being responsible for the bulk of these deaths [6, 129]. Like most cancers, CRC advances through various stages altering and/or utilising molecules associated with various biochemical pathways to gradually progress from being a benign polyp through an adenocarcinoma and finally to becoming metastatic cancer.

Several proteins families including growth factors (e.g., TGFβ, VEGF, EGFR), integrins (e.g., αvβ6, αvβ1, αvβ3, and α6β4), proteolytic enzymes and their regulators (e.g., plasmin, uPAR, PAI-1, cathepsins, MMPs to name but a few), MAPK pathway members (e.g., ERK1/2, Ras, JNK, p38), Wnt and Notch signaling have been implicated as dysfunctional in CRC.

The primary aim of this thesis was to contribute to new knowledge regarding the role TGFβ has in model systems of cancer where we have artificially reduced the expression levels of two known activator system of TGFβ, namely integrin β6 and the uPA protease receptor uPAR. This was achieved by employing state-of-the-art proteomics, cell signalling assays (i.e., AlphaScreen® SureFire® Assay) and multiplexing technologies (i.e., Proseek Multiplex Oncology I kit), in conjunction with sophisticated bioinformatics using a panel of cultured human CRC cell lines and clinically staged CRC plasma samples.

As outlined in earlier chapters, our group and several others have published that β6 and uPAR play a significant role in CRC [69, 71, 154, 158, 185, 190-193, 376, 377] as interaction partners. Additionally, β6 (a direct activator of TGFβ) and uPAR (an indirect activator of latent TGFβ through the uPA-driven activation of cell-surface plasmin) can influence TGFβ activation and subsequent cancer-related biologies. The body of work began in our group after Saldanha *et al.,* using ovarian cancer (OVCA429) cells observed β6 integrin subunit as the dominant protein in a co-immunoprecipitation (co-IP) experiment with anti-uPAR antibodies. In a subsequent reverse IP using anti-β6 antibodies co-purification of uPAR was demonstrated, and since then our group has relentlessly shown other evidence confirming the uPAR•β6 interaction [180].

The uPAR•αvβ6 interaction was recently further investigated by Ahn *et al.*, (our group; Publication VII of this thesis in Appendix II) using proximity ligation assay (PLA) and peptide array studies. This interaction in the ovarian cancer cells (OVCA429) and CRC cell lines (SW480 and HT29 subclones) was first confirmed using PLA and was observed to

occur at cell surface. PLA was performed using the anti-uPAR R4 and anti-αvβ6 6.4B4 monoclonal antibodies. Subsequent, peptide array studies identified six potential αvβ6 binding sites spanning across all three domains of uPAR [185]. Further *in silico* analysis of the peptide array data determined that domain II and III of uPAR are accessible for binding with αvβ6. Interestingly, Chaurasia *et al.,* had observed that the 9-mer peptide derived from domain III (residues G262-Q270 from Uniprot KB: Q03405) of uPAR bound to α5β1 [378]. To confirm these observations from PLA and peptide array studies, Sowmya *et al.,* (our group) undertook structural modelling to generate a three-dimensional structure of integrin αvβ6. This is quite remarkable as the crystal structure for αvβ6 has not been reported and therefore this homology model reported by Sowmya *et al.,* offers a glimpse of the αvβ6 structure [186]. Subsequent docking studies, using this homology model, confirmed the site of αvβ6 interaction to be in domain III of uPAR [186]. Furthermore, six (S229, E230, T248, G249, T250, E255) out of the 27 residues identified by peptide array study were consistent with the docking results that further strengthens the uPAR•αvβ6 interaction.

Furthermore functional blocking of β6 using Clone 6.3G9 antibody inhibited uPA-stimulated ERK1/2 phosphorylation and cell proliferation in OVCA429 cells [180]. However, both β6 and uPAR cannot participate directly in downstream signalling as they both lack intracellular kinase domains and require accessory/adaptor proteins to exert signalling effects. Saldanha *et al.,* proposed that the αvβ6 and uPAR interaction might influence TGFβ activation which can then regulate cell proliferation and tumourigenesis [180], as they obtained some (currently unpublished data) suggesting TGFbR2 co-immunoprecipitated as well. This lead to the novel hypothesis of the uPAR•αvβ6•TGFβ1 interactome which is under investigation in this thesis. Another proteomic study (by our research group) using the SW480 CRC cell lines determined TGFβ1 expression to be significantly increased upon the overexpression of β6 (SW480^{β6OE} cells) [149] adding considerable credence to our proposal. Considering these novel observations collectively, it was crucial to study these proteins in combination in order to fully comprehend their role/s in CRC.

Therefore, this thesis aimed to investigate the role of TGFβ1 in the proposed hypothetical uPAR•αvβ6•TGFβ1 interactome using CRC cell lines that have β6 and uPAR expression artificially altered. This was primarily achieved by performing a combination of cell signalling assays, cancer cell behaviour assays and LC-MS/MS-based proteomics.

The first study of this thesis (Chapter 3, Study I) demonstrated that CRC cells that express β6 at varying levels (SW480^{β6OE}, HT29^{Mock}, HT29^{β6AS}) [146, 379] have the ability to incorporate recombinant L-TGFβ1 and PLG zymogens as part the hypothetical uPAR•αvβ6•TGFβ1 interactome *in cellulo* and induce phenotypic changes required for cancer progression. Previous studies have shown that expression of β6 increases proliferation and invasion through its unique cytoplasmic tail that can mediate ERK1/2 signalling activity [146, 379]. In agreement, treatment of β6 expressing cells with L-TGFβ1 and/or PLG significantly enhanced proliferation, wound healing, migration and invasion phenotypes. Interestingly, ERK1/2 signalling activity was amplified upon treatment with L-TGFβ1 and/or PLG, indicating the additive effects of these molecules through the uPAR•αvβ6•TGFβ1 interactome. These observations align with previous reports by Agrez *et al.,* and Ahmed *et al.,* [146, 379]. Additionally, TGFβ has been implicated in crosstalk with the ERK1/2 pathway [380-382] and the observed amplification of ERK activity could be due to β6 expression and TGFβ1 crosstalk. TGFβ1 has also been shown to induce ERK-mediated phosphorylation of Smad2 and Smad3 [382]. Interestingly, an increased Smad2 and Akt1/2/3 signalling activity was observed when β6 was expressed which was not significantly altered upon treatment with L-TGFβ1 and/or PLG. These results suggest a significant role for β6 and TGFβ1 in the uPAR/αvβ6/TGFβ1 interactome and highlight the importance of investigating the direct and indirect (as a result of crosstalk) signalling activity associated with various proteins implicated in cancer biology. The current study also demonstrated the diversity and complexity of signalling utilised by cancer cells to survive and eventually metastasise. This study, however, did not reveal the full extent of alterations to proteins required to maintain cancer phenotypes as that necessitated a more detailed proteomic investigation of these cell lines.

The proteomic alterations associated with phenotypic changes observed in the previous study, were subsequently investigated in a high-throughput quantitative proteomic experiment (Chapter 3, Study II). In that study, however, the SW480 and HT29 CRC subclone cells were treated solely with <u>active</u> TGFβ1 as this allowed for an investigation of phenotypic and proteomic changes solely exerted by active TGFβ1 and not associated with activation of normally L-TGFβ1 that could introduce additional variables. Cell-based assays determined that cells expressing β6 when treated with TGFβ1 exhibited significantly enhanced proliferation, wound healing, migration and invasion and supported some of the observations shown in Chapter 3 as well as those observed by Agrez *et al.,* and Ahmed *et al.,* [146, 379]. The subsequent proteomic study was performed on plasma membrane-

enriched cell samples to elucidate the TGFβ-mediated alterations in proteins, cellular pathways, processes, and behaviours when β6 is expressed. The high-throughput quantitative proteomics approach using iTRAQ following TGFβ treatment identified at least 2,050 proteins for each cell line comparison. Several of the significantly altered proteins were associated with cytoskeletal remodelling, cell migration, invasion, adhesion, and cellular stress were observed to be differentially up- or down-regulated in a TGFβ-integrin β6-dependent manner. The biological significance of these results was displayed through Ingenuity Pathway Analysis (IPA) and showed that the eukaryotic translation initiation factor 2 (eIF2) signalling pathway (previously associated with cancer [383-385]) was significantly altered when β6 subunit is expressed. These findings further demonstrate that β6 in the presence of active TGFβ1 potentiates pathways that are required to sustain the proliferative and invasive phenotypes required to attain malignancy at a later stage.

The SW480 and HT29 subclone cells endogenously express uPAR and therefore were ideal to investigate the uPAR•αvβ6•TGFβ1 interactome. Although, it was not possible from the two previous studies of this thesis (Chapter 3, Study I & II) to determine if the observed phenotypic and proteomic changes were influenced by any associations between TGFβ1 and uPAR or β6 and uPAR. The possible associations between TGFβ1 and uPAR were evaluated using HCT116 CRC cells (Chapter 4) that endogenously express uPAR (HCT116^{WT}) but not β6 integrin. Additionally, the HCT116^{WT} has a subclone where the uPAR expression has been stably and artificially suppressed by approximately 50% (HCT116^{uPARAS}) [376]. Interestingly, HCT116^{WT} cells upon treatment with TGFβ did not show significant alterations to proliferation or invasion, although HCT116^{uPARAS} cells exhibited a decreased proliferation (~24%↓) following TGFβ treatment and invasion (~20%↓) following SB431542 (a TGFβ receptor I kinase inhibitor) or dual SB431542 and TGFβ treatment. Interestingly, Brattain *et al.,* reported the parent HCT116 cells to be tumorigenic to athymic nude mice when trypsinised or scrapped cells in tissue culture medium without any serum were given as subcutaneous injections [386]. Likewise, Wang *et al.,* also reported pulmonary metastases to occur in 63-78% of athymic nude mice injected with the HCT116^{WT} cells and injection with the antisense transfected clones, 3′-AS7 and 5′-AS, showed pulmonary metastases in only 19% and 9% of the mice respectively [387]. The observations from the current study clearly align with these mice studies, wherein proliferation and invasion was more pronounced in HCT116^{WT} cells with higher uPAR expression, suggesting a possible tumorigenic activity, which was reduced when uPAR expression was artificially decreased by ~50% [376].

These interesting observations were then validated by proteomics using a similar approach employed in Chapter 3, Study II where the membrane enriched samples following TGFβ treatment were analysed using iTRAQ. This high-throughput quantitative proteomics approach identified approximately 1,700 proteins. IPA of the significantly altered proteins demonstrated several related to cytoskeletal signalling, cell adhesion, migration, cell death and survival, protein trafficking and (once again) the eIF2 signalling pathway components as being affected in either in a TGFβ-dependent or TGFβ-independent manner. This study in particular identified that cells expressing uPAR (HCT116^{WT}) do not respond significantly to TGFβ treatments whereas those with lower uPAR levels (HCT116$^{uPAR-AS}$) respond more readily. These observations suggest a possible malignant phenotype of the HCT116^{WT} cells in a TGFβ-independent manner and a possible TGFβ-dependant growth suppression in the HCT116$^{uPAR-AS}$ cells.

Interestingly, the eIF2 signalling was observed to be significantly altered, in both proteomic studies performed in this thesis, in a TGFβ-β6 or uPAR or TGFβ-uPAR dependent manner. The treatment of β6-expressing (SW480^{β6OE} and HT29 subclones) cells with active TGFβ1 identified several eIF2 and eIF4 signalling pathway members including eIF2A, eukaryotic translation initiation factor 2 subunit alpha (eIF2S1), eukaryotic translation initiation factor 2 subunit beta (eIF2S2), eukaryotic translation initiation factor 2 subunit gamma (eIF2S3), and KRAS to be significantly up-regulated. Likewise, several ribosomal proteins related to eIF2 signalling were altered when the HCT116$^{uPAR-AS}$ cells were treated with TGFβ. The eIF2 signalling complex, is made up of the eIF2S1, eIF2S2, and eIF2S3 subunits and controls stress-related signals to regulate global and specific mRNA translation, and thus protein synthesis [388]. The up-regulation of these eIF2 subunits indicates a potential need to sustain increased protein expression levels required for the abnormal functioning of cancer cells. However, the increased protein levels cannot be achieved without eIF4 which is necessary to deliver the mRNA to eIF3 for translation into polypeptide [385]). Although eIF4 related molecules were not observed in the current SW480 and HT29 proteomic study, eukaryotic translation initiation factor 4 gamma 1 (eIF4G1) was observed to be up-regulated in our previous proteomic study using the SW480 subclones [389] and other studies in breast [390] and lung [391] epithelial cancers. Interestingly, TGFβ treatment of the HCT116^{WT} resulted in down-regulation eIF4G1 (0.60↓). eIF4G1 is the most abundant member of the eIF4G scaffold protein family, whose elevated expression in yeast has been shown to promote direct mRNA-ribosome interaction and translation of mRNAs with longer polyA tails, thereby promoting mRNA translation efficiency [392-394]. It is also a component of the eIF4F

complex essential for mRNA translation. Additionally, previous studies have shown that the down-regulation of eIF4G1 in mammalian and yeast cells resulted in decreased mRNA translation of multiple mRNAs but was not completely inhibited [392, 395]. The observations from the HCT116 proteomic study suggests that TGFβ may be exerting growth inhibitory effects and the presence of uPAR seems to abrogate those effects to promote growth in an uPAR-dependent manner.

Taken together, the results from the signalling and proteomic studies demonstrate that molecules from the hypothesised uPAR•αvβ6•TGFβ1 interactome contribute to alterations required for malignant phenotype lending more credence to the existence of this hypothetical interactome. TGFβ1 in a β6-dependant manner further enhanced the alterations of proteins and signalling activity required to maintain the malignant phenotype essential for progression towards a metastatic stage in the SW480 and HT29 cells, whilst uPAR by itself was able to promote these changes in the HCT116 cells.

Therefore, understanding the expression levels of these molecules through the use of non-invasive tests could be useful as they may serve as potential markers for CRC. This prompted the investigation of TGFβ and uPAR expression levels in a clinical setting using human blood plasma samples from Dukes' stage A-D CRC patients (n=60) and unaffected normal control plasmas (n=15) (Chapter 5). These samples were analysed using the Proseek Multiplex Oncology I kit that evaluated the expression of 92 putative cancer-related proteins including Latency-associated peptide TGFβ1 (LAP TGFβ1) and uPAR from just 1μL of human plasma. The observations from this study indicated no significant difference in expression of LAP-TGFβ1 and uPAR in plasma between various stages in this set of samples. However, the study identified 8 oncoproteins (CEA, IL-8, prolactin, amphiregulin, PDGF-BB, IL-6, CXCL11 and CXCL5) to be significantly different amongst various CRC stages. In particular, CEA, IL-8 and prolactin were found to differentiate unaffected controls from non-malignant (Dukes' A + B) and malignant (Dukes' C + D) stages and reported as potential CRC biomarkers in the published manuscript in Chapter 5. These identified biomarkers could potentially be implemented in the development of a multi-protein biomarker panel that could be used for early diagnosis of CRC.

Taken together, the cell signalling assays and high-throughput proteomic studies (Chapter 3 & 4) provided insight into the biomolecular deregulations that can be exerted by TGFβ during CRC. The observations reported in these studies opened up avenues for initiating a knowledge-driven search for protein markers. This lead to the identification of three

potential CRC biomarkers (Chapter 5) that could serve as direct targets for developing new diagnostic and therapeutic assays for CRC. Overall, the observations reported in this thesis have enhanced our understanding of how TGFβ drives/alters the fundamental cellular processes required for the progression of CRC to a metastatic stage and will pave way to further research to fully elucidate its role in cancer itself.

6.2 Proteins as Biomarkers for CRC

Cancer biomarkers are used to screen for primary cancers, distinguish benign from malignant or different types of malignancies from one another, determine prognosis for patients who have been diagnosed with cancer, and monitor status the disease, either to detect recurrence or determine response or progression to therapy [34]. Various molecules, such as proteins, peptides, microRNAs and DNA amongst others, can be used as biomarkers. A multitude of potential biomarkers for CRC have been identified and reported in the literature (Chapter 1, Table 2). For example, carcinoembryonic antigen (CEA) is employed as a routine marker to monitor CRC recurrence. Most commonly it is used to monitor CRC patients, following adjuvant therapy, with the goal of detecting liver metastases [35, 396].

The modern high-throughput LC-MS/MS-based proteomics, utilized to study the global membrane proteome profiles of TGFβ-treated colorectal adenocarcinoma cells with artificially modified β6 and uPAR expression, identified several altered proteins and perturbed pathways that provided broad insights into the role of TGFβ in CRC biology. The proteomic studies identified several cytoskeletal keratins, actin associated proteins, cell proliferation, migration, adhesion and cellular stress and cell death associated proteins to be significantly altered, amongst which were several proteins that have suggested to be biomarkers by the American Society of Clinical Oncology (ASCO). For instance, annexin A2 was reported to be used a diagnostic and prognostic marker for CRC [397, 398]. The expression of annexin A2 observed in proteomic studies conferred with previous observations reported in [341, 399, 400]. Several keratins (KRT1, KRT2, KRT5, KRT6A, KRT8, KRT9, KRT10, KRT17, KRT18, KRT19, KRT20) were also identified in the proteomic studies and have been previously reported to be markers for diagnosis, disease progression, prognosis, and efficacy of CRC. Karantza *et al.,* has published a detailed review on the role of keratins in cancer and illustrates the use of keratins as diagnostic and prognostic markers for various cancers including CRC [401]. Within the SW480 and HT29 proteomic study three S100 proteins (A6, A8 and A9) were identified and were also listed as potential markers for diagnosis and efficacy by ASCO. Yang *et al.,* have shown that S100-A6 is up-regulated in gastric cancer [402]. Another study by Zhang *et al.,* reported that high

levels of S100-A6 in serum could be used as prognostic marker in gastric cancer [403]. It is therefore agreeable that some of the potential biomarkers identified in these proteomic studies could potentially be used as markers for processes that are altered in an uPAR/αvβ6/TGFβ dependent manner during CRC progression. However, a validation of these proteins as potential biomarkers is required to determine the actual the significance and utility in diagnosis and prognosis of CRC.

Utilising emerging Proximity Extension Assay (PEA) technology that is employed in the Proseek Multiplex Oncology I kit, the examination of CRC patient plasmas for 92 putative cancer-related analytes as potential biomarkers of CRC identified 8 oncoproteins (CEA, IL-8, prolactin, amphiregulin, PDGF-BB, IL-6, CXCL11 and CXCL5) to be significantly different amongst various CRC stages. Amongst these, only CEA, IL-8 and prolactin were able to significantly differentiate unaffected controls from non-malignant (Dukes' A + B) and malignant (Dukes' C + D) stages. CEA is currently employed as a routine marker for CRC prognosis, disease-free survival and therapeutic response and monitor CRC recurrence and/or metastases during postoperative follow-up [396, 404]. The observed high plasma CEA levels significantly correlate with the presence of metastatic CRC and is not an effective biomarker for early stage disease (Dukes' A). IL-8 expression was found to significantly correlate with tumour size, depth of infiltration, liver metastases and tumour stage [57, 405, 406] as seen in this study. Interestingly, Sun *et al.,* reported that IL-8 in a dose dependent manner increased cell migration of the HT29 and WiDr colon cancer cell lines through the [ERK1/2]-[Ets-1]-[αvβ6] signalling axis [407]. The increased ERK1/2 phosphorylation observed by Sun *et al.,* correlate with the cell signalling study performed in this thesis (Chapter 3, Study I) and also validate the findings reported here. Additional, immunohistochemical analysis of 139 primary CRC samples by Sun *et al.,* demonstrated that IL-8 expression directly proportional to αvβ6 expression [407]. Elevated levels of prolactin levels has been observed in serum, several tumour specimens and suggested to correlate with CRC malignancy [408, 409], and the observation in the current study confers with previous reports. These observations from the Olink Proseek study further strengthen the previously suggested role of these molecules as biomarkers for CRC.

In summary, the significantly regulated cancer-associated proteins observed in the proteomic studies are clearly strong biomarker candidates for CRC. However, further work is required to understand their genuine marker potential using a larger cohort of CRC patient samples (e.g., blood, plasma, tissue, stools).

6.3 Future directions

The identification of molecules involved in deregulation of CRC-related biomolecular process presented in this thesis represents exciting findings that are mostly congruent with observations reported in the existing literature. However, many of these findings warrant further exploration and validation by targeted proteomic experiments that will enable a better understanding of the role/s of TGFβ, uPAR and β6 and their underlying regulatory mechanisms in cancer. Examples of rational follow-up experiments that can be performed following on from the efforts disseminated in this work are briefly described below:

- **Co-immunoprecipitation (Co-IP) experiments** can be performed to examine the interactions between TGFβ signalling components and uPAR/β6. Co-IP approach that was employed (on OVCA429 cells) by Saldanha *et al.,* [180] should be used to examine the uPAR•β6 interaction in CRC. This can be further extended to examine the interacting partners of TGFβ and its receptor as well. Following, the pull down of the interacting partners using appropriate antibodies as bait proteins they should be identified using SWATH enabled ABSCIEX Triple TOF® 6600 mass spectrometer following a 1D SDS-PAGE slice-and-dice protein extraction or SCX separation. These data should allow for determination of the uPAR, β6, TGFβ and TGFβ receptor/s interacting partners in CRC.

- **Cross-linking mass spectrometry (X-MS)**, can be used to stabilise the protein interactions *in cellulo* using various cross linkers such as disuccinimidyl suberate (DSS), bis(sulfosuccinimidyl) suberate (BS3) or sulfo-N-hydroxylsuccinimide-SS-Biotin. The cell lysate obtained after cross-linking should directly or after co-IP experiments be analysed on using a high mass accuracy instrument such as the ABSCIEX Triple TOF® 6600. The mass spectra should then be searched using xQuest [410], a search engine for identification of peptides from cross-linked samples.

- **Peptide array interaction analysis** of TGFβ receptors could also be undertaken to determine their interacting proteins. Peptide arrays containing 15- or 18-mer peptides with at least 8- to 10-mer amino acid overlap should be prepared on PVDF or Nitrocellulose membrane blotting papers with a 0.2 μm pore size. These arrays should then be treated with 'potential' interacting partners identified from co-IP or X-MS experiments to determine the binding specificity, affinity and the site on the receptors.

- **Structural modelling or crystal structure analysis** should then be performed to analyse the interactions between the TGFβ receptors and partners identified in the previous suggested experiments. The analysis of those using a three-dimensional model will strengthen validity of the observed interactions.

- **Mouse models** should then be used to validate these interactions in an *in vitro* system. The proposed interactions can be functionally blocked using antibodies, peptide inhibitors, siRNAs or chemical inhibitors to examine the associated downstream effects.

- All CRC cell lines used in this thesis were colorectal adenocarcinomas that were of Dukes' stage B (non-metastatic) and the expression of β6 and uPAR was artificially altered in these cell lines. Although, the observations from these cell lines are helpful to understand their role in CRC, it would be interesting to alter/inhibit the expression of αvβ6, uPAR, TGFβ and TGFβ receptor/s expression in various metastatic CRC cell lines. These observations should then be confirmed using immunocompromised mouse CRC xenograft models.

- Post-translational modifications such as glycosylation is a very common process by which the proteins are stabilised in the cell. It would be very interesting to study the *N*- and *O*-glycosylation changes that are associated with treatment of TGFβ to the cell lines used in this thesis. Although, glycoproteomics technologies are fairly new and not yet fully matured (compared to proteomics), they could be applied in their current state to identify and quantitate TGFβ-mediated glycosylation changes. Similar approaches that were used by Sethi *et al.,* [411] can be employed.

- The cancer-associated proteins identified by the global proteomics approach could be accurately quantified using targeted proteomics experiments such as SRM and MRM to complement the iTRAQ quantitative approach used in this thesis. These specific and significantly more sensitive protein quantitation methods could allow for validation of the potential candidate CRC biomarkers suggested in this thesis.

- Determining the (consistent) molecular patterns from a higher number of biological replicates would add confidence to this set of biomarker candidates and establish a more accurate and reliable understanding of these molecular alterations associated with the early stages of CRC where the diagnosis is particularly required.

- The studies performed this thesis used a limited number of cell lines and plasma samples. It would be valuable to perform these experiments using a large cohort of different samples (e.g., tissue, blood, plasma, urine, stools, cell lines) obtained from

normal healthy individuals and CRC patients. Potential variables such as age, gender, ethnic background, disease history, etc should also be taken into consideration. This large scale study will prove to be a significant task yet is crucial to understanding the biology of CRC

6.4 Conclusion

In conclusion, this thesis has demonstrated the capacity of targeted cell signalling assays in combination with high-throughput modern proteomics technologies to better understand the TGFβ-associated protein alterations in CRC. Furthermore, the use of the Olink Proseek Oncology kit to identify biomarkers from just 1μL of plasma is remarkable.

The knowledge gleaned from this PhD thesis has opened up a range of unanswered research avenues that need to be explored. This indeed is typically the result of system-wide "discovery type" studies trying to map entire populations of biomolecules from complex set of samples such as partially enriched cell lysate and un-fractionated plasma samples used in this thesis. Modern multiplexing technologies are slowly making their way into the more targeted and hypothesis-driven research areas. However, proteomics will still remain is a powerful tool that enables discovery based understanding of a disease as complex as cancer.

Overall, this thesis has demonstrated the immense power of high-throughput modern proteomic and multiplexing technologies to gain insights into the TGFβ associated CRC pathogenesis at detailed molecular level and to identify avenues for disease biomarker exploration. Future initiatives building on the observations reported in this thesis will take us a step closer to understanding the prevalent and fatal disease we have named 'cancer'.

REFERENCES

1. Boyle, P., B. Levin, and World Health Organization., *World cancer report 2008*. 2008, Lyon, France: International Agency for Research on Cancer (IARC), Distributed by WHO Press. 510.
2. Ruddon, R.W., *Cancer Biology*. 2007: Oxford University Press, USA. 568.
3. National Cancer Institute. *What Is Cancer?* [cited 2015 19 May]; Available from: http://www.cancer.gov/cancertopics/cancerlibrary/what-is-cancer.
4. Hanahan, D. and R.A. Weinberg, *The hallmarks of cancer.* Cell, 2000. **100**(1): p. 57-70.
5. Torre, L.A., et al., *Global cancer statistics, 2012.* CA Cancer J Clin, 2015. **65**(2): p. 87-108.
6. Ferlay, J., et al., *Cancer incidence and mortality worldwide: Sources, methods and major patterns in GLOBOCAN 2012.* Int J Cancer, 2015. **136**(5): p. E359-86.
7. Stewart, B.W., C.P. Wild, and World Health Organization, *World cancer report 2014*. 2014, Lyon, France: International Agency for Research on Cancer (IARC), Distributed by WHO Press. 630.
8. Cunningham, D., et al., *Colorectal cancer.* The Lancet, 2010. **375**(9719): p. 1030-1047.
9. Shelton, B.K., *Introduction to colorectal cancer.* Semin Oncol Nurs, 2002. **18**(2 Suppl 2): p. 2-12.
10. Health, D.o. *About bowel cancer*. 2015 [cited 2015 07 June]; Available from: http://www.health.gov.au/internet/screening/publishing.nsf/Content/about-bowel-cancer.
11. Kim, S.E., et al., *Sex- and gender-specific disparities in colorectal cancer risk.* World J Gastroenterol, 2015. **21**(17): p. 5167-5175.
12. Amersi, F., M. Agustin, and C.Y. Ko, *Colorectal cancer: epidemiology, risk factors, and health services.* Clinics in colon and rectal surgery, 2005. **18**(3): p. 133-40.
13. Kune, G.A. and L. Vitetta, *Alcohol consumption and the etiology of colorectal cancer: a review of the scientific evidence from 1957 to 1991.* Nutrition and cancer, 1992. **18**(2): p. 97-111.
14. Ferrari, P., et al., *Lifetime and baseline alcohol intake and risk of colon and rectal cancers in the European prospective investigation into cancer and nutrition (EPIC).* Int J Cancer, 2007. **121**(9): p. 2065-72.
15. Botteri, E., et al., *Smoking and colorectal cancer: a meta-analysis.* JAMA : the journal of the American Medical Association, 2008. **300**(23): p. 2765-78.
16. Giovannucci, E., *An updated review of the epidemiological evidence that cigarette smoking increases risk of colorectal cancer.* Cancer epidemiology, biomarkers & prevention : a publication of the American Association for Cancer Research, cosponsored by the American Society of Preventive Oncology, 2001. **10**(7): p. 725-31.
17. Carr, P.R., et al., *Meat subtypes and their association with colorectal cancer: Systematic review and meta-analysis.* Int J Cancer, 2015.
18. Jung, A., *Colon and Rectum Normal Anatomy and Congenital Variants*, in *Abdominal Imaging*, B. Hamm and P. Ros, Editors. 2013, Springer Berlin Heidelberg. p. 785-796.
19. *Layers of Bowel Wall*. 2015 14 June; Available from: http://training.seer.cancer.gov/colorectal/anatomy/layers.html.
20. *Basic Anatomy*. 2015 14 June; Available from: http://www.hopkinscoloncancercenter.org/CMS/CMS_Page.aspx?CurrentUDV=59&CMS_Page_ID=B6ACAEF5-52D3-4CC1-88CC-CEB21F5ABBCD.
21. Majumdar, S.R., R.H. Fletcher, and A.T. Evans, *How does colorectal cancer present[quest] symptoms, duration, and clues to location.* Am J Gastroenterol, 1999. **94**(10): p. 3039-3045.
22. Astin, M., et al., *The diagnostic value of symptoms for colorectal cancer in primary care: a systematic review.* Br J Gen Pract, 2011. **61**(586): p. e231-43.

23. Fijten, G.H., et al., *Predictive value of signs and symptoms for colorectal cancer in patients with rectal bleeding in general practice.* Family Practice, 1995. **12**(3): p. 279-286.
24. Mor, V., et al., *Pre-diagnostic symptom recognition and help seeking among cancer patients.* J Community Health, 1990. **15**(4): p. 253-66.
25. Irvin, T.T. and M.G. Greaney, *Duration of symptoms and prognosis of carcinoma of the colon and rectum.* Surg Gynecol Obstet, 1977. **144**(6): p. 883-6.
26. McDermott, F.T., et al., *Prognosis in relation to symptom duration in colon cancer.* Br J Surg, 1981. **68**(12): p. 846-9.
27. Etzioni, R., et al., *The case for early detection.* Nat Rev Cancer, 2003. **3**(4): p. 243-52.
28. Meyerhardt, J.A. and R.J. Mayer, *Systemic therapy for colorectal cancer.* N Engl J Med, 2005. **352**(5): p. 476-87.
29. Davis, N.C. and R.C. Newland, *Terminology and classification of colorectal adenocarcinoma: the Australian clinico-pathological staging system.* Aust N Z J Surg, 1983. **53**(3): p. 211-21.
30. *Esophageal cancer*. 2015 25 June; Available from: http://www.hpvvaccination.com/p/esophageal-cancer.html.
31. Weber, T.K. and N.J. Petrelli, *Local excision for rectal cancer: an uncertain future.* Oncology (Williston Park), 1998. **12**(6): p. 933-43; discussion 944, 947.
32. Shah, R., et al., *Biomarkers for early detection of colorectal cancer and polyps: systematic review.* Cancer Epidemiol Biomarkers Prev, 2014. **23**(9): p. 1712-28.
33. *NCI Dictionary of Cancer Terms*. 2015 14 June; Available from: http://www.cancer.gov/publications/dictionaries/cancer-terms?cdrid=45618.
34. Henry, N.L. and D.F. Hayes, *Cancer biomarkers.* Mol Oncol, 2012. **6**(2): p. 140-6.
35. Locker, G.Y., et al., *ASCO 2006 update of recommendations for the use of tumor markers in gastrointestinal cancer.* J Clin Oncol, 2006. **24**(33): p. 5313-27.
36. Allegra, C.J., et al., *American Society of Clinical Oncology provisional clinical opinion: testing for KRAS gene mutations in patients with metastatic colorectal carcinoma to predict response to anti-epidermal growth factor receptor monoclonal antibody therapy.* J Clin Oncol, 2009. **27**(12): p. 2091-6.
37. Fung, K.Y., et al., *Colorectal cancer biomarkers: to be or not to be? Cautionary tales from a road well travelled.* World J Gastroenterol, 2014. **20**(4): p. 888-98.
38. Fuzery, A.K., et al., *Translation of proteomic biomarkers into FDA approved cancer diagnostics: issues and challenges.* Clin Proteomics, 2013. **10**(1): p. 13.
39. Vikram, R. and R.B. Iyer, *PET/CT imaging in the diagnosis, staging, and follow-up of colorectal cancer.* Cancer imaging : the official publication of the International Cancer Imaging Society, 2008. **8 Spec No A**: p. S46-51.
40. Walsh, J.M. and J.P. Terdiman, *Colorectal cancer screening: scientific review.* JAMA : the journal of the American Medical Association, 2003. **289**(10): p. 1288-96.
41. Wickham, R. and Y. Lassere, *The ABCs of Colorectal Cancer.* Seminars in Oncology Nursing, 2007. **23, Supplement 1**(0): p. 1-8.
42. Winawer, S.J., *The multidisciplinary management of gastrointestinal cancer. Colorectal cancer screening.* Best practice & research. Clinical gastroenterology, 2007. **21**(6): p. 1031-48.
43. Burch, J.A., et al., *Diagnostic accuracy of faecal occult blood tests used in screening for colorectal cancer: a systematic review.* Journal of medical screening, 2007. **14**(3): p. 132-7.
44. Ouyang, D.L., et al., *Noninvasive testing for colorectal cancer: a review.* The American journal of gastroenterology, 2005. **100**(6): p. 1393-403.
45. Claridge, L.C., *Barium enema and diagnosis of colorectal cancer.* BMJ, 2011. **343**: p. d7704.
46. Fung, K.Y., et al., *Blood-based protein biomarker panel for the detection of colorectal cancer.* PLoS One, 2015. **10**(3): p. e0120425.
47. Tagi, T., et al., *Dermokine as a novel biomarker for early-stage colorectal cancer.* J Gastroenterol, 2010. **45**(12): p. 1201-11.

48.   Babel, I., et al., *Identification of MST1/STK4 and SULF1 proteins as autoantibody targets for the diagnosis of colorectal cancer by using phage microarrays.* Mol Cell Proteomics, 2011. **10**(3): p. M110 001784.

49.   Bujanda, L., et al., *Evaluation of alpha 1-antitrypsin and the levels of mRNA expression of matrix metalloproteinase 7, urokinase type plasminogen activator receptor and COX-2 for the diagnosis of colorectal cancer.* PLoS One, 2013. **8**(1): p. e51810.

50.   Mahboob, S., et al., *A novel multiplexed immunoassay identifies CEA, IL-8 and prolactin as prospective markers for Dukes' stages A-D colorectal cancers.* Clin Proteomics, 2015. **12**(1): p. 10.

51.   Fentz, A.K., et al., *Detection of colorectal adenoma and cancer based on transthyretin and C3a-desArg serum levels.* Proteomics Clin Appl, 2007. **1**(6): p. 536-44.

52.   Kim, H.J., et al., *Identification of S100A8 and S100A9 as serological markers for colorectal cancer.* J Proteome Res, 2009. **8**(3): p. 1368-79.

53.   Japink, D., et al., *CEA in activated macrophages. New diagnostic possibilities for tumor markers in early colorectal cancer.* Anticancer Res, 2009. **29**(8): p. 3245-51.

54.   Nielsen, H.J., et al., *Plasma TIMP-1 and CEA in detection of primary colorectal cancer: a prospective, population based study of 4509 high-risk individuals.* Scand J Gastroenterol, 2011. **46**(1): p. 60-9.

55.   Sole, X., et al., *Discovery and validation of new potential biomarkers for early detection of colon cancer.* PLoS One, 2014. **9**(9): p. e106748.

56.   Kawamura, M., et al., *CXCL5, a promoter of cell proliferation, migration and invasion, is a novel serum prognostic marker in patients with colorectal cancer.* Eur J Cancer, 2012. **48**(14): p. 2244-51.

57.   Rubie, C., et al., *Correlation of IL-8 with induction, progression and metastatic potential of colorectal cancer.* World J Gastroenterol, 2007. **13**(37): p. 4996-5002.

58.   Wilson, S., et al., *Serum matrix metalloproteinase 9 and colorectal neoplasia: a community-based evaluation of a potential diagnostic test.* Br J Cancer, 2012. **106**(8): p. 1431-8.

59.   Mroczko, B., et al., *The diagnostic value of matrix metalloproteinase 9 (MMP-9) and tissue inhibitor of matrix metalloproteinases 1 (TIMP-1) determination in the sera of colorectal adenoma and cancer patients.* Int J Colorectal Dis, 2010. **25**(10): p. 1177-84.

60.   Pedersen, J.W., et al., *Seromic profiling of colorectal cancer patients with novel glycopeptide microarray.* Int J Cancer, 2011. **128**(8): p. 1860-71.

61.   Chen, J.S., et al., *Detection of autoantibodies against Rabphilin-3A-like protein as a potential biomarker in patient's sera of colorectal cancer.* Clin Chim Acta, 2011. **412**(15-16): p. 1417-22.

62.   De Chiara, L., et al., *Serum CD26 is related to histopathological polyp traits and behaves as a marker for colorectal cancer and advanced adenomas.* BMC Cancer, 2010. **10**: p. 333.

63.   Mulder, S.A., et al., *Tumor pyruvate kinase isoenzyme type M2 and immunochemical fecal occult blood test: performance in screening for colorectal cancer.* Eur J Gastroenterol Hepatol, 2007. **19**(10): p. 878-82.

64.   Shastri, Y.M., et al., *Comparison of an established simple office-based immunological FOBT with fecal tumor pyruvate kinase type M2 (M2-PK) for colorectal cancer screening: prospective multicenter study.* Am J Gastroenterol, 2008. **103**(6): p. 1496-504.

65.   Koss, K., D. Maxton, and J.A. Jankowski, *Faecal dimeric M2 pyruvate kinase in colorectal cancer and polyps correlates with tumour staging and surgical intervention.* Colorectal Dis, 2008. **10**(3): p. 244-8.

66.   Haug, U., et al., *Tumour M2-PK as a stool marker for colorectal cancer: comparative analysis in a large sample of unselected older adults vs colorectal cancer patients.* Br J Cancer, 2007. **96**(9): p. 1329-34.

67.   Shastri, Y.M., et al., *Prospective multicenter evaluation of fecal tumor pyruvate kinase type M2 (M2-PK) as a screening biomarker for colorectal neoplasia.* Int J Cancer, 2006. **119**(11): p. 2651-6.

68. Tonus, C., G. Neupert, and M. Sellinger, *Colorectal cancer screening by non-invasive metabolic biomarker fecal tumor M2-PK.* World J Gastroenterol, 2006. **12**(43): p. 7007-11.

69. Ahn, S.B., et al., *Correlations between integrin alphanubeta6 expression and clinico-pathological features in stage B and stage C rectal cancer.* PLoS One, 2014. **9**(5): p. e97248.

70. Magnusson, K., et al., *SATB2 in combination with cytokeratin 20 identifies over 95% of all colorectal carcinomas.* Am J Surg Pathol, 2011. **35**(7): p. 937-48.

71. Ahn, S.B., et al., *Epithelial and stromal cell urokinase plasminogen activator receptor expression differentially correlates with survival in rectal cancer stages B and C patients.* PLoS One, 2015. **10**(2): p. e0117786.

72. Kanaan, Z., et al., *A plasma microRNA panel for detection of colorectal adenomas: a step toward more precise screening for colorectal cancer.* Ann Surg, 2013. **258**(3): p. 400-8.

73. Wang, Q., et al., *Plasma miR-601 and miR-760 are novel biomarkers for the early detection of colorectal cancer.* PLoS One, 2012. **7**(9): p. e44398.

74. Ng, E.K., et al., *Differential expression of microRNAs in plasma of patients with colorectal cancer: a potential marker for colorectal cancer screening.* Gut, 2009. **58**(10): p. 1375-81.

75. Zheng, G., et al., *Serum microRNA panel as biomarkers for early diagnosis of colorectal adenocarcinoma.* Br J Cancer, 2014. **111**(10): p. 1985-92.

76. Kanaan, Z., et al., *Plasma miR-21: a potential diagnostic marker of colorectal cancer.* Ann Surg, 2012. **256**(3): p. 544-51.

77. Huang, Z., et al., *Plasma microRNAs are promising novel biomarkers for early detection of colorectal cancer.* Int J Cancer, 2010. **127**(1): p. 118-26.

78. Takai, T., et al., *Fecal cyclooxygenase 2 plus matrix metalloproteinase 7 mRNA assays as a marker for colorectal cancer screening.* Cancer Epidemiol Biomarkers Prev, 2009. **18**(6): p. 1888-93.

79. Lee, B.B., et al., *Aberrant methylation of APC, MGMT, RASSF2A, and Wif-1 genes in plasma as a biomarker for early detection of colorectal cancer.* Clin Cancer Res, 2009. **15**(19): p. 6185-91.

80. Azuara, D., et al., *Novel methylation panel for the early detection of colorectal tumors in stool DNA.* Clin Colorectal Cancer, 2010. **9**(3): p. 168-76.

81. Han, M., et al., *Novel blood-based, five-gene biomarker set for the detection of colorectal cancer.* Clin Cancer Res, 2008. **14**(2): p. 455-60.

82. Cassinotti, E., et al., *DNA methylation patterns in blood of patients with colorectal cancer and adenomatous colorectal polyps.* Int J Cancer, 2012. **131**(5): p. 1153-7.

83. Leung, W.K., et al., *Detection of hypermethylated DNA or cyclooxygenase-2 messenger RNA in fecal samples of patients with colorectal cancer or polyps.* Am J Gastroenterol, 2007. **102**(5): p. 1070-6.

84. Tanzer, M., et al., *Performance of epigenetic markers SEPT9 and ALX4 in plasma for detection of colorectal precancerous lesions.* PLoS One, 2010. **5**(2): p. e9061.

85. Pack, S.C., et al., *Usefulness of plasma epigenetic changes of five major genes involved in the pathogenesis of colorectal cancer.* Int J Colorectal Dis, 2013. **28**(1): p. 139-47.

86. Imperiale, T.F., et al., *Multitarget stool DNA testing for colorectal-cancer screening.* N Engl J Med, 2014. **370**(14): p. 1287-97.

87. Ahlquist, D.A., et al., *Next-generation stool DNA test accurately detects colorectal cancer and large adenomas.* Gastroenterology, 2012. **142**(2): p. 248-56; quiz e25-6.

88. Chen, W.D., et al., *Detection in fecal DNA of colon cancer-specific methylation of the nonexpressed vimentin gene.* J Natl Cancer Inst, 2005. **97**(15): p. 1124-32.

89. Glockner, S.C., et al., *Methylation of TFPI2 in stool DNA: a potential novel biomarker for the detection of colorectal cancer.* Cancer Res, 2009. **69**(11): p. 4691-9.

90. Kalimutho, M., et al., *A simplified, non-invasive fecal-based DNA integrity assay and iFOBT for colorectal cancer detection.* Int J Colorectal Dis, 2011. **26**(5): p. 583-92.

91. Zhang, J., et al., *Detection of methylated tissue factor pathway inhibitor 2 and human long DNA in fecal samples of patients with colorectal cancer in China.* Cancer Epidemiol, 2012. **36**(1): p. 73-7.

92. Melotte, V., et al., *N-Myc downstream-regulated gene 4 (NDRG4): a candidate tumor suppressor gene and potential biomarker for colorectal cancer.* J Natl Cancer Inst, 2009. **101**(13): p. 916-27.

93. Lofton-Day, C., et al., *DNA methylation biomarkers for blood-based colorectal cancer screening.* Clin Chem, 2008. **54**(2): p. 414-23.

94. Warren, J.D., et al., *Septin 9 methylated DNA is a sensitive and specific blood test for colorectal cancer.* BMC Med, 2011. **9**: p. 133.

95. Johnson, D.A., et al., *Plasma Septin9 versus fecal immunochemical testing for colorectal cancer screening: a prospective multicenter study.* PLoS One, 2014. **9**(6): p. e98238.

96. Toth, K., et al., *Detection of methylated SEPT9 in plasma is a reliable screening method for both left- and right-sided colon cancers.* PLoS One, 2012. **7**(9): p. e46000.

97. deVos, T., et al., *Circulating methylated SEPT9 DNA in plasma is a biomarker for colorectal cancer.* Clin Chem, 2009. **55**(7): p. 1337-46.

98. Grutzmann, R., et al., *Sensitive detection of colorectal cancer in peripheral blood by septin 9 DNA methylation assay.* PLoS One, 2008. **3**(11): p. e3759.

99. Wang, D.R. and D. Tang, *Hypermethylated SFRP2 gene in fecal DNA is a high potential biomarker for colorectal cancer noninvasive screening.* World J Gastroenterol, 2008. **14**(4): p. 524-31.

100. Zhang, H., Y.C. Song, and C.X. Dang, *Detection of hypermethylated spastic paraplegia-20 in stool samples of patients with colorectal cancer.* Int J Med Sci, 2013. **10**(3): p. 230-4.

101. Lind, G.E., et al., *SPG20, a novel biomarker for early detection of colorectal cancer, encodes a regulator of cytokinesis.* Oncogene, 2011. **30**(37): p. 3967-78.

102. Lange, C.P., et al., *Genome-scale discovery of DNA-methylation biomarkers for blood-based detection of colorectal cancer.* PLoS One, 2012. **7**(11): p. e50266.

103. Mori, Y., et al., *Novel candidate colorectal cancer biomarkers identified by methylation microarray-based scanning.* Endocr Relat Cancer, 2011. **18**(4): p. 465-78.

104. *Treating colon/rectum cancer Topics*. 2015 14 June; Available from: http://www.cancer.org/cancer/colonandrectumcancer/detailedguide/colorectal-cancer-treating-by-stage-colon.

105. Andre, T., et al., *Improved overall survival with oxaliplatin, fluorouracil, and leucovorin as adjuvant treatment in stage II or III colon cancer in the MOSAIC trial.* J Clin Oncol, 2009. **27**(19): p. 3109-16.

106. Saridaki, Z., et al., *A triplet combination with irinotecan (CPT-11), oxaliplatin (LOHP), continuous infusion 5-fluorouracil and leucovorin (FOLFOXIRI) plus cetuximab as first-line treatment in KRAS wt, metastatic colorectal cancer: a pilot phase II trial.* Br J Cancer, 2012. **107**(12): p. 1932-7.

107. Cunningham, D., et al., *Cetuximab monotherapy and cetuximab plus irinotecan in irinotecan-refractory metastatic colorectal cancer.* N Engl J Med, 2004. **351**(4): p. 337-45.

108. Tabernero, J., et al., *Phase II trial of cetuximab in combination with fluorouracil, leucovorin, and oxaliplatin in the first-line treatment of metastatic colorectal cancer.* J Clin Oncol, 2007. **25**(33): p. 5225-32.

109. Tabernero, J., et al., *RAISE: A randomized, double-blind, multicenter phase III study of irinotecan, folinic acid, and 5-fluorouracil (FOLFIRI) plus ramucirumab (RAM) or placebo (PBO) in patients (pts) with metastatic colorectal carcinoma (CRC) progressive during or following first-line combination therapy with bevacizumab (bev), oxaliplatin (ox), and a fluoropyrimidine (fp).* 2015: 2015 Gastrointestinal Cancers Symposium.

110. Punt, C.J., *New options and old dilemmas in the treatment of patients with advanced colorectal cancer.* Ann Oncol, 2004. **15**(10): p. 1453-9.

111. Vincent, T.L. and R.A. Gatenby, *An evolutionary model for initiation, promotion, and progression in carcinogenesis.* International journal of oncology, 2008. **32**(4): p. 729-37.

112. Devi, P.U., *Basics of Carcinogenesis.* Health Adm., 2004. **17**(1): p. 16-24.
113. Rous, P. and J.G. Kidd, *Conditional Neoplasms and Subthreshold Neoplastic States : A Study of the Tar Tumors of Rabbits.* The Journal of experimental medicine, 1941. **73**(3): p. 365-90.
114. Mottram, J.C., *A sensitising factor in experimental blastogenesis.* The Journal of Pathology and Bacteriology, 1944. **56**(3): p. 391-402.
115. Berenblum, I. and P. Shubik, *A new, quantitative, approach to the study of the stages of chemical cartinogenesis in the mouse's skin.* British journal of cancer, 1947. **1**(4): p. 383-91.
116. Vogelstein, B., et al., *Genetic alterations during colorectal-tumor development.* The New England journal of medicine, 1988. **319**(9): p. 525-32.
117. Fearon, E.R. and B. Vogelstein, *A genetic model for colorectal tumorigenesis.* Cell, 1990. **61**(5): p. 759-67.
118. Christie, M. and O. Sieber, *Pathways of Carcinogenesis*, in *ABC of Colorectal Cancer*, A. Young, R. Hobbs, and D. Kerr, Editors. 2011, Wiley-Blackwell.
119. Young, A., R. Hobbs, and D. Kerr, *ABC of Colorectal Cancer*. 2011: Blackwell Publishing Ltd.
120. Vogelstein, B. and K.W. Kinzler, *The multistep nature of cancer.* Trends Genet, 1993. **9**(4): p. 138-41.
121. Stoffel, E.M., et al., *Hereditary colorectal cancer syndromes: American Society of Clinical Oncology Clinical Practice Guideline endorsement of the familial risk-colorectal cancer: European Society for Medical Oncology Clinical Practice Guidelines.* J Clin Oncol, 2015. **33**(2): p. 209-17.
122. Cheah, P.Y., *Hypotheses for the etiology of colorectal cancer--an overview.* Nutr Cancer, 1990. **14**(1): p. 5-13.
123. Miyoshi, Y., et al., *Somatic mutations of the APC gene in colorectal tumors: mutation cluster region in the APC gene.* Hum Mol Genet, 1992. **1**(4): p. 229-33.
124. Watson, P. and H.T. Lynch, *Extracolonic cancer in hereditary nonpolyposis colorectal cancer.* Cancer, 1993. **71**(3): p. 677-85.
125. Schwitalle, Y., et al., *Immunogenic peptides generated by frameshift mutations in DNA mismatch repair-deficient cancer cells.* Cancer Immun, 2004. **4**: p. 14.
126. Boland, C.R., et al., *A National Cancer Institute Workshop on Microsatellite Instability for cancer detection and familial predisposition: development of international criteria for the determination of microsatellite instability in colorectal cancer.* Cancer Res, 1998. **58**(22): p. 5248-57.
127. Davies, R.J., R. Miller, and N. Coleman, *Colorectal cancer screening: prospects for molecular stool analysis.* Nat Rev Cancer, 2005. **5**(3): p. 199-209.
128. Chambers, A.F., A.C. Groom, and I.C. MacDonald, *Dissemination and growth of cancer cells in metastatic sites.* Nature reviews. Cancer, 2002. **2**(8): p. 563-72.
129. Mehlen, P. and A. Puisieux, *Metastasis: a question of life or death.* Nature reviews. Cancer, 2006. **6**(6): p. 449-58.
130. Cairns, R.A., R. Khokha, and R.P. Hill, *Molecular mechanisms of tumor invasion and metastasis: an integrated view.* Current molecular medicine, 2003. **3**(7): p. 659-71.
131. Sugarbaker, P.H., *Metastatic inefficiency: the scientific basis for resection of liver metastases from colorectal cancer.* Journal of surgical oncology. Supplement, 1993. **3**: p. 158-60.
132. Weiss, L., *Metastatic inefficiency.* Advances in cancer research, 1990. **54**: p. 159-211.
133. Wittekind, C. and M. Neid, *Cancer invasion and metastasis.* Oncology, 2005. **69 Suppl 1**: p. 14-6.
134. Hart, I.R. and I.J. Fidler, *Role of organ selectivity in the determination of metastatic patterns of B16 melanoma.* Cancer research, 1980. **40**(7): p. 2281-7.
135. Nicolson, G.L., *Organ specificity of tumor metastasis: role of preferential adhesion, invasion and growth of malignant cells at specific secondary sites.* Cancer metastasis reviews, 1988. **7**(2): p. 143-88.

136. Yeaman, C., et al., *Cell polarity: Versatile scaffolds keep things in place.* Current biology : CB, 1999. **9**(14): p. R515-7.

137. Radisky, D.C., *Epithelial-mesenchymal transition.* Journal of cell science, 2005. **118**(Pt 19): p. 4325-6.

138. Klymkowsky, M.W. and P. Savagner, *Epithelial-mesenchymal transition: a cancer researcher's conceptual friend and foe.* The American journal of pathology, 2009. **174**(5): p. 1588-93.

139. Voulgari, A. and A. Pintzas, *Epithelial-mesenchymal transition in cancer metastasis: mechanisms, markers and strategies to overcome drug resistance in the clinic.* Biochimica et biophysica acta, 2009. **1796**(2): p. 75-90.

140. Samarasinghe, B. *The Hallmarks of Cancer 6: Tissue Invasion and Metastasis*. 2013 21 June; Available from: http://blogs.scientificamerican.com/guest-blog/the-hallmarks-of-cancer-6-tissue-invasion-and-metastasis/.

141. Kohn, E.C. and L.A. Liotta, *Molecular insights into cancer invasion: strategies for prevention and intervention.* Cancer research, 1995. **55**(9): p. 1856-62.

142. Liotta, L.A. and E.C. Kohn, *Invasion and Metastases*, in *Holland-Frei Cancer Medicine*, R.C. Bast, Jr., et al., Editors. 2000, BC Decker: Hamilton.

143. nanostring. *Key Features and Genes Involved in Cancer Progression*. 2015 14 June; Available from: http://www.nanostring.com/products/pancancer_progression/cancer_progression.

144. Okegawa, T., et al., *The role of cell adhesion molecule in cancer progression and its application in cancer therapy.* Acta Biochim Pol, 2004. **51**(2): p. 445-57.

145. Bendas, G. and L. Borsig, *Cancer cell adhesion and metastasis: selectins, integrins, and the inhibitory potential of heparins.* Int J Cell Biol, 2012. **2012**: p. 676731.

146. Agrez, M., et al., *The alpha v beta 6 integrin promotes proliferation of colon carcinoma cells through a unique region of the beta 6 cytoplasmic domain.* The Journal of cell biology, 1994. **127**(2): p. 547-56.

147. Ahmed, N., et al., *Alpha(v)beta(6) integrin-A marker for the malignant potential of epithelial ovarian cancer.* The journal of histochemistry and cytochemistry : official journal of the Histochemistry Society, 2002. **50**(10): p. 1371-80.

148. Brooks, P.C., R.A. Clark, and D.A. Cheresh, *Requirement of vascular integrin alpha v beta 3 for angiogenesis.* Science, 1994. **264**(5158): p. 569-71.

149. Cantor, D., et al., *Overexpression of alphavbeta6 integrin alters the colorectal cancer cell proteome in favor of elevated proliferation and a switching in cellular adhesion that increases invasion.* J Proteome Res, 2013. **12**(6): p. 2477-90.

150. Huhtala, P., et al., *Cooperative signaling by alpha 5 beta 1 and alpha 4 beta 1 integrins regulates metalloproteinase gene expression in fibroblasts adhering to fibronectin.* The Journal of cell biology, 1995. **129**(3): p. 867-79.

151. Seguin, L., et al., *Integrins and cancer: regulators of cancer stemness, metastasis, and drug resistance.* Trends Cell Biol, 2015. **25**(4): p. 234-40.

152. Gille, J. and R.A. Swerlick, *Integrins: role in cell adhesion and communication.* Annals of the New York Academy of Sciences, 1996. **797**: p. 93-106.

153. Hynes, R.O., *Integrins: versatility, modulation, and signaling in cell adhesion.* Cell, 1992. **69**(1): p. 11-25.

154. Ramos, D.M., D. Dang, and S. Sadler, *The role of the integrin alpha v beta6 in regulating the epithelial to mesenchymal transition in oral cancer.* Anticancer Res, 2009. **29**(1): p. 125-30.

155. Ganguly, K.K., et al., *Integrins and metastasis.* Cell Adh Migr, 2013. **7**(3): p. 251-61.

156. Mizejewski, G.J., *Role of integrins in cancer: survey of expression patterns.* Proc Soc Exp Biol Med, 1999. **222**(2): p. 124-38.

157. Sheldrake, H.M. and L.H. Patterson, *Strategies to inhibit tumor associated integrin receptors: rationale for dual and multi-antagonists.* J Med Chem, 2014. **57**(15): p. 6301-15.

158. Bandyopadhyay, A. and S. Raghavan, *Defining the role of integrin alphavbeta6 in cancer.* Curr Drug Targets, 2009. **10**(7): p. 645-52.

159. Giancotti, F.G. and E. Ruoslahti, *Integrin signaling.* Science, 1999. **285**(5430): p. 1028-32.

160. Chicurel, M.E., et al., *Integrin binding and mechanical tension induce movement of mRNA and ribosomes to focal adhesions.* Nature, 1998. **392**(6677): p. 730-3.

161. Schwartz, M.A. and R.K. Assoian, *Integrins and cell proliferation: regulation of cyclin-dependent kinases via cytoplasmic signaling pathways.* Journal of cell science, 2001. **114**(Pt 14): p. 2553-60.

162. Giancotti, F.G., *Integrin signaling: specificity and control of cell survival and cell cycle progression.* Current opinion in cell biology, 1997. **9**(5): p. 691-700.

163. Schwartz, M.A., M.D. Schaller, and M.H. Ginsberg, *Integrins: emerging paradigms of signal transduction.* Annual review of cell and developmental biology, 1995. **11**: p. 549-99.

164. Varner, J.A. and D.A. Cheresh, *Integrins and cancer.* Current opinion in cell biology, 1996. **8**(5): p. 724-30.

165. Meredith, J.E., Jr. and M.A. Schwartz, *Integrins, adhesion and apoptosis.* Trends in cell biology, 1997. **7**(4): p. 146-50.

166. Dedhar, S., *Integrins and tumor invasion.* BioEssays : news and reviews in molecular, cellular and developmental biology, 1990. **12**(12): p. 583-90.

167. Akiyama, S.K., K. Olden, and K.M. Yamada, *Fibronectin and integrins in invasion and metastasis.* Cancer metastasis reviews, 1995. **14**(3): p. 173-89.

168. Mahabeleshwar, G.H., et al., *Integrin signaling is critical for pathological angiogenesis.* The Journal of experimental medicine, 2006. **203**(11): p. 2495-2507.

169. Friedlander, M., et al., *Definition of two angiogenic pathways by distinct alpha v integrins.* Science, 1995. **270**(5241): p. 1500-2.

170. Bates, R.C., et al., *Transcriptional activation of integrin beta6 during the epithelial-mesenchymal transition defines a novel prognostic indicator of aggressive colon carcinoma.* The Journal of clinical investigation, 2005. **115**(2): p. 339-47.

171. Niu, J., et al., *Integrin expression in colon cancer cells is regulated by the cytoplasmic domain of the beta6 integrin subunit.* Int J Cancer, 2002. **99**(4): p. 529-37.

172. Song, J., et al., *beta1 integrin modulates tumor growth and apoptosis of human colorectal cancer.* Oncol Rep, 2014. **32**(1): p. 302-8.

173. Song, J., et al., *beta1 integrin mediates colorectal cancer cell proliferation and migration through regulation of the Hedgehog pathway.* Tumour Biol, 2015. **36**(3): p. 2013-21.

174. Oh, B.Y., et al., *Role of beta1-Integrin in Colorectal Cancer: Case-Control Study.* Ann Coloproctol, 2014. **30**(2): p. 61-70.

175. Lei, Y., et al., *Proteomics identification of ITGB3 as a key regulator in reactive oxygen species-induced migration and invasion of colorectal cancer cells.* Mol Cell Proteomics, 2011. **10**(10): p. M110 005397.

176. Beaulieu, J.F., *Integrin alpha6beta4 in colorectal cancer.* World J Gastrointest Pathophysiol, 2010. **1**(1): p. 3-11.

177. Breuss, J.M., et al., *Expression of the beta 6 integrin subunit in development, neoplasia and tissue repair suggests a role in epithelial remodeling.* J Cell Sci, 1995. **108 (Pt 6)**: p. 2241-51.

178. Munger, J.S., et al., *The integrin alpha v beta 6 binds and activates latent TGF beta 1: a mechanism for regulating pulmonary inflammation and fibrosis.* Cell, 1999. **96**(3): p. 319-28.

179. Bristow, R.E., et al., *Altered expression of transforming growth factor-beta ligands and receptors in primary and recurrent ovarian carcinoma.* Cancer, 1999. **85**(3): p. 658-68.

180. Saldanha, R.G., et al., *Proteomic identification of lynchpin urokinase plasminogen activator receptor protein interactions associated with epithelial cancer malignancy.* J Proteome Res, 2007. **6**(3): p. 1016-28.

181. Morgan, M.R., et al., *The integrin cytoplasmic-tail motif EKQKVDLSTDC is sufficient to promote tumor cell invasion mediated by matrix metalloproteinase (MMP)-2 or MMP-9.* J Biol Chem, 2004. **279**(25): p. 26533-9.

182. Huang, X.Z., et al., *Inactivation of the integrin beta 6 subunit gene reveals a role of epithelial integrins in regulating inflammation in the lung and skin.* J Cell Biol, 1996. **133**(4): p. 921-8.

183. Rakoff-Nahoum, S., *Why cancer and inflammation?* Yale J Biol Med, 2006. **79**(3-4): p. 123-30.

184. Smith, H.W. and C.J. Marshall, *Regulation of cell signalling by uPAR.* Nature reviews. Molecular cell biology, 2010. **11**(1): p. 23-36.

185. Ahn, S.B., et al., *Characterization of the interaction between heterodimeric alphavbeta6 integrin and urokinase plasminogen activator receptor (uPAR) using functional proteomics.* J Proteome Res, 2014. **13**(12): p. 5956-64.

186. Sowmya, G., et al., *A site for direct integrin alphavbeta6.uPAR interaction from structural modelling and docking.* J Struct Biol, 2014. **185**(3): p. 327-35.

187. Solberg, H., et al., *The murine receptor for urokinase-type plasminogen activator is primarily expressed in tissues actively undergoing remodeling.* J Histochem Cytochem, 2001. **49**(2): p. 237-46.

188. Romer, J., et al., *The receptor for urokinase-type plasminogen activator is expressed by keratinocytes at the leading edge during re-epithelialization of mouse skin wounds.* The Journal of investigative dermatology, 1994. **102**(4): p. 519-22.

189. de Bock, C.E. and Y. Wang, *Clinical significance of urokinase-type plasminogen activator receptor (uPAR) expression in cancer.* Med Res Rev, 2004. **24**(1): p. 13-39.

190. Pyke, C., et al., *Immunohistochemical detection of the receptor for urokinase plasminogen activator in human colon cancer.* Histopathology, 1994. **24**(2): p. 131-8.

191. Boonstra, M.C., et al., *Expression of uPAR in tumor-associated stromal cells is associated with colorectal cancer patient prognosis: a TMA study.* BMC Cancer, 2014. **14**: p. 269.

192. Illemann, M., et al., *Urokinase-type plasminogen activator receptor (uPAR) on tumor-associated macrophages is a marker of poor prognosis in colorectal cancer.* Cancer Med, 2014. **3**(4): p. 855-64.

193. Guo, H., et al., *Prognostic role of urokinase plasminogen activator receptor in gastric and colorectal cancer: A systematic review and meta-analysis.* Onco Targets Ther, 2015. **8**: p. 1503-9.

194. Ranson, M., et al., *Increased plasminogen binding is associated with metastatic breast cancer cells: differential expression of plasminogen binding proteins.* Br J Cancer, 1998. **77**(10): p. 1586-97.

195. Hilska, M., et al., *Prognostic significance of matrix metalloproteinases-1, -2, -7 and -13 and tissue inhibitors of metalloproteinases-1, -2, -3 and -4 in colorectal cancer.* International journal of cancer. Journal international du cancer, 2007. **121**(4): p. 714-23.

196. Sun, G., et al., *TGF-beta Promotes Colorectal Cancer Cell Growth In Vitro and In Vivo.* Hepato-gastroenterology, 2012. **60**(123).

197. Goustin, A.S., et al., *Growth factors and cancer.* Cancer Res, 1986. **46**(3): p. 1015-29.

198. Witsch, E., M. Sela, and Y. Yarden, *Roles for growth factors in cancer progression.* Physiology (Bethesda), 2010. **25**(2): p. 85-101.

199. Lyons, R.M., J. Keski-Oja, and H.L. Moses, *Proteolytic activation of latent transforming growth factor-beta from fibroblast-conditioned medium.* The Journal of cell biology, 1988. **106**(5): p. 1659-65.

200. Harland, R.M., *The transforming growth factor beta family and induction of the vertebrate mesoderm: bone morphogenetic proteins are ventral inducers.* Proceedings of the National Academy of Sciences of the United States of America, 1994. **91**(22): p. 10243-6.

201. Parsons, R., et al., *Microsatellite instability and mutations of the transforming growth factor beta type II receptor gene in colorectal cancer.* Cancer research, 1995. **55**(23): p. 5548-50.

202. Eppert, K., et al., *MADR2 maps to 18q21 and encodes a TGFbeta-regulated MAD-related protein that is functionally mutated in colorectal carcinoma.* Cell, 1996. **86**(4): p. 543-52.

203. Beck, H.N., et al., *Bone morphogenetic protein-5 (BMP-5) promotes dendritic growth in cultured sympathetic neurons.* BMC neuroscience, 2001. **2**: p. 12.

204. Xiong, B., et al., *Transforming growth factor-beta1 in invasion and metastasis in colorectal cancer.* World J Gastroenterol, 2002. **8**(4): p. 674-8.

205. Liao, R.Y., et al., *TGFBR1*6A/9A polymorphism and cancer risk: a meta-analysis of 13,662 cases and 14,147 controls.* Molecular biology reports, 2010. **37**(7): p. 3227-32.

206. Fleming, N.I., et al., *SMAD2, SMAD3 and SMAD4 mutations in colorectal cancer.* Cancer research, 2013. **73**(2): p. 725-35.

207. Salomon, D., *Transforming growth factor beta in cancer: Janus, the two-faced god.* J Natl Cancer Inst, 2014. **106**(2): p. djt441.

208. Akhurst, R.J., *TGF beta signaling in health and disease.* Nature genetics, 2004. **36**(8): p. 790-2.

209. Hogan, B.L., *Bone morphogenetic proteins: multifunctional regulators of vertebrate development.* Genes & development, 1996. **10**(13): p. 1580-94.

210. Risbridger, G.P., J.F. Schmitt, and D.M. Robertson, *Activins and inhibins in endocrine and other tumors.* Endocrine reviews, 2001. **22**(6): p. 836-58.

211. Woodruff, T.K. and J.P. Mather, *Inhibin, activin and the female reproductive axis.* Annual review of physiology, 1995. **57**: p. 219-44.

212. Ling, N., et al., *Pituitary FSH is released by a heterodimer of the beta-subunits from the two forms of inhibin.* Nature, 1986. **321**(6072): p. 779-82.

213. Vale, W., et al., *Purification and characterization of an FSH releasing protein from porcine ovarian follicular fluid.* Nature, 1986. **321**(6072): p. 776-9.

214. de Kretser, D.M., *Inhibin.* Molecular and cellular endocrinology, 1990. **69**(2-3): p. C17-20.

215. Jones, C.M., et al., *Nodal-related signals induce axial mesoderm and dorsalize mesoderm during gastrulation.* Development, 1995. **121**(11): p. 3651-62.

216. Meno, C., et al., *lefty-1 is required for left-right determination as a regulator of lefty-2 and nodal.* Cell, 1998. **94**(3): p. 287-97.

217. Mehler, M.F., et al., *Bone morphogenetic proteins in the nervous system.* Trends in neurosciences, 1997. **20**(7): p. 309-17.

218. Wozney, J.M., et al., *Novel regulators of bone formation: molecular clones and activities.* Science, 1988. **242**(4885): p. 1528-34.

219. Daluiski, A., et al., *Bone morphogenetic protein-3 is a negative regulator of bone density.* Nature genetics, 2001. **27**(1): p. 84-8.

220. David, L., et al., *Bone morphogenetic protein-9 is a circulating vascular quiescence factor.* Circulation research, 2008. **102**(8): p. 914-22.

221. Buxton, P., et al., *Growth/differentiation factor-5 (GDF-5) and skeletal development.* The Journal of bone and joint surgery. American volume, 2001. **83-A Suppl 1**(Pt 1): p. S23-30.

222. Francis-West, P.H., et al., *BMP/GDF-signalling interactions during synovial joint development.* Cell and tissue research, 1999. **296**(1): p. 111-9.

223. Francis-West, P.H., et al., *Mechanisms of GDF-5 action during skeletal development.* Development, 1999. **126**(6): p. 1305-15.

224. O'Keeffe, G.W., P. Dockery, and A.M. Sullivan, *Effects of growth/differentiation factor 5 on the survival and morphology of embryonic rat midbrain dopaminergic neurones in vitro.* Journal of neurocytology, 2004. **33**(5): p. 479-88.

225. Settle, S.H., Jr., et al., *Multiple joint and skeletal patterning defects caused by single and double mutations in the mouse Gdf6 and Gdf5 genes.* Developmental biology, 2003. **254**(1): p. 116-30.

226. Lee, K.J., M. Mendelsohn, and T.M. Jessell, *Neuronal patterning by BMPs: a requirement for GDF7 in the generation of a discrete class of commissural interneurons in the mouse spinal cord.* Genes & development, 1998. **12**(21): p. 3394-407.

227. McPherron, A.C., A.M. Lawler, and S.J. Lee, *Regulation of skeletal muscle mass in mice by a new TGF-beta superfamily member.* Nature, 1997. **387**(6628): p. 83-90.

228. Shi, Y. and J.P. Liu, *Gdf11 facilitates temporal progression of neurogenesis in the developing spinal cord.* The Journal of neuroscience : the official journal of the Society for Neuroscience, 2011. **31**(3): p. 883-93.

229. Lee, Y.J., et al., *Growth differentiation factor 11 signaling controls retinoic acid activity for axial vertebral development.* Developmental biology, 2010. **347**(1): p. 195-203.

230. Gad, J.M. and P.P. Tam, *Axis development: the mouse becomes a dachshund.* Current biology : CB, 1999. **9**(20): p. R783-6.

231. McPherron, A.C., A.M. Lawler, and S.J. Lee, *Regulation of anterior/posterior patterning of the axial skeleton by growth/differentiation factor 11.* Nature genetics, 1999. **22**(3): p. 260-4.

232. Kedem, A., et al., *Growth differentiating factor 9 (GDF9) and bone morphogenetic protein 15 both activate development of human primordial follicles in vitro, with seemingly more beneficial effects of GDF9.* The Journal of clinical endocrinology and metabolism, 2011. **96**(8): p. E1246-54.

233. Dong, J., et al., *Growth differentiation factor-9 is required during early ovarian folliculogenesis.* Nature, 1996. **383**(6600): p. 531-5.

234. Peng, J., et al., *Growth differentiation factor 9:bone morphogenetic protein 15 heterodimers are potent regulators of ovarian functions.* Proceedings of the National Academy of Sciences of the United States of America, 2013. **110**(8): p. E776-85.

235. Josso, N., et al., *Anti-mullerian hormone: the Jost factor.* Recent progress in hormone research, 1993. **48**: p. 1-59.

236. Wu, M.Y. and C.S. Hill, *Tgf-beta superfamily signaling in embryonic development and homeostasis.* Dev Cell, 2009. **16**(3): p. 329-43.

237. Feng, X.H. and R. Derynck, *Specificity and versatility in tgf-beta signaling through Smads.* Annu Rev Cell Dev Biol, 2005. **21**: p. 659-93.

238. Nawshad, A., et al., *Transforming growth factor-beta signaling during epithelial-mesenchymal transformation: implications for embryogenesis and tumor metastasis.* Cells Tissues Organs, 2005. **179**(1-2): p. 11-23.

239. Mercado-Pimentel, M.E. and R.B. Runyan, *Multiple transforming growth factor-beta isoforms and receptors function during epithelial-mesenchymal cell transformation in the embryonic heart.* Cells Tissues Organs, 2007. **185**(1-3): p. 146-56.

240. Moses, H.L., E.Y. Yang, and J.A. Pietenpol, *Regulation of epithelial proliferation by TGF-beta.* Ciba Found Symp, 1991. **157**: p. 66-74; discussion 75-80.

241. Massague, J., *TGFbeta in Cancer.* Cell, 2008. **134**(2): p. 215-30.

242. Roberts, A.B. and M.B. Sporn, *The Transforming Growth Factor-βs*, in *Peptide Growth Factors and Their Receptors I*, M. Sporn and A. Roberts, Editors. 1990, Springer Berlin Heidelberg. p. 419-472.

243. Coffey, R.J., Jr., et al., *Selective inhibition of growth-related gene expression in murine keratinocytes by transforming growth factor beta.* Mol Cell Biol, 1988. **8**(8): p. 3088-93.

244. Shi, M., et al., *Latent TGF-beta structure and activation.* Nature, 2011. **474**(7351): p. 343-9.

245. Brown, P.D., et al., *Physicochemical activation of recombinant latent transforming growth factor-beta's 1, 2, and 3.* Growth factors, 1990. **3**(1): p. 35-43.

246. Jullien, P., T.M. Berg, and D.A. Lawrence, *Acidic cellular environments: activation of latent TGF-beta and sensitization of cellular responses to TGF-beta and EGF.* International journal of cancer. Journal international du cancer, 1989. **43**(5): p. 886-91.

247. Barcellos-Hoff, M.H., *Radiation-induced transforming growth factor beta and subsequent extracellular matrix reorganization in murine mammary gland.* Cancer research, 1993. **53**(17): p. 3880-6.

248. Barcellos-Hoff, M.H. and T.A. Dix, *Redox-mediated activation of latent transforming growth factor-beta 1.* Molecular endocrinology, 1996. **10**(9): p. 1077-83.

249. Barcellos-Hoff, M.H., et al., *Transforming growth factor-beta activation in irradiated murine mammary gland.* The Journal of clinical investigation, 1994. **93**(2): p. 892-9.

250. Lyons, R.M., et al., *Mechanism of activation of latent recombinant transforming growth factor beta 1 by plasmin.* The Journal of cell biology, 1990. **110**(4): p. 1361-7.

251. Yu, Q. and I. Stamenkovic, *Cell surface-localized matrix metalloproteinase-9 proteolytically activates TGF-beta and promotes tumor invasion and angiogenesis.* Genes Dev, 2000. **14**(2): p. 163-76.

252. Horimoto, M., et al., *Identification of a transforming growth factor beta-1 activator derived from a human gastric cancer cell line.* British journal of cancer, 1995. **72**(3): p. 676-82.

253. Murphy-Ullrich, J.E. and M. Poczatek, *Activation of latent TGF-beta by thrombospondin-1: mechanisms and physiology.* Cytokine & growth factor reviews, 2000. **11**(1-2): p. 59-69.

254. Schultz-Cherry, S. and J.E. Murphy-Ullrich, *Thrombospondin causes activation of latent transforming growth factor-beta secreted by endothelial cells by a novel mechanism.* The Journal of cell biology, 1993. **122**(4): p. 923-32.

255. Mu, D., et al., *The integrin alpha(v)beta8 mediates epithelial homeostasis through MT1-MMP-dependent activation of TGF-beta1.* The Journal of cell biology, 2002. **157**(3): p. 493-507.

256. Munger, J.S., et al., *Interactions between growth factors and integrins: latent forms of transforming growth factor-beta are ligands for the integrin alphavbeta1.* Mol Biol Cell, 1998. **9**(9): p. 2627-38.

257. Laiho, M., et al., *Responsiveness to transforming growth factor-beta (TGF-beta) restored by genetic complementation between cells defective in TGF-beta receptors I and II.* The Journal of biological chemistry, 1991. **266**(14): p. 9108-12.

258. Boyd, F.T. and J. Massague, *Transforming growth factor-beta inhibition of epithelial cell proliferation linked to the expression of a 53-kDa membrane receptor.* J Biol Chem, 1989. **264**(4): p. 2272-8.

259. O'Grady, P., et al., *Transforming growth factor beta (TGF-beta) type V receptor has a TGF-beta-stimulated serine/threonine-specific autophosphorylation activity.* J Biol Chem, 1992. **267**(29): p. 21033-7.

260. O'Grady, P., et al., *Purification of a new type high molecular weight receptor (type V receptor) of transforming growth factor beta (TGF-beta) from bovine liver. Identification of the type V TGF-beta receptor in cultured cells.* J Biol Chem, 1991. **266**(13): p. 8583-9.

261. Bilandzic, M. and K.L. Stenvers, *Betaglycan: a multifunctional accessory.* Molecular and cellular endocrinology, 2011. **339**(1-2): p. 180-9.

262. Blobe, G.C., et al., *A novel mechanism for regulating transforming growth factor beta (TGF-beta) signaling. Functional modulation of type III TGF-beta receptor expression through interaction with the PDZ domain protein, GIPC.* The Journal of biological chemistry, 2001. **276**(43): p. 39608-17.

263. Lee, J.D., et al., *The type III TGF-beta receptor suppresses breast cancer progression through GIPC-mediated inhibition of TGF-beta signaling.* Carcinogenesis, 2010. **31**(2): p. 175-83.

264. Mitchell, E.J., K. Lee, and M.D. O'Connor-McCourt, *Characterization of transforming growth factor-beta (TGF-beta) receptors on BeWo choriocarcinoma cells including the identification of a novel 38-kDa TGF-beta binding glycoprotein.* Mol Biol Cell, 1992. **3**(11): p. 1295-307.

265. Derynck, R. and X.H. Feng, *TGF-beta receptor signaling.* Biochimica et biophysica acta, 1997. **1333**(2): p. F105-50.

266. Velasco-Loyden, G., J. Arribas, and F. Lopez-Casillas, *The shedding of betaglycan is regulated by pervanadate and mediated by membrane type matrix metalloprotease-1.* The Journal of biological chemistry, 2004. **279**(9): p. 7721-33.

267. Mendoza, V., et al., *Betaglycan has two independent domains required for high affinity TGF-beta binding: proteolytic cleavage separates the domains and inactivates the neutralizing activity of the soluble receptor.* Biochemistry, 2009. **48**(49): p. 11755-65.

268. Lin, H.Y., et al., *Expression cloning of the TGF-beta type II receptor, a functional transmembrane serine/threonine kinase.* Cell, 1992. **68**(4): p. 775-85.

269. Massague, J., *The transforming growth factor-beta family.* Annu Rev Cell Biol, 1990. **6**: p. 597-641.

270. Massague, J., *TGF-beta signal transduction.* Annu Rev Biochem, 1998. **67**: p. 753-91.

271. Gilboa, L., et al., *Oligomeric structure of type I and type II transforming growth factor beta receptors: homodimers form in the ER and persist at the plasma membrane.* The Journal of cell biology, 1998. **140**(4): p. 767-77.

272. Attisano, L., et al., *Identification of human activin and TGF beta type I receptors that form heteromeric kinase complexes with type II receptors.* Cell, 1993. **75**(4): p. 671-80.

273. Oh, S.P., et al., *Activin receptor-like kinase 1 modulates transforming growth factor-beta 1 signaling in the regulation of angiogenesis.* Proceedings of the National Academy of Sciences of the United States of America, 2000. **97**(6): p. 2626-31.

274. Ebisawa, T., et al., *Characterization of bone morphogenetic protein-6 signaling pathways in osteoblast differentiation.* Journal of cell science, 1999. **112 (Pt 20)**: p. 3519-27.

275. Yamashita, H., et al., *Osteogenic protein-1 binds to activin type II receptors and induces certain activin-like effects.* The Journal of cell biology, 1995. **130**(1): p. 217-26.

276. Macias-Silva, M., et al., *Specific activation of Smad1 signaling pathways by the BMP7 type I receptor, ALK2.* The Journal of biological chemistry, 1998. **273**(40): p. 25628-36.

277. Visser, J.A., et al., *The serine/threonine transmembrane receptor ALK2 mediates Mullerian inhibiting substance signaling.* Molecular endocrinology, 2001. **15**(6): p. 936-45.

278. ten Dijke, P., et al., *Identification of type I receptors for osteogenic protein-1 and bone morphogenetic protein-4.* The Journal of biological chemistry, 1994. **269**(25): p. 16985-8.

279. Cheng, S.K., et al., *EGF-CFC proteins are essential coreceptors for the TGF-beta signals Vg1 and GDF1.* Genes & development, 2003. **17**(1): p. 31-6.

280. Oh, S.P., et al., *Activin type IIA and IIB receptors mediate Gdf11 signaling in axial vertebral patterning.* Genes & development, 2002. **16**(21): p. 2749-54.

281. Yeo, C. and M. Whitman, *Nodal signals to Smads through Cripto-dependent and Cripto-independent mechanisms.* Molecular cell, 2001. **7**(5): p. 949-57.

282. Franzen, P., et al., *Cloning of a TGF beta type I receptor that forms a heteromeric complex with the TGF beta type II receptor.* Cell, 1993. **75**(4): p. 681-92.

283. Miyazono, K., *TGF-beta receptors and signal transduction.* Int J Hematol, 1997. **65**(2): p. 97-104.

284. Nishitoh, H., et al., *Identification of type I and type II serine/threonine kinase receptors for growth/differentiation factor-5.* The Journal of biological chemistry, 1996. **271**(35): p. 21345-52.

285. Erlacher, L., et al., *Cartilage-derived morphogenetic proteins and osteogenic protein-1 differentially regulate osteogenesis.* Journal of bone and mineral research : the official journal of the American Society for Bone and Mineral Research, 1998. **13**(3): p. 383-92.

286. Gouedard, L., et al., *Engagement of bone morphogenetic protein type IB receptor and Smad1 signaling by anti-Mullerian hormone and its type II receptor.* The Journal of biological chemistry, 2000. **275**(36): p. 27973-8.

287. Moore, R.K., F. Otsuka, and S. Shimasaki, *Molecular basis of bone morphogenetic protein-15 signaling in granulosa cells.* The Journal of biological chemistry, 2003. **278**(1): p. 304-10.

288. Reissmann, E., et al., *The orphan receptor ALK7 and the Activin receptor ALK4 mediate signaling by Nodal proteins during vertebrate development.* Genes & development, 2001. **15**(15): p. 2010-22.

289. Chapman, S.C., et al., *Properties of inhibin binding to betaglycan, InhBP/p120 and the activin type II receptors.* Molecular and cellular endocrinology, 2002. **196**(1-2): p. 79-93.

290. Wiater, E. and W. Vale, *Inhibin is an antagonist of bone morphogenetic protein signaling.* The Journal of biological chemistry, 2003. **278**(10): p. 7934-41.

291. Rosenzweig, B.L., et al., *Cloning and characterization of a human type II receptor for bone morphogenetic proteins.* Proceedings of the National Academy of Sciences of the United States of America, 1995. **92**(17): p. 7632-6.

292. Liu, F., et al., *Human type II receptor for bone morphogenic proteins (BMPs): extension of the two-kinase receptor model to the BMPs.* Molecular and cellular biology, 1995. **15**(7): p. 3479-86.

293. Lopez-Casillas, F., J.L. Wrana, and J. Massague, *Betaglycan presents ligand to the TGF beta signaling receptor.* Cell, 1993. **73**(7): p. 1435-44.

294. Wrana, J.L., et al., *TGF beta signals through a heteromeric protein kinase receptor complex.* Cell, 1992. **71**(6): p. 1003-14.

295. Akhurst, R.J. and R. Derynck, *TGF-beta signaling in cancer--a double-edged sword.* Trends Cell Biol, 2001. **11**(11): p. S44-51.

296. Wakefield, L.M. and A.B. Roberts, *TGF-beta signaling: positive and negative effects on tumorigenesis.* Curr Opin Genet Dev, 2002. **12**(1): p. 22-9.

297. Grady, W.M., et al., *Mutational inactivation of transforming growth factor beta receptor type II in microsatellite stable colon cancers.* Cancer research, 1999. **59**(2): p. 320-4.

298. Bellam, N. and B. Pasche, *Tgf-beta signaling alterations and colon cancer.* Cancer Treat Res, 2010. **155**: p. 85-103.

299. Levy, L. and C.S. Hill, *Alterations in components of the TGF-beta superfamily signaling pathways in human cancer.* Cytokine & growth factor reviews, 2006. **17**(1-2): p. 41-58.

300. Rosman, D.S., et al., *TGFBR1*6A enhances the migration and invasion of MCF-7 breast cancer cells through RhoA activation.* Cancer Res, 2008. **68**(5): p. 1319-28.

301. Qi, P., et al., *-509C>T polymorphism in the TGF-beta1 gene promoter is not associated with susceptibility to and progression of colorectal cancer in Chinese.* Colorectal Dis, 2010. **12**(11): p. 1153-8.

302. Chung, S.J., et al., *Transforming growth factor-[beta]1 -509T reduces risk of colorectal cancer, but not adenoma in Koreans.* Cancer Sci, 2007. **98**(3): p. 401-4.

303. Fang, F., et al., *TGFB1 509 C/T polymorphism and colorectal cancer risk: a meta-analysis.* Med Oncol, 2010. **27**(4): p. 1324-8.

304. Liu, Y., et al., *Transforming growth factor beta-1 C-509T polymorphism and cancer risk: a meta-analysis of 55 case-control studies.* Asian Pacific journal of cancer prevention : APJCP, 2012. **13**(9): p. 4683-8.

305. Wang, Y., et al., *An updated meta-analysis on the association of TGF-beta1 gene promoter -509C/T polymorphism with colorectal cancer risk.* Cytokine, 2013. **61**(1): p. 181-7.

306. Berndt, S.I., et al., *Transforming growth factor beta 1 (TGFB1) gene polymorphisms and risk of advanced colorectal adenoma.* Carcinogenesis, 2007. **28**(9): p. 1965-70.

307. Liu, Y., W. Zhou, and D.W. Zhong, *Meta-analyses of the associations between four common TGF-beta1 genetic polymorphisms and risk of colorectal tumor.* Tumour biology : the journal of the International Society for Oncodevelopmental Biology and Medicine, 2012. **33**(4): p. 1191-9.

308. Sparks, R., et al., *TGFbeta1 polymorphism (L10P) and risk of colorectal adenomatous and hyperplastic polyps.* Int J Epidemiol, 2004. **33**(5): p. 955-61.

309. Xu, W.Q., et al., *Expression of TGF-beta1, TbetaRII and Smad4 in colorectal carcinoma.* Exp Mol Pathol, 2007. **82**(3): p. 284-91.

310. Friedman, E., et al., *High levels of transforming growth factor beta 1 correlate with disease progression in human colon cancer.* Cancer Epidemiol Biomarkers Prev, 1995. **4**(5): p. 549-54.

311. Robson, H., et al., *Transforming growth factor beta 1 expression in human colorectal tumours: an independent prognostic marker in a subgroup of poor prognosis patients.* Br J Cancer, 1996. **74**(5): p. 753-8.

312. Tsushima, H., et al., *High levels of transforming growth factor beta 1 in patients with colorectal cancer: association with disease progression.* Gastroenterology, 1996. **110**(2): p. 375-82.

313. Shim, K.S., et al., *Elevated serum levels of transforming growth factor-beta1 in patients with colorectal carcinoma: its association with tumor progression and its significant decrease after curative surgical resection.* Cancer, 1999. **85**(3): p. 554-61.

314. Markowitz, S., et al., *Inactivation of the type II TGF-beta receptor in colon cancer cells with microsatellite instability.* Science, 1995. **268**(5215): p. 1336-8.

315. Pasche, B., et al., *Somatic acquisition and signaling of TGFBR1*6A in cancer.* JAMA, 2005. **294**(13): p. 1634-46.

316. Takagi, Y., et al., *Somatic alterations of the SMAD-2 gene in human colorectal cancers.* Br J Cancer, 1998. **78**(9): p. 1152-5.

317. Ohtaki, N., et al., *Somatic alterations of the DPC4 and Madr2 genes in colorectal cancers and relationship to metastasis.* Int J Oncol, 2001. **18**(2): p. 265-70.

318. Boulay, J.L., et al., *Combined copy status of 18q21 genes in colorectal cancer shows frequent retention of SMAD7.* Genes Chromosomes Cancer, 2001. **31**(3): p. 240-7.

319. Sjoblom, T., et al., *The consensus coding sequences of human breast and colorectal cancers.* Science, 2006. **314**(5797): p. 268-74.

320. Ku, J.L., et al., *Genetic alterations of the TGF-beta signaling pathway in colorectal cancer cell lines: a novel mutation in Smad3 associated with the inactivation of TGF-beta-induced transcriptional activation.* Cancer letters, 2007. **247**(2): p. 283-92.

321. Fukushima, T., et al., *Mutational analysis of TGF-beta type II receptor, Smad2, Smad3, Smad4, Smad6 and Smad7 genes in colorectal cancer.* J Exp Clin Cancer Res, 2003. **22**(2): p. 315-20.

322. Miyaki, M., et al., *Higher frequency of Smad4 gene mutation in human colorectal cancer with distant metastasis.* Oncogene, 1999. **18**(20): p. 3098-103.

323. Boulay, J.L., et al., *SMAD7 is a prognostic marker in patients with colorectal cancer.* Int J Cancer, 2003. **104**(4): p. 446-9.

324. Pulleyn, L.J., et al., *TGFbeta1 allele association with asthma severity.* Hum Genet, 2001. **109**(6): p. 623-7.

325. Silverman, E.S., et al., *Transforming growth factor-beta1 promoter polymorphism C-509T is associated with asthma.* Am J Respir Crit Care Med, 2004. **169**(2): p. 214-9.

326. Grainger, D.J., et al., *Genetic control of the circulating concentration of transforming growth factor type beta1.* Hum Mol Genet, 1999. **8**(1): p. 93-7.

327. Yokota, M., et al., *Association of a T29-->C polymorphism of the transforming growth factor-beta1 gene with genetic susceptibility to myocardial infarction in Japanese.* Circulation, 2000. **101**(24): p. 2783-7.

328. Awad, M.R., et al., *Genotypic variation in the transforming growth factor-beta1 gene: association with transforming growth factor-beta1 production, fibrotic lung disease, and graft fibrosis after lung transplantation.* Transplantation, 1998. **66**(8): p. 1014-20.

329. Cambien, F., et al., *Polymorphisms of the transforming growth factor-beta 1 gene in relation to myocardial infarction and blood pressure. The Etude Cas-Temoin de l'Infarctus du Myocarde (ECTIM) Study.* Hypertension, 1996. **28**(5): p. 881-7.

330. Wasinger, V.C., et al., *Progress with gene-product mapping of the Mollicutes: Mycoplasma genitalium.* Electrophoresis, 1995. **16**(7): p. 1090-4.

331. Wilkins, M.R., et al., *From proteins to proteomes: large scale protein identification by two-dimensional electrophoresis and amino acid analysis.* Biotechnology (N Y), 1996. **14**(1): p. 61-5.

332. Wilkins, M.R., et al., *Progress with proteome projects: why all proteins expressed by a genome should be identified and how to do it.* Biotechnol Genet Eng Rev, 1996. **13**: p. 19-50.

333. Edman, P., *A method for the determination of amino acid sequence in peptides.* Arch Biochem, 1949. **22**(3): p. 475.

334. Maher, S., F.P.M. Jjunju, and S. Taylor, *Colloquium: 100 years of mass spectrometry: Perspectives and future trends.* Reviews of Modern Physics, 2015. **87**(1): p. 113-135.

335. Tanaka, K., et al., *Protein and polymer analyses up to m/z 100 000 by laser ionization time-of-flight mass spectrometry.* Rapid Communications in Mass Spectrometry, 1988. **2**(8): p. 151-153.

336. Fenn, J.B., et al., *Electrospray ionization for mass spectrometry of large biomolecules.* Science, 1989. **246**(4926): p. 64-71.

337. Deterding, L.J., et al., *Nanoscale separations combined with tandem mass spectrometry.* J Chromatogr, 1991. **554**(1-2): p. 73-82.

338. Hunt, D.F., et al., *Protein sequencing by tandem mass spectrometry.* Proc Natl Acad Sci U S A, 1986. **83**(17): p. 6233-7.

339. Eng, J.K., A.L. McCormack, and J.R. Yates, *An approach to correlate tandem mass spectral data of peptides with amino acid sequences in a protein database.* J Am Soc Mass Spectrom, 1994. **5**(11): p. 976-89.

340. Perkins, D.N., et al., *Probability-based protein identification by searching sequence databases using mass spectrometry data.* Electrophoresis, 1999. **20**(18): p. 3551-3567.

341. Ghosh, D., et al., *Identification of key players for colorectal cancer metastasis by iTRAQ quantitative proteomics profiling of isogenic SW480 and SW620 cell lines.* J Proteome Res, 2011. **10**(10): p. 4373-87.

342. Xue, H., et al., *Identification of serum biomarkers for colorectal cancer metastasis using a differential secretome approach.* J Proteome Res, 2010. **9**(1): p. 545-55.

343. de Wit, M., et al., *Cell surface proteomics identifies glucose transporter type 1 and prion protein as candidate biomarkers for colorectal adenoma-to-carcinoma progression.* Gut, 2012. **61**(6): p. 855-64.

344. Lin, Q., et al., *iTRAQ analysis of colorectal cancer cell lines suggests Drebrin (DBN1) is overexpressed during liver metastasis.* Proteomics, 2014. **14**(11): p. 1434-43.

345. Shin, J., et al., *Discovery of melanotransferrin as a serological marker of colorectal cancer by secretome analysis and quantitative proteomics.* J Proteome Res, 2014. **13**(11): p. 4919-31.

346. Zou, X., et al., *Up-regulation of type I collagen during tumorigenesis of colorectal cancer revealed by quantitative proteomic analysis.* J Proteomics, 2013. **94**: p. 473-85.

347. Tsai, M.H., et al., *Identification of secretory gelsolin as a plasma biomarker associated with distant organ metastasis of colorectal cancer.* J Mol Med (Berl), 2012. **90**(2): p. 187-200.

348. Murakoshi, Y., et al., *Plasma biomarker discovery and validation for colorectal cancer by quantitative shotgun mass spectrometry and protein microarray.* Cancer Sci, 2011. **102**(3): p. 630-8.

349. Huber, L.A., K. Pfaller, and I. Vietor, *Organelle proteomics: implications for subcellular fractionation in proteomics.* Circ Res, 2003. **92**(9): p. 962-8.

350. Ramsby, M.L. and G.S. Makowski, *Differential detergent fractionation of eukaryotic cells. Analysis by two-dimensional gel electrophoresis.* Methods Mol Biol, 1999. **112**: p. 53-66.

351. McQuade, L.R., et al., *Improved membrane proteomics coverage of human embryonic stem cells by peptide IPG-IEF.* J Proteome Res, 2009. **8**(12): p. 5642-9.

352. Wissing, J., et al., *Enrichment of hydrophobic proteins via Triton X-114 phase partitioning and hydroxyapatite column chromatography for mass spectrometry.* Electrophoresis, 2000. **21**(13): p. 2589-93.

353. Han, C.L., et al., *An informatics-assisted label-free approach for personalized tissue membrane proteomics: case study on colorectal cancer.* Mol Cell Proteomics, 2011. **10**(4): p. M110 003087.

354. Chen, J.S., et al., *Comparison of membrane fraction proteomic profiles of normal and cancerous human colorectal tissues with gel-assisted digestion and iTRAQ labeling mass spectrometry.* FEBS J, 2010. **277**(14): p. 3028-38.

355.   Kume, H., et al., *Discovery of colorectal cancer biomarker candidates by membrane proteomic analysis and subsequent verification using selected reaction monitoring (SRM) and tissue microarray (TMA) analysis.* Mol Cell Proteomics, 2014. **13**(6): p. 1471-84.

356.   Edelmann, M.J., *Strong cation exchange chromatography in analysis of posttranslational modifications: innovations and perspectives.* J Biomed Biotechnol, 2011. **2011**: p. 936508.

357.   Dole, M., et al., *Molecular Beams of Macroions.* The Journal of Chemical Physics, 1968. **49**(5): p. 2240-2249.

358.   Karas, M., et al., *Matrix-assisted ultraviolet laser desorption of non-volatile compounds.* International Journal of Mass Spectrometry and Ion Processes, 1987. **78**(0): p. 53-68.

359.   El-Aneed, A., A. Cohen, and J. Banoub, *Mass Spectrometry, Review of the Basics: Electrospray, MALDI, and Commonly Used Mass Analyzers.* Applied Spectroscopy Reviews, 2009. **44**(3): p. 210-230.

360.   Glish, G.L. and R.W. Vachet, *The basics of mass spectrometry in the twenty-first century.* Nat Rev Drug Discov, 2003. **2**(2): p. 140-50.

361.   Ho, C.S., et al., *Electrospray ionisation mass spectrometry: principles and clinical applications.* Clin Biochem Rev, 2003. **24**(1): p. 3-12.

362.   Yates, J.R., C.I. Ruse, and A. Nakorchevsky, *Proteomics by mass spectrometry: approaches, advances, and applications.* Annu Rev Biomed Eng, 2009. **11**: p. 49-79.

363.   Miller, P.E. and M.B. Denton, *The quadrupole mass filter: Basic operating concepts.* Journal of Chemical Education, 1986. **63**(7): p. 617.

364.   Wolff, M.M. and W.E. Stephens, *A Pulsed Mass Spectrometer with Time Dispersion.* Review of Scientific Instruments, 1953. **24**(8): p. 616-617.

365.   Brown, R.S. and J.J. Lennon, *Mass resolution improvement by incorporation of pulsed ion extraction in a matrix-assisted laser desorption/ionization linear time-of-flight mass spectrometer.* Anal Chem, 1995. **67**(13): p. 1998-2003.

366.   Yates, J.R., 3rd, *Mass spectrometry and the age of the proteome.* J Mass Spectrom, 1998. **33**(1): p. 1-19.

367.   Gillet, L.C., et al., *Targeted data extraction of the MS/MS spectra generated by data-independent acquisition: a new concept for consistent and accurate proteome analysis.* Mol Cell Proteomics, 2012. **11**(6): p. O111 016717.

368.   Wiese, S., et al., *Protein labeling by iTRAQ: a new tool for quantitative mass spectrometry in proteome research.* Proteomics, 2007. **7**(3): p. 340-50.

369.   Shiio, Y. and R. Aebersold, *Quantitative proteome analysis using isotope-coded affinity tags and mass spectrometry.* Nat Protoc, 2006. **1**(1): p. 139-45.

370.   Ong, S.E., et al., *Stable isotope labeling by amino acids in cell culture, SILAC, as a simple and accurate approach to expression proteomics.* Mol Cell Proteomics, 2002. **1**(5): p. 376-86.

371.   Stewart, II, T. Thomson, and D. Figeys, *18O labeling: a tool for proteomics.* Rapid Commun Mass Spectrom, 2001. **15**(24): p. 2456-65.

372.   Shen, Y., N.N. Senzer, and J.J. Nemunaitis, *Use of Proteomics Analysis for Molecular Precision Approaches in Cancer Therapy.* Drug Target Insights, 2008. **3**(DTI-3-Nemunaitis-et-al): p. 55-66.

373.   Tweedie-Cullen, R.Y. and M. Livingstone-Zatchej, *Quantitative analysis of protein expression using iTRAQ and mass spectrometry.* 2008.

374.   Shilov, I.V., et al., *The Paragon Algorithm, a next generation search engine that uses sequence temperature values and feature probabilities to identify peptides from tandem mass spectra.* Mol Cell Proteomics, 2007. **6**(9): p. 1638-55.

375.   Tang, W.H., I.V. Shilov, and S.L. Seymour, *Nonlinear fitting method for determining local false discovery rates from decoy database searches.* J Proteome Res, 2008. **7**(9): p. 3661-7.

376.   Ahmed, N., et al., *Downregulation of urokinase plasminogen activator receptor expression inhibits Erk signalling with concomitant suppression of invasiveness due to loss of uPAR-beta1 integrin complex in colon cancer cells.* Br J Cancer, 2003. **89**(2): p. 374-84.

377. Yang, G.Y., et al., *Integrin alpha v beta 6 mediates the potential for colon cancer cells to colonize in and metastasize to the liver.* Cancer Sci, 2008. **99**(5): p. 879-87.

378. Chaurasia, P., et al., *A region in urokinase plasminogen receptor domain III controlling a functional association with alpha5beta1 integrin and tumor growth.* J Biol Chem, 2006. **281**(21): p. 14852-63.

379. Ahmed, N., et al., *Direct integrin alphavbeta6-ERK binding: implications for tumour growth.* Oncogene, 2002. **21**(9): p. 1370-80.

380. Cheruku, H.R., et al., *Transforming growth factor-β, MAPK and Wnt signaling interactions in colorectal cancer.* EuPA Open Proteomics, 2015(0).

381. Hayashida, T., M. Decaestecker, and H.W. Schnaper, *Cross-talk between ERK MAP kinase and Smad signaling pathways enhances TGF-beta-dependent responses in human mesangial cells.* FASEB J, 2003. **17**(11): p. 1576-8.

382. Hough, C., M. Radu, and J.J. Dore, *Tgf-beta induced Erk phosphorylation of smad linker region regulates smad signaling.* PLoS One, 2012. **7**(8): p. e42513.

383. Koromilas, A.E., *Roles of the translation initiation factor eIF2alpha serine 51 phosphorylation in cancer formation and treatment.* Biochim Biophys Acta, 2015. **1849**(7): p. 871-880.

384. Hamamura, K., et al., *Attenuation of malignant phenotypes of breast cancer cells through eIF2alpha-mediated downregulation of Rac1 signaling.* Int J Oncol, 2014. **44**(6): p. 1980-8.

385. Zheng, Q., J. Ye, and J. Cao, *Translational regulator eIF2alpha in tumor.* Tumour Biol, 2014. **35**(7): p. 6255-64.

386. Brattain, M.G., et al., *Heterogeneity of malignant cells from a human colonic carcinoma.* Cancer Res, 1981. **41**(5): p. 1751-6.

387. Wang, Y., et al., *Inhibition of colon cancer metastasis by a 3'- end antisense urokinase receptor mRNA in a nude mouse model.* Int J Cancer, 2001. **92**(2): p. 257-62.

388. Stolboushkina, E.A. and M.B. Garber, *Eukaryotic type translation initiation factor 2: structure-functional aspects.* Biochemistry (Mosc), 2011. **76**(3): p. 283-94.

389. Cantor, D., et al., *Overexpression of alphavbeta6 integrin alters the colorectal cancer cell proteome in favor of elevated proliferation and a switching in cellular adhesion that increases invasion.* Journal of proteome research, 2013. **12**(6): p. 2477-90.

390. Nathan, C.O., et al., *Elevated expression of eIF4E and FGF-2 isoforms during vascularization of breast carcinomas.* Oncogene, 1997. **15**(9): p. 1087-94.

391. Seki, N., et al., *Expression of eukaryotic initiation factor 4E in atypical adenomatous hyperplasia and adenocarcinoma of the human peripheral lung.* Clin Cancer Res, 2002. **8**(10): p. 3046-53.

392. Badura, M., et al., *DNA damage and eIF4G1 in breast cancer cells reprogram translation for survival and DNA repair mRNAs.* Proc Natl Acad Sci U S A, 2012. **109**(46): p. 18767-72.

393. Clarkson, B.K., W.V. Gilbert, and J.A. Doudna, *Functional overlap between eIF4G isoforms in Saccharomyces cerevisiae.* PLoS One, 2010. **5**(2): p. e9114.

394. Park, E.H., et al., *Depletion of eIF4G from yeast cells narrows the range of translational efficiencies genome-wide.* BMC Genomics, 2011. **12**: p. 68.

395. Ramirez-Valle, F., et al., *eIF4GI links nutrient sensing by mTOR to cell proliferation and inhibition of autophagy.* J Cell Biol, 2008. **181**(2): p. 293-307.

396. Litvak, A., et al., *False-positive elevations of carcinoembryonic antigen in patients with a history of resected colorectal cancer.* J Natl Compr Canc Netw, 2014. **12**(6): p. 907-13.

397. Gurluler, E., et al., *Serum annexin A2 levels in patients with colon cancer in comparison to healthy controls and in relation to tumor pathology.* Med Sci Monit, 2014. **20**: p. 1801-7.

398. Yang, T., et al., *Prognostic and diagnostic significance of annexin A2 in colorectal cancer.* Colorectal Dis, 2013. **15**(7): p. e373-81.

399. Bertucci, F., et al., *Gene expression profiling of colon cancer by DNA microarrays and correlation with histoclinical parameters.* Oncogene, 2004. **23**(7): p. 1377-91.

400. Duncan, R., et al., *Characterisation and protein expression profiling of annexins in colorectal cancer.* Br J Cancer, 2008. **98**(2): p. 426-33.

401. Karantza, V., *Keratins in health and cancer: more than mere epithelial cell markers.* Oncogene, 2011. **30**(2): p. 127-38.

402. Yang, Y.Q., et al., *Upregulated expression of S100A6 in human gastric cancer.* J Dig Dis, 2007. **8**(4): p. 186-93.

403. Zhang, J., et al., *S100A6 as a potential serum prognostic biomarker and therapeutic target in gastric cancer.* Dig Dis Sci, 2014. **59**(9): p. 2136-44.

404. Fakih, M.G. and A. Padmanabhan, *CEA monitoring in colorectal cancer. What you should know.* Oncology (Williston Park), 2006. **20**(6): p. 579-87; discussion 588, 594, 596 passim.

405. Terada, H., T. Urano, and H. Konno, *Association of interleukin-8 and plasminogen activator system in the progression of colorectal cancer.* Eur Surg Res, 2005. **37**(3): p. 166-72.

406. Bunger, S., et al., *Toward standardized high-throughput serum diagnostics: multiplex-protein array identifies IL-8 and VEGF as serum markers for colon cancer.* J Biomol Screen, 2011. **16**(9): p. 1018-26.

407. Sun, Q., et al., *Interleukin-8 promotes cell migration through integrin alphavbeta6 upregulation in colorectal cancer.* Cancer Lett, 2014. **354**(2): p. 245-53.

408. Chauhan, A., et al., *Prognostic value of prolactin in postoperative colorectal carcinoma.* Gastrointest Cancer Res, 2008. **2**(5): p. 260-1.

409. Soroush, A.R., et al., *Plasma prolactin in patients with colorectal cancer.* BMC Cancer, 2004. **4**: p. 97.

410. Pang, S.S., et al., *The structural basis for autonomous dimerization of the pre-T-cell antigen receptor.* Nature, 2010. **467**(7317): p. 844-8.

411. Sethi, M.K., et al., *Comparative N-glycan profiling of colorectal cancer cell lines reveals unique bisecting GlcNAc and alpha-2,3-linked sialic acid determinants are associated with membrane proteins of the more metastatic/aggressive cell lines.* J Proteome Res, 2014. **13**(1): p. 277-88.

APPENDICES

Appendix I – Expression of TGFβ receptors 1 and 2 in the cell lines used in this thesis
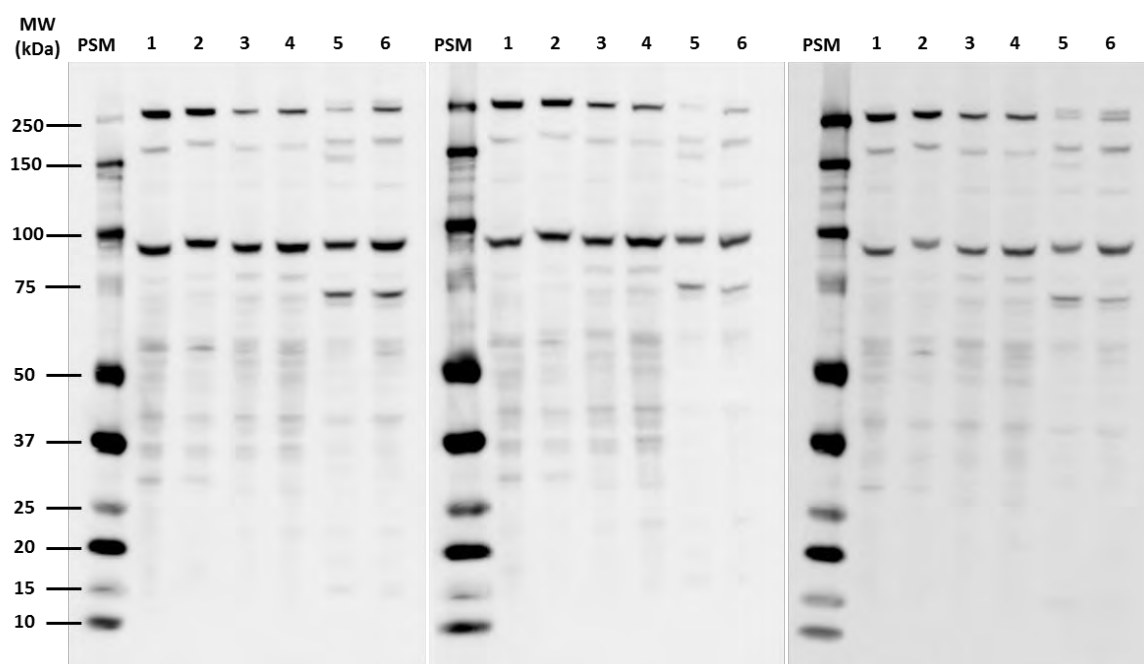
Appendix I Figure 1 – Expression TGFβ receptor 1 (TGFβR1) in all the six cell lines used in this thesis examined by Werstern blotting using anti-TGFβ RI antibody (V-22; Cat #: sc-398) from Santa Cruz Biotechnology. 50 µg or whole cell lysate was loaded into each well. All the cell lines were identified to express the TGFβR1 and the dimeric form of the receptors identified in the Western blot. PSM: prestained Western marker; Lane 1: HCT116^{WT}; Lane 2: HT29^{uPARAS}; Lane 3: SW480^{Mock}; Lane 4: SW480^{β6OE}; Lane 5: HT29^{Mock}; and Lane 6: HT29^{β6AS}
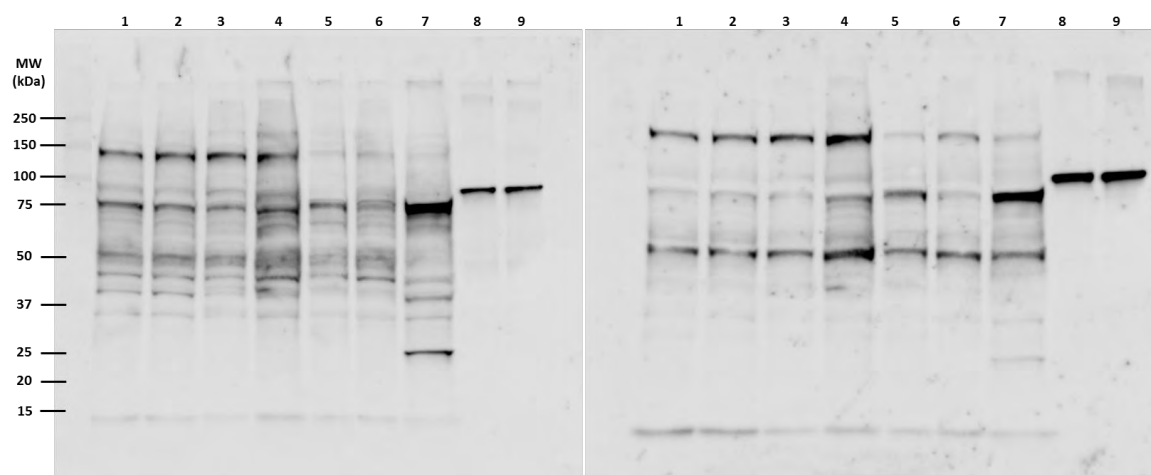
Appendix I Figure 2 – Expression TGFβ receptor 2 (TGFβR2) in all the six cell lines used in this thesis examined by Werstern blotting using anti-TGFβ RII antibody (c-16; Cat #: sc-220) from Santa Cruz Biotechnology. 50 μg or whole cell lysate was loaded into each well. All the cell lines were identified to express the TGFβR2 around the 75 kDa as reported by the antibody manufacturer (Source: http://datasheets.scbt.com/sc-220.pdf). Breast cancer cell line MCF-7 was used as positive control cell lysate as it is known to express the TGFβR2. Recombinant TGFβR2 was also used. Lane 1: HCT116^{WT}; Lane 2: HT29^{uPARAS}; Lane 3: SW480^{Mock}; Lane 4: SW480^{β6OE}; Lane 5: HT29^{Mock}; Lane 6: HT29^{β6AS}; Lane 7: MCF-7 cell lysate; Lane 8: 180 ng recombinant TGFβR2; and Lane 9: 200 ng recombinant TGFβR2

Appendix II – Characterization of the interaction between heterodimeric alphavbeta6 integrin and urokinase plasminogen activator receptor (uPAR) using functional proteomics. Publication VII of this thesis.

Characterization of the Interaction between Heterodimeric αvβ6 Integrin and Urokinase Plasminogen Activator Receptor (uPAR) Using Functional Proteomics

Seong Beom Ahn,[†,∇] Abidali Mohamedali,[‡,∇] Samyuktha Anand,[‡,∇] Harish R. Cheruku,[†] Debra Birch,[‡] Gopichandran Sowmya,[‡] David Cantor,[†] Shoba Ranganathan,[‡] David W. Inglis,[§] Ronald Frank,[∥] Michael Agrez,[⊥] Edouard C. Nice,[#] and Mark S. Baker*,[†]

[†]Australian School of Advanced Medicine, Faculty of Human Sciences, [‡]Department of Chemistry and Biomolecular Sciences, and [§]Department of Engineering, Faculty of Science, Macquarie University, Sydney, NSW 2109, Australia

[∥]Department of Chemical Biology, Helmholtz Centre for Infection Research, Inhoffen Strasse, 738124 Braunschweig, Germany

[⊥]Division of Surgery, John Hunter Hospital, Newcastle, NSW 2310, Australia

[#]Department of Biochemistry and Molecular Biology, Monash University, Melbourne, VIC 3800, Australia

ABSTRACT: Urokinase plasminogen activator receptor (uPAR) and the epithelial integrin αvβ6 are thought to individually play critical roles in cancer metastasis. These observations have been highlighted by the recent discovery (by proteomics) of an interaction between these two molecules, which are also both implicated in the epithelial–mesenchymal transition (EMT) that facilitates escape of cells from tissue barriers and is a common signature of cancer metastases. In this study, orthogonal in cellulo and in vitro functional proteomic approaches were used to better characterize the uPAR·αvβ6 interaction. Proximity ligation assays (PLA) confirmed the uPAR·αvβ6 interaction on OVCA429 (ovarian cancer line) and four different colon cancer cell lines including positive controls in cells with de novo β6 subunit expression. PLA studies were then validated using peptide arrays, which also identified potential physical sites of uPAR interaction with αvβ6, as well as verifying interactions with other known uPAR ligands (e.g., uPA, vitronectin) and individual integrin subunits (i.e., αv, β1, β3, and β6 alone). Our data suggest that interaction with uPAR requires expression of the complete αβ heterodimer (e.g., αvβ6), not individual subunits (i.e., αv, β1, β3, or β6). Finally, using in silico structural analyses in concert with these functional proteomics studies, we propose and demonstrate that the most likely unique sites of interaction between αvβ6 and uPAR are located in uPAR domains II and III.

KEYWORDS: functional proteomics, uPAR, αvβ6 integrin, proximity ligation assay, peptide array, ovarian cancer, colorectal cancer
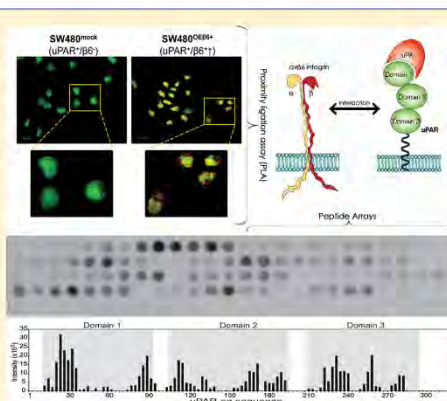
■ INTRODUCTION

A hallmark of epithelial cancer metastasis is the ability of cancer cells to migrate and infiltrate distant organs. Key stages during metastasis include detachment of the tumor cell from neighboring cells and the basement membrane, intravasation of cell(s) to the blood or lymphatic system, invasion of the migrated cell into a new environment, readhesion, and finally angiogenesis.[1] At the molecular level, the epithelial–mesenchymal transition (EMT) is thought to be a pivotal biological process that facilitates tissue remodeling and metastatic progression. Normal epithelial cells undergo numerous biochemical alterations during EMT, including loss of cell polarity, loss of cell–cell adhesion, suppression of E-cadherin, and an increase in cell migration and invasiveness.[2] EMT is facilitated by degradation of extracellular matrix (ECM) structures, allowing cancer cells to escape and potentially colonize secondary sites in the body.[2] Degradation of ECM is now thought to be one of the most complex and important mechanisms that drives EMT, but how this occurs is not yet fully understood. The matrix metalloproteinase (MMP) family and the serine protease plasminogen activation cascade are two major matrix degrading protease families implicated in epithelial cancer metastasis (e.g., breast, endometrial, hepato-

5956

cellular, colorectal, pancreatic, gastric, renal, brain, and lung).[3] Both the MMPs and the plasmin are found as inactive zymogens (pro-MMPs and plasminogen, respectively), which are spatially and temporally (spatiotemporally) activated in a series of steps.[4] Inactive plasminogen can be converted to active plasmin by urokinase plasminogen activator (uPA) on its major receptor the uPA-receptor (uPAR), where it is relatively "shielded" from inhibitors when located on the cell surface. Plasmin degrades many ECM components including fibrin, fibronectin, laminin, and the protein core of proteoglycans,[4] while also activating MMP-1, MMP-3, and MMP-9 among many proteases that consequently degrade additional ECM components.[5] To understand the regulation and consequences of ECM degradation in the tumor microenvironment, it was essential to determine cell surface interacting proteins. Using immunoprecipitation and mass spectrometry, we recently elucidated a cell surface uPAR interactome using an ovarian cancer cell line (OVCA429) with the novel discovery of the interaction of uPAR and integrin αvβ6,[5] subsequently shown as uPAR·αvβ6. This was further validated by Western blot analysis. Interestingly, both of these cell surface proteins have been implicated in many aspects of the biology of epithelial cancer and its progression.[5]

From more than 8000 membrane proteins predicted from the human protein-coding genes,[6] uPAR has been suggested to be one of a few multifunctional multi-interacting cell surface receptors that is known to be involved in, among other things, ECM degradation, growth factor activation, and downstream cellular signaling.[7] A glycosylphosphotidylinositol (GPI) linker anchors the three domains (DI, DII, and DIII) of the mature uPAR protein to the extracellular surface of the plasma membrane. These three domains form a thick-fingered glove-like structure that provides a central pocket for the binding of the cognate ligand protease, uPA.[8] Equally this shape reveals a large contralateral external surface potentially facilitating interactions with other proteins.[8] While initial studies focused exclusively on regulation of plasmin activation by uPAR, 42 proteins (9 extracellular proteins and 33 lateral interacting partners) have now been proposed to interact with uPAR.[9] This exhaustive list suggests that uPAR may have evolved multiple different ligand specificities involved in the regulation of many biologies, like proteolysis, cell migration, proliferation, cell signaling, as well as other yet to be explored cell behaviors. Indeed, in the past decade, extensive evidence has suggested that uPAR is implicated in cell adhesion, proliferation, migration, tissue remodeling, and regulation of signaling pathways (e.g., MAP kinase, Ras pathways),[7] which are important features not only of ubiquitous developmental pathways, but more importantly for cancer metastasis. High expression of the uPAR antigen has been observed in many cancers (including breast, ovarian, colon, and lung[10,11]). In colorectal cancer (CRC), a high level of uPAR has been suggested as a prognostic factor for poor survival.[11] Additionally, up-regulation of uPA in metastasis and its subsequent roles in the degradation of the ECM have further suggested uPAR and its interacting partners are central to processes that lead to metastasis, including EMT.[12]

As uPAR possesses no intrinsic intracellular domain, it is commonly thought that downstream cellular signaling pathways influenced by uPAR must be mediated through lateral interactions with transmembrane proteins (e.g., integrins). Indeed, 11 integrins (out of a total of 24) have been suggested to directly interact with uPAR,[9] and many of these studies have

implicated these interactions in some role in cancer metastasis.[13] A major function of integrins that relates them directly to cell adhesion in cancer metastasis is in cellular traction, where the β subunit embeds itself across the cell membrane and mechanically links integrins to the cytoskeleton and ECM.[13] Integrins also regulate molecular processes related to cell morphology, proliferation, survival, migration, and invasion, mostly by engaging in crucial intracellular signaling.[13]

This study focuses specifically on the αvβ6 integrin, a transmembrane heterodimer receptor expressed exclusively on the surface of epithelial cells. The αvβ6 integrin is involved in a bidirectional manner in the signal cascade system, sending signals from the cells to the ECM and vice versa via a series of protein binding partners, which include fibronectin, cytotactin, tenascin, vitronectin (Vn), and TGFβ1.[14] High expression of αvβ6 has been demonstrated in various cancers including CRC, liver, ovarian, gastric, thyroid, cervical squamous, and endometrial cancer, where its expression is often correlated with poor patient survival.[15,16] Several studies have implicated αvβ6 in cell proliferation, migration, and invasion,[16,17] with some reports suggesting the involvement of αvβ6 through activation and up-regulation of various MMP-driven proteolytic pathways.[16] Furthermore, it has been conclusively demonstrated that αvβ6 activates nascent latent transforming growth factor, TGF-β1,[18] which can also up-regulate MMP pathways,[19] leading to similar outcomes.

Our central hypothesis here is that, when coexpressed, uPAR and αvβ6 function cooperatively as a single membrane proteomic machine (as uPAR·αvβ6). In this study, we confirm the originally observed uPAR·αvβ6 interaction by functional proteomics using two orthogonal techniques, proximity ligation assays (PLA) and peptide arrays. In detail, PLA is an in cellulo technique that allows direct detection of protein−protein interactions due to the close proximity of the binding partners, and the in vitro peptide array method was used to locate potential specific interacting sites in uPAR·αvβ6 using an offset 15-mer sequential array of uPAR peptides across the whole protein sequence to find binding sites using HRP-labeled αvβ6 or other ligands (i.e., uPA, Vn, and integrin subunits). Furthermore, using an in silico structural analysis tool (ICM bioinformatics software), we were able to map putative sites of uPAR and αvβ6 interaction. This study not only validates the uPAR·αvβ6 interactions observed by proteomics in CRC and ovarian cancer cells, but also opens significant new avenues for functional targeting of similar interactions that may play key roles in epithelial cancer metastasis and provide unique therapeutic options.

■ MATERIALS AND METHODS

Antibodies and Recombinant Proteins

Monoclonal antibodies (mAb) against human uPAR (clone R4, IgG1) were purchased from DAKO (Glostrup, Denmark). The mAb against the β6 subunit of the human αvβ6 integrin (clone 6.4B4, IgG1) was obtained from Biogen Idec (Cambridge, MA).[20] Isotype control, IgG1, was purchased from R&D Systems (Minneapolis, MN). The full length recombinant proteins that were used for the peptide array were uPA and integrin αvβ6 (R&D Systems); vitronectin (Merck Millipore, MA); and integrin αv, β6, β1, and β3 (Abnova, Taipei City, Taiwan).

358

Cell Culture

The ovarian and colon cancer cell lines expressing uPAR and varying levels of $\beta6$ used for the experiments were: ovarian, OVCA429[21] (uPAR[+], $\beta6^3$); colorectal, HT29[mock] (uPAR[+], $\beta6^3$), HT29[$\beta6AS$] (uPAR[+], $\beta6^+\downarrow$), SW480[$\beta6OE$] (uPAR[+], $\beta6^+\uparrow$), and SW480[mock] (uPAR[+], $\beta6^-$).[22,23] The OVCA429 cells were cultured in DMEM (Invitrogen) media supplemented with 10% FBS, 100 μg/mL penicillin, 100 μg/mL streptomycin, 10 mM HEPES, and 6 mM L-glutamine. The HT29[mock] and HT29[$\beta6AS$] cells were cultured in RPMI media (Invitrogen, San Diego, CA) supplemented with 10% FBS and 2.5 μg/mL puromycin. The SW480[$\beta6OE$] and SW480[mock] cells were cultured in DMEM supplemented with 4.5 g/L glucose, 10% FBS, and 500 μg/mL Geneticin G418 (Invitrogen). The cells were seeded at 2×10^5 cells/mL and were grown until ~50% confluence prior to immunofluorescence and PLA experiments. All cells were grown at 37 °C in 5% CO_2 (v/v) in biological triplicates.

Immunofluorescence (IF)

The presence and/or absence of uPAR and $\beta6$ in all five cell lines were confirmed using IF. When cell cultures reached ~50% confluence, the cells were fixed using 2% paraformaldehyde for 10 min, washed with 0.1 M glycine in PBS, and incubated with blocking solution (9% goat serum, 1% BSA in PBS) for 1 h at room temperature. The cells were then incubated with anti-uPAR R4 (5 μg/mL) and anti-$\alpha v\beta6$ 6.4B4 (5 μg/mL) antibodies for 1 h at 37 °C followed by incubation with Alexa Fluor 488 goat Anti-Mouse IgG (H+L) (Invitrogen) as secondary antibody (4 μg/mL), for 1 h at 37 °C. Cell nuclei were counter stained with the blue fluorescent DAPI (Invitrogen) nucleic acid stain (300 nM) for 10 min and mounted on glass slides in Gelmount (ProScitech, Australia). The cells were analyzed using a UPLSAPO 40× objective (N.A. 0.95) on a fluorescence microscope (BX63, Olympus, Tokyo). All image capture was conducted using a XM10, monochrome cooled CCD camera and CELLSENS dimensions software (Olympus, Tokyo).

Proximity Ligation Assay (PLA)

The assay was performed according to manufacturer's instructions (Olink Bioscience, Uppsala, Sweden). Briefly, the PLUS oligonucleotide probe was conjugated to anti-uPAR R4 and its isotype control (IgG1), while the MINUS oligonucleotide probe was conjugated to anti-$\alpha v\beta6$ 6.4B4 and its corresponding isotype control (IgG1). Cells were fixed using 2% paraformaldehyde in PBS and blocked using blocking solution (9% goat serum, 1% BSA in PBS). Oligonucleotide probe conjugated antibodies were introduced to the cells and incubated for 1 h, followed by incubation with the ligation solution for 30 min, followed by amplification solution (contains Cy5 fluorophore) for 100 min. Cells were counter stained with SYBR Green1 stain and mounted. The PLUS and MINUS oligonucleotide conjugated IgG1 mAbs were used as negative controls.

PLA Imaging

The cells were imaged using an Olympus Fluoview 300 confocal laser scanning system equipped with an inverted microscope (IX70, Olympus Tokyo). A 40× UPLAN APO objective (NA 0.95) was used for analysis of all slides. SYBR Green1 stain was excited using a 488 nm argon laser and the emission signal detected using 510 and 530 nm interference filters. The Cy5 dye was excited using the 633 nm HeNe laser,

and the emission signal was detected using a long pass 610 barrier filter. Three sets of images, in the X, Y, and Z dimensions (10 optical slices with a spacing of 0.5 μm), were captured for each replicate and image analysis performed on the extended XYZ images, using Duolink Image Tool software (Olink Bioscience). The number of protein interaction signals (seen as red spots) per cell was calculated for each image. Aggregated cells were counted manually to avoid miscalculation. A student t test was performed to establish the statistical significance of uPAR·$\alpha v\beta6$ for each cell line.

uPAR Peptide Array

A cellulose-bound array of 108 spots of 15-mer peptides covering the complete uPAR sequence of 331 amino acids with a 3 amino acid shift was synthesized using SPOT synthesis.[24,25] The uPAR peptide arrays were blocked with 5% skim milk followed by incubation with HRP conjugated recombinant proteins (HRP-RPs) for 4 h. HRP-RPs were prepared by a Lightning-Link HRP conjugation kit (Innova Biosciences) as per the manufacturer's instructions. Unbound HRP-RPs was washed off, and bound HRP-RPs was detected using Super-Signal West Femto Chemiluminescent Substrate (Thermo Scientific). Images were captured using a Fujifilm CS3000 imager in chemiluminescence mode with the intensity adjusted such that the darkest spots were slightly below saturation. The images were then analyzed using MultiGuage software (FujiFilm). A quantitative intensity value for each spot was calculated using the following formula:

$$intensity = (AU - BG)/t$$

where "AU" is the measured intensity of each spot, "BG" is the background, and "t" is the time of exposure of the imaging. The uPAR peptide array with $\alpha v\beta6$ was performed in triplicate to confirm reproducibility.

Bioinformatics Analysis of uPAR Interaction

The known crystal structures (PDB ID: 3BT1) of uPAR, uPA, and Vn complex[26] were analyzed using the ICM bioinformatics software (Internal Coordinate Mechanics).[27] First, the uPAR regions that bound to $\alpha v\beta6$ on the peptide array were graphically visualized using ICM. These regions were then subjected to manual analysis to determine residues with favorable side-chain orientations. The residues with favorable side-chain orientations were then reanalyzed to determine $\alpha v\beta6$ residues potentially accessible to the outer surface of uPAR based on hydrophobicity.

■ RESULTS AND DISCUSSION

Previous proteomics studies using immunoprecipitation, mass spectrometry, and Western blot analysis, using the ovarian cancer cell line OVCA429,[5] demonstrated that uPAR potentially interacts with other membrane associated proteins, including the $\alpha v\beta6$ integrin heterodimer. Many of the proteins identified in that study had been previously implicated in either the biology of cancer metastasis, the regulation of plasminogen activation, or as prognostic indicators of poor cancer patient survival (e.g., α-enolase, $\alpha v\beta6$, uPAR). Specifically, uPAR and $\alpha v\beta6$ have been independently implicated in both cancer biology (e.g., proliferation, TGFβ activation, cell adhesion, migration, proteolysis, and invasion) and poor epithelial cancer patient prognosis (colorectal, breast, prostate, lung, and ovarian cancer).[7] Coexpression of uPAR and $\alpha v\beta6$ in the OVCA429 and other cell lines is now well established.[8] Studies using flow cytometry have also independently confirmed the expression of
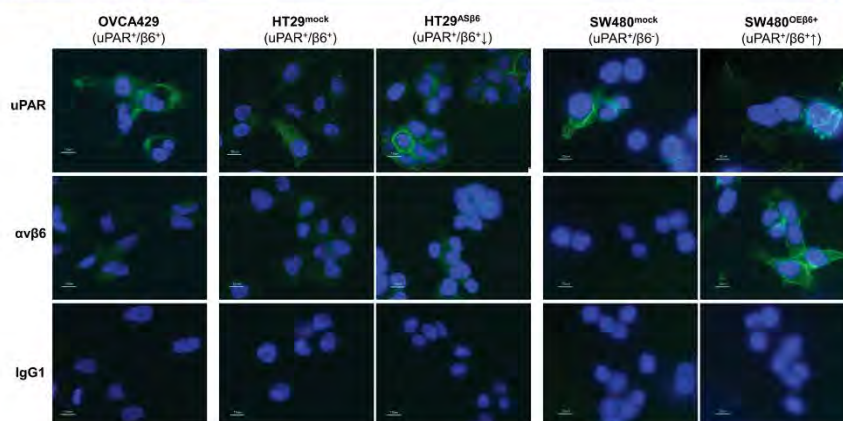
359

Figure 1. A representation of the cell surface expression of uPAR and $\alpha v\beta6$ for five different cell lines as SW480 $\beta6$OE, SW480 mock, OVCA-429, HT-29 mock, and HT-29 $\beta6$AS each expressing varying levels of $\beta6$. The third row represents the antibody control (IgG1). Nuclei were stained with DAPI, while proteins were detected with a secondary antibody conjugated to Alexa 488.
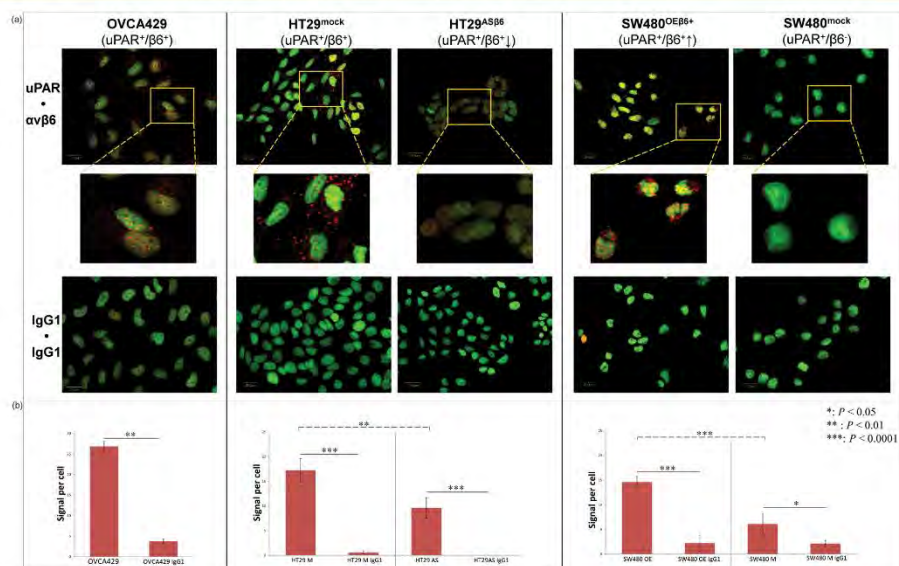

Figure 2. Proximity ligation assay images of the cells shown in (A) where the red spots represent the interaction between uPAR·$\alpha v\beta6$. A signal for the interaction of the uPAR·$\alpha v\beta6$ corresponding to the level of $\beta6$ in the cell seems to be observed as compared to the IgG1 isotype control. (B) This observation was quantified by measuring the number of spots per cell. The results showed a significant decrease in interaction when the level of $\beta6$ was reduced by 35% (in HT-29 $\beta6$AS cells) ($p < 0.05$). Similarly, a significant increase in interactions was observed when $\beta6$ was up-regulated in SW480 $\beta6$OE cells.

both of these antigens on the cell surface.[23,28−30] However, correlations of tumor tissue coexpression and relationships with cancer stage, differentiation status, and patient clinical outcomes (including survival) remain to be explored. The confirmation of a direct uPAR·$\alpha v\beta6$ interaction would suggest

a novel paradigm that potentially explains how and why these membrane proteins share critical aspects of tumor biology and would assist in the development of novel therapeutics to prevent cancer metastasis.[29]
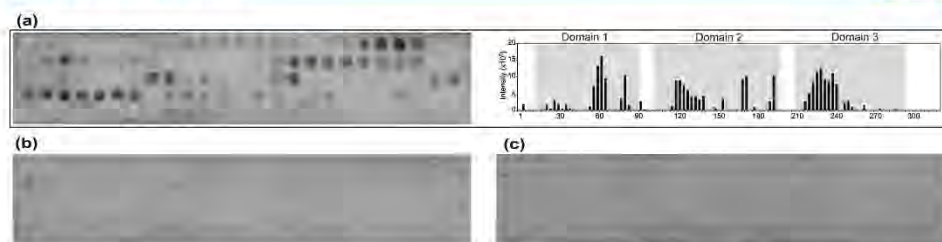
Figure 3. (a) uPAR peptide array incubated with $\alpha v \beta 6$ and corresponding intensity plot indicating locations of binding on the three domains of uPAR with the more intense spot (semiquantitatively indicated on the bar chart) indicating a stronger affinity for the heterodimer to the corresponding uPAR peptide. The same peptide array incubated with αv (b) and $\beta 6$ (c) integrins separately, neither of which showed any binding to the array.

The aim of the present study was to functionally validate our previous proteomic studies[5] on IP pull downs of the specific interacting sites of uPAR·$\alpha v \beta 6$ by using two diverse orthogonal biochemical techniques: PLA for in cellulo studies and peptide arrays for in vitro analysis of the specific interacting sites. To validate the uPAR·$\alpha v \beta 6$ interaction, ovarian (OVCA429) and four colon cancer cell lines were employed (HT29^mock, HT29^$\beta 6AS$, SW480^$\beta 6OE$, and SW480^mock). The dysregulation of uPAR and $\beta 6$ in these cell lines has been previously demonstrated by various techniques not limited to but including flow cytometry, Western blot, and PET analysis.[29,31–33]

Immunofluorescence and PLA Confirm the Presence of uPAR·$\alpha v \beta 6$ Interactions

In this study, immunofluorescence (IF) was used to demonstrate the presence of uPAR and $\alpha v \beta 6$ on the cell surface using anti-uPAR R4 and anti-$\alpha v \beta 6$ 6.4B4 mAbs. Consistent with previous studies, these results demonstrated that uPAR was expressed on the cell surface of all cell lines, while $\alpha v \beta 6$ was expressed on SW480^$\beta 6OE$, HT29^mock, HT29^$\beta 6AS$, and OVCA429, but was not on SW480^mock (Figure 1). No binding (no fluorescence) was observed with the negative isotype control IgG1 antibody (Figure 1) as control.

Proximity ligation is an emerging technology that has been used to visualize and simultaneously quantify P-P interactions occurring in situ.[34] Proteins in close proximity (30–40 nm) are fluorescently detected using rolling circle amplification of ligatable DNA primers attached to secondary antibodies that bind a pair of epitope-specific monoclonal antibodies.[34,35] In our study, primary antibodies were directed against uPAR and $\alpha v \beta 6$. Expression of integrin $\beta 6$ is restricted to epithelial cells, and it is only known to dimerize with the αv subunit.[36] Therefore, to identify whether interaction with uPAR could be demonstrated quantitatively, we examined other cell lines in which relative expression levels of the $\beta 6$ integrin were modulated. The cell lines used expressed uPAR with varying levels of integrin $\beta 6$ expression. For example, cells that did not express $\beta 6$ (i.e., SW480^mock) were compared to those in which integrin $\beta 6$ had been engineered to be overexpressed (SW480^$\beta 6OE$). In addition, cells that endogenously expressed $\beta 6$ (HT29^mock) were compared to subclones of the same cell line in which $\beta 6$ expression had been deliberately and stably reduced by ~80% (i.e., HT29^$\beta 6AS$)[29] (Figure 2).

To allow statistical analyses, the assay was performed in biological triplicate for all cell lines, and three images were acquired for each replicate. A significant number of positive spots were observed localized to the cell surface as anticipated (Figure 2). The OVCA429, SW480^$\beta 6OE$, and HT29^mock cell lines showed strong signals for the uPAR·$\alpha v \beta 6$ interaction, whereas the HT29^$\beta 6AS$ cell line showed much weaker signals ($p < 0.05$) (Figure 2a), which is in agreement with the reduced $\beta 6$ expression previously reported.[29] The SW480^mock cell line, where $\beta 6$ is completely absent, showed no apparent uPAR·$\alpha v \beta 6$ PLA signal (Figure 2a). An analysis of the average signal obtained per cell as compared to the corresponding isotype controls demonstrated that the signals obtained from uPAR·$\alpha v \beta 6$ were significantly greater ($p < 0.05$) than the control (Figure 2b).

The results for the OVCA429 cell line were similar to those we had obtained previously.[5] For the colon cancer cell lines, PLA data showed a significant decrease in interaction when the level of $\alpha v \beta 6$ was reduced; concordantly, a significant increase in interaction was observed when $\alpha v \beta 6$ was up-regulated.

In all cases, our PLA results were in good agreement with previous expression data,[29] showing that quantitative uPAR·$\alpha v \beta 6$ PLA signal could be altered simply by decreasing or increasing the expression level of $\beta 6$ present on the cell surface. All isotype controls were negative. However, while collectively these data show close proximity of uPAR and $\beta 6$ indicative of an interaction, the possibility that other "bridging" proteins may be involved in direct interactions with either partner in uPAR·$\alpha v \beta 6$ could not be conclusively excluded. To eliminate this possibility, direct uPAR·$\alpha v \beta 6$ was probed using an orthogonal technique, peptide arrays.

Peptide Arrays Map Potential Sites of uPAR·$\alpha v \beta 6$ Interaction

Peptide arrays are cost-efficient, accurate, and reliable one-dimensional reconstructions that allow mapping of potential peptidyl binding sites of labeled full length interacting proteins.[37] They have been widely used to analyze large arrays of synthetic peptides on cellulose membranes, facilitating the rapid screening of diverse biomolecule probes.[38] SPOT synthesis[24] was used in this study to generate an array composed of 108 sequential overlapping (3 residues) 15-mer peptides (along the linear uPAR expressed protein sequence) arranged successively on a cellulose membrane. This was used to map the potential binding sites of uPAR and the heterodimeric $\alpha v \beta 6$ integrin, as well as the individual integrin subunits (αv and $\beta 6$). While this method involves a reduction of the three-dimensional uPAR structure into single linear overlapping 15-mer peptides, the method has been used
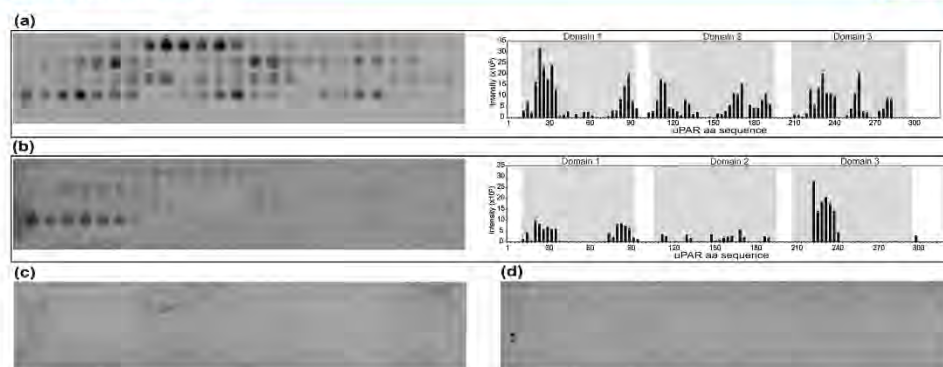
361

Figure 4. (a) uPAR peptide array incubated with uPA and corresponding intensity plot indicating locations of binding on the three domains of uPAR with the more intense spot (semiquantitatively indicated on the bar chart) indicating a stronger affinity for the heterodimer to the corresponding uPAR peptide. The same peptide array incubated with vitronectin, another known binding partner of uPAR, and its corresponding intensity plot (b) and the β1 (c) and β3 (d) integrins separately, neither of which again, as monomers, showed any binding to the array.

Table 1. Potential uPAR and Integrin αvβ6 Interaction Sites[a]

uPAR domain	region identified from peptide array	possible surface residues identified	overlapping residues binding to Vn (uPA)
I	61 ELVEKSCTHSEKTNRTLS 78	E61, V63, K65, S70, E71, N74, T76, S78	S78 (T76)
	82 GLKITSLTEVVCGLD 96	I85, S87, T89, V91, L95	I85, S87 (T89)
II	121 GSSDMSCERGRHQSLQCRSPE 141	M125, R129, R131, H132, S134, Q136, R138	Q136, R138
	172 LPGCPGSNGFHNNDTFHF 189	S178, N184, D185, F187, F189	none
	193 CNTTKCNEGPILELE 207	N194, T195, K197, E200, P202, E207, N208	none
III	229 SEETFLIDCRGPMNQCLVATGTHEPKN 255	S229, E230, L234, D236, D238, N242, Q243, V246, T248, T250, T254	none

[a]Regions binding to integrin αvβ6 on the peptide array and possible surface residues were identified by manual analysis of the uPAR crystal structure. The last column lists known overlapping binding residues to Vn and uPA (in parentheses). Amino acid residue numbers correspond to full uPAR sequence from UniProt KB (ID: Q03405).

successfully to identify linear specific binding sequences involved in many P-P interactions.[24]

In this study, a GUI (graphical user interface) was developed to semiquantitatively determine the binding affinity of the labeled species (e.g., HRP-labeled αvβ6) to the uPAR peptide array based on the intensity of positive spots identified (Figure 3a). Overall, our data showed that integrin αvβ6 binds to peptides emanating from all three uPAR domains (DI, DII, and DIII); in particular, positive binding of labeled-αvβ6 was located within the following uPAR amino acid sequences: uPAR DI at E61-R75 and G82-D96, uPAR DII at G121-E141, L172-F189, and C193-E207, and uPAR DIII at S229-N255.

In control experiments using identical protein concentrations, the individual integrin protein subunits αv (Figure 3b) or β6 (Figure 3c) did not bind to any region of the uPAR peptide array, in contrast to the αvβ6 dimer.

The peptide array was also used to identify the binding sites of other potential uPAR partners, uPAR's cognate protease ligand uPA and the well-established binding partner Vn. The integrin subunits β1 and β3 were also examined to determine if they were able to bind as individual integrin subunits in contrast to the data observed for β6 (Figure 3C).

These data showed that uPA could bind through domain I, C16-V51, I85-T108; domain II, S112-H150, C169-P210; and domain III, M226-Y258 and I283-V300, (Figure 4a), while Vn

was found to bind to domain I, G22-V51, G82-R105; domain II, L116-H150, L172-E207; and domain III, G226-N255 (Figure 4b). As observed for individual subunits αv and β6, neither β1 nor β3 (Figure 4c and d) showed any detectable binding to the uPAR peptide array.

Structural Mapping of Interacting Sites Reveals Pockets of uPAR·αvβ6 Interactions

Six potential binding sites were located on the uPAR sequence from the collective peptide array data. These sites were found to be spread across all three domains of uPAR and covered almost 35% of the uPAR sequence. Interestingly, a number of the sequences found to bind to αvβ6 integrin have previously been implicated in interactions with either Vn and/or uPA (Table 1).[7] To narrow potential docking/binding sites for integrin αvβ6, an in silico structural analysis of where these six sites were located on the uPAR crystal structure was undertaken and mapped using ICM software (Figure 5a). This was followed by a manual identification of uPAR regions with residues containing favorable side-chain orientations and then investigated for potential residues that could be accessed on the outer surfaces of uPAR (Table 1).

Initial uPAR residue side-chain orientation analysis revealed that approximately 39% of the αvβ6 interacting uPAR residues identified on peptide arrays possessed side chains found in favorable orientations (i.e., surface accessible). However,
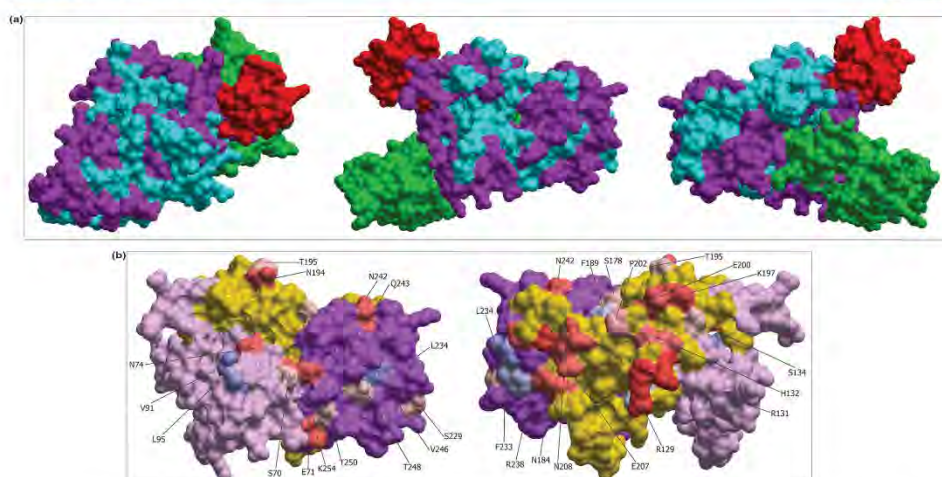
Figure 5. (a) The space-filling crystal structure of uPAR (magenta) with red indicating vitronectin, green indicating uPA, and cyan showing regions of uPAR binding to $\alpha v\beta 6$ from uPAR peptide array in three different views. (b) Crystal structure of uPAR only indicating its three domains (light pink, domain I; yellow, domain II; magenta, domain III) overlaid with predicted hydrophobicity labeled in red (residues with H-bond acceptor potential) and blue (residues with H-bond donor potential). The intensity of red and blue shows how strong or weak the H-bond formation potential is, and the numbers correspond to the amino acid sequence of uPAR without the signal peptide. A total of 14 potential residues as sites of binding can be observed on domain II, while 11 can be observed on domain III.

further manual analysis revealed that many of these residues were inaccessible. Only the favorable residues were then subjected to physicochemical (hydrophobicity) analysis (Figure 5). Figure 5b illustrates the hydrophobic nature of the residues identified. It was noted that most of the identified residues had hydrogen (H-) bond acceptor potential (red residues) with some residues having the potential to be H-bond donors (blue residues), while very few residues showed any potential to form H-bonds. Those with acceptor or donor H-bond potentials should prove better binding sites than those with low or no H-bond acceptor potential.

It was clear from this analysis that some residues identified in regions of uPAR domain I (E61 to R75 and G82 to D96) that had been previously suggested to be required for interaction with Vn and/or the receptor's cognate protease ligand uPA[26,39] were buried inside the outer surfaces of uPAR. Residues Q136 and R128, and L172, P173, and H188 in uPAR domain II, which have been previously demonstrated to be required for interaction with Vn and uPA, respectively, were found to be surface accessible.[26,39]

This study revealed that most of the domain II and III residues identified from the arrays could potentially be sites of $\alpha v\beta 6$ integrin interaction. Interestingly, a previous study addressing interactions between integrin $\alpha 5\beta 1$ and uPAR suggested that integrin $\alpha 5\beta 1$ directly interacts with uPAR domain III across the sequence G262-Q270 and the interaction was lost when a single amino acid alanine substitution (S267A) was introduced.[40] Our data suggest that although domains II and III maybe accessible for integrin binding, domain III appears to be a more favorable site, should other ligands be available.

While binding of uPA to its cognate receptor uPAR is a high affinity interaction $(K_d = 4 \times 10^{-10}\ \mathrm{M})$,[41] significant external

regions of uPAR remain available for binding to other potential interacting partners (e.g., Vn and various integrins like $\alpha 3\beta 1$, $\alpha_M\beta 2$, $\alpha v\beta 1$, $\alpha 5\beta 1$, $\alpha v\beta 3$[42]). The uPA and Vn sites indicated from the peptide array showed ~70% overlap with binding sites already published,[26,39] including data obtained from alanine scanning mutagenesis experiments.[9] A detailed structural docking study has been performed to recapitulate and confirm these findings on the interaction of uPAR and $\alpha v\beta 6$.[43]

■ IMPLICATIONS AND FUTURE DIRECTIONS

The most likely binding sites for $\alpha v\beta 6$ to uPAR, based on the crystal structure of uPAR (bound to uPA and Vn) coupled with information arising from our peptide array data and a manual analysis of potential binding sites by side-chain orientation and hydrophobicity, appeared to be neighboring adjacent integrin binding sites that were previously identified.[40] An additional advantage of the use of peptide arrays in this study over screening by site directed protein–protein interaction libraries or molecular modeling is that not only are potential binding sites identified, but lead peptide antagonists also determined. These can subsequently be used as tools to address the specific interaction under study.[44] Structural analysis coupled with the previous study on interaction of uPAR with $\alpha 5\beta 1$[40] suggests that uPAR domain III may be a favorable binding site for "all" uPAR-binding integrins. Experiments using blocking peptides against the domain III region of uPAR to determine the precise binding site of uPAR and integrin $\alpha v\beta 6$ are currently ongoing.

For cell motility, invasion, proliferation, and adhesion, it is essential for uPAR to interact with transmembrane proteins for transmission of specific signals across cell membranes to activate appropriate intracellular second messenger systems. Thus, interaction of uPAR with $\alpha v\beta 6$ and other integrins not

363

only couples the proteolytic activation (by binding with uPA) with cell signaling but also localizes the proteolysis to the cell surface.[7] Interactions between uPAR and $\alpha v \beta 6$ could potentially have profound implications on the promotion of cancer cell metastasis by activating a series of specific signaling pathways. For example, uPAR is involved in the Ras-ERK pathway, which is known to directly induce EMT in cells.[7,45] The association of uPAR with integrins like $\alpha 3 \beta 1$, $\alpha v \beta 1$, $\alpha 5 \beta 1$, $\alpha v \beta 3$ has been studied to varying degrees. It has been shown that uPAR interaction with $\beta 1$ activates both FAK and ERK/ MAPK pathways,[40] while interaction with $\beta 3$ activates the Rac pathway.[46] Similarly, studies have shown that disruption of a uPAR and $\alpha v \beta 3$ integrin interaction selectively inhibits Vn-induced cell migration,[9,47] implying that $\alpha v \beta 6$ might also modulate cell migration in some comparable manner.

High expression of $\alpha v \beta 6$ is associated with poor prognosis in many cancer types, including colon cancer.[48] Several studies have implicated $\beta 6$ in cell proliferation, migration, and invasion,[49−51] although the mechanisms by which these processes occur remain unclear. Some reports have suggested involvement of $\alpha v \beta 6$ in MMP pathways as a means by which ECM degradation is facilitated.[16,52] For example, Fyn kinase, which associates with $\alpha v \beta 6$, recruits FAK, thereby activating the Rac/ERK/MAPK pathways, which in turn activate MMP3.[50] There is also evidence showing that $\alpha v \beta 6$ activates transforming growth factor TGF$\beta 1$ by a mechanism involving torsional stress (not proteolysis), which leads to up-regulation of MMP pathways.[53] In addition, a direct interaction between $\alpha v \beta 6$-P-ERK2 has been conclusively established[29] and shown to mediate MMP-9 secretion in colon cancer cells.[29]

It is possible that the pathways activated, seemingly independently by uPAR and $\alpha v \beta 6$, could indeed be activated collectively with proteins found in membranes forming the uPAR·$\alpha v \beta 6$ complex. Indeed, in our initial study several other proteins were identified by proteomics to be binding to uPAR.[5] Targeting $\alpha v \beta 6$ integrin has the additional benefit that it is exclusively expressed in epithelial restricted tumors. It is possible that by therapeutically targeting the uPAR·$\alpha v \beta 6$, the $\alpha v \beta 6$ signaling pathway can be uncoupled from the plasmin activity, potentially leading to a disruption of the pathways involved in EMT resulting in decreased metastasis.

This study provides the detailed groundwork for an analysis of the uPAR·$\alpha v \beta 6$ interaction aimed at using it as a potential novel therapeutic cancer target. Further alternative and complementary techniques could be used to elucidate P·P interactions and to identify significant pathways affected by the interaction. When combined with the approaches taken here, methods like cross-linking mass spectrometry[54] in conjunction with competition studies using peptide arrays and surface plasmon resonance analysis (e.g., BIAcore, Proteon) could be used to analyze the binding kinetics of potential interactants. Indeed, preliminary studies using complementary peptides to block the sites of binding followed by functional assays (migration, proliferation, etc.) on related cell lines have been shown to induce biological and morphological effects (data not shown). The consequences of ablating such interactions can be investigated in mouse models of CRC enabling an in vivo approach.

■ AUTHOR INFORMATION

Corresponding Author

*Phone: +61 2 9850 8211. Fax: +61 2 9812-3600. E-mail: mark.baker@mq.edu.au.

Author Contributions

▽These authors contributed equally.

Notes

The authors declare no competing financial interest.

■ REFERENCES

(1) Nguyen, D. X.; Bos, P. D.; Massague, J. Metastasis: from dissemination to organ-specific colonization. *Nat. Rev. Cancer* **2009**, *9*, 274−84.

(2) Kalluri, R.; Weinberg, R. A. The basics of epithelial-mesenchymal transition. *J. Clin. Invest.* **2009**, *119*, 1420−8.

(3) Pepper, M. S. Role of the matrix metalloproteinase and plasminogen activator-plasmin systems in angiogenesis. *Arterioscler., Thromb., Vasc. Biol.* **2001**, *21*, 1104−17.

(4) Cox, G.; Steward, W. P.; O'Byrne, K. J. The plasmin cascade and matrix metalloproteinases in non-small cell lung cancer. *Thorax* **1999**, *54*, 169−79.

(5) Saldanha, R. G.; Molloy, M. P.; Bdeir, K.; Cines, D. B.; Song, X.; Uitto, P. M.; Weinreb, P. H.; Violette, S. M.; Baker, M. S. Proteomic identification of lynchpin urokinase plasminogen activator receptor protein interactions associated with epithelial cancer malignancy. *J. Proteome Res.* **2007**, *6*, 1016−28.

(6) Fagerberg, L.; Jonasson, K.; von Heijne, G.; Uhlen, M.; Berglund, L. Prediction of the human membrane proteome. *Proteomics* **2010**, *10*, 1141−9.

(7) Smith, H. W.; Marshall, C. J. Regulation of cell signalling by uPAR. *Nat. Rev. Mol. Cell Biol.* **2010**, *11*, 23−36.

(8) Llinas, P.; Le Du, M. H.; Gardsvoll, H.; Dano, K.; Ploug, M.; Gilquin, B.; Stura, E. A.; Menez, A. Crystal structure of the human urokinase plasminogen activator receptor bound to an antagonist peptide. *EMBO J.* **2005**, *24*, 1655−63.

(9) Eden, G.; Archinti, M.; Furlan, F.; Murphy, R.; Degryse, B. The urokinase receptor interactome. *Curr. Pharm. Des.* **2011**, *17*, 1874−89.

(10) Mekkawy, A. H.; Morris, D. L.; Pourgholami, M. H. Urokinase plasminogen activator system as a potential target for cancer therapy. *Future Oncol.* **2009**, *5*, 1487−99.

(11) Seetoo, D. Q.; Crowe, P. J.; Russell, P. J.; Yang, J. L. Quantitative expression of protein markers of plasminogen activation system in prognosis of colorectal cancer. *J. Surg. Oncol.* **2003**, *82*, 184−93.

(12) Rabbani, S. A.; Mazar, A. P. The role of the plasminogen activation system in angiogenesis and metastasis. *Surg. Oncol. Clin. N. Am.* **2001**, *10*, 393−415.

(13) Hynes, R. O. Integrins: versatility, modulation, and signaling in cell adhesion. *Cell* **1992**, *69*, 11−25.

364

(14) Giancotti, F. G.; Ruoslahti, E. Integrin signaling. *Science* **1999**, 285, 1028−32.

(15) Liu, S.; Liang, B.; Gao, H.; Zhang, F.; Wang, B.; Dong, X.; Niu, J. Integrin alphavbeta6 as a novel marker for diagnosis and metastatic potential of thyroid carcinoma. *Head Neck Oncol.* **2013**, 5, 7.

(16) Bandyopadhyay, A.; Raghavan, S. Defining the role of integrin alphavbeta6 in cancer. *Curr. Drug Targets* **2009**, 10, 645−52.

(17) Bates, R. C. The alphaVbeta6 integrin as a novel molecular target for colorectal cancer. *Future Oncol.* **2005**, 1, 821−8.

(18) Annes, J. P.; Munger, J. S.; Rifkin, D. B. Making sense of latent TGFbeta activation. *J. Cell Sci.* **2003**, 116, 217−24.

(19) Gu, X.; Niu, J.; Dorahy, D. J.; Scott, R.; Agrez, M. V. Integrin alpha(v)beta6-associated ERK2 mediates MMP-9 secretion in colon cancer cells. *Br. J. Cancer* **2002**, 87, 348−51.

(20) Weinreb, P. H.; Simon, K. J.; Rayhorn, P.; Yang, W. J.; Leone, D. R.; Dolinski, B. M.; Pearse, B. R.; Yokota, Y.; Kawakatsu, H.; Atakilit, A.; Sheppard, D.; Violette, S. M. Function-blocking integrin alpha(v)-beta(6) monoclonal antibodies - Distinct ligand-mimetic and non-ligand-mimetic classes. *J. Biol. Chem.* **2004**, 279, 17875−17887.

(21) Tsao, S. W.; Mok, S. C.; Fey, E. G.; Fletcher, J. A.; Wan, T. S.; Chew, E. C.; Muto, M. G.; Knapp, R. C.; Berkowitz, R. S. Characterization of human ovarian surface epithelial cells immortalized by human papilloma viral oncogenes (HPV-E6E7 ORFs). *Exp. Cell Res.* **1995**, 218, 499−507.

(22) Agrez, M.; Chen, A.; Cone, R. I.; Pytela, R.; Sheppard, D. The alpha v beta 6 integrin promotes proliferation of colon carcinoma cells through a unique region of the beta 6 cytoplasmic domain. *J. Cell Biol.* **1994**, 127, 547−56.

(23) Weinacker, A.; Chen, A.; Agrez, M.; Cone, R. I.; Nishimura, S.; Wayner, E.; Pytela, R.; Sheppard, D. Role of the integrin alpha v beta 6 in cell attachment to fibronectin. Heterologous expression of intact and secreted forms of the receptor. *J. Biol. Chem.* **1994**, 269, 6940−8.

(24) Frank, R. The SPOT-synthesis technique. Synthetic peptide arrays on membrane supports–principles and applications. *J. Immunol. methods* **2002**, 267, 13−26.

(25) Frank, R. Spot-Synthesis - an easy technique for the positionally addressable, parallel chemical synthesis on a membrane support. *Tetrahedron* **1992**, 48, 9217−9232.

(26) Huai, Q.; Zhou, A.; Lin, L.; Mazar, A. P.; Parry, G. C.; Callahan, J.; Shaw, D. E.; Furie, B.; Furie, B. C.; Huang, M. Crystal structures of two human vitronectin, urokinase and urokinase receptor complexes. *Nat. Struct. Mol. Biol.* **2008**, 15, 422−3.

(27) Abagyan, R.; Totrov, M.; Kuznetsov, D. ICM−A new method for protein modeling and design: Applications to docking and structure prediction from the distorted native conformation. *J. Comput. Chem.* **1994**, 15, 488−506.

(28) Li, Y.; Wood, N.; Yellowlees, D.; Donnelly, P. K. Cell surface expression of urokinase receptor in normal mammary epithelial cells and breast cancer cell lines. *Anticancer Res.* **1999**, 19, 1223−8.

(29) Ahmed, N.; Niu, J.; Dorahy, D. J.; Gu, X.; Andrews, S.; Meldrum, C. J.; Scott, R. J.; Baker, M. S.; Macreadie, I. G.; Agrez, M. V. Direct integrin alphavbeta6-ERK binding: implications for tumour growth. *Oncogene* **2002**, 21, 1370−80.

(30) Niu, J.; Gu, X.; Ahmed, N.; Andrews, S.; Turton, J.; Bates, R.; Agrez, M. The alphaVbeta6 integrin regulates its own expression with cell crowding: implications for tumour progression. *Int. J. Cancer* **2001**, 92, 40−8.

(31) Moreau, M.; Mourah, S.; Dosquet, C. beta-Catenin and NF-kappaB cooperate to regulate the uPA/uPAR system in cancer cells. *Int. J. Cancer* **2011**, 128, 1280−92.

(32) Ronne, E.; Behrendt, N.; Ploug, M.; Nielsen, H. J.; Wollisch, E.; Weidle, U.; Dano, K.; Hoyer-Hansen, G. Quantitation of the receptor for urokinase plasminogen activator by enzyme-linked immunosorbent assay. *J. Immunol. Methods* **1994**, 167, 91−101.

(33) Persson, M.; Madsen, J.; Ostergaard, S.; Jensen, M. M.; Jorgensen, J. T.; Juhl, K.; Lehmann, C.; Ploug, M.; Kjaer, A. Quantitative PET of human urokinase-type plasminogen activator receptor with 64Cu-DOTA-AE105: implications for visualizing cancer invasion. *J. Nucl. Med.* **2012**, 53, 138−45.

(34) Weibrecht, I.; Leuchowius, K. J.; Clausson, C. M.; Conze, T.; Jarvius, M.; Howell, W. M.; Kamali-Moghaddam, M.; Soderberg, O. Proximity ligation assays: a recent addition to the proteomics toolbox. *Expert Rev. Proteomics* **2010**, 7, 401−9.

(35) Thymiakou, E.; Episkopou, V. Detection of signaling effector-complexes downstream of bmp4 using PLA, a proximity ligation assay. *J. Visualized Exp.* **2011**.

(36) Breuss, J. M.; Gillett, N.; Lu, L.; Sheppard, D.; Pytela, R. Restricted distribution of integrin beta 6 mRNA in primate epithelial tissues. *J. Histochem. Cytochem.* **1993**, 41, 1521−7.

(37) Li, S. S.; Wu, C. Using peptide array to identify binding motifs and interaction networks for modular domains. *Methods Mol. Biol.* **2009**, 570, 67−76.

(38) Maier, R. H.; Maier, C. J.; Rid, R.; Hintner, H.; Bauer, J. W.; Onder, K. Epitope mapping of antibodies using a cell array-based polypeptide library. *J. Biomol. Screening* **2010**, 15, 418−26.

(39) Barinka, C.; Parry, G.; Callahan, J.; Shaw, D. E.; Kuo, A.; Bdeir, K.; Cines, D. B.; Mazar, A.; Lubkowski, J. Structural basis of interaction between urokinase-type plasminogen activator and its receptor. *J. Mol. Biol.* **2006**, 363, 482−95.

(40) Chaurasia, P.; Aguirre-Ghiso, J. A.; Liang, O. D.; Gardsvoll, H.; Ploug, M.; Ossowski, L. A region in urokinase plasminogen receptor domain III controlling a functional association with alpha5beta1 integrin and tumor growth. *J. Biol. Chem.* **2006**, 281, 14852−63.

(41) Vassalli, J. D.; Baccino, D.; Belin, D. A cellular binding site for the Mr 55,000 form of the human plasminogen activator, urokinase. *J. Cell Biol.* **1985**, 100, 86−92.

(42) Blasi, F.; Carmeliet, P. uPAR: a versatile signalling orchestrator. *Nat. Rev. Mol. Cell Biol.* **2002**, 3, 932−43.

(43) Sowmya, G.; Khan, J. M.; Anand, S.; Ahn, S. B.; Baker, M. S.; Ranganathan, S. A site for direct integrin alphavbeta6.uPAR interaction from structural modelling and docking. *J. Struct. Biol.* **2014**, 185, 327−35.

(44) Hruby, V. J. Designing peptide receptor agonists and antagonists. *Nat. Rev. Drug Discovery* **2002**, 1, 847−58.

(45) Jo, M.; Eastman, B. M.; Webb, D. L.; Stoletov, K.; Klemke, R.; Gonias, S. L. Cell signaling by urokinase-type plasminogen activator receptor induces stem cell-like properties in breast cancer cells. *Cancer Res.* **2010**, 70, 8948−58.

(46) Smith, H. W.; Marra, P.; Marshall, C. J. uPAR promotes formation of the p130Cas-Crk complex to activate Rac through DOCK180. *J. Cell Biol.* **2008**, 182, 777−90.

(47) Degryse, B.; Orlando, S.; Resnati, M.; Rabbani, S. A.; Blasi, F. Urokinase/urokinase receptor and vitronectin/alpha(v)beta(3) integrin induce chemotaxis and cytoskeleton reorganization through different signaling pathways. *Oncogene* **2001**, 20, 2032−43.

(48) Bates, R. C. Colorectal cancer progression: integrin alphavbeta6 and the epithelial-mesenchymal transition (EMT). *Cell Cycle* **2005**, 4, 1350−2.

(49) Ramos, D. M.; But, M.; Regezi, J.; Schmidt, B. L.; Atakilit, A.; Dang, D.; Ellis, D.; Jordan, R.; Li, X. Expression of integrin beta 6 enhances invasive behavior in oral squamous cell carcinoma. *Matrix Biol.* **2002**, 21, 297−307.

(50) Li, X.; Yang, Y.; Hu, Y.; Dang, D.; Regezi, J.; Schmidt, B. L.; Atakilit, A.; Chen, B.; Ellis, D.; Ramos, D. M. Alphavbeta6-Fyn signaling promotes oral cancer progression. *J. Biol. Chem.* **2003**, 278, 41646−53.

(51) Ramos, D. M.; Dang, D.; Sadler, S. The role of the integrin alpha v beta6 in regulating the epithelial to mesenchymal transition in oral cancer. *Anticancer Res.* **2009**, 29, 125−30.

(52) Morgan, M. R.; Thomas, G. J.; Russell, A.; Hart, I. R.; Marshall, J. F. The integrin cytoplasmic-tail motif EKQKVDLSTDC is sufficient to promote tumor cell invasion mediated by matrix metalloproteinase (MMP)-2 or MMP-9. *J. Biol. Chem.* **2004**, 279, 26533−9.

(53) Xu, J.; Lamouille, S.; Derynck, R. TGF-beta-induced epithelial to mesenchymal transition. *Cell Res.* **2009**, 19, 156−72.

(54) Tang, X.; Bruce, J. E. A new cross-linking strategy: protein interaction reporter (PIR) technology for protein-protein interaction studies. *Mol. BioSyst.* **2010**, 6, 939−47.

365

Appendix III – An improved method for the detection and enrichment of low-abundant membrane and lipid raft-residing proteins Publication VIII of this thesis

Technical note

An improved method for the detection and enrichment of low-abundant membrane and lipid raft-residing proteins

Alison Kan, Abidali Mohamedali, Sock Hwee Tan, Harish R. Cheruku,
Iveta Slapetova[1], Ling Y. Lee, Mark S. Baker*

Department of Chemistry & Biomolecular Sciences, Faculty of Science, Macquarie University, NSW 2109, Australia

ABSTRACT

A high degree of optimisation is required in native co-immunoprecipitation (co-IP) experiments with added challenges for low-abundant membrane proteins and masking by IgG molecules. Although in vivo tagged-protein purification avoids the IgG masking problem, modifying the terminus of the protein may result in conformational and post-translational modification changes. In this paper, we propose a method which combines four key aspects to improve the solubility and enrichment of low-abundant plasma membrane proteins using the urokinase plasminogen activator receptor (uPAR) as an example. As this GPI-linked receptor predominantly resides in lipid rafts (LR), we used a modified RIPA lysis buffer containing the non-ionic detergent, octyl-glucoside which solubilizes LRs to extract uPAR. This is followed by a modified crosslinking co-IP which covalently crosslinks the antibodies to the beads. Crosslinking allowed for a significant increase in the detection of uPAR with minimal IgG contamination using on-bead digestion or acid elution followed by digestion and analysis on high-throughput one-dimensional (nanoLC) MS/MS instrument (AbSciex 5600). To the best of our knowledge, this method of isolation is the first to be done to increase the yield of a low-abundant membrane protein and may be useful for the purification of other non-raft and raft-residing membrane proteins.

© 2012 Elsevier B.V. All rights reserved.

In conventional co-IP, captured complexes are eluted and separated out on 1D-SDS-PAGE (sodium dodecyl sulphate gel electrophoresis) and several gel pieces (typically between 12–24 per lane) are cut out (slice-and-dice) [1,2] for protein identification by mass spectrometry (MS) [3,4]. Although the co-IP procedure is relatively simple and straightforward, the antibody tends to be eluted off with the bound proteins. As the antibody molecules are one of the most predominant proteins in the co-IP procedure, masking of low abundant proteins on the SDS-PAGE gel is inevitable, making protein detection in this region near impossible. If the protein happens to reside in the 25 and 55 kDa regions, further masking is observed. In addition, since antibody molecules are heavily glycosylated, the antibody can also be found all along the electrophoresed lane resulting in very high background which affects signal:noise ratio. As such, masking by the antibody poses a significant problem in conventional co-IP experiments.

Carboxyl (C)- or amine (N)-terminal affinity fused-protein purifications have been used to avoid antibody masking and to increase the yield and purity of bait and associating proteins by

* Corresponding author at: Australian Proteome Analysis Facility, Faculty of Science, Research Park Drive, Macquarie University, 2109, NSW, Australia. Tel.: +61 2 9850 8211; fax: +61 2 9850 8313.
E-mail addresses: i.slapetova@unsw.edu.au (I. Slapetova), mark.baker@mq.edu.au (M.S. Baker).
[1] Current address: Biomolecular Imaging Facility, Lowy Cancer Research Centre, University of New South Wales, NSW 2052, Australia.

the addition of a biological motif such as polyhistidine, gluta-thione S-transferase (GST), and FLAG [5]. This process involves genetic modification of the bait protein in vivo by the addition of an affinity tag at the C- or N-terminus of the protein with co-IP being performed using either a biological or chemical ligand to the tag. When using a chemical ligand, this procedure avoids the problem of contaminating antibody in the elution and reduces background significantly [6,7]. However as the tagged protein is expressed in vivo, the terminus is no longer accessible for posttranslational modifications (PTMs). For GPI-anchored proteins such as the urokinase plasminogen activator receptor (uPAR), the addition of the glycolipid GPI anchor is inhibited and delivery of the protein to the cell surface for protein:protein interaction cannot occur. Moreover, modification at the N-terminus may result in misfolding of the protein to inhibit other PTMs such as glycosylation or block specific sites of protein interactions. In such situations, native co-IP proce-dure using crosslinked antibodies to bait native proteins is the preferred choice.

Covalent conjugation of the antibody to the beads in co-IP allows for native proteins to be eluted with minimal antibody interference. Crosslinkers vary in their spacer arms and target specific side groups ranging from carbohydrate to amine and sulfhydrals. DMP is commonly used in co-IP experiments as this chemical is a water-soluble, 9-angstrom (Å) crosslinker which reacts with amine groups but retains an overall neutral charge, thereby allowing for unmodified native binding to the bait protein. DMP is also non-cleavable so the antibody is retained on the beads during elution, allowing for other proteins to be detected which otherwise would have been masked by the antibody.

Non-ionic detergents such as triton X-100, NP-40, and Brij are commonly used to lyse the cell by solubilising the plasma and intracellular membranes to release cytosolic and subcellular organelle proteins. Despite the effectiveness of these detergents in many cell solubilising applications, detergent-resistant mem-branes (lipid rafts; LR) are insoluble to many non-ionic detergents [8], and as such, downstream quantitative analyses using these detergents may not be sufficient. GPI-linked proteins such as uPAR are known to predominantly reside in LRs [9–12] but also shuttle out [10,11,13]. As such the use of common non-ionic detergents is not suitable for the complete solubilisation of these proteins. For co-IP analysis on LR-residing proteins, it is essential that most (if not all) of the protein is solubilized to allow for a more comprehensive and accurate analysis. Fortunately, non-ionic detergents such as octyl-glucoside (OG) has been shown to solubilize LRs [14] and is therefore suitable for cell lysis requiring native conditions. In this study, OG was selected as the detergent of choice for testing due to its superior properties as a lipid raft membrane solubilizing agent compared to other non-ionic detergents such as another excellent membrane-solubilizing detergent, digitonin [8,15–18]. Moreover, digitonin is toxic and has been reported to be unsuitable for permeabilization of the membrane in the presence of Ca^{2+} ions [18], which is required for some protein:protein interactions such as those involved in calcium cell signalling pathways in lipid rafts [19,20].

In this paper, we attempted to address the solubility and antibody masking issues in native co-IPs in a three-step approach using uPAR for our analysis. Firstly, we modified the cell lysis buffer for maximal solubility by including OG as one of the key ingredients. We tested two different commonly used lysis buffers and a modified OG-containing RIPA buffer (see Supplementary data) on uPAR and several other proteins representing three subcellular locations including the plasma membrane, LR, and cytosol. The expression levels of these proteins were determined to provide a comparison of the degree of solubility of the various detergent solutions tested. Conventional RIPA buffer is often used in co-IP experiments due to its ability to reduce back-ground noise (false positives) with no adverse effects on protein degradation [21]. Other detergents containing only NP-40/Tween-20 or 2% OG were also tested but they were not superior to the triton X-100-containing buffer or the modified RIPA buffer tested, respectively (data not shown). Our results indicate that all of the proteins tested were present in all three buffers but at different levels, representing the amount solubilized. There was a significant increase in intensities of the plasma membrane proteins uPAR and transferring receptor (Tfr) when OG-containing buffer was used (P<0.05, Fig 1i and ii). This suggests that the presence of 2% OG in the modified RIPA buffer improves solubility of membrane proteins. uPAR protein appears as multiple bands between 35–55 kDa or streaks (at high loading concentrations) in western blots due to the highly N-glycosylated nature of the protein [22]. When the expression of another lipid raft residing protein caveolin-1 (cav-1) was analysed, the levels were significantly lower for triton X-100 lysed cells compared to either RIPA- or OG-lysed cells (P<0.05). No significant differences were observed for the cytosolic protein, β-actin. Unlike cav-1, uPAR [23–25] and Tfr [26] are highly N-linked glycosylated and these high-mannose containing carbohydrates may be affecting the solubility of these proteins. Previous analysis in our lab showed that uPAR and Tfr expression were significantly higher when deglycosylated (data not shown) and suggests that N-glycosylation may restrict solubility to a certain degree in Triton X-100 detergent. There was no preferen-tial solubilising of the various glycosylated forms of uPAR and Tfr; suggesting that modified RIPA buffer containing 2% OG is suitable for solubilising N-glycosylated PM proteins.

Secondly, we covalently conjugated the antibody to the beads using dimethyl pimelimidate dihydrochloride (DMP). Results indicate that samples crosslinked (CL) to the beads immunoprecipitated down a significantly higher proportion of uPAR (P<0.05) with a drastic reduction in IgG molecules (P<0.01) compared to non-crosslinked (NCL) beads (Fig. 2i and ii). Several elution conditions were also tested on CL beads 10–30 mM DMP crosslinking conditions to determine the elution efficiency against background (IgG molecules) (Fig. 2iii–v, Table 2). Results showed that the use of 20 mM DMP was the best for eluting uPAR (Fig 2iii and v, Fig. 2i). Higher concentrations of DMP (40 or 50 mM) were also tested but there were no differences in relative uPAR signal intensity (uPAR/IgG$_1$) when compared to 30 mM (data not shown). The use of 0.1% formic acid and 0.1% NH_4OH at 20 mM DMP eluted significantly more uPAR compared to NCL or at 10 or 30 mM DMP (Fig. 2iv) (P≤0.01). Relative uPAR intensity at 10 mM DMP was also significantly higher when compared to the other groups for both of these elutions (P≤0.01). At 1× LDS-SB, relative uPAR intensity at 20 mM DMP was only significantly higher when compared to 30 mM and NCL samples. No significant differences were observed across the four treatment groups when eluted with 1× LDS-SB containing DTT.
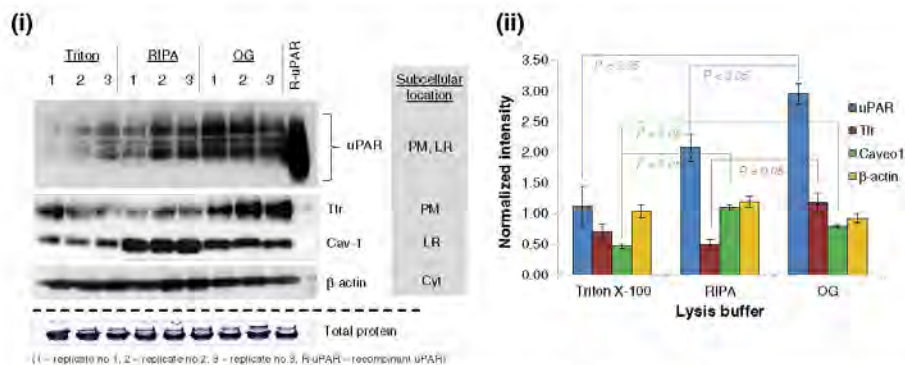
Fig. 1 – Western blotting results of representative proteins in triplicates normally residing within the plasma membrane and cytosol. i. Western immunoblotting images obtained for the three types of lysis buffers denoted as Triton (containing 1% Triton X-100), RIPA (radioimmunoassay buffer), and OG (modified RIPA buffer containing 2% octyl-glucoside). Known subcellular locations of the mature forms of the representative proteins are depicted in the shaded box. PM — plasma membrane, LR — lipid raft, and Cyt — cytosol. R-uPAR: positive control is recombinant His-tagged uPAR. Total protein intensities were derived from cell lysates that were electrophoresed (SDS-PAGE) into the 4% stacking region followed by Coomassie staining. ii. Bar graph denoting the average normalised intensities (protein intensity/total protein intensity) (±SEM) across the triplicate samples. Comparisons were performed on triplicate protein samples across the three lysis buffers where P≤0.05 using Kruskal–Wallis test followed by a posthoc Mann–Whitney U test.

All glycosylated forms of uPAR were identified in the co-IP, indicating that crosslinking did not affect the way the antibodies were associating with uPAR. Despite the recommended 50 mM DMP concentration for crosslinking suggested by the manufacturer, we found that less than half of that concentration (20 mM) gave the highest signal-to-noise ratio (uPAR:IgG₁). This ratio significantly decreased when at least 30 mM DMP was used. This may be because at higher DMP concentrations, the crosslinker may be masking regions on the antibody required for uPAR and/or uPAR complex binding, thereby reducing/preventing these proteins from associating with the antibody. Moreover, the concentration of crosslinker used not only had little or no effect on the binding efficiency of the antibody to the bait protein (uPAR) but also improved the yield. The use of DMP is suitable for co-IP as it is an irreversible, denaturant–resistant chemical and so regions blocked by the crosslinker sites are not exposed to trypsin and enzymatic digestion of the antibody is minimized. When co-IP samples were sequentially eluted, we showed that uPAR eluted much more efficiently in 0.1% formic acid than in 0.1% NH₄OH. Formic acid is an ideal elution buffer for hydrophobic proteins such as PM proteins as it has a strong proton donation ability that solubilizes hydrophobic proteins efficiently [27–29]. In addition, proteins dissolved in formic acid maintain their native structure and are metabolically active and so can be used for downstream enzymatic analyses [30,31]. This is ideal as uPAR eluted in 0.1% formic acid at 37 °C with very little IgG and non-specific protein contamination and the CL Ab: IP bead complex can potentially be regenerated and used for future co-IP experiments. In addition, formic acid is compatible with downstream MS analysis and so sample clean-up and

purification is not required. Elution of CL samples with 1× LDS-SB containing DTT is not suitable for downstream MS analysis as a substantial amount of IgG₁ molecules, especially IgG₁ L chain, were eluted off. This may be because the L chain portion, held together by disulphide bonds, dissociated from the antibody complex in the presence of the reducing agent, DTT. The predominant amount of IgG₁ molecules in the NCL sample eluted in the first two elutions (0.1% formic acid and 0.1% NH₄OH) but CL samples were more resistant to these conditions and so very little IgG₁ molecules eluted off.

Finally, instead of eluting uPAR-bound complexes from beads and performing a slice-and-dice analysis, we performed tryptic digestion directly on the beads for MS analysis. This technique, affinity purification and mass spectrometry (AF–MS), has been successfully applied previously [7] but not in the study of membrane proteins. This technique avoids protein loss during the various stages of the slice-and-dice analysis and hence allows for more proteins to be identified during MS. The use of a high-throughput nanoLC-tandem mass spectrometry (MS/MS) instrument (AbSciex 5600) [32] for the detection of these proteins allows for a one-dimensional (nanoLC) MS/MS analysis, avoiding the initial SDS-PAGE separation step altogether. Our results showed a total of eight unique uPAR peptides (UniProt ID: Q03405 Protein ID: UPAR_HUMAN, M.W.: 37 kDa) were identified in CL uPAR co-IP samples with 32% coverage (Fig 2vi). No uPAR peptides were observed in IgG samples. For NCL co-IP sample using uPAR antibody R4 (NCL-R4), 12 unique peptides for both IgG₁ heavy (gamma) (UniProt ID: P01869, Protein ID: IGH1M_MOUSE, M.W.: 43 kDa) and 2 for light (kappa) chain (UniProt ID: P01837, Protein ID: IGKC_MOUSE,
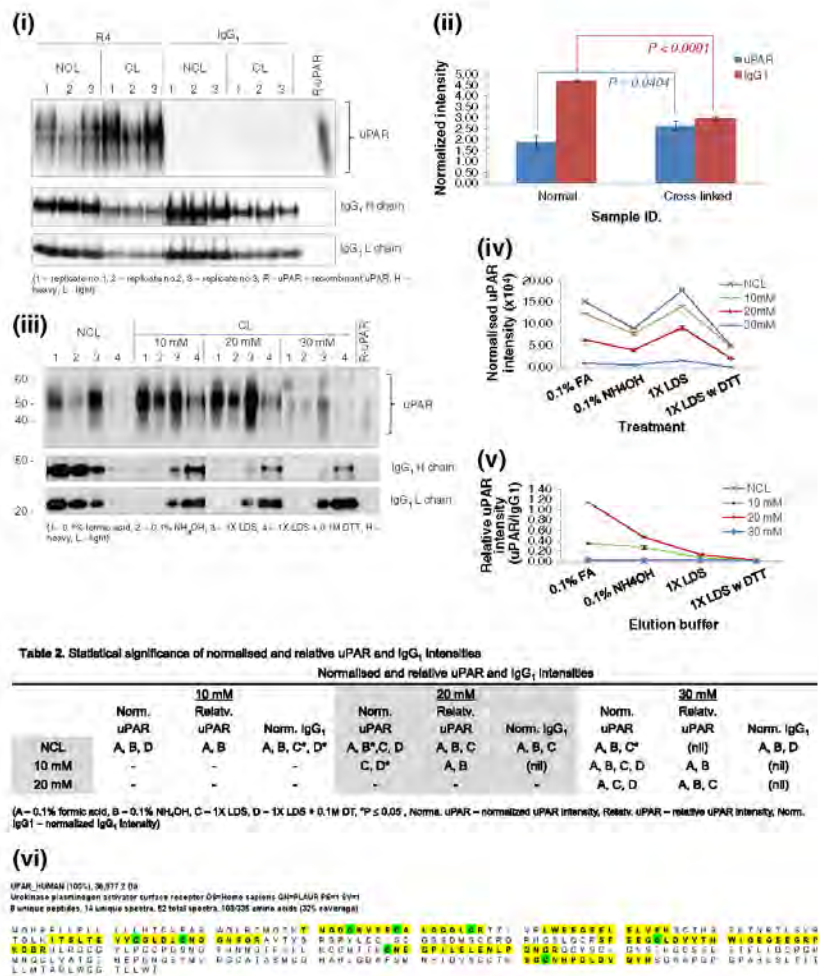
Fig. 2 – Western immunblotting and mass spectrometry results of co-IP experiments performed on triplicate samples lysed with modified RIPA buffer (containing 2% OG). i. CL and NCL samples were eluted under specified conditions in 1× LDS buffer containing 0.1 M DTT at 95 °C for 10 min. Eluates were from triplicate co-IP experiments were immunoblotted using HRP-anti-uPAR and HRP-anti-mouse antibodies. ii. Bar graph denoting the mean normalised intensities (uPAR intensity-recombinant uPAR intensity/IgG1 intensity) obtained across the triplicate samples for uPAR co-IP and for IgG₁ H and L chains (±SEM, one-tailed t-test). iii. Representative images of CL and NCL co-IP samples that were DSP-crosslinked (10, 20, and 30 mM) and sequentially eluted with various buffers and immunoblotted with anti-uPAR-HRP and anti-mouse-HRP antibodies. The blot was stripped prior to immunblotting with anti-mouse-HRP. iv. Line graph denoting the normalised uPAR intensities (uPAR/recombinant uPAR) obtained across the triplicate samples for CL and NCL uPAR co-IPs (±SEM, one-tailed t-test). v. Line graph denoting the relative uPAR intensities (uPAR/IgG₁) obtained across the triplicate samples for CL and NCL uPAR co-IPs (±SEM, one-tailed t-test). *Inset table 2 with figure.* Table representing comparison groups where statistical significance of P ≤ 0.05 was identified using multifactorial ANOVA with Tukey's posthoc test. vi. Protein sequence coverage of the full-length amino acid sequence of uPAR for CL sample. Yellow shading denotes regions of peptide sequences that matched to the uPAR full-length protein sequence. Green shading denotes cysteine residues identified within the matched peptide sequences. Details of the methods used can be found in Supplementary data.

M.W.: 12 kDa) were detected. Only 7 unique peptides for heavy chain were detected for CL sample (CL-R4). For the IgG$_1$ co-IP samples, there were no differences observed in the number of unique peptides for IgG heavy chain for both CL (CL-IgG$_1$) and NCL (NCL-IgG$_1$) samples. There was also an absence of light chain IgG$_1$ peptides observed.

In summary, using 2% OG in our modified RIPA lysis buffer coupled with crosslinking of the antibody to the beads significantly increased the yield of the bait protein, uPAR and together with on-bead digestion and high resolution MS increased the sensitivity for detection of uPAR with very little interference from IgG$_1$ molecules. We believe that the modifications made in the co-IP performed can also be applied for the interatomic analysis of other plasma membrane-residing proteins.

Acknowledgments

Appendix A. Supplementary data

Supplementary data to this article can be found online at http://dx.doi.org/10.1016/j.jprot.2012.11.019.

REFERENCES

[1] Shevchenko A, Wilm M, Vorm O, Mann M. Mass spectrometric sequencing of proteins silver-stained polyacrylamide gels. Anal Chem 1996;68:850–8.

[2] Shevchenko A, Tomas H, Havlis J, Olsen JV, Mann M. In-gel digestion for mass spectrometric characterization of proteins and proteomes. Nat Protoc 2006;1:2856–60.

[3] Berggard T, Linse S, James P. Methods for the detection and analysis of protein-protein interactions. Proteomics 2007;7: 2833–42.

[4] Phizicky EM, Fields S. Protein-protein interactions: methods for detection and analysis. Microbiol Rev 1995;59:94–123.

[5] Lichty JJ, Malecki JL, Agnew HD, Michelson Horowitz DJ, Tan S. Comparison of affinity tags for protein purification. Protein Expr Purif 2005;41:98–105.

[6] Gingras A-C, Aebersold R, Raught B. Advances in protein complex analysis using mass spectrometry. J Physiol 2005;563:11–21.

[7] Gingras A-C, Gstaiger M, Raught B, Aebersold R. Analysis of protein complexes using mass spectrometry. Nat Rev Mol Cell Biol 2007;8:645–54.

[8] Brown DA, Rose JK. Sorting of GPI-anchored proteins to glycolipid-enriched membrane subdomains during transport to the apical cell surface. Cell 1992;68:533–44.

[9] Kiyan J, Smith G, Haller H, Dumler I. Urokinase-receptor-mediated phenotypic changes in vascular smooth muscle cells require the involvement of membrane rafts. Biochem J 2009;423:343–51.

[10] Cunningham O, Andolfo A, Santovito ML, Iuzzolino L, Blasi F, Sidenius N. Dimerization controls the lipid raft partitioning of uPAR/CD87 and regulates its biological functions. EMBO J 2003;22:5994–6003.

[11] Raghu H, Sodadasu PK, Malla RR, Gondi CS, Estes N, Rao JS. Localization of uPAR and MMP-9 in lipid rafts is critical for migration, invasion and angiogenesis in human breast cancer cells. BMC Cancer 2010;10:647.

[12] Sitrin RG, Johnson DR, Pan PM, Harsh DM, Huang J, Petty HR, et al. Lipid raft compartmentalization of urokinase receptor signaling in human neutrophils. Am J Respir Cell Mol Biol 2004;30:233–41.

[13] Sahores M, Prinetti A, Chiabrando G, Blasi F, Sonnino S. uPA binding increases UPAR localization to lipid rafts and modifies the receptor microdomain composition. Biochim Biophys Acta 2008;1778:250–9.

[14] Garner AE, Smith DA, Hooper NM. Visualization of detergent solubilization of membranes: implications for the isolation of rafts. Biophys J 2008;94:1326–40.

[15] Baron C, Thompson TE. Solubilization of bacterial membrane proteins using alkyl glucosides and dioctanoyl phosphatidylcholine. Biochim Biophys Acta 1975;382: 276–85.

[16] Stubbs GW, Smith Jr HG, Litman BJ. Alkyl glucosides as effective solubilizing agents for bovine rhodopsin. A comparison with several commonly used detergents. Biochim Biophys Acta 1976;426:46–56.

[17] Zhang G, Neubert TA. Use of detergents to increase selectivity of immunoprecipitation of tyrosine phosphorylated peptides prior to identification by MALDI quadrupole-TOF MS. Proteomics 2006;6:571–8.

[18] Karl J, Gottfried C, Tramontina F, Dunkley P, Rodnight R, Goncalves CA. GFAP phosphorylation studied in digitonin-permeabilized astrocytes: standardization of conditions. Brain Res 2000;853:32–40.

[19] Burgoyne RD, Geisow MJ. The annexin family of calcium-binding proteins. Review article. Cell Calcium 1989;10:1–10.

[20] Kretsinger RH. Calcium-binding proteins. Annu Rev Biochem 1976;45:239–66.

[21] Harlow E, Lane D. Antibodies: a laboratory manual. Cold Spring Harbor Laboratory Press; 1988. p. 499.

[22] Ploug M, Rahbek-Nielsen H, Nielsen PF, Roepstorff P, Dano K. Glycosylation profile of a recombinant urokinase-type plasminogen activator receptor expressed in Chinese hamster ovary cells. J Biol Chem 1998;273:13933–43.

[23] Behrendt N, Ronne E, Ploug M, Petri T, Lober D, Nielsen LS, et al. The human receptor for urokinase plasminogen activator. NH2-terminal amino acid sequence and glycosylation variants. J Biol Chem 1990;265:6453–60.

[24] Ploug M, Ronne E, Behrendt N, Jensen AL, Blasi F, Dano K. Cellular receptor for urokinase plasminogen activator. Carboxyl-terminal processing and membrane anchoring by glycosyl-phosphatidylinositol. J Biol Chem 1991;266: 1926–33.

[25] Moller LB, Ploug M, Blasi F. Structural requirements for glycosyl-phosphatidylinositol anchor attachment in the cellular receptor for urokinase plasminogen activator. Eur J Biochem 1992;208:493–500.

[26] Hayes GR, Williams A, Costello CE, Enns CA, Lucas JJ. The critical glycosylation site of human transferrin receptor contains a high-mannose oligosaccharide. Glycobiology 1995;5:227–32.

[27] Collinson SK, Emody L, Muller KH, Trust TJ, Kay WW. Purification and characterization of thin, aggregative fimbriae from Salmonella enteritidis. J Bacteriol 1991;173:4773–81.

[28] Sage HJ, Singer SJ. The properties of bovine pancreatic ribonuclease in ethylene glycol solution. Biochemistry 1962;1: 305–17.

[29] Whittaker GR, Meredith DM. Purification of the structural proteins of herpes simplex virus type 1 by reverse-phase high performance liquid chromatography. Arch Virol 1990;114: 271-6.

[30] Um IC, Kweon HY, Lee KG, Park YH. The role of formic acid in solution stability and crystallization of silk protein polymer. Int J Biol Macromol 2003;33:203-13.

[31] Klingman KL, Murphy TF. Purification and characterization of a high-molecular-weight outer membrane protein of

Moraxella (Branhamella) catarrhalis. Infect Immun 1994;62: 1150-5.

[32] Andrews GL, Simons BL, Young JB, Hawkridge AM, Muddiman DC. Performance characteristics of a new hybrid quadrupole time-of-flight tandem mass spectrometer (TripleTOF 5600). Anal Chem 2011;83:5442-6.

2

Reagents and cell line

4   All chemicals were purchased from Sigma-Aldrich (Sydney, Australia) except for octyl-glucoside (OG), which
     was obtained from Enzo Life Sciences (NY, USA) and DMP (dimethyl pimelimidate dihydrochloride), which

6   was from Pierce® (ThermoScientific, IL, USA). For the IP procedure, magnetic protein G beads were used
     (Cat. no. 28-9440-08) (GE Healthcare Biosciences, Uppsala, Sweden) and anti-uPAR antibody Clone R-4

8   (mouse IgG1, Abcam Pty Ltd, MA, USA) and mouse IgG1 isotype control antibody (MAB002) were used. For
     western immunoblotting, the antibodies used included: 3 ug/mL of unconjugated #AF807 for uPAR (goat

10   polyclonal, R&D systems, MN, USA), 1 μg/mL of clone H68.4 for transferring receptor (Tfr) (SantaCruz
     Biotechnology, CA, USA), 1 μg/mL of ab2910 for caveolin-1 (cav-1) (Abcam®, MA, USA), 1:1000 dilution of

12   ab133633 for carcino embryonic antigen (CEA) (Abcam®, MA, USA), 1:1000 dilution of clone AC-15-HRP for
     β-actin (Sigma-Aldrich®, MO, USA) and 1:1000 dilution of donkey anti-goat HRP conjugated secondary

14   antibody (HAF109) from R&D systems, MN, USA. The epithelial ovarian cancer cell line, OVCA429, was a
     kind gift from Dr. Robert Bast (MD Andersen Cancer Research Centre, Houston, USA). Sequencing-grade

16   trypsin (Cat. #V511, Promega Corp., MA, USA) was used for tryptic digestion of samples for MS analysis.

18   *Lysis conditions*
     Cells were grown in Dulbecco's modified eagle medium supplemented with 10% fetal bovine serum in either

20   6-well plates or 15-cm cell cultures dishes (for IP) at 37°C with 5% CO_2 till approximately 80% confluent.
     Media was discarded and washed 3 times with 15 mL ice-cold 1X PBS, pH 7.2 to remove residual medium.

22   Two-hundred microliter (for 6-well plates) and 1 mL (for 15cm dishes) of lysis buffer (50 mM Tris, pH 7.0,
     150 mM NaCl, 10 mM $CaCl_2$, 100 uM EDTA) containing 1X protease inhibitor cocktail (P8340; Sigma-

24   Aldrich, Sydney, Australia) and 1X phosphatase inhibitor cocktail (P5726; Sigma-Aldrich, Sydney, Australia)
     with various detergent components (Table S1) were added to the plate/dish and incubated for 30 min at 4°C

26   with occasional shaking. OG and the protease and phosphatase inhibitor cocktails were added just prior to
     cell lysis. Cells were then harvested by scraping into 1.5 mL low-protein binding microfuge tubes and

28   centrifuged at 1,500 x g for 15 min at 4°C to pellet nuclei. The supernatant was then transferred into new
     low-protein binding tubes and frozen at -80°C until used.

30

Table S1. Detergent components of the three lysis buffers used‡

Buffer description	Detergent components‡
Triton lysis buffer	1% Triton X-100. 10 mM $CaCl_2$
RIPA lysis buffer	1% NP-40, 0.5% sodium deoxycholate, 0.1% sodium dodecyl sulphate (SDS), 10 mM $CaCl_2$
OG lysis buffer	2% octyl-glucoside, 0.5% NP-40, 0.5% sodium deoxycholate, 0.1% SDS, 10 mM $CaCl_2$

‡*all concentrations are by weight per volume*

32

Protein quantification and immunoprecipitation

34   Cell lysates were diluted 10-fold and protein quantified using Pierce® BCA protein assay kit
     (ThermoScientific, IL, USA) according to manufacturer's instructions. Immunoprecipitation was performed

36   according to manufacturer's instructions (28953763AA) with modifications. Specifically, the pH of the binding
     and wash buffer (tris buffered saline; TBS) was at pH 7.0 instead of pH 7.5. All mixing steps were performed

38   with gentle end-over-end mixing to allow for homogenous mixing of beads in the solution. All buffers used in
     the crosslinking procedure were prepared fresh. Briefly, 10 μL of a 20% magnetic bead slurry (2 μL bead

40   volume) was washed with 1 mL TBS. This is followed by incubation with either five μg of R4 antibody or IgG1
     isotype control in 500 μL TBS for 1 h at room temperature. The buffer was then removed and washed twice

42   with 1X PBS, pH 7.2. After this, one millilitre cell lysate was pre-cleared with two μL mouse IgG1-conjugated
     beads containing 200 μg total protein for 1 h at 4°C. Subsequently, the antibody was covalently conjugated

44   to the beads via crosslinking as follows. The antibody-bead complex was washed with 500 μL of 200 mM

triethanolamine, pH 8.9 (crosslink solution A). The liquid was then removed and 500 μL of 10 mM DMP in
crosslink solution A was added and incubated for 15 min at room temperature with mixing. The solution was
then replaced with one mL of 100 mM ethanolamine, pH 8.9 (crosslink solution B) and incubated for 15 min
at room temperature with mixing. The liquid was replaced with 500 μL of elution buffer (2 M urea, 0.1 M
glycine-HCl, pH 2.5) and immediately washed twice with an equal volume of wash buffer (2 M urea, 50 mM
Tris-HCl, pH 7.0, 150 mM NaCl). The pre-cleared lysate was then added to the cross-linked beads and
incubated at 4°C for overnight with mixing. The lysate (flow-through) was then removed and the beads
washed three times with 1 mL TBS containing 0.01% triton X-100.

Western immunoblotting

Proteins were eluted off the beads by boiling in 10 μL of 4X NuPAGE LDS sample buffer (LDS-SB) (Life
Technologies Australia Pty Ltd., VIC, Australia) at 95°C for 10 min. Alternatively for serial elution's, the beads
were first incubated with 10 μL of 0.1% formic acid at 37°C for 10 min and then neutralized with 1 μL of 0.1M
ammonium bicarbonate (AMBIC), pH 8.0, followed by another 10 min with 10 μL of 0.1% ammonium
hydroxide (NH4OH), then with 10 μL of 1X LDS-SB at 95°C for 10 min, and then finally in 10 μL of 1X LDS-
SB containing 100 mM dithiothreitol (DTT) at 95°C for 10 min. The eluants were then loaded onto a 4-12%
NuPAGE Bis-Tris precast gel (Life Technologies Australia Pty Ltd., VIC, Australia) and subjected to SDS-
PAGE under reducing conditions (100 uM DTT) for 45 min at 200V constant till dye front reached the bottom.
Proteins were transferred onto PVDF membrane using Rapid Transfer buffer (AMRESCO Inc., OH, USA)
according to manufacturer's instructions at 20 V constant for 20 min. Western immunoblotting was performed
using the SNAP i.d.® system (Merck Ltd., VIC, Australia). Briefly, the membrane was blocked with 0.5% ECL
Advance Blocking Reagent (GE Healthcare Australia Pty. Ltd., NSW, Australia). For IP, two microgram per
mL of anti-uPAR antibody conjugated to horseradish peroxidase (HRP) was added and incubated for 20 min
prior to washing. HRP-conjugation was performed using the Lightning-Link™ HRP conjugation kit (Innova
Biosciences Ltd, Cambridge, UK) according to manufacturers instructions. Chemiluminescence detection
was performed by adding SuperSignal® West Femto maximum sensitivity substrate (Thermo Fisher
Scientific, VIC, Australia) and the blot imaged using a Luminescent Image Analyzer LAS-3000 (Fujifilm
Australia, NSW, Australia). For stripping of blot, Restore™ western blot stripping buffer (ThermoScientific, IL,
USA) was added for 10 min at room temperature with shaking before proceeding to western immunoblotting.

Tryptic digestion and mass spectrometry analysis

The beads (after IP) were resuspended in 100 μL of 25 mM AMBIC and reduced with 10 mM DTT for 90 min
at 37°C followed by alkylation with 55 mM iodoacetamide at room temperature for 45 min in the dark.
Assuming a 5 μg total protein eluate, a 1:50 ratio (100 ng) of sequencing grade trypsin was then added and
the beads incubated at room temperature overnight with gentle rotation. The digested peptides were then
water bath sonicated for 5 min. The supernatant was then transferred to a new tube. 150 μL of 50 mM
triethylammonium bicarbonate buffer (TEAB) was added to the beads and sonicated again before
transferring to the existing tube containing the digest. A final concentration of 1% formic acid was added to
the digest and concentrated down to 10 μL.

Digests were analysed on a nano LC-MS/MS (Eksigent Ultra nanoLC system, Eksigent; AB SCIEX™
TripleTOF® 5600 mass spectrometry, MA, USA). The sample was injected onto a peptide trap (Michrome
peptide Captrap) for pre-concentration and desalted with 0.1% formic acid, 2% ACN, at 5 μL/min for 10 min.
The peptide trap was then switched into line with the analytical column. Peptides were eluted from the
column using a linear solvent gradient, with steps, from mobile phase A: mobile phase B (98:2) to mobile
phase A:mobile phase B (60:40) where mobile phase A is 0.1% formic acid and mobile phase B is 90%
ACN/0.1% formic acid at 600 nL/min over a 140 min period. The reverse phase nanoLC eluent was
subjected to positive ion nanoflow electrospray analysis in an information dependant acquisition mode (IDA).
In IDA mode, a TOFMS survey scan was acquired (m/z 350 - 1500, 0.25 sec) with the 15 most intense
multiply charged ions (counts >150) in the survey scan sequentially subjected to MS/MS analysis. MS/MS
spectra were accumulated for 50 millisec in the mass range m/z 100 – 1500 with the total cycle time of 1.05
sec.

100 ***Data analysis***

For non-parametric analysis, Kruskal-Wallis test was used to compare between the groups followed by a
102 posthoc Mann-Whitney U test. For parametric analysis, multifactorial ANOVA was used with Tukey's posthoc
test. Values were considered statistically significant when $P \leq 0.05$. The experimental nanoLC ESI MS/MS
104 data were submitted to ProteinPilot V4.2 (AB SCIEX™, MA, USA) for data processing using *Homo sapiens*
and *Mus musculus* species. Bias correction was selected and the detected protein threshold (unused
106 ProtScore) was set at larger than 1.3 ($\geq 95\%$ confidence). FDR (False discovery rate) analysis was selected.
Generated MGF files were submitted to Mascot Daemon server (*Homo sapiens* - SwissProt_2012.fasta, Jun
108 2012; Mus musculus - SwissProt_2012x database selected for *Mus musculus*, Jun 2012) with monoisotopic
fragment and parent tolerance at 0.1 Da and 50 ppm, respectively. Variable modifications were set at +16 on
110 M (oxidation) and +57 on C (carbamidomethyl) with maximum missed cleavage at 1. Generated Mascot log
files were then submitted to Scaffold™ (version 3.5.1) (Proteome Software Inc., OR, USA) and 95% peptide
112 confidence was selected.

114

Appendix IV – Ethics approval

MACQUARIE UNIVERSITY

Research Office
Ethics
Research Hub, Buliding C5C East
MACQUARIE UNIVERSITY NSW 2109 AUSTRALIA

Phone +61 (0)2 9850 6848
Phone 2 +61 (0)2 9850 8612
Fax +61 (0)2 9850 4465
Email ethics.secretariat@ro.mq.edu.au

30 October 2012

Prof Mark Baker
Department of Chemistry and Biomolecular Sciences
Faculty of Science
MACQUARIE UNIVERSITY

Reference: 5201200702

Dear Prof Baker,

FINAL APPROVAL

Title of project: "Deep drilling of the low abundance human plasma proteome for candidate biomarkers of colorectal cancer onset, Stage and clinical progression" (Ethics Ref: 5201200702)

Thank you for your recent correspondence. Your response has addressed the issues raised by the Human Research Ethics Committee and you may now commence your research.

This research meets the requirements of the National Statement on Ethical Conduct in Human Research (2007). The National Statement is available at the following web site:

http://www.nhmrc.gov.au/_files_nhmrc/publications/attachments/e72.pdf.

The following personnel are authorised to conduct this research:

A/Prof Edouard Nice
Dr Charlie Ahn
Mr Harish Reddy Cheruku
Mrs Sadia Mahboob
Ms Sock Tan
Prof Mark Baker

NB. STUDENTS: IT IS YOUR RESPONSIBILITY TO KEEP A COPY OF THIS APPROVAL EMAIL TO SUBMIT WITH YOUR THESIS.

Please note the following standard requirements of approval:

1.   The approval of this project is conditional upon your continuing compliance with the National Statement on Ethical Conduct in Human Research (2007).

2.   Approval will be for a period of five (5) years subject to the provision of annual reports.

Progress Report 1 Due: 30 October 2013
Progress Report 2 Due: 30 October 2014
Progress Report 3 Due: 30 October 2015
Progress Report 4 Due: 30 October 2016
Final Report Due: 30 October 2017

www.research.mq.edu.au/researchers/ethics/human_ethics

NB. If you complete the work earlier than you had planned you must submit a Final Report as soon as the work is completed. If the project has been discontinued or not commenced for any reason, you are also required to submit a Final Report for the project.

Progress reports and Final Reports are available at the following website:

http://www.research.mq.edu.au/for/researchers/how_to_obtain_ethics_approval/human_research_ethics/forms

3.   If the project has run for more than five (5) years you cannot renew approval for the project. You will need to complete and submit a Final Report and submit a new application for the project. (The five year limit on renewal of approvals allows the Committee to fully re-review research in an environment where legislation, guidelines and requirements are continually changing, for example, new child protection and privacy laws).

4.   All amendments to the project must be reviewed and approved by the Committee before implementation. Please complete and submit a Request for Amendment Form available at the following website:

http://www.research.mq.edu.au/for/researchers/how_to_obtain_ethics_approval/human_research_ethics/forms

5.   Please notify the Committee immediately in the event of any adverse effects on participants or of any unforeseen events that affect the continued ethical acceptability of the project.

6.   At all times you are responsible for the ethical conduct of your research in accordance with the guidelines established by the University. This information is available at the following websites:

http://www.mq.edu.au/policy/

http://www.research.mq.edu.au/for/researchers/how_to_obtain_ethics_approval/human_research_ethics/policy

If you will be applying for or have applied for internal or external funding for the above project it is your responsibility to provide the Macquarie University's Research Grants Management Assistant with a copy of this email as soon as possible. Internal and External funding agencies will not be informed that you have final approval for your project and funds will not be released until the Research Grants Management Assistant has received a copy of this email.

Please retain a copy of this letter as this is your official notification of final ethics approval.

Yours sincerely

Dr Karolyn White
Director of Research Ethics
Chair, Human Research Ethics Committee

Fwd: Ethics application ref: 5201200702 - Amendment Approved

SADIA MAHBOOB <sadia.mahboob@students.mq.edu.au>   Thu, Jul 23, 2015 at 11:15 AM
To: Harish Cheruku <harish.cheruku@mq.edu.au>

———— Forwarded message ————
From: **Ethics Secretariat** <ethics.secretariat@mq.edu.au>
Date: Mon, Sep 16, 2013 at 1:29 PM
Subject: Re: Ethics application ref: 5201200702 - Amendment Approved
To: SADIA MAHBOOB <sadia.mahboob@students.mq.edu.au>
Cc: Mark Baker <mark.baker@mq.edu.au>

Dear Sadia

Thank you for your email and apologies for the oversight.

The addition of the following personnel to the project has been approved:

1. Mr David Cantor
2. Ms Bhooma Venkatraman

Please do not hesitate to contact the Ethics Secretariat if you have any questions.

Kind regards
Fran

On Mon, Sep 16, 2013 at 1:18 PM, SADIA MAHBOOB <sadia.mahboob@students.mq.edu.au> wrote:
> Dear Nicola
>
> Thanks a lot for the approval of amendment. Just wanted to confirm that we have also requested to
> include two new students in the application. Their details have been included in the amendment form.
> Please ;et me know if you need any further details about the requested amendments.
>
> Thanks and regards
> Sadia
>
>
> On Mon, Sep 16, 2013 at 11:35 AM, Ethics Secretariat <ethics.secretariat@mq.edu.au> wrote:
>
>> Dear Professor Baker
>>
>> RE: "Deep drilling of the low abundance human plasma proteome for candidate biomarkers of colorectal
>> cancer onset, Stage and clinical progression"
>>
>> Thank you for submitting an amendment to the above application on the 4th September 2013.
>>
>> The following amendments to the above study have been approved:
>>
>> 1. The application of a new methodology (Proseek technology developed by Olink, Upsala, Sweden) to
>> analyse the samples.
>>
>> This HREC is constituted and operates in accordance with the National Health and Medical Research
>> Council's (NHMRC) *National Statement on Ethical Conduct in Human Research (2007)* (the National
>> Statement) and the CPMP/ICH Note for Guidance on Good Clinical Practice (Guidance Note).
>>
>> Please ensure that a copy of this approval correspondence is forwarded to all the investigators listed on

the project.

The HREC wishes you every success in your research.

Regards

Nicola Myton
Human Research Ethics Officer (Health)

—

Ethics Secretariat
Research Office
Level 3, Research Hub, Building C5C East
Macquarie University
NSW 2109 Australia
T: +61 2 9850 6848
F: +61 2 9850 4465
http://www.mq.edu.au/research

—

Sadia Mahboob
PhD Student
Cancer Proteomics & Biomarker Group
Department of Chemistry & Biomolecular Sciences
Faculty of Science
Macquarie University
Building F7B, Room 233
Office: +61-2-9850-1176
Fax: +61-2-9850-8313

—
—

Ethics Secretariat
Research Office
Level 3, Research Hub, Building C5C East
Macquarie University
NSW 2109 Australia
T: +61 2 9850 6848
F: +61 2 9850 4465
http://www.mq.edu.au/research

–
Sadia Mahboob
PhD Student
Cancer Biology & Human Proteomics Research Group
Australian School of Advanced Medicine
Faculty of Medicine and Health Science
2 Technology Place,
Macquarie University. NSW 2109, AUSTRALIA
Email: sadia.mahboob@students.mq.edu.au

Appendix V – Biosafety certificate

MACQUARIE
UNIVERSITY

Biosafety and
Biohazards Workshop

This is to certify that

Harish Cheruku

has successfully completed the above workshop which was conducted by the
Macquarie University Institutional Biosafety Committee and
Biohazards Safety Committee on 10 April 2012

Dr Subra Vemulpad
Chair, Institutional Biosafety Committee
April 2012

Expiry Date:
April 2015